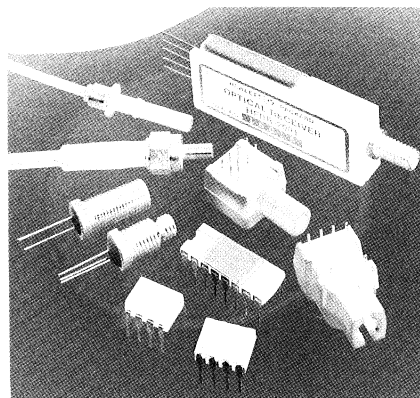
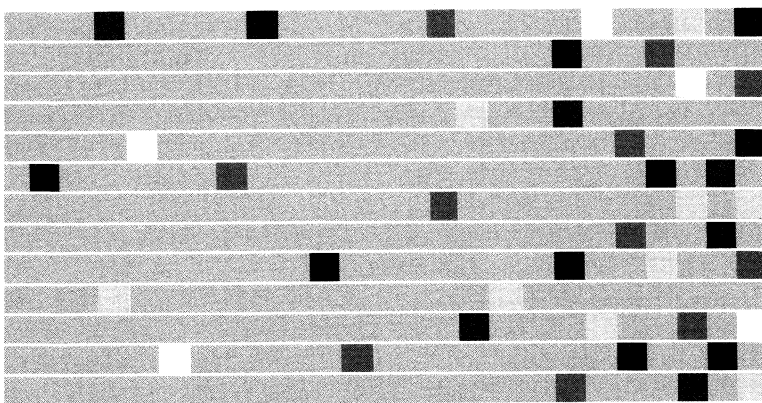


Optocouplers and Fiber Optics Applications Handbook



HEWLETT
PACKARD

This handbook is designed to give you a variety of applications information for designing with HP's high performance optocouplers and fiber optic components. There are four sections for Optocouplers and five for Fiber Optic Components.

Chapters one and five are entitled Optocoupler Technology and Fiber Optic Technology. On the first two pages of each of these two chapters is a description of the HP product families and their performance characteristics. This is designed to help you narrow your product choice. The following

chapters are then organized according to product family. Product selection guides in the front of each chapter give you brief specifications of the product part numbers. Articles and Application Notes concerning these product families follow the selection guides.

The appendix contains information on where HP sales and service offices are located worldwide as well as locations of HP's authorized distributors for off-the-shelf delivery of HP components.

Optocouplers and Fiber Optics Applications Handbook

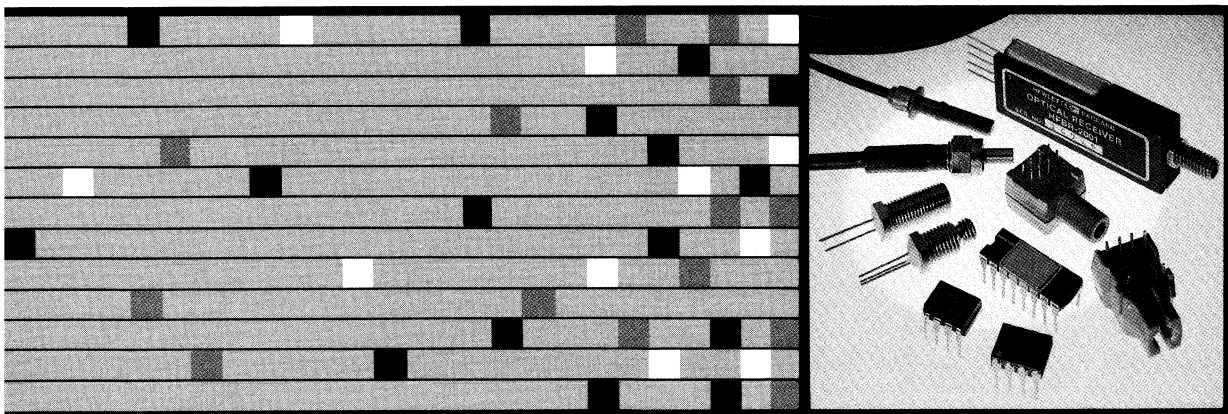
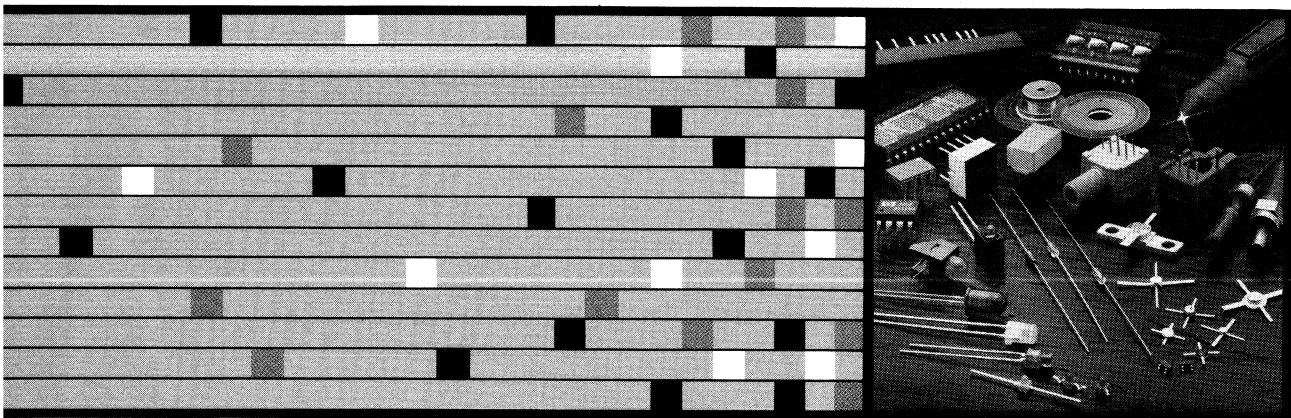


Table of Contents

	Page
HP Components: A Brief Sketch	iv
HP: Helping You in Application and Design	v
Optocoupler Technology	1
HP Optocoupler Families: A Description	2
Consideration of CTR Variations in Optocoupler Circuit Designs	3
Digital Data Transmission Using Optically Coupled Isolators	19
Optocouplers for Digital Data Transmission	55
Hermetic/MIL STD Optocouplers	63
Selection Guide	64
Screening Programs	65
Radiation Immunity of HP Optocouplers	69
High Speed/High Gain Optocouplers	73
Selection Guide	74
CMOS Circuit Design Using HP Optocouplers	76
Performance of the 6N135, 6N136 and 6N137 Optocouplers in Short to Moderate Length Digital Data Transmission	79
Linear Applications of Optocouplers	88
High Speed Optocoupler vs. Pulse Transformer	92
Coming in at 20 MBaud, An Optocoupler IC Doubles the Data Transfer Rate	94
Applications for Low Input Current, High Gain Optocouplers	98
Application Specific Optocouplers	103
Selection Guide	104
Applications Circuits for HCPL-3700 and HCPL-2601	105
Threshold Sensing for Industrial Control Systems with the HCPL-3700 Interface Optocoupler	107
Ring Detection with the HCPL-3700 Optocoupler	120
Interfacing from Industrial Control Systems to Microprocessor	124
Designing with the HCPL-4100 and HCPL-4200 Current Loop Optocouplers	133
Fiber Optic Technology	153
HP Fiber Optic Families: A Description	154

	Page
Optical Fiber or Wire: The Designer's Dilemma or a Clear Choice	156
HP's Connector Assembly Tooling Kit Simplifies Connector Attachment to Fiber Optic Cable	159
Design Considerations for Fiber Optic Data Communications Systems	163
General Concerns for LAN Fiber Optic Cable Installation	167
Use of Standard Modulation Codes for Fiber Optic Link Optimization	173
Reliability Considerations in Designing Fiber Optic Transmitters	177
Fiber Optic Multiplexer Clusters Signals from 16 RS-232-C Channels	180
Threshold Detection of Visible and Infrared Radiation with PIN Photodiodes	184
Plastic Snap-in Fiber Optic Components	191
Selection Guide	192
An Introduction to Plastic Fiber Optic Technology	193
Low Cost Miniature Fiber Optic Components	199
Selection Guide	200
Using 200 μ m PCS Optical Fiber with HP Components	201
Fiber Optic SMA Connector Technology	208
Fiber/Cable Selection for LED Based Local Communications Systems	210
Baseband Video Transmission with Low Cost Fiber Optic Components	213
High Performance, Low Cost, Third Generation Fiber Optic Components	215
Miniature Fiber Optic Components	225
Selection Guide	226
Using 50/125 μ m Optical Fiber with HP Components	227
High Speed Fiber Optic Link Design with Discrete Components	231
High Performance Fiber Optic Modules	245
Selection Guide	246
Digital Data Transmission with the HP Fiber Optic System	247
Appendix	267
HP Components US Sales Offices	268
HP Worldwide Sales and Service Offices	269
HP Authorized Components Distributors	276
Application Note Number/Title Cross Reference	280
Solder Flux Considerations	281
HP Fiber Optic Test Equipment Summary	282



Hewlett-Packard Components: A Brief Sketch

In 1964, Hewlett-Packard established a new division having the charter of developing and producing state-of-the-art electronic components for internal use. By 1975, both microwave and optoelectronic devices contributed to the growing business of Hewlett-Packard and the Components Group was formed. Today there are three divisions: the Optoelectronics division, Optical Communications division and Microwave Semiconductor division. In addition to these three divisions there is a specialized team of people to develop, manufacture and market bar code components.

The products of the Components Group are vertically integrated, from the growing of LED crystals to the development of the

various onboard integrated circuits to package design. Vertical integration insures that HP quality is maintained throughout product development and manufacturing.

Over 5200 employees are dedicated to HP Components, including manufacturing facilities in Malaysia and Singapore, factory and marketing support in San Jose, California and a world-wide sales force. Marketing operations for Europe are located in Boeblingen, Germany.

Each field sales office is staffed with engineers trained to provide technical assistance. An extensive communications network links field with factory to assure that each customer can quickly attain the information and help needed.

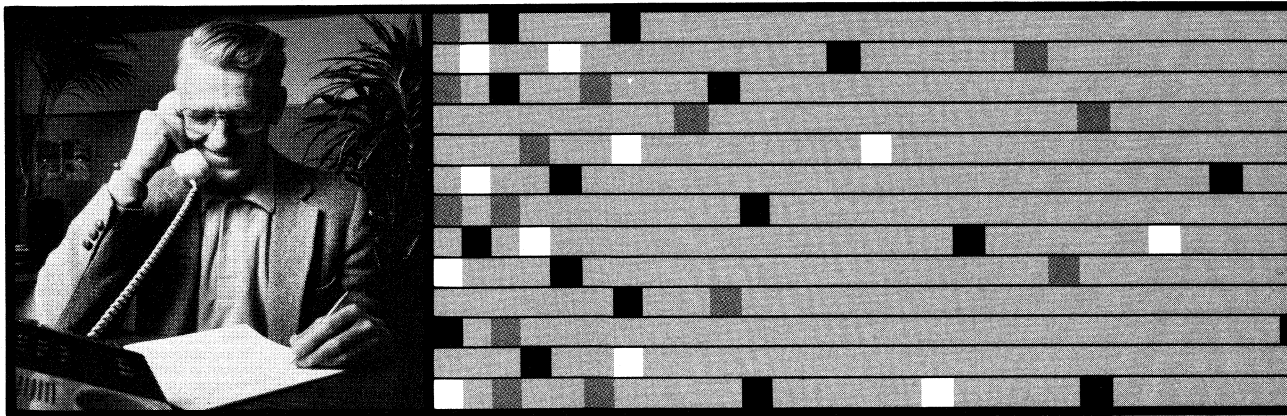
HP: Helping You in Application and Design.

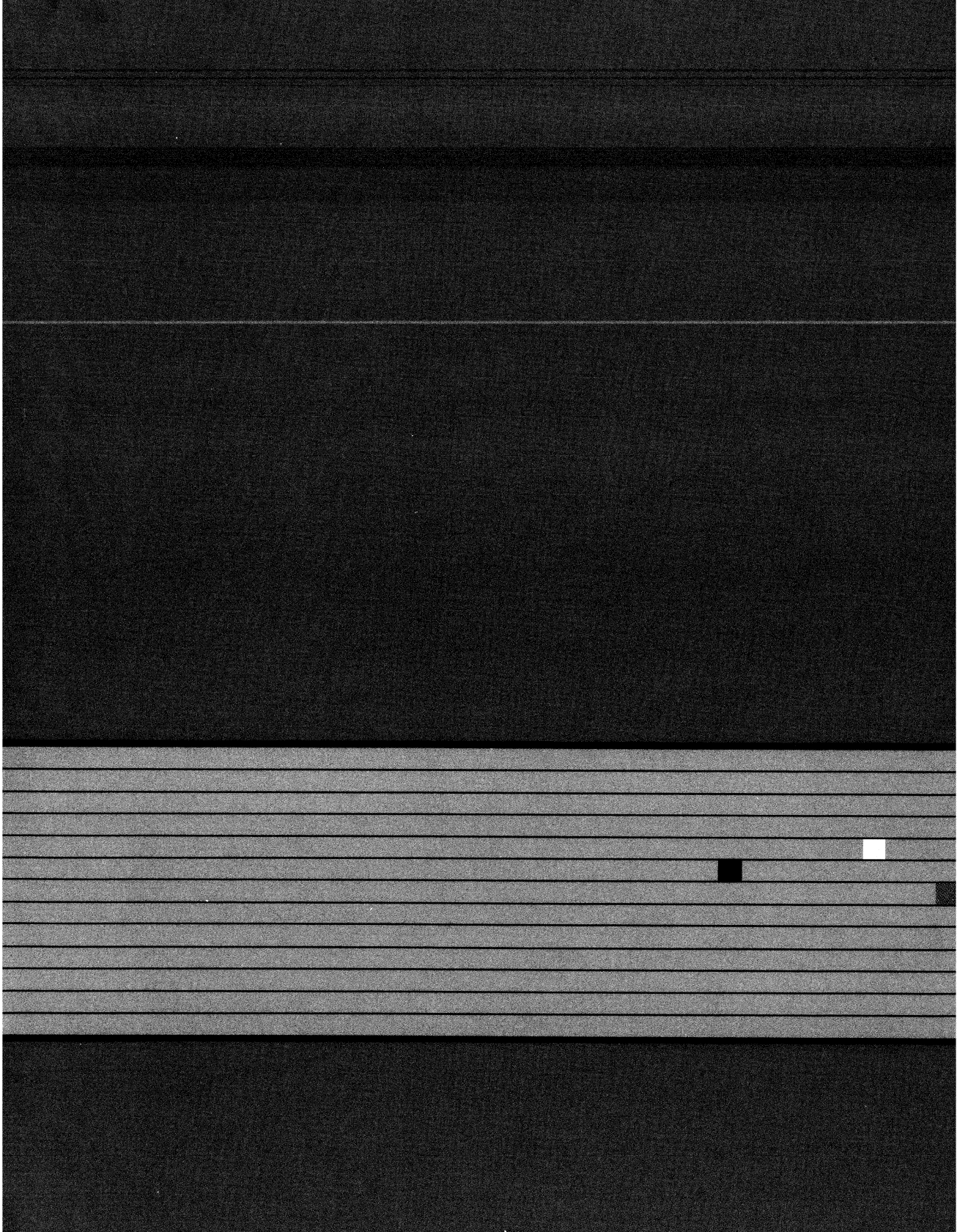
The applications staff for HP optical communication components is dedicated to providing technical support for you. This includes being available by phone 8:00 a.m. to 5:00 p.m. Pacific time, at (408) 435-6679. These engineers total over 30 years of experience.

In addition to answering your questions by phone, they have authored the information in this handbook. They write articles published

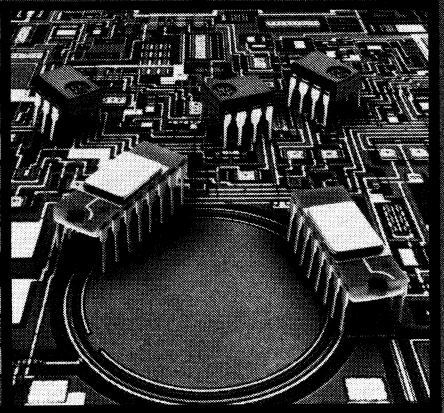
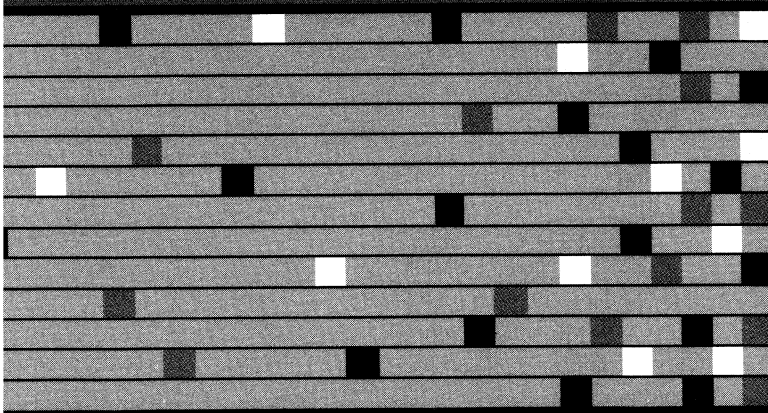
in technical publications and presented at conferences. They train our field sales force and design seminars to help you stay abreast of the latest advances in the application of the technology.

All of these activities are focused on helping you, wherever you live. Operations in Boeblingen, Germany, Japan, and many other countries in the world have applications engineers ready to serve your needs.





Optocoupler Technology



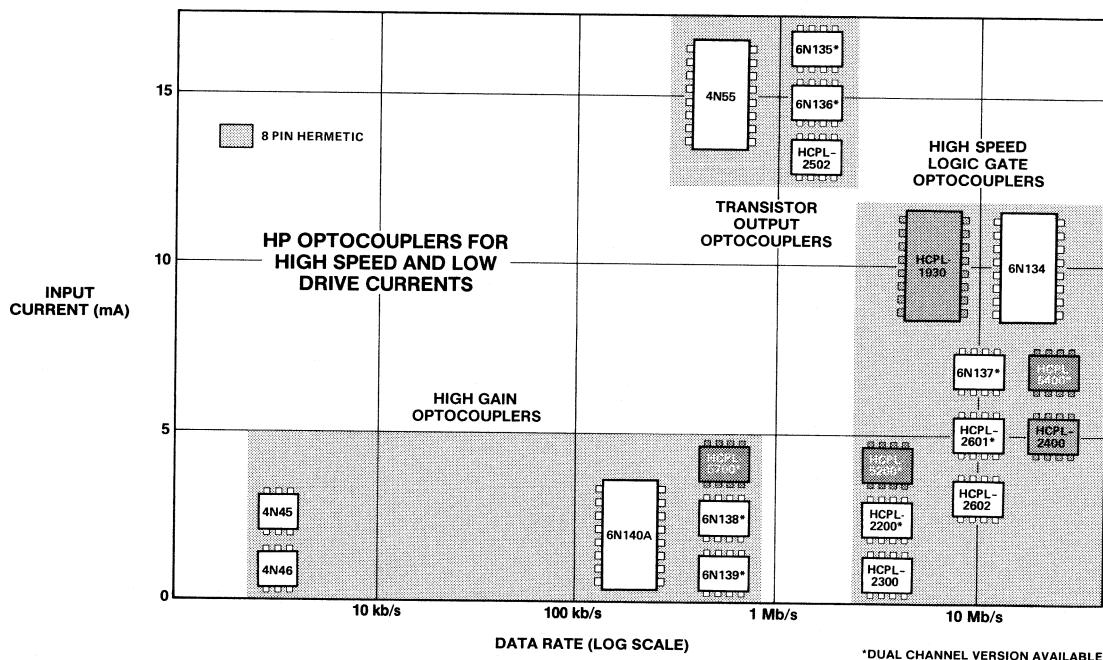
HP Optocoupler Families: A Description

HP offers a broad range of high performance optocouplers designed to provide isolation for system interfaces for a wide variety of applications. By utilizing the latest technology and by building in the quality and reliability required for today's marketplace, HP optocouplers are the first choice of the world's leading suppliers of telecommunications, computer and industrial control equipment. HP optocouplers not only provide solutions in commercial environments but also in military/high reliability environments including space applications (Class S).

All HP optocouplers in plastic packages meet the Underwriter's Laboratory requirement for a working voltage of 220 V ac. Our Option 010 meets U.L.'s specification for a 2500 V ac., 1 minute tested optocoupler. Both types are recognized by U.L. file number E55361.

Whether you need high speed logic compatibility, ac/dc threshold sensing or isolated 20 mA current loop transmitters and receivers, HP has a quality optocoupler for your application.

Hewlett-Packard High Performance Optocouplers





Consideration of CTR Variations in Optocoupler Circuit Designs

INTRODUCTION — Optocouplers Aging Problem

A persistent, and sometimes crucial, concern of designers using optocouplers is that of the current transfer ratio, CTR, changing with time. The CTR is defined as the ratio of the output current, I_O , of the optocoupler divided by the input current, I_F , to the light emitting diode expressed as a percentage value at a specified input current. The resulting optocoupler's gain change, ΔCTR^+ , with time is referred to as CTR degradation. This change, or degradation, must be accounted for if long, functional lifetime of a system is to be guaranteed.

A number of different sources for this degradation will be explained in the next section, but numerous studies have demonstrated that the predominant factor for degradation is reduction of the total photon flux being emitted from the LED, which, in turn, reduces the device's CTR. This degradation occurs to some extent in all optocouplers.

$$^+\Delta CTR = CTR_{\text{final}} - CTR_{\text{initial}} \quad (1)$$

Causes

The main cause for CTR degradation is the reduction in efficiency of the light emitting diode within the optocoupler. Its quantum efficiency, η , defined as the total photons per electron of input current, decreases with time at a constant current. The LED current is comprised primarily of two components, a diffusion current component, and a space-charge recombination current:

$$I_F(V_F) = \underbrace{A e^{\frac{qV_F}{kT}}}_{\text{Diffusion}} + \underbrace{B e^{\frac{qV_F}{2kT}}}_{\text{Space-Charge Recombination}} \quad (2)$$

where A and B are independent of V_F , q is electron

charge, k is Boltzmann's constant, T is temperature in degrees Kelvin, and V_F is the forward voltage across the light emitting diode.

The diffusion current component is the important radiative current and the non-radiative current is the space-charge recombination current. Over time, at fixed V_F , the total current increases through an increase in the value of B. From another point of view, with fixed total current, if the space-charge recombination current increases, due to an increase in the value of B, then the diffusion current, the radiative component, will decrease. The specific reasons for this increase in the space-charge recombination current component with time are not fully understood.

The reduction in light output through an increase in the proportion of recombination current at a specific I_F is due to both the junction current density, J, and junction temperature, T_J . In any particular optocoupler, the emitter current density will be a function of not only the required current necessary to produce the desired output, but also of the junction geometry and of the resistivity of both the P and N regions of the diode. For this reason, it is important not to operate a coupler at a current in excess of the manufacturer's maximum ratings. The junction temperature is a function of the coupler packaging, power dissipation and ambient temperature. As with current density, high T_J will promote a more rapid increase in the proportion of recombination current.

The junction and IC detector temperature of Hewlett-Packard optocouplers can be calculated from the following expressions:

$$T_J = T_A + \theta_{11} (V_F I_F) + \theta_{12} (V_O I_O + V_{CC} I_{CC})$$

$$T_D = T_A + \theta_{21} (V_F I_F) + \theta_{22} (V_O I_O + V_{CC} I_{CC}) \quad (3)$$

where the T_J is the junction temperature of the LED emitter, T_D is the junction temperature of the detector IC, T_A is ambient temperature, and the internal thermal resistances are $\theta_{11} = \theta_{22} = 370^\circ \text{C/W}$, and $\theta_{12} = \theta_{21} = 170^\circ \text{C/W}$. V_F , I_F are the forward LED voltage and current; V_O , I_O are the output stage voltage, and current and V_{CC} , I_{CC} are the power supply voltage and current to the device. In general, it is desirable to maintain $T_J \leq 125^\circ \text{C}$.

A useful model can be constructed to describe the basic optocoupler's parameters which are capable of influencing the current transfer ratio. The 6N135 optocoupler, Figure 1 is the simplest device and one which is easily accessible for needed parameter measurements. However, any optocoupler can be modeled in this fashion within its linear region. Figure 1 shows the system block diagram which yields the relationship of input current, I_F , to output current, I_O . The resulting expression for CTR is:

$$\text{CTR} = \frac{I_O}{I_F} (100\%) = K R \eta (I_F, t) \beta (I_P, t) \quad (4)$$

where K represents the total transmission factor of the optical path, generally considered a constant as is R, the responsivity of the photodetector, defined in terms of electrons of photocurrent per photon. η is the quantum efficiency of the emitter defined as the photons emitted per

electron of input current and depends upon the level of input current, I_F , and upon time. Finally, β is the gain of the output amplifier and is dependent upon I_P , the photocurrent, and time. Temperature variations would, of course, cause changes in η , β as well.

From Equation (4), a normalized change in CTR, at constant I_F , can be expressed as:

$$\frac{\Delta \text{CTR}}{\text{CTR}} = \left(\frac{\Delta \eta}{\eta} \right)_{I_F} + \left(\frac{\Delta \eta}{\eta} \right)_{I_F} \left(\frac{\partial \ln \beta}{\partial \ln I_P} \right)_t + \left(\frac{\Delta \beta}{\beta} \right)_{I_P} \quad (5)$$

The first term, $\Delta \eta / \eta$, represents the major contribution to ΔCTR due to the relative emitter efficiency change; generally, over time, $\Delta \eta$ is negative. This change is strongly related to the input current level, I_F , as discussed earlier and more elaboration will be given later. The second term, $(\Delta \eta / \eta)_{I_F} (\partial \ln \beta / \partial \ln I_P)_t$, represents a second order effect of a shift, positive or negative, in the operating point of the output amplifier as the emitter efficiency changes. The third term, $(\Delta \beta / \beta)_{I_P}$, is a generally negligible effect which represents a positive or negative change in the output transistor gain over time. The parameters K and R are considered constants in this model.

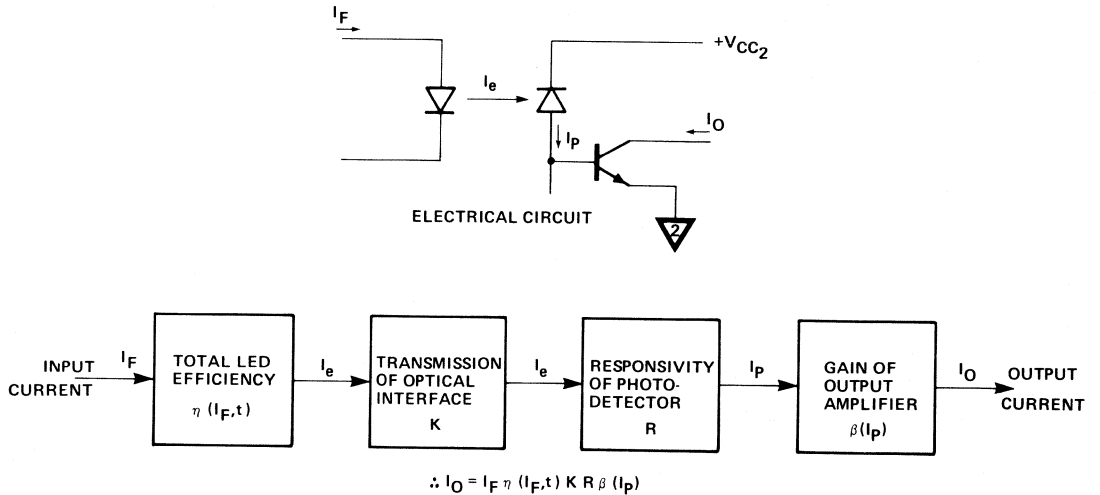


Figure 1. System Model for an Optocoupler

Degradation Model

In this section, an extensive test program conducted at Hewlett-Packard to characterize the CTR degradation of optocouplers is discussed. The development which will follow is mainly of interest to those concerned with reliability and quality assurance. From the basic data, the CTR degradation equations will be developed in order to predict the percentage change in CTR with time. Complete data and analysis of CTR degradation will be found in an internal Hewlett-Packard report.

This study is based on a total of 640 optocouplers of the 6N135 type (Figure 1) with 700nm GaAs_{0.7}P_{0.3} LEDs from twenty different epitaxial growth lots representing a range of n-type doping and radiance. The 6N135 allows access to measurement of the emitter degradation via the relative percentage change in photodiode current, $\Delta I_p/I_p$, as well as output amplifier β change. Stress currents of $I_{FS} = .6, 7.5, 25$ and 40 mA were applied to different groups of optocouplers, and at each measurement time of $t = 0, 24, 168, 1000, 2000, 4000$ and $10,000$ hours, measurement currents of $I_{FM} = .5, 1.6, 7.5, 25$ and 40 mA were used to determine the CTR.

The important results to be noted are the following. First, a factor of major significance in the study of CTR degradation is the ΔCTR varies as a function of the ratio of $I_{FS}/I_{FM} \equiv R$. Large values of R will result in greater CTR degradation than at lower R values with the same magnitude of I_{FS} . However, knowledge of the ratio of I_{FS}/I_{FM} alone does not give a complete picture of degradation because ΔCTR is also dependent upon the absolute magnitude of the stress current, $|I_{FS}|$. The following data will allow the derivation of the necessary equations with which to predict ΔCTR as a function of I_{FS}, I_{FM} and time.

Figure 2 displays the mean and mean plus 2σ values of emitter degradation versus R for 1K, 4K, and 10K hours at 25°C . Accelerated degradation can be seen at larger R values.

The data of Figure 2 can be replotted to illustrate the percentage degradation versus time as a function of R . Figure 3 illustrates the mean and mean plus 2σ distribution with $R = 1$ and 50 .

From this curve, a useful expression which relates the average degradation in emitter efficiency to time is obtained for the mean or mean plus 2σ distributions. [The symbol "D" will refer to CTR degradation due solely to emitter degradation, $\Delta\eta/\eta$, whereas $\Delta CTR/CTR$ will refer to total CTR degradation as expressed in Equation (5)].

$$\bar{D}_x \text{ or } \bar{D}_x + 2\sigma \equiv \frac{-\Delta I_p}{I_p} = A_0 R^{\alpha} t^n(R) \text{ in \% for } I_{FS} = \bar{I}_{FS} \quad (6)$$

where t is in 10^3 hours and A_0 and α differ for mean or mean plus 2σ . Equation (6) represents an average degradation corresponding to a specific R, t , and an average stress current \bar{I}_{FS} . A knowledge of \bar{I}_{FS} and the actual device operating stress I_{FS} can be utilized to correct \bar{D} to a value D which reflects the actual absolute magnitude of I_{FS} . This will be shown in the development of Equations (11) and (13). The data shows that \bar{I}_{FS} increases with R and can be represented as follows:

$$\bar{I}_{FS}(R) = 14.13 + 9.06 \log_{10} R, \text{ mA}, T_A = 25^\circ\text{C} \quad (7)$$

$$\bar{I}_{FS}(R) = 10.5 + 5.76 \log_{10} R, \text{ mA}, T_A = 85^\circ\text{C} \quad (8)$$

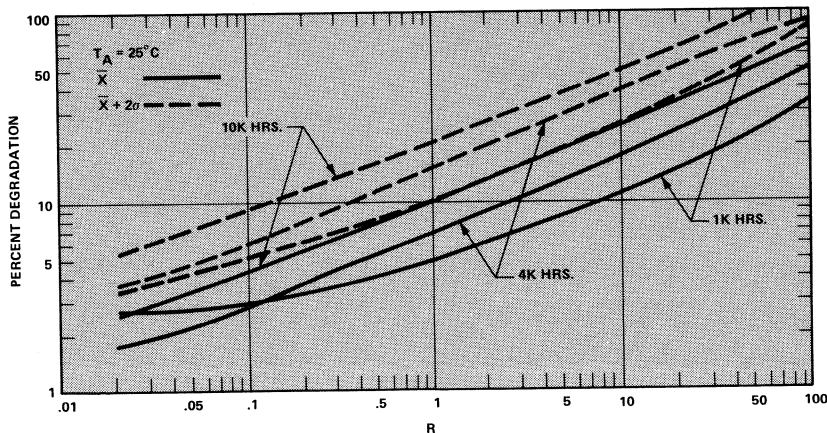


Figure 2. Emitter Degradation vs. R (Ratio of Stress Current to Measurement Current) for 1k, 4k, and 10k Hours, Mean, Mean + 2σ Distribution, $T_A = 25^\circ\text{C}$.

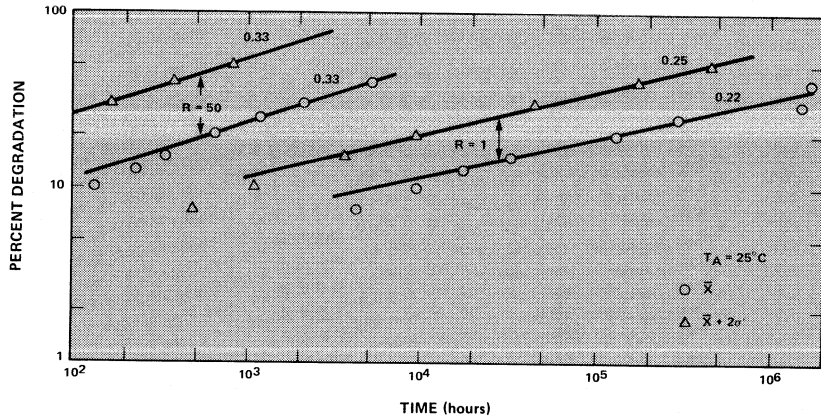


Figure 3. Emitter Degradation vs. Time at $R = 1$ and $R = 50$ for Mean, Mean + 2σ Distributions, $T_A = 25^\circ\text{C}$

These equations are obtained from averaged degradation data versus I_{FS} at different measurement times.

The expression for $n(R)$ was found to obey the relationship

$$n(R) = .0475 \log_{10} R + .25 \quad (9)$$

A_0 and α were determined from degradation data versus R and are found in Figure 7, "Matrix of Coefficients."

Equation (6) gives a direct relationship between the average degradation, \bar{D} , and time. As mentioned earlier, the magnitude of the stress current also determines the amount of degradation. In order to allow for the effect of $|I_{FS}|$, empirical observations were made on D at different I_{FS} and at different times for several values of R . The dependence of degradation on stress current is linear up to $I_{FS} = 40$ mA, for all values of R . From these observations, the average rate of change, or slope, $S(R, t)$, of degradation D with I_{FS} over time was found to behave in the following fashion for any R :

$$S \equiv \frac{\partial D}{\partial I_{FS}} = \alpha(R) \log_{10} t + \beta(R) \quad \%/mA \quad (10)$$

where t is in 10^3 hours, the coefficients $\alpha(R)$ and $\beta(R)$ can be found on Figure 7.

Along with Equation (10), the mean distribution degradation, $\bar{D}_{\bar{x}}$, can be estimated for any specific stress current, I_{FS} , ratio R , and time t via the subsequent expression:

$$D_{\bar{x}} = \bar{D}_{\bar{x}} + S [I_{FS} - \bar{I}_{FS}] \quad \% \quad (11)$$

or substituting Equation (6),

$$D_{\bar{x}} = A_0 R^\alpha t^{n(R)} + S [I_{FS} - \bar{I}_{FS}] \quad \% \quad (12)$$

where, again, $\bar{D}_{\bar{x}}$ is the average degradation at time t , in units of 10^3 hours, corresponding to an average stress current, \bar{I}_{FS} , given by Equations (7) and (8); I_{FS} is the actual stress current. In equation (12) $R = I_{FS}/I_{FM}$; S is the expression (10) for the change of slope of D versus I_{FS} with time; $n(R)$ is a power of t , given by Equation (9), and A_0 , α are found in Figure 7.

Equation (11) gives the mean distribution degradation by using an average degradation value, $\bar{D}_{\bar{x}}$ (first term), corresponding to the ratio of I_{FS}/I_{FM} , or an average stress current, \bar{I}_{FS} , and then applying a correction quantity (second term) to $\bar{D}_{\bar{x}}$ due to the magnitude of the actual stress current, I_{FS} , yielding the actual degradation $D_{\bar{x}}$.

The expression for the mean + 2σ distribution degradation, $D_{\bar{x} + 2\sigma}$, (worst case) is almost of the same form as Equation (11). The dissimilarity arises from the fact that the standard deviation, σ , is dependent upon the stress current, I_{FS} , the ratio R , and upon time. This complex dependency was analytically deduced from the data to be the following expression:

$$D_{\bar{x} + 2\sigma} = \bar{D}_{\bar{x} + 2\sigma} + [S + 2P] [I_{FS} - \bar{I}_{FS}] \quad \% \quad (13)$$

or substituting Equation (6)

$$D_{\bar{x} + 2\sigma} = A_0 R^\alpha t^{n(R)} + [S + 2P] [I_{FS} - \bar{I}_{FS}] \quad \% \quad (14)$$

where $\bar{D}_{\bar{x} + 2\sigma}$ is the average degradation for $\bar{x} + 2\sigma$ distribution corresponding to the average stress current \bar{I}_{FS} ,

Equations (7) and (8). In equation (14) A_0 and α are found in Figure 7 under the $\bar{x} + 2\sigma$ category. S [Equation (10)] represents the slope to correct for actual I_{FS} versus \bar{I}_{FS} current levels, and P [Equation (15)] is the new term which is a slope to correct for the σ variation with I_{FS} , R and t. The coefficients $\gamma(R)$, $\delta(R)$ in P are found in Figure 7.

$$P = \gamma(R) \log_{10} t + \delta(R) \quad \%/\text{mA} \quad (15)$$

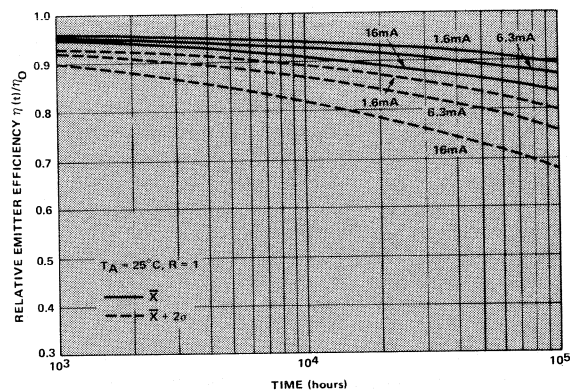
where t is in 10^3 hours.

The degradation Equations (11) and (13) are considered accurate for the ranges of $I_{FS} \leq 40$ mA and $R \leq 20$; outside this range, the model does not predict degradation as well. Hence, check to see if I_{FS} and R satisfy the above conditions. If I_{FS} or R exceed these limits, prediction of D will be, in general, greater than the actual degradation due to large values for S and P which do not reflect actual S and P. If \bar{I}_{FS} is approximately equal to the actual I_{FS} , then the second term in the degradation equations need not be determined. Otherwise, the second term needs to be determined to obtain true emitter degradation, D. If $I_{FS} < \bar{I}_{FS}$, then the degradation, D, will be less than the degradation, \bar{D} , corresponding to \bar{I}_{FS} , and vice versa when $I_{FS} > \bar{I}_{FS}$. A quick and coarse estimate for degradation \bar{D} can be obtained by using $\bar{D} = A_0 R^{\alpha} t^{n(R)}$ for a specific R with approximate values for $\alpha \approx 0.4$ and $n \approx 0.3$. Figure 4 represents plots of Equations (11) and (13) for $R = 1$ and $I_{FS} = 1.6, 6.3$, and 16 mA at both $T_A = 25^\circ\text{C}$ and $T_A = 85^\circ\text{C}$. These plots are very useful in making a quick approximation of D for the specific conditions for which the plots have been made. These conditions represent the recommended operating conditions for the three HP optocoupler families.

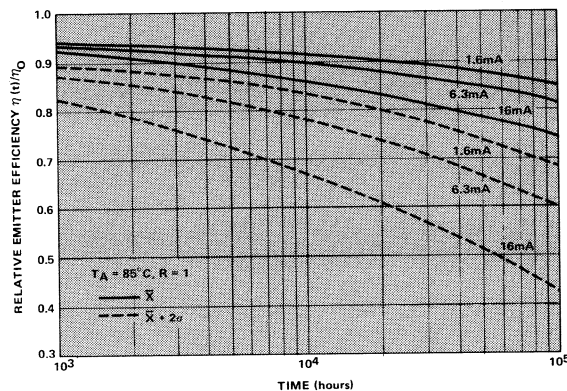
This discussion of reliability data and its interpretation with model equations is qualified to specific optocouplers, 6N135 and 6N138, where continuous LED operation was maintained, and extrapolation of data for times beyond 10,000 hours is assumed to be valid. Different types of LEDs or preparation processes may produce different results than those presented in this section. These expressions only incorporate the first order effect, emitter degradation $\Delta\eta/\eta$, whereas comments about higher order effects upon total CTR degradation will be given in the following section. With these expressions for degradation, accelerated testing may be accomplished by employing large values of R. Such testing can provide a means by which to determine acceptable emitter lots for optocoupler fabrication, acceptable degradation performed for lot selection, or predict functional lifetime expectance for optocouplers under specific operational conditions.

An important point to note is that the total operational life of an optocoupler is greater than the worst case mean plus 2σ distribution implies. Specifically, the worst case degradation given in Figures 4a (25°C) and 4b (85°C) are for the continuous operation of the 6N135 optocoupler.

The actual lifetime for an optocoupler is greater than Figures 4a and 4b would indicate since the majority of units will be centered around the mean distribution lifetime. Secondly, the optocoupler which is operated at some signal duty factor less than 100%, for example 50%, would increase the optocoupler's life by a factor of two. Third, the fact that an optocoupler is used within equipment which may have a typical 2000 hours per year (8 hours/day – 5 days/week – 50 weeks/year) instrument or system operating time, could expect to increase the optocoupler's life by another factor of 4.4 in terms of years of useful life.



a



b

Figure 4. Calculated Curves of Relative Emitter Efficiency vs. Time for $R = 1$: $I_{FS} = I_{FM} = 1.6, 6.3$, and 16 mA which are Recommended I_F for 6N138, 6N137, and 6N135 Optocouplers Respectively. Mean, Mean + 2σ Distributions. a) $T_A = 25^\circ\text{C}$, b) $T_A = 85^\circ\text{C}$.

The appropriate operating time considerations will vary depending upon the designer's knowledge of the system in which the optocoupler will be used. The operating lifetime of an optocoupler can be expressed, for a maximum allowable degradation at a particular I_FS, by using Figures 4a and 4b for t_{continuous} lifetime and the following expression:

$$t_{\text{continuous lifetime}} = \left[t_{\text{system lifetime}} \right] \left[\frac{\text{Data Duty Factor}}{\text{System Use Data Factor}} \right] \quad (16)$$

Another equally important point to observe is that of the worst case conditions under which the optocoupler is used. As will be illustrated in the design examples, the worst possible combination of variations in V_{CC1}, V_{CC2}, R_{IN}, CTR, R_L, I_{IL}, and temperature still result in the optocoupler functioning over an extended length of time (10⁵ hours) for a particular maximum allowable degradation. However, the likelihood of seven parameters all deviating in their worst directions at the same time is extremely remote. A thorough statistical error accumulation analysis would illustrate that this worst-worst case is not a representative situation from which to design.

Higher Order Effects

The first order effect of emitter degradation, Δη/η, has a pronounced influence upon the ΔCTR as explained in the previous sections; however, consideration of higher order effects is important as well.

Consider the second term in Equation (5) (Δη/η)_{I_F} (∂lnβ/∂lnI_P)_t, the emitter degradation part has been explained; however, (∂lnβ/∂lnI_P)_t represents a shift in the operating point of the output amplifier of an optocoupler. The term (∂lnβ/∂lnI_P) can be rewritten as (1/2.3β) (∂β/∂log₁₀I_P) which is more convenient to use with the accompanying typical curves of β versus log₁₀I_P for the two optocouplers 6N135 and 6N138, given in Figure 5a.

If the operating photocurrent, I_P, is to the right of the maximum β point of either curve, then with reduced emitter efficiency over time, I_P will decrease, but the increasing β will tend to compensate for this degradation. However, if the operating I_P is to the left of the maximum β and then I_P decreases, the β change will accentuate the emitter's degradation, yielding a larger CTR loss. The magnitude of the contributions of ∂lnβ/∂lnI_P to overall CTR degradation can be illustrated by the following examples.

Consider a 6N138 optocoupler of Figure 5c operating at its recommended I_F = 1.6 mA which corresponds to an I_P ≈ 1.6μA. (An I_F to I_P relationship for Hewlett-Packard optocouplers is 1 mA input current yields approximately 1μA of photodiode current.) At I_P = 1.6μA, the slope of the V_{CE} = 5V curve is equal to -15,000 and the

gain is β = 26,000; hence, ∂lnβ/∂lnI_P ≈ -0.25. If, for instance, the emitter degradation Δη/η is -10%, then the second order term would improve the overall CTR degradation, i.e.,

$$\frac{\Delta \text{CTR}}{\text{CTR}} = \left(\frac{\Delta \eta}{\eta} \right) + \left(\frac{\Delta \eta}{\eta} \right) \left(\frac{\partial \ln \beta}{\partial \ln I_P} \right) + \dots = -10\% + 2.5\% = -7.5\% \quad (17)$$

This improvement is what was expected while operating on the right side of the β maximum. In fact, with an I_F = 4 mA or I_P ≈ 4μA, the term ∂lnβ/∂lnI_P = -0.8, and again, if Δη/η = -10%, the resulting ΔCTR/CTR = -2%, nearly cancelling the emitter's degradation.

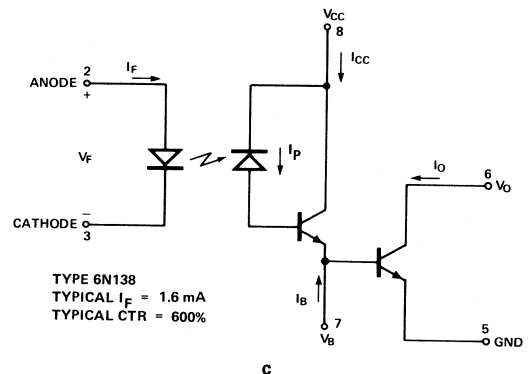
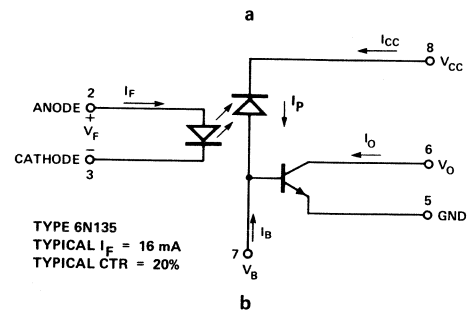
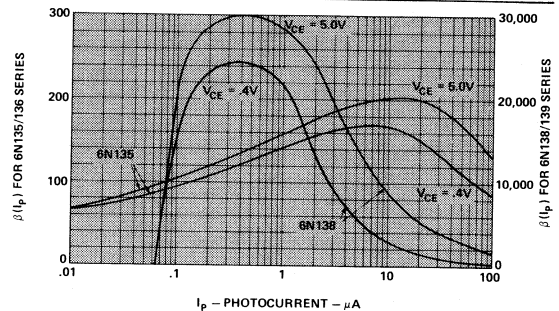


Figure 5. a) Typical DC Current Gain, β, vs. Photocurrent, I_P, for 6N135 and 6N138 Optocouplers. Current Diagrams and Typical Values of I_F and CTR for Hewlett-Packard Optocouplers, b) 6N135, c) 6N138.

With the 6N135 optocoupler, Figure 5b operating at $I_F = 10\text{ mA}$, or $I_P \approx 10\mu\text{A}$, which corresponds to the maximum β point on the $V_{CE} = .4\text{V}$ curve, the slope is zero and the total CTR degradation is basically the emitter's degradation.

Another subtle effect is seen from the third term in Equation (5), $(\Delta\beta/\beta)I_P$, over time. At constant I_P , β can increase or decrease by a few percent over 10,000 hours. This change is so small that the third term is generally neglected.

For the optocouplers containing an output amplifier, such as the 6N137, which switches abruptly about a particular threshold input current, the actual emitter degradation can be determined from Equations (11) and (13). An appropriate $I_{F\text{initial}}$ can be determined to provide for adequate guard band current which will allow the optocoupler emitter to degrade while maintaining sufficient I_P to switch the amplifier. An actual design procedure to determine the needed $I_{F\text{initial}}$ for proper operation of Hewlett-Packard optocouplers is given in the design examples section.

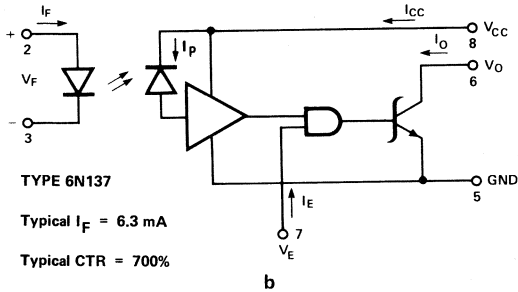
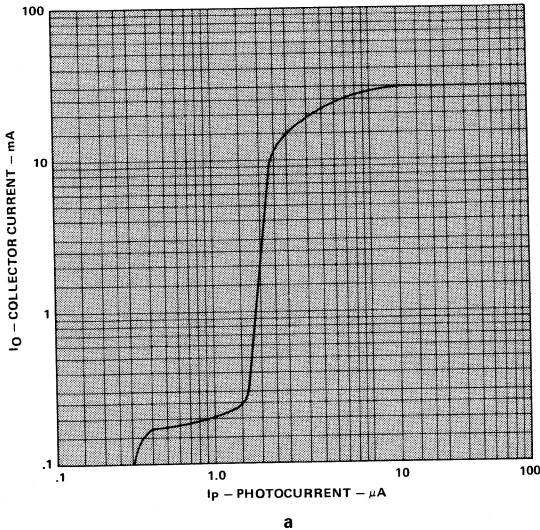


Figure 6. a) Typical Output Current, I_O , vs. Photocurrent, I_P , for 6N137 Optocoupler.
b) Circuit Diagram and Typical Values of I_F and CTR for 6N137 Optocoupler.

MATRIX OF COEFFICIENTS						
	25° C		85° C			
	\bar{X}	$\bar{X} + 2\sigma$	\bar{X}		$\bar{X} + 2\sigma$	
			$R < 6$	$6 \leq R$	$R < 8$	$8 \leq R$
A_o	4.95	9.7	6.8	5.0	15.0	11.0
α	.388	.428	.302	.467	.284	.430
	25° C		85° C			
	$R \leq 1$	$R \geq 1$	$R \leq 1$		$R \geq 1$	
$\alpha(R)$.19 R .052	.19 R .32	.32 R .08		.32 R .30	
$\beta(R)$.055	.055 R .68	.11 R .25		.11 R .65	
	25° C		85° C			
$\gamma(R)$.063 R .30		.154 R .26			
$\delta(R)$.081 R .38		.196 R .39			

Figure 7. Matrix of Coefficients.

Procedure for Calculation of CTR Degradation

1. Specify I_{FS} , I_{FM}

2. Determine $R = I_{FS}/I_{FM} \leq 20$
 $I_{FS} \leq 40 \text{ mA}$

Degradation Model Equations (11) and (13) Valid

3. First Approximation of Degradation

$$\bar{D}_{\bar{x}} = A_0 R^{\alpha} t^n \quad (\%) \quad \text{with } \alpha \approx .4, A_0 \text{ (Figure 7)}$$

or
 $\bar{x} + 2\sigma$

$n \approx .3, t \text{ in } 10^3 \text{ hours}$
 $(\bar{D} \text{ corresponds to } \bar{I}_{FS})$

4. Calculate $\bar{I}_{FS} = \begin{cases} 14.13 + 9.06 \log_{10} R @ 25^\circ \text{C} \text{ mA} & \text{Equation (7)} \\ 10.5 + 5.76 \log_{10} R @ 85^\circ \text{C} \text{ mA} & \text{Equation (8)} \end{cases}$

If $I_{FS} \approx \bar{I}_{FS}$, Step 6 and the second terms in Equations (11) and (13) do not need to be calculated.

5. Calculate $n(R) = .0475 \log_{10} R + .25$

6. Calculate $S = \alpha(R) \log_{10} t + \beta(R) \quad \%/mA$
 $P = \gamma(R) \log_{10} t + \delta(R) \quad \%/mA$

$\alpha(R), \beta(R)$
 $\gamma(R), \delta(R)$

Figure 7
 $t \text{ in } 10^3 \text{ hours}$

7. Calculate Mean, Mean + 2σ Degradation (No Approximation)

$$D_{\bar{x}} = A_0 R^{\alpha} t^{n(R)} + S [I_{FS} - \bar{I}_{FS}] \quad \% \quad \text{Equation (11)}$$

$$D_{\bar{x} + 2\sigma} = A_0 R^{\alpha} t^{n(R)} + [S + 2P] [I_{FS} - \bar{I}_{FS}] \quad \% \quad \text{Equation (13)}$$

(A_0, α via Figure 7, $t \text{ in } 10^3 \text{ hours}$)

8 For Second Order Effect, Determine Slope

$$\frac{\partial \ln \beta}{\partial \ln I_P} = \frac{1}{2.3\beta} \frac{\partial \beta}{\partial \log_{10} I_P}$$

Figure 5a – typical curves with an approximation for HP optocouplers of $I_F = 1 \text{ mA}$ yields $I_P \approx 1 \mu A$

9a. Total CTR Degradation for Mean Distribution

$$\frac{\Delta CTR}{CTR} = D_{\bar{x}} + D_{\bar{x}} \left(\frac{\partial \ln \beta}{\partial \ln I_P} \right)$$

9b. Total CTR Degradation for Mean + 2σ Distribution

$$\frac{\Delta CTR}{CTR} = D_{\bar{x} + 2\sigma} + D_{\bar{x} + 2\sigma} \left(\frac{\partial \ln \beta}{\partial \ln I_P} \right)$$

Practical Application

A very common application of an optocoupler is to function as the interfacing element between digital logic. In this section, the designer will be shown an approach which will insure the initial and long term performance of such an interface, and take into account the practical aspects of the system that surrounds it. These system elements include the data rate, the logic families being interfaced, the variations of the power supply, the tolerances of the components used, the operational temperature range, and lastly the expected lifetime of the system.

The system data speed can be considered as the primary selection criteria for selecting a specific optocoupler family. Figure 9 lists the ranges of data rates for four Hewlett-Packard optocoupler families when driven at specified LED input current, I_F . With this table, and the knowledge of the system data rate requirements, it is possible to select an optimum coupler.

An example of an optocoupler interconnecting two logic gates is shown in Figure 8. A logic low level is insured when the saturated output sinking current, I_O , is greater than the combined sourcing currents of the pull-up resistor, and the logic low input current, I_{IL} , of the interconnecting gate. Using the coupler specifications selected from Figure 9 and the corresponding CTR (MIN) from Figure 10,

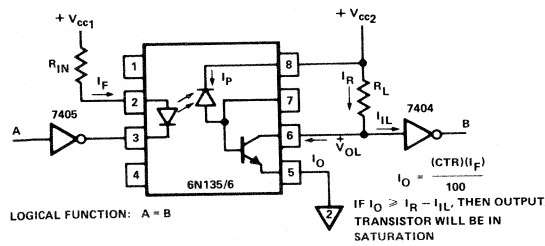


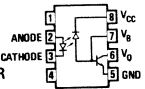
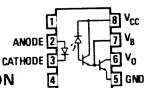
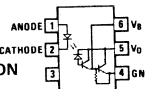
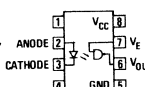
Figure 8. Typical Digital Interface Using an Optocoupler.

$$I_F (\text{MIN}) = \frac{V_{cc1} (\text{MIN}) - V_F (\text{MAX}) - V_{OL}}{R_{in} (\text{MAX})} \tag{18}$$

$$I_F (\text{MAX}) = \frac{V_{cc1} (\text{MAX}) - V_F (\text{MIN}) - V_{OL}}{R_{in} (\text{MIN})} \tag{19}$$

$$I_F = \frac{I_O \times 100}{CTR (\text{MIN})} \tag{20}$$

$$R_{in} = \frac{V_{cc1} - V_F - V_{OL}}{I_F} \tag{21}$$

FAMILY	NRZ DATA RATE BITS/S	INPUT CURRENT – I _F						
		.5mA	1.0mA	1.6mA	7.5mA	10mA	12mA	16mA
6N135/6 SINGLE TRANSISTOR	 MIN						333k	
	TYP						2M	
6N138/9 SPLIT DARLINGTON	 MIN	12k		22k			125k	
	TYP	100k		200k			840k	
4N45/6 DARLINGTON	 MIN					1.8k		
	TYP		640			6.5k		
6N137 OPTICALLY COUPLED GATE	 MIN				6.7M			
	TYP				10M			

FAMILY		% CTR @ $I_F = (\text{mA})$						TEMP °C	V_{OL}
		.5	1.0	1.6	5	10	16		
SINGLE TRANSISTOR	6N135						7	25	0.4
	6N136						19		
SPLIT DARLINGTON	6N138		300					0-70	0.4
	6N139	400	500					0-70	0.4
DARLINGTON	4N45		250			200		0-70	1.0
	4N46	350	500			200		0-70	1.0
OPTICALLY COUPLED GATE	6N137				400			0-70	0.6

Figure 10. Optocoupler CTR (MIN).

it is possible to determine from Equation (20) the minimum initial value of I_F for the coupler. The design criteria is that $I_O \geq I_{IL} + I_R$ for the V_{IL} specified in Figure 11.

Using Equation (21), the typical value of R_{in} can be calculated for the selected I_F and the logic low output voltage, V_{OL} , of the driving gate. The V_{OL} of the logic family is given in Figure 11. The next step is to determine the worst case value of the LED input current, I_F , resulting from the tolerance variations of the LED current limiting resistor, R_{in} , and the power supply voltage, V_{cc1} . The conditions of $I_F(\text{MIN})$ and the initial CTR(MIN) are then used to determine the initial worst case value of $I_{O(\text{MIN})}$. Conversely, the worst case CTR degradation will occur when the LED is stressed at $I_F(\text{MAX})$ conditions; thus, $I_F(\text{MAX})$ will be used to determine the worst case degradation of the optocoupler performance. Using the maximum V_{cc1} and the minimum R_{in} will accomplish this worst case calculation, as shown in Equation (19).

TTL FAMILY	I_{IL}	V_{IL}	I_{IH}	V_{IH}	I_{OL}	V_{OL}	I_{OH}	V_{OH}
74S	-2 mA	.8V	50 μ A	2V	20 mA	.5V	-1000 μ A	2.7V
74H	-2 mA	.8V	50 μ A	2V	20 mA	.4V	- 500 μ A	2.4V
74	-1.6 mA	.8V	40 μ A	2V	16 mA	.4V	- 400 μ A	2.4V
74LS	-36 mA	.8V	20 μ A	2V	8 mA	.5V	- 400 μ A	2.7V
74L	-18 mA	.7V	10 μ A	2V	3.6 mA	.4V	- 200 μ A	2.4V

Figure 11. Logic Interface Parameters.

The change in CTR from the initial value at time $t=0$ to a final value at some later time can be compensated by

choosing a value of R_L which is consistent with $I_{O(\text{MIN})} - mI_{IL}$ at the end of system life. Equation (22) describes this worst case calculation.

(22)

$$R_L(\text{MIN}) \geq \frac{V_{cc2}(\text{MAX}) - V_{OL}}{\left[\frac{I_F(\text{MIN}) \cdot \text{CTR}(\text{MIN}) \left(1 - \frac{D_x + 2\sigma}{100} \right)}{100} - mI_{IL} \right]}$$

$D_x + 2\sigma$ = worst case CTR degradation

The selection of the maximum value of R_L is also of important in that its value insures that the collector is pulled up to the logic one voltage conditions, V_{IH} , under the conditions of maximum I_{OH} of the coupler, and the I_{IH} of the interconnecting gate.

(23)

$$R_L(\text{MAX}) \leq \frac{V_{cc2}(\text{MIN}) - V_{OH}}{I_{OH}(\text{MAX}) + mI_{IH}}$$

The selection of the value of R_L between the boundaries of $R_L(\text{MIN})$, and $R_L(\text{MAX})$ has certain trade offs. As in any open collector logic system, T_{PLH} increases with increasing R_L . Conversely, as R_L is increased above $R_{L(\text{MIN})}$, a larger guardband between $I_{O(\text{MIN})}$ and $I_{IL} + I_R$ is achieved. Engineering judgement should be employed here to achieve the optimum trade off for desired performance.

Using the coefficient Figure 7 and Equations (11) and (13), the following examples are developed to demonstrate the methods of optocoupler system design in the presence of the mean and mean plus two sigma CTR degradation.

Example 1.

System Specifications

Data Rate	20 k bit NRZ
Logic Family	Standard TTL
Power Supply 1 & 2	5V \pm 5
Component Tolerances	\pm 5%
Temperature Range	0 – 70°C
Expected System Lifetime	350 k hr (40 yr) at 50% system use time and 50% Data Duty Factor

Interface Specifications

Coupler 6N139

CTR (MIN)	= 500% @ $I_F = 1.6$ mA
V_{OL} (MAX)	= .4V @ $I_F = 1.6$ mA
I_{OH} (MAX)	= 250 μ A @ $V_{cc2} = 7$ V
V_F (MAX)	= 1.7V @ $I_F = 1.6$ mA
V_F (MIN)	= 1.4V @ $I_F = 1.6$ mA
V_F (TYP)	= 1.6V @ $I_F = 1.6$ mA

Logic Standard TTL

I_{IL}	= 1.6 mA	I_{IH}	= 40 μ A
V_{IL}	= .8V	V_{IH}	= 2V
I_{OL}	= 16 mA	I_{OH}	= 400 μ A
V_{OL}	= .4V	V_{OH}	= 2.4V

Step 1. R_{in} (TYP)

$$R_{in} = \frac{V_{cc1} - V_F (TYP) - V_{OL}}{I_F (TYP)} \quad (24)$$

$$R_{in} = \frac{5.0 - 1.6 - .4}{1.6 \times 10^{-3}} = 1.87k\Omega, \text{ select } 1.8k\Omega \pm 5\%$$

$R_{(MIN)} = 1710\Omega$
 $R_{(MAX)} = 1890\Omega$

Step 2. I_F (MAX)

$$I_F (MIN) = \frac{V_{cc1} (MIN) - V_F (MAX) - V_{OL}}{R_{in} (MAX)} \quad (25)$$

$$I_F (MIN) = \frac{4.75 - 1.7 - .4}{1890\Omega} = 1.4 \text{ mA}$$

Step 3. I_F (MAX)

$$I_F (MAX) = \frac{V_{cc1} (MAX) - V_F (MIN) - V_{OL}}{R_{in} (MIN)} \quad (26)$$

$$I_F (MAX) = \frac{5.25 - 1.4 - .4}{1710\Omega} = 2.02 \text{ mA}$$

Step 4. Determine continuous operation time for LED emitter.

$$t_{\text{continuous lifetime}} = \left[t_{\text{system lifetime}} \right] \left[\text{Data Duty Factor} \right] \left[\text{System Use Duty Factor} \right]$$

$$= (40 \text{ yr} \times 8.76 \text{ k hr/yr})(50\%)(50\%)$$

$$t_{\text{continuous lifetime}} = 87.60 \text{ K hr}$$

Step 5. Obtain the mean and mean + 2 σ CTR degradation at I_F (MAX) and $t_{\text{continuous lifetime}}$ either as an approximation from Figure 4 or by calculations as shown below.

Step 5a. Determine $D_{\bar{x}}$

$$D_{\bar{x}} = A_o t^{.25} + S [I_{FS} - \bar{I}_{FS}] \quad (27)$$

$$D_{\bar{x}} = 4.95 t_{(k \text{ hr})}^{.25} + [.186 \log t_{(k \text{ hr})} + .055]$$

$$[I_F (MAX) - 14.13 \text{ mA}]$$

$$D_{\bar{x}} = 4.95 (87.6)^{.25} + (.186 \log 87.6 + .055)$$

$$(2.02 \text{ mA} - 14.13 \text{ mA})$$

$$D_{\bar{x}} = 10.10\% \text{ for 40 yr system operation}$$

Step 5b. Determine $\bar{D}_{x+2\sigma}$

$$D_{\bar{x}+2\sigma} = A_o t^{.25} + [S + 2P] [I_{FS} + \bar{I}_{FS}] \quad (28)$$

$$D_{\bar{x}+2\sigma} = 9.7 t_{(k \text{ hr})}^{.25} + [2 (.063 \log t_{(k \text{ hr})} + .081)]$$

$$\begin{aligned}
& + (.186 \log t_{(k \text{ hr})} + .055)] \\
& \times [I_F (\text{MAX}) - 14.13 \text{ mA}] \\
D_{\bar{x}} + 2\sigma &= 9.7 (87.6)^{.25} + [2 (.063 \log 87.6 + .081) \\
& + (.186 \log 87.6 + .055)] \\
& \times [2.02 \text{ mA} - 14.13 \text{ mA}]
\end{aligned}$$

$$D_{\bar{x}} + 2\sigma = 19.71\%$$

Step 6. Guardband the worst case value of CTR degradation.

It is often desirable to add some additional operating margin over and above conditions dictated by simple worst case analysis. The use of engineering judgement to increase the worst possible CTR degradation by an additional 5% margin would insure that the entire distribution would fall within the analysis. Thus,

$$D_{\bar{x}} + 2\sigma + 5\% = 24.71\%$$

Step 7. Selecting $R_L (\text{MIN})$ for guardbanded worst case

$$D_{\bar{x}} + 2\sigma + 5\% \quad , \quad m = 1$$

(22)

$$R_L (\text{MIN}) \geq \frac{V_{cc2} (\text{MAX}) - V_{OL}}{\frac{I_F (\text{MIN}) \cdot \text{CTR} (\text{MIN}) \left(1 - \frac{D_{\bar{x}} + 2\sigma + 5\%}{100}\right)}{100} - m I_{IL}}$$

$$R_L (\text{MIN}) \geq \frac{5.25 - .4}{\frac{1.4 \times 10^{-3} \cdot 500\% \left(1 - \frac{19.71\%}{100}\right)}{100} - 1 (1.6 \text{ mA})}$$

$$R_L (\text{MIN}) = 1.32k\Omega$$

Step 8. Select $R_L (\text{MAX})$

$$R_L (\text{MAX}) \leq \frac{V_{cc2} (\text{MIN}) - V_{OH}}{I_{OH} (\text{MAX}) + m I_{IH}} \quad (29)$$

$$R_L (\text{MAX}) \leq \frac{4.75 - 2.4}{250\mu\text{A} + 40\mu\text{A}} = 8.1k$$

The range of R_L is from $1.32k\Omega$ to $8.1k\Omega$. It is desirable to select a pull-up resistor which optimizes both speed performance and additional I_O guardband. This criteria leads to a tradeoff between a value close to $R_L (\text{MIN})$ for speed performance and one bordering near $R_L (\text{MAX})$ for I_O guardbanding. In this design example, the system's lifetime has a higher priority than does the moderate speed performance demanded from the optocoupler. An R_L of $3.3k\Omega \pm 5\%$ is selected under this condition.

An additional guardband of 5% was added to the worst case $D_{\bar{x}} + 2\sigma$ CTR degradation guardband to insure that even a greater percentage of the distribution would be accounted for. The actual percentage difference between $I_{OL} (\text{MAX})$ and $I_O (\text{MIN})$ at the end of system life is shown below:

(30)

$$I_O (\text{MIN}) = \frac{\text{CTR} (\text{MIN}) \cdot I_F (\text{MIN}) \left(1 - \frac{D_{\bar{x}} + 2\sigma}{100}\right)}{100}$$

(31)

$$I_{OL} (\text{MAX}) = \frac{V_{cc2} (\text{MAX}) - V_{OL}}{R_L (\text{TYP} - 5\%)} + m I_{IL}$$

$$\% \text{ Guardband} = \left[1 - \frac{I_{OL} (\text{MAX})}{I_O (\text{MIN})}\right] \times 100 \quad (32)$$

For the example shown, the additional end of system life I_O guardband results from the selection of an R_L greater than the $R_L (\text{MIN})$ as shown in Steps 9, 10, and 11.

Step 9. $I_O (\text{MIN})$ at end of system life

$$I_O (\text{MIN}) = \frac{500\% \cdot 1.4 \text{ mA} \cdot \left(1 - \frac{19.71\%}{100}\right)}{100} = 5.65 \text{ mA}$$

Step 10. $I_{OL} (\text{MAX})$ for worst case of $I_R (\text{MAX}) + I_{IL}$

(33)

$$I_{OL} (\text{MAX}) = \frac{5.25 - .4}{3.13k\Omega} + 1.6 \text{ mA} = 3.14 \text{ mA}$$

Step 11. % Guardband

$$\% = 1 - \frac{3.14 \text{ mA}}{5.65 \text{ mA}} \times 100 = 44.4\% \quad (34)$$

Thus, this circuit interface design offers an additional 44.4% I_O guardband beyond the 19.71% required to compensate for the CTR change caused by 86.7k hr of continuous operation at an I_F (MAX) of 2 mA. This extra guardband results from having chosen an $R_L = 3.3k$ rather than the lowest allowable value of R_L plus the engineering guardband chosen in Step 6.

Example 2.

System Specifications

Data Rate	250K bit NRZ
Logic Family	TTL to LSTTL
Power Supply 1 and 2	5V \pm 5%
Component Tolerance	\pm 5%
Temperature Range	25°C
Expected System Lifetime	175 k hr (20 yr) at 50% System Use Time and 50% Data Duty Factor

Interface Conditions

Coupler 6N136

CTR(MIN)	= 19% @ $I_F = 16$ mA
V_{OL}	= .4V
I_{OH}	= 500 nA @ $V_{cc2} = 5.0V$
V_F (TYP)	= 1.6V @ $I_F = 16$ mA
V_F (MIN)	= 1.5V @ $I_F = 16$ mA
V_F (MAX)	= 1.7V @ $I_F = 16$ mA

Logic LSTTL

I_{IL}	= .36 mA	I_{OL}	= 8 mA
V_{IL}	= .8V	V_{OL}	= .5V
I_{IH}	= 40 μ A	I_{OH}	= 400 μ A
V_{IH}	= 2V	V_{OH}	= 2.7V

Again using Figure 7, the data rate dictates the use of a 6N136 at an I_F (TYP) of 16 mA. Using the same 12 step worst case analysis, it is possible to determine the values of R_{in} , R_L and the degree of guardbanding of I_O at end of system lifetime.

Step 1. $R_{in} = 187\Omega$, select $180\Omega \pm 5\%$
 R_L (MIN) = 179 Ω
 R_L (MAX) = 189 Ω

Step 2. I_F (MIN) = 14.02 mA

Step 3. I_F (MAX) = 19 mA

Step 4. System Lifetime

$t = 43.8k$ hr

Step 5. $D_{\bar{x}}$ and $D_{\bar{x} + 2\sigma}$ for I_F (MAX) of 19 mA

by calculation or from Figure 4

$$\left. \begin{array}{l} D_{\bar{x}} = 14.5\% \\ D_{\bar{x} + 2\sigma} = 28.5\% \end{array} \right\} \begin{array}{l} 43.8k \text{ hr} \\ \text{continuous lifetime} \end{array}$$

Step 6. Engineering Guardband of 5%,

$D_{\bar{x} + 2\sigma} + 5\% = 33.5\%$

Step 7. R_L selection with guardbanding of $D_{\bar{x} + 2\sigma} + 5\%$

R_L (MIN) = 3.44k Ω

Step 8. R_L (MAX) = 50k Ω

Step 9. R_L (TYP) = 5.1k $\Omega \pm 5\%$, R_L (TYP - 5%)
= 4.84k Ω , R_L (MAX + 5%)
= 5.35k Ω

Step 10. End of System Life I_O (MIN)

I_O (MIN) = 1.5 mA

Step 11. I_{OL} (MAX) = 1.36 mA

Step 12. Engineering % Guardband of I_O (MIN) = 9.3%

Example 3.

If a particular design requirements specifies a maximum tolerable degradation over a system lifetime, the optimum value of I_F (TYP) can be obtained from Figure 12. For example, if a maximum acceptable degradation, $D_{\bar{x} + 2\sigma}$, is 40%, and a continuous operation of 400k hr is desired, this curve specifies that I_F (TYP) should be less than or equal to 10 mA. A 400k hr continuous operation with 100% system duty factor as might be encountered in telephone switching equipment is equivalent to 45 years of system lifetime.

If a 6N139 split Darlington were used to interface an LSTTL logic gate with the system specifications stated, a collector pull-up resistor of as low as 160 Ω could be used. If an R_L of 1k were selected, this optocoupler would offer an additional end of life guardband of 81.8%. This worst case analysis points out that with the knowledge of selecting proper values of R_L , the CTR performance of the

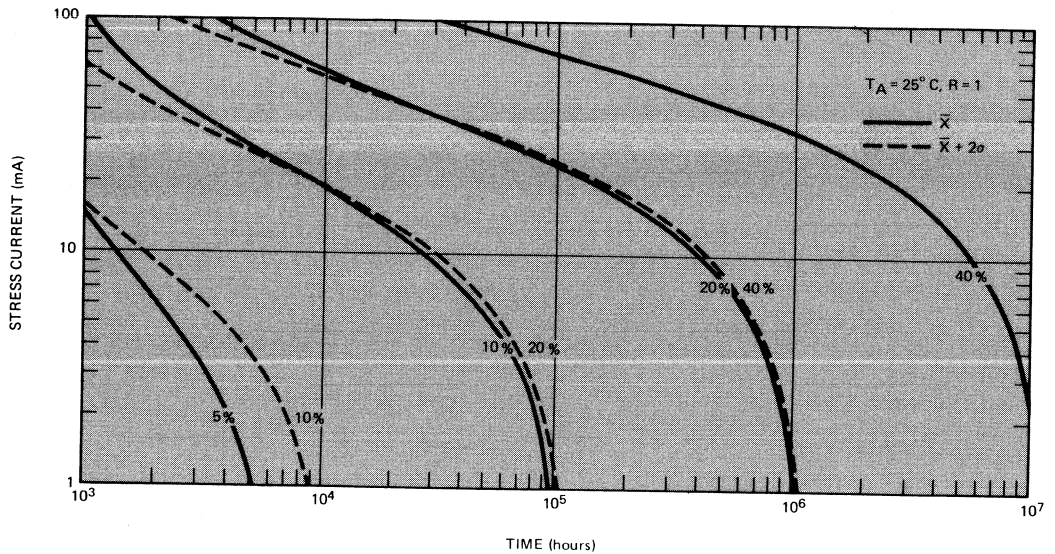


Figure 12. Stress Current (I_{FS}) vs. Time vs. % Degradation.

coupler far exceeds the normal MTBF requirements for most commercial electronic systems.

Consideration of the Optically Coupled Gate

System data speed requirements in the multi-megabit range can also be communicated through an optocoupler. The first three coupler families listed in Figure 9 are not applicable in these very high speed data interface applications; however, the optically coupled gate, 6N137, will function to speeds of up to 10 MHz. This type of coupler differs in operation from the single transistor and Darlington style units in that it exhibits a non-linear transfer relationship of I_F to I_O . This is shown in Figure 13. The relationship is described as a minimum threshold of LED input current, I_{Fth} which is required to cause the output transistor to sink the current supplied by the pull-up resistor and interconnected gate. As the LED degrades, the effect is that a larger value of I_{Fth} is required to create the same detector photodiode current necessary to switch the output gate.

In the previous interface examples, the worst case analysis and guardbanding is based on the output collector current, I_O . With the optically coupled gate, worst case guardbanding is concerned with the selection of the initial value of the I_F , which at end of system lifetime will generate the necessary threshold photocurrent demanded by the gate's amplifier to change state.

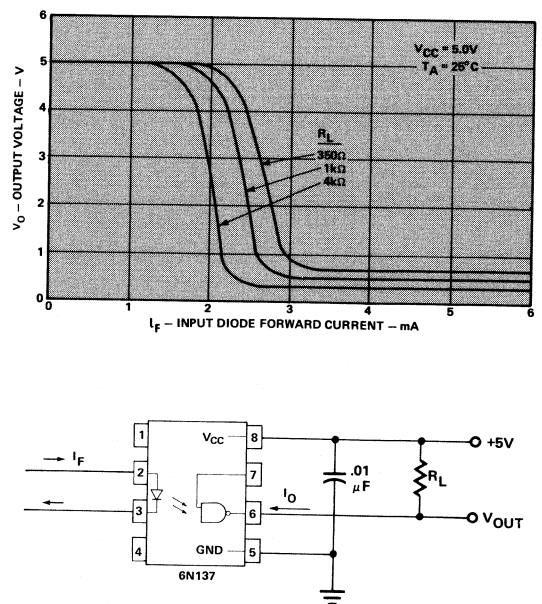


Figure 13. 6N137 Input - Output Characteristics.

The calculation of the required I_F to allow for worst case LED degradation is approached by guardbanding the guaranteed minimum isolator input current, I_{FH} , for a specified I_{OL} and V_{OL} interface. Equation (35) shows the relationship of the I_P to I_F for this coupler.

$$I_P \propto (I_F)^n, \text{ where } 1.1 \leq n \leq 1.3 \quad (35)$$

Using the concept that the guardbanding of the initial value of I_F will result in a similarly guardbanded I_P , the relationship presented in Equation (36) results:

$$\left[1 - \frac{D_{\bar{x}} + 2\sigma}{100} \right] = \left[\frac{I_{PH}}{I_P} \right] = \left[\frac{I_{FH}}{I_F} \right]^n \quad (36)$$

$$I_F = \frac{I_{FH}}{\left[1 - \frac{D_{\bar{x}} + 2\sigma}{100} \right]^{1/n}} \quad (37)$$

The previous interface example showed that the first term of the $D_{\bar{x}} + 2\sigma$ equation dominated the magnitude of the worst case degradation. This term, $A_0 R^{\alpha} t^{n(R)}$, i.e., $(9.7 \text{ t(k hr)})^{.25}$, does not contain an I_F current dependent term; thus, an approximation of the worst case LED degradation can be made that relates to the system's lifetime. This initial value of $D_{\bar{x}} + 2\sigma$ can be used in Equation (37) to calculate the initial value of the I_F . With this initial I_F , a more accurate degradation value can be calculated using Equation (28). This procedure results in an iterative process to zero in on a value of I_F that will insure reliable operation.

The following example will illustrate this approach.

Example 4.

System Specifications

Data Rate	6 MHz NRZ
Logic Family	LSTTL to TTL
Power Supply 1 and 2	5V \pm 5%
Component Tolerance	\pm 5%
Temperature Range	0 – 70°C
Expected System Lifetime	203k hr (23 yr) at 50% System Use Time and 50% Data Duty Factor

Step 1. Determine the continuous operation time for LED emitter

$$\begin{aligned} t_{\text{continuous lifetime}} &= \left[t_{\text{system lifetime}} \right] \left[\frac{\text{Data Duty Factor}}{\text{System Use Factor}} \right] \\ &= \left[23 \text{ yr} \right] \left[\frac{8.76 \text{ k hr/yr}}{50\%} \right] \left[50\% \right] \\ &= 50.3 \text{ k hr} \end{aligned}$$

Step 2. Calculate the worst case LED degradation

$$D_{\bar{x}} + 2\sigma \approx 9.7 \text{ t(k hr)}^{.25}$$

$$D_{\bar{x}} + 2\sigma \approx 9.7 (50.3)^{.25}$$

$$D_{\bar{x}} + 2\sigma \approx 26\%$$

Step 3. Calculate the first approximation of guardbanded I_F , $n = 1.2$

$$I_F = \frac{I_{FH}}{\left[1 - \frac{(\approx D_{\bar{x}} + 2\sigma)}{100} \right]^{1/n}} = \frac{5 \text{ mA}}{.78} = 6.41 \text{ mA}$$

Step 4. Calculate input resistor R_{in}

$$R_{in} \leq \frac{V_{cc1}(\text{MIN}) - V_F(\text{MAX}) - V_{OL}}{I_F}$$

$$R_{in} \leq \frac{4.75 - 1.7 - .4}{.00641}$$

$$R_{in} \leq 413\Omega \text{ select } R_{in} = 390\Omega \pm 5\%$$

$$R_{in}(\text{MAX})$$

$$R_{in}(\text{MAX}) = 409\Omega$$

$$R_{in}(\text{MIN}) = 370\Omega$$

Step 5. Calculate the $I_F(\text{MAX})$

$$I_F(\text{MAX}) = \frac{V_{cc1}(\text{MAX}) - V_F(\text{MIN}) - V_{OL}}{R_{in}(\text{MIN})}$$

$$I_F = \frac{5.25 - 1.4 - .4}{370}$$

$$I_F = 9.32 \text{ mA}$$

Step 6. Calculate the worst case $D_{\bar{x}} + 2\sigma$ for $I_F(\text{MAX})$

$$D_{\bar{x}} + 2\sigma = 25.8\% + .747 (9.32 \text{ mA} - 14.13 \text{ mA})$$

$$D_{\bar{x}} + 2\sigma = 22.2\%$$

Step 7. Calculate the new minimum required I_F at end of life based on degradation found in Step 6.

$$I_{F(EOL)} = \frac{I_{FH}}{\left[1 - \frac{22.2}{100}\right]^{1/1.2} \cdot .81} = \frac{5}{.81} = 6.16 \text{ mA}$$

Step 8. Calculate I_F (MIN)

$$I_F (\text{MIN}) = \frac{V_{cc1} (\text{MIN}) - V_F (\text{MAX}) - V_{OL}}{R_{in} (\text{MAX})}$$

$$I_F (\text{MIN}) = \frac{4.75 - 1.7 - .4}{409}$$

$$I_F (\text{MIN}) = 6.47 \text{ mA}$$

Step 9. R_L (MIN) , $m = 1$

$$R_L (\text{MIN}) = \frac{V_{cc2} (\text{MAX}) - V_{OL}}{I_{OL} (\text{MIN}) - mI_{IL}}$$

$$= \frac{5.25 - .6}{.016 - .0016}$$

$$R_L (\text{MIN}) = 332\Omega$$

Step 10. R_L (MAX) , $m = 1$

$$R_L (\text{MAX}) = \frac{V_{cc2} (\text{MAX}) - V_{OH}}{I_{OH} (\text{MAX}) + mI_{IH}}$$

$$R_L (\text{MAX}) = \frac{4.75 - 2.4}{250\mu A + 40\mu A}$$

$$R_L (\text{MAX}) = 8.1k\Omega$$

Step 11. Minimum % Emitter Degradation Guardband

$$\%(\text{MIN}) = \left[1 - \frac{I_F (\text{EOL})}{I_F (\text{MIN})} \right] 100 \quad (38)$$

$$4.8\% = \left[1 - \frac{6.16 \text{ mA}}{6.47 \text{ mA}} \right] 100$$

where I_F (EOL) represents the switching threshold at the end of life.

Step 12. Maximum % Emitter Degradation Guardband

$$\%(\text{MAX}) = \left[1 - \frac{I_F (\text{EOL})}{I_F (\text{MAX})} \right] 100 \quad (39)$$

$$34\% = \left[1 - \frac{6.16 \text{ mA}}{9.32 \text{ mA}} \right] 100$$

The conclusions that are to be drawn from this analysis are that as long as the I_F (MAX) is less than $I_{FS} = 14.13 \text{ mA}$, the worst-worst case CTR degradation may be calculated using only the first term, $A_0 R^{\alpha} t^n(R)$, of the $D_{\bar{X}} + 2\sigma$ case. In the example presented, 26% degradation was determined from the first term, and when the more accurate calculation using Equation (28) was used, a 22% degradation resulted. The end of life I_F guardband may be calculated using Equations (38) and (39). Using Equation (38), the minimum guardband is 5.7%, and with Equation (39), the maximum guardband is 35%.



HEWLETT
PACKARD

REPRINTED FROM
EDN
EXCLUSIVELY
FOR DESIGNERS
AND DESIGN MANAGERS
IN ELECTRONICS
A CAHNS PUBLICATION
A DIVISION OF REED PUBLISHING U.S.A.

Digital Data Transmission Using Optically Coupled Isolators

Designer's Guide to: Optoisolators — Part 1

Optically coupled isolators are extremely versatile in digital data transmission lines. In this article we examine lines and drivers.

The interaction between telemetry systems, computers and IC technology has given birth to a fantastic amount of data. The systems have been alternately feeding and needing each other with one purpose in mind—faster, more accurate data transfer. Unfortunately, in designing a system to transmit digital data, the designer too often finds his digital transmission lines plagued by a host of problems.

When connections are made between various modules of a digital data system, the ground loop often produces an offset or ground shift. Circulating currents in data communication systems between a remote computer terminal and a CPU, for example, can spell disaster. Another problem that can haunt the unwary designer is common-mode interference. The optically coupled isolator (OCI) offers a convenient, effective and economical solution to both of these problems.

Indeed, the advantages of OCI's are truly impressive: Unlike transformers, OCI's can hold a given logic state indefinitely; unlike relays, they have high data rate capability (dc to beyond 10 M-bits/sec); and unlike differential-amplifier data receptors, OCI's can tolerate high common-mode voltages (up to 2500V). The OCI has no inductive coupling, has small capacitive coupling, generates no EMI and has no mechanical contacts. Furthermore, it can withstand shock and vibration, requires little power and is IC-compatible.

Optical couplers electrically isolate two circuits, yet permit the transfer of data through a transparent insulation. On the input side of an OCI, a LED or IRED emits photons; on the receiving side, a photodetector (phototransistor

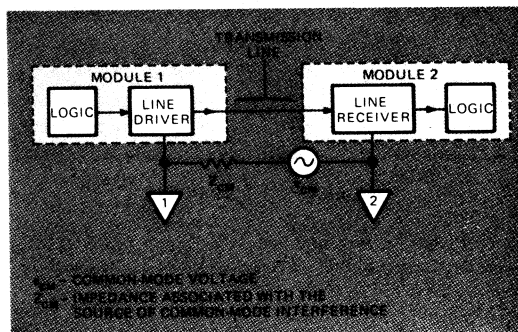


Fig. 1—Driver, transmission line and receiver comprise the functional elements of every data transmission system. The line driver converts the logic levels of Module 1 (transmitting module) to the configuration and amplitude best suited to the transmission line and receiver, while the line receiver converts received data to the levels required by the logic in Module 2 (receiving module).

or PIN photodiode) converts the optical signal to an electrical signal by switching the detector.

Our tutorial, 4-part Designer's Guide series will center on drivers, lines and receivers. This article will explore drivers and transmission lines, while the second will cover passive terminations. Active terminations and enhancement of common-mode rejection are the subject of the third article, with the fourth installment centering on data rate enhancement and multiplex applications.

Rather than restricting our discussion to performance obtainable with particular circuits, we will emphasize broadly applicable design principles and circuit analysis. By referring to data sheets, you can then apply the principles presented to different OCI's in other circuits.

It takes three to communicate

Three functional elements (**Fig. 1**) exist in every digital data system: a line driver, the transmission line and a line receiver.

A line driver accepts as its input the logic levels developed in the transmitting module (Module 1 in **Fig. 1**) and converts them to a form that is compatible with the transmission line and line receiver. The transmission line simply connects the line driver to the line receiver, but its characteristics can profoundly influence system performance with regard to bandwidth,

line and the receiver module logic levels. Let's consider the line driver first.

Put an OCI in the driver's seat

Transmission lines and line receivers require line drivers that produce signals of the optimum configuration and amplitude. Briefly, configuration considerations include current/voltage sourcing or sinking, balanced or single-ended system, and polarity reversing or nonreversing. Amplitude consideration, on the other hand, takes into account current or voltage threshold requirements at the receiver, impedance of the transmission line and interference amplitude (the latter being especially important in single-ended systems).

Current or voltage sinking. For systems requiring such a configuration, the optoisolator can serve as the line driver. Some types of OCI's have outputs that can function as simple 2-terminal switches, as shown in **Fig. 2a**. However, because the current flowing in the line is relatively low, the system is more vulnerable to interference than it would be if higher line current was used. To obtain higher line current and data rate, an optoisolator could still be used, but the system would then require an additional wire to bring V_{CC2} from Module 2 to power the amplifier in the output of the optoisolator (**Fig. 2b**). You could

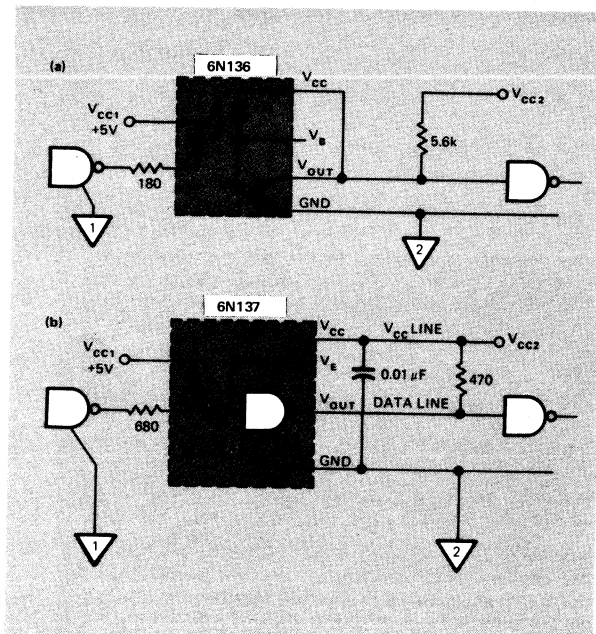


Fig. 2—Opto-isolators can function as line drivers. Using one as a 2-terminal switch (a) is the direct approach, but it suffers from greater noise interference due to low line current. You can achieve higher line current and data rates by carrying Module 2's supply voltage back to Module 1 through a third line (b).

common-mode rejection and compatibility with the line driver. At the opposite end of the transmission line, the line receiver responds to the signals delivered through the line and converts them to be compatible with the logic levels required in the receiving module (Module 2).

As far as establishing error-free performance, the receiver is typically the most important element of the system; and it is in the design of line receivers where optoisolators are usually found. For this reason, most of this series will deal with making the optoisolator input and output compatible, respectively, with the driver/

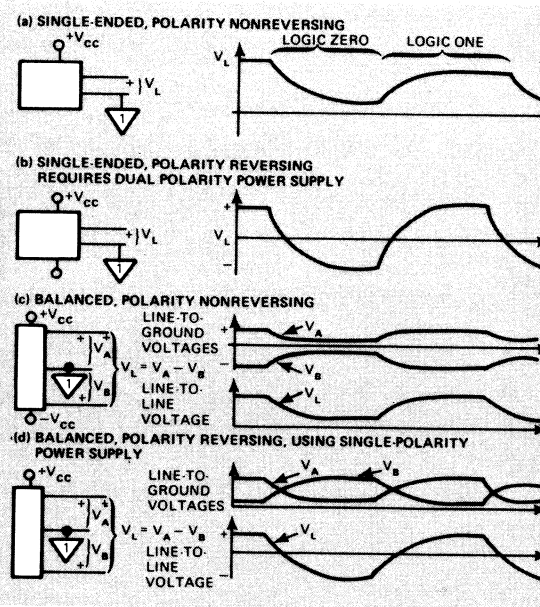


Fig. 3—Both single-ended or balanced drivers can be either polarity nonreversing or polarity reversing. Balanced systems (c and d) are generally preferred because receiver common-mode rejection subtracts out the common line noise. As a result, balanced systems provide greater common-mode rejection for given line currents.

obtain still higher line current, but a lower data rate, by using a high gain optoisolator such as the 6N138/6N139 instead of the 6N137.

Current or voltage sourcing line drivers (conventional types) are the most commonly used, mainly because they provide higher line currents than is possible with optoisolator inputs. We will say more about them later.

Balanced or single ended. With 2-conductor transmission lines (either coax or unshielded twisted pair), the driver may be either single-ended or differential. A balanced system requires a differential line driver and is often preferred because it offers higher immunity to electromagnetically induced interference (EMI) by causing the interference to appear in common mode, while the desired signal is differential mode.

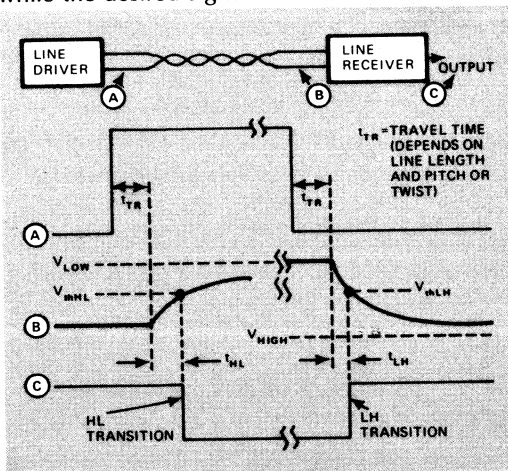


Fig. 4—A square pulse generated at line drive (A) possesses steel edges that are exponentially rounded by the skin-effect and dielectric losses of the transmission line. Since the line receiver switches at a threshold V_{th} , the line introduces a delay time (transit time t_{TR} plus rise time t_{HL}) as seen in B. After time $t_{TR} + t_{HL}$ has elapsed the receiver makes a HIGH-to-LOW (HL) transition. On the trailing edge of the pulse, the reverse takes place

Polarity reversing or nonreversing. Both balanced and single-ended systems may be operated with either polarity reversing or polarity non-reversing signals. In a single-ended system, one side is usually connected to Ground 1 (of Module 1) and the line voltage appearing in response to changes in the logic state can be seen in **Figs. 3a** and **3b**.

For balanced systems, the voltage on each line can be referred to Ground 1. But what is significant in this case is the line-to-line voltage, since a conductor carrying Ground 1 is not necessarily brought to the receiving end. The line-to-ground and line-to-line voltages for balanced systems under varying logic states appear

in **Figs. 3c** and **3d**.

Amplitude considerations for line drivers should take account of the current (or voltage) required by the line receiver. Obviously, optoisolators cannot be operated unless the line voltage (V_L) exceeds the operating voltage of the terminating circuit. Operating voltage can vary from as little as 1.5V (V_F of the optoisolator's input diode) to as much as 2.4V for an active termination.

The characteristic impedance of the transmission line affects amplitude considerations. Low impedance lines, such as coaxial, require a fairly large current drive capability to develop the voltage required by the line receiver.

Finally, there's the matter of noise. Ideally, the desired signal is carried at voltages and currents much larger than the noise amplitude. By designing the threshold of the line receiver to respond only to the high amplitudes produced by the desired signal, the lower amplitude of the interference becomes quite insignificant. The need for high amplitude signals will prove greater in single-ended than in balanced systems. This is so because in balanced systems interference is coupled with equal phase and amplitude into both sides and can be easily subtracted out in a differential receiver.

Amplitude balancing is desirable for data rate optimization. That is, with respect to the logic transition threshold, the asymptote for a HIGH should exceed the LOW-to-HIGH (LH) threshold to the same extent that the LOW asymptote exceeds the HIGH-to-LOW (HL) threshold (**Fig. 4**).

Note the inversion

Referring to **Fig. 4**, have you noticed what appears at first to be a polarity discrepancy between waveforms and nomenclature in this figure and others? Obviously it is not, since it stems from the standard specification of optoisolator propagation delay. For example, t_{PHL} is the propagation delay for a HIGH-to-LOW transition at the output of the optoisolator. In most applications with the most commonly used types of optoisolators, a LOW output requires a HIGH input voltage (or current), taking the forward voltage (and current) of the input diode as positive. Thus, an HL delay is associated with a rising input voltage.

Table 1 lists TTL and MOS line drivers suitable for lines terminated with OCI's. Other line drivers can be constructed from discrete components. Keep in mind that because line receivers using OCI's have high thresholds, you should use drivers with nonreversing output polarities and with amplitude characters such that logic ONE and logic ZERO line voltages deviate equidistantly

TYPE NO.	INPUT SIGNAL	POWER SUPPLY	OUTPUT CHARACTERISTICS		COMMENTS	TYPICAL APPLICATION
			"HIGH" STATE	"LOW" STATE		
FOR HIGH DATA RATES — TO 15M bit/sec						
DM 9830 μA 9814	TTL TTL	+5V +5V	LOW-Z SOURCE 40 mA, +3V	LOW-Z SINK 120 mA, +0.5V	BOTH HAVE INTERNAL PHASE SPLITTER; 9814 HAS SEPARABLE SOURCE/SINK	TWISTED PAIR SHIELDED DIFFERENTIAL—POLARITY REVERSING
μA 9821	TTL	+5V TO +14V	LOW-Z OR 130Ω E _o = 2.5 TO 11.5V	LOW-Z OR 130Ω E _o = 0	INTERNAL RES. AVAILABLE FOR BACKMATCH TYP. TWISTED PAIR, UNSHIELDED	TWISTED PAIR, UNSHIELDED DIFFERENTIAL—POLARITY REVERSING
LM 75324 75325	TTL TTL	+5 TO 17V +5 TO 24V	400 mA SOURCE 800 mA SOURCE	400 mA SINK 800 mA SINK	MEMORY DRIVERS—BOTH NEED EXTERNAL PHASE SPLITTER FOR DIFFERENTIAL OUTPUT	EXTERNAL BACK MATCH, DIFFERENTIAL—REVERSING OR NONREVERSING
75451 75452 75453 75454	TTL TTL TTL TTL	+5V +5V +5V +5V	OPEN COLLECTOR V _{ceo} > 30V	SINK 300 mA	NAND AND NOR OR FOR DIFFERENTIAL OPERATION NEED EXTERNAL PHASE SPLITTER UNLESS USED IN OR/NOR OR AND/NAND PAIRS	EXTERNAL BACK MATCH, DIFFERENTIAL—REVERSING OR NONREVERSING
FOR MEDIUM DATA RATES — TO 1 Mbit/sec						
MC 75113	TTL	+5V, -6V	SOURCE/SINK 20 mA	SOURCE/SINK OPEN	CURRENT-SOURCE FOR HI-Z _o LINES	DIFFERENTIAL—NONREVERSING
75491	MOS	UP TO +10V	SOURCE 50 mA OPEN COLLECTOR	OPEN EMITTER SINK 50 mA	QUAD LED DRIVER—w/ EXTERNAL PHASE SPLITTER CAN BE DIFFERENTIAL LINE DRIVER	SINGLE-END QUAD OR DUAL DIFFERENTIAL DRIVER
75492	MOS	UP TO +10V	OPEN COLLECTOR	SINK 250 mA	HEX LED DRIVER—w/ EXTERNAL PHASE SPLITTER & PULL-UP RESISTOR MAKES LINE DRIVER	SINGLE-END HEX OR TRIPLE DIFFERENTIAL DRIVER
FOR LOW DATA RATES — TO 50k bit/sec						
MC 1488 μA 9816	TTL	+9, -9	+5V, 300Ω	-6V, 300Ω	QUAD TRIPLE BOTH HAVE 10 mA LIMITER 9816 HAS "INHIBIT" INPUTS	RS-232-C UNBALANCED, POLARITY—REVERSING
75109 75110	TTL	+5, -5	OFF	3.5-7.0 mA SINK 6.5-15 mA SINK	INTERNAL PHASE SPLIT; NEED EXTERNAL PULL-UP RESISTOR; CURRENT LIMIT OUTPUT	DIFFERENTIAL—POLARITY—REVERSING

Table 1—Integrated drivers for lines terminated with optoisolators.

above and below the threshold voltage. Drivers with polarity reversing output need only have enough amplitude to exceed the threshold with either polarity; balancing is then achieved by using a pair of OCL's operating in a balanced, split-phase circuit. This technique will be discussed in detail later.

Impedance Considerations. Where the possibility exists of high EMI, you should make the driver output impedance to Ground 1 either low with respect to the characteristic impedance of the line, or balanced with respect to Ground 1. With this advice, we come to the second element of the data transmission system—the transmission line itself.

Meanwhile, on down the line. . .

In choosing a cable for data transmission, you should consider four factors: the characteristic impedance (Z_0 , in ohms), the dc resistance of line (R_w , in ohms per unit length), bandwidth or data rate capability and effectiveness against common-mode interference. Of course, there are also the usual considerations of cost, availability, ruggedness, size, and so forth. But these are not areas of concern since they do not directly affect performance (except for cost and size).

Characteristic Impedance (Z_0) becomes an important consideration only when low loss cable is used in a high speed system with distances less than 50 meters. As a rule, coaxial cables have the lowest characteristic impedance, followed by

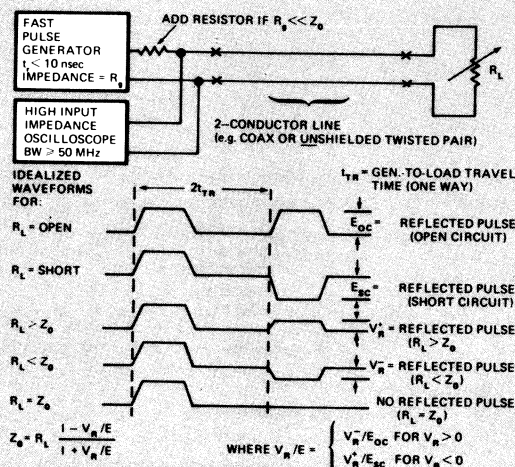


Fig. 5—In the time domain reflectometry (TDR) method for measuring characteristic impedance (Z_0) of a 2-conductor transmission line (single-ended or balanced unshielded line), both the waveform of the generated pulse and its reflection appear on the scope, separated by twice the transit time. Only one value of R_L need be used in the measurements provided $R_L \neq Z_0$.

shielded twisted pair, then by unshielded twisted pair. The characteristic impedance of these cables remains the same regardless of the length, while dc resistance is proportional to length.

If the characteristic impedance is not listed by the manufacturer, you can measure it easily by

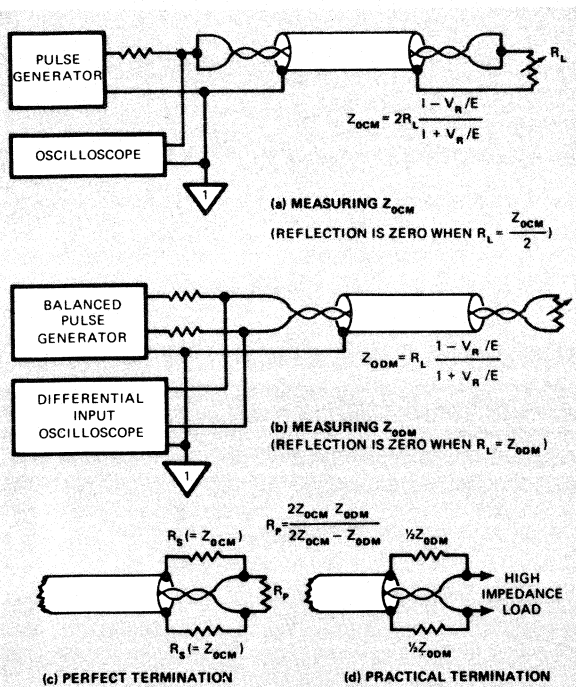


Fig. 6—To measure common-mode (Z_{0CM}) and differential-mode (Z_{0DM}) characteristic impedance of a shielded twisted pair, use the TDR method and circuits of a and b. Then calculate Z_{0CM} and Z_{0DM} and use this information, in turn, to design a perfect (c) or practical (d) termination. Perfect terminations absorb all incident energy from the driver and line, while practical terminations reflect back an insignificant amount.

the time domain reflectometry (TDR) method (Fig. 5). Set the pulse duration short enough to permit observation of the baseline as well as the reflection. On the other hand, the sweep time must be greater than $2t_{TR}$, the travel time for the pulse edge to go from scope to load and back. Keep in mind that propagation velocity for coaxial cable is less than 0.3 m/nsec while for twisted pair lines, the velocity may be much slower, depending on the pitch of the twist. At a velocity of 0.2 m/nsec, a cable of 10 meters will have a round trip time ($2t_{TR}$) of 100 nsec.

Twist it, shield it—and you get two

Shielded twisted pair line, because of the shield, has two characteristic impedances: common mode (Z_{0CM}) and differential mode (Z_{0DM}). Once again, you can use TDR techniques to measure these impedances, with the circuits of Fig. 6 and the pulse generator, oscilloscope and waveforms of Fig. 5. Notice, however, that the measurements do not directly yield the resistor value to be used in the termination. Rather, they

are used as in Fig. 6 to compute the resistance values needed for a perfect termination. Common-mode signals are terminated with $R_s = Z_{0CM}$ from each line to ground (shield). Differential-mode signals are terminated with Z_{0DM} from line to line, so R_p in parallel with $2Z_{0CM}$ provides a net line-to-line resistance of Z_{0DM} .

$$R_p = (2Z_{0CM} Z_{0DM}) / (2Z_{0CM} - Z_{0DM}) \quad (1)$$

Because of parasitic impedances in the apparatus, the waveforms you observe in TDR may not be as clean as those represented in Fig. 5. To obtain accurate information, we recommend that you perform the TDR measurement for several values of R_L , selected so that some of them cause positive reflections and others negative. Then take as Z_0 the average obtained by calculating Z_0 for each observation according to:

$$Z_0 = R_L(1 - V_R/|E|) / (1 + V_R/|E|) \quad (2)$$

Here V_R is the reflected pulse when R_L is connected, while E is the reflected pulse when the line is open (for $R_L > Z_0$) or shorted (for $R_L < Z_0$).

DC resistance (R_w) of the line is important to the extent that it limits the dc current available at the termination. Note that the total line resistance to be considered is the "loop resistance" encountered as current flows to and from the load. It shows up at the termination as part of the source internal resistance; the remainder is the internal resistance of the line driver. For designing a resistive termination, this internal resistance information can be represented either as a "source line" for graphical solutions or as a Thevenin or Norton Equivalent circuit. You obtain the data in a dc (not pulsed) measurement (Fig. 7).

Bandwidth, or data rate capability, of the transmission line is affected by the line's resistance. But other loss factors also affect the transient response. The waveforms of Fig. 4 illustrate the delay in response to step transient signals. (Travel or transit time is not included as part of the logic delay because it is the same for both HL or LH transitions.)

The amplitude of the line driver output and the threshold of the line receiver can affect the logic delay. For this reason, although the transmission line affects the data rate capability, a data rate figure cannot be stated for the cable alone unless the threshold of the line receiver is exactly halfway between the HIGH-state and LOW-state levels. And even if $V_{thLH} = V_{thHL} = (V_{HIGH} + V_{LOW})/2$, the delay can be distorted if the time between logic changes is less than that required for the transient to reach steady state at V_{HIGH} or V_{LOW} . At any rate, it is worthwhile examining the

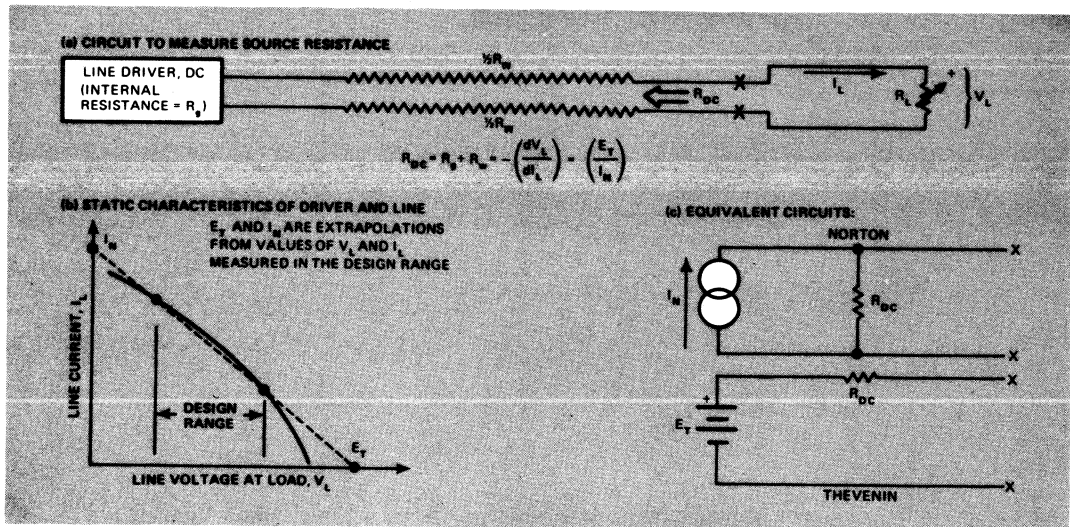


Fig. 7—To obtain the dc resistance looking backward into the line (a) from the termination, vary R_L and plot line current vs.

line voltage (b). Extrapolate to obtain I_N and E_T . This yields R_{DC} , from which you can draw the dc equivalent circuit (c).

effects of cable properties on logic delay.

Attenuation of a line depends on frequency and the length and quality of the line. Fig. 8 illustrates some typical attenuation characteristics.

Notice that the curves have a slope of "one-half," that is, α_0 changes by $\sqrt{10}$, or half a decade per decade of frequency. While this relationship doesn't hold for all types of cable, it is based on the theoretical analysis of skin effect and has been substantially verified by measurements.

So, if attenuation data is not available, you can make a single measurement at a high frequency and use it to provide a curve of α_0 vs. frequency. With this information and the curve in Fig. 9, you can then compute the values of t_{PHL} and t_{PLH} if the line length, line driver amplitude, and line receiver thresholds are known.

Measuring attenuation step by step

To measure the attenuation characteristic (α_0)

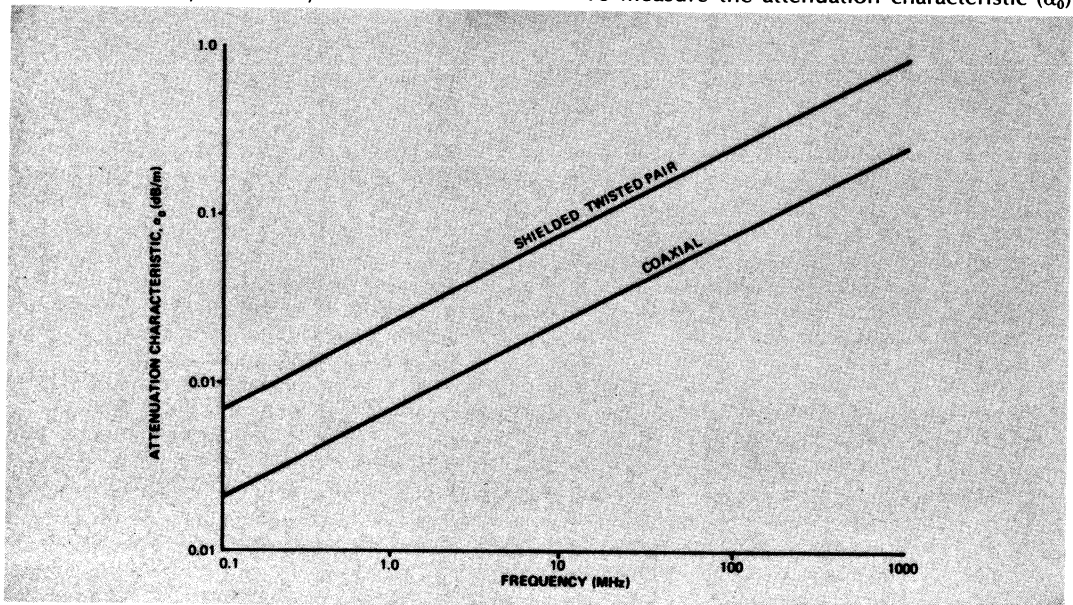


Fig. 8—Transmission line attenuation as a function of frequency graph can be used to obtain f_0 , which is then used to calculate the delay time (see example).

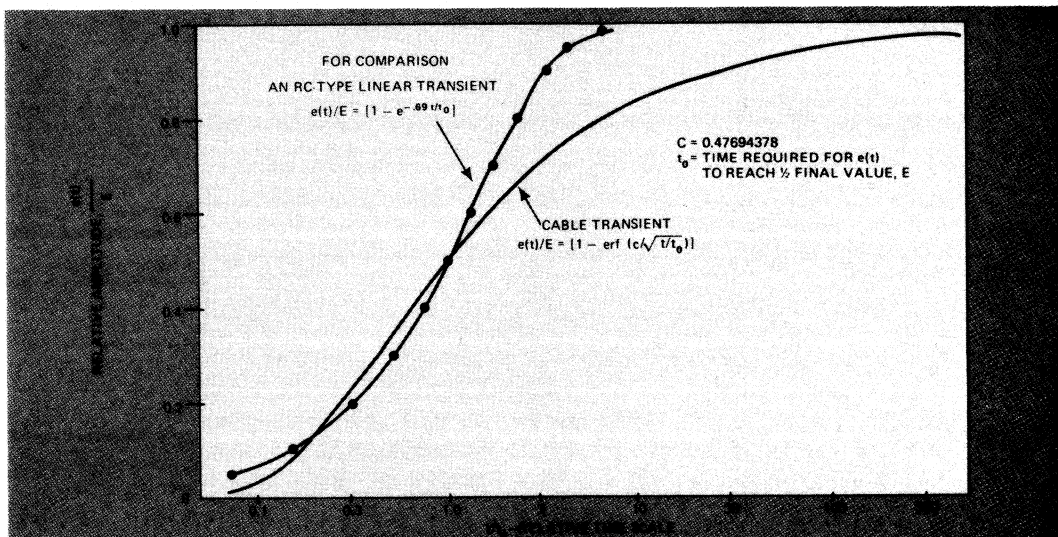


Fig. 9—Normalized transmission line response curve to a step change, E obtains the cable-imposed HL or LH delay when switching thresholds and asymptotic levels are applied. This curve is used to obtain t/t_0 in calculating the delay time (see example).

for a particular sample of transmission line:

1. Measure the characteristic impedance (Z_0) of the transmission line as explained earlier,
2. Set a signal generator to some convenient frequency (f_0) and select a convenient amplitude to be held fixed during measurement,
3. Measure the voltage across a load resistor ($R_L = Z_0$),
 - (a) With no transmission line, measure V_0 ,
 - (b) With a line of length, l , inserted between the generator and R_L , measure V_l ,
4. Finally, calculate α_0 according to:

$$\alpha_0 = (1/l) 20 \log_{10} (V_0/V_l) \quad (3)$$

α_0 has the units db/m for l measured in meters. To improve the accuracy of this measurement:

- a. Make the generator impedance approximately Z_0 ,
- b. Use a high impedance voltmeter,
- c. Measure at several different lengths,
- d. Repeat the measurement for several values of f_0 , and, plotting $\log \alpha_0$ against $\log f_0$, verify that your results are similar to Fig. 8 (i.e., slope ≈ 0.5).

Now let's tackle propagation delay

Propagation delay imposed by a particular type of transmission line of length l can be estimated using the α_0 vs. f_0 curve (such as Fig. 8) and the normalized time response curve of Fig. 9. The procedure is as follows:

1. Calculate α_0 for the length of cable to be used:

$$\alpha_0 = 6\text{dB}/l \text{ (in meters)} \quad (4)$$

2. With α_0 from Eq. 3, enter Fig. 8 (or a curve for the actual cable to be used) and read off a value of f_0 , then compute t_0 :

$$t_0 = 0.164/f_0 \quad (5)$$

Here t_0 is in seconds when f_0 is in Hz.

3. You determine the propagation delay for a cable of the length selected in step 1 from the normalized curve in Fig. 9. This curve does not include source-to-load travel time; the time delay imposed by the cable response is measured from the time when energy begins to arrive at the termination. To find the delay for a HIGH-to-LOW transition t_{HL} , note the value of (t/t_0) in Fig. 9 at which

$$e(t)/E = (V_{\text{HIGH}} - V_{\text{thHL}})/(V_{\text{HIGH}} - V_{\text{LOW}}) \quad (6)$$

where V_{HIGH} and V_{LOW} are the asymptotic voltages and V_{thHL} is the HIGH-to-LOW threshold voltage.

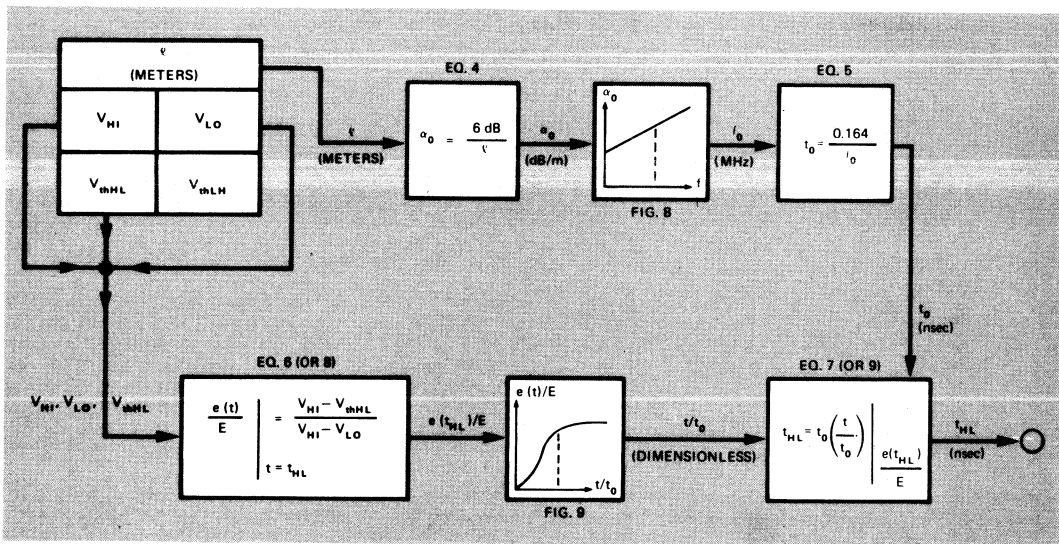
Then, with this value of (t/t_0) , you can calculate the delay from

$$t_{HL} = t_0 \times (t/t_0) \quad (7)$$

where t_0 is the value found in step 2, Eq. 5.

The delay for a LOW-to-HIGH transition is found similarly. From Fig. 9 find (t/t_0) at which

$$e(t)/E = (V_{\text{LOW}} - V_{\text{thLH}})/(V_{\text{LOW}} - V_{\text{HIGH}}) \quad (8)$$



Procedural flowchart summarizes the steps (see example) to follow in determining the cable delay time (t_{HL} or t_{LH}). Starting from known factors (l , V_{HI} , V_{LO} , V_{thHL} and V_{thLH}), merely follow the flow and perform the calculations of each operator box. You can also work backwards: by knowing the steady state and threshold voltages and delay time, you can obtain cable length (l).

Here V_{thLH} is the LOW-to-HIGH threshold. Then, with this value of (t/t_0), you again calculate the delay

$$t_{LH} = t_0 \times (t/t_0) \quad (9)$$

An example makes it clear

Let's apply this procedure to a typical example that could crop up in a real-life situation. A $\mu A9614$ or DM8830 line driver with 75m of shielded twisted pair line with approximate load matching that has $V_{HIGH} = -2.14V$, $V_{LOW} = +2.14V$. (Inversion through the optoisolator accounts for the apparent polarity disparity.) For one side of the balanced pair, $V_{thHL} = V_{thLH} = 1.5V$.

1. From **Eq. 4**, calculate $\alpha_0 = 6\text{dB}/75\text{m} = 0.08\text{ dB/m}$
2. From **Fig. 8**, for $\alpha_0 = 0.08\text{ dB/m}$, read $f_0 = 14.2\text{ MHz}$. Then from **Eq. 5**, calculate $t_0 = 0.164/14.2\text{ MHz} = 11.55\text{ nsec}$
3. For t_{HL} , from **Eq. 6**, calculate:

$$e(t_{HL})/E = (-2.14 - 1.5)/(-2.14 - 2.14) = 0.85$$
Enter **Fig. 9** with $e(t)/E = 0.85$. Read off $(t/t_0) = 13$, and from **Eq. 7**, calculate:

$$t_{HL} = (11.55\text{ nsec} \times 13) = 150\text{ nsec}.$$

If we want to, we can work backwards. From given asymptotic (steady state) and threshold voltages, the value of $e(t)/E$ is calculated from **Eq. 6** or **8**, and a value of t/t_0 is read from **Fig. 9**. Applying the desired delay time to **Eq. 7** or **9** yields a value of t_0 , and **Eq. 5** yields f_0 . With this value of f_0 , **Fig. 8** and **Eq. 4** can be used to

determine either the maximum length of cable or the necessary cable characteristics for a desired length to achieve the desired delay.

Why not save some time?

Eqs. 4-9 and **Figs. 8** and **9** can also be used to examine effects of threshold and asymptotic voltage adjustments on delay times. While it is not likely that calculated results will agree precisely with measured performance, this procedure can save a great deal of design time by eliminating some possible causes of excessive propagation delay. Note, though, that you must remember that total propagation delay (t_{TPHL} or t_{TPLH}) includes that of the isolator itself (t_{PHL} or t_{PLH}). For example:

$$t_{TPHL}(\text{total}) = t_{HL}(\text{cable}) + t_{PHL}(\text{isolator}) \quad (10)$$

$$t_{TPLH}(\text{total}) = t_{LH}(\text{cable}) + t_{PLH}(\text{isolator}) \quad (11)$$

If the isolator delay times are relatively small, the importance of the cable-imposed delay time is emphasized. From **Fig. 9** and **Eqs. 6** and **8** it is clear that threshold voltages may profoundly influence the cable-imposed delay. Ideally, the HL and the LH thresholds should be balanced, so **Eqs. 6** and **8** yield equal values of $e(t)/E$, resulting in balanced delays. The use of hysteresis in the termination tends to give larger values in both **Eqs. 6** and **8**, whether balanced or not, while the use of peaking in the termination tends to reduce both. Thus, while hysteresis is helpful in prevent-

ing errors due to noise (either common mode or differential mode), its adverse effect on data rate should be considered.

Interference protection. A final, but important, cable consideration is its property of common-mode rejection (CMR). The cable cannot relieve the effects of common-mode signals generated within the equipment being interconnected, but it can reduce the effects of induced interference. Either inductively or capacitively induced common-mode signals are less likely to occur in balanced lines than those that are single ended. If we rank lines in descending order of CMR effectiveness, we rate shielded twisted pair first, then unshielded twisted pair and finally coaxial.

If your system requires a data rate capability that only coaxial line can provide, but if the coaxial line does not give adequate CMR, then a pair of coaxial lines should be used for each channel. By driving the two coaxial lines in opposite phase, a balanced system is obtained, having the data rate capability of coaxial line and a CMR at least as good as shielded twisted pair. We will reserve a more detailed discussion of CMR enhancement for a later article. □

References

1. "Performance of the 6N135, 6N136, and 6N137 Optocouplers..." Application Note AN-948, Hewlett-Packard.
2. Dreher, Thad, "Cabling fast pulses? Don't trip on the steps," *The Electronic Engineer*, Aug. 1969, pp. 11-75.

Part 2 of this series will examine resistive terminations to achieve on/off steady-state conditions, optimize data rate and reduce reflections in short, low-loss lines.

Designer's Guide to: Optoisolators — Part 2

If you're looking for simplicity and economy in your line terminations, the resistive road is the one to take.

Ignore proper termination of a high-speed digital transmission line and you'll pay several times over: either the line receiver won't switch or line reflections will play a game of Russian Roulette with the receiver, producing multiple switching. Or your high-speed printer will crawl at half speed. Or any of a dozen other unpleasant surprises will await you.

With an optoisolator as the active element in a line receiver, designing a resistive termination becomes more complicated than merely connecting a terminating resistor across the line. This is because you must account for forward voltage (V_F) and forward current (I_F) requirements of the optoisolator input diode. There's little current flow until the diode voltage exceeds V_F . Then V_F remains substantially constant as current increases. Input current must be high enough for proper operation of the photodetector and output circuit, but it must not exceed maximum ratings.

Three Commandments of termination design

Three design objectives must be considered when terminating any line:

1. Proper ON/OFF steady-state conditions (I_F);
2. Threshold adjustment (I_{Fth}) for optimum data rate (unequal thresholds will time-distort data pulses);
3. Load matching to reduce reflections in low-loss, high-speed lines less than 50 meters long.

The first design objective is mandatory! You must always meet it or the optoisolator will simply not provide sufficient drive for the logic—possibly even none at all. Objectives 2 and 3 are desirable but not always mandatory; in some cases they may be impossible. For example, you can't balance thresholds with a single isolator if polarity-reversing drive is used.

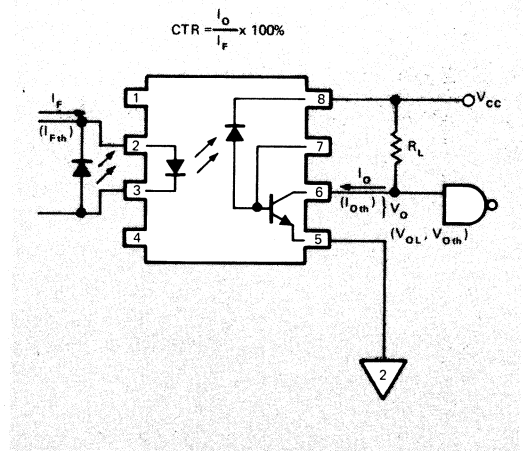


Fig. 1—Proper steady-state current drive (I_F) is determined by the maximum I_O needed to drive the output logic, as well as V_{CE} , V_{OL} , and current transfer ratio (CTR). Designing for extra drive (up to 20%) will compensate for CTR degradation.

Generally, while a 3-resistor termination meets all three objectives, a 1-resistor meets only one (1), and a 2-resistor termination meets two (1 and 2 or 1 and 3).

Proper min./max. current limits must be observed to ensure reliable optoisolator switching. The minimum current for some types of isolators is established by the manufacturer. For others, it depends on the isolator's current transfer ratio (CTR) and the output logic drive requirements.

When selecting input current (I_F), you should allow

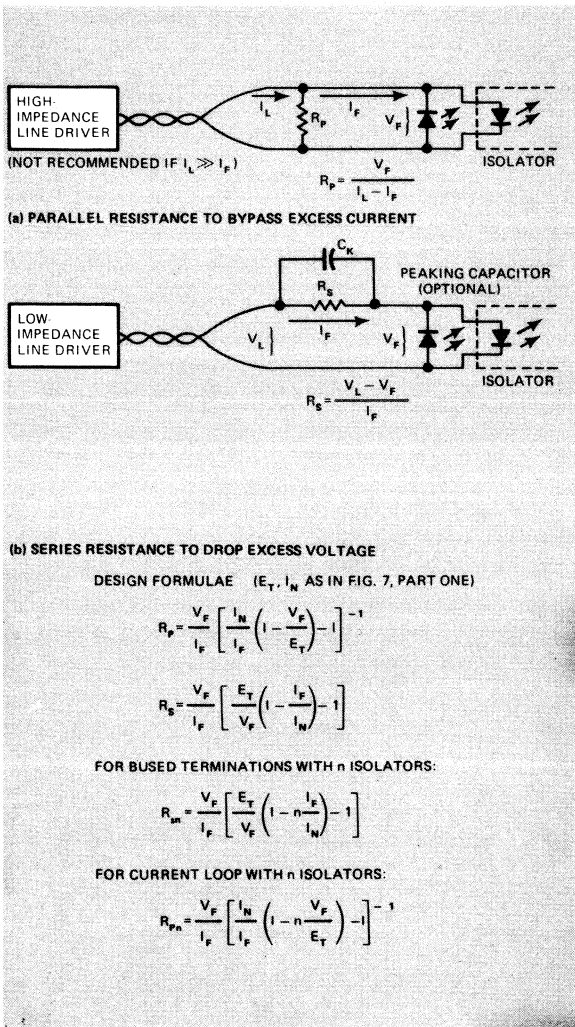


Fig. 2—One-resistor terminations will meet design Objective 1 (steady state). Parallel-resistance circuit (a) possesses poor regulation, but responds more rapidly. Series-resistance termination (b) handles a wider range of source voltages but is inherently slower. Its response time can be improved by shunting the series resistor with a peaking capacitor (C_K), provided an anti-parallel LED is placed across the optoisolator input to discharge C_K . Otherwise, the anti-parallel LED is employed only with polarity-reversing drive.

for CTR degradation. CTR decreases rapidly at high levels of input current. Typically, at $I_F > 20$ mA, allow an extra 20%. But at $I_F < 2$ mA, a 5% margin is adequate for more than 20,000 hrs. of proper operation.

To design a termination, begin with the heart of the receiving module—the optoisolator—and find a nominal value for the minimum input current (Fig. 1). For the steady ON state, the voltage drop

across R_L must be large enough to make V_O adequately low with respect to the logic family used at the output.

Calculate the maximum value of I_O , taking account of the tolerance on R_L and maximum V_{CC} . Then divide by the minimum CTR to arrive at the proper value of I_F . However, since the manufacturer sometimes specifies a minimum CTR for only one value of I_F , you might want to try an alternate (and preferred) procedure. Use the known value of I_F and the minimum CTR to find the minimum value of R_L :

$$I_F \geq I_O (\text{max.}) \times \left[\frac{100\%}{\text{CTR} (\text{min.})} \right] =$$

$$\left[\frac{V_{CC} (\text{max.}) - V_{OL} (\text{min.})}{R_L (\text{min.})} \right] \times \left[\frac{100\%}{\text{CTR} (\text{min.})} \right] \quad (1)$$

For the steady OFF state, reduce the input current to a value at which the output is at a proper logic HIGH level.

Protect the input diode from excessive reverse current when using polarity-reversing drive. The best way is to shunt the input diode with a LED having the same forward voltage as the isolator input diode, but with opposite polarity (Fig. 1).

One-resistor termination—the economy line

If the transmission line is long, has a high resistance and carries a low data rate, then Objective 1 is your only worry. Therefore, the 1-resistor termination is your choice, and design of the termination will be as simple as in Fig. 2, leaving you nothing further than a decision between the two versions.

Parallel-resistance termination (Fig. 2a) permits the input photodiode to face a lower source resistance and, thereby, to respond more rapidly. But since the circuit trades speed for poorer regulation, it should be avoided unless the open-circuit voltage, E_T , is several hundred mV greater than V_F . Also, the line current I_L must not be more than twice the value of I_F .

Series-resistance termination (Fig. 2b) can handle a broader tolerance on the resistance value and source characteristics. Although the high source resistance imposed on the input diode tends to reduce the speed of response, connecting a peaking capacitor (C_K) in parallel with R_s can compensate for this effect.

Both series- and parallel- resistance terminations in reverse-polarity should have an anti-parallel diode across the input of the opto-isolator, since reverse current may reduce the CTR by heating the input diode. If you use a peaking capacitor in the series termination, always use the anti-parallel LED — whether the drive is reversing or not. This gives the peaking capacitor a chance to discharge for maximum peaking.

When multiple terminations are on one line

Can several optoisolators operate on the same

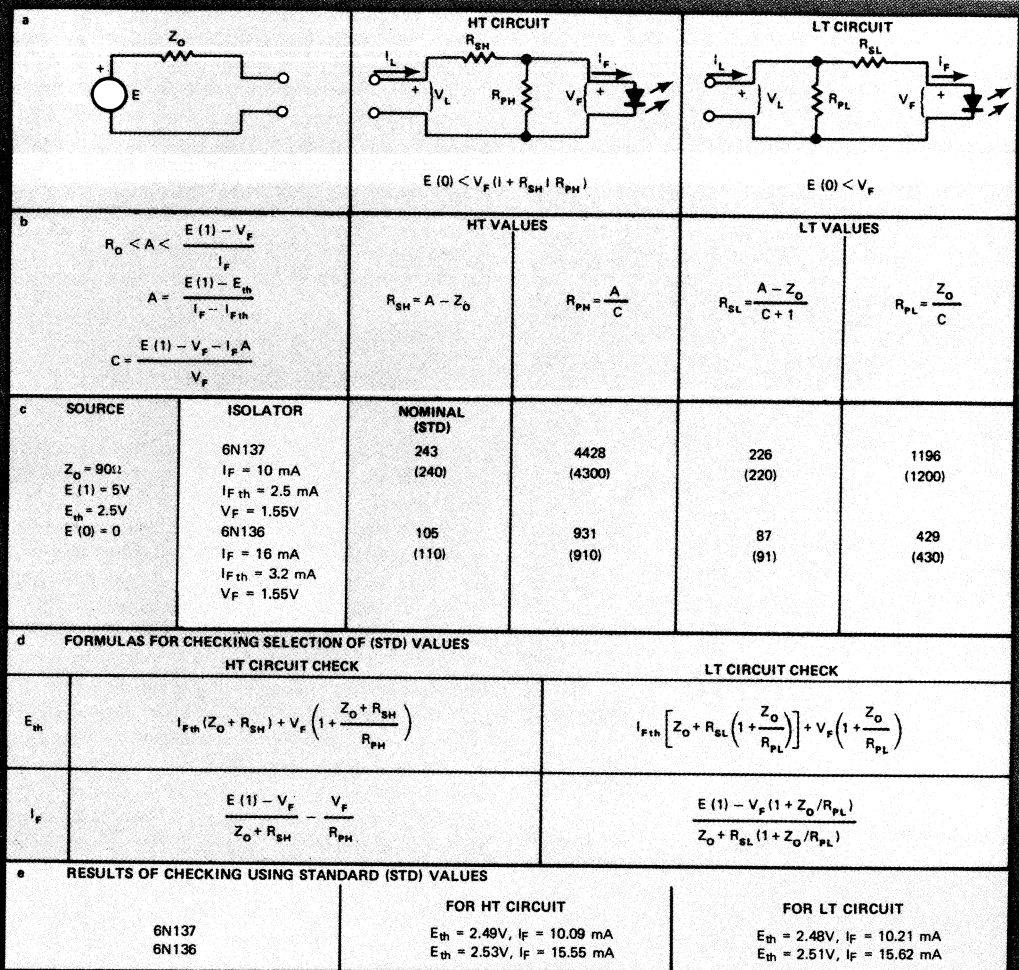


Fig. 3—Two-resistor termination circuits (a) for a back-matched ($R_0 = Z_0$), polarity nonreversing system. Obtain the line impedance, optoisolator data and steady-state threshold values. Calculate 'A' and 'C', making sure that 'A' falls within the calculated limits (b). Then calculate the series and parallel resistance (b) and

choose the closest standard values as illustrated in the two examples (c). To be sure threshold and steady-state conditions are still met by the standard values, calculate E_{th} and I_F (d) as demonstrated in the two examples (e).

transmission line? Yes, but be sure to use the series-resistance termination with a separate resistance (and, if required, an anti-parallel LED) for each isolator input. To find the value of resistance to be used for bused terminations, refer to the formula for R_{sn} in Fig. 2. Obviously, if $I_F \ll I_{n}$, the value of R_{sn} will not change much as n , the number of terminations, varies. Under these conditions, terminations can be added or removed without disturbing existing ones.

The parallel-resistance termination is not suitable for busing. However, it could be used in a current loop, with several isolator inputs connected in series and a separate R_{pn} across each.

What's threshold adjustment?

Between the steady-state extremes for logic ZERO and logic ONE, a voltage level exists at which transition occurs. The amplitude of this threshold level, relative to the asymptotic levels (upper and lower extremes), can seriously affect propagation delay. To correct this, raise the threshold to lengthen HL (High-Low) delay and shorten LH delay or vice versa. Remember, for optimum error-free data rate, the overall delays should balance; or, in a word, $t_{FPHL} = t_{PLH}$.

In cases where cable-imposed delays greatly exceed isolator delays, threshold adjustment can work wonders. Where cable delays are negligible relative

to isolator delays, though, threshold adjustment will still influence HL and LH delays as described above, although the amount of influence can't be calculated.

To find the threshold level for the output circuit (Fig. 1), I_{Fth} is substituted into Eq. 1 to yield:

$$I_{Fth} = I_{Oth} (typ.) \times \left(\frac{100\%}{CTR (typ.)} \right) = \left[\frac{V_{CC} (typ.) - V_{Oth} (typ.)}{R_L (typ.)} \right] \times \left[\frac{100\%}{CTR (typ.)} \right] \quad (2)$$

Since the values called for are typical rather than maximum or minimum, it may be necessary to obtain them empirically.

Are two resistors better than one?

If you find your data rate is high enough to be time-distorted by unequal leading- and trailing-edge thresholds, you have an unbalanced system. Except for isolated cases, the old 1-resistor trick won't work here.

First, find I_F and I_{Fth} from Eqs. 1 and 2. Then decide how to arrange the two resistors (Fig. 3), either in the High Threshold (HT) or Low Threshold (LT) termination. Incidentally, the HT and LT designations refer to the voltage threshold at which the isolator input diode begins to conduct significantly.

In making your choice, remember that for significant diode conduction (hence, impedance lowering), the LT circuit requires only that $V_L > V_F$; while the lower impedance HT circuit requires that $V_L > V_F (1 + R_{SH}/R_{PH})$.

The design relationships of Fig. 3 hold for a back-matching system ($R_g = Z_0$) with negligible wire resistance. $E(1)$ is the open-circuit voltage for isolator-ON state, and $E(0)$ is the open-circuit voltage for the isolator-OFF state. To place the threshold voltage at any desired midway value, use a resistor network at the driver to raise $E(0)$ to the required voltage, such that:

$$\frac{E_{th} = [E(1) + E(0)]}{2} \quad (3)$$

The only limitation on $E(0)$ is that V_L be less than the impedance threshold value, which requires $E(0) < V_F$ for the LT circuit, and $E(0) < V_F (1 + R_{SH}/R_{PH})$ for the HT.

For designing the HT circuit, follow the design expressions in Fig. 3. If you care to verify the expressions, solve for R_{SH} and R_{PH} in the pair of simultaneous equations resulting when E_{th} and I_{Fth} are substituted for $E(1)$ and I_F in the HT circuit equation:

$$\frac{E(1) - V_F}{Z_0 + R_{SH}} - \frac{V_F}{R_{PH}} = I_F \quad (4)$$

The design expressions for the LT circuit are found by solving for R_{PL} and R_{SL} in the pair of simultaneous equations obtained by substituting E_{th} and I_{Fth} for $E(1)$ and I_F in the LT circuit equation:

$$\frac{(E(1) - I_F Z_0)}{\left(\frac{1 + Z_0}{R_{PL}} \right)} - I_F R_{SL} = V_F \quad (5)$$

As a matter of interest, notice that as the value of "A" (Fig. 3) approaches either of its limits, the HT and LT circuits become identical, reducing to either a series or parallel 1-resistor termination. On the other hand, if "A" falls outside the prescribed limits, the first method fails and a solution for the selected value of E_{th} does not exist.

To remedy this situation, substitute E_{th} from Eq. 3 into the expression for "A" and its limits (Fig. 3). This yields:

$$Z_0 < \frac{(E(1) - E(0))}{2(I_F - I_{Fth})} < \frac{(E(1) - V_F)}{I_F} \quad (6)$$

When the system is not back matched or when the wire resistance is significant, a specific solution for either the HT or the LT circuit becomes too complicated. Instead, use the following alternate approximation procedure that converges onto the solution.

Obtain E_T for both the ONE and ZERO state and use them as $E(1)$ and $E(0)$, respectively. Terminate the line with a variable resistor and plot line current as a function of line voltage (Fig. 7 of Part 1). Next, project the linear portion of the curve to both axes and read I_N and E_T . For Z_0 use $R_{DC} = E_T/I_N$. Then apply the equations in Fig. 3 to compute resistor values. Try the circuit, don't be surprised if it doesn't work. Recompute, if necessary, selecting a different value of E_{th} . Keep at it until you obtain values that produce a balanced delay.

Reflecting on the problem

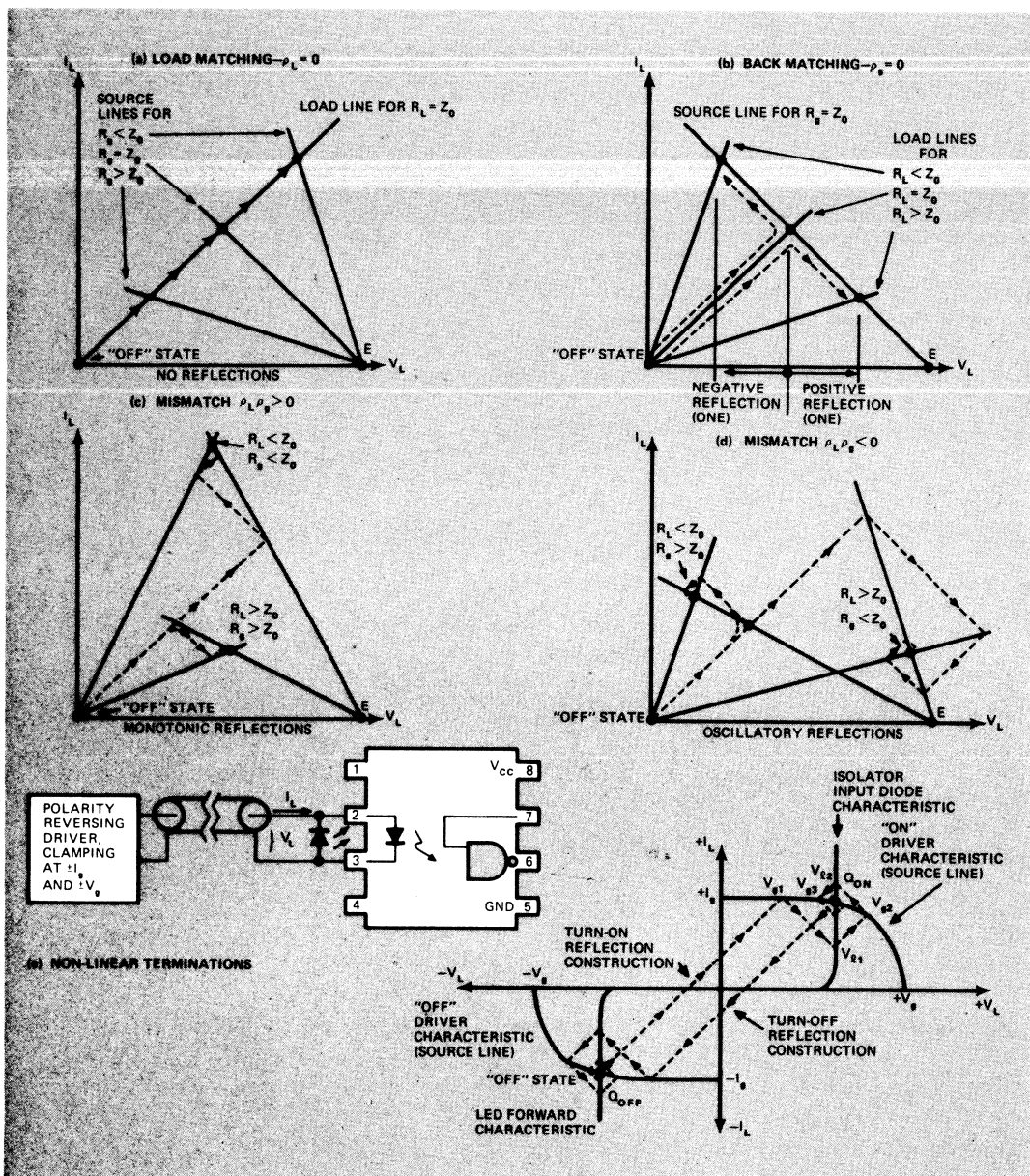
In high-speed data transmission lines under 50 meters, reflections can kill your system. Reflection occurs when a transient propagating along a transmission line encounters an impedance not equal to the line's characteristic impedance. And just as echoes can make conversation unintelligible in a canyon, so too, can these electrical reflections transform data flow into gibberish. If this is your problem, consider these two alternatives.

One method uses "load matching" to make the termination impedance match the line, so all incident energy is absorbed. Presto, no reflection! On the other hand, "back matching" matches the drive (generator) impedance to the line. One reflection may occur, but is absorbed at the driver.

For linear impedances, the magnitude and polarity of reflections can be computed from the reflection coefficients ρ_r and ρ_k :

$$\rho_r = \frac{(R_r - Z_0)}{(R_r + Z_0)} \quad \rho_k = \frac{(R_g - Z_0)}{(R_g + Z_0)} \quad (7)$$

$$(\Delta \vec{V}_L) = \rho_r (\Delta \vec{V}_L) \quad (\Delta \vec{V}_L) = \rho_g (\Delta \vec{V}_L) \quad (8)$$



$(\Delta \bar{V}_L)$ is a transient propagating toward the load and $(\Delta \bar{V}_L)$ is a transient propagating toward the generator. R_L is at the load and R_g is at the driver.

Incidentally, the above reflection coefficients apply only to the line voltage step change, ΔV_L .

Have nonlinearities got you down? If so, you will find it more practical to use a graphical construction to examine reflections. This technique can handle nonlinear impedances because it takes account of the instantaneous line voltage (and current) as well as of the step change. Construct the graph (**Fig. 4**) on linear coordinates of line current (I_L) and line voltage (V_L). First, draw the "load line"—the V-I characteristic of the load (positive current flows into the LOAD). Next, construct the "source lines"—one for logic ONE (ON) state and another for logic ZERO (OFF) state. These are the V-I characteristics of the source (positive current flows from the source into the line). Finally, graph the reflections.

Incidentally, we show the driver characteristics represented in **Fig. 4e** only for illustration. Yes, the circuit can be used, but it would prove a disaster in any high-speed system.

Various combinations of load/source match/mismatch for polarity nonreversing drive provide better solutions to the problem. In order of desirability, they are:

- **BEST—Fig. 4a**—load matching allows no reflections regardless of source mismatch polarity or magnitude.
- **NEXT BEST—Fig. 4b**—back matching allows one reflection regardless of load mismatch polarity or magnitude.
- **TOLERABLE—Fig. 4c**—double mismatch, same polarity, $\rho_L \rho_g > 0$ —may have several re-reflections, but both source and load terminal voltages approach steady-state condition monotonically, so the only effect is a data rate limitation depending on magnitude of $\rho_L \rho_g$.
- **POTENTIALLY DISASTROUS—Fig. 4d**—double mismatch opposite polarity, $\rho_L \rho_g < 0$ —oscillatory re-reflections; not only is data rate limited, but there is high risk that a single HL or LH transition may produce multiple transitions (HL — LH — HL) in the output circuit, especially with a short (< 50m) line. □

This Designer's Guide series has now expanded to five parts. The third part will continue the discussion of resistive terminations, focusing on load matching with 2-resistor terminations and applications for 3-resistor terminating networks.

Designer's Guide to: Optoisolators — Part 3

These design procedures permit 2- and 3-resistor terminations to adjust threshold, match impedances and boost system performance.

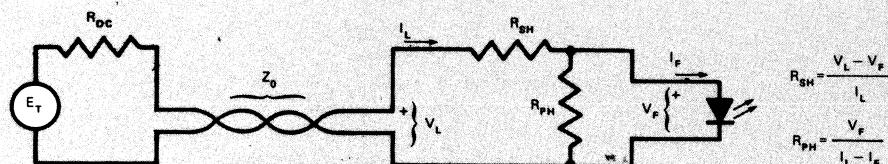
Last issue we covered 1- and 2-resistor termination designs; this article delves into 3-resistor designs and the use of 2-resistor circuits in impedance-matching. As we saw, there are three design objectives in termination design: forward isolator drive (I_F), threshold balancing and impedance matching. One-resistor terminations meet only the first goal; two resistors meet two goals; while three resistors meet all three goals.

Matching loads? Two resistors will do!

Under certain conditions, a 1-resistor termination can simultaneously satisfy Objective 1 and Objective 3 (load matching):

- If $R_g < Z_0$ and $R_p < Z_0$, (Fig. 2a, Part 2)
- If $R_g > Z_0$ and $R_s > Z_0$, (Fig. 2b, Part 2)

In general, however, two resistors are required to satisfy the two objectives (1 and 3, Part 2). As we already know, Eq. 1 simply establishes the proper value



E_T — SOURCE VOLTAGE, DC, OPEN-CIRCUIT
 R_{DC} — SOURCE RESISTANCE, DC, INCLUDES TRANS. LINE RESISTANCE
 Z_0 — CHARACTERISTIC IMPEDANCE OF LINE TO BE MATCHED
 V_L, I_L — LINE VOLTAGE, CURRENT AT TERMINATION
 V_F — STEADY STATE FORWARD VOLTAGE, ISOLATOR INPUT
 I_F — CURRENT REQUIREMENT OF OPTO ISOLATOR

CASE 1: $V_L / I_L = Z_0$ AT STEADY STATE

$$R_{SH} = Z_0 \frac{V_F}{I_L} \quad R_{PH} = \frac{V_F}{I_L - I_F} \quad \text{WHERE} \quad I_L = \frac{E_T}{R_{DC} + Z_0}$$

CHECK: FIND I_F AS BELOW, THEN $\frac{V_L}{I_L} = \frac{V_F}{I_F + V_F/R_{PH}} + R_{SH} \stackrel{?}{=} Z_0$

CASE 2: $(dV_L/dI_L) = Z_0$ FOR $V_L < V_{TURN-ON}$

$$R_{SH} = \frac{Z_0 + A}{2} - B \quad \text{WHERE } B = +\sqrt{\left(\frac{Z_0 - A}{2}\right)^2 + \frac{V_F}{I_F}(R_{DC} + Z_0)}$$

$$R_{PH} = \frac{Z_0 - A}{2} + B \quad A = \left(\frac{E_T}{I_F} - R_{DC}\right) \quad \text{CHECK: } R_{SH} + R_{PH} \stackrel{?}{=} Z_0$$

CASE 3: $(dV_L/dI_L) = Z_0$ FOR $V_L > V_{TURN-ON}$

$$R_{SH} = Z_0 \quad R_{PH} = \frac{V_F}{\frac{E_T - V_F}{R_{DC} + Z_0} - I_F} \quad \text{CHECK: } R_{SH} \stackrel{?}{=} Z_0$$

$$\text{CHECK FOR } I_F, \text{ ALL CASES: } I_F = \frac{E_T - V_F}{R_{DC} + R_{SH}} - \frac{V_F}{R_{PH}}$$

Fig. 1—Approximate load matching for HT circuits. Dynamic resistance of the terminating circuit ($\partial V_L / \partial I_L$) changes as the optoisolator switches ON. These three cases are calculated differently as shown.

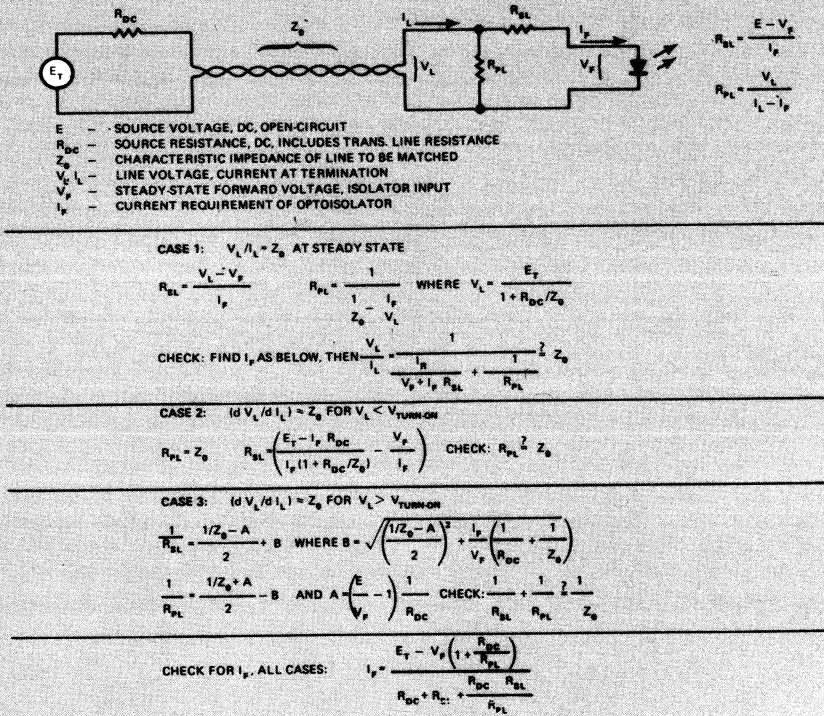


Fig. 2—Approximate load-matching LT circuit design formulas. After calculating series and parallel resistances, select the closest standard values and check I_F with these values to determine if the practical circuit is satisfactory.

for I_F . The dynamic resistance of the termination changes as the isolator input diode goes from OFF to ON. To satisfy Objective 3 (approximate load matching), we must consider three cases produced by this change of dynamic resistance of the termination:

CASE 1: $V_L/I_L = Z_0$. The reflection coefficient, which is the ratio of voltage in the reflected wave to the incident wave, changes from positive to negative as the input diode turns ON. This is the best choice for a back-matched driver or one of unknown reflection coefficient; and though it may permit oscillatory reflections, they will be of low amplitude. That's not bad, considering it's the easiest termination to design.

CASE 2: $\partial V_L / \partial I_L \leq Z_0$. The reflection coefficient changes from zero to negative as the input diode turns ON. This permits a larger reflection than CASE 1, but prevents oscillatory reflection for a driver with $R_k < Z_0$.

CASE 3: $\partial V_L / \partial I_L \geq Z_0$. Reflection coefficient changes from positive to zero as the input diode turns ON. This permits a larger reflection than CASE 1, but prevents oscillatory reflection for a driver with $R_k > Z_0$.

An HT or an LT circuit can satisfy these three conditions. The expressions for selecting R_{SH} and R_{PH} for the HT circuit are given in Fig. 1; the expressions for R_{PL} and R_{SL} for the LT circuit, in Fig. 2.

For CASE 1, the design expressions that result from the circuit equations are as follows.

For the HT circuit:

$$R_{SH} = \frac{(V_L - V_F)}{I_L} \quad (1)$$

$$R_{PH} = \frac{V_F}{(I_L - I_F)}$$

For the LT circuit:

$$R_{SL} = \frac{(V_L - V_F)}{I_F} \quad (2)$$

$$R_{PL} = \frac{V_L}{(I_L - I_F)}$$

V_L and I_L have the values resulting when a resistor whose value is Z_0 is connected to the source (including cable) whose characteristics are determined as in Fig. 7 of Part 1:

$$V_L = E_T \left(1 + \frac{E_T}{I_N Z_0} \right)^{-1} \quad (3)$$

$$I_L = \left(\frac{E_T}{Z_0} \right) \left(1 + \frac{E_T}{I_N Z_0} \right)^{-1}$$

E_T and I_N are measured for the logic state that turns the isolator input diode ON, so $E_T = E(1)$; the assumption is that $E(0)$ is low enough to produce turnoff.

For CASE 2 and CASE 3, the design expressions

result from the assumption that the dynamic resistance of the isolator input diode is infinite below turn-on and a short-circuit above turn-on. Applying this condition to the circuit equations yields the following relations:

For the HT circuit:

$$\left(\frac{E_T - V_F}{I_N + R_{SH}} \right) - \frac{V_F}{R_{PH}} = I_F$$

CASE 2: $R_{SH} + R_{PH} = Z_0$ (4)

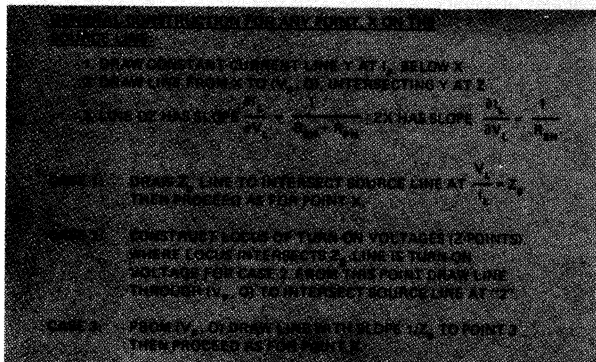
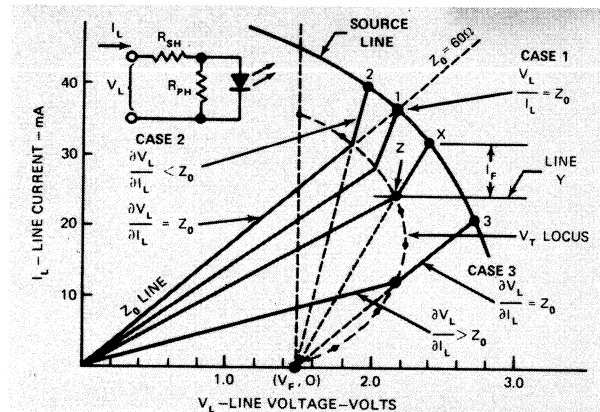


Fig. 3—Graphical construction procedure for an HT circuit with a nonlinear source.

CASE 3: $R_{SH} = Z_0$

For the LT circuit:

$$\left(\frac{I_N - I_F}{\left(\frac{I_N}{E_T} + \frac{1}{R_{PL}} \right)} \right) - (I_F R_{SL}) = V_F$$

Case 2: $R_{PL} = Z_0$ (5)

CASE 3: $\frac{1}{R_{PL}} + \frac{1}{R_{SL}} = \frac{1}{Z_0}$

E_T and I_N are described earlier for Eq. 3. Figs. 1 and 2 summarize HT and LT circuit design formulas, approximate matching and steady-state requirements.

Graphical solutions for load matching are the only practical, handy tools available to design with nonlinear sources. Even with linear sources, there's an advantage to working with graphical solutions—they literally make the design tradeoffs clearly visible! (For further design of load-match terminations, refer to Fig. 3 of Part 2 and Fig. 3 of this article).

Consider the HT vs. LT circuit

So you've decided the 2-resistor termination is for your line receiver, have you? Well, you still must make one more decision: High Threshold vs. the Low Threshold circuit. Consider the advantages of both before making your choice.

In general, HT and LT circuits have the same relative merits, respectively, as the parallel and series 1-resistor terminations, and for the same reason. The HT circuit is faster, but more vulnerable to driver variations and resistor tolerances. Thus it's not suitable for busing.

If you want to go the bus route, be advised that busing with the LT circuit is possible within the limits of available current from the driver. When busing n isolators, obtain the values of R_{PL} and R_{SL} . How? Simply substitute $n \times I_F$ for I_F in the formulas of Fig. 2, or the graphical construction of Fig. 4. Then, in series

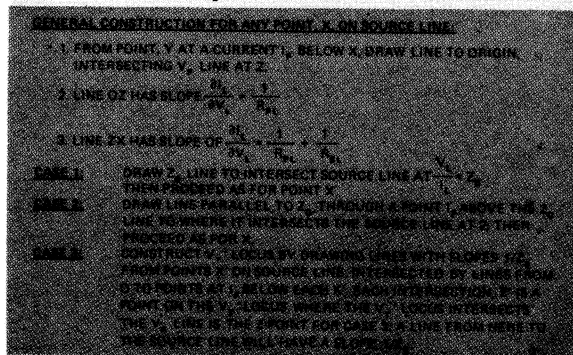
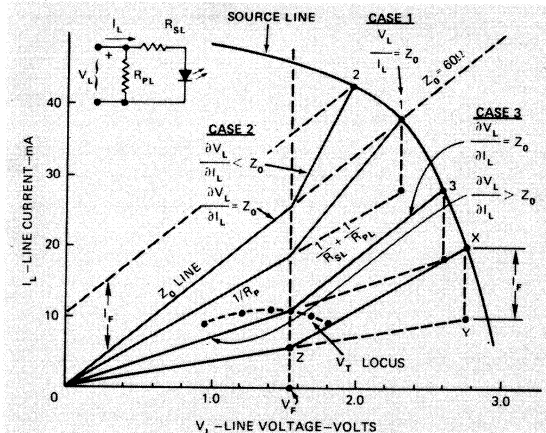


Fig. 4—Graphical construction procedure for a LT circuit with a nonlinear source.

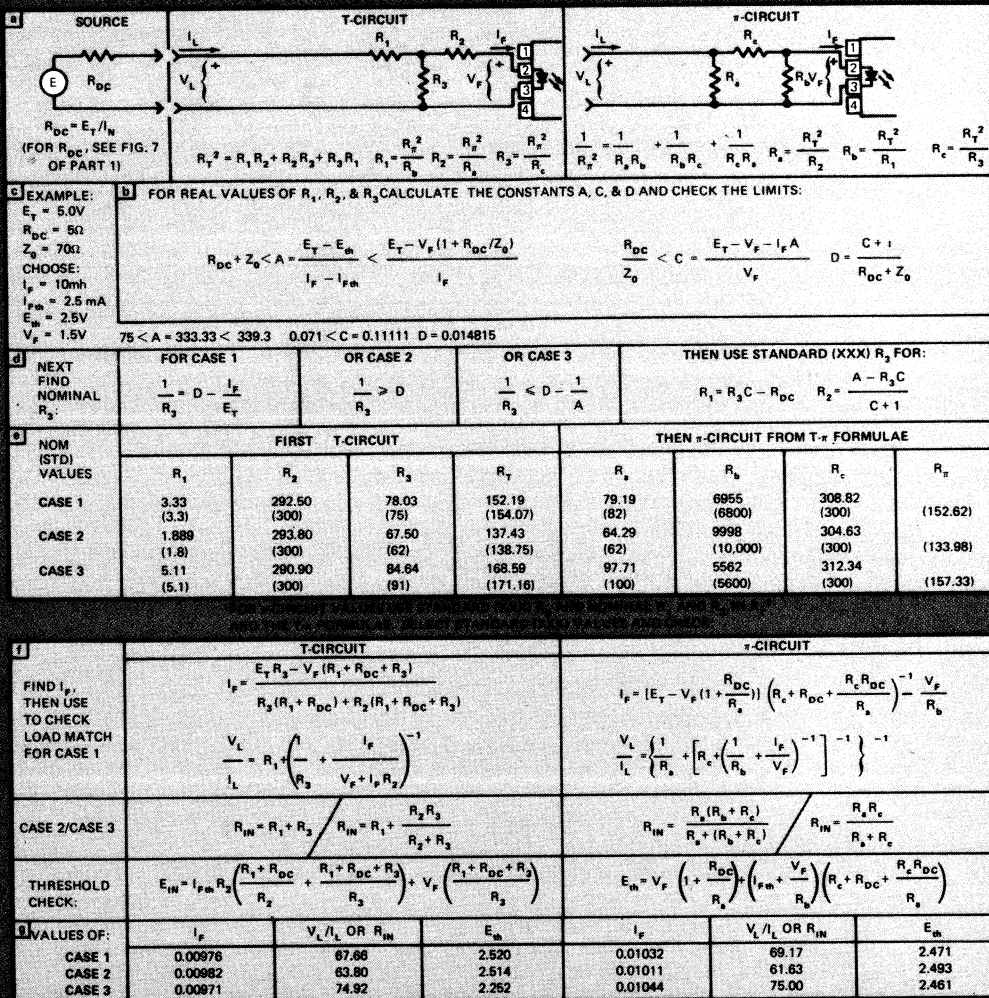


Fig. 5—This 3-resistor termination design procedure calculates the T-circuit first, then converts to π -values (a) and determines which set of nominal values are closest to standard resistors. First, calculate 'A', 'C' and 'D' and be sure they fall within the limits (b) as demonstrated by the example (c). Second, calculate R_2

and then solve for both R_1 , R_2 (d) and R_T , as in the example (e). Fourth, convert to the π -circuit. Finally, select standard resistor values and check I_F , V_L/I_L and E_{th} for the three cases (f) as in the example (g).

with each isolator input use $n \times R_{SL}$, where R_{SL} is the value obtained by making the $n \times I_F$ substitution. Finally, connect a single R_{PL} (serving the n isolators) across the line.

If you're lucky, the current (I_F) required by the isolator will be such a small fraction of the current available that busing can be done without making any resistor value adjustment. If so, fine.

For current-loop designs, neither the HT nor the LT circuit is very good and the parallel 1-resistor circuit described earlier must be used. If this won't meet the objectives of your line and receiver, then consider using active or 3-resistor terminations.

Believe me, three is best

As we saw earlier, 2-resistor terminations can

handle Objectives 1 and 2 or Objectives 1 and 3. Yes, in special situations (wonder of wonders!) it just *might* happen that a 2-resistor termination could meet all three objectives—but don't count on it. As a rule of thumb, it takes a 3-resistor termination to meet all three objectives.

Fig. 5 shows the circuit to be used and expressions for computing the nominal resistor values. The basic expressions are given only for the T-circuit because those for the π -circuit are unwieldy. Since the T and π -circuits are electrically identical, the T- π transformation can be used to obtain nominal π -circuit resistance values that may be closer to standard ones than the nominal values computed for the T circuit. Then the π -T transformation can be used to check the design.

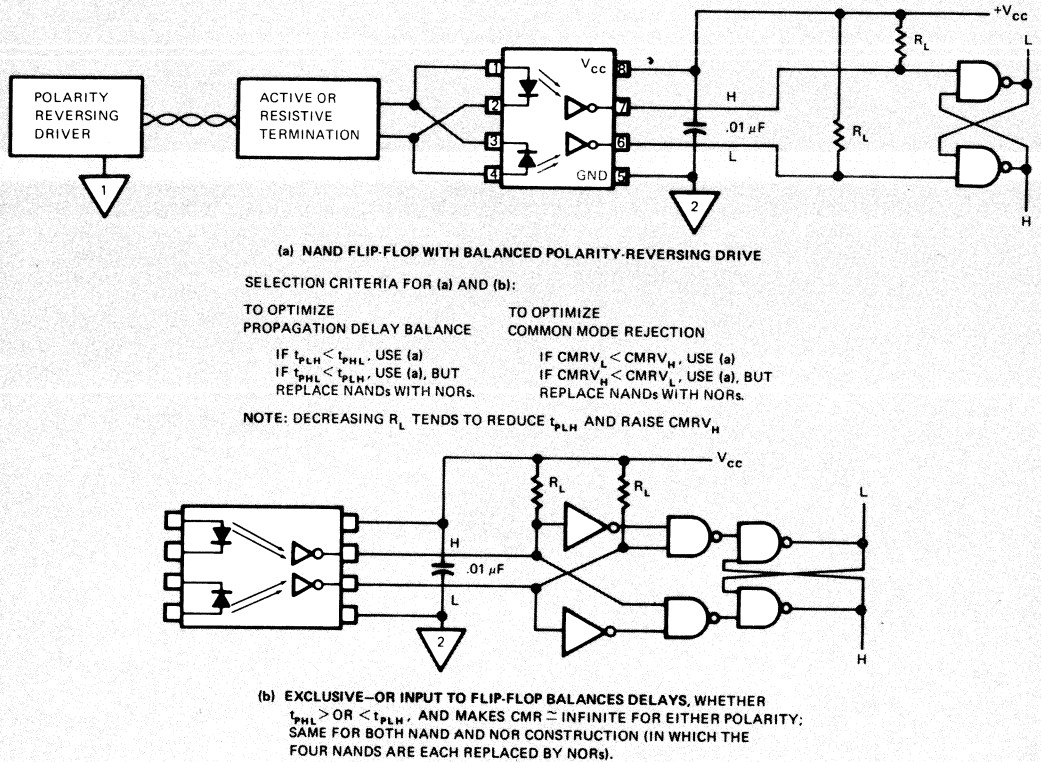


Fig. 6—Balanced resistive terminations can enhance both common-mode rejection (CMR) and propagation delay balance, as well as make threshold adjustment unnecessary. Whenever polarity-reversing drive is employed, the anti-parallel LED used

(Fig. 2) may be replaced by the input diode of a second (identical) optoisolator to enhance common-mode rejection, balance propagation delay and make threshold adjustment unnecessary.

With respect to threshold and steady-state requirements, the values of R_1 and R_2 in terms of R_3 are found by solving the pair of simultaneous equations obtained by substituting E_{th} for E_T and I_{Fth} for I_F in the circuit equation:

$$\frac{[E_T - (V_F + I_F R_2)]}{(R_1 + R_{DC})} = \frac{(V_F + I_F R_2)}{R_3 + I_F} \quad (6)$$

where E_T and R_{DC} are found as in Fig. 7 of Part 1. Then, for load matching, obtain R_3 by applying the conditions for CASE 1, CASE 2 or CASE 3. For CASE 1:

$$\left(\frac{V_L}{I_L}\right) = Z_0 = R_1 + \left[\frac{I_F}{(V_F + I_F R_2)} + \frac{1}{R_3}\right]^{-1} \quad (7)$$

$$\left(\frac{\partial V_L}{\partial I_L}\right)_{(OFF)} = R_1 + R_3 \leq Z_0 \quad (8)$$

$$\left(\frac{\partial V_L}{\partial I_L}\right)_{(ON)} = R_1 + \frac{R_2 R_3}{(R_2 + R_3)} \geq Z_0 \quad (9)$$

Why not use a dual optoisolator?

Referring back to Fig. 2 of Part 2, we see an anti-

parallel LED across the optoisolator. We recommend the LED whenever polarity-reversing drive is used to protect the isolator from excessive reverse bias. However, a superior alternative is to use the input diode of a second identical isolator. In such a design, the two isolators will have balanced, split-phase input currents when a balanced polarity-reversing driver is used. Connect the outputs shown in Fig. 6 using a NAND (or NOR) flip-flop.

Since the 2-isolator termination is more complex, is it really worth it? A casual look reveals several impressive benefits. Assuming that the isolators are similar, with this design it's unnecessary to perform threshold adjustment to obtain balanced delays. Of course, threshold adjustment may still be worth considering simply to reduce both HL and LH delays. Properly choosing R_L according to the criteria in the figure will give your design the best of two worlds by optimizing both delay balance and CMR. That's a bargain!

Limitations of resistive terminations

A resistive-termination design is simple and economical. But, ah yes, ever since Pandora opened

her box, all good things have had their shortcomings. Resistive terminations have their share of curses, so before you decide they're for your system, know the limitations.

To start, consider the narrow range of applicability—for example, one driver or one cable of fixed length. And when variations among different drivers of the same type number start causing deviations from desired operating levels, you're in trouble. Resistor adjustments then become necessary, slowing down production and increasing the chances for error. The same goes for variations in the length and type of cable.

Worst of all, if the driver characteristics or line resistance ever change from your design values—it makes no difference if the changes are due to changes in production, operating environment or a field change—and you forget just once to adjust the resistor values, any of four curses will plague your system:

1. The receiver will sit inactive when input current drops too low;
2. Or, too much input current will degrade the CTR and send the optoisolator to an early grave;
3. Delays will become more excessively unbalanced or, if a balanced 2-isolator termination

is used, the delays, though balanced, may make your system crawl in slow motion;

4. Those reflections that never affected your longer line may become a scourge when a shorter line is substituted, perhaps years later in a design change.

The only advantages to resistive terminations are freedom from overkill—simplicity and low cost. When you need transmission system flexibility, the best solution is an active termination. □

References

1. Sorensen, H., "Optoisolator developments are making your design chores simpler," EDN, Dec. 20, 1973, pp. 36-44.
2. *Optoelectronics Designer's Catalog*, Hewlett-Packard.

The fourth article in this 5-part series explores when to use active terminations and explains how to design them. It also will cover CMR enhancement.

Designer's Guide to: Optoisolators — Part 4

When terminating resistors cannot meet data line requirements, use an active termination. Optimizing CMR enhances system performance.

Active terminations provide many advantages over terminating resistors. Active types regulate the isolator input current with an active element and a feedback path. Because of this, they can adapt the isolator input to driver and transmission line conditions—even when these conditions vary over a broad range.

This article will first address the termination needs when environmental conditions render resistive terminations inadequate. Then we will

review how common-mode signals degrade system performance and discuss some methods for enhancing common-mode rejection.

Do you really need an active termination?

The process of choosing between a resistive termination and an active one should be made only after examining system constraints. If the driver, line and isolator will not suffer from wide variations in their characteristics, then resistive

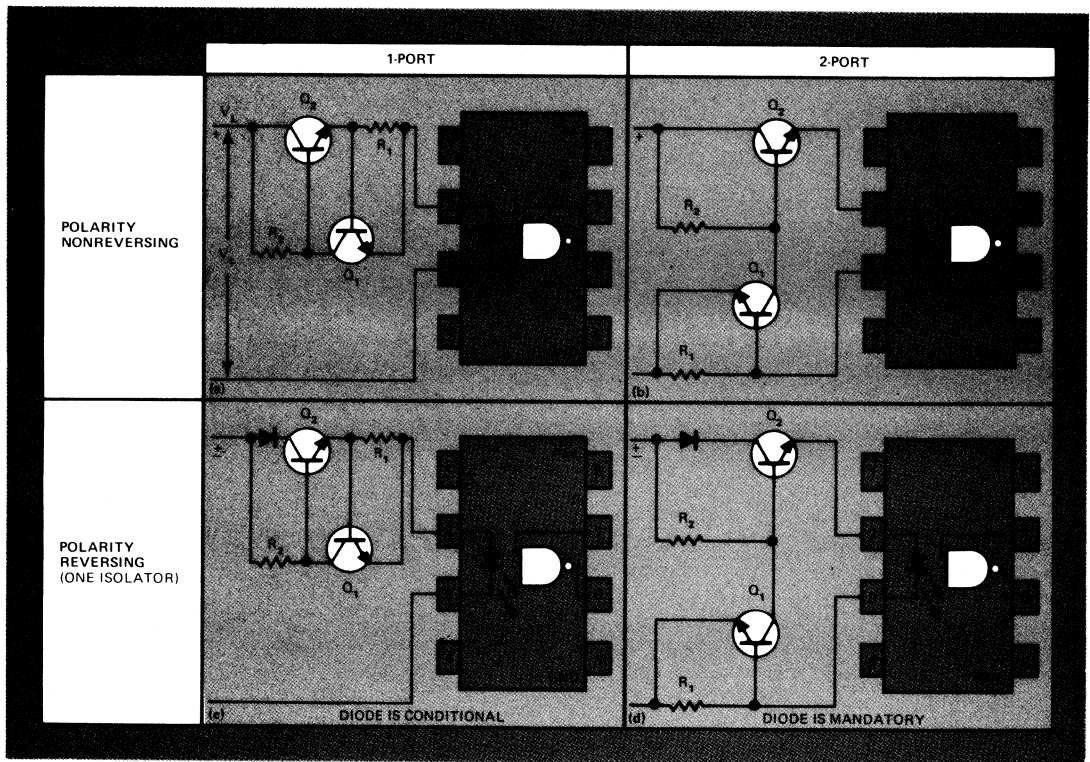


Fig. 1—Current-clamp regulators regulate current flow with a series pass transistor, Q_2 , which receives self-biasing current through R_2 . With increasing current, the emitter-base voltage on Q_1 increases, causing Q_1 to remove base current from Q_2 .

The 2-port regulators shunt the incremental current increase across the isolator input and offer improved regulation over that of the one-ports.

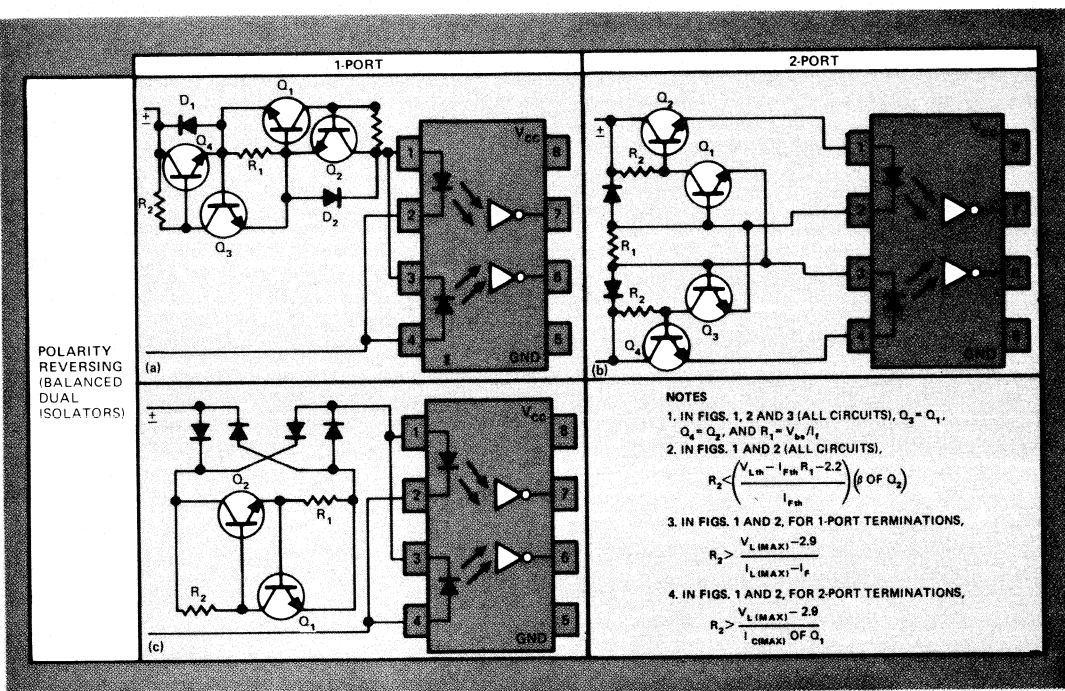


Fig. 2—Balanced dual-isolator, current-clamp regulators provide load balancing when a polarity-reversing driver is used. The 1-port termination (a) is merely a combination of two simple one-ports of Fig. 1a, but with a common R_1 . The

two-port is, likewise, made of two simple two-ports of Fig. 1b. Bridge regulator (c) is a 1-port regulator of Fig. 1a across the diode bridge.

terminations provide the most cost-effective solution. Active terminations should be used in the following situations:

- Busing, where changing the number of stations influences the current available to the termination.
- Power supply fluctuations at the driver.
- Changing the length of transmission line, where line resistance is a significant part of the source resistance.
- Temperature changes on long lines ($\Delta R/R \approx 0.4\%/^{\circ}\text{C}$ for copper wire).
- Design flexibility requiring the same termination to be operated by any of several types of drivers.
- Data rate enhancement when a long or lossy line degrades the rise time at the termination.
- Mismatch reflections causing excessive variation in terminal voltage/current.

Although active terminations require higher terminal voltage and data rate for very short, low-loss lines, and cost more, your only concern in an active termination design is proper steady-state ON current. Threshold adjustment becomes unnecessary, since with a voltage-clamp regulator the threshold is lower than for a resistive termination. Load matching can also be neglected

because terminal voltage or current variations produced by reflections are attenuated at the regulator, leaving the isolator unaffected. And where reflections must be controlled, a series or shunt resistor added to the active termination will do the trick.

Basically, active terminations fall into two categories: current and voltage-clamp regulators. Both circuits perform current regulation, but the current-clamp regulators let the line voltage rise, while the voltage-clamp regulators allow the line current to rise.

Current regulators provide high dynamic Z

Current-clamp regulators are series-pass circuits. Figs. 1 a-d and 2 a-c show seven different current-clamp regulators. Of these, the first two (Fig. 1a and b) show most clearly the basic principles on which the other five are based.

The one-port regulator of Fig. 1a consists of a series-pass transistor (Q_2), a self-biasing resistor (R_2) and a feedback resistor (R_1). With minimal voltage, Q_2 conducts, receiving base current through R_2 . As line voltage rises to $V_F + 2V_{be} \approx 2.9\text{V}$, line current becomes high enough so that the voltage drop across R_1 turns Q_1 ON. This, in turn, limits base current to Q_2 by bypassing much of

the current through Q_1 . As line voltage rises above 2.9V, only a slight increase in current occurs, depending on the value of R_2 . Therefore, line (isolator) current is fairly well regulated at V_{be}/R_1 .

The current-clamp circuit of **Fig. 1a** has no problem handling reverse-polarity line drivers—providing, of course, that reverse voltage doesn't exceed the reverse breakdown voltage of the isolator input diode. Should this possibility exist, connect a diode with adequate breakdown voltage in series with the input termination (**Fig. 1c**). Note, however, that in the 2-port polarity-reversing current-clamp regulator of **Fig. 1d**, the series diode is mandatory.

Compared to the one-port, the two-port (**Fig. 1b**) provides better current regulation. When the line rises above 2.9V, the additional increment of line current ($\Delta V_L/R_2$) is bypassed around the isolator rather than through it as in the one-port. R_2 can be a lower value in a 2-port circuit, thus providing a faster response time. For data rate enhancement, two peaking capacitors are needed—one from the collector to emitter of Q_2 and another across R_1 .

A 2-way road needs a dual regulator

A balanced dual-isolator termination must be regulated in both directions. This can be accomplished by connecting two isolators in opposite phase (**Fig. 2**) to provide both load balancing and split-phase outputs to improve common-mode rejection.

If the line voltage amplitude is marginal, it's best to connect two regulators into an anti-parallel configuration to feed the anti-parallel-connected input diodes of two isolators (not shown). However, if ample line current is available, use the regulators of **Fig. 2a** or **b**. Since these paired regulators share feedback resistor R_1 , component count is slightly reduced. However, the operating voltage is now higher by one additional V_{be} .

As shown in **Fig. 2c**, a bridge rectifier further reduces component count by using one current-clamp regulator. However, operating voltage is higher by 2 V_{be} than that required by previously discussed current-clamp regulators.

Because current-clamp circuits present a high dynamic load resistance, they are better than voltage-clamp types if the line driver has a

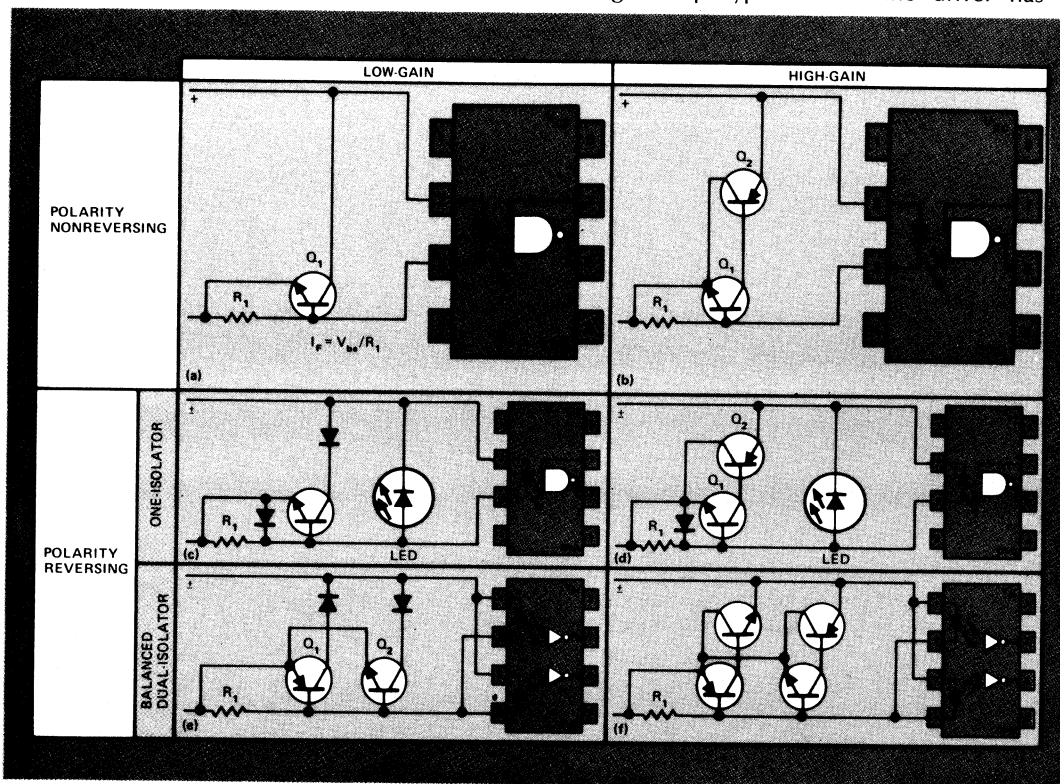


Fig. 3—Voltage-clamp regulators are generally better than current-clamp because of lower turn-ON voltage. The shunt-type regulator maintains constant voltage by conducting more heavily, shunting the excess current across the line. The

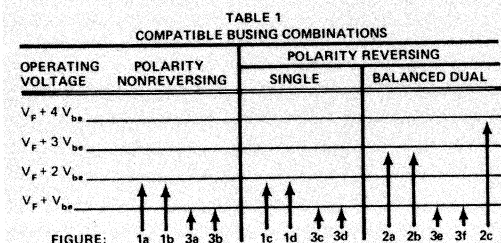
high-gain circuits on the right provide better regulation than the low-gain terminations. One-isolator circuits (**c** and **d**) use an anti-parallel LED to protect the isolator photodiode from excess reverse voltage.

positive reflection coefficient. As it turns out, such a high-impedance driver makes a low-speed system anyway, and, therefore, response speed is unimportant.

When you need a high-speed regulator...

Of all active terminating circuits, voltage-clamp regulators (Fig. 3) are generally better than the current-clamp variety. This is because turn-ON occurs at a lower line voltage of $V_L = V_F$, rather than $V_L = V_F + V_{be}$ or more, as required by series-clamp circuits.

As shown in Fig. 3a, the termination begins conducting when line voltage exceeds $V_F \approx 1.5V$. As line current increases beyond V_F , the isolator input current rises until the voltage drop across R_1 is high enough to activate Q_1 , which then shunts additional increments of line current, clamps the line voltage at $V_F + V_{be} \approx 2.2V$, and regulates the isolator input current at $I_F = V_{be}/R_1$.



Actually, as line current rises above I_F , some slight increase in line voltage and isolator current will occur, depending on the β of Q_1 . However, if this slight increase in line voltage causes inadequate regulation of I_F , the high-gain circuit of Fig. 3b should be used. The latter also turns ON at V_F and clamps at $V_F + V_{be}$, but, because of higher gain, regulates better.

With its lower turn-ON voltage, a voltage-clamp regulator performs better than a current-clamp regulator in high-speed operation—and it's not necessary to use a high-speed transistor. Paradoxically, a slow transistor actually permits faster switching. This is because the slower transistor allows a current peak to enter the isolator input until the transistor comes on and regulates the current. These current peaks, of course, must not exceed the maximum ratings of the isolator input diode.

Operation of the reversing, 1-isolator system of Fig. 3c and d is the same, except in reverse polarity. At this instant, current flows through the LED, thus keeping the reverse-polarity line voltage at a safe level. The collector diode of Fig. 3c prevents Q_1 from turning ON in reverse. In Fig. 3d, this function is performed by the base-emitter

junction of the pnp transistor.

If reverse-polarity line current exceeds the maximum rating of the LED, you should use the circuits of Fig. 3e and f, substituting a LED for the input of the second isolator. The current in the substitute LED will, of course, be regulated as would the input current of the second isolator.

The previously mentioned active terminations provide good design flexibility when busing enters the picture. Table 1 shows combinations directly compatible and modifications that permit other busing combinations. The only limit on the number of terminations is set by available line current and voltage.

At this point, let's look at a problem that has given more than one designer many a sleepless night.

How to murder a signal

If your data transmission-line prototype is connected and running, and all your module receives is spurious garbage, common-mode voltage could be the culprit. The differential-mode signal could be drowning in a sea of noise.

Eliminating the effects of common-mode signals is a major task confronting all designers of data transmission lines.

Common-mode interference is sometimes inherent in the system design. More often than not, though, it is incidental. Examples of inherent common-mode signals include:

- Floating equipment with its common point offset from ambient ground. The offset is the common-mode voltage, being common to all points in the floating unit with respect to ambient ground.
- Equipment having a line noise filter. The capacitors in the filter place the chassis at a potential somewhere between the potential of each power line. With one side of the power line at ambient ground (e.g. 115V line), the chassis is offset by approximately 58V. Even if power line voltages are balanced to ground (e.g. 220V line), filter capacitors may not be balanced, thus causing an offset.

Examples of incidental common-mode signals include:

- Offset current coupled through interwinding capacitance of a power transformer.
- Electro-magnetically induced (EMI) interference coupled from equipment or adjacent lines.
- Offset voltages caused by flow of ground-loop currents in the interconnecting wires between modules.

Common-mode voltage in a data transmission system is measured with respect to the common point of the receiving unit's output circuit. The

isolator input diode draws current and produces photons only in response to the differential mode signal. Unfortunately, another effect enters the picture—common-mode capacitance, C_{CM} , which capacitively couples the common-mode signal, e_{CM} , to the base of the output amplifier proportionately to the current flowing in C_{CM} , or: $i_{CM} = C_{CM} (de_{CM}/dt)$.

Too steep an edge means trouble...

Common-mode rejection (CMR) properties of the isolator are given as rate of change of e_{CM} and

maximum tolerable rate of change determines the CMR property. It is given in either CMRV or CMTR.

Common-mode rejection voltage (CMRV) is the maximum tolerable common-mode ac voltage. But beware of CMRV specs given for only a single frequency, as this invariably gives a false impression of the CMR property. As a function of frequency, CMRV has a slope of -1 on log-log scales, continuing to the cutoff frequency of the output transistor (or amplifier). Beyond the cutoff frequency, the CMRV curve assumes a positive slope.

Common-mode transient rejection (CMTR) describes the maximum tolerable rate of rise (or fall) of transient changes in common-mode voltage and is usually given in volts per microsecond. Positive-going transients tend to turn the output ON when it should be OFF, while negative-going transients tend to turn the output OFF when it should remain ON.

Once again, a false impression of the CMTR property results if CMTR is provided for only one condition of transient amplitude (or duration). The reason is that an arbitrarily high rate of rise (or fall) can be tolerated for a sufficiently small amplitude (or short duration). A curve of $\partial e_{CM}/\partial t$ vs. e_{CM} (for both negative and positive transient slopes) provides a complete description of CMTR.

Tools for enhancing CMR

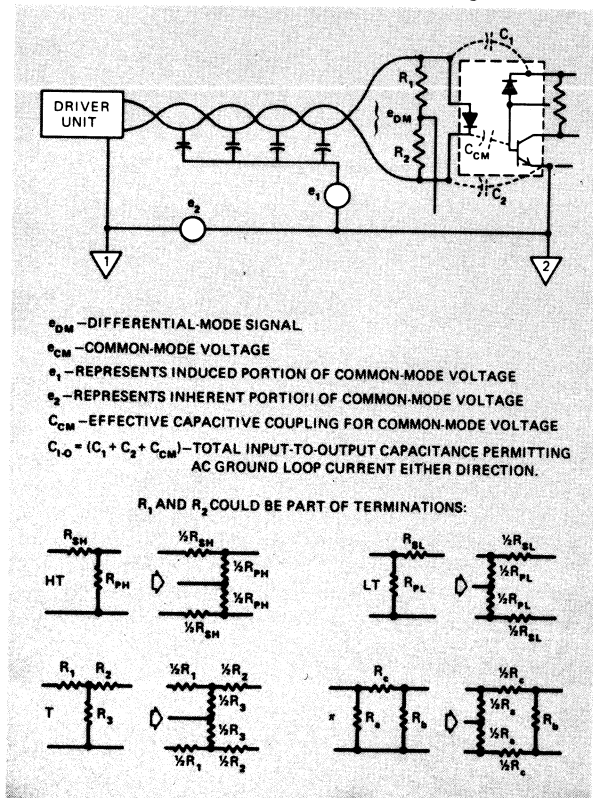
Methods of reducing the effects of EMI include using a twisted-pair line, a shield, good pc-board layout and "trick" circuits.

A **twisted-pair line** reduces common-mode voltage by balanced coupling. When e_1 is not coupled equally to both sides of the line, the net unbalance appears as a differential mode signal, as shown in Fig. 4. A twisted line pair helps to equalize the coupling of both electric and magnetic EMI. Also, balancing the impedance of each wire to Ground 1 further equalizes coupling.

A **shield**, unlike the twisted pair, does not balance coupling; instead, it reduces the net unbalance of the coupling e_1 to the lines.

Where would you connect the shield? To Ground 1? If so, you've just made a common mistake. Unfortunately, this won't protect your system, since connecting the shield to Ground 1 is good practice **ONLY** if the internal impedance to Ground 1 is the same at both output terminals. But since these internal impedances are usually unbalanced, it is a better idea to let the shield float. If not—and if internal impedances are sufficiently unbalanced—a shield connection to Ground 1 may prove worse than no shield at all! So, where should you connect the shield?

To reduce the effects of e_1 , the **BEST** place to



influence the output. As we know, the output should be at a logic HIGH when the differential mode signal, e_{DM} , is in the OFF state, and at a logic LOW when e_{DM} is ON. For each of these two states, a maximum tolerable rate of change of the common-mode signal exists, which, if exceeded, may cause trouble in the form of excessive deviation in the output logic state voltage. This

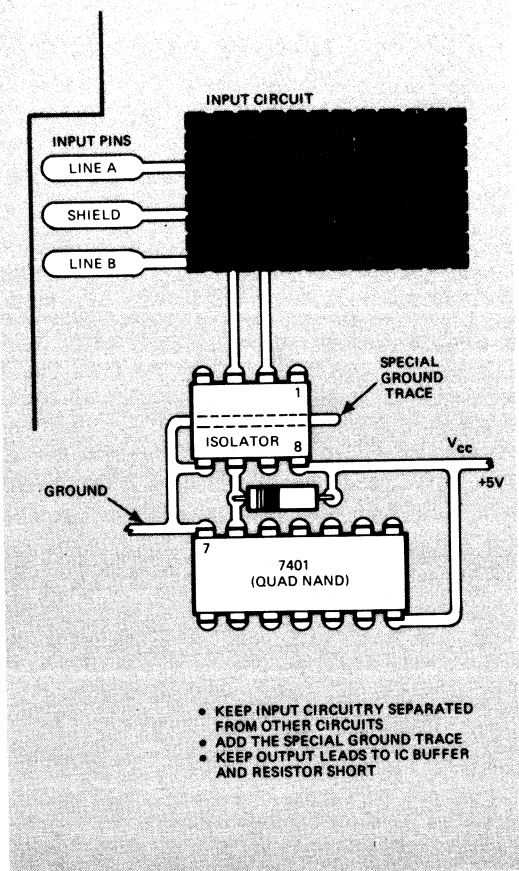


Fig. 5—Circuit board layout can raise common-mode rejection. Input circuitry, obviously, should be separated from all other circuitry. Capacitive coupling between input diode and the transistor base can be lessened by running a ground trace beneath the input and output pins. And, of course, output leads to the IC buffer and resistor should be kept short.

connect the shield is at Ground 2. However, if e_2 is a very high voltage, a shield connected to Ground 2 while the line inside is referred to Ground 1 can cause insulation failure. If e_2 is a high dc voltage, the benefit of a Ground 2 shield connection can be obtained without the insulation-failure hazard by connecting the shield to Ground 2 via a capacitor with a suitable voltage rating.

The NEXT-to-BEST point for shield connection is a tap on a resistance across the line, such as the junction of R_1 and R_2 in Fig. 4. R_1 and R_2 may be part of a resistive termination; such line-to-line resistance may be added to an active termination without disrupting its function—providing the

resistance is high enough. Usually R_1 and R_2 will be of equal value, but if the common-mode interference coupling is unbalanced, adjust the tap on the resistance ($R_1 + R_2$) to the point at which e_{CM} is smallest.

The following list ranks shield terminations in the above order of their effectiveness against EMI:

BEST

- To Gnd 2 (but may pose insulation hazard).
- To junction of R_1 and R_2 adjusted for minimum e_{CM} .
- To Gnd 1 with balanced source impedance.

MOST PRACTICAL

- To nothing—floating (not connected, either end).
- To junction of $R_1 = R_2$.

WORST

- To Gnd 1 with unbalanced source impedance.

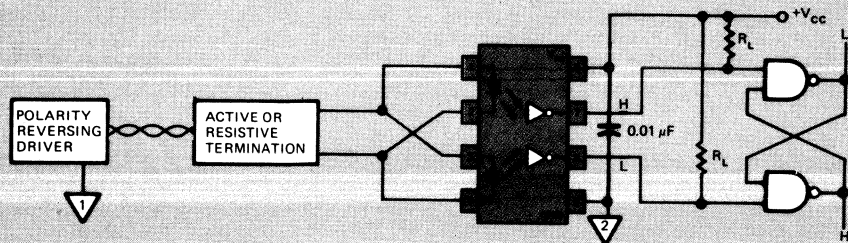
A good board layout is a must. The effect of common-mode voltage (e_{CM}) can be reduced by good layout of the circuit board, as shown in Fig. 5. Position all input circuitry as far as possible from all output circuitry. A ground trace between the isolator pin rows helps to direct electric coupling away from the output of the isolator. This ground trace forms a capacitive coupling parallel to C_{CM} and terminates on output ground rather than on the isolator output circuit.

Running a piece of wire across the isolator parallel to the pin rows, connected to output ground at each end, also helps (for the same reason). Last of all, if insulation “creep” distance is critical, insulated wire can be used instead of a ground trace.

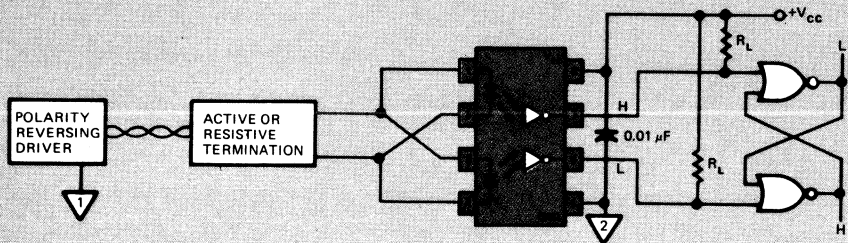
Try a trick or two

With an isolator having a single-stage amplifier (transistor or phototransistor) operated with the emitter grounded, the C_{CM} coupling can be neutralized. This trick requires a neutralizing capacitor, C_N , from the input side (anode, cathode or common point) to the collector pin. As seen in Fig. 4, the collector current resulting from e_{CM} will be $-\beta C_{CM}(de_{CM}/dt)$, while the current into the collector from the neutralizing capacitor will be $+C_N(de_{CN}/dt)$. Perfect neutralization requires $C_N = \beta C_{CM}$. But, as far as CMR is concerned, approximate neutralization is better than none.

There are other concerns. Adding C_N increases the ac ground-loop current and the insulation of C_N must withstand e_{CM} . If the required value of C_N is small enough, a gimmick can be used. (“Gimmick” is the old-timer’s term for a capacitor formed by twisting together two pieces of insulated wire.) Neutralization works best with polarity nonreversing drive, especially if the input diode is prebiased. If polarity reversing drive is used,



(a) NAND FLIP-FLOP WITH BALANCED POLARITY-REVERSING DRIVE



(b) NOR FLIP-FLOP WITH BALANCED POLARITY-REVERSING DRIVE

SELECTION CRITERIA FOR (a) AND (b):

TO OPTIMIZE

PROPAGATION DELAY BALANCE

USE (a) IF $t_{PLH} < t_{PHL}$

USE (b) IF $t_{PHL} < t_{PLH}$

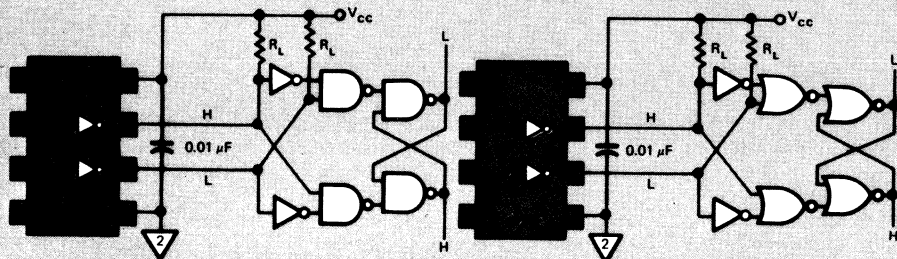
TO OPTIMIZE

COMMON-MODE REJECTION

USE (a) IF $CMR_{VL} < CMR_{VH}$

USE (b) IF $CMR_{VH} < CMR_{VL}$

NOTE: DECREASING R_L TENDS TO REDUCE t_{PLH} AND RAISE CMR_{VH}



(c) EXCLUSIVE-OR INPUT TO FLIP-FLOP BALANCES DELAYS, WHETHER $t_{PHL} > \text{OR} < t_{PLH}$, AND MAKES CMR \approx INFINITE FOR EITHER POLARITY; SAME FOR BOTH NOR AND NAND CONSTRUCTION.

Fig. 6—Output circuit techniques for CMR enhancement. Use (a) or (b) if isolator properties and/or common mode transient polarities are known. Use (c) for infinite CMR and inherently balanced delays.

other circuit tricks must be considered.

Circuit "tricks" in the output circuit can raise the CMR. They are based on the fact that CMRV and CMTR of the isolator are higher when the output is in the logic LOW state. All such circuits require a pair of isolators driven in split phase, such as with a reversing-polarity driver.

When a NOR-gate R-S flip-flop (Fig. 6b) has been triggered by a logic HIGH at one of its inputs, then the outputs (both of them) are immune to any subsequent changes. Since the isolator is more likely to hold a LOW in the face of interference, the NOR-gate flip-flop enhances the CMR of such a pair. This is true because common-mode transients produce output tran-

sients of the same phase on each side, whereas a flip-flop requires opposite-phase inputs. As a result, these opposite-phase inputs occur only in response to the desired differential-mode signal.

Another benefit of using a flip-flop output is that the delay times to logic HIGH and to logic LOW are equalized to the extent that both isolators have the same t_{PLH} . Given two isolators with the same drive conditions, it's more likely that t_{PLH} (of #1) = t_{PLH} (of #2) than it is that t_{PLH} = t_{PHL} of either of them.

The choice of NAND or NOR construction (Fig. 6) depends on the propagation delay and CMR properties of the isolator, along with the input requirements of R-S flip-flops. In a NAND flip-

flop, simultaneous HIGH inputs are of no concern. However simultaneous LOW inputs will drive both inputs HIGH, a condition to be avoided. Conversely, in a NOR flip-flop, simultaneous LOW inputs are tolerable, while simultaneous HIGH inputs drive both outputs LOW and should be avoided. With a balanced dual-isolator termination, if $t_{PLH} < t_{PHL}$, the NAND flip-flop should be used, with propagating delays balanced at t_{PHL} . This is because the isolator outputs cannot be simultaneously LOW. If $t_{PHL} < t_{PLH}$, the isolator outputs cannot be simultaneously HIGH, so the NOR flip-flop should be used and propagation delays balanced at t_{PLH} .

A final word on common-mode rejection

The isolator outputs will be simultaneously HIGH if $e_{CM} > CMRV_L$ and simultaneously LOW if $e_{CM} > CMRV_H$. For isolators with $CMRV_L < CMRV_H$, the NAND flip-flop is preferred because it can tolerate the simultaneous HIGH's occurring at $e_{CM} > CMRV_L$. Should e_{CM} exceed $CMRV_H$, the resulting simultaneous LOW's at the NAND flip-flop inputs will drive both outputs HIGH. However, when e_{CM} drops, they will return to the proper states as required by the differential mode signal on the transmission line. As might be expected, the improper logic state caused by a common-mode transient is only momentary.

For isolators with $CMRV_H < CMRV_L$, a NOR flip-flop is better (except for polarity). The reason is the same as before, since the improper logic state resulting from excessive e_{CM} is momentary.

These momentary improper logic states can be prevented by adding exclusive-OR logic to the inputs of the flip-flop as shown in **Fig. 6c**. Moreover, the exclusive-OR-ed flip-flop will automatically balance propagation delays. As far as CMR and delay balance are concerned, it makes absolutely no difference whether NOR or NAND gates are used. Keep in mind that if a NAND flip-flop is used, the exclusive-OR-ing must be done with NAND gates; and for a NOR flip-flop, with NOR gates. □

The next and final article will explore data rate enhancement and multiplexing.

Reference

1. Sorensen, Hans, "Opto-isolator developments are making your design chores simpler," *EDN*, December 20, 1973.

Designer's Guide to: Optoisolators — Part 5

Here are several powerful techniques that increase data rates and open new horizons in multiplexing. How many can you use?

When data rate is slower that it should be, the culprit can be the driver, the transmission line or the receiver. Generally, the driver is not a serious limitation, therefore we will ignore it. The line will delay the arrival of the data, but aside from degrading rise/fall times, it cannot affect the data rate. The receiver, however, is where the action takes place, and a poor design here can seriously degrade data rate. This article will offer several solutions to the problem of data rate degradation.

How are your thresholds?

Threshold adjustment was already discussed in **Part 4**. As you recall, balanced thresholds are desirable because they maintain equal time delays and prevent time-distortion of data pulses. Threshold adjustment also can enhance data rate.

Fig. 2 of this part shows how to use threshold offset. The shield of a twisted-pair shielded cable carries the offset voltage from driver to terminal. Even if the offset voltage E_c equals zero, the shield return connection is still beneficial. This is because the line-to-ground voltage for logic HIGH exceeds line-to-line voltage, thereby lowering the threshold (as compared to the steady-state terminal voltage). The termination becomes more vulnerable to common-mode voltage whenever a shield return connection is used—especially if $E_c > 0$. Therefore be sure to use an exclusive-OR-ed flip-flop output circuit.

If a single isolator and polarity-reversing drive are used in the termination, then delay balance is obtained only if negative offset is introduced as in **Fig. 1a**. Also, if the drive is nonreversing, a proper choice of resistors in a 2-resistor HT or LT circuit will balance delays.

With paired isolators (**Fig. 6, Part 4**), balancing is not a problem. However, if you are seeking the maximum in data rate, adjust the threshold for each side of the pair. To see this, compare the delays in **Fig. 1b** with those of **Fig. 1c**, where offset is applied, and with **Fig. 1d**, where peaking is used.

When line-to-line voltage is polarity reversing,

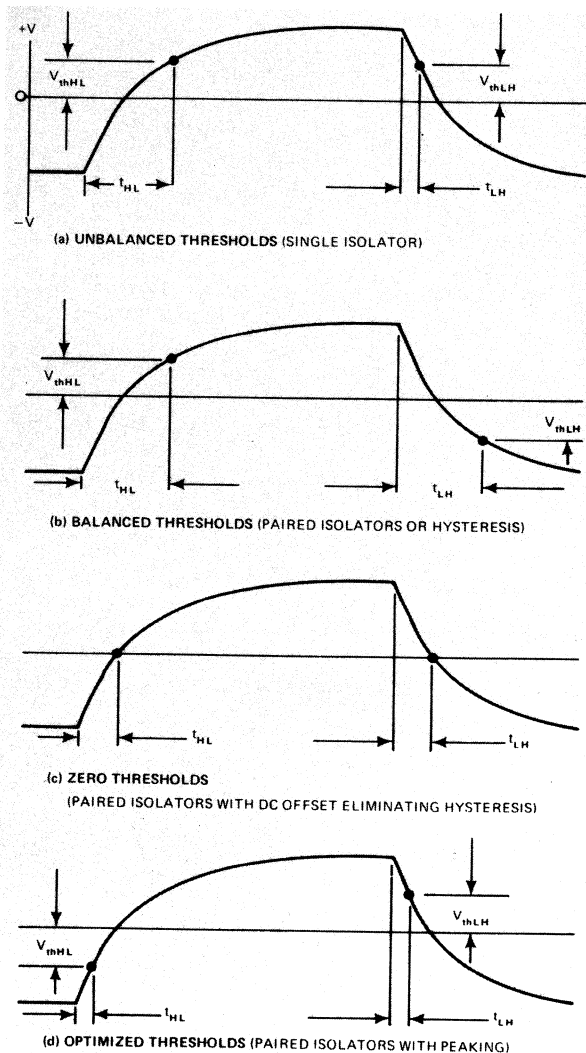


Fig. 1—Threshold affects data rate as well as propagation delay. When $V_{thHL} = V_{thLH} > 0$, the delays cannot be equal (a); while if $V_{thHL} = -V_{thLH} < 0$, the delays will balance (b). For $V_{thHL} = -V_{thLH} = 0$, the delays will also balance (c). Notice the location of the thresholds (d) when $V_{thHL} = -V_{thLH} < 0$.

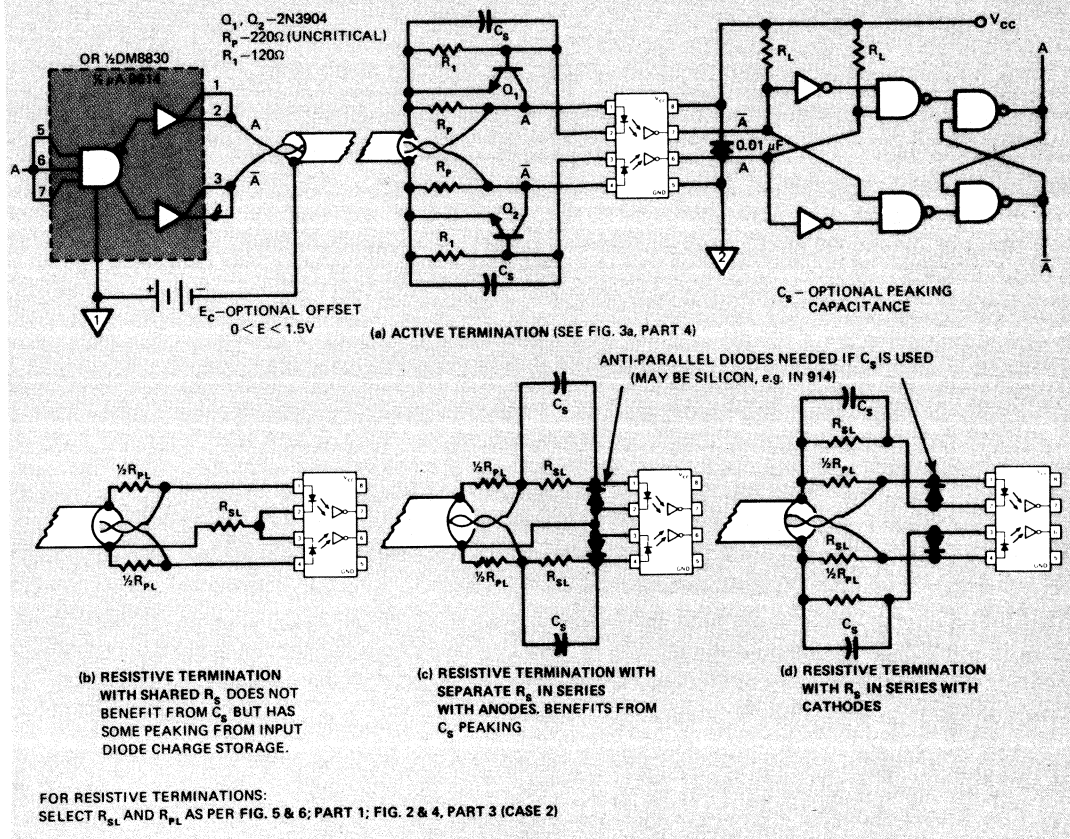


Fig. 2—Using the shield return allows offset for the isolator inputs.

termination of each side of the line to the shield can be a single-ended, polarity-nonreversing design. This is because the line-to-shield voltages are split-phase polarity nonreversing. For the active termination of Fig. 2a, the two diodes that handle polarity reversal are eliminated. The termination consists merely of two shunt-pass active terminations for each line.

The same concept of threshold adjustment applies to resistive terminations (Fig. 2b, c, d). Find R_{sL} by applying Case 2 (Fig. 2 and 4, Part 3), where Z₀ is Z_{odm} as seen in Fig. 6, Part 1.

Peaking—the key to isolator speed

The delay involved in turning on the output transistor, t_{PHL}, can be shortened by driving the input diode at a higher current. This forces a higher photocurrent into the isolator amplifier input.

To shorten the delay involved in turning off the output transistor, t_{PLH}, quickly turn off the input diode and wait for the transistor to turn-off. The

time required for turn-off depends on how hard the transistor was turned on, so shortening t_{PHL} lengthens t_{PLH}, unless the higher drive current used in shortening t_{PHL} is only momentary. This “peaking” technique increases data rate by providing a momentary surge of forward current during turn-on, reducing to a minimum the acceptable forward current in the steady state. A high momentary forward current is produced by a transmission line with a low characteristic impedance and a low driver internal resistance. Back matching will prove unnecessary if you use the terminations suggested here.

Can peaking affect threshold?

If the high-state and low-state voltage drops across a current-limiting resistance are significantly different, connecting a capacitor (C_s) in parallel with the current-limiting resistance gives peaking. This peaking effect is a threshold shift (Fig. 3).

When V_L is negative, the input voltage becomes

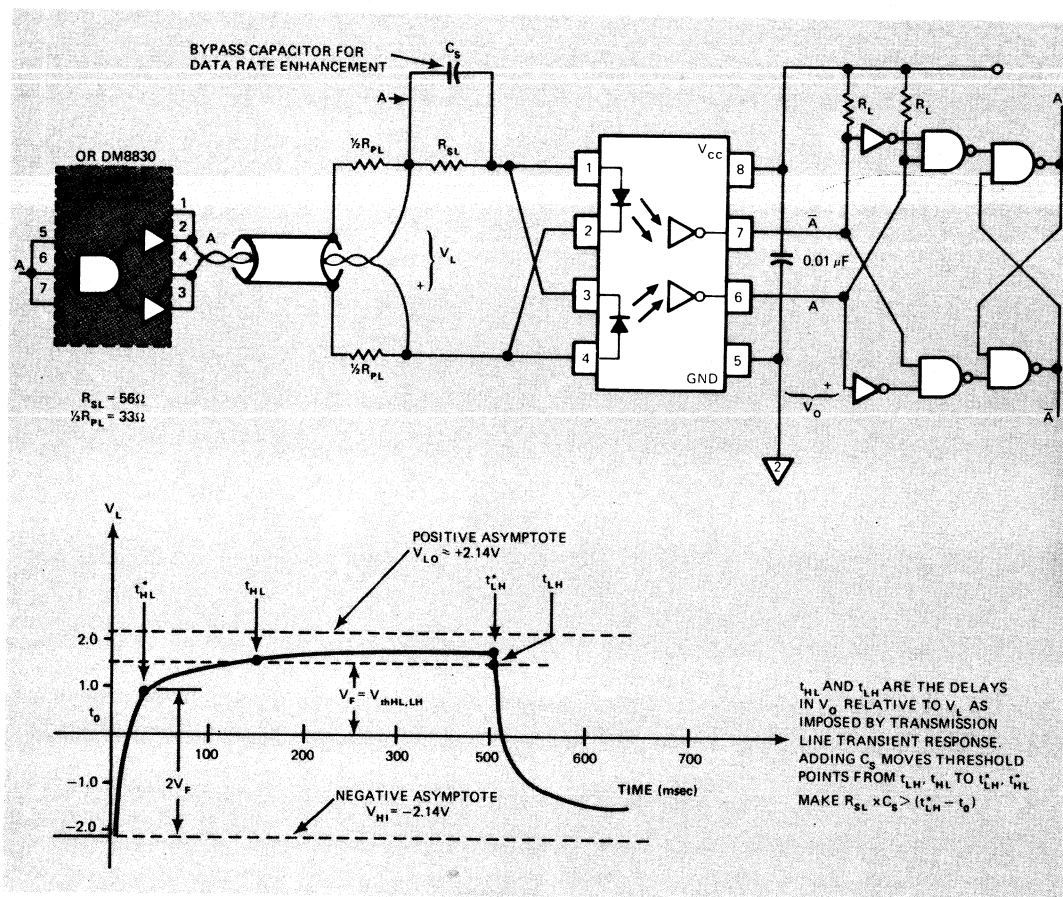


Fig. 3—Peaking capacitor, C_S , increases data rate in a balanced data transmission system with resistive termination.

$-V_F$. Without peaking, V_L rises from its asymptotic negative value to $+1.5V$ before the lower isolator can begin to turn on. On the other hand, with a peaking capacitor, turn-on begins when voltage across the lower isolator input changes from $-V_F$ to $+V_F$. Note that C_S should be large enough so that its voltage does not change very much during the interval $(t_{HL} - t_0)$. The effect of peaking in this case is to shorten t_{HL} .

Without the peaking capacitor, turn-off begins only when V_L drops to the threshold. But with a peaking capacitor, turn-off begins as soon as V_L drops. Because this makes the termination more vulnerable to negative common-mode transients, we recommend an exclusive-OR-ed flip-flop for the output circuits.

Enter "resistive peaking"

As we saw in Part 2, a peaking capacitor paralleled with the series resistor of any resistive termination causes a momentary forward-current

surge. Unfortunately, this, in turn, can cause oscillatory, re-reflections from the driver when you use the simple series circuit (Fig. 2b, Part 2), or the HT and LT terminations for threshold adjustment (Fig. 3, Part 2).

If Case 2 (Part 3) is applied, the 3-resistor π or T circuit can be used. But it makes no sense to design a π or T for threshold and load match and then to upset both with a peaking capacitor. That leaves the HT and LT terminations designed for load matching Case 2 (Fig. 2 and Figs. 1-4, Part 3). Of these, LT terminations benefit most from peaking.

One exception is the circuit of Fig. 2b. Here the current in R_{SL} has the same polarity for both logic states. As a result, insufficient voltage change exists for a peaking capacitor in parallel with the resistor to be effective. Still, this circuit has some peaking. During steady state, the ON input diode has a charge stored in it—the charge necessary to support I_F . Thus, when the line-to-line voltage

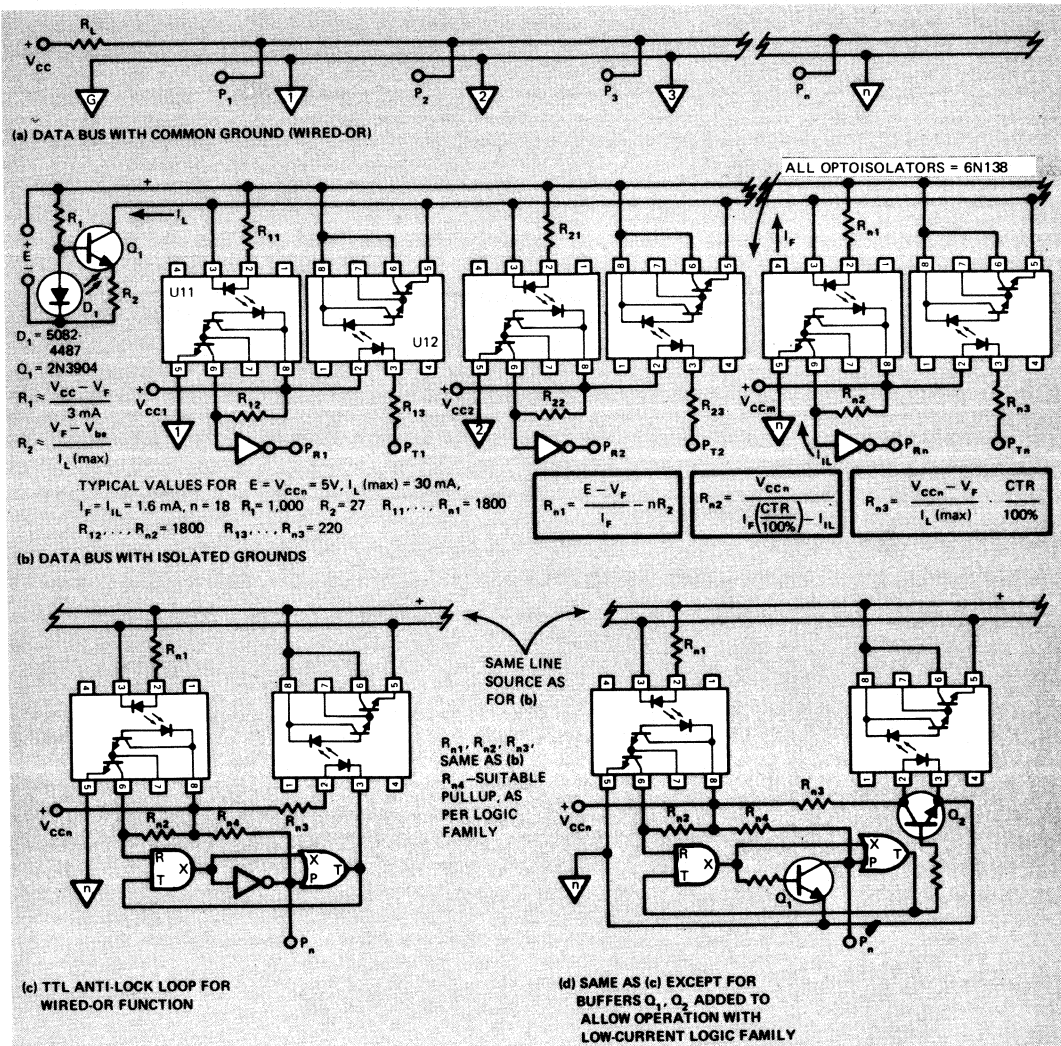


Fig. 4—Moderate data rate multiplexing with high CTR optoisolators is shown. The data bus with isolated grounds (b) has separate terminals at each station for receiving (P_R) and transmitting (P_T). The same terminal in each station of the TTL anti-lock loop (c) can transmit and receive.

reverses polarity, this stored charge is transferred to the other diode, thereby reducing its turn-on time.

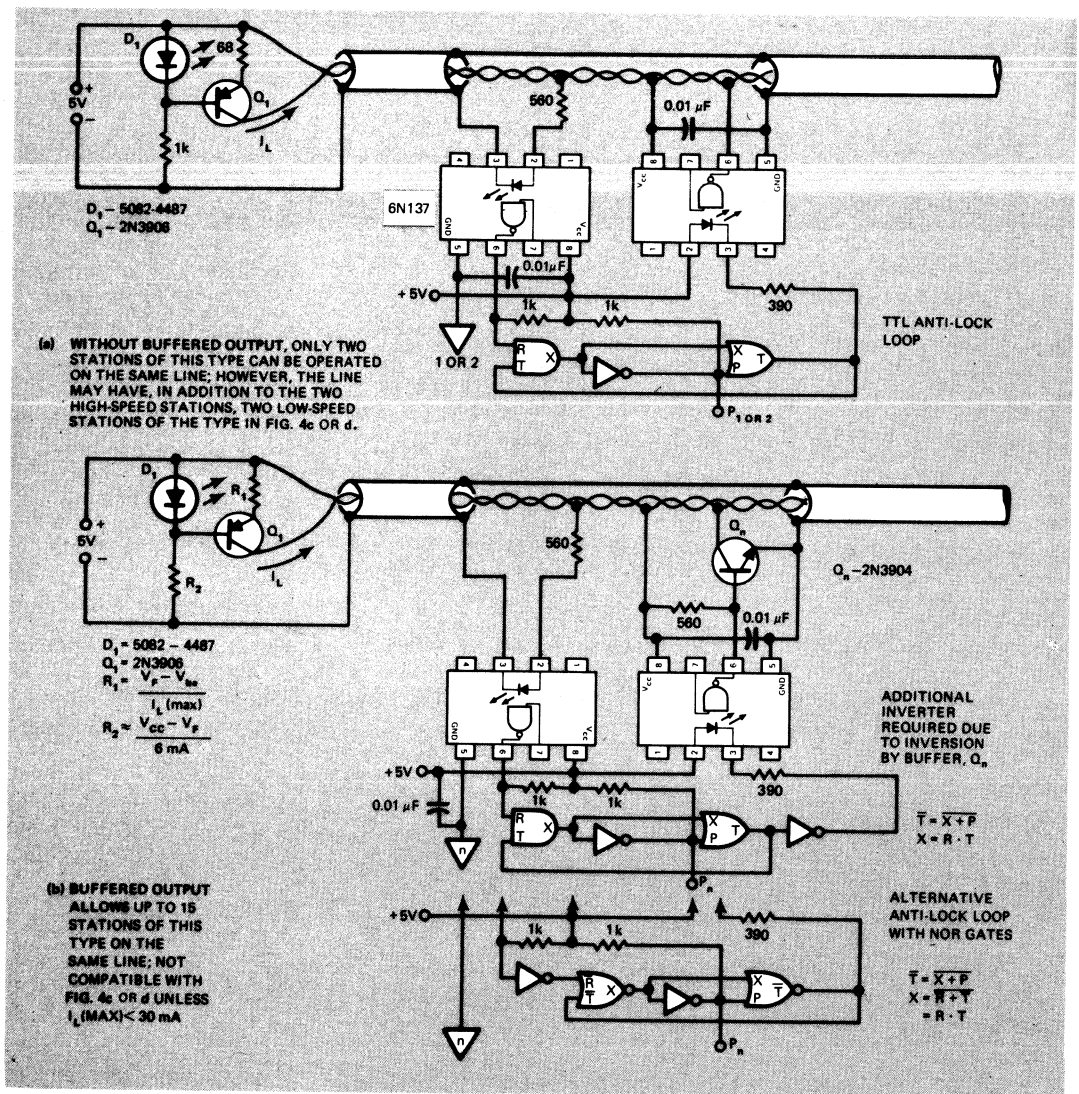
What is the best value for the peaking capacitor? That depends on the shape of the turn-on transient, so a specific formula doesn't exist. Peaking capacitance for polarity-nonreversing drive should be a good deal larger than that required in polarity-reversing drive. Anti-parallel diodes allow C_S to charge and discharge, even if polarity is nonreversing.

To obtain the greatest benefits from peaking, try the circuit in Fig. 3, where the polarity on the

peaking capacitor is reversed. Peaking capacitance is optional in Fig. 2, where the main data rate enhancement comes from threshold control. In particular, since polarity on the peaking capacitor in Fig. 2c and 2d is not reversed, C_S is of little incremental value.

A refresher on active peaking

The voltage-clamp regulators of Fig. 3, Part 4, lag line voltage, thereby allowing a momentary surge into the isolator diode. On turn-off, the shunt transistor lags again, remaining on briefly. This helps to drain the charge from the isolator



diode, thus hastening turn-off.

To further enhance both effects (especially in **Fig. 3 c-f, Part 4**, where voltage across R_1 reverses polarity), place a capacitor in parallel with R_1 .

For the one-port, current clamp terminations shown in **Part 4**, you should connect a peaking capacitor in parallel with the entire regulator. Two-port regulators, on the other hand, need more than one peaking capacitor and should have a capacitor in parallel with R_1 . In addition, circuits of **Fig. 1b** and **d, Part 4** should have a capacitor from the input diode anode to the + or the \pm line terminal. The circuit given in **Fig. 2b, Part 4** should

have two additional capacitors—one from each input diode anode to the collector of its regulating transistor.

Multiplexing—how optoisolators fit

Data goes only in one direction on a simplex data transmission line, from one driver to one or more receivers. In multiplexing, however, data exchanges in both directions from any of several stations on the line to all other receivers on the line.

Bused multiplexing, as shown in **Fig. 4a**, is a wired-OR arrangement. Each of the terminal

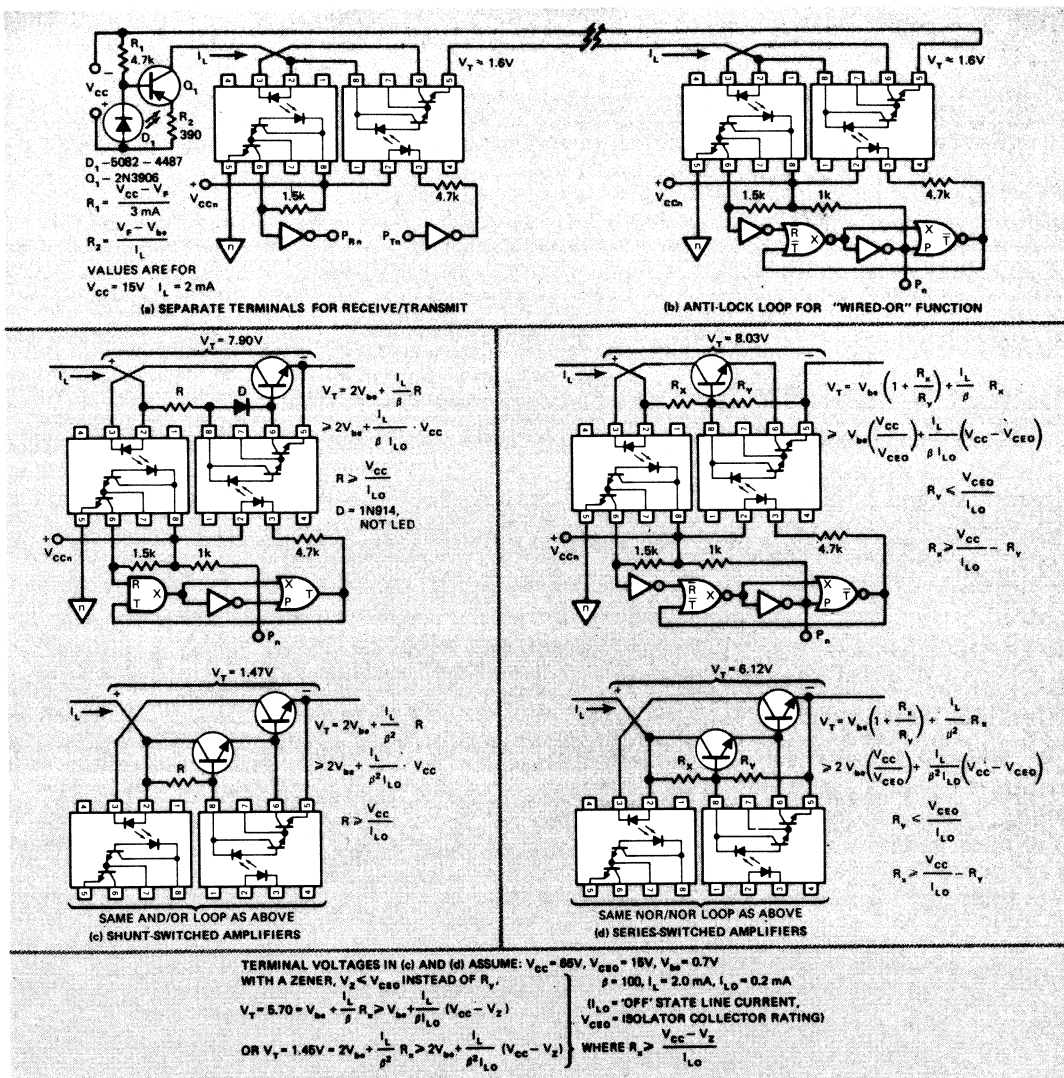


Fig. 6—Current loop multiplexing, otherwise difficult to utilize, poses no serious problems for the designer when optoisolators are used.

points (P_1, P_2, \dots, P_n) are at a quiescent HIGH state. Since the transmitter/receivers share a common ground and V_{CC} , applying a LOW at any point causes a LOW to appear at all others.

Ground looping can create common-mode interference and may require that these common connections be separated as shown in **Fig. 4b**. Here one isolator is the transmitter; the other, a receiver. When a LOW is applied to P_{Tn} , the transmitting isolator drops the line voltage by sinking all the current available from the line source. This causes all receiving points ($P_{R1}, P_{R2}, \dots, P_{Rn}$) to go LOW. This differs from the

arrangement of **Fig. 4a** because in **4b** the transmit and receive points (P_{Tn} and P_{Rn}) at each station are not common. Though the logic is the same, these points cannot be connected without locking everything LOW.

You can obtain common transmit/receive points by using the AND/OR anti-lock loop shown in **Fig. 4c** (for TTL). The loop requires an open-collector inverter, whose input remains LOW even when a LOW is applied at P_{in} , thereby ensuring that its output will go HIGH when the LOW is removed from P_{in} .

In the quiescent state, R is LOW, making X

LOW, with P_n and T becoming HIGH. If another station transmits a LOW, R goes HIGH, causing a HIGH, HIGH input at the AND gate. X goes HIGH, making P_n a LOW. However, T remains HIGH because $T = X + \bar{X}$ (unless a LOW is internally applied at P_n).

In transmitting, $T = X + P_n$. Since X is LOW, applying a LOW at P_n makes T go LOW. T is applied at the AND gate, so X will remain LOW, even though R goes HIGH when T drops LOW (and thereby turning on the "transmit" isolator). Since data can be both transmitted and received at P_n , the wired-OR is achieved.

The anti-loop (**Fig. 4d**) can be made compatible with other logic families (even CMOS) that lack the current-sinking capability of TTL. Since the isolated interconnection takes place at the bus, you can have one station operated by TTL while another is operated by LTTL, LSTTL, CMOS, etc. The only requirement for isolated wired-OR is an anti-lock loop that makes the logic family in any station compatible with the transmit isolator's drive requirement.

Data rates, limited mainly by the isolators used, can be improved by using a high-speed isolator as shown in **Fig. 5a**. There is a price, though, and it takes the form of a third connector in the bus. This extra connector supplies power to the amplifier in the transmit isolator. Since the current-sinking capability of the transmit isolator limits the number of stations, you should add a buffer as given in **Fig. 5b**.

Current-loop multiplexing is next to impossible without optoisolators. Because potential builds up around the loop, level shift adjustments are needed when stations are added or removed (unless relays are used).

With optoisolators, however, current loop multiplexing becomes quite simple and is similar to bus multiplexing, although in transmitting the loop is opened; whereas, in multiplexing the bus is shorted. As can be seen in **Fig. 6a**, separate transmit and receive points can be used at each station. If a common transmit/receive point is needed, you must use the anti-lock loop (**Fig. 6b**).

The voltage rating on the isolator collector limits the number of stations in a current loop. To increase the number of stations, it may prove necessary to raise the voltage rating by using circuits such as **Fig. 6c** or **d**. □

This fifth and final article concludes EDN's optoisolator digital transmission line series.

Optocouplers for Digital Data Transmission Systems

The optocoupler is a component which is coupled by means of photons. The electrical input signal is converted in the transmitter part of the optocoupler into radiant energy and transmitted through an electrically insulating material to the receiver section. The "optical signal", the received radiant energy, is converted back into an electrical signal in the receiver.

In an optocoupler, the three components — transmitter, transmission path, and receiver — are integrated in one case.

TYPES OF OPTOCOUPLES FOR DIGITAL APPLICATIONS

In a phototransistor optocoupler (Figure 1), a light-emitting diode (LED) is coupled optically with a phototransistor in a small case. This permits transfer of electrical signals without dc connection and without a common ground connection. Any interference signals which are present are suppressed to a great degree.

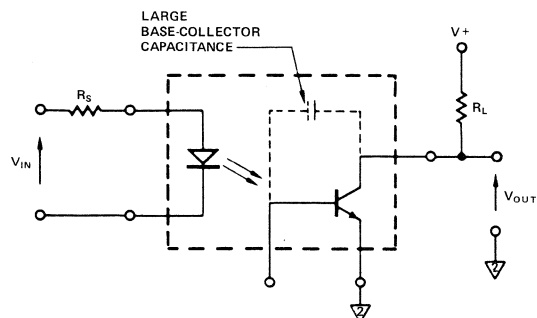


Figure 1. Typical Phototransistor Optocoupler

In order to achieve a high optical coupling to the phototransistor, the base area must be very large, which means that the base-collector capacitance is also very large. This capacitance has a major effect on the transmission speed of the optocoupler. If a load resistor R_L is connected, as shown in Figure 1, then the so-called Miller effect causes long pulse rise and fall times.

In order to achieve higher switching speeds, the phototransistor is replaced by a photodiode and an amplifying transistor on a common chip (Figure 2). This reduces the "Miller" capacitance. The pulse rise and fall times are shortened by this means by approximately 4000%, while retaining an equivalent voltage gain.

Other optocoupler configurations may contain additional components which increase the gain (allowing reduced input current) and simultaneously retain a high transmission speed.

In Figure 3, an emitter-follower stage is added. This makes it possible to operate with lower input currents between

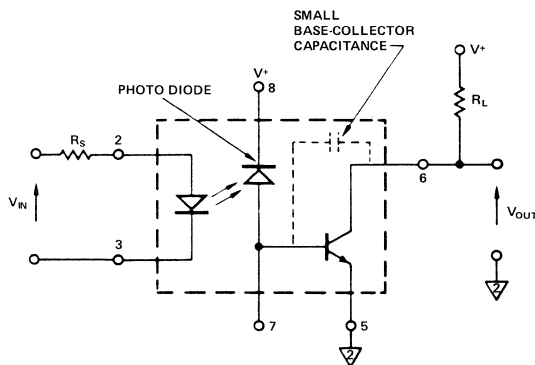


Figure 2. Photodiode/Transistor Optocoupler

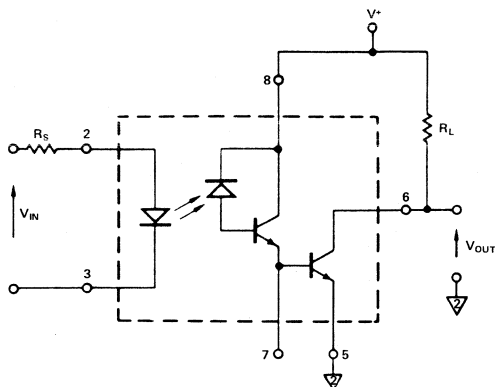


Figure 3. Split Darlington Transistor Optocoupler

0.5 and 1.6 mA. At the same time, the output current is sufficient to drive TTL gates and load resistance. This configuration is called a "split" Darlington circuit to distinguish it from a Darlington circuit in which the collector of the second transistor is connected to the collector of the first transistor. This results in a low saturation voltage (below 0.4 V) with a high degree of coupling. This combination makes it possible to reach medium transmission speeds (up to 300 kbaud), about one hundred times that which can be reached with full Darlington optocouplers.

If the photodiode, cascaded amplifier, and Schottky transistor are integrated on one chip, the result is an optocoupler such as that shown in Figure 4. This type achieves the highest transmission speeds (up to 20 Mbaud). The integrated amplifier presents a very low input impedance to the photo diode and does not become saturated. The amplifier output drives a high speed switching transistor. The gain/band width product can be maximized by optimization of the LED/photodiode switching speed and of the coupling efficiency. Optocouplers of this type have delay times of 30 ns with an input current of 5 mA. A digital gate inserted in the circuit can enable or disable the output of the optocoupler. Some optocouplers also permit "Tri-state" outputs.

CURRENT TRANSFER RATIO

The current transfer ratio (CTR) of an optocoupler is a dimension for the coupling efficiency between the input and output currents. It is specified at a certain level of the input or output current and is:

$$CTR = \frac{I_{OUT}}{I_{IN}} \times 100\%$$

This often has a value of less than 100%, as simple photo-transistor optocouplers have transmission losses. In newly developed versions, the gain may be above 100%.

CTR is a function of the input level, as shown in Figure 5. This curve is similar to the h_{FE}/I_C characteristic of a typical transistor.

It is also possible to show the output current I_{OUT} as a function of I_{IN} , as shown in Figure 6. This curve permits

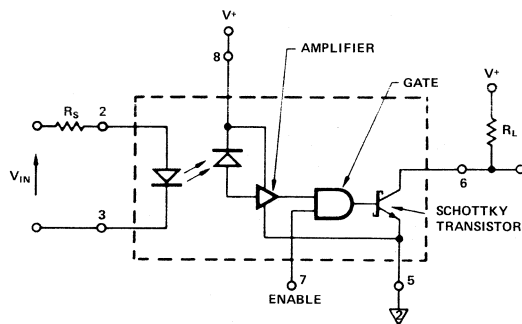


Figure 4. Optocoupler with Integrated Circuit

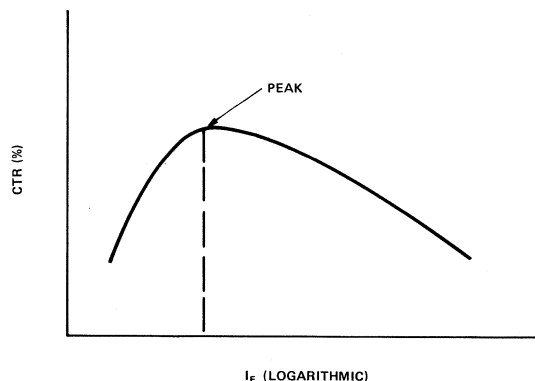


Figure 5. Typical CTR Curve as a Function of I_F

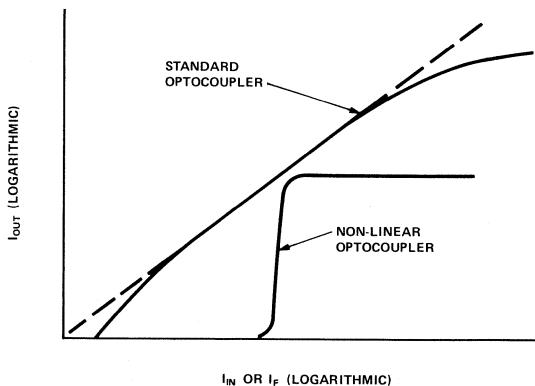


Figure 6. Typical I_{OUT} Curve as a Function of I_F

the designer to determine the value of I_{IN} for a given I_{OUT} . In the case of optocouplers with extremely non-linear characteristics, this curve has a step shape. Here, no output level appears until a threshold value in the circuit is reached. After this, the output level reaches its maximum level very rapidly.

Degradation of the CTR was, in the past, a major problem. Today, hysteresis circuits for threshold value adjustment are used more and more in the development of digital applications in order to circumvent this phenomenon. The reduction of the input current I_{IN} to values around 150 μA also contributes decisively to the reduction of the CTR degradation.

COMMON-MODE REJECTION (CMR)

The basic function of an optocoupler is to isolate one part of a system or circuit from another part. This is done by electrical disconnection of the normally required ground return. Under these conditions, a voltage difference may occur between the ground voltages of the input and output sides. This voltage is called the common-mode voltage, as it is common to both input lines. Figure 7 shows the most simple example of a common-mode voltage which is fed into an optocoupler. Ideally, there should be no change in V_{OUT} at the output, regardless of the amplitude and frequency of the common-mode signal voltage (e_{cm}), if no input signal is provided. The "effective" common-mode capacitance provides a path for e_{cm} . This capacitance, with a typical value of 0.1 pF, is very low. It can be reduced by a factor of approximately 10 by inclusion of electrical shielding between the LED and the photodetector.

Figure 8 shows the typical common-mode response for a sinusoidal input. It shows the maximum e_{cm} , as a function of the frequency, at which no error signal appears at the output. This common-mode signal voltage is very high at low frequencies, drops to a minimum at a specific fre-

quency, and then rises again to a very high value due to the frequency response limitation of the output amplifier.

Figure 9 shows a voltage step which can be applied to the input instead of the sinusoidal voltage. This can be increased until an error voltage is generated at the output. From this, a specification called the common-mode transient rejection is derived. This transient rejection is a function of the amplitude (maximum voltage) of the change and of the rate of voltage change. It is expressed as $V/\mu s$. Optocouplers with good characteristics with respect to common-mode suppression have values of 1000 $V/\mu s$. Very good optocouplers reach values of 10,000 $V/\mu s$. This behavior is not caused by the peak value of the common-mode current, but by the total charge transfer through the effective common-mode capacitance, which generates an output error signal.

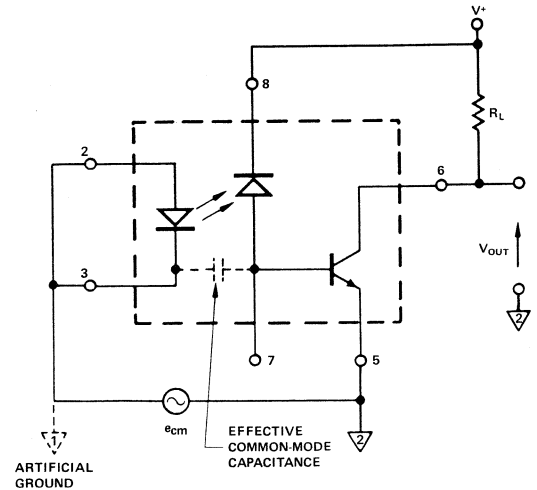


Figure 7. Circuit for Representation of Common-Mode Rejection

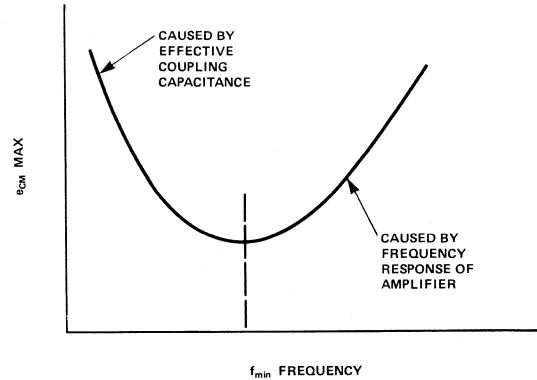


Figure 8. Sinusoidal Common-Mode Rejection Curve

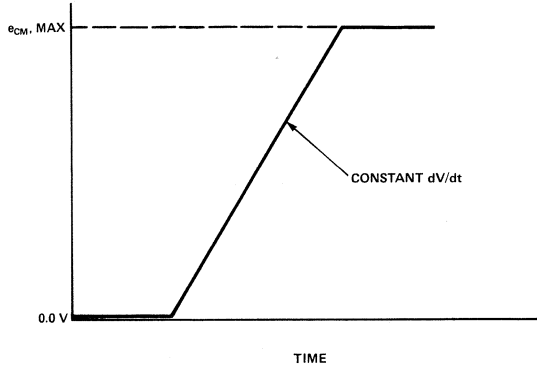


Figure 9. Typical Test Voltage for Transient Rejection

In the data sheets, the delay time could be specified in

These delay times are shown in Figures 10 and 11. The delay time which is shown in Figure 11 is of particular importance for designers of digital circuits, as it shows a



typical digital interface. It shows the measurement of the propagation time of the input-to-output response from "low" to "high" (t_{PLH}) and from "high" to "low" (t_{PHL}). Today, there are already optocouplers such as the HCPL-2400 from Hewlett-Packard which have such short delay times that data rates of up to 20 Mb/s can be achieved. In optocouplers with transistor outputs, the LED drive current I_F and the value of the pull-up resistor R_L contribute, in addition to the selection of the optocoupler, to determination of the maximum possible data rate. Basically, it can be said that the propagation time is reduced as the value of R_L is reduced. However, an optocoupler is restricted by the maximum permissible value of I_F and a minimum value of the current transfer ratio, and thus a minimum value of R_L .

DIGITAL APPLICATIONS

One of the most important applications for optocouplers in digital systems is their use instead of pulse transformers or integrated line receivers. In addition to dc transmission behavior, optocouplers offer simple circuit construction, and lower weight and smaller space requirements than a pulse transformer. In other applications, they offer a far higher common-mode rejection than IC line receivers.

This is a very important factor in designs with long lines or in environments subject to interference. Figure 12 shows the circuit of an optocoupler in an LSTTL to LSTTL interface. The maximum data transmission rate is 10 Mbaud. The internal shielding in the optocoupler provides a common-mode rejection of 1000 V/ μ s. The drive current I_F for the LED is 5 mA.

The use of an optocoupler as a line receiver is shown in Figure 13. This circuit is TTL-compatible and is driven by standard TTL gates. The maximum data rate is 40 kbaud with a maximum line length of 1500 m.

A special application of optocouplers is their use in line current interfaces. Current loops are used as they permit long transmission distances of up to 10 km with low data rates. They are quite insensitive to external interference and can be implemented cheaply. The usual 20 mA current loops are often restricted in their data rate to 5 to 10 kbaud, even over short distances. The use of special 20 mA transmitter and receiver optocouplers, such as HCPL-4100/4200 made by Hewlett-Packard, permit implementation of distances of up to 400 m at a data rate of 20 kbaud.

Data transmission via current loops can be implemented in one of three ways: simplex, half-duplex, and full-duplex. The simplest loop configuration is the simplex point-to-

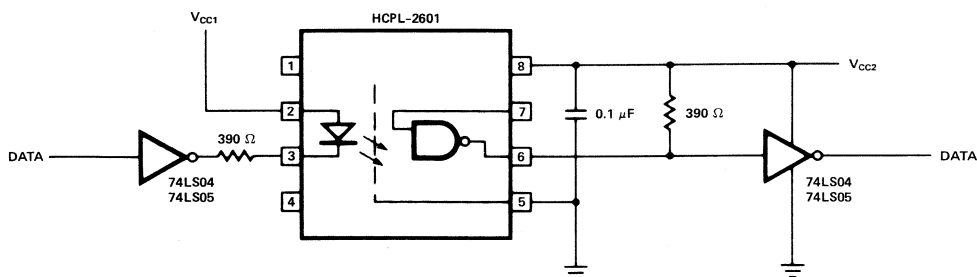


Figure 12. LSTTL to LSTTL Optocoupler Interface

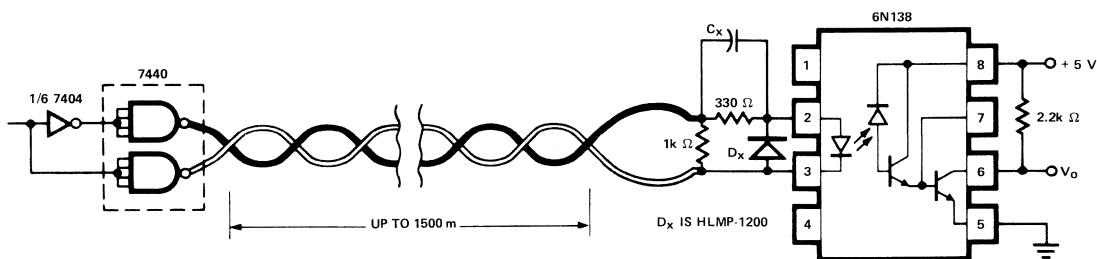


Figure 13. Line Receiver for 1-1500 m

point connection. The data flow in only one direction from the transmitter via the current loop to the receiver. This configuration is shown in Figure 14. Figure 14a shows an isolated, active line current interface transmitter, together with an isolated HCPL-4200 receiver. Figure 14b shows an isolated HCPL-4100 line current interface transmitter connected to an unisolated, active receiver. A typical point-to-point application is the use of a 20 mA current loop for communication between a computer and a remote printer. In order to achieve a full-duplex data connection, both circuits shown in Figure 14 would be used together for

simultaneous, bi-directional data transmission, the isolated parts being at one end of the link and the unisolated parts at the other end (Figure 15). Figure 16 shows the configuration of a half-duplex, point-to-point connection. Here, the data cannot be transmitted simultaneously in both directions. However, this configuration has the advantage that only one current loop is required. The use of optocouplers in such applications permits simple implementation of potential isolation and also a considerable reduction in the interference sensitivity.

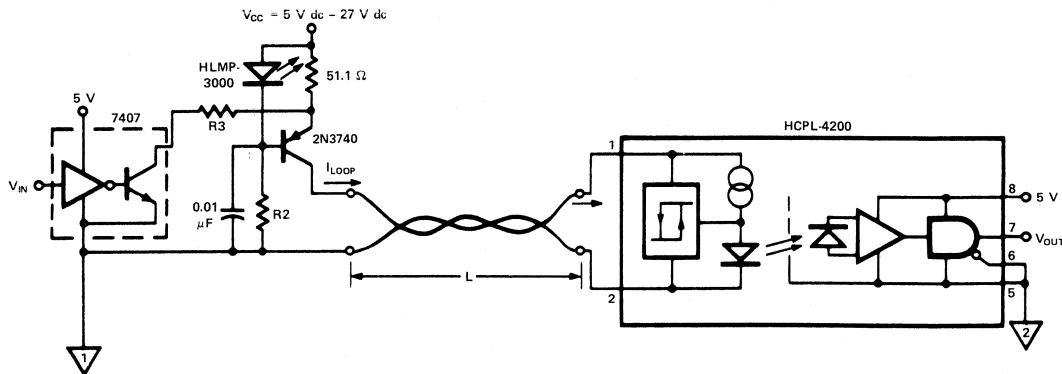


Figure 14a. Unisolated, Active Transmitter with Isolated HCPL-4200 Receiver for Simplex Point-to-Point 20 mA Current Loop

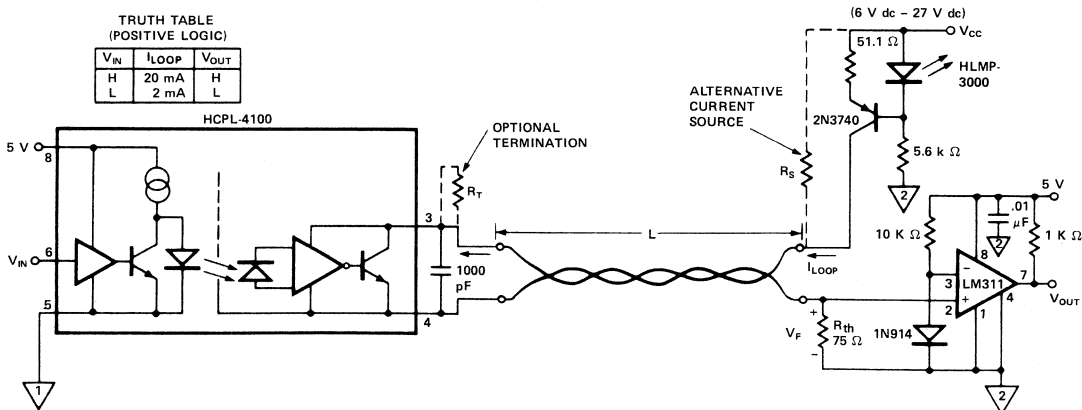


Figure 14b. Unisolated, Active Receiver with Isolated HCPL-4100 Transmitter for Simplex Point-to-Point 20 mA Current Interface

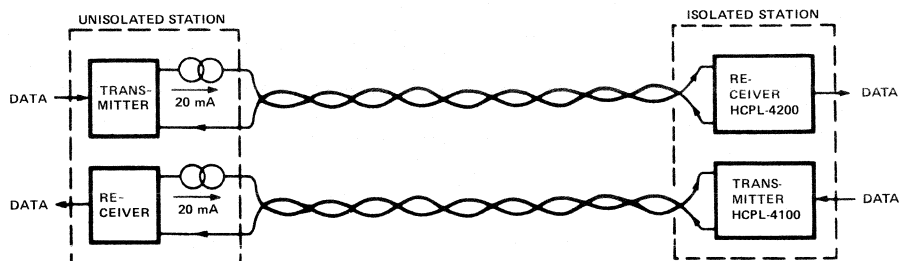


Figure 15. Configuration of a Full-Duplex Point-to-Point Current Loop System.

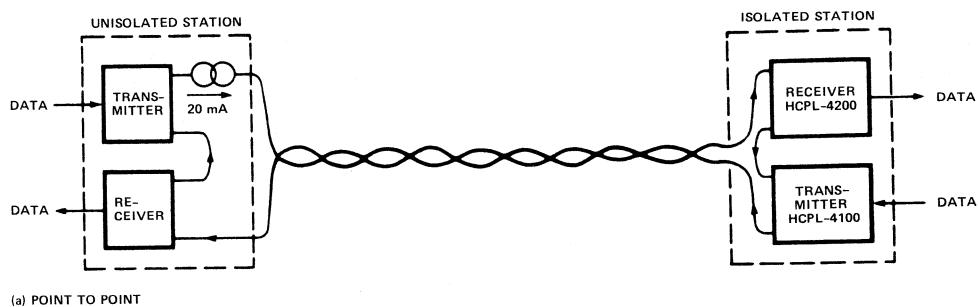
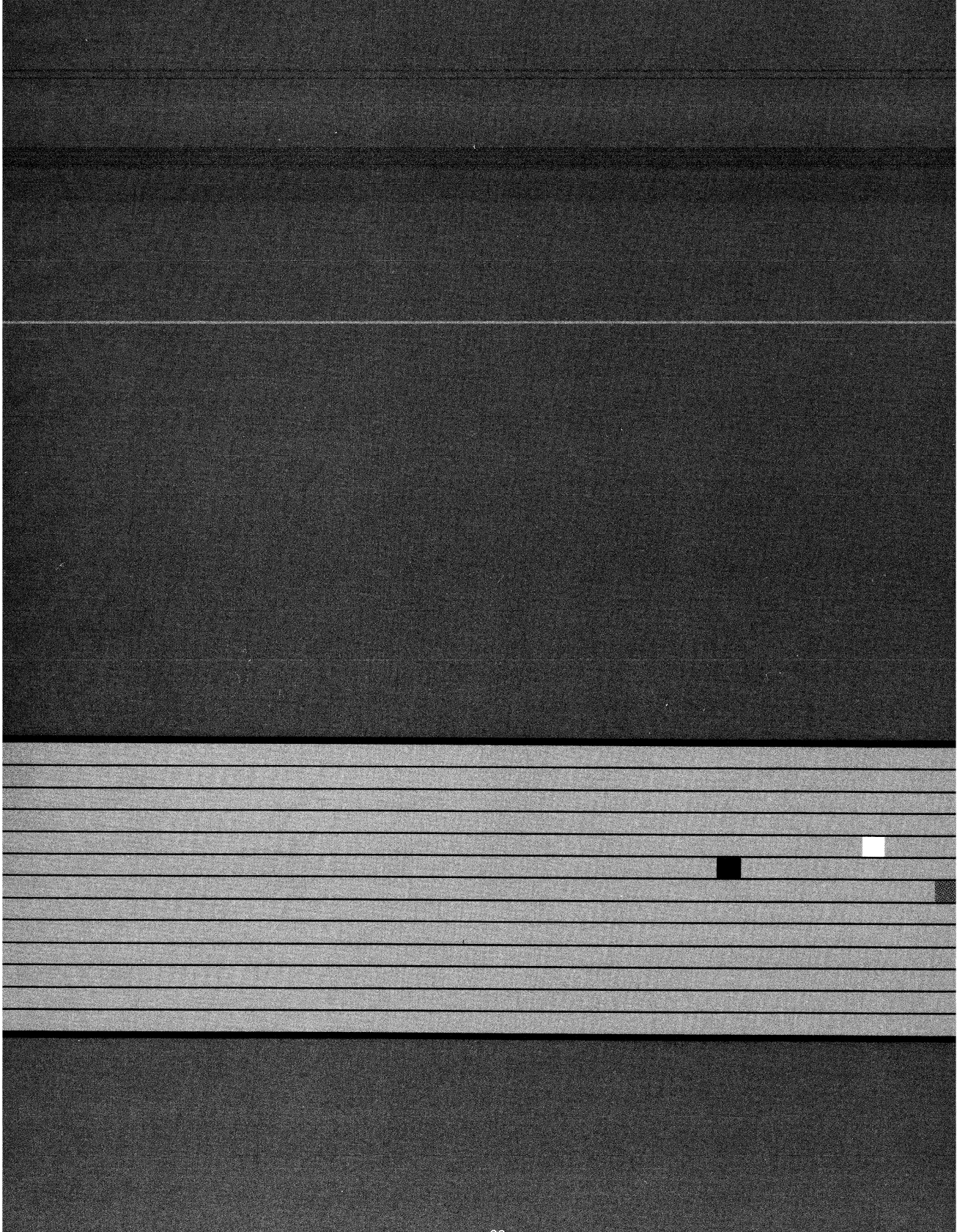
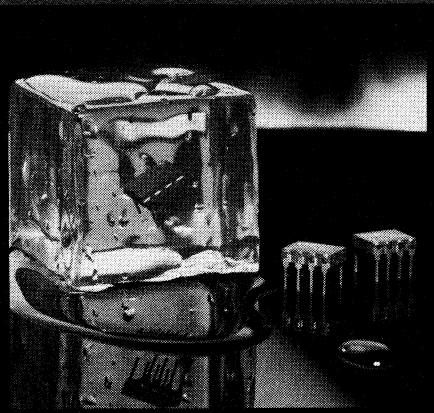
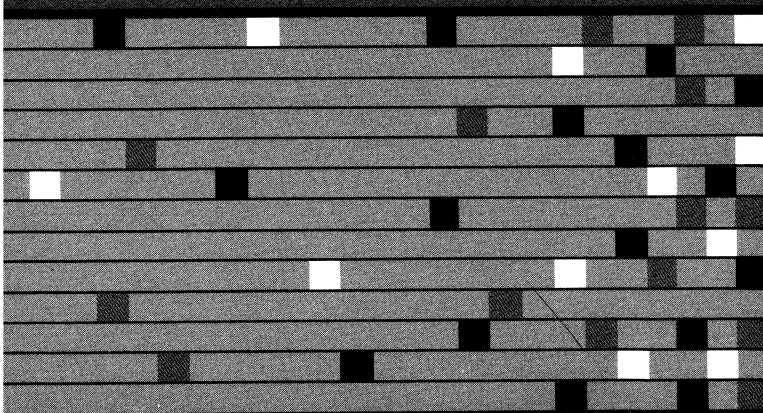


Figure 16. Point-to-Point Half-Duplex Current Loop System.



Hermetic/MIL STD
Optocouplers



Hermetic/MIL STD Optocouplers

Device	Description	Application	Typical Data Rate (NRZ)	Current Transfer Ratio	Specified Input Current	Withstand Test Voltage
	6N134	Dual Channel Hermetically Sealed Optically Coupled Logic Gate	10M bit/s	400% Typ.	10 mA	1500 V dc
	8102801EC	DESC Approved 6N134				
	6N134TXV	TXV — Screened				
	6N134TXVB	TXVB — Screened with Group B Data				
	HCPL-1930	Dual Channel Hermetically sealed High CMR Line Receiver Optocoupler	10M bit/s	400% Typ.	10 mA	1500 Vdc
	HCPL-1931	MIL-STD-883 Class B Part				
	HCPL-5700	Single Channel Hermetically Sealed High Gain Optocoupler	60k bit/s	200% Min.	0.5 mA	500 V dc
	HCPL-5701	MIL-STD-883 Class B Part				
	HCPL-5730	Dual Channel Hermetically Sealed High Gain Optocoupler				
	HCPL-5731	MIL-STD-883 Class B Part				
	6N140A (6N140)	Hermetically Sealed Package Containing 4 Low Input Current, High Gain Optocouplers	100k bit/s	300% Min.	0.5 mA	1500 V dc
	8302401EC	DESC Approved 6N140A				
	6N140A/883B (6N140/883B)	MIL-STD-883 Class B Part				
	6N140TXV	TXV — Hi-Rel Screened				
	6N140TXVB	TXVB — Hi-Rel Screened with Group B Data				
	4N55	Dual Channel Hermetically Sealed Analog Optical Coupler	700k bit/s	9% Min.	16 mA	1500 V dc
	4N55/883B	MIL-STD-883 Class B Part				
	4N55TXV	TXV — Hi-Rel Screened				
	4N55TXVB	TXVB — Hi-Rel Screened with Group B Data				

Hermetic Optocoupler Product Qualification

MIL-STD-883 Class B Test Program

The following 100% Screening and Quality Conformance Inspection programs show in detail the capabilities of our 4N55, 6N134, 6N140A, HCPL-5701, and 5731 optocouplers. This program will help customers understand the tests included in Methods 5004 and 5005 of MIL-STD-883 and to help in the design of special product

drawings where this testing is required. The 4N55/883B, 5701/883B, 5731 883B, 8102801EC and 8302401EC (DESC Selected Item Drawings for the 6N134 and 6N140A respectively) have standardized test programs suitable for product use in military, high reliability applications and are the preferred devices by military contractors.



100% Screening

MIL-STD-883, METHOD 5004 (CLASS B DEVICES)

Test Screen	Method	Conditions
1. Precap Internal Visual	2010	Condition B, DESC Parts
2. High Temperature Storage	1008	Condition C, $T_A = 150^\circ\text{C}$, Time = 24 Hours minimum
3. Temperature Cycling	1010	Condition C, -65°C to $+150^\circ\text{C}$, 10 cycles
4. Constant Acceleration	2001	Condition A, 5K Gs, Y_1 axis only, 16 pin DIP, Condition E, 30K Gs, Y_1 axis only, 8 pin DIP
5. Fine Leak	1014	Condition A
6. Gross Leak	1014	Condition C
7. Interim Electrical Test	—	Group A, Subgroup 1, except I/O (optional)
8. Burn-In	1015	Condition B, Time = 160 Hours minimum, $T_A = 125^\circ\text{C}$ Burn-in conditions are product dependent and are given in the individual data sheets.
9. Final Electrical Test Electrical Test Electrical Test Electrical Test	—	Group A, Subgroup 1, 5% PDA applies Group A, Subgroup 2 Group A, Subgroup 3 Group A, Subgroup 9
10. External Visual	2009	

Quality Conformance Inspection

Group A electrical tests are product dependent and are given in the individual

device data sheets. Group A and B testing is performed on each inspection lot.

GROUP A TESTING MIL-STD-883, METHOD 5005 (CLASS B DEVICES)

	LTPD
Subgroup 1 Static tests at $T_A = 25^\circ\text{C}$	2
Subgroup 2 Static tests at $T_A = +125^\circ\text{C}$	3
Subgroup 3 Static tests at $T_A = -55^\circ\text{C}$	5
Subgroups 4, 5, 6, 7 and 8 These subgroups are non-applicable to this device type	
Subgroup 9 Switching tests at $T_A = 25^\circ\text{C}$	2
Subgroup 10 Switching tests at $T_A = +125^\circ\text{C}$	3
Subgroup 11 Switching tests at $T_A = -55^\circ\text{C}$	5

GROUP B TESTING MIL-STD-883, METHOD 5005 (CLASS B DEVICES)

Test	Method	Conditions	LTPD
Subgroup 1 Physical Dimensions (Not required if Group D is to be performed)	2016		2 Devices/ 0 Failures
Subgroup 2 Resistance to Solvents	2015		4 Devices/ 0 Failures
Subgroup 3 Solderability (LTPD applies to number of leads inspected — no fewer than 3 devices shall be used.)	2003	Soldering Temperature of $245 \pm 5^{\circ}\text{C}$ for 10 seconds	15 (3 Devices)
Subgroup 4 Internal Visual and Mechanical	2014		1 Device/ 0 Failures
Subgroup 5 Bond Strength (1) Thermocompression (performed at precap, prior to seal. LTPD applies to number of bond pulls from a minimum of 4 devices).	2011	(1) Test Condition D	15 (4 Devices)
Subgroup 6 Internal water vapor content (Not applicable — per footnote of MIL-STD)	—		—
Subgroup 7 Fine Leak Gross Leak	1014	Test Condition A Test Condition C	5
Subgroup 8* Electrical Test Electrostatic Discharge Sensitivity Electrical Test	3015	Group A, Subgroup 1, except I _{I-O} Group A, Subgroup 1	15

*(To be performed at initial qualification only)

Group C testing is performed on a periodic basis from current manufacturing every 3 months.

GROUP C TESTING MIL-STD-883, METHOD 5005 (CLASS B DEVICES)

Test	Method	Conditions	LTPD
Subgroup 1 Steady State Life Test	1005	Condition B, Time = 1000 Hours Total $T_A = +125^{\circ}\text{C}$ Burn-in conditions are product dependent and are given in the individual device data sheets.	5
Endpoint Electricals at 168 hours and 504 hours		Group A, Subgroup 1, except I _{I-O}	
Endpoint Electricals at 1000 hours		Group A, Subgroup 1	
Subgroup 2 Temperature Cycling	1010	Condition C, -65°C to $+150^{\circ}\text{C}$, 10 cycles	15
Constant Acceleration	2001	Condition A, 5KG's, Y ₁ axis only	
Fine Leak	1014	Condition A	
Gross Leak	1014	Condition C	
Visual Examination	1010	Per visual criteria of Method 1010	
Endpoint Electricals		Group A, Subgroup 1	

Group D testing is performed on a periodic basis from current manufacturing every 6 months.

GROUP D TESTING MIL-STD-883, METHOD 5005 (CLASS B DEVICES)

Test	Method	Conditions	LTPD
Subgroup 1 Physical Dimensions	2016		15
Subgroup 2 Lead Integrity	2004	Test Condition B2 (lead fatigue)	15
Subgroup 3 Thermal Shock	1011	Condition B, (-55° C to +125° C) 15 cycles min.	15
Temperature Cycling	1010	Condition C, (-65° C to +150° C) 100 cycles min.	
Moisture Resistance	1004		
Fine Leak	1014	Condition A	
Gross Leak	1014	Condition C	
Visual Examination		Per visual criteria of Method 1004 and 1010	
Endpoint Electricals		Group A, Subgroup 1	
Subgroup 4 Mechanical Shock	2002	Condition B, 1500G, t = 0.5 ms, 5 blows in each orientation	15
Vibration Variable Frequency	2007	Condition A min.	
Constant Acceleration	2001	Condition A, 5KGs, Y ₁ axis only, 16 pin DIP, Condition E, 30 KGs, Y ₁ axis only, 8 pin DIP	
Fine Leak	1014	Condition A	
Gross Leak	1014	Condition C	
Visual Examination	1010	Per visual criteria of Method 1010	
Endpoint Electricals		Group A, Subgroup 1	
Subgroup 5 Salt Atmosphere	1009	Condition A min.	15
Fine Leak	1014	Condition A	
Gross Leak	1014	Condition C	
Visual Examination	1009	Per visual criteria of Method 1009	
Subgroup 6 Internal Water Vapor Content	1018	5,000 ppm maximum water content at 100° C	3 Devices (0 failures) 5 Devices (1 failure)
Subgroup 7 Adhesion of lead finish	2025		15
Subgroup 8 Lid Torque (Applicable to 8 pin DIP only)	2024		5 Devices (0 failures)

Plastic Optocouplers

Hewlett-Packard supplies plastic optocouplers with high reliability testing for commercial/industrial applications requiring prolonged operational life. Two of the most frequently requested 100% preconditioning and screening programs are given. The first program has burn-in and electrical test only, the second program adds temperature storage and temperature cycling. Either program is

available for HP's plastic optocouplers. Electrical testing is to catalog conditions and limits and will include 100% DC parameters, sample testing of input-output insulation leakage current and appropriate AC parameters. Contact your local field representative for pricing and availability of these programs.

PLASTIC OPTOCOUPERS PRECONDITIONING AND SCREENING 100%

COMMERCIAL BURN-IN**

Examinations or Tests	MIL-STD-883 Methods	Conditions
1. Commercial Burn-in	1015	$T_A = 70^\circ\text{C}$, 160 hours per designated circuit.
2. Electrical Test		Per specified conditions and min./max. limits at $T_A = 25^\circ\text{C}$

SCREENING PROGRAM**

Examinations or Tests	MIL-STD-883 Methods	Conditions
1. High Temperature Storage	1008	24 hours at 125°C
2. Temperature Cycling	1010	10 cycles, -55°C to $+125^\circ\text{C}$
3. Burn-in	1015	$T_A = 70^\circ\text{C}$, 160 hours per designated circuit
4. Electrical Test		Per specified conditions and min./max. limits at $T_A = 25^\circ\text{C}$
5. External Visual	2009	

**Contact your field salesman for details.



Radiation Immunity of Hewlett-Packard Optocouplers

This application note describes the immunity of Hewlett-Packard optocouplers to the effects of high radiation environments, such as those encountered in military and space applications. According to MIL-HDBK-279,

"Optical isolators (i.e. optocouplers) are a combination of a GaAs LED and either a photodiode or phototransistor. The isolators containing phototransistors are more sensitive to irradiation than those containing photodiodes."^[1]

HP optocouplers use photodiodes, whereas many optocouplers use phototransistors in their designs. Several HP optocouplers have been exposed to high levels of neutron fluence and gamma radiation. The results of these tests, presented here, show that HP optocouplers are relatively immune to high radiation levels and are thus well-suited for applications where radiation hardness is desirable.

RADIATION FUNDAMENTALS

An optocoupler, as any solid state electronic device, degrades in performance as a result of exposure to radiation. The extent of degradation depends upon the type of radiation encountered, as well as exposure level and duration.

Radiation Types: Particles and Photons

There are two basic types of radiation: particles and photons. Particles (neutrons, protons, and electrons) have mass, energy, and sometimes charge. Photons (gamma rays, x-rays) are bundles of electromagnetic energy with no mass or charge. Particle radiation is measured in terms of fluence (particles/area), whereas photon radiation is measured in terms of total dose (rads [Si]) and dose rate (rads[Si]/sec). One rad is the radiation absorbed dose which releases 100 ergs of energy per gram of absorbing material, in this case silicon (Si).

Radiation Environments: Space and Military

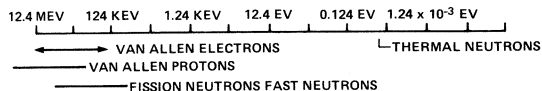
Radiation environments typically consist of both particles and photons. Natural space radiation contains high-energy gamma rays, Van Allen protons and electrons which combine to give a significant total dose over time. Maximum

fluences are 10^4 protons/cm² (3 rad/hour equivalent) and 10^{10} electrons/cm² (100 rad/hour equivalent).^[2] In contrast, military radiation environments caused by a nuclear blast last less than one microsecond. Huge neutron fluences (10^{12} neutrons/cm²) and gamma ray dose rates of 10^9 rads [Si]/sec characterize this environment.^[3]

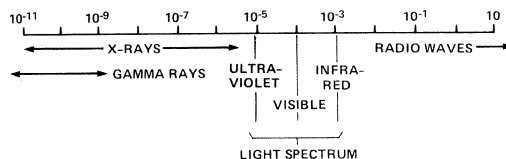
Radiation Damage: Displacement and Ionization

The ability of radiation to penetrate matter and cause damage varies as a function of mass, energy, and charge. Neutrons and protons have more mass than electrons and are therefore more harmful. Radiation occurs over a broad spectrum (Figure 1), but energies of 0.1 MeV or greater cause significant damage. Charged particles (protons, electrons) have much shorter penetration depths than do neutrons and gamma rays of the same energy. Neutrons are largely responsible for permanent displacement damage in optocouplers, whereas transient ionization damage is mostly due to gamma radiation.

FOR PARTICLES AND PHOTONS ENERGY (ELECTRON VOLTS)



FOR PHOTONS WAVELENGTH (CENTIMETERS)



FREQUENCY (HERTZ)

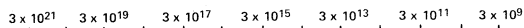


Figure 1. Radiation Spectrum Nomograph

High-energy neutrons strike and displace atoms from their normal positions in the crystal lattice, resulting in a vacancy and an interstitial atom. These defects are equivalent to semiconductor impurities; they have energy levels in the forbidden gap and can act as recombination centers.^[4] Consequently, carrier lifetimes decrease and the material's effective resistivity increases. These effects combine to impair device performance in a permanent way. In optocouplers, fluences above 10^{12} neutrons/cm² lead to dimmer LEDs, reduced optical channel transmittance, decreased photodiode efficiency, and less transistor gain.^[5]

High-energy gamma rays impart energy to electrons (and holes) in the crystal lattice, exciting them to nonequilibrium (ionized) states. During exposure, photocurrent surges are produced in the depletion regions of reverse-biased pn junctions. These surges are dose rate dependent and can induce an erroneous high ("off") to low ("on") output transition. At dose rates above 10^9 rads(Si)/sec, photocurrents in the 1 — 1000 mA range occur which can cause device latch-up and burn out. At all dose rates, the accumulated total dose leads to noticeable (but not irreversible) degradation. Total doses as low as 10^4 rads(Si) can impair optocoupler performance through increased leakage currents.^[6]

OPTOCOUPLER RADIATION RESPONSE

Radiation tests have been performed on a variety of HP optocouplers under a wide range of conditions over the last ten years. In every case, the primary conclusion is that the HP photo IC design yields superior immunity to high radiation levels.

Note: This document contains new data not available for the previous publication of AN 1023. As radiation data becomes available, it will be included in subsequent versions.

Figure 2 illustrates the difference between photodiode and phototransistor style optocouplers. The former distinguishes the optical detection and amplification functions with separate photodiode and transistor stages. This design permits shallower diffusion depths and a smaller transistor base area. Phototransistor optocouplers, on the other hand, maximize the base area for increased optical coupling. This scheme makes the device very susceptible to radiation. At the same radiation level, the device with the smaller exposed sensitive area will experience less radiation damage and hence perform better.^[7]

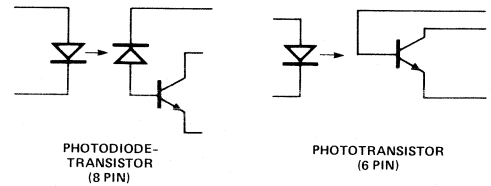


Figure 2. Photodiode and Phototransistor Optocoupler Schematics

CTR (Current Transfer Ratio) is a convenient figure of merit for measuring optocoupler performance. It is defined as the ratio of output collector current (I_O) to input forward LED current (I_F) expressed as a percent. A handy overall transfer characteristic, it gives us the device gain in the "on" state. We will examine CTR degradation, calculated as change in CTR (final CTR — initial CTR) divided by the initial value.

The following HP hermetic optocouplers demonstrate stable operation after exposure to the following radiation levels:

1. **Neutron Fluence:** 4.0×10^{12} neutrons/cm² (8)
Devices Tested: 6N134, 6N140, 4N55
2. **Gamma Total Dose:** 3.0×10^5 rads (Si) (9)
Device Tested: 6N134

Only the 6N134 was tested for immunity to total dose radiation. Since it experienced negligible (<5%) CTR degradation we expect that the device's true total dose hardness limit is higher (over 10^6 rads (Si)). Furthermore, since the 6N140 and 4N55 exhibit responses similar to the 6N134 when exposed to harsh neutron radiation, we expect their total dose immunity to be high as well. Tested devices were not taken to destruction, so the true radiation hardness limits of the devices are not known at this time.

Figure 3 illustrates the radiation performance of the 6N140 and 4N55. As expected, neutrons cause more severe and permanent damage than gamma rays. Performance degrades with increasing radiation level. At the same radiation level, CTR degradation is more pronounced at lower drive current (I_F).

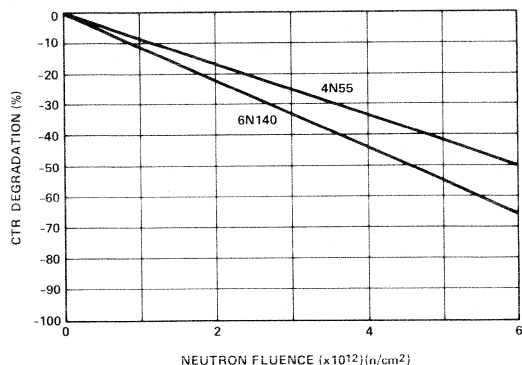


Figure 3. HP Optocoupler Neutron Fluence Response

This data reinforces our confidence in the HP optocoupler design as intrinsically superior in terms of radiation hardness. With shallower photodiode and transistor base diffusion depths than those of phototransistor optocouplers, the HP device minimizes the capture volume exposed to harmful radiation.

Table 1. Radiation Hardness Assurance Levels

RHA Level Designator	Radiation and Total Dose (rads)	Level of Neutron Fluence (n/cm ²)
/	No RHA	No RHA
M	3000	2×10^{12}
D	10^4	2×10^{12}
R	10^5	1×10^{12}
H	10^6	1×10^{12}

Table 1 shows the US Government RHA (radiation hardness assurance) levels for JAN qualified Class B (military) and Class S (space) microelectronic devices^[10]. Levels M and D generally apply to military components, whereas levels R and H are important for devices used in space applications. The radiation data presented here demonstrate that HP hermetic optocouplers continue to operate up to and beyond the highest RHA neutron fluence level. In addition, the data suggest that the devices will pass the RHA gamma total dose levels as well. In fact, MIL-HDBK-279 states that "in general, optical isolators are within manufacturer's specification to 10^6 rads."^[11]

CONCLUSION

In summary, HP optocouplers offer superior immunity to the effects of a variety of high radiation environments, making them a logical choice for military and space applications

where radiation hardness is desirable. We wish to thank the staff of the Nuclear Effects Laboratory of White Sands Missile Range, White Sands, New Mexico, for their support.

APPENDIX

Military Documents Relating to Radiation Testing and Device Qualification

1. MIL-STD-883C, "Test Methods and Procedures for Microelectronics", 25 Aug. 1983.

Group E: Radiation Hardness Assurance Tests

Method 1017.2, Neutron Irradiation

Method 1019.2, Steady State Total Dose Procedure

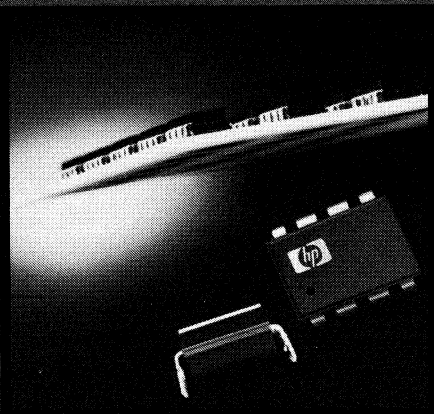
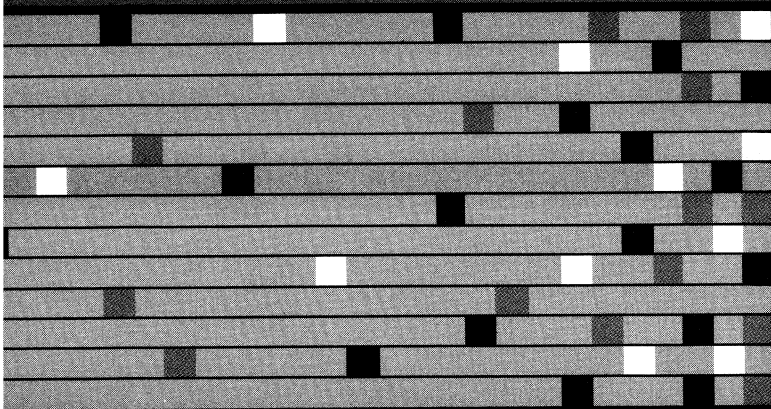
2. MIL-HDBK-280, "Neutron Hardness Assurance Guidelines for Semiconductor Devices and Microcircuits", 1984.
3. MIL-HDBK-279, "Total-Dose Hardness Assurance Guidelines for Semiconductor Devices and Microcircuits", 1984.
4. MIL-M-38510F, "Military Specification Microcircuits, General Specification for", 31 Oct. 1983.

NOTES AND REFERENCES

1. MIL-HDBK-279, 1984, p.41.
2. Myers, David K., "Space and Nuclear Environments and Their Effects on Semiconductors", *Electronic Engineer*, Sept., 1967
3. Rose, Marion, "Nuclear Hardening of Weapons Systems" (Parts I, II, and III), *Defense Electronics*, Sept., Oct., Nov., 1979.
4. Grove, Andrew S., *Physics and Technology of Semiconductor Devices*, Wiley, 1967, p.143.
5. Tirado, Joseph, "Rad-Tolerant ICs Are Available Off The Shelf", *Defense Electronics*, Dec., 1984, p.56.
6. Soda, K.J., Barnes, C.E., Kiehl, R.A., "The Effect of Gamma Irradiation on Optical Isolators", *IEEE Transactions on Nuclear Science*, Vol. NS-22, No. 6, Dec., 1975, p.2475.
7. Epstein, A.S., and Trimmer, P.A., "Radiation Damage and Annealing Effects in Photon Coupled Isolators", *IEEE Transactions on Nuclear Science*, Vol. NS-19, p.391.
8. Radiation data courtesy of the Nuclear Effects Laboratory, White Sands Missile Range, White Sands, New Mexico.
9. Price, William E., et. al., "Total-Dose Radiation Effects Data for Semiconductor Devices", *Jet Propulsion Laboratory Publication 81-66*, Volume 1, August, 1981, pp. 6-168, 169.
10. MIL-M-38510F, p.11.
11. MIL-HDBK-279, p.41.



High Speed/High Gain Optocouplers



High Speed/High Gain Optocouplers

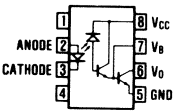


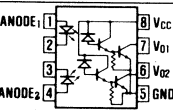


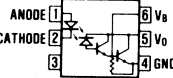


High Gain Family — This family offers high (800%) current transfer ratios and encompasses both conventional 6 pin, Darlington output devices and 8 pin “split collector” detector devices for logic compatible V_{OL} . These optocouplers are useful in low power applications and in long length or multidrop line receivers where input currents are low.

Transistor Output Family — HP's unique integrated photo IC technology brings orders of magnitude better speed performance than attainable with phototransistor type optocouplers by reducing the base-collector

(Miller) capacitance. This family of devices also offers improved linearity for analog signal isolation and is compatible with most logic families.

Logic Gate Family — In order to simplify interfacing optocouplers to logic systems, HP offers the broadest range of logic gate output optocouplers. These products offer data rates from 1 Mb/s to 10 Mb/s, high common mode rejection as well as features like 3-state outputs, low drive currents and wide V_{CC} ranges to simplify designs with popular logic families.

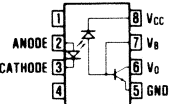
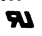
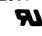
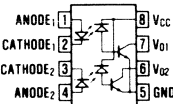
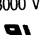
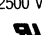
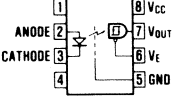


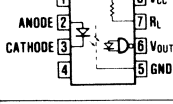


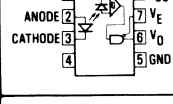


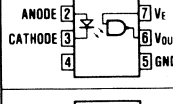


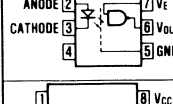


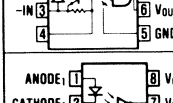


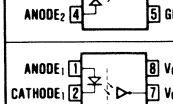
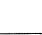

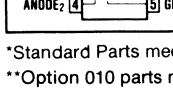
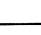
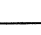
High Gain Optocouplers

Device	Description	Application ^[1]	Typical Data Rate (NRZ)	Current Transfer Ratio	Specified Input Current	Withstand Test Voltage	
						Standard*	Option 010**
	6N138	Line Receiver, Low Current Ground Isolation, TTL/TTL, LSTTL/TTL, CMOS/TTL	100k bit/s	300% Min.	1.6 mA	3000 V dc 	2500 V ac 
	6N139	Line Receiver, Ultra Low Current Ground Isolation, CMOS/LSTTL, CMOS/TTL, CMOS/CMOS		400% Min.	0.5 mA		
	HCPL-2730	Line Receiver, Polarity Sensing, Low Current Ground Isolation	100k bit/s	300% Min.	1.6 mA	3000 V dc 	2500 V ac 
	HCPL-2731			400% Min.	0.5 mA		
	4N45	AC Isolation, Relay-Logic Isolation	3k bit/s	250% Min.	1.0 mA	3000 V dc 	2500 V ac 
	4N46			350% Min.	0.5 mA		

Optocoupler Options

Option	Description
010	Special construction and testing to ensure the capability to withstand 2500 V ac input to output for one minute. Testing is recognized by Underwriters Laboratories, Inc. (File No. E55361). This specification is required by U.L. in some applications where working voltages can exceed 220 V ac.
100	Surface mountable optocoupler in a standard sized dual-in-line package with leads trimmed (butt joint). Provides an optocoupler which is compatible with surface mounting processes.

High Speed Optocouplers

Device	Description	Application[1]	Typical Data Rate (NRZ)	Current Transfer Ratio	Specified Input Current	Withstand Test Voltage	
						Standard*	Option 010**
	6N135	Transistor Output	1 M bit/s	7% Min.	16 mA	3000 V dc 	2500 V ac 
	6N136						
	HCPL-4502						
	HCPL-2502	Pin 7 Not Connected					
	SL5505	Telephone circuits. Approved by CNET	1 M bit/s	15% Min. 40% Max.	16 mA	1500 V dc	
	HCPL-2530	Dual Channel Transistor Output	1 M bit/s	7% Min.	16 mA	3000 V dc 	2500 V ac 
	HCPL-2531						
	HCPL-2200	Low Input Current Optically Coupled Logic Gate 3 State Output VCC = 20 V Max.	5 M bit/s	4 TTL Loads	1.6 mA	3000 V dc 	2500 V ac 
	HCPL-2300	Low Input Current. High Speed Opto-Coupler	8 M bit/s	5 TTL Loads	0.5 mA	3000 V dc 	2500 V ac 
	HCPL-2400	20 MBaud, High Common Mode Rejection, Optically Coupled Logic Gate 3 State Output	40 M bit/s	5 TTL Loads	5.0 mA	3000 V dc 	2500 V ac 
	6N137	Optically Coupled Logic Gate	10 M bit/s	8 TTL Loads	5.0 mA	3000 V dc 	2500 V ac 
	HCPL-2601	High Common Mode Rejection, Optically Coupled Logic Gate	10 M bit/s	8 TTL Loads	5.0 mA	3000 V dc 	2500 V ac 
	HCPL-2602	Optically Coupled Line Receiver	10 M bit/s	8 TTL Loads	5.0 mA	3000 V dc 	2500 V ac 
	HCPL-2630	Dual Channel Optically Coupled Gate	10 M bit/s	8 TTL Loads	5.0 mA	3000 V dc 	2500 V ac 
	HCPL-2631	Dual Channel, High Common Mode Rejection, Optically Coupled Logic Gate	10 M bit/s	8 TTL Loads	5.0 mA	3000 V dc 	2500 V ac 

*Standard Parts meet the UL1440 V ac test for 1 minute.
**Option 010 parts meet the UL 2500 V ac test for 1 minute.

HIGH SPEED/
HIGH GAIN
OPTOCOUPERS



CMOS Circuit Design Using Hewlett-Packard Optocouplers

INTRODUCTION

The purpose of this bulletin is to provide the CMOS designer with a set of useful interface circuits incorporating Hewlett-Packard optocouplers. HP offers a wide variety of optocouplers suitable for use in the low current, low power CMOS design environment. Typical applications include logic system isolation, ground loop elimination, logic level translation, microprocessor system interface, computer-peripheral interface, and line receiver applications.

HEWLETT-PACKARD CMOS COMPATIBLE OPTOCOUPLEDERS

The HCPL-2300 optocoupler (Table 1, Figure 1) offers the unique combination of low LED operating drive current of 0.5 mA at a 5 MBd data rate. Power supply voltage is rated at +7 V max and the open collector output is rated at +18 volts. A 1K Ω internal pull-up resistor eliminates the need for an external pull-up resistor, if so desired. An internal shield, which shunts capacitively coupled common mode noise to ground, improves common mode transient immunity.

The HCPL-2200 optocoupler (Table 1, Figure 2) has +20 V maximum power supply and output voltage ratings. At a drive current of 1.6 mA, a 2.5 MBd data rate is achievable. The HCPL-2200 also features the internal shield to improve common mode transient immunity.

The 6N139 optocoupler (Table 1, Figure 3) has a low input drive current requirement of 0.5 mA, as well as +18 V power supply and output voltage capabilities. The data rate can be increased to 100 KBd by connecting a 51K Ω emitter-base bypass resistor between pins 5 and 7. This resistor provides an alternate path for output current to flow, which shortens transition times and effectively increases data rate capability.

The HCPL-2731 optocoupler (Table 1, Figure 4) performs as a dual channel version of the 6N139 and features an internal emitter-base bypass resistor. The power supply and output voltages are also rated at +18 V max.

RECOMMENDED CIRCUIT DESIGNS

The shunt drive interface circuit (Table 1, Figure 5) provides optimal speed performance, protection against leakage current through the LED, and reduced common mode influences associated with switching a floating LED. The diode, D1, is required for active devices to ensure that the

drive current originates from the power supply and not the device output. The low forward voltage of the diode, D1, ensures that the LED remains off when the driver switches low. The capacitor, C_p, can be used with the HCPL-2300 to correct pulse width distortion by substantially delaying the turn-on time of the LED while leaving the turn-off time nearly the same.

The active CMOS series drive (Table 1, Figure 6) does not require a diode, thus saving the designer one component. The capacitor, C_p, functions as a peaking capacitor by effectively dumping charge to and from the HCPL-2300 LED when switching. This circuit, however, does not provide protection from leakage current and its switching action is slightly slower due to the total interruption of current rather than the re-direction of it as seen in the shunt drive circuit.


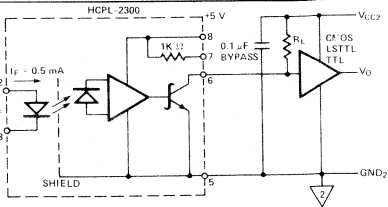
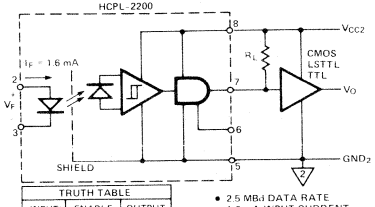
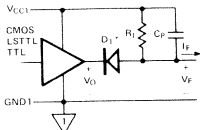
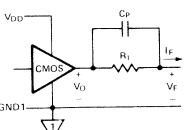
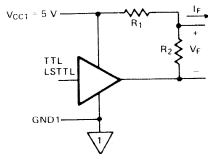
The open collector LSTTL/TTL series drive interface circuit (Table 1, Figure 7) also provides leakage current protection. The resistor, R₂, shunts up to 250 μ A of leakage current away from the optocoupler input terminals, protecting the LED from undesired conduction when the driver output transistor is in the off state.

On the output side, a pull-up resistor is required for use with the open collector HCPL-2300, 6N139, and HCPL-2731. A pull-up resistor is recommended for use in CMOS designs with the HCPL-2200 to improve data rate, but is optional due to the device's three-state output.

The circuit parameters of Table 1 were obtained with low power dissipation as the main design objective, in keeping with CMOS characteristics. However, data rate capability can be improved with increased I_F and I_O. When R_i and R_L are decreased in value, the respective RC time constants which correspond to the input and output circuitry decrease to an optimum value. This yields faster transition times, lower pulse width distortion and higher data rate capability at the expense of greater power dissipation.

To choose an optocoupler and drive circuit suitable for a particular application, the designer should select the optocoupler which best matches the data rate and input current requirements. Then, a drive circuit can be chosen: shunt drive is recommended for speed and leakage current protection; series drive is recommended if the designer wants to minimize the number of components. The individual component values are then selected according to the power supply voltages indicated in Table 1.

Table 1. Optocoupler Circuit Configurations for use in CMOS Circuit Design

<div><p>OPTOCOUPERS</p></div>	<div><ul style="list-style-type: none">• 5 MBd DATA RATE• 0.5 mA INPUT CURRENT• INTERNAL SHIELD FOR GUARANTEED COMMON MODE REJECTION• OPTIONAL INTEGRATED PULL-UP RESISTOR</div> <p>Figure 1. HCPL-2300</p>						<div><p>TRUTH TABLE</p><table><tr><th>INPUT</th><th>ENABLE</th><th>OUTPUT</th></tr><tr><td>H</td><td>H</td><td>Z</td></tr><tr><td>L</td><td>H</td><td>H</td></tr><tr><td>L</td><td>L</td><td>L</td></tr></table><ul style="list-style-type: none">• 2.5 MBd DATA RATE• 1.6 mA INPUT CURRENT• THREE STATE OUTPUT</div> <p>Figure 2. HCPL-2200</p>						INPUT	ENABLE	OUTPUT	H	H	Z	L	H	H	L	L	L																															
	INPUT	ENABLE	OUTPUT																																																				
H	H	Z																																																					
L	H	H																																																					
L	L	L																																																					
<table><tr><td>V_{CC1} (V dc)</td><td>R_I (KΩ)</td><td>C_P</td><td>D_1</td><td>V_{CC2} (V dc)</td><td>R_L (KΩ)</td><td>V_{CC1} (V dc)</td><td>R_I (KΩ)</td><td>D_1</td><td>V_{CC2} (V dc)</td><td>R_L (KΩ)</td></tr><tr><td>+5</td><td>6.19</td><td>20 pF</td><td>1N5711</td><td>+5</td><td>1.00 Internal</td><td>+5</td><td>2.15</td><td>1N916</td><td>+5</td><td>1.1</td></tr><tr><td>+10</td><td>14.7</td><td>20 pF</td><td>1N5711</td><td>+10</td><td>2.37</td><td>+10</td><td>5.11</td><td>1N916</td><td>+10</td><td>2.37</td></tr><tr><td>+15</td><td>21.5</td><td>20 pF</td><td>1N5711</td><td>+15</td><td>3.16</td><td>+15</td><td>8.25</td><td>1N916</td><td>+15</td><td>3.83</td></tr></table>												V_{CC1} (V dc)	R_I (K Ω)	C_P	D_1	V_{CC2} (V dc)	R_L (K Ω)	V_{CC1} (V dc)	R_I (K Ω)	D_1	V_{CC2} (V dc)	R_L (K Ω)	+5	6.19	20 pF	1N5711	+5	1.00 Internal	+5	2.15	1N916	+5	1.1	+10	14.7	20 pF	1N5711	+10	2.37	+10	5.11	1N916	+10	2.37	+15	21.5	20 pF	1N5711	+15	3.16	+15	8.25	1N916	+15	3.83
V_{CC1} (V dc)	R_I (K Ω)	C_P	D_1	V_{CC2} (V dc)	R_L (K Ω)	V_{CC1} (V dc)	R_I (K Ω)	D_1	V_{CC2} (V dc)	R_L (K Ω)																																													
+5	6.19	20 pF	1N5711	+5	1.00 Internal	+5	2.15	1N916	+5	1.1																																													
+10	14.7	20 pF	1N5711	+10	2.37	+10	5.11	1N916	+10	2.37																																													
+15	21.5	20 pF	1N5711	+15	3.16	+15	8.25	1N916	+15	3.83																																													
<div><p>*DIODE D1 NOT REQUIRED FOR UNITS WITH OPEN-COLLECTOR OUTPUT.</p></div> <p>Figure 5. CMOS/LSTTL/TTL Shunt Drive Circuit</p>	<table><tr><td>V_{DD} (V dc)</td><td>R_I (KΩ)</td><td>C_P</td><td>V_{CC2} (V dc)</td><td>R_L (KΩ)</td><td>V_{CC1} (V dc)</td><td>R_I (KΩ)</td><td>V_{CC2} (V dc)</td><td>R_L (KΩ)</td></tr><tr><td>+5</td><td>5.11</td><td>20 pF</td><td>+5</td><td>1.00 Internal</td><td rowspan="2">+5</td><td rowspan="2">7.5</td><td>+5</td><td>1.1</td></tr><tr><td>+10</td><td>13.3</td><td>20 pF</td><td>+10</td><td>2.37</td><td>+10</td><td>2.37</td></tr><tr><td>+15</td><td>19.6</td><td>20 pF</td><td>+15</td><td>3.16</td><td>+15</td><td>7.5</td><td>+15</td><td>3.83</td></tr></table>											V_{DD} (V dc)	R_I (K Ω)	C_P	V_{CC2} (V dc)	R_L (K Ω)	V_{CC1} (V dc)	R_I (K Ω)	V_{CC2} (V dc)	R_L (K Ω)	+5	5.11	20 pF	+5	1.00 Internal	+5	7.5	+5	1.1	+10	13.3	20 pF	+10	2.37	+10	2.37	+15	19.6	20 pF	+15	3.16	+15	7.5	+15	3.83										
V_{DD} (V dc)	R_I (K Ω)	C_P	V_{CC2} (V dc)	R_L (K Ω)	V_{CC1} (V dc)	R_I (K Ω)	V_{CC2} (V dc)	R_L (K Ω)																																															
+5	5.11	20 pF	+5	1.00 Internal	+5	7.5	+5	1.1																																															
+10	13.3	20 pF	+10	2.37			+10	2.37																																															
+15	19.6	20 pF	+15	3.16	+15	7.5	+15	3.83																																															
<div><p>NOTE: USE OF THIS DRIVE CIRCUIT WILL REDUCE DATA RATE CAPABILITY BY APPROXIMATELY 20%.</p></div> <p>Figure 6. Active CMOS Series Drive Circuit</p>	<table><tr><td>V_{CC1} (V dc)</td><td>R_1 (KΩ)</td><td>R_2 (KΩ)</td><td>V_{CC2} (V dc)</td><td>R_L (KΩ)</td><td>V_{CC1} (V dc)</td><td>R_1 (KΩ)</td><td>R_2 (KΩ)</td><td>V_{CC2} (V dc)</td><td>R_L (KΩ)</td></tr><tr><td>+5</td><td>3.48</td><td>3.16</td><td>+5</td><td>1.0 Internal</td><td>+5</td><td>1.33</td><td>3.16</td><td>+5</td><td>1.1</td></tr><tr><td colspan="4"></td><td>+10</td><td>2.37</td><td colspan="3"></td><td>+10</td><td>2.37</td></tr><tr><td colspan="4"></td><td>+15</td><td>3.16</td><td colspan="3"></td><td>+15</td><td>3.83</td></tr></table>											V_{CC1} (V dc)	R_1 (K Ω)	R_2 (K Ω)	V_{CC2} (V dc)	R_L (K Ω)	V_{CC1} (V dc)	R_1 (K Ω)	R_2 (K Ω)	V_{CC2} (V dc)	R_L (K Ω)	+5	3.48	3.16	+5	1.0 Internal	+5	1.33	3.16	+5	1.1					+10	2.37				+10	2.37					+15	3.16				+15	3.83		
V_{CC1} (V dc)	R_1 (K Ω)	R_2 (K Ω)	V_{CC2} (V dc)	R_L (K Ω)	V_{CC1} (V dc)	R_1 (K Ω)	R_2 (K Ω)	V_{CC2} (V dc)	R_L (K Ω)																																														
+5	3.48	3.16	+5	1.0 Internal	+5	1.33	3.16	+5	1.1																																														
				+10	2.37				+10	2.37																																													
				+15	3.16				+15	3.83																																													
<div><p>Figure 7. Open-Collector TTL/LSTTL Series Drive Circuit with Leakage Current Protection</p></div>																																																							

HIGH SPEED/
HIGH GAIN
OPTOCOUPERS

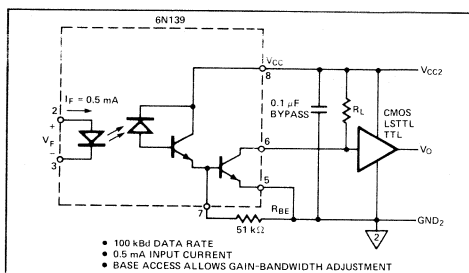


Figure 3. 6N139

V _{CC1} (V dc)	R _I (KΩ)	D ₁	R _{BE} (KΩ)	V _{CC2} (V dc)	R _L (KΩ)
+5	6.81	1N916	51.0	+5	1.1
+10	16.2	1N916	51.0	+10	2.37
+15	26.1	1N916	51.0	+15	3.83

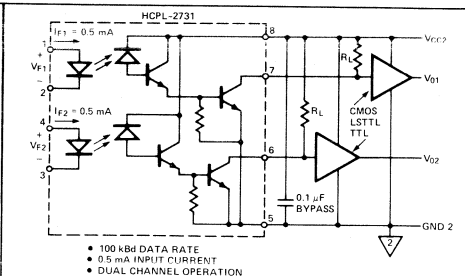


Figure 4. HCPL-2731

V _{CC1} (V dc)	R _I (KΩ)	D ₁	V _{CC2} (V dc)	R _L (KΩ)
+5	6.81	1N916	+5	1.1
+10	16.2	1N916	+10	2.37
+15	26.1	1N916	+15	3.83

V _{CC1} (V dc)	R _I (KΩ)	R _{BE} (KΩ)	V _{CC2} (KΩ)	R _L (KΩ)
+5	6.19	51.0	+5	1.1
+10	16.2	51.0	+10	2.37
+15	23.7	51.0	+15	3.83

V _{CC1} (V dc)	R ₁ (KΩ)	R ₂ (KΩ)	R _{BE} (KΩ)	V _{CC2} (V dc)	R _L (KΩ)
+5	3.16	3.16	51.0	+5	1.1
				+10	2.37
				+15	3.83



Performance of the 6N135, 6N136 and 6N137 Optocouplers in Short To Moderate Length Digital Data Transmission Systems

This application note assists system designers by describing the performance to be expected from the use of HP 6N135-6N137 optocouplers as a line receiver in a TTL-TTL compatible NRZ¹ data transmission link. It describes several useful total systems including line driver, cable, terminations and TTL compatible connections. The systems described utilize inexpensive cable and operate satisfactorily over the range of transmission distances from 1 ft. to 300 ft. Over this range of distances, the data rate varies from 0.6 megabits per second to 19 megabits per second largely limited by coupler performance at short distances, and cable losses at longer distances.

¹ Non-return to zero

HIGH SPEED/
HIGH GAIN
OPTOCOUPERS

INTRODUCTION

Optocouplers can function as excellent alternatives to integrated circuit line receivers in digital data transmission applications. Their major advantages consist of superior common-mode noise rejection and true ground isolation between the two subsystems. For example, a conventional line receiver is limited to a $\pm 20V$ common-mode noise rejection at best from DC over its operating frequency range, while an optocoupler can achieve rejections of $\pm 2.5kV$ at 60Hz.

A conventional optocoupler that utilizes a photo-transistor is limited in its minimum total switching time. At the higher data rates, above 200-500 kbits/s, these delay times can become very significant. The HP 6N135 and 6N136 utilize an integrated photo-diode and transistor to produce lower total switching time. The HP 6N137 adds an integrated amplifier within its package to decrease these delay times still further. All three units can produce data rates well in excess of 500 kbits/s, while the 6N137 can couple an isolated 9.5MHz (19M bits/s) clock from its input to its output. These data rates are achieved with common-mode noise voltage rejection in excess of that provided by most types of line receivers at all frequencies.

The information contained in this application note covers the performance of optocoupler line receiver circuits; however, it does not describe design details. These details are covered in Application Note 947 "Digital Data Transmission Using Optically Coupled Isolators".

This application note describes the basic design elements of a data transmission link and presents several examples of total systems that will be useful to systems designers at distances that range from 1 ft. to 300 ft. and have a mod-

erate overall cost. First, a few measures of performance are defined to allow systems to be compared with one another. Second, the elements of an optocoupler data transmission system are discussed. Third, circuit examples and demonstrated performance of a selected set of systems are presented for the various transmission distances. This presentation includes schematics, representative waveforms at intermediate circuit points, and a summary performance table. It compares the results of passive (resistive) terminations with active terminations that improve overall performance at the longer transmission distances. Fourth, the trade-offs that were made to arrive at the selected system components are described. Along with the trade-offs, there is a discussion of approaches to increase performance by selection of other circuit components or by "peaking" a given length system.

DEFINITIONS OF PERFORMANCE

In data transmission systems that utilize optocouplers, there are no standardized definitions that allow performance capability to be specified. The major performance parameters that are of interest are data rate capability, usually specified in bits per second; and immunity to common mode noise at the coupler input, usually specified as AC or DC common mode voltage rejection in volts, or transient voltage noise rejection in volts/microsecond.

To arrive at a definition of maximum data rate capability requires that the total system be specified including all components, and in addition, data modulation and demodulation techniques. In order to compare the various systems presented in the application note, it is necessary to define some useful terms.

One commonly used modulation technique for digital data transmission is NRZ, or non-return-to-zero transmission. In the most common form of this technique, a twisted pair transmission line is driven by a balanced driver with an alternating plus or minus voltage signal. A number of integrated circuits are available to provide the drive signals and create a straightforward design.

One potential measure of system performance for NRZ, and potentially other modulation techniques as well, is the measurement of the maximum 50% duty cycle clock frequency that the system will pass. Since a clock represents a total 1/0 and 0/1 transition each full cycle, this square wave provides two bits of data for each cycle. As the upper clock frequency limit of a system using couplers is reached, the duty cycle will change from 50%. The MAXIMUM CLOCK DATA RATE is found by observing the system output as a function of a square wave input until the output distorts to a 10% duty cycle and multiplying this frequency by two (two bits/cycle). At this input frequency, the system data rate is very close to its absolute maximum and any potential recovery of a signal at a higher data rate is impractical. A more detailed definition of this term appears in the glossary.

Another parameter indicative of the performance of a system is to measure the system transient response in its worst case condition. The step response of a transmission system using isolators is a function of the duty cycle and repetition rate. For NRZ, if this term is properly defined, it can indicate a worst case maximum data rate that the system will faithfully transmit, regardless of the combination of ones and zeroes in the data bit stream. This step response term will be referred to as the STEP TRANSIENT DATA RATE MAXIMUM. It assumes that the pulse propagation delay down the transmission line is essentially constant, and defines a data rate maximum at which a single bit of data in a stream of all zeroes and a one, or all ones and a zero may be successfully sent through the system. This is simulated by placing a very low frequency square wave input into the line. Then the circuit delay time from a pulse received at the *end* of the line until the system output makes a transition is measured. This delay time is a function of the cable output risetime and the delays experienced in the coupler and its associated circuitry. The specific delay times are called t_{PHL} and t_{PLH} , indicating delay times for a 1/0 and 0/1 transition respectively. The STEP TRANSIENT DATA RATE MAXIMUM is defined as the inverse of t_{PLH} or t_{PHL} , whichever is longer. In general, this data rate will be lower than the MAXIMUM CLOCK DATA RATE. A more exact definition of t_{PHL} , t_{PLH} and STEP TRANSIENT DATA RATE appears in the glossary.

The parameters used to define worst-case common mode noise immunity are measured for the coupler and associated circuitry without the transmission cable. The common mode voltage rejection is a function of frequency and indicates the maximum AC steady state signal voltage common to both inputs and output ground that will not create an error in the output. This rejection reaches a minimum at some frequency. The transient voltage noise immunity is

a measure of the maximum rate of rise (or fall) that can be placed across the common input terminals and output ground without producing an error voltage in the output. This term is a function of the input pulse magnitude and rate of rise for an optocoupler and is stated as a dv/dt minimum in volts per microsecond. Further definitions of these terms appear in the glossary. It should be noted that common mode characteristics of such systems are largely determined by the point at which the noise enters the transmission system. Common mode rejection for a total system would be expected to improve with increasing distance between the common mode insertion point and the input to optocoupler.

ELEMENTS OF AN OPTOCOUPLER DATA TRANSMISSION SYSTEM

The basic elements of an optocoupler transmission system are:

- ☐ Line Driver
- ☐ Transmission Cable
- ☐ Line Termination Circuit
- ☐ Optocoupler
- ☐ TTL Interface Circuit

In order that the performance of systems using the 6N135-6N137 optocouplers might be demonstrated, component elements had to be defined for several systems. These elements are chosen to be TTL compatible at the input and the output. They are also chosen to produce high performance, be moderate in cost, and work over a range of distances of one foot to 300 feet. This can then maximize the utility to systems designers of the circuits demonstrated, thus allowing them to be used without change in a variety of specific applications to produce a known level of performance.

CIRCUIT EXAMPLES AND DEMONSTRATED PERFORMANCE

To reduce the number of complete systems upon which performance is demonstrated to a practical number, a basic representative set of elements must be selected or designed. This includes a single line driver and cable type with performance measurements taken at three transmission distances — 1 ft., 100 ft., and 300 ft. It also includes two termination types, active and passive, and three types of couplers with companion TTL interface circuits. This produces six total data transmission systems upon which data rate performance can be observed at the three transmission distances. Figure 1 illustrates the line driver and cable combination selected. Figure 2 illustrates the pulse response of this driver/cable combination. Figures 3 through 8 indicate the line termination, coupler, and TTL interface circuitry for the various terminations. Included are representative waveforms measured on the three passive termination systems at the 300 ft. transmission distance. Table 1 outlines the critical parameters of the cable used and Tables 2, 3, and 4 summarize the performance demonstrated on all of the transmission systems.

The performance tabulated for the 1 ft. transmission length is indicative of that which might be achieved by a system with negligible performance degradation in the cable. The performance at 100 ft. and 300 ft. indicates the decrease in data rate due to cable losses as the transmission distance increases. This decrease is the most critical data rate limitation and is indicative of the change in performance of systems using low cost cable. Clearly evident in the tables is the increase in performance of the active termination at the 300 ft. transmission distance. Note also that the data rate of the system utilizing the 6N137 at short transmission distances is less with the active than with the passive termination. This decrease is due to the additional delay added by the active termination.

These performance tables can be used to select a design suitable for an application required by a system designer. For example, assume it is desired to design a data transmission system of variable lengths up to 100 ft. and data rates of up to 1.6 Mbits/s. The circuit shown in Figure 4 and the line driver and cable shown in Figure 1 could be selected to assure this level of performance.

SELECTION OF DEMONSTRATION CIRCUIT ELEMENTS

The foregoing systems exemplify achievable performance and incorporate a number of design decisions which are discussed in this section.

LINE DRIVER

Line Drivers generate the signal that is sent down the transmission line. They have limits as to voltage swing, output impedance, and switching time. A good compromise is provided by National Semiconductor's DM 8830. Any similar device with a low output impedance such as the Fairchild 9614 would operate satisfactorily. These devices are TTL input compatible, require no external components, are relatively inexpensive and readily available. They provide adequate performance and produce directly a dual rail (inverting and non-inverting) output.

For systems requiring higher data rates, more sophisticated

and expensive drivers can be selected or designed. Figure 9 illustrates a circuit that has a higher current output and produces a higher data rate than an integrated driver. It uses several components, but does not require a supply voltage above the standard TTL 5 volts. To obtain still higher data rates, the driver line voltage output must be increased. This in turn requires a supply voltage above 5 volts. The National Semiconductor LH 0002C is an example of an integrated circuit that can be used to produce directly a higher line voltage. Numerous other discrete circuits could be designed.

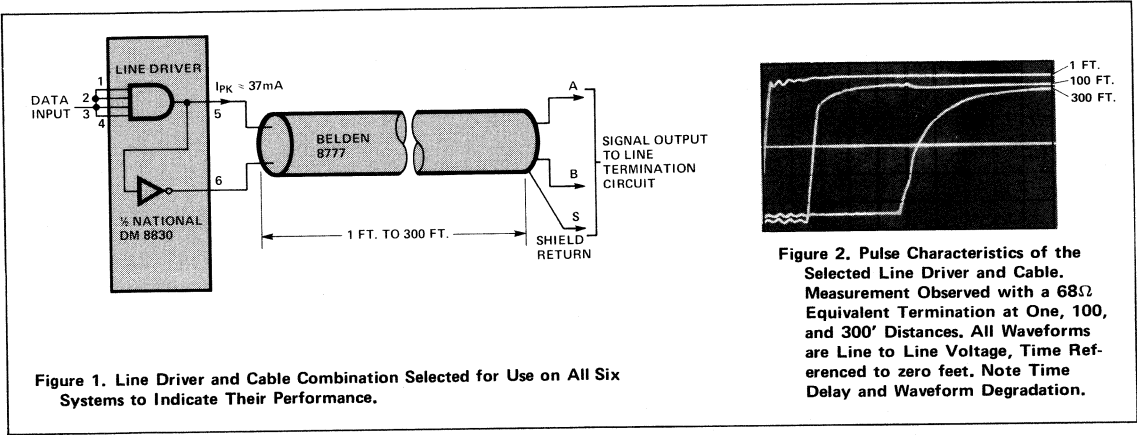
TRANSMISSION CABLE

Transmission cables are very critical in the overall system. They can decrease the effect of extraneous noise voltages on system performance by providing shielding. They also greatly affect the signal losses as the transmission length increases. By controlling these losses, cables can permit a single set of system elements to function adequately for both long and short transmission distances. The critical performance parameters of a transmission cable include cost, transmission length, line series resistance (DC losses), high frequency losses, type and amount of shielding and characteristic impedance.

The Belden type 8777 is representative of a relatively well-shielded, inexpensive cable with typical transmission loss. The important characteristics of this cable are summarized in Table 1.

If it is desired to attain higher performance, the line cost becomes considerably more expensive and tends to dominate system costs. These higher performance cables utilize a large conductor size to lower DC losses, and provide considerably lower losses at high frequencies. Examples of such a cable would be Belden 9269 (IBM 32392), Belden 9250 or their equivalents.

The pulse response of the DM 8830 and the Belden 8777 illustrates the waveform degradation of signals sent down this driver/transmission line pair, regardless of the line receiver employed. Figure 1 illustrates this circuit combination, and Figure 2 illustrates the pulse waveform degradation at 1 ft., 100 ft., and 300 ft. into a 68Ω equivalent load.



LINE TERMINATION CIRCUIT

The line termination circuit converts the voltage arriving at the end of the line to a current impulse to drive the coupler emitter diode. In these system examples, performance of both passive and active circuits was measured.

A passive circuit consists of a set of resistors to match the line to its characteristic impedance and to convert the line voltage to a current. The circuits illustrated here were designed to provide good performance at 300 ft., while not exceeding the coupler input drive current maximum at the 1 ft. line length condition. With this design criterion, these circuits are useful over this *range* of transmission cable lengths. These design characteristics required that two resistive line termination circuits be designed for the three isolators. They are illustrated in Figures 3, 4, and 5.

An improvement in the performance of a resistive termination can be obtained by peaking the line to operate at a specific length as shown in Figure 10. This technique allows the coupler to operate from the peak to peak voltage at the end of the line. To avoid overdriving the coupler, the peaking capacitor value must be minimized. It is chosen by observing the circuit delay time t_{PLH} and selecting the smallest value of capacitor that significantly decreases this delay. With this technique, performance can be expected to improve by as much as 20-30% or more, but the values of peaking capacitor tend to vary with many of the characteristics of components in all of the elements of the system. These include driver output voltage, line length, line losses, coupler delay, etc. This in turn requires each individual system to have a selected value of peaking capacitor.

An active termination utilizes a transistor to act as a line voltage to coupler input current regulator. This technique ignores any attempt to match the line, but instead converts any incoming voltage to a suitable current, once the circuit threshold voltage is exceeded. This tends to decrease circuit sensitivity to line length and other line voltage variations. The delay of an active circuit can limit the maximum system data rate, especially for short transmission distances. But, in general, their use can improve the maximum data rate at the longer distances. In the system examples, two active termination circuits were designed and are illustrated in Figures 6, 7 and 8.

Improving the performance of the active circuit consists of finding transistors and circuit designs to perform the voltage to input current regulation function without limiting overall system performance.

OUTPUT TO TTL INTERFACE

The 6N136 and 6N137 have sufficiently high input to output coupling efficiency (CTR) that the only component required to interface the optocoupler to a TTL input gate is a pull-up resistor. The 6N135 has a somewhat lower CTR and requires an external transistor and resistor to interface with a TTL gate input. The actual circuit configuration and values required for these interface circuits are illustrated in Figures 3 through 8. The circuits illustrate, in general, the optimum interface for a TTL-TTL compatible circuit. Performance could be improved through the use of lower pull-up resistor values in the coupler output collectors and high speed TTL compatible comparators.

Table 1

IMPORTANT LINE CHARACTERISTICS OF BELDEN 8777

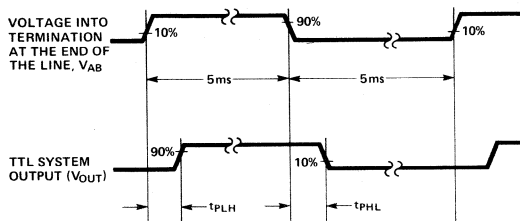
- Three sets of two conductor, twisted and individually foil shielded, 22 gauge wire
- Z_0 (Measured Characteristic Impedance)—68 Ω line to line
- Line-to-line capacitance — 30pF/ft.
- Line Resistance — 3.2 Ω /100 ft. (per conductor pair)
- Attenuation at 10MHz \approx 4 dB/100 ft.
- Delay \approx 1.5 nsec/ft.
- Cost \approx 5¢/ft./Transmission Pair

GLOSSARY

1. **DATA RATE** – This term is typically stated in bits per second and has no standardized definition when used in reference to optocouplers. It is related to the minimum pulse transition time that will be passed by the system and detected. This in turn is related to the distortion or change in duration the pulse experiences upon passing through the system.
2. **STEP TRANSIENT DATA RATE MAXIMUM** – This term, stated in bits per second, is a function of the maximum delay experienced by a 0/1 or a 1/0 transition in passing through the optocoupler. The step transient data rate maximum is defined as:

$$\text{STEP TRANSIENT DATA RATE (MAX)} = \frac{1}{t_{\text{PHL}}} \text{ or } \frac{1}{t_{\text{PLH}}}$$

whichever is smaller. Where t_{PLH} and t_{PHL} are measured at the coupler termination input (end of the line) and the TTL output and are defined as follows:



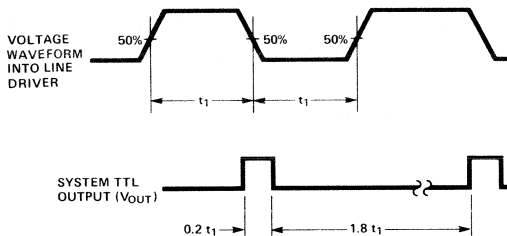
The t_{PHL} and t_{PLH} measured under these conditions approach the maximum delay that will be experienced by data sent through the isolator.

3. **MAXIMUM CLOCK DATA RATE** – This term defines the maximum data rate at which a 50% duty cycle square wave (clock) will be distorted to a 90%/10% pulse. It is

very close to the maximum alternating 1/0 and 0/1 transition that can be passed by the system. It is defined mathematically as:

$$\text{MAXIMUM CLOCK DATA RATE} = \frac{1}{t_1}$$

where t_1 is defined as:



4. **COMMON MODE REJECTION VOLTAGE** – This term is defined as the maximum sinusoidal voltage at a given frequency that can be applied *simultaneously* to both inputs with respect to output ground and not produce an error signal in the system output. In optocouplers, the value of this voltage is very high at low frequencies and decreases with increasing frequency until it reaches a minimum. The effect is caused by the effective inter-circuit capacitance of the emitter and detector chips, and the detector gain and bandwidth. (See Figure 11.)
5. **COMMON MODE dv/dt REJECTION MINIMUM** – This term is defined as the maximum rate of change of voltage that can be applied to both inputs *simultaneously* with respect to output ground and not produce an error in the system output. Note that this parameter is a function of the duration of the change, or equivalently the pulse amplitude. The stated values in this application note are for a 10V step pulse amplitude generated by a source having a controlled risetime and falltime (e.g., HP 8007B). (See Figure 11.)

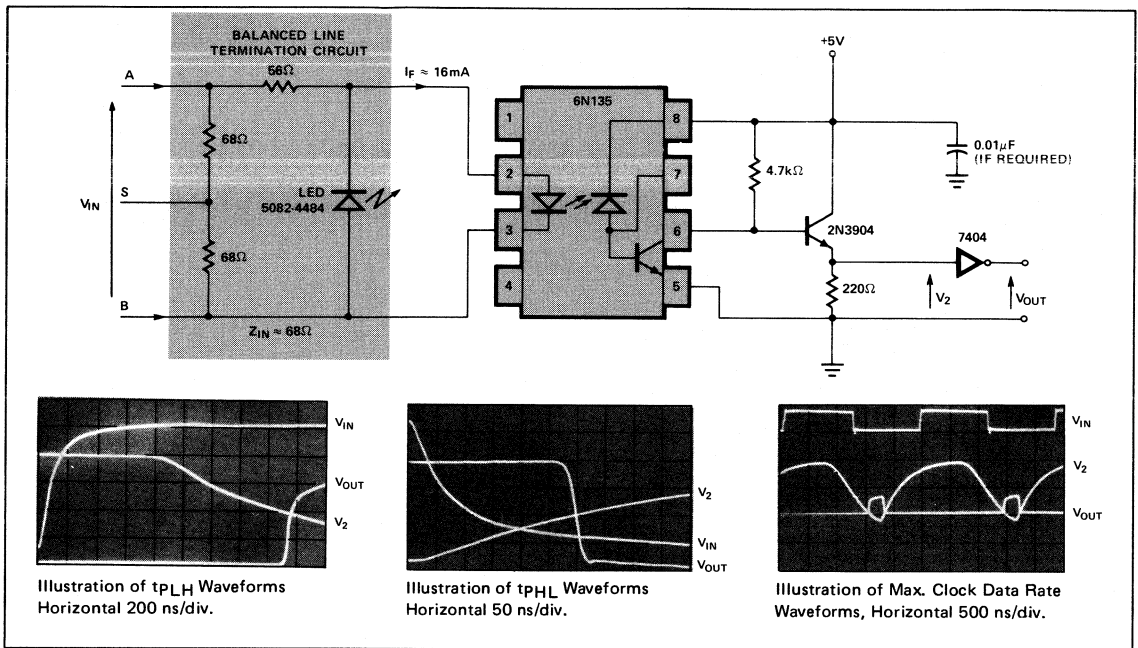


Figure 3. TTL Compatible Passive (Resistive) Termination for the 6N135 and Photographs Indicating Measured Performance at the End of the 300 Ft. Transmission Cable.

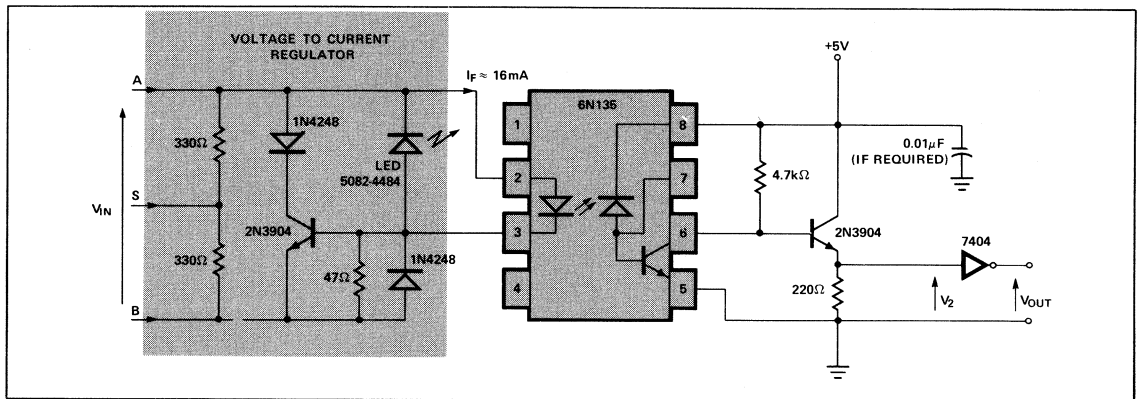


Figure 6. TTL Compatible Active Termination for the 6N135.

Table 2. Summary of Performance of 6N135 Data Transmission Systems at 1, 100, and 300 ft.

Termination	Transmission Distance (ft)	t _{PLH} (ns)	t _{PHL} (ns)	Step Transient Data Rate Max. (Mbits/s)	Clock Data Rate Max. (Mbits/s)	Worst Case Common Mode Noise Rejection	
						Sinusoidal	dV/dt
RESISTIVE (PASSIVE) Fig. 3	1	475	500	2.0	11.2	≤10kHz: 5.0kV pk-pk 1MHz: 84V pk-pk min.	250V/μs min.
	100	900	425	1.1	3.0		
	300	1700	300	0.6	0.8		
ACTIVE Fig. 6	1	500	330	2.0	5.3	≤10kHz: 5.0kV pk-pk 1MHz: 84V pk-pk min.	250V/μs min.
	100	580	270	1.7	4.0		
	300	875	330	1.1	1.6		

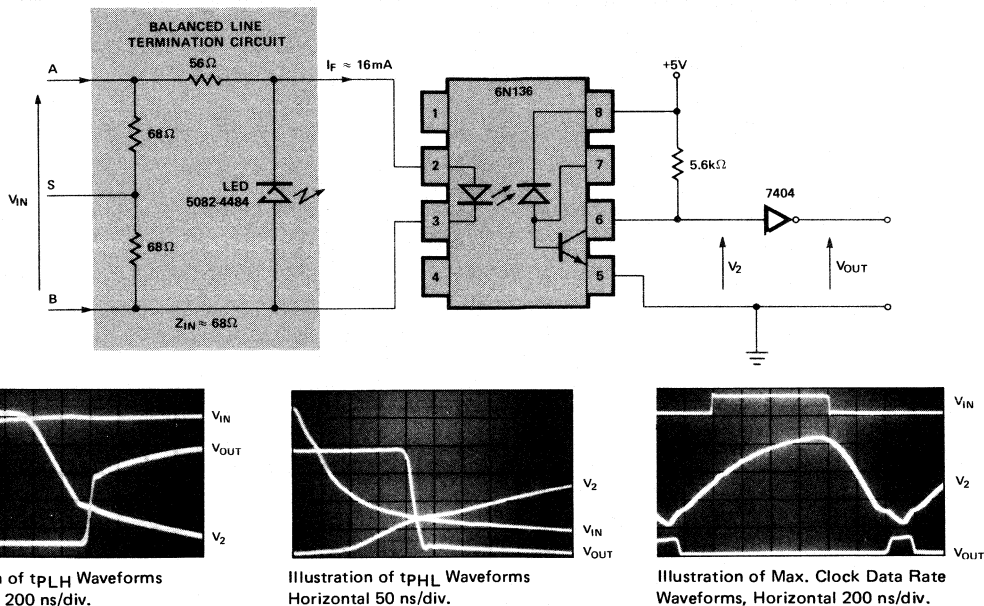


Figure 4. TTL Compatible Passive (Resistive) Termination for the 6N136 and Photographs Indicating Measured Performance at the End of the 300 Ft Cable.

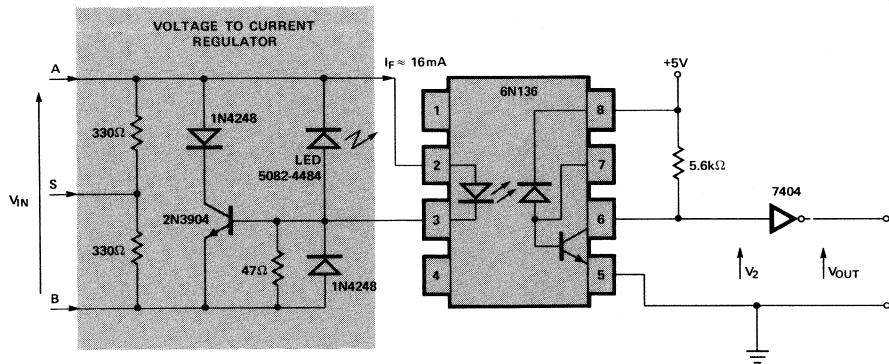


Figure 7. TTL Compatible Active Termination for the 6N136.

Table 3. Summary of Performance of 6N136 Data Transmission Systems at 1, 100, and 300 ft.

	Transmission Distance (ft)	tp _{LH} (ns)	tp _{HL} (ns)	Step Transient Data Rate Max. (Mbits/s)	Clock Data Rate Max. (Mbits/s)	Worst Case Common Mode Noise Rejection	
						Sinusoidal	dV/dt
RESISTIVE (PASSIVE) Fig. 4	1	320	270	2.7	10.0	<10kHz: 5.0kV pk-pk 1MHz: 84V pk-pk min.	250V/μs min.
	100	640	265	1.6	4.0		
	300	1200	220	0.8	1.2		
ACTIVE Fig. 7	1	375	250	2.7	6.6	<10kHz: 5.0kV pk-pk 1MHz: 84V pk-pk min.	250V/μs min.
	100	440	250	2.3	5.0		
	300	700	250	1.4	2.4		

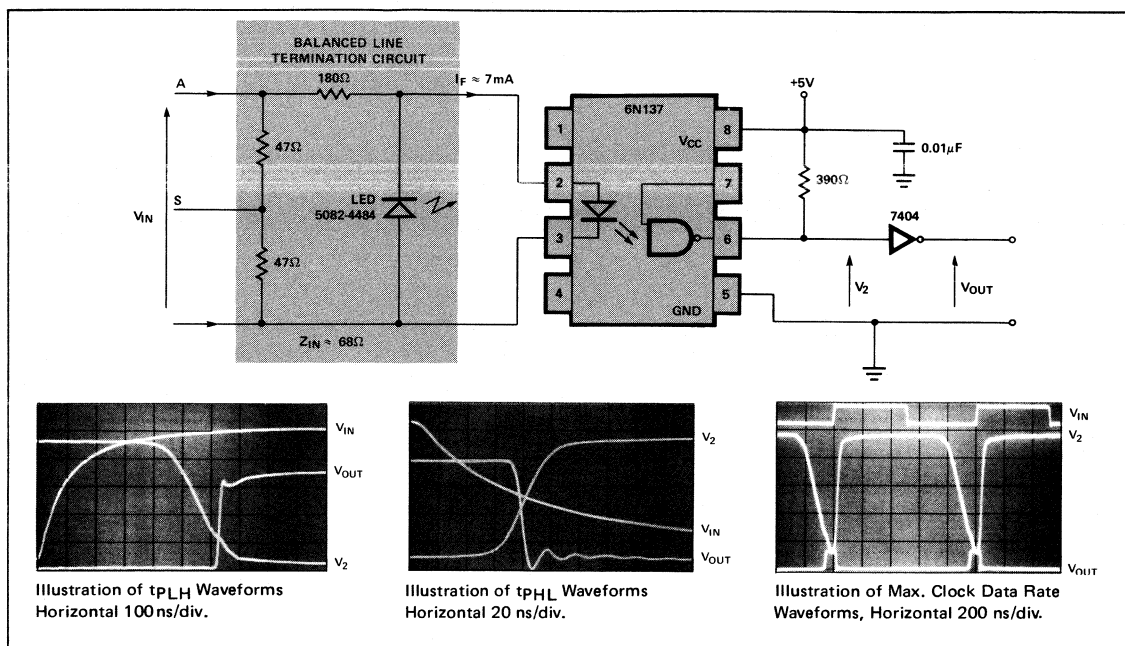


Figure 5. TTL Compatible Passive (Resistive) Termination for the 6N137 and Photographs Indicating Measured Performance at the End of the 300 Ft. Transmission Cable.

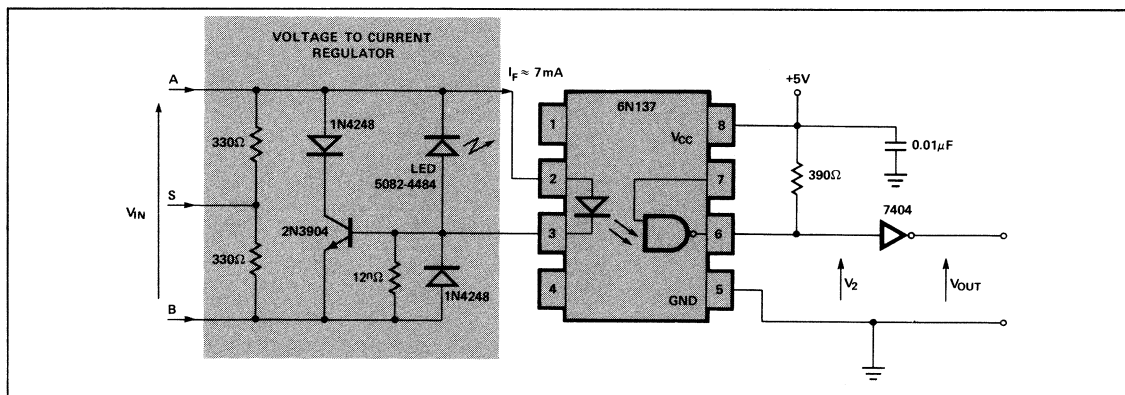


Figure 8. TTL Compatible Active Termination for the 6N137.

Table 4. Summary of Performance of 6N137 Data Transmission Systems at 1, 100, and 300 ft.

	Transmission Distance (ft)	t_{PLH} (ns)	t_{PHL} (ns)	Step Transient Data Rate Max. (Mbits/s)	Clock Data Rate Max. (Mbits/s)	Worst Case Common Mode Noise Rejection	
						Sinusoidal	dV/dt
RESISTIVE (PASSIVE)	1	105	70	9.5	19.0	<10kHz: 5.0kV pk-pk 8MHz: 22V pk-pk min.	40V/ μ s min.
	100	170	70	5.8	8.0		
	300	625	70	1.6	2.0		
ACTIVE	1	190	65	5.3	11.0	<10kHz: 5.0kV pk-pk 8MHz: 22V pk-pk min.	40V/ μ s min.
	100	190	70	5.3	13.2		
	300	275	80	3.9	8.2		

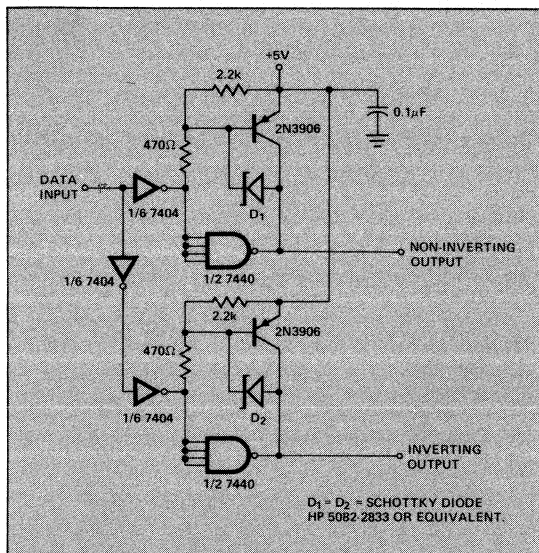


Figure 9. High Output Voltage Swing, High Current, Wide Bandwidth Line Driver that Operates From a 5 Volt Supply and Produces a >8.5V Pk to Pk Pulse into 300 Ft. of Belden 8777 at 10 MHz.

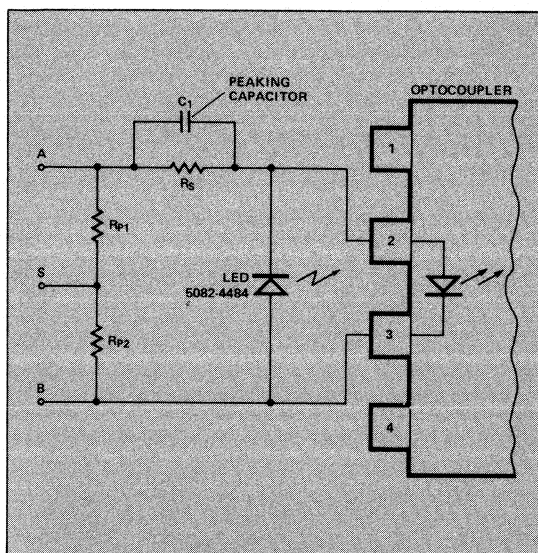


Figure 10. An Example of Circuit Peaking to Improve the Performance of the Passive Termination. C_1 is Chosen for the Minimum Value that Significantly Reduces Input to Output Delay Time. In General, C_1 Must be Selected Individually For Each System.

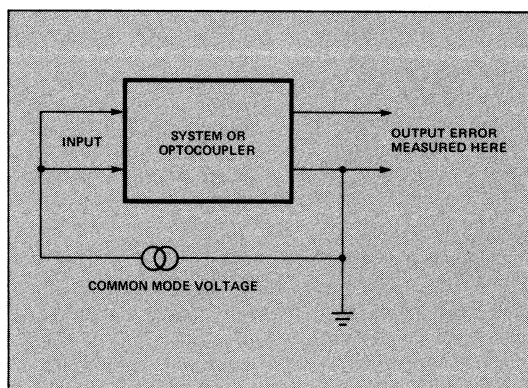


Figure 11. Common Mode Measurement Circuit.

HIGH SPEED/
HIGH GAIN
OPTOCOUPLES



Linear Applications of Optocouplers

Optocouplers are useful in applications where analog or DC signals need to be transferred from one module to another in the presence of a large potential difference or induced noise between the ground or common points of these modules.

Potential applications are those in which large transformers, expensive instrumentation amplifiers or complicated A/D conversion schemes are used. Examples are: sensing circuits (thermocouples, transducers ...), patient monitoring equipment, power supply feedback, high voltage current monitoring, adaptive control systems, audio amplifiers and video amplifiers.

HP's optocouplers have integrated photodetector/amplifiers with speed and linearity advantages over conventional phototransistors. In a photo transistor, the photodetector is the collector-base junction so the capacitance impairs the collector rise time. Also, amplified photocurrent flows in the collector-base junction and modulates the photo-response, thereby causing non-linearity. The photodetector in an HP optocoupler is a separately integrated diode so its photoresponse is not affected by amplified photocurrent and its capacitance does not impair speed. Some linear isolation schemes employ digital conversion techniques (A/D-D/A, PWM, PCM, etc.) in which the higher speed of the integrated photodetector permits better linearity and bandwidth.

The 6N135/6N136 is recommended for single channel AC analog designs. The HCPL-2530/31 is recommended for dual channel DC linear designs. The 6N135/6 series or the 6N137 series are recommended for digital conversion schemes.

If the output transistor is biased in the active region, the current transfer relationship for the 6N135 series optocoupler can be represented as:

$$I_C = K \left(\frac{I_F}{I_F'} \right)^n$$

where I_C is the collector current; I_F is the input LED current; I_F' is the current at which K is measured; K is the collector current when $I_F = I_F'$; and n is the slope of I_C vs. I_F on logarithmic coordinates.

The exponent n varies with I_F , but over some limited range of ΔI_F , n can be regarded as a constant. The current transfer relationship for an opto isolator will be linear only if n equals one.

For the 6N135 series optocoupler, n varies from approximately 2 at input currents less than 5mA to approximately 1 at input currents greater than 16mA. For AC coupled applications, reasonable linearity can be obtained with a single optocoupler. The optocoupler is biased at higher levels of input LED current where the ratio of incremental photodiode current to incremental LED current ($\partial I_D / \partial I_F$) is more nearly constant.

For better linearity and stability, servo or differential linearization techniques can be used.

The servo linearizer forces the input current of one optocoupler to track the input current of the second optocoupler by servo action. Thus, if $n_1 \approx n_2$ over the excursion range, the non linearities will cancel and the overall transfer function will be linear. In the differential linearizer, an input signal causes the input current of one optocoupler to increase by the same amount that input current of the second optocoupler is decreased. If $n_2 \approx n_1 \approx 2$, then a gain increment in the first optocoupler will be balanced by a gain decrement in the second optocoupler and the overall transfer function will be linear. With these techniques, matching of K will not effect the overall linearity of the circuit but will simplify circuit realization by reducing the required dynamic range of the zero and offset potentiometers.

Gain and offset stability over temperature is dependent on the stability of current sources, resistors, and the optocoupler. For the servo technique, changes of K over temperature will have only a small effect on overall gain and offset as long as the ratio of K_1 to K_2 remains constant. With the differential technique, changes of K over temperature will cause a change in gain of the circuit. Offset will remain stable as long as the ratio of K_1 to K_2 remains constant. In the AC circuit, since $(\partial I_D / \partial I_F)$ varies with temperature, the gain will also vary with temperature. A thermister can be used in the output amplifiers of the Differential and AC circuits to compensate for this change in gain over temperature.

There are also several digital techniques to transmit an optocoupler analog signal. Optocouplers can be used to transmit a frequency or pulse width modulated signal. In these applications, overall circuit bandwidth is determined by the required linearity as well as the propagation delay of the optocoupler. The 6N137 series optocoupler features propagation delays typically less than 50ns and

the 6N135 series optocoupler features propagation typically less than 300ns.

In several places the circuits shown call for a current source. They can be realized in several ways. If V_{CC} is stable, the current source can be a mirror type circuit as shown in Figure 1.

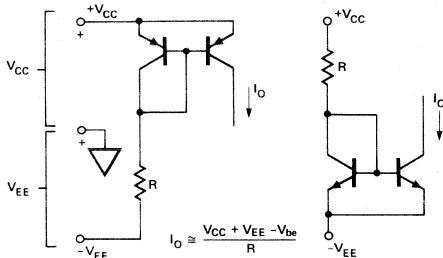


Figure 1.

If V_{CC} is not stable, a simple current source such as the ones shown in Figure 2 can be realized with an LED as a voltage reference. The LED will approximately compensate the transistor over temperature since $\Delta V_{be}/\Delta T \approx \Delta V_F/\Delta T = -2\text{mV}/^\circ\text{C}$:

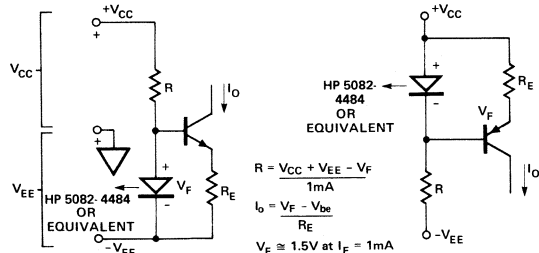


Figure 2.

SERVO ISOLATION AMPLIFIER

The servo amplifier shown in Figure 3 operates on the principle that two optocouplers will track each other if their gain changes by the same amount over some operating region. U_2 compares the outputs of each optocoupler and forces I_{F2} through D_2 to be equal to I_{F1} through D_1 . The constant current sources bias each I_F at 3mA quiescent current. R_1 has been selected so that I_{F1} varies over the range of 2mA to 4mA as V_{IN} varies from -5V to $+5\text{V}$. R_1 can be adjusted to accommodate any desired range. With $V_{IN}=0$, R_2 is adjusted so that $V_{OUT}=0$. Then with V_{IN} at some value, R_4 can be adjusted for a gain of 1. Values for R_2 and R_4 have been picked for a worst case spread of optocoupler or current transfer ratios. The transfer function of the servo amplifier is:

$$V_{OUT} = R_4 \left[\left(\frac{I_{F2}}{I_{F1}} \right)^2 \left(\frac{K_1 R_2 (I_{CC1})^{n_1}}{K_2 R_3 (I_{F1})^{n_1}} \right)^{1/n_2} \left(1 + \frac{V_{IN}}{R_1 I_{CC1}} \right)^{n_1/n_2} - I_{CC2} \right]$$

After zero adjustment, this transfer function reduces to:

$$V_{OUT} = R_4 I_{CC2} \left[(1+x)^n - 1 \right], \text{ where } x = \frac{V_{IN}}{R_1 I_{CC1}}, n = \frac{n_1}{n_2}$$

The non linearities in the transfer function where $n_1 \neq n_2$ can be written as shown below. For example, if $|x| \leq .35$, $n = 1.05$, then the linearity error is 1% of the desired signal.

$$\frac{\text{linearity error}}{\text{desired signal}} = \frac{(1+x)^n - n x - 1}{n x}$$

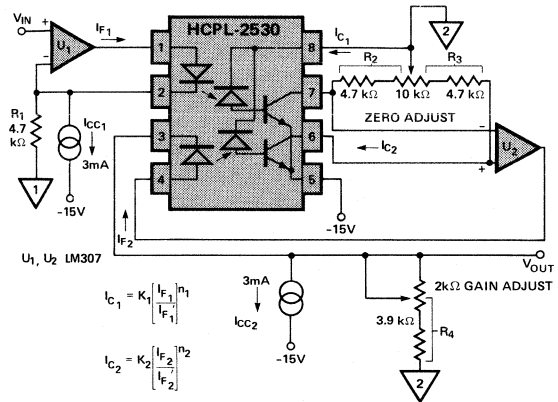


Figure 3. Servo Type DC Isolation Amplifier.

Typical Performance for the Servo Linearized DC Amplifier:

- 1% linearity for 10V p-p dynamic range
- Unity voltage gain
- 25 kHz bandwidth (limited by U_1 , U_2)
- Gain drift: $-.03\%/^\circ\text{C}$
- Offset drift: $\pm 1\text{mV}/^\circ\text{C}$
- Common mode rejection: 46dB at 1 kHz
- 500V DC insulation (3000V if 2 single couplers are used)

DIFFERENTIAL ISOLATION AMPLIFIER

The differential amplifier shown in Figure 4 operates on the principle that an operating region exists where a gain increment in one optocoupler can be approximately balanced by a gain decrement in the second optocoupler. As I_{F1} increases due to changes in V_{IN} , I_{F2} decreases by an equal amount. If $n_1 = n_2 = 2$, then the gain increment caused by increases in I_{F1} will be balanced by the gain decrement caused by decreases in I_{F2} . The constant current source biases each I_F at 3mA quiescent current. R_1 and R_2 are designed so that I_F varies over the range of 2mA to 4mA as V_{IN} varies from -5V to $+5\text{V}$. R_1 and R_2 can be adjusted to accommodate any desired dynamic range. U_3 and U_4 are used as a differential current amplifier:

$$V_{OUT} = R_5 [(R_3/R_4) I_{C1} - I_{C2}]$$

R_3 , R_4 , R_5 have been picked for an amplifier with a gain of 1 for a worst case spread of coupler current transfer ratios. The transfer function of the differential amplifier is:

$$V_{OUT} = R_5 \left[\left(\frac{K_1 R_3}{R_4} \right) \left(\frac{I_{CC}}{2 I_{F1}} \right)^{n_1} \left(1 + \frac{V_{IN}}{R I_{CC}} \right)^{n_1} - K_2 \left(\frac{I_{CC}}{2 I_{F2}} \right)^{n_2} \left(1 - \frac{V_{IN}}{R I_{CC}} \right)^{n_2} \right]$$

if $R \equiv R_1 \equiv R_2$

HIGH SPEED/
HIGH GAIN
OPTOCOUPLES

After zero adjustment, this transfer function reduces to:

$$V_{OUT} = R_5 K' \left[\left(1 + \frac{V_{IN}}{R I_{CC}} \right)^{n_1} - \left(1 - \frac{V_{IN}}{R I_{CC}} \right)^{n_2} \right]$$

$$\text{where } K' = \frac{K_1 R_3}{R_4} \left(\frac{I_{CC}}{2 I_{F1}} \right)^{n_1} = K_2 \left(\frac{I_{CC}}{2 I_{F2}} \right)^{n_2}$$

The non linearities in the transfer function when $n_1 \neq n_2 \neq 2$ can be written as shown below. For example, if $|x| \leq .35$, $n_1 = 1.9$, $n_2 = 1.8$, then the linearity error is 1.5% of the desired signal.

$$\frac{\text{linearity error}}{\text{desired signal}} = \frac{(1+x)^{n_1} - (1-x)^{n_2} - (n_1 + n_2)x}{(n_1 + n_2)x}, \text{ where } x = \frac{V_{IN}}{R I_{CC}}$$

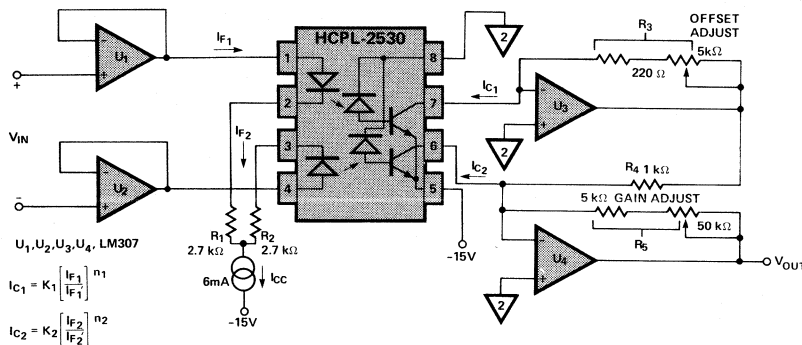


Figure 4. Differential Type DC Isolation Amplifier.

Typical Performance of the Differential Linearized DC Amplifier:

3% linearity for 10V p-p dynamic range
 Unity voltage gain
 25 kHz bandwidth (limited by U_1, U_2, U_3, U_4)
 Gain drift: $-4\%/^{\circ}\text{C}$
 Offset drift: $\pm 4\text{mV}/^{\circ}\text{C}$
 Common mode rejection: 70dB at 1 kHz
 3000V DC insulation

AC COUPLED AMPLIFIER

In an AC circuit, since there is no requirement for a DC reference, a single optocoupler can be utilized by biasing the optocoupler in a region of constant incremental CTR ($\partial I_D / \partial I_F$). An example of this type of circuit is shown in Figure 5. Q_1 is biased by R_1, R_2 and R_3 for a collector quiescent current of 20mA. R_3 is selected so that I_F varies from 15mA to 25mA for V_{IN} of 1V p-p. Under these

operating conditions, the 6N136 operates in a region of almost constant incremental CTR. Linearity can be improved at the expense of signal-to-noise ratio by reducing I_F excursions. This can be accomplished by increasing R_3 , then adding a resistor from the collector of Q_1 to ground to obtain the desired quiescent I_F of 20mA. Q_2 and Q_3 form a cascade amplifier with feedback applied through R_4 and R_6 . R_6 is selected as V_{be}/I_3 with I_3 selected for maximum gain bandwidth product of Q_3 . R_7 is selected to allow maximum excursions of V_{OUT} without clipping. R_5 provides DC bias to Q_3 . Closed loop gain ($\Delta V_{OUT} / \Delta V_{IN}$) can be adjusted with R_4 . The transfer function of the amplifier is:

$$\frac{V_{OUT}}{V_{IN}} \cong \left(\frac{\partial I_D}{\partial I_F} \right) \left(\frac{1}{R_3} \right) \left(\frac{R_4 R_7}{R_6} \right)$$

Typical Performance of the Wide Bandwidth AC Amplifier:

2% linearity over 1V p-p dynamic range
 Unity voltage gain
 10 MHz bandwidth
 Gain drift: $-6\%/^{\circ}\text{C}$
 Common mode rejection: 22dB at 1 MHz
 3000V DC insulation

DIGITAL ISOLATION TECHNIQUES

Digital conversion techniques can be used to transfer an analog signal between two isolated systems. With these techniques, the analog signal is converted into some digital form and transmitted through the optocoupler. This digital information is then converted back to the analog signal at the output. Since the optocoupler is used only as a switch, the overall circuit linearity is primarily dependent on the accuracy by which the analog signal can be converted into digital form and then back to the analog signal. However, the overall circuit bandwidth is limited by the propagation delays of the optocoupler.

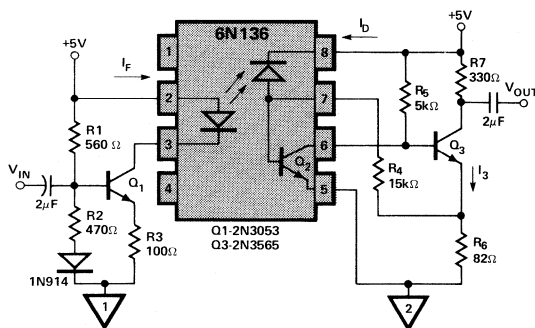


Figure 5. Wide Bandwidth AC Isolation Amplifier.

Figure 6 shows a pulse width modulated scheme to isolate an analog signal. The oscillator operates at a fixed frequency, f , and the monostable multivibrator varies the duty factor of the oscillator proportional to the input signal, V_{IN} . The maximum frequency at which the oscillator can be operated is determined by the required linearity of the circuit and the propagation delay of the opto isolators:

$$(t_{\max} - t_{\min}) \text{ (required linearity)} \geq |t_{PLH} - t_{PHL}|$$

At the output, the pulse width modulated signal is then converted back to the original analog signal. This can be

accomplished with an integrator circuit followed by a low pass filter or through some type of demodulator circuit that gives an output voltage proportional to the duty factor of the oscillator.

Figure 7 shows a voltage to frequency conversion scheme to isolate an analog signal. The voltage to frequency converter gives an output frequency proportional to V_{IN} . The maximum frequency that can be transmitted through the optocoupler is approximately:

$$f_{\max} \approx \frac{1}{t}, \text{ where } t = t_{PLH} \text{ or } t_{PHL}, \text{ whichever is larger.}$$

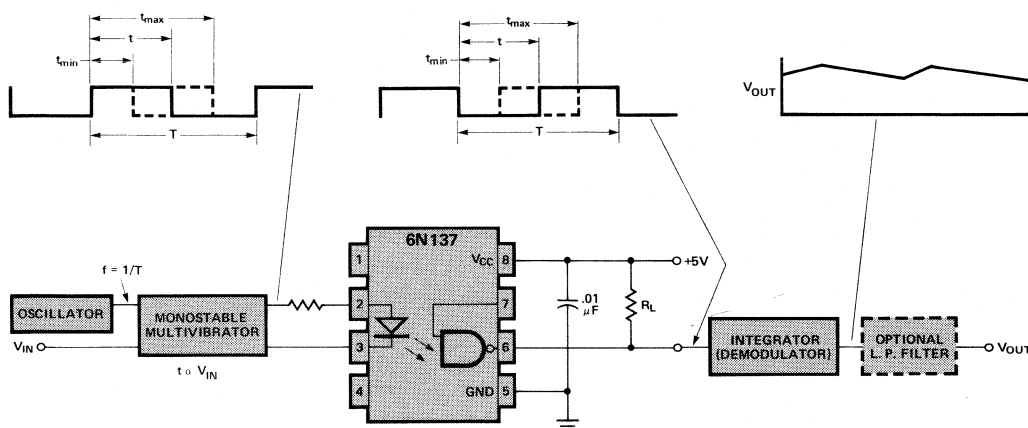


Figure 6. Pulse Width Modulation.

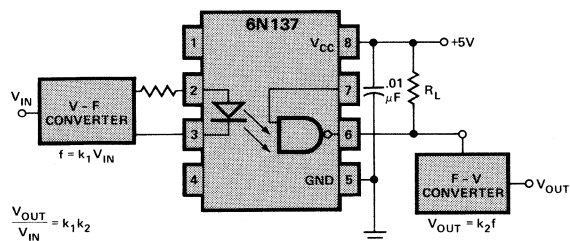


Figure 7. Voltage to Frequency Conversion.

At the output, the frequency is converted back into a voltage. The overall circuit linearity is dependent only on the linearity of the V-F and F-V converters.

Another scheme similar to voltage to frequency conversion is frequency modulation. A carrier frequency, f_o , is modulated by Δf such that $f_o \pm \Delta f$ is proportional to V_{IN} . Then at the output, V_{OUT} is reconstructed with a phase locked loop or similar circuit.

One further scheme to isolate an analog signal is to use A-D and D-A converters and transfer the binary or BCD information through optocoupler. The information can be transmitted through the optocoupler in parallel or serial format depending on the outputs available from the A-D converter. If serial outputs are not available, the A-D outputs can be converted into serial form with a PISO shift register and transmitted through one high speed optocoupler. This scheme becomes economical especially where high resolution is required allowing several optocouplers to be replaced with one high speed optocoupler. Refer to HP Application Note 947 for further discussion of digital data transmission techniques.



High Speed Optocouplers vs. Pulse Transformers

INTRODUCTION

For data rates over 1 MBaud, there are several optocouplers supplied by Hewlett-Packard containing high speed logic gates in the detector integrated circuit. These logic gate optocouplers, which include the HCPL-2200, HCPL-2300, HCPL-2400, and HCPL-2600 families, have typical data rates ranging from 5 MBaud to 40 MBaud, depending on the family. Common Mode Transient Immunity, a measure of the digital isolation capability of the optocoupler, ranges from 50 to 10,000 V/ μ s, depending on the product. The HCPL-2630 and HCPL-2631 are dual channel versions of the 6N137 and HCPL-2601, respectively. (See Table 1.) For data rates higher than 10 MBaud the only existing component for optical isolation is the HCPL-2400. It is guaranteed to operate at 20 MBaud over the temperature range 0° to 70° C, with typical data rates being much higher.

Isolation is also obtainable using the magnetic coupling available with transformers. Pulse transformers, which are transformers designed to operate at high data rates, are generally much more difficult to design with relative to an optocoupler solution. The advantages of using an optocoupler fall generally into two categories: 1) maintaining waveform fidelity and 2) obtaining high common mode rejection. (See Table 2.)

WAVEFORM FIDELITY

In many applications it is difficult to obtain a usable waveform with a pulse transformer (See Figure 1). This is essentially due to three factors: waveform "droop," effects of the turns ratio on risetime, and backswing.

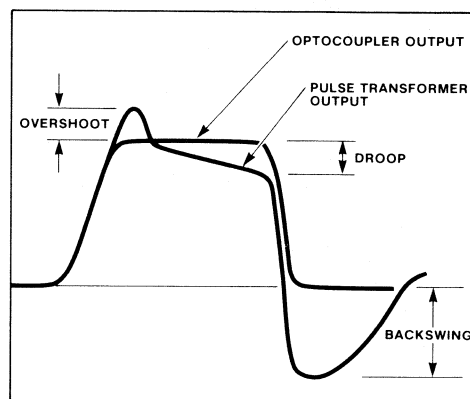


Figure 1: Optocoupler and
Pulse Transformer Output Waveforms

Transformers experience "droop" or "sag" inversely proportional to the time constant made up of the mutual inductance and the equivalent resistance. The transformer must be designed so that the magnitude of the droop does not exceed an allowable threshold or fraction of the initial amplitude. The larger the mutual inductance the less will be the droop, but the better the flux coupling then has to be. This usually results in a higher primary to secondary capacitance which reduces common mode transient immunity and dielectric withstand voltage.

Table 1. Logic Gate Optocouplers

Product	Typical Data Rate [1]	Recommended Input Current	Typical Common Mode Transient Immunity [2]
HCPL-2200	5 Mbit/s	1.6 mA	$\pm 10,000$ V/ μ s
HCPL-2300	10 Mbit/s	0.5 mA	± 400 V/ μ s
6N137 HCPL-2630	10 Mbit/s	5 mA	± 50 V/ μ s, -150 V/ μ s
HCPL-2601 HCPL-2631	10 Mbit/s	5 mA	$\pm 10,000$ V/ μ s
HCPL-2400	40 Mbit/s	4-8 mA	$\pm 10,000$ V/ μ s

Notes: 1. At 25° C and recommended operating conditions for the particular product

2. $V_{cm} = 50$ V (peak)

Table 2. Optocoupler Advantages

Characteristic of Optocoupler	Advantage of Characteristic
1) Ease in obtaining waveform fidelity (Fig. 1)	Does not constrain data format or duty cycle. Does not require elaborate encode/decode functions.
A. No waveform "droop"	Does not constrain duty cycle. No tradeoff between "allowable" droop and transformer speed, which limits performance.
B) No turns ratio effect on capacitance	Pulse transformers need unity turns ratio to maintain speed, constraining input and output waveforms.
C) No backswing	Without compensation, backswing may be harmful to sensitive circuitry. Also, backswing constrains duty cycle.
2) Typically higher common mode transient immunity relative to many pulse transformers	Does not require the extra complexity, increased board space, and decrease in performance necessary to achieve high common mode transient immunity with pulse transformers.

Higher interwinding dielectric strength can be achieved by increasing the size of the transformer, which has the detrimental effect of increasing the risetime of the signal and the physical board space required.

A transformer with a turns ratio near unity must be used for high speed applications because of the fact that capacitance at the secondary will be multiplied by the square of the turns ratio and added to the primary capacitance. The equation is:

$$C_{eq} = C_{primary} + C_{secondary} \times N^2$$

C_{eq} is the combination of the distributed capacitance of the primary and secondary windings looking into the primary. (A similar equation could also be written for C_{eq} looking into the secondary.)

$C_{primary}$ is the distributed capacitance of the primary, including source capacitance.

$C_{secondary}$ is the distributed capacitance of the secondary, including load impedance.

N is the turns ratio (n_2/n_1). n_1 = turns in primary,
 n_2 = turns in secondary.

This equivalent capacitance will then detrimentally effect the risetime. Having a unity turns ratio is generally not a problem when using transformers for isolation, but it does imply an added constraint when considering what voltages and currents must be available at the primary to achieve a logic level signal at the output.

Pulse transformers exhibit backswing upon the opening of a switch in series with their primary which may require a clamping diode to limit its magnitude, possibly to prevent damage to adjoining circuitry. Even so, the negative volt-time area must be equal to the positive volt-time area, which imposes limits on threshold settings for signals if the range of the dc-component variation is an appreciable fraction of the amplitude. Thresholds must be low enough to accommodate a high duty factor, and attempts to circumvent this limitation by using high thresholds and high drive amplitudes encounter the limitation of core

saturation. A larger core reduces the chance of saturation, but results in an increase in the risetime.

The final conclusion is that the pulse transformer is not useful for data formats like non-return to zero (NRZ) where the duty factor can vary from zero up to near 100% (long stream of logic 1's). The data must therefore be encoded with a limited duty factor range, by using codes like Manchester, biphase, or Miller. These codes require more elaborate decoding and encoding circuitry. There are no constraints on the data format when using the HCPL-2400, or any other high speed optocoupler.

COMMON MODE TRANSIENT IMMUNITY

As was previously mentioned, pulse transformers have a primary to secondary capacitance that is typically higher than that of the high speed logic gate families, particularly the HCPL-2200, HCPL-2601/31, and the HCPL-2400 families. This means that fast transients are more likely to be coupled through to the secondary. To obtain high common mode transient immunity in pulse transformers there are usually two approaches. One is to introduce an electrostatic shield between the primary and secondary. However, it is generally difficult to manufacture a small transformer with a shield, so cost will increase substantially. The second method is to employ two transformers in a series manner, so that signals are coupled through two transformers. This design becomes very complex relative to an optocoupler design, and requires more components and board space.

CONCLUSION

The high speed logic gate optocouplers have applications in many areas, including data communications, telecommunications, instrumentation, and industrial control. They can replace pulse transformers, or allow for the replacement of several lower speed optocouplers in parallel with a serial interface. They can therefore result in significant reductions in power consumption, component count, and board space requirements.

Coming in at 20 Mbaud, an Optocoupler IC Doubles the Data Transfer Rate

By teaming an AlGaAs emitter with a three-state detector, an optocoupler also manifests 10,000-V/ μ s common-mode noise immunity and 2500-V rms insulation.

By teaming an AlGaAs emitter with a three-state detector, an optocoupler also manifests 10,000-V/ μ s common-mode noise immunity and 2500-V rms insulation.

Optocouplers have armed the designers of data communication systems with new weapons to meet today's stringent requirements for data rate, insulation, and common-mode immunity. What's more, these components are replacing the pulse transformer, while improving on that old standby's waveform fidelity, NRZ data handling, and TTL compatibility.

Of course, data-handling optocouplers have had their own shortcomings. Many could not provide more than a few hundred volts of input-to-output insulation. Most were not matched from device to device and generally could not be

used in high-speed parallel-line applications. None could consistently manage data rates exceeding 10 Mbaud over temperature, and few had a common-mode transient immunity exceeding a hundred volts or so per microsecond.

All that is changed with an optocoupler that delivers a guaranteed data rate of 20 Mbaud over temperature, has a typical common-mode immunity of 10,000 V/ μ s, and supplies an insulation of 2500 V rms. Central to the success of the HCPL-2400 optocoupler is an aluminum gallium arsenide LED with low junction capacitances that emits an optical signal with an 820-nm wavelength. The three-state detector IC, which accompanies the LED, is isolated from it by a dielectric of silicone gel. The detector includes a differential amplifier with hysteresis that matches both TTL and HCMOS logic levels (Fig. 1). Pairing the emitter with the detector not only yields speed, but affords a good degree of noise immunity and input protection as well.

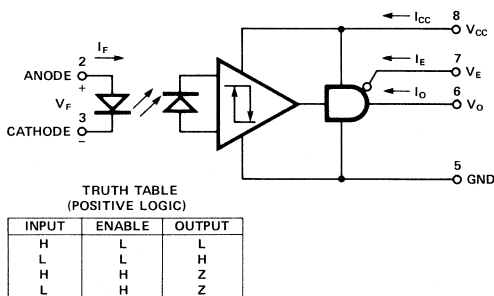


Figure 1. A fast switching LED and a matching three-state Schottky TTL detector with hysteresis are at the core of the HCPL-2400 optocoupler. Providing 2.5 kV of dc insulation, and a typical common-mode noise immunity to 10,000 V/ μ s, the component switches NRZ input signals at 20 to 40 Mbaud with minimal distortion.

THREE PARAMETERS IMPORTANT

To better predict the behavior of the high-speed interfaces that use the optocoupler, designers are provided with three frequently ignored parameters — minimum propagation delay, pulse-width distortion, and channel distortion. Those parameters effectively simplify the design of a circuit within the maximum-to-minimum timing window of the system's switching specifications.

Both pulse-width and channel distortion depend heavily on propagation delay. That delay, typically 33 ns, indicates the amount of time a device needs to respond to an input signal. In a notable departure from previous optocoupler specifications, which dealt only with maximum (worst-case) values, those for this component list the minimum propagation delay as well. In reality, a signal that arrives at a point too early in a circuit is just as harmful to system

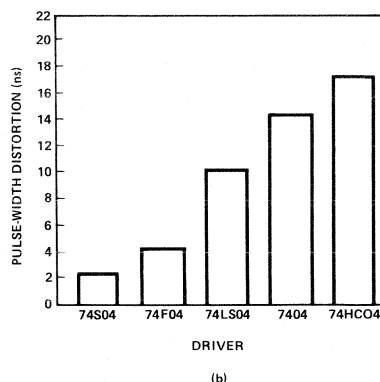
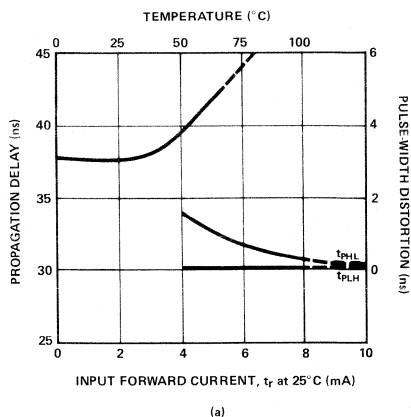


Figure 2. Propagation delays and pulse-width distortion (t_{PHL} - t_{PLH}), inherently low in the HCPL-2400, can be maintained by holding the forward driving current through the LED to 7 or 8 mA and operating the device at temperatures below 35°C or so (a). Low pulse-width distortion can be secured by driving the optocoupler with Schottky or FAST logic (b).

operation as one that arrives too late; the end result — faulty timing or distortion — is the same. In any case, by using only worst-case specifications when working with windows, designers assume a lower-boundary condition of zero for minimum propagation delay. The value of most devices, of course, is nowhere near that low. Knowing both the minimum and maximum propagation delays allows the designer to work with a more realistic window.

If the device's propagation delay in moving from a low to a high logic state (t_{PLH}) differs from that of the high-to-low transition (t_{PHL}), then pulse-width distortion exists. In other words, the input signal's duty factor at input and output is not conserved. Expressed as a percentage, pulse-width distortion is equal to $100(t_{PLH}-t_{PHL})/T$, where T is the period of the driving signal. The higher the pulse-width distortion, the more difficult it is to recover the data stream without error. Typically, the maximum data rate allowable is that at which distortion is 20% to 30%; the actual value depends on the protocol and coding used.

Pulse-width distortion essentially depends on three factors: temperature, forward current through the LED, and the LED's switching speed (Fig. 2a). The typical pulse-width distortion of the optocoupler is a relatively low 3 ns, allowing data to be transmitted at 40 MBaud. That rate assumes that the LED is driven by fast logic devices, such as Schottky (Fig. 2b).

Channel distortion describes the worst-case variation in propagation delay from device to device under identical operating conditions. The need for low channel distortion arises when two or more identical optocouplers must perform in applications such as the transmission of data along parallel lines. The optocoupler generates maximum

variations in t_{PHL} and t_{PLH} of 25 ns; typically, it can be held at 8 ns or below over 0° to 70°C.

A COUPLER'S GOOD CONNECTIONS

Uses for optocouplers abound: digital communication between a computer and peripheral, local networking, and any situation in which a circuit demands a floating ground. Signal sources in test equipment, for example, might connect to several separate stations.

To maximize the data rates often required in such systems, the user must understand the interrelation of the optocoupler's pulse-width distortion and the various circuit parameters that affect its speed. Consider the optical connection between a crystal oscillator and a microprocessor (Fig. 3). Here the oscillator provides a two-phase signal to the processor's clock inputs, X_1 and X_2 . In doing so, it follows the recommended driving technique for high-speed applications.

In this example, the drive requirements of the microprocessor are such that X_1 must be switched low for a period of at least 40 ns during each data transfer cycle. From a design standpoint, the engineer must account for duty-cycle variations introduced by the optocoupler, for it ultimately sets the oscillator's maximum allowable frequency.

Because the maximum pulse-width distortion for the HCPL-2400 is 15 ns, the clock signal feeding to the optocoupler must at least equal the minimum low time plus the pulse-width distortion time, or 55 ns (40 ns + 15 ns). The duty cycle of the crystal oscillator modifies this value; if the duty cycle is 50%, then the minimum clock period becomes 2 X 55 ns, or 110 ns. Thus, the clock frequency cannot exceed 9.1 MHz. The crystal oscillator in this circuit

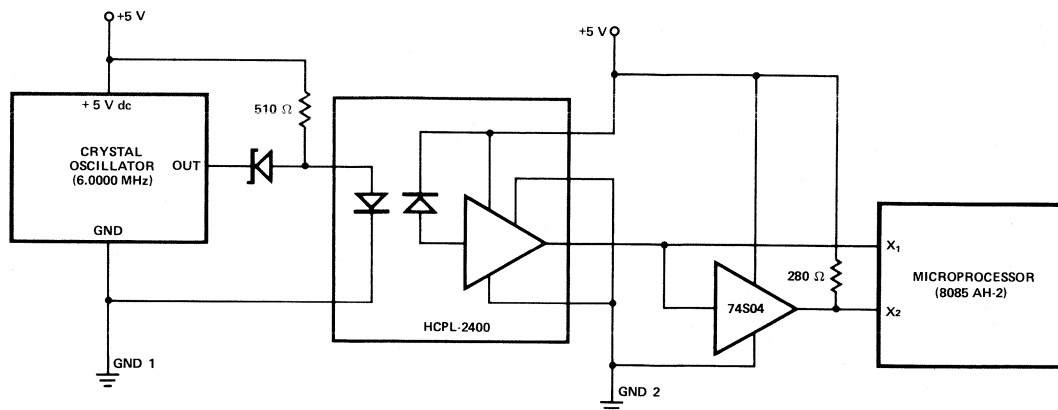


Figure 3. A floating oscillator-to-microprocessor interface needs few external parts. Clock-speed constraints imposed by the 8085 microprocessor are ultimately determined only by the optocoupler's pulse-width distortion and the oscillator's duty cycle.

has a duty cycle that nominally varies between 40% and 60% from unit to unit. For the most reliable performance, the maximum operating frequency should thus be limited to 7.2 MHz (0.4/55 ns).

In analog-to-digital converters, designers should isolate the two portions of a circuit so that interference generated by digital switching and clock signals is not coupled to the analog section. That task is more difficult for systems that employ parallel data and control lines. Knowing the channel distortion ultimately maximizes the reliability of the circuit.

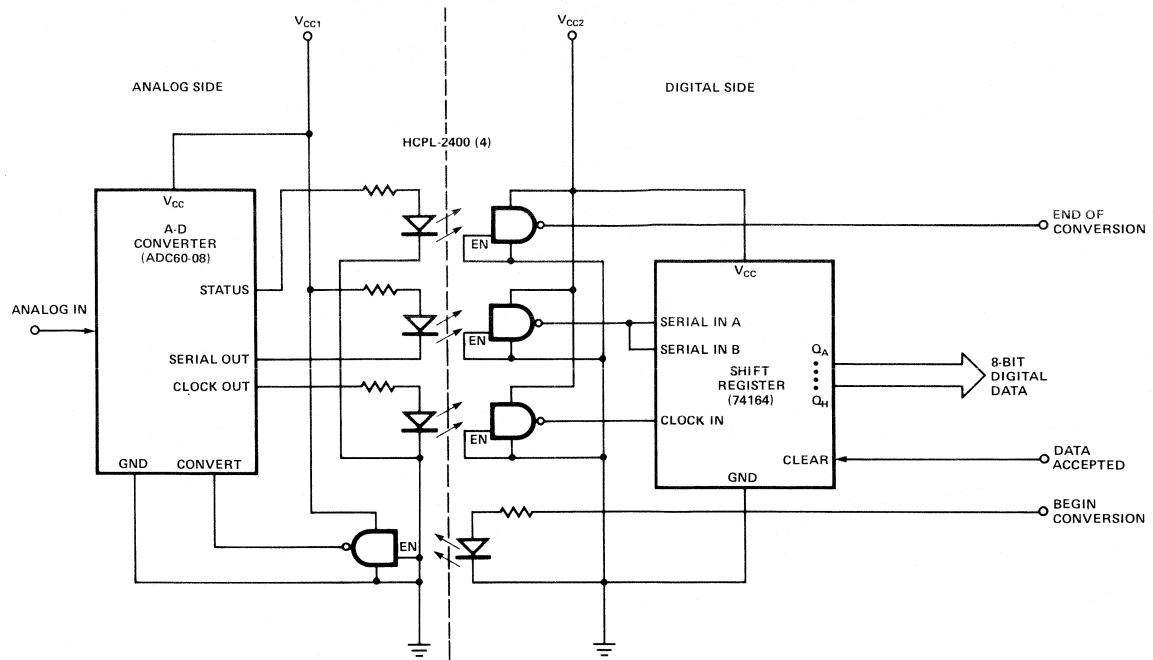
CHANNELING AWAY DISTORTION

An interface between an analog-to-digital converter and an 8-bit serial-in, parallel-out shift register illustrates the point (Fig. 4). In this case, a converter works with four optocouplers and a shift register to deliver an 8-bit word to the central processor. The converter's serial output feeds the LED of the optocoupler, driving the shift register in a way that preserves its phase at the output. One optocoupler supplies the clock signal for the register; the other two coordinate the system timing. Clearly the clock, control, and data signals must keep pace with each other as they pass through the optocouplers to minimize data transfer errors and achieve maximum circuit speed. Accordingly, the optocouplers' channel distortion must be small and of a known value.

Each clock cycle in this example takes 95 ns, during which time the clock is high for 50 ns and low for 45 ns. By the time the clock signal arrives at the shift register, it is inverted and delayed; the serial data at the input to the register is not inverted but is similarly skewed.

For example, let time t_1 be the nominal time between the data signal's rising edge and the clock's trailing edge at the input to the register. Time t_2 is the nominal delay between a valid low output of the data signal and the timing edge of the clock. Further, t_3 is the interval from the time that the valid data high signal reaches the input of the shift register and the rising edge of the clock. Time t_3 is thus equal to t_1 , plus or minus the optocoupler's 25-ns maximum channel distortion, and its sign depends on the signal's polarity.

In this circuit, t_1 equals 43 ns and t_2 equals 51 ns; thus t_3 lies between 18 and 68 ns. Similarly, the range for time t_4 , the period between the data low at the register input and the rising edge of the clock signal, is equal to t_2 plus the optocoupler's maximum channel distortion. It lies between 26 to 76 ns (51 ns \pm 25 ns). The lower boundary of these two windows, 18 ns, exceeds the minimum data setup time for the register, which is 15 ns. Consequently, the circuit will work at that clock rate under all conditions, because the optocoupler was designed and manufactured so that it would track well from unit to unit.



HIGH SPEED/
HIGH GAIN
OPTOCOUPERS

Figure 4. Optocouplers achieve isolation and high speed in the parallel-line interface of this rudimentary data processing circuit. The circuit works at 10 MHz, thanks to low variations in each optocoupler's actual channel distortion.



Applications for Low Input Current, High Gain Optocouplers

Optically coupled isolators are useful in applications where large common mode signals are encountered. Examples are: line receivers, logic isolation, power lines, medical equipment and telephone lines. This application note has at least one example in each of these areas for the 6N138/9 series high CTR couplers.

HP's 6N138/9 series couplers contain a high gain, high speed photodetector that provides a minimum current trans-

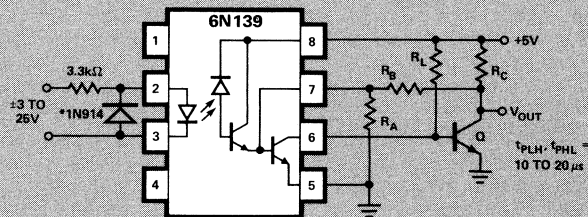
fer ratio (CTR) of 300% at input currents of 1.6 mA for the 6N138 and 400% at 0.5 mA for the 6N139. The excellent low input current CTR enables these devices to be used in applications where low power consumption is required and those applications that do not provide sufficient input current for other couplers. Separate pin connections for the photodiode and output transistor permit high speed operation and TTL compatible output. A base access terminal allows a gain bandwidth adjustment to be made.

RS-232C COMPATIBLE LINE RECEIVER

- 2500V 60Hz Common Mode Rejection
- Allows use of Low Cost Line
- Full 40kbs Data Rate for Line Lengths up to 5000'
- Hysteresis for Increased Noise Immunity

*ANTIPARALLEL DIODE IS NEEDED ONLY IF REVERSE LINE VOLTAGE EXCEEDS 15V (TO PREVENT HIGH REVERSE VOLTAGE FROM CAUSING POWER DISSIPATION IN EXCESS OF INPUT DIODE MAXIMUM RATING).

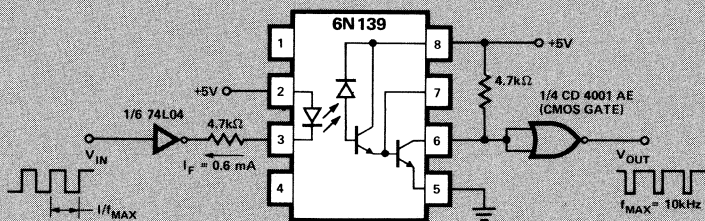
REMOVE R_A AND R_B FOR NO HYSTERESIS



R_A	R_B	R_C	R_L	Q
680kΩ	1.5MΩ	1.8kΩ	15kΩ	2N3904

LOW POWER INTERFACE

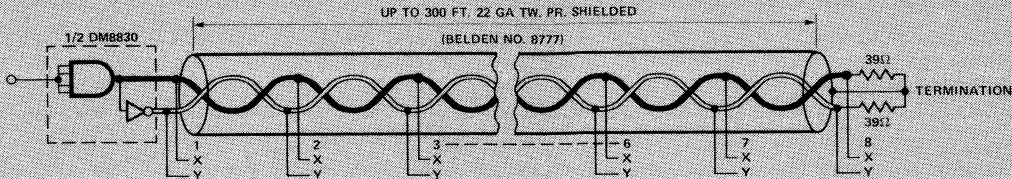
- Operation at $I_F \geq 0.5\text{mA}$
- 10kHz f_{MAX}
- Low Power Consumption



f_{MAX} IS THE FREQUENCY AT WHICH A 50% DUTY FACTOR AT THE INPUT IS DEGENERATED TO 10% OR 90% DUTY FACTOR AT THE OUTPUT.

LINE RECEIVER FOR PARTY LINE

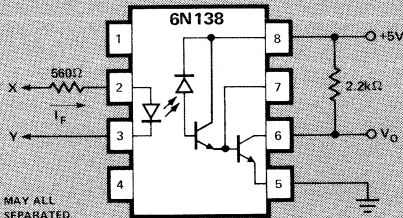
- 1-8 Receivers can be used with circuit shown
- Uses conventional IC Line Driver
- Total Line Length 1-300'
- Typical Data Rate —180kbs
($t_{PHL}, t_{PLH} = 3 \mu\text{sec}$)
- Allows use of Low Cost Line



ISOLATOR LOADS MAY BE DISTRIBUTED RANDOMLY ALONG THE LENGTH OF THE LINE, OR ALL MAY BE LUMPED AT THE END. I_F FOR 1 AND 8 ISOLATOR LOADS WOULD BE 2.7 AND 1.8mA RESPECTIVELY.

PROPAGATION DELAY: $t_{PHL}, t_{PLH} = 0.5$ to $5 \mu\text{s}$

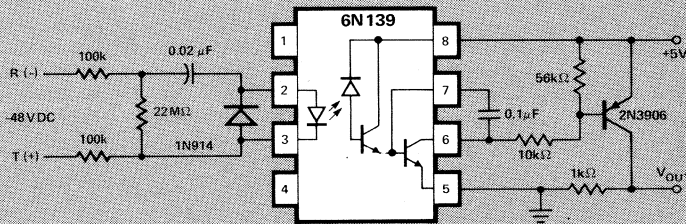
OUTPUT GROUNDS MAY ALL BE ELECTRICALLY SEPARATED.



HIGH SPEED/
HIGH GAIN
OPTOCOUPLED

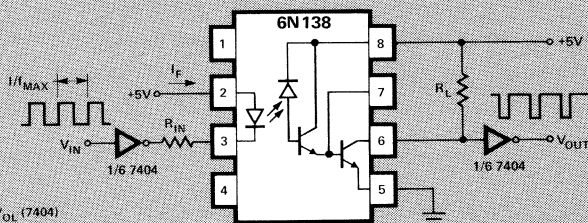
TELEPHONE RING DETECTOR

- Discriminates between Ring and Dial Signals
- Minimal Line Loading
- 2500V Insulation from Telephone Line
- Small Size
- Integrator Included



TTL TO TTL INTERFACE

- Direct Input and Output Compatibility
- Adjustable Data Rate
- High Fan-Out



$$I_F = \frac{5V - V_F - V_{OL}(7404)}{R_{IN}}$$

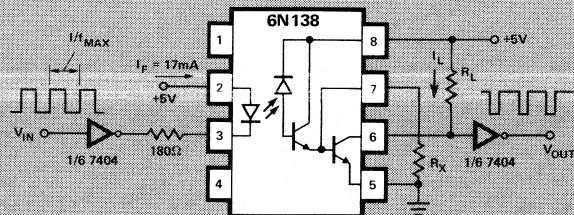
FOR HIGHER FANOUT WITH COMPARABLE DATA RATES USE SMALLER VALUES OF R_{IN} .

f_{MAX} IS THE FREQUENCY AT WHICH A 50% DUTY FACTOR AT THE INPUT IS DEGENERATED TO 10% OR 90% DUTY FACTOR AT THE OUTPUT.

$R_L (\Omega)$	$R_{IN} (\Omega)$	I_F (mA)	f_{MAX} (kHz)
2200	1800	1.7	40
270	390	8	125
100	180	17	250

GAIN/SPEED TRADE OFF

- Obtain Maximum Speed at Required Gain
- Single Resistor Required
- Use same device for Multiple Applications

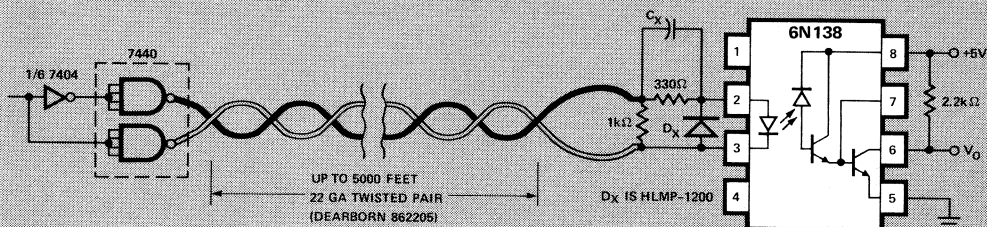


f_{MAX} IS THE FREQUENCY AT WHICH A 50% DUTY FACTOR AT THE INPUT IS DEGENERATED TO 10% or 90% DUTY FACTOR AT THE OUTPUT.

$R_X (\Omega)$	$R_L (\Omega)$	$I_L (mA)$	$f_{MAX} (kHz)$
NONE	100	46	250
820	1000	4.6	650

1-5000 FT. LINE RECEIVER

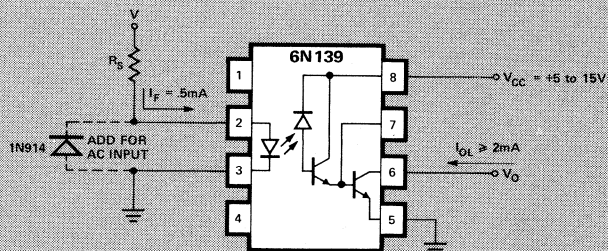
- Drive with Standard TTL Buffer Gate
- 2500V 60Hz Common Mode Rejection
- Allows use of Low Cost Line
- 40kbs Data Rate
- TTL Compatible Output



PROPAGATION DELAY: WITHOUT C_X , D_X , $t_{PLH} = 2$ to $5 \mu s$; $t_{PHL} = 25 \mu s$
WITH D_X , $C_X > 0.002 \mu F$, $t_{PLH} = 2 \mu s$; $t_{PHL} = 7 \mu s$

HIGH VOLTAGE STATUS INDICATOR

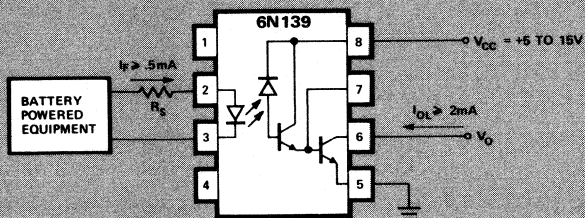
- Low Power Consumption
- TTL Compatible Output
- High Speed
- Use for Power Turn On Anticipation Circuit, 117V Line Monitor or Other High Voltage Sensing



V(Vdc or Vrms)	R_S	$V \cdot I_F (mW)$
24	47k Ω	11
48	100k Ω	22
117	220k Ω	62
230	470k Ω	113

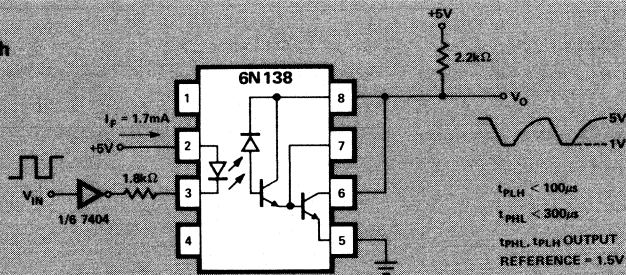
MEDICAL EQUIPMENT ISOLATION

- Low Power Consumption
- 2500V 60Hz Isolation
- Digital or Analog Operation

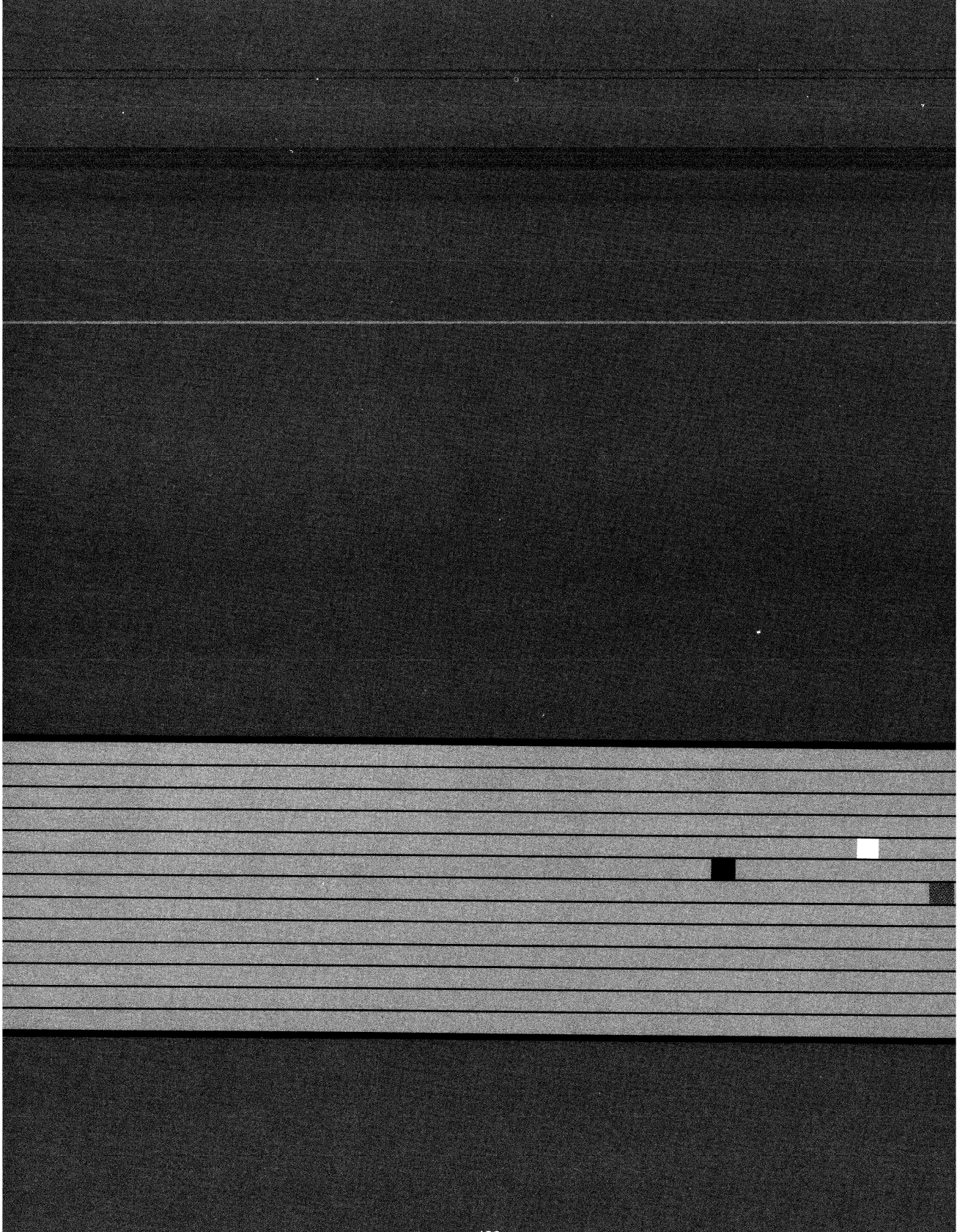


CONVENTIONAL DARLINGTON

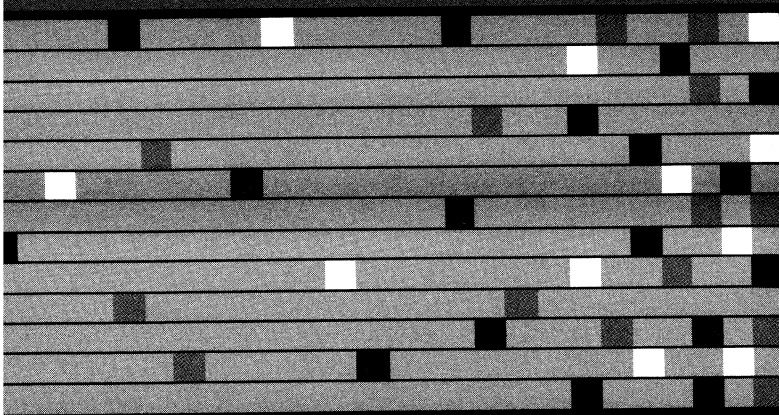
- No Bias Supply Required
- Base Lead available for Gain/Bandwidth Adjust
- Data Rates of 2kbs



HIGH SPEED/
HIGH GAIN
OPTOCOUPLES



Application Specific Optocouplers

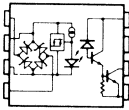




Application Specific Optocouplers

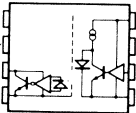


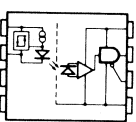
A fundamental part of HP's optocoupler product strategy is to examine common customer needs for optical isolation and develop products which provide a complete solution for those applications. Using our photo IC technology, we have integrated into the optocouplers many of the circuit functions

normally implemented discretely. This not only saves our customers money but reduces board space and design time. Examples of these complete solutions include our ac/dc threshold sensing coupler (HCPL-3700) and our 20 mA current loop couplers (HCPL-4100, HCPL-4200).

AC/DC to Logic Interface Optocoupler

Device	Description	Application[1]	Typical Data Rates	Input Threshold Current	Output Current	Withstand Test Voltage	
						Standard*	Option 010**
	HCPL-3700 AC/DC to Logic Threshold Sensing Interface Optocoupler	Limit Switch Sensing, Low Voltage Detector, Relay Contact Monitor	4 KHz	2.5 mA TH+ 1.3 mA TH-	4.2 mA	3000 V dc 	2500 V ac 

20 mA Current Loop Optocouplers

Device	Description	Application[1]	Typical Data Rates	Input Characteristics	Output Characteristics	Withstand Test Voltage	
						Standard*	Option 010**
	HCPL-4100 Optically Coupled 20 mA Current Loop Transmitter	Isolated 20 mA Current Loop in: • Computer Peripherals • Industrial Control Equipment • Data Communication Equipment	20 kBd (at 400 metres)	TTL/CMOS	27 V Max. Compliance Voltage	3000 V dc 	2500 V ac 
	HCPL-4200 Optically Coupled 20 mA Current Loop Receiver			6.5 mA Typ. Threshold Current	3 State Output		

*Standard Parts meet the UL1440 V ac test for 1 minute.

**Option 010 parts meet the UL 2500 V ac test for 1 minute.

Optocoupler Options

Option	Description
010	Special construction and testing to ensure the capability to withstand 2500 V ac input to output for one minute. Testing is recognized by Underwriters Laboratories, Inc. (File No. E55361). This specification is required by U.L. in some applications where working voltages can exceed 220 V ac.
100	Surface mountable optocoupler in a standard sized dual-in-line package with leads trimmed (butt joint). Provides an optocoupler which is compatible with surface mounting processes.



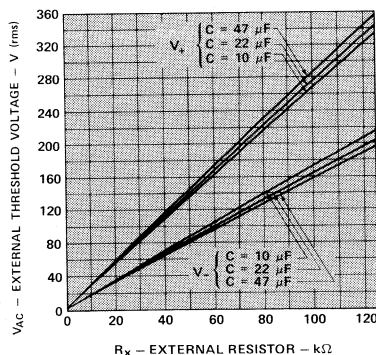
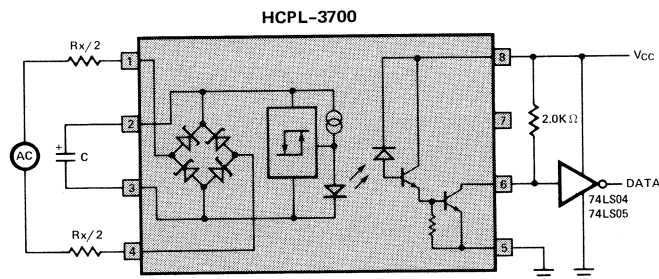
Applications Circuits for HCPL-3700 and HCPL-2601

The HCPL-3700 and HCPL-2601 are versatile members of HP's High Performance Optocoupler family. The following circuits will help you start using HP Optocouplers.

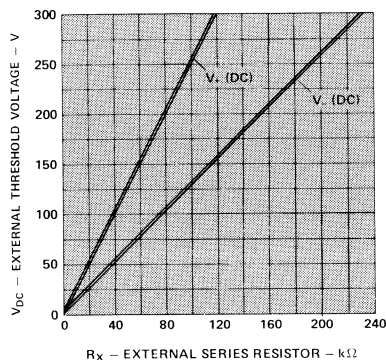
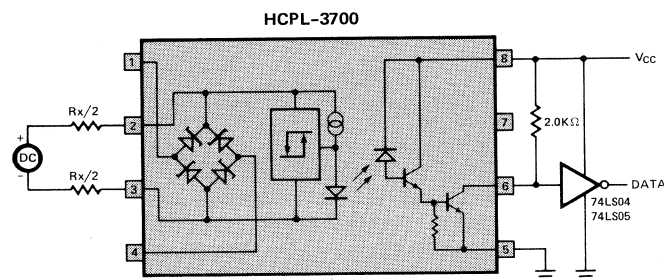
THRESHOLD SENSING INTERFACE OPTOCOUPLER — HCPL-3700

- Programmable Sense Voltage with Hysteresis
- LSTTL and CMOS Compatible Output
- AC or DC Input
- Recognized under the Components Program of Underwriters Laboratories, Inc. (File No. E55361)

AC INPUT



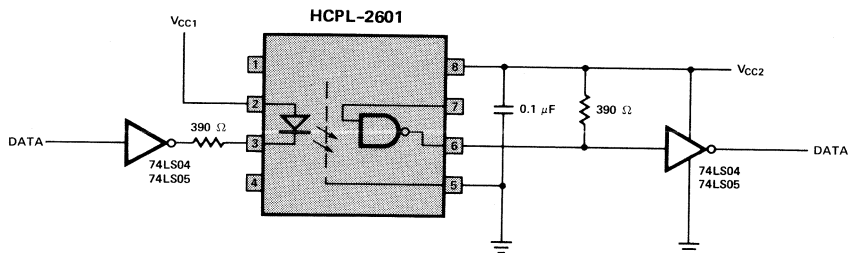
DC INPUT



For additional information see HP Application Note 1004.

LSTTL TO LSTTL OPTOCOUPLER INTERFACE — HCPL-2601

- 10 MBaud Speed Typical
- Shield provides 1 KV/ μ s Common Mode Noise Immunity
- Low Input Current Required: 5 mA
- Recognized under the Components Program of Underwriters Laboratories, Inc. (File No. E55361)



Other HP single channel logic compatible optocouplers are 6N136, 6N137, 6N138, HCPL-2200, and HCPL-2503. Dual channel logic compatible optocouplers are HCPL-2531, HCPL-2630, and HCPL-2700.

For additional optocoupler applications consult the HP Optocoupler Selection Guide.



Threshold Sensing For Industrial Control Systems With the HCPL-3700 Interface Optocoupler

INTRODUCTION

The use of electronic logic circuitry in most applications outside of a controlled environment very quickly brings the design engineer into contact with the problems and hazards involved in interfacing between the logic function and the controlled function. These problems have always been particularly evident in the field of industrial control where the electrically "noisy" environment produced by motors, power lines, lightning and other sources of interference may mask the desired signal, and in some cases even result in the destruction of the logic control system itself. In these situations, the designer must resort to solutions which will provide isolation between the logic system and the input or output function. Traditional methods of isolation involve the use of such devices as capacitors, relays, transformers, and optocouplers. Of these methods, the optocoupler provides an ideal combination of speed, dc response, high common mode rejection, and low input to output coupling capacitance.

In the implementation of an interface from an electrically noisy environment into logic systems, it is often desirable, if not mandatory, to establish some current or voltage switching point or threshold at which the input signal is considered true. Since the input, or feedback, signal in industrial control systems may be ac or dc and may range from low, 5 volt, levels to 110 or 240 volts ac, the design of such a threshold switching system can become more than a trivial problem. This is especially true when using the optocoupler, considering the relatively large range of current transfer ratio (CTR) found in most devices.

The problem of establishing an input switching threshold is resolved in the design of the Hewlett-Packard HCPL-3700 optocoupler. This device combines an ac or dc voltage and/or current detection function with a high insulation voltage optocoupler in a single eight pin plastic dual in-line package.

As shown in the block diagram of Figure 1, this device con-

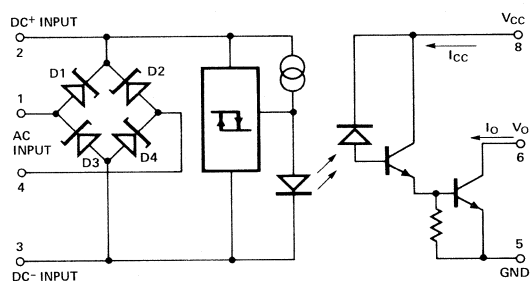


Figure 1. Block Diagram of the HCPL-3700

sists of a full-wave bridge rectifier and threshold detection, integrated circuit, an LED, and an optically coupled detector integrated circuit. The detector circuit is a combination of a photodiode and a high current gain, split Darlington, amplifier.

The input circuit will operate from an ac or dc source and provide a guaranteed, temperature compensated threshold level with hysteresis. The device may be programmed for higher switching thresholds through the use of a single external resistor.

With threshold level detection provided prior to the optical isolation path and subsequent gain stage, variations in the current transfer ratio of the device with time or from unit to unit are no longer important.

In addition to allowing ac or dc input signals, the Zener diodes of the bridge circuit also provide input voltage clamping to protect the threshold circuitry and LED from over voltage/current stress conditions. The LED current is provided by a switched current source.

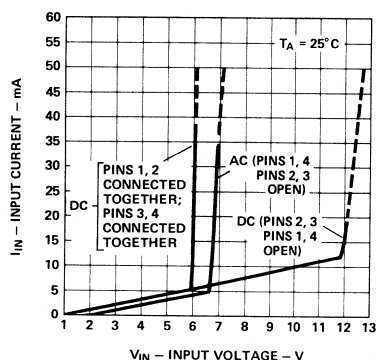
The HCPL-3700 optocoupler output is an open collector, high gain, split Darlington configuration. The output is compatible with TTL and CMOS logic levels. High common mode rejection, or transient immunity of $600\text{V}/\mu\text{s}$, allows excellent isolation. Insulation capability is 3000 volts dc. The recommended operating temperature range is 0°C to 70°C .

The HCPL-3700 meets the requirements of the industrial control environment for interfacing signals from ac or dc power equipment to logic control electronics. Isolated monitoring of relay contact closure or relay coil voltages, monitoring of limit or proximity switch operation or sensor signals for temperature or pressure, etc., can be accomplished by the HCPL-3700. The HCPL-3700 may also be used for sensing low power line voltage (Brown Out) or loss of line power (Black Out).

Device Characteristics

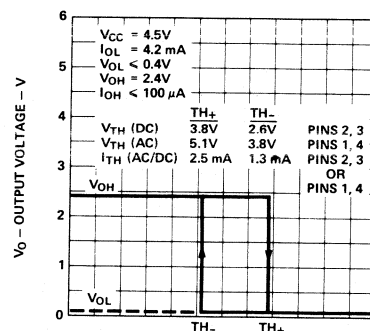
The function of the HCPL-3700 can best be understood through a review of the input V/I function and the input to output transfer function. Figure 2 shows the input characteristics, I_{IN} (mA) versus V_{IN} (volts), for both the ac and dc cases.

The dc input of the HCPL-3700 appears as a 1000Ω resistor in series with a one volt offset. If the ac pins (1, 4) are left unconnected, the dc input voltage can increase to 12V (two Zener diode voltages) before the onset of input voltage clamping occurs. If the ac pins (1, 4) are connected to ground or to dc pins (2, 3) respectively, the dc input voltage will clamp at 6.0V (one Zener diode voltage). Under clamping conditions, it is important that the maximum input current limits not be exceeded. Also, to prevent excessive current flow in a substrate diode, the dc input can not be backbiased more than -0.5V . The choice of the input voltage clamp level is determined by the requirements of the system design. The advantages of clamping the input at a low voltage level is in limiting the magnitude of forward current to the LED as well as limiting the input power



NOTE: AC VOLTAGE VALUES REPRESENT INSTANTANEOUS PEAK.

Figure 2. Typical Input Characteristics, I_{IN} vs. V_{IN}



NOTE: AC VOLTAGE VALUES REPRESENT INSTANTANEOUS PEAK.

Figure 3. Typical Transfer Characteristics of the HCPL-3700

to the device during large voltage or current transients in the industrial control environment. The internal limiting will in some cases eliminate the need for additional protection components.

The ac input appears similar to the dc input except that the circuit has two additional diode forward voltages. The ac input voltage will clamp at 6.7V (one Zener diode voltage plus one forward biased diode voltage), and is symmetric for plus or minus polarity. The ac voltage clamp level can not be changed with different possible dc pin connections.

The transfer characteristic displayed in Figure 3 shows how the output voltage varies with input voltage, or current, levels. Hysteresis is provided to enhance noise immunity, as well as to maintain a fast transition response (t_r , t_f) for slowly changing input signals.

The hysteresis of the device is given in voltage terms as $V_{HYS} = V_{TH+} - V_{TH-}$, or in terms of current as $I_{HYS} = I_{TH+} - I_{TH-}$. The optocoupler output is in the high state until the input voltage (current) exceeds V_{TH+} (I_{TH+}). The output state will return high when the input voltage (current) becomes less than V_{TH-} (I_{TH-}).

As is shown in Figure 3, the HCPL-3700 has preprogrammed ac and dc switching threshold levels. Higher input switching thresholds may be programmed through the use of a single series input resistance as defined in Equation (1). In some cases, it may be desirable to split this resistance in half to achieve transient protection on each input lead and reduce the power dissipation requirement of each of the resistors.

Figure 4 illustrates three typical interface situations which a designer may encounter in utilizing a microprocessor as a controller in industrial environments.

Example 1. A dc voltage applied to the motor is monitored as an indication of proper speed and/or load condition.

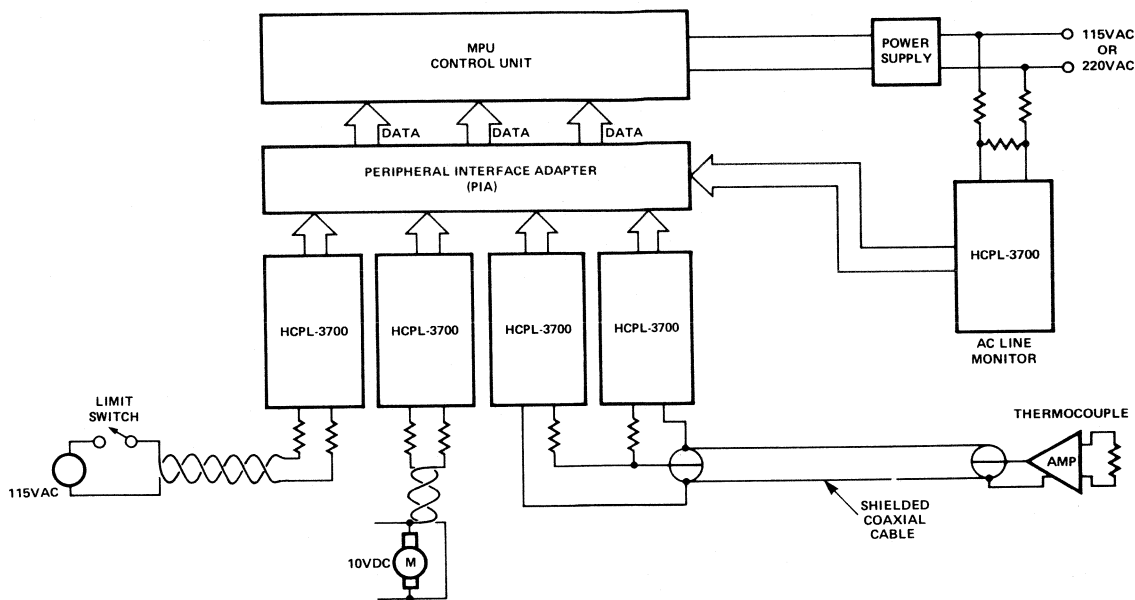


Figure 4. Applications of the HCPL-3700 for Interfacing AC and DC Voltages to a Microprocessor

Example 2. A limit switch uses a 115V ac or 220V ac control loop to improve noise immunity and because it is a convenient high voltage for that purpose.

Example 3. An HCPL-3700 is used to monitor a computer power line to sense a loss of line power condition. Use of a resistive shunt for improvement of threshold accuracy is analyzed in this example.

Also illustrated is an application in which two HCPL-3700's are used to monitor a window of safe operating temperatures for some process parameters. This example also requires a rather precise control of the optocoupler switching threshold. An additional dedicated leased line system example is also shown (Example 4).

Example 1. DC Voltage Sensing

The dc motor monitor function is established to provide an indication that the motor is operating at a minimum desired speed prior to the initiation of another process phase. If the applied voltage, V_M , is greater than 5V, it is assumed that the desired speed is obtained. The maximum applied voltage in the system is 10V. The HCPL-3700 circuit configuration for this dc application is shown in Figure 5.

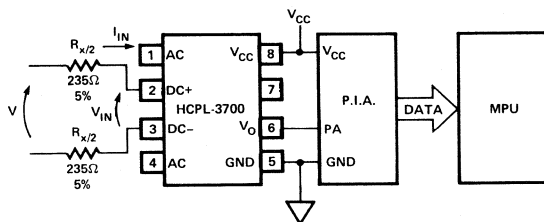


Figure 5. Interfacing a DC Voltage to an MPU using the HCPL-3700

NOTE: See Appendix for a definition of terms and symbols for this and all other examples.

The following conditions are given for the external voltage threshold level and input requirements of the HCPL-3700:

External Voltage Levels — V_M

$$V_+ = 5V \text{ dc (50\%)}$$

$$V_{\text{peak}} = 10V \text{ dc}$$

HCPL-3700 Input Levels

$$V_{TH+} = 3.8V$$

$$V_{TH-} = 2.6V$$

$$V_{ICH3} = 12V$$

$$I_{TH+} = 2.5mA$$

$$I_{TH-} = 1.3mA$$

For the 5V threshold, R_x is calculated via the expression:

$$R_x = \frac{V_+ - V_{TH+}}{I_{TH+}} \quad (1)$$

$$= \frac{5V - 3.8V}{2.5mA}$$

$$R_x = 480\Omega \quad (470\Omega \pm 5\%)$$

The resultant lower threshold level is formed by using the following expression:

$$V_- = I_{TH-} R_x + V_{TH-} \quad (2)$$

$$= (1.3mA) 470\Omega + 2.60V$$

$$V_- = 3.21V$$

With the possible unit to unit variations in the input threshold levels as well as $\pm 5\%$ tolerance variations with R_x , the variation of V_+ is $+12.4\%$, -15% and V_- varies $+14\%$, -23.5% . (NOTE: With a low, external, voltage threshold level, V_+ , which is comparable in magnitude to the V_{TH+} voltage threshold level of the optocoupler ($V_+ \leq 10V_{TH+}$) the tolerance variations are not significantly improved by the use of a 1% precision resistor for R_x . However, at a large external voltage threshold level compared to V_{TH+} ($V_+ > 10V_{TH+}$), the use of a precision 1% resistor for R_x does reduce the variation of V_+ .)

For simultaneous selection of external upper, V_+ , and lower, V_- , voltage threshold points a combination of a series and parallel input resistors can be used. Refer to the example on "ac operation with improved threshold control and accuracy" for detailed information.

Calculation of the maximum power dissipation in R_x is determined by knowing which of the following inequalities is true:

$$\frac{V_+}{V_{peak}} > \frac{V_{TH+}}{V_{IHC}} \quad (V_{IN} \text{ will not clamp}) \quad (3)$$

$$\frac{V_+}{V_{peak}} < \frac{V_{TH+}}{V_{IHC}} \quad (V_{IN} \text{ will clamp}) \quad (4)$$

where V_{IHC} is the particular input clamp voltage listed on the data sheet.

For this dc application with ac pins (1, 4) open, input voltage clamping will not occur, i.e.,

$$\frac{V_+}{V_{peak}} > \frac{V_{TH+}}{V_{IHC3}}$$

$$\frac{5V}{10V} > \frac{3.8V}{12.0V}$$

Consequently, a conservative value for the maximum power dissipation in R_x for the unclamped input voltage condition ignoring the input offset voltage is given by:

$$P_{R_x} = \frac{\left[V_{peak} \left(\frac{R_x}{R_x + 1 \text{ k}\Omega} \right) \right]^2}{R_x} \quad (\text{Unclamped Input}) \quad (5)$$

$$= \frac{\left[10V \left(\frac{470\Omega}{1470\Omega} \right) \right]^2}{470\Omega}$$

$$P_{R_x} = 21.8mW$$

If $V_+/V_{peak} < V_{TH+}/V_{IHC}$ was true (clamped input voltage condition), then the formula for the maximum power dissipation in R_x becomes:

$$P_{R_x} = \frac{(V_{peak} - V_{IHC})^2}{R_x} \quad (\text{Clamped Input}) \quad (6)$$

The maximum input current or power must be determined to ensure that it is within the maximum input rating of the HCPL-3700. For the clamped input voltage condition,

$$I_{IN} = \frac{V_{peak} - V_{IHC}}{R_x} < I_{IN}(\text{max}) \quad (7)$$

or

$$P_{IN} = V_{IHC} (I_{IN}) < P_{IN}(\text{max}) \quad (8)$$

Clamped
Condition

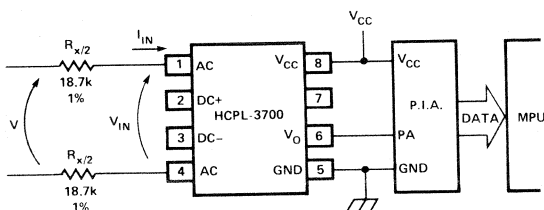


Figure 6. Interfacing an AC Voltage to an MPU using the HCPL-3700

For the unclamped input voltage condition, the maximum input current, or power will not be exceeded, because maximum input current and power will occur only under clamp conditions.

An output load resistance is not needed in this application because the peripheral interface adapter, such as MC6821, has an internal pullup resistor connected to its input.

Example 2. AC Operation

As shown in Figure 6, an ac application is that of a monitored 115V ac limit switch. Ac sensing is commonly used and the HCPL-3700 conveniently provides an internal rectification circuit. With the HCPL-3700 interfacing to the P.I.A., a choice can be made not to filter the ac signal or to filter the ac signal at the input or output of the device. All three conditions will be explored. Simplicity is obtained with no filtering at all, but software detection techniques must be used. Output filtering is a standard method, but may present problems with slow RC rise time of the output waveform when TTL logic is used. Input filtering avoids the RC rise time problem of output filtering, but introduces an extra time delay at the input.

AC Operation With No Filtering

In this example, a V_+ value of 98V is selected based on a criteria of 60% of V_{peak} . Monitoring a limit switch for a 60% level of the signal will give sufficient noise immunity from an open 115V ac line while allowing the HCPL-3700 to turn on under low line voltage conditions of -15% from nominal values when the limit switch is closed.

The value of R_x for the upper threshold detection level without the filter capacitor, C, across the dc input, can be obtained from the following expression.

$$R_x = \frac{V_+ - V_{TH+}}{I_{TH+}} \quad \begin{array}{l} V_{TH+} = 5.1V \\ \text{(ac instantaneous)} \\ I_{TH+} = 2.5mA \end{array} \quad (9)$$

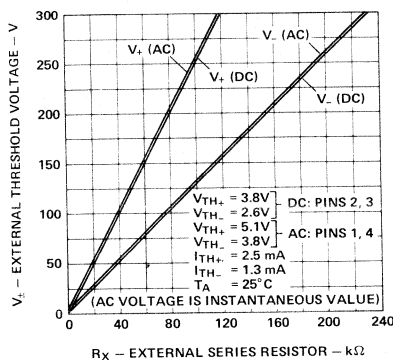


Figure 7. Typical External Threshold Characteristic, V_{\pm} - vs. R_x

$$R_x = \frac{98V - 5.1V}{2.5mA}$$

$$R_x = 37.2k\Omega \quad (\text{use } R_x/2 = 18.7k\Omega, 1\% \text{ resistor for each input lead})$$

The resulting lower threshold point is

$$\begin{aligned} V_- &= I_{TH-} R_x + V_{TH-} \\ &= (1.3mA)(37.4k\Omega) + 3.8V \end{aligned} \quad (10)$$

$$V_- = 52.4V \quad (32\% \text{ of peak input voltage})$$

Figure 7 provides a convenient, graphical choice for the external series resistor, R_x , and a particular external threshold voltage V_{\pm} .

The corresponding R_x value and output waveform of the HCPL-3700 for a $V_+ = 98V$ (60% of peak) is shown in Figure 8.

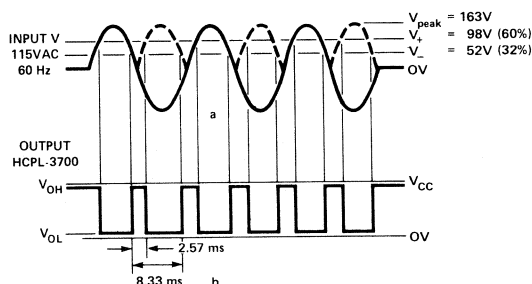


Figure 8. Output Waveforms of the HCPL-3700 Design in Figure 7 with no Filtering Applied

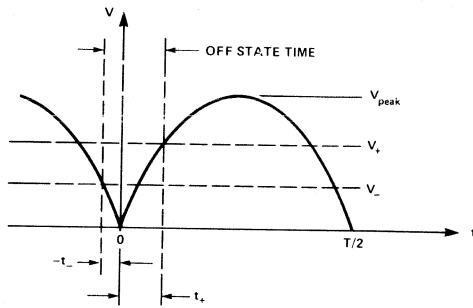


Figure 9. Determination of Off/On State Time

To determine the time in the high state, refer to Figure 9 and Equation (11).

Due to symmetry of sinusoidal waveform, the high state time is $t_- + t_+$ where t_{\pm} is given by:

$$t_{\pm} = \frac{T}{360^\circ} \sin^{-1} \left(\frac{V_{\pm}}{V_{\text{peak}}} \right) \quad (11)$$

where arc sine is in degrees and T = period of sinusoidal waveform.

In the unfiltered condition, the output waveform of Figure 8 must be used as sensed information. Software can be created in which the microprocessor will examine the waveform from the optocoupler at specific intervals to determine if ac is present or absent at the input to the HCPL-3700. This technique eliminates the problem of filtering, and accompanying delays, but requires more sophisticated software implementation in the microprocessor.

Input Filtering for AC Operation

A convenient method by which to achieve a continuous output low state in the presence of the applied ac signal is to filter the input dc terminals (pins 2–3) with a capacitance C while the ac signal is applied to the ac input (pins 1–4) of the full wave rectifier bridge. Input filtering allows flexibility in using the HCPL-3700 output for direct interfacing with TTL or CMOS devices without the slow rise time which would be encountered with output filtering. In addition, the input filter capacitor provides extra transient and contact bounce filtering. Because filtering is done after R_x , the capacitor working voltage is limited by the V_{IHC2} clamp voltage rating which is 6.7V peak for ac operation. The disadvantage of input filtering is that this technique introduces time delays at turn on and turn off of the optocoupler due to initial charge/discharge of the input filter capacitor.

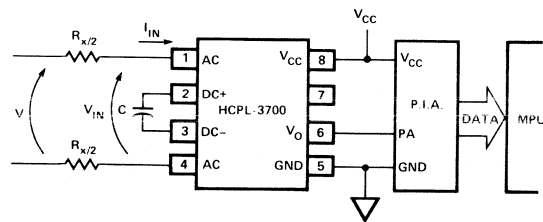


Figure 10. Input Filtering with the HCPL-3700

The application of ac input filtering is illustrated in Figure 10 and is described in the following example. The ac input conditions are the same as in the previous example of the 115V ac limit switch.

The minimum value of capacitance C to ensure proper ac filtering is determined by the parameters of the optocoupler. At low ac input voltage, the capacitor must charge to at least $V_{\text{TH}+}$ in order to turn on, but must not discharge to $V_{\text{TH}-}$ during the discharge cycle. A conservative estimate for the minimum value of C is given by the following equations.

$$V_{\text{TH}+} - V_{\text{TH}-} = V_{\text{TH}+} e^{-t/\tau}, \quad \tau = R_{\text{IN}} C_{\text{min}} \quad (12)$$

where R_{IN} is the equivalent input resistance of the HCPL-3700.

$$C_{\text{min}} = \frac{t}{R_{\text{IN}} \ln \left(\frac{V_{\text{TH}+}}{V_{\text{TH}+} - V_{\text{TH}-}} \right)} \quad (13)$$

with $R_{\text{IN}} = 1\text{k}\Omega$, $V_{\text{TH}+} = 3.8\text{V}$, $V_{\text{TH}-} = 2.6\text{V}$ and $t = 8.33\text{ms}$ for 60 Hz or $t = 10\text{ms}$ for 50 Hz.

$$C_{\text{min}} = 7.23\mu\text{F} \text{ for } 60 \text{ Hz}$$

$$C_{\text{min}} = 8.68\mu\text{F} \text{ for } 50 \text{ Hz}$$

To ensure proper filtering, the recommended value of C should be large enough such that with the tolerance variation, C will always be greater than C_{min} (C should otherwise be kept as small as possible to minimize the inherent delay times which are encountered with this technique). Since the filter capacitor affects the input impedance, a slightly different value of R_x is required for the input filtered condition. Figure 11 shows the R_x versus V_{\pm} threshold voltage for $C = 10\mu\text{F}$, $22\mu\text{F}$, and $47\mu\text{F}$. For an application of monitoring a 115V RMS line for 65% of nominal voltage condition (75V RMS), an $R_x = 26.7\text{k}\Omega \pm 1\%$ with $C = 10\mu\text{F}$ will yield the desired threshold. The power dissipation for R_x is determined from the clamped

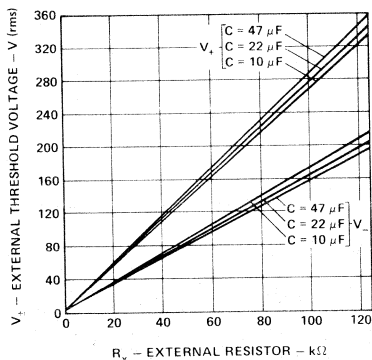


Figure 11. External Threshold Voltage versus R_X for Applications Using an Input Filter Capacitor C (Figure 10)

condition ($V_+/V_{\text{peak}} < V_{\text{TH+}}/V_{\text{ICH2}}$) and is 455mW (see Figure 6) which suggests $R_x/2$ of 1/2 watt resistors for each input lead.

Example 3. AC Operation with Improved Threshold Control and Accuracy

Some applications may occur which require threshold level detection at specific upper and lower threshold points. The ability to independently set the upper and lower threshold levels will provide the designer with more flexibility to meet special design criteria. As illustrated in Figure 12, a computer power line is monitored for a power failure condition in order to prevent loss of memory information during power line failure.

In this design, the HCPL-3700 optocoupler monitors the computer power line and the output of the optocoupler is interfaced to a TTL Schmitt trigger gate (7414).

In the earlier ac application of the HCPL-3700 (limit switch example), a single external series resistor, R_x , was used to determine one of the threshold levels. The other threshold level was determined by the hysteresis of the device, and not the designer. A potential problem of single threshold

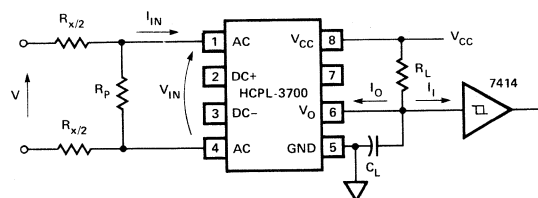


Figure 12. An AC Power Line Monitor with Simultaneous Selection of Upper and Lower Threshold Levels and Output Filtering

selection with 115V line application would be to determine R_x for a lower threshold level of 50% of nominal peak input voltage, only to find that the upper threshold level is 90% of peak input voltage. With the possible ac line voltage variations (+10%, -15%), it would be possible that the optocoupler could never reach the upper threshold point with an ac line that is at -15% of nominal value. To give the designer more control over both threshold points, a combination of series resistance, R_x , and parallel resistance, R_p , may be used, as shown in Figure 12.

Two equations can be written for the two external threshold level conditions. At the upper threshold point,

$$V_+ = R_x \left(I_{TH+} + \frac{V_{TH+}}{R_p} \right) + V_{TH+} \quad (14)$$

and at the lower threshold point,

$$V_- = R_x \left(I_{TH-} + \frac{V_{TH-}}{R_p} \right) + V_{TH-} \quad (15)$$

Solving these equations for R_x and R_p yield the following expressions:

$$R_x = \frac{V_{TH-}(V_+) - V_{TH+}(V_-)}{I_{TH+}(V_{TH-}) - I_{TH-}(V_{TH+})} \quad \begin{matrix} (16) \\ (16) \end{matrix}$$

$$R_p = \frac{V_{TH-}(V_+) - V_{TH+}(V_-)}{I_{TH+}(V_- - V_{TH-}) + I_{TH-}(V_{TH+} - V_+)} \quad (17)$$

Equations (16) and (17) are valid only if the conditions of Equations (18) or (19) are met. The desired external voltage threshold levels, V_+ and V_- , are established and the values for $V_{TH\pm}$ and $I_{TH\pm}$ are found from the data sheet. With the $V_{TH\pm}$, $I_{TH\pm}$ values, the denominator of R_X , Equation (16) is checked to see if it is positive or negative. If it is positive, then the following ratios must be met:

$$\frac{V_+}{V_-} \geq \frac{V_{TH+}}{V_{TH-}} \text{ and } \frac{V_+ - V_{TH+}}{V_- - V_{TH-}} < \frac{I_{TH+}}{I_{TH-}} \quad (18)$$

Conversely, if the denominator of R_x Equation (16) is negative, then the following ratios must hold:

$$\frac{V_+}{V_-} \leq \frac{V_{TH+}}{V_{TH-}} \text{ and } \frac{V_+ - V_{TH+}}{V_- - V_{TH-}} > \frac{I_{TH+}}{I_{TH-}} \quad (19)$$

Consider that the computer power line is monitored for a 50% line drop condition and a 75% line presence condition. The 115V 60 Hz ac line (163V peak) can vary from 85% (139V) to 110% (179V) of nominal value.

Require:

$$V_- = 81.5V \quad (50\%) \quad - \quad \text{Turn off threshold}$$

$$V_+ = 122.5V \quad (75\%) \quad - \quad \text{Turn on threshold}$$

Given:

$$V_{TH+} = 5.1V \quad I_{TH+} = 2.5mA \quad V_{IHC2} = 6.7V$$

$$V_{TH-} = 3.8V \quad I_{TH-} = 1.3mA$$

Using the Equations (16, 17) for R_x , R_p with the conditions of Equations (18, 19) being met yields

$$R_x = 17.4 \text{ k}\Omega \quad \text{use } 18 \text{ k}\Omega \quad 5\%$$

$$R_p = 1.2 \text{ k}\Omega \quad \text{use } 1.2 \text{ k}\Omega \quad 5\%$$

To complete the input calculations for maximum input current, I_{IN} , to the device and maximum power dissipation in R_x and R_p , a check must be made to determine if the input voltage will clamp at peak applied voltage. Using Equations (3) and (4) to determine if a clamp or no clamp exists, it is found that the ratios

$$0.75 = \frac{V_+}{V_{peak}} \approx \frac{V_{TH+}}{V_{IHC2}} = 0.76$$

indicate that V_{IN} slightly entered clamp condition. In this application, the operating input current, I_{IN} , is given approximately by

$$I_{IN} = \frac{V - \frac{V_{IHC2}}{\sqrt{2}}}{R_x} - \frac{\frac{V_{IHC2}}{\sqrt{2}}}{R_p} < I_{IN} \text{ (max)} \quad (20)$$

$$= \frac{115V - \frac{6.7V}{\sqrt{2}}}{18 \text{ k}\Omega} - \frac{\frac{6.7V}{\sqrt{2}}}{1.2 \text{ k}\Omega}$$

$$I_{IN} = 2.18mA \text{ RMS} < 34.3mA$$

Power dissipation in R_x is determined from the following equation,

$$P_{R_x} = \frac{\left(V - \frac{V_{IHC2}}{\sqrt{2}} \right)^2}{R_x} \quad (21)$$

which yields 0.675W. With the clamp condition existing, the maximum power dissipation for R_p is 18.7mW which is determined from

$$P_{R_p} = \frac{\left(\frac{V_{IHC2}}{\sqrt{2}} \right)^2}{R_p} \quad (22)$$

Output Filtering

The advantages of filtering at the output of the HCPL-3700 are that it is a simple method to implement. The output waveform introduces only one additional delay time at turn off condition as opposed to the input filtering method which introduces additional delay times at both the turn on and turn off conditions due to initial charge or discharge of the input filter capacitor. The disadvantage of output filtering is that the long transition time, t_r , which is introduced by the output RC filter requires a Schmitt trigger logic gate to buffer the output filter circuit from the subsequent logic circuits to prevent logic chatter problems. The determination of load resistance and capacitance is illustrated in the following text.

The following given values specify the interface conditions.

HCPL-3700

$$V_{OL} = 0.4V$$

$$I_{OL} = 4.2mA$$

$$I_{OH} = 100\mu A \text{ max}$$

$$V_{CC} = 5.0V \pm 5\%$$

7414

$$\left. \begin{array}{l} V_{T+} \text{ (min)} = 1.5V \\ V_{T+} \text{ (max)} = 2.0V \end{array} \right\} \begin{array}{l} \text{Schmitt trigger upper} \\ \text{threshold level} \end{array}$$

$$I_{IH} = 40\mu A \text{ max}$$

$$I_{IL} = -1.2mA \text{ max}$$

With the current convention shown in Figure 12, the minimum value of R_L which ensures that the output transistor remains in saturation is:

$$\begin{aligned} R_L \text{ (min)} &\geq \frac{V_{CC} \text{ (max)} - V_{OL}}{I_{OL} + I_{IL}} \\ &= \frac{5.25V - 0.4V}{4.2mA - 1.2mA} = 1.62 \text{ k}\Omega \end{aligned} \quad (23)$$

The maximum value for R_L is calculated allowing for a guardband of 0.4V in $V_{T+} \text{ (max)}$ parameter, or $V_{IH} = V_{T+} \text{ (max)} + 0.4V$.

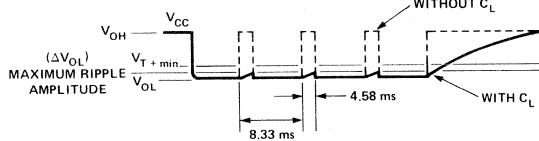


Figure 13. Output Waveforms of the HCPL-3700

$$R_L (\text{max}) \leq \frac{V_{CC} (\text{min}) - V_{IH}}{I_{OH} - I_{IH}} \quad (24)$$

$$= \frac{4.75\text{V} - 2.4\text{V}}{0.1\text{mA} + 0.04\text{mA}} = 16.8 \text{ k}\Omega$$

R_L is chosen to be 1650Ω .

C_L can be determined in the following fashion. As illustrated in Figure 8, the output of the optocoupler will be in the high state for a specific amount of time dependent upon the selected V_+ levels. In this example, $V_+ = 122.5\text{V}$ (75%) and $V_- = 81.5\text{V}$ (50%) and allowing for a minimum peak line voltage of 138V (-15%), the high state time (without C_L) is from Equation (11), 4.58ms . With the appropriate C_L value, the output waveform (solid line) shown in Figure 13 is filtered.

The maximum ripple amplitude above V_{OL} is chosen to be 0.6V ; that is, $V_{OL} + \Delta V_{OL} = 1.0\text{V}$. This gives a 0.5V noise margin before $V_{T+} (\text{min}) = 1.5\text{V}$ is reached. The exponential ripple waveform is caused by the C_L being charged through R_L and input resistance, R_{INTTL} , of TTL gate. An expression for the allowable change in V_{OL} can be written:

$$\Delta V_{OL} = (V_{OH} - V_{OL}) (1 - e^{-t/\tau}) \quad (25)$$

where $\tau = R'_L C_L$ with R'_L equal to parallel combination of R_L and R_{INTTL} .

Below $V_{T+} = 1.5\text{V}$ (min), R_{INTTL} is constant and nominally $6 \text{ k}\Omega$. Hence:

$$R'_L = \frac{R_L R_{INTTL}}{R_L + R_{INTTL}} \quad (26)$$

$$= \frac{(1.65 \text{ k}\Omega) (6 \text{ k}\Omega)}{1.65 \text{ k}\Omega + 6 \text{ k}\Omega}$$

$$R'_L = 1.29 \text{ k}\Omega$$

Solving Equation (25) for τ yields

$$\tau = \frac{t}{\ln \left(\frac{V_{OH} - V_{OL}}{V_{OH} - V_{OL} - \Delta V_{OL}} \right)} \quad (27)$$

and substituting previous parameter values and using $V_{OH} = V_{CC} - (I_{OH} + I_{IH}) R_L$ results in

$$= \frac{4.58\text{ms}}{\ln \left(\frac{4.8\text{V} - 0.4\text{V}}{4.8\text{V} - 0.4\text{V} - 0.6\text{V}} \right)}$$

$$\tau = 31.24\text{ms}$$

C_L can be calculated directly,

$$C_L = \frac{\tau}{R'_L} \quad (28)$$

$$= \frac{31.24\text{ms}}{1.29 \text{ k}\Omega}$$

$$C_L = 24.2\mu\text{F} \quad \text{use } 27\mu\text{F} \pm 10\%$$

$$\text{or } 33\mu\text{F} \pm 20\%$$

With this value of C_L , the time the $R'_L C_L$ filter network takes to reach V_{T+} of the TTL gate is found as follows.

$$V_{OL} + (V_{OH} - V_{OL}) (1 - e^{-t/\tau}) = V_{T+} \quad (29)$$

Solving for t ,

$$t = \tau \ln \left(\frac{V_{OH} - V_{OL}}{V_{OH} - V_{T+} (\text{min})} \right) \quad (30)$$

and substituting $V_{OH} = 4.8\text{V}$, $V_{OL} = 0.4\text{V}$, $V_{T+} (\text{min}) = 1.5\text{V}$, and $\tau = 31.24\text{ms}$ yields

$$t = 9.0\text{ms}$$

This is the delay time that the system takes to respond to the ac line voltage going below the 50% (V_-) threshold level. In essence, the response time is slightly more than a half cycle (8.33ms) of 60 Hz ac line with worst case line variation taken into account. This delay time is acceptable for system power line protection. In this example, a complete worst case analysis was not performed. A worst case analysis should be done to ensure proper function of the circuit over variations in line voltage, unit to unit device parameter variations, component tolerances and temperature.

Threshold Accuracy Improvement

In the above example on output filtering, the two external threshold levels were selected for turn on conditions at $V_+ = 122.5\text{V}$ (75%) and turn off at $V_- = 81.5\text{V}$ (50%). The calculated external resistor values were $R_X = 17.4\text{ k}\Omega$ and $R_P = 1.2\text{ k}\Omega$. Using standard 5% resistors of $18\text{ k}\Omega$ and $1.2\text{ k}\Omega$ respectively, the upper threshold voltage was actually 126.6V nominal.

Examination of the worst possible combination of variations of the HCPL-3700 optocoupler V_{TH+} , I_{TH+} , levels from unit to unit, and the $\pm 5\%$ variations of R_X and R_P can result in the V_+ level changing +23% to -25% from design nominal.

If higher threshold accuracy is desired, it can be accomplished by decreasing the value of R_P in order to allow R_P to dominate the input resistance variations of the optocoupler. Using a 1% resistor for R_P and resistance of sufficiently small magnitude, the V_+ tolerance variations can be significantly improved. The following analysis will allow the designer to obtain nearly optimum threshold accuracy from unit to unit. It should be noted that the HCPL-3700 demonstrates excellent threshold repeatability once the external resistors are adjusted for a particular level and unit. The compromise which is made for the added control on threshold accuracy is that more input power must be consumed within the R_P , R_X resistors.

In Figure 14, assume the circuit is at the upper threshold point. At constant V_{TH+} , it is desired to maintain I_+ to within $\pm 5\%$ variation of nominal value while allowing $\pm 1\%$ variation in I_{P+} . With this requirement, Equations (31) and (32) can be written and solved for the magnitude of I_{P+} which is needed to maintain the desired condition on I_+ . I_+ is the sum of I_{P+} and I_{TH+} .

$$1.05 I_+ = 1.01 I_{P+} + I_{TH+} (\text{max}) \quad (31)$$

$$0.95 I_+ = 0.99 I_{P+} + I_{TH+} (\text{min}) \quad (32)$$

} at constant V_{TH+}

where

$$I_{TH+} (\text{max}) = 3.11\text{mA}$$

$$I_{TH+} (\text{min}) = 1.96\text{mA}$$

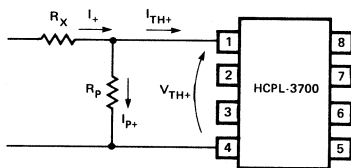


Figure 14. Threshold Accuracy Improvement through the Use of External R_X and R_P Resistors

Solving for I_{P+} yields

$$I_{P+} = 11.2\text{mA},$$

and

$$R_P = \frac{V_{TH+}}{I_{P+}} \quad (33)$$

$$= \frac{5.1\text{V}}{11.2\text{mA}}$$

$$R_P = 433\Omega \quad (\text{use } 453\Omega, 1\% \text{ resistor})$$

This new value of R_P replaces the earlier $R_P = 1.2\text{ k}\Omega$, and the circuit requires a new R_X value to maintain the same V_+ threshold level.

$$R_X = \frac{V_+ - V_{TH+}}{I_+} \quad \text{where } I_+ = I_{P+} + I_{TH+} \quad (34)$$

$$= 11.2\text{mA} + 2.5\text{mA}$$

$$= \frac{122.5\text{V} - 5.1\text{V}}{13.7\text{mA}}$$

$$R_X = 8.57\text{ k}\Omega \quad (\text{use } 8.66\text{ k}\Omega, 1\% \text{ resistor})$$

With the possible variation of $\pm 1\%$ in R_P and R_X , as well as unit to unit variations in the optocoupler V_{TH+} , I_{TH+} , the upper threshold level V_+ will vary significantly less than in the 5% resistor design case. The variations in V_+ , which is given by $V_+ = R_X I_+ + V_{TH+}$, where $I_+ = I_{P+} + I_{TH+}$, are compared in Table 1.

Table 1 illustrates the possible improvements in V_+ tolerance as R_X and R_P are adjusted to limit the variation of the external input threshold current, I_+ , to the resistor network and optocoupler. This table is centered at a nominal external input threshold voltage of $V_+ = 122.5\text{V}$. It is the designer's compromise to keep power consumption low, but threshold accuracy high.

NOTE: The above method for selection of R_P and R_X can be adapted for applications where larger sense currents (wet sensing) may be appropriate.

Example 4. Dedicated Lines for Remote Control

In situations involving a substantial separation between the signal source and the receiving station, it may be desirable to lease a dedicated private line metallic circuit (dc path) for supervisory control of remote equipment. The HCPL-3700 can provide the interface requirements of voltage threshold detection and optical isolation from the metallic line to the remote equipment. This greatly reduces the expense of using a sophisticated modem system over a convention telephone line.

R_x	T O L.	R_p	T O L.	I_+ TOLERANCE	V_+ TOLERANCE		MAXIMUM TOTAL POWER IN $R_x + R_p$ (RMS)
18 k Ω	5%	1.2 k Ω	5%	+17.5% -21.2%	+ 23%	- 25%	0.69 W
8.66 k Ω	1%	453 Ω	1%	$\pm 5\%$	+12.7%	-19.3%	1.45 W
4.32 k Ω	1%	205 Ω	1%	$\pm 3\%$	+11.2%	-18.9%	2.92 W
2.15 k Ω	1%	97.5 Ω	1%	$\pm 2\%$	+10.6%	-18.8%	5.89 W

Table 1. Comparison of the V_+ Threshold Accuracy Improvement versus R_x and R_p and Power Dissipation for a Nominal $V_+ = 122.5$ V

Figure 15 represents the application of the HCPL-3700 for a line which is to control tank levels in a water district.

Some comments are needed about dedicated metallic lines. The use of a private metallic line places restrictions upon the designer's signal levels. The line in this example would be used in the interrupted dc mode (duration of each interruption greater than one second), the maximum allowed voltage between any conductor and ground is ≤ 135 volts. Maximum current should be limited to 150mA if the cable has compensating inductive coils in it. Balanced operation of the line is strongly recommended to reduce possible cross talk interference as well as to allow larger signal magnitudes to be used. Precaution also should be taken to protect the line and equipment. The line needs to be fused to ensure against equipment failure causing excessive current to flow through telephone company equipment. In addition, protection from damaging transients must be taken via spark gap arrestors and commercial transient suppressors. Details of private line metallic circuits can be founded in the American Telephone and Telegraph Company publication 43401.

In this application, a 48V dc floating power source supplies the signal for the metallic line. The HCPL-3700 upper voltage threshold level is set for $V_+ = 36$ V (75%). Consequently, R_x is

$$R_x = \frac{V_+ - V_{TH+}}{I_{TH+}} \quad (35)$$

$$= \frac{36\text{V} - 3.8\text{V}}{2.5\text{mA}}$$

$$= 12.9 \text{ k}\Omega \quad (\text{use } R_x/2 = 6.49 \text{ k}\Omega, 1\% \text{ resistor in each input level})$$

The resulting lower voltage threshold level is

$$V_- = R_x I_{TH-} + V_{TH-} \quad (36)$$

$$= 13 \text{ k}\Omega (1.3\text{mA}) + 2.6\text{V}$$

$$V_- = 19.5\text{V}$$

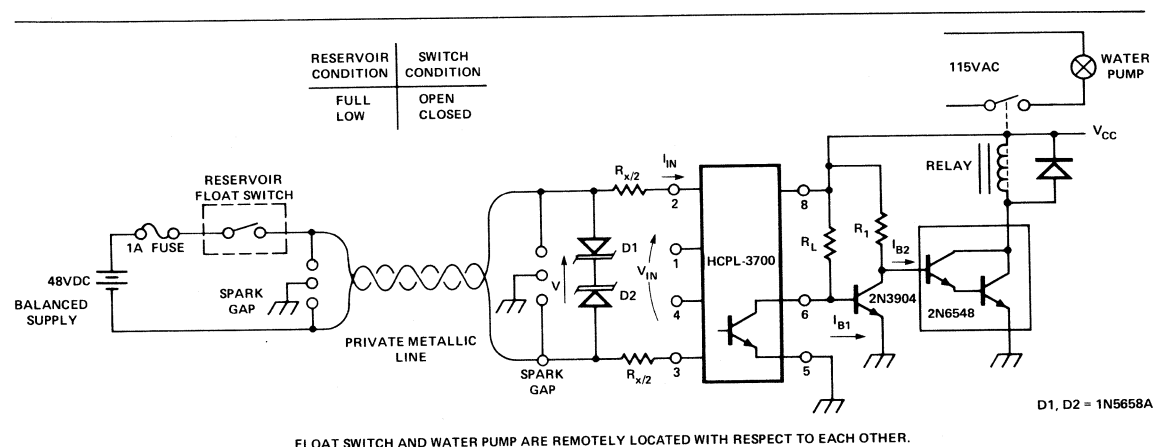


Figure 15. Application of the HCPL-3700 to Private Metallic Telephone Circuits for Remote Control

yielding $V_{HYS} = 16.5V$. The average induced ac voltage from adjacent power lines is usually less than 10 volts (reference ATT publication 43401) which would not falsely turn on, or off, the HCPL-3700, but could affect conventional optocouplers.

Under normal operation (full reservoir), the optocoupler is off. When the float switch is closed (low reservoir), the optocoupler output (V_{OL}) needs inversion, via a transistor, to drive the power Darlington transistor which controls a motor starting relay. The relay applies ac power to the system water pump. With $V_{CC} = 10V$, $I_{B2} = 0.5mA$, $I_{B1} = 0.5mA$.

$$R_1 = \frac{V_{CC} - 2V_{BE}}{I_{B2}} \quad (37)$$

$$= \frac{10V - 1.4V}{0.5mA}$$

$$R_1 = 17.2 \text{ k}\Omega$$

$$(R_1 = 18 \text{ k}\Omega)$$

$$R_L = \frac{V_{CC} - V_{BE}}{I_{B1}} \quad (38)$$

$$= \frac{10V - 0.7V}{0.5mA}$$

$$R_L = 18.6 \text{ k}\Omega$$

$$(R_L = 18 \text{ k}\Omega)$$

For this application, the ac inputs could also be used, which would remove any concern about the polarity of the input signal.

General Protection Considerations for the HCPL-3700

The HCPL-3700 optocoupler combines a unique function of threshold level detection and optical isolation for interfacing sensed signals from electrically noisy, and potentially harmful, environments. Protection from transients which could damage the threshold detection circuit and LED is provided internally by the Zener diode bridge rectifier and an external series resistor. By examination of Figure 1, it is seen that an input ac voltage clamp condition will occur at a maximum of a Zener diode voltage plus a forward biased diode voltage.

At clamp condition, the bridge diodes limit the applied input voltage at the device and shunt excess input current which could damage the threshold detection circuit or cause excessive stress to the LED.

The HCPL-3700 optocoupler can tolerate significant input current transient conditions. The maximum dc input current into or out of any lead is 50mA. The maximum

input surge current is 140mA for 3ms at 120 Hz pulse repetition rate, and the maximum input transient current is 500mA for 10 μ s at 120 Hz pulse repetition rate. The use of an external series resistor, R_X , provides current limiting to the device when a large voltage transient is present. The amplitude of the acceptable voltage transient is directly proportional to the value of R_X .

However, in order to protect the HCPL-3700 when the input voltage to the device is clamped, the maximum input current must not be exceeded. An external means by which to enhance transient protection can be seen in Figure 16.

A transient $R_X C_P$ filter can be formed with C_P chosen by the designer to provide a sufficiently low break point for the low pass filter to reduce high frequency transients. However, the break point must not be so low as to attenuate the signal frequency. Consider the previous ac application where no filtering was used. In that application, $R_X = 37.4 \text{ k}\Omega$, and if the bandwidth of the transient filter needs to be 600 Hz, then C_P is:

$$C_P = \frac{1}{2\pi f R_X} \quad (39)$$

$$C_P = 0.0071\mu F \quad (\text{use } 0.0068\mu F \text{ capacitor @ } 50V \text{ dc})$$

Should additional protection be needed, a very effective external transient suppression technique is to use a commercial transient suppressor, such as a Transzorb[®], or metal oxide varistor, MOV[®], at the input to the resistor network prior to the optocoupler. The Transzorb[®] will provide extremely fast transient response, clamp the input voltage to a definite level, and absorb the transient energy. Selection of a Transzorb[®] is made by ensuring that the reverse stand off voltage is greater than the continuous peak operating voltage level. Transzorbs[®] can be stacked in series or parallel for higher peak power ratings. Depending upon the designer's potential transient problems, a solution may warrant the expense of a commercial suppression device.

Thermal Considerations

Thermal considerations which should be observed with the HCPL-3700 are few. The plastic 8 pin DIP package is designed to be operated over a temperature range of -25°C to 85°C. The absolute maximum ratings are established for

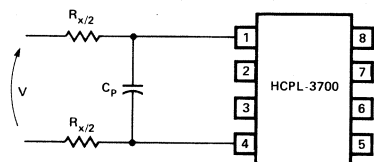


Figure 16. $R_X C_P$ Transient Filter for the HCPL-3700

a 70°C ambient temperature requiring slight derating to 85°C. In general, if operation of the HCPL-3700 is at ambient temperature of 70°C or less, no heat sinking is required. However, for operation between 70°C and 85°C ambient temperature, the maximum ratings should be derated per the data sheet specifications.

Mechanical and Safety Considerations

Mechanical Mounting Considerations

The HCPL-3700 optocoupler is a standard 8 pin dual-in-line plastic package designed to interface ac or dc power systems to logic systems. This optocoupler can be mounted directly onto a printed circuit board by wave soldering.

Electrical Safety Considerations

Special considerations must be given for printed circuit board lead spacing for different safety agency requirements. Various standards exist with safety agencies (U.L., V.D.E., I.E.C., etc.) and should be checked prior to PC board layout. The HCPL-3700 optocoupler component is recognized under the Component Program of Underwriters Laboratories, Inc. in file number E55361. This file qualifies the component to specific electrical tests to 220V ac operation.

The spacing required for the PC board leads depends upon the potential difference that would be observed on the board. Some standards that could pertain to equipment which would use the HCPL-3700 are UL1244, Electrical and Electronic Measuring and Testing Equipment, UL1092, Process Control Equipment, and IEC348, Electronic Measuring Apparatus. Spacing for the worst case in an uncontrolled environment with a 2000 volt-amperes maximum supplying source rating must be 3.2mm (0.125 inches) for 51 – 250 volts RMS potential difference over a surface (creepage distance), and 3mm (0.118 inches)

through air (bare wire). These separations are between any uninsulated live part and uninsulated live part of opposite polarity, or uninsulated ground part other than the enclosure or an exposed metal part.

An uncontrolled environment is an environment which has contaminants, chemical vapors, particulates or any substances which would cause corrosion, decrease resistance between PC board traces or, in general, be an unhealthy environment to human beings.

For 0 – 50 volts RMS, the spacing is 1.6mm (0.063 inches) through air or over surfaces.

Electrical Connectors

The HCPL-3700 provides the needed isolation between a power signal environment and a control logic system. However, there exists a physical requirement to actually interconnect these two environments. This interconnection can be accomplished with barrier strips, edge card connectors, and PCB socket connectors which provide the electrical cable/field wire connection to the I/O logic system. These connectors provide for easy removal of the PC board for repair or substitution of boards in the I/O housing and are needed to satisfy the safety agency (U.L., V.D.E., I.E.C.) requirements for spacing and insulation. Connectors are readily available from many commercial manufacturers, such as Connection Inc., Buchanan, etc. The style of connector to choose is dependent upon the application for which the PC board is used. If possible it is wise to choose a style which does not mount to the PC board. This would enable the PC card to be removed without having to disconnect field wires. The use of connectors which are called “gas tight connectors” provide for good electrical and mechanical reliability by reducing corrosion effects over time.

APPENDIX I. List of Parameters

- V ≡ Externally Applied Voltage
- V₊ ≡ External Upper Threshold Voltage Level
- V_− ≡ External Lower Threshold Voltage Level
- V_{IHC1} = Device* Input Voltage Clamp Level; Low Voltage DC Case
- V_{IHC2} = Low Voltage AC Case
- V_{IHC3} = High Voltage DC Case
- I_{IN} = Device Input Current
- V_{IN} = Device Input Voltage
- V_{TH+} = Device Upper Voltage Threshold Level
- V_{TH−} = Device Lower Voltage Threshold Level
- I_{TH+} = Device Upper Input Current Threshold Level
- I_{TH−} = Device Lower Input Current Threshold Level
- R_x = External Series Resistor for Selection of External Threshold Level
- R_p = External Parallel Resistor for Simultaneous Selection/Accuracy Improvement of External Threshold Voltage Levels
- I₊ = Total Input Current at Upper Threshold Level to External Resistor Network (R_x, R_p) and Device
- I_{p+} = Current in R_p at Upper Threshold Levels
- V_{peak} = Peak Externally Applied Voltage
- V_O = Output Voltage of Device

- V_{OL} = Output Low Voltage of Device
- V_{OH} = Output High Voltage of Device
- I_{OH} = Output High Leakage Current of Device
- I_{OL} = Output Low Sinking Current of Device
- I_{IH} = Input High Current of Driven Gate
- I_{IL} = Input Low current of Driven Gate
- V_{CC} = Positive Supply Voltage
- R_{IN} = Input Resistance of HCPL-3700
- V_{T+} ≡ Schmitt Trigger Upper Threshold Voltage of TTL Gate (7414)
- R_L = Output Pullup Resistance
- C_L = Output Filter Capacitance
- C = Input Filter Capacitor
- TH₊ = Upper Threshold Level
- TH_− = Lower Threshold Level
- P_{R_x} = Power Dissipation in R_x
- P_{IN} = Power Dissipation in HCPL-3700 Input IC
- PA = Input Signal Port to P.I.A.
- t₊ = Turn On Time
- t_− = Turn Off Time
- T = Period of Waveform
- C_p = Similar to R_p

*Device = HCPL-3700



Ring Detection with the HCPL-3700 Optocoupler

The field of telecommunications has reached the point where the efficient control of voice channels is essential. People in business are communicating to a larger extent over telephone, and they are requiring lower cost, easy, and quick access to phone lines. These requirements, coupled with the evolution of the modem, automatic phone answering equipment, and communication between computers over public lines, have resulted in the introduction of electronic control and private automatic branch exchange (PABX) systems. There must, however, be isolation between the sensitive, microprocessor-based, control circuitry and the higher voltage, transient-prone transmission line. Optocouplers, or optical isolators, are effective, reliable, and inexpensive devices for achieving this protection and isolation. An area where optocouplers can be used to great advantage is in the ring detection portion of the control circuitry, and that will be the emphasis of this report.

THE NATURE OF THE RING SIGNAL

Ring detection is the first operation necessary in completing the connection between the central office and the individual telephone. Figure 1 illustrates a simplified version of this connection.

When a request to connect a particular line comes to the central office, the ring signal is transmitted on the tip and ring of the requested line until an off-hook condition is detected through the presence of a dc loop current. The nature of this ring signal is addressed in the Federal Communications Commission's Part 68, in section 312 (On-hook Impedance Limitations). Essentially, the ringing signal is a sinusoidal wave of frequency ranging from 15.3 to 68.0 Hz. The amplitude of the ring signal, which is superimposed upon a dc voltage between tip and ring of -48 V, can vary from 40 to 150 VRMS. The ac impedance must be greater

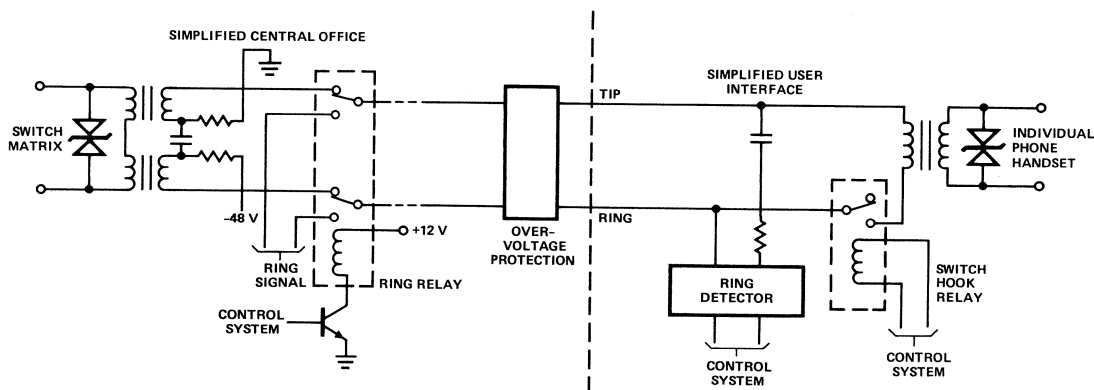


Figure 1. Simplified Central Office-to-User Interface

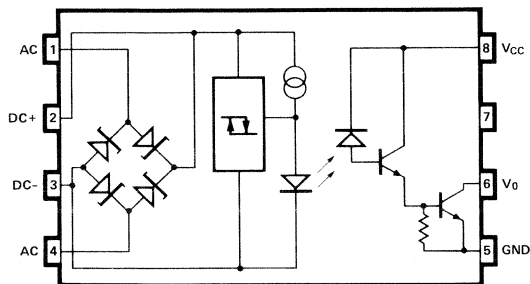


Figure 2. Schematic Diagram of HCPL-3700

than 1600 Ω . Due to the fact that the central exchange detects an off-hook condition by the presence of a dc current, the dc impedance presented by the ring detection circuitry must be very high. Part 68 states that "the dc resistance between tip and ring conductors, and between each of the tip and ring conductors and earth ground shall be greater than 10 M Ω for dc voltages up to and including 100 V."

Regulations are slightly different in Europe, with voltage amplitudes varying from 30 VRMS to 100 VRMS at a nominal frequency of 25 Hz.

Therefore, the ring signal is obviously not logic compatible and cannot be interfaced directly to electronic circuitry. Furthermore, lightning-induced transients, in the form of a very high voltage, underdamped sinusoid, as well as other environmentally induced transients such as dial pulses from other extensions on the same line, must also be protected against. The ring detector must output a logic compatible signal in the presence of ring signal with amplitude anywhere within the U.S. or European regulations, and also discriminate between this signal and any transient that might be present on the transmission line.

THE HCPL-3700: EASY THRESHOLD DETECTION AND FILTERING

The HCPL-3700 offers a complete, optimal solution to the ring detect problem with a minimal amount of external components needed. This optocoupler features a Zener

diode full-wave bridge rectifier at the input, followed by a hysteresis buffer and constant current source to drive the LED. The LED is turned on or off at prescribed voltage and current thresholds. These thresholds can be adjusted by the insertion of a series impedance. The output stage of the optocoupler is a photodetector and a split-Darlington amplifier circuit. A schematic diagram of the HCPL-3700 is shown in Figure 2.

To turn the LED on, which results in an output low state, the positive threshold must be exceeded. The correct external impedance must be used to ensure that this switching occurs at the desired point, according to the following equation:

$$Z_{EXT} = (V_{+}(MIN) - V_{TH}(MAX) +) / I_{TH}(MAX) + \quad (1)$$

where $V_{TH}(MAX) +$ and $I_{TH}(MAX) +$ are given in the data sheet and $V_{+}(MIN)$ is the desired switching point. (If detection of a ring signal of 40 VRMS minimum is desired, this value would be $40 \times \sqrt{2} = 56.6$ V.)

To meet the requirement of presenting a very high dc impedance to the central office, it is advantageous to ac couple the ring signal. This is accomplished by using a series capacitor. This capacitor, in conjunction with series resistance, creates the impedance required to set the threshold of the HCPL-3700 and to meet the ac impedance requirement. The impedance is then approximated as follows:

$$Z_{EXT} \cong (R_{EXT}^2 + \left[\frac{1}{2\pi f RING C} \right]^2)^{0.5} \quad (2)$$

If we choose a capacitor of 2.2 μ F, and assume a minimum ringing frequency of 15 Hz and a minimum amplitude of 40 VRMS, then we can calculate a value for the external resistance using equations (1) and (2).

$$R_{EXT} = ((V_{+}(MIN) - V_{TH}(MAX) +) / I_{TH}(MAX) +)^2 - (1 / 2\pi f RING C)^2)^{0.5} \\ R_{EXT} = 15700 \Omega. \quad (3)$$

The external resistance is then split up equally between the tip and the ring lines in order to provide a balanced line termination and transient suppression on both lines. Figure 3 shows the equivalent circuit using the results from equation (3).

The power dissipation required of the resistors must also be taken into account. The Zener diode bridge at the input of

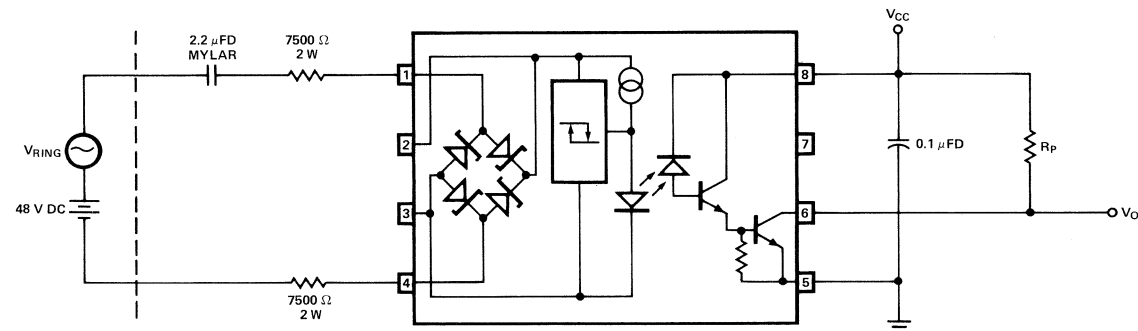


Figure 3. Equivalent Circuit for Detection of 40 V rms Signal

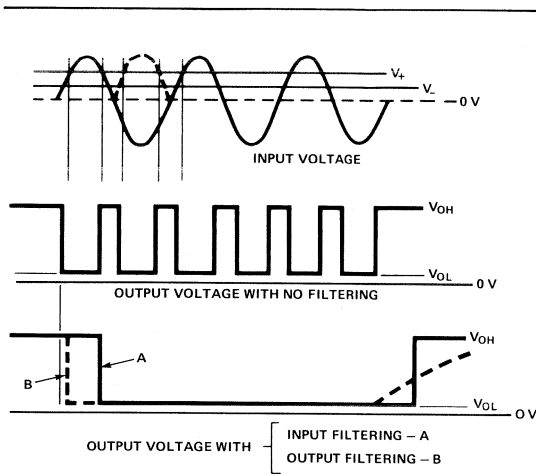


Figure 4. Waveforms for Input and Output Filtering

the HCPL-3700 clamps the voltage across the ac inputs at approximately 7 V. The amount of power that then must be dissipated by each of the two external resistors is:

$$P = ((V_{RING(MAX)} - 7)/2)^2/R \quad (4)$$

where R is $R_{EXT}/2$. If the peak amplitude of the ring signal is 150 VRMS, then each resistor must dissipate 1.4 watts. A 2-watt resistor will provide extra protection. At the level of current present in the circuit, there is no danger of exceeding the maximum current rating of the optocoupler.

The output signal is essentially a square wave of frequency twice that of the input signal. To obtain a signal that is at logic low throughout the duration of the ring signal some type of filtering is required. This filtering can either be done at the input or the output of the HCPL-3700. Figure 4 shows the waveforms that would be obtained with input or output filtering.

If filtering is done on the output, the result will be a signal that begins to respond very quickly to a change in the ring signal but has very slow transitions. A comparator with hysteresis would then be needed at the output to digitize the signal. If filtering were done at the input, the output would not respond as quickly to a change in the ring signal but the edges would be much quicker. A comparator would not be needed. Since a slight delay in detection of the ring signal is generally tolerable, the input filtering technique is preferred. There is the added benefit of filtering, which follows from the fact that ring detection is slightly delayed. This benefit is that quick-edged transients with amplitudes in the range of the ring signal will not affect the output signal. The filter will eliminate them.

Input filtering is accomplished through the insertion of a capacitor across the dc inputs of the optocoupler (pins 2 and 3). Because the frequency of the ring signal can go down as low as 15 Hz, this capacitor should be 33 μ F. The voltage rating should be greater than 7 V, the clamping voltage of the Zener diode bridge rectifier. The introduction of this capacitor results in about a 30% reduction in the amplitude of the voltage detected by the optocoupler. This means that in order to maintain the desired effective threshold of operation, the external impedance must be lowered. Equation (1) given previously now becomes:

$$Z_{EXT} = ((V_+(MIN)) (0.7) - V_{TH(MAX)})/I_{TH(MAX)} + \quad (5)$$

Then, relating equations (2) and (5) we get the following equation which is similar to equation (3):

$$R_{EXT} = (((V_+(MIN)) (0.7) - V_{TH(MAX)})/I_{TH(MAX)})^2 - (1/2\pi f_{RING} C)^2)^{0.5} \quad (6)$$

Using the same values used previously, we obtain a value for R_{EXT} of 9845 Ω . The final equivalent circuit with filtering is then shown in Figure 5.

The power dissipation required of the resistors is reduced somewhat, to the point where 1 watt resistors could prove sufficient.

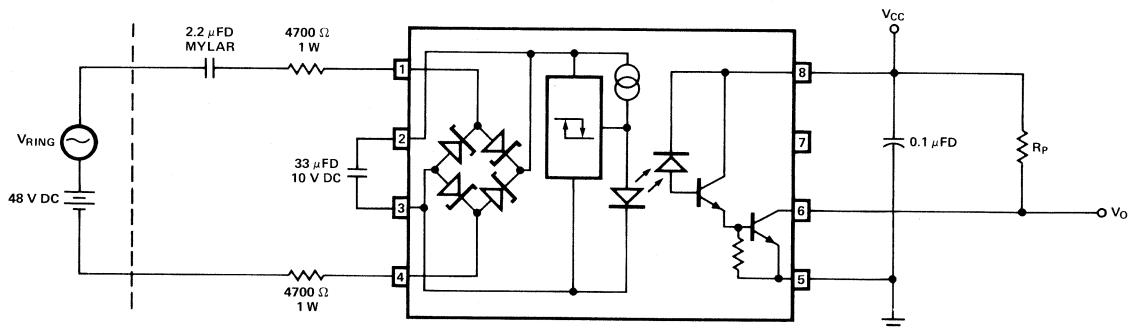


Figure 5. Equivalent Circuit with Input Filtering

THE HEWLETT-PACKARD HCPL-3700 VERSUS OTHER RING DETECTION TECHNIQUES

The HCPL-3700 optocoupler is a power-to-logic optocoupler which is very suitable for interfaces like ring detection where high voltage signals are monitored by sensitive electronics. It requires the least amount of external circuitry, and contains internal circuitry that allows for the most easily controllable switching point and higher reliability. Figure 6 illustrates another optocoupler design alternative which has "back-to-back" LED's that transmit light to a single photodetector.

This type of optocoupler design has several disadvantages compared to the HCPL-3700. It is evident from the diagram of this optocoupler that input filtering is not possible. Input filtering with the HCPL-3700 is only possible because of the dc input, which allows for a capacitor to be added to integrate the already rectified signal. There is no way to integrate the ac signal after it is rectified at the input of the "back-to-back" optocoupler alternative. Therefore, in order to present a "clean," digital signal to the following logic circuitry, output filtering must be done. This output filtering must include not only a capacitor but a comparator with hysteresis. Also, in looking at the data sheet the minimum guaranteed On-State RMS Input Current far exceeds the maximum guaranteed Off-State RMS Input Current. There is not a well defined threshold, which further amplifies the need for a comparator.

Another consideration, which affects reliability of the optocoupler and therefore reliability of the system, is the amount of forward current that the LED is subject to. Degradation in the light output of the LED due to high current levels reduces switching stability by raising the "effective" threshold

over time. Each LED in the "back-to-back" optocoupler design experiences the full excursion of the half-wave rectified current signal. This means that, in order to ensure detection of a ring signal of the minimum amplitude specified by FCC Part 68, the circuit would have to be designed in such a way that the maximum current level experienced by the LED's could be stressful and could lead to accelerated degradation. With the HCPL-3700, threshold detection is performed prior to the LED by the buffer (with hysteresis), and the LED is driven by a switched current source at low current levels. Degradation is therefore much lower. More information on LED degradation can be found in the Hewlett-Packard Application Note 1002, "Consideration of CTR Variations in Optically Coupled Isolator Designs."

There also exist integrated circuit packages specifically designed for ring detection applications. This family of ring detectors does not employ optical coupling and is less immune to transients than the HCPL-3700. An application report on this ring detector states that "when used in series with the proper resistor and capacitor, these devices will withstand 1500 V/200 μ s transients." This translates to 7.5 V/ μ s which, when compared to the HCPL-3700 values of -600 V/ μ s for Common Mode Transient Immunity at Logic Low Output and 4000 V/ μ s for CMTI at Logic High Output, is extremely low. To obtain an isolated ring detection circuit with this product, the application report recommends a single phototransistor optocoupler at the output. For the straightforward ring detection application, the HCPL-3700 is preferable for ease of design, number of external components required, isolation capabilities, and reliability.

SUMMARY

More and more aspects of the telecommunications industry are being automated, meaning that sensitive electronic devices are being interfaced with higher voltage, electrically-noisy circuitry. Ring detection is one area where this interface occurs. The sensitivity and expense of electronic equipment requires that this interface have high isolation capabilities, high performance capabilities, and a degree of versatility. Optical isolation with high performance optocouplers provides this.

For an integrated ring detection solution incorporating ease of design, a lower component count, and better predictability and reliability, the HCPL-3700 is optimal. The HCPL-3700 optocoupler contains a full-wave Zener diode bridge rectifier which, when combined with the correct input series impedance, provides a controllable, low-level current to an LED when a ring signal is present. With proper input filtering, consisting of a simple capacitor across the dc input, the output will be a digital, logic-compatible signal. A comparator is not required for interface to logic gates or microprocessors.

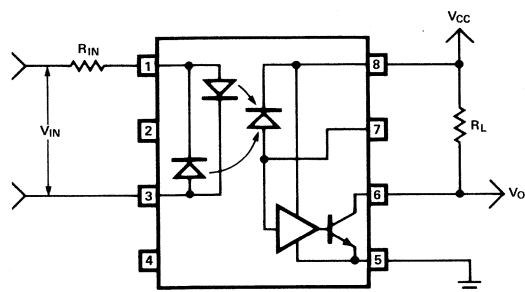


Figure 6. "Back-to-Back" Optocoupler

Interfacing from Industrial Control Systems to Microprocessors

Within the world of industrial and process control systems, there arises a need to interface from a power system, or large signal system, to a standard logic or microprocessor system. The interface must provide isolation, insulation, and level detection. Isolation is a requirement to keep systems electrically separate yet allow functional interconnection of the systems. Insulation capability prevents damage to either system which is referenced to different voltage levels. Level detection provides the needed discrimination between noise and signal.

Of these three interface characteristics, isolation and level detection pose the most important problems to solve. The range of problems includes high level noise, transients, capacitively coupled cross talk, large common mode signals, ground loops, wide range of sensed voltage, reliability, and safety.

Various methods of isolation include the use of a relay, capacitor, transformer, and optocoupler. Each method has its respective advantages and disadvantages in attempting to provide a workable solution to the problems of isolation and level detection. The advantage of an electromechanical relay is that isolation is provided by a physical separation of points. However, the major disadvantage of a relay is, ultimately, poor mechanical and electrical reliability. Even the use of a cleaning current (wetting current) for the relay contacts does not alleviate long term electrical reliability problems.

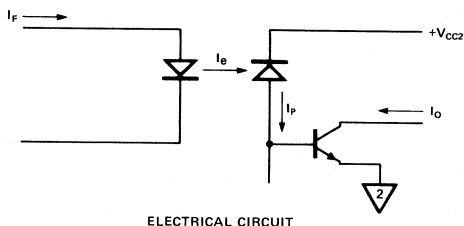


Figure 1. Basic Optocoupler Used for Isolation, 6N135.

The capacitor provides a simple means to isolate two systems, essentially blocking dc levels but allowing ac signals to couple between systems. Long term dc voltage stress across the capacitor, or frequent charge/discharge of a capacitor, will ultimately degrade these components.

Transformers have moderately small input to output capacitance which provides for reduced ground loop current. However, only limited bandwidth ac signals are coupled between systems.

An optocoupler provides the best combination of speed (20 Mbits/sec), dc response, high common mode rejection capability, and very low input-output capacitance. The only disadvantage which an optocoupler can present is that of the change in current transfer ratio (CTR) over operating life. This disadvantage can be compensated at initial design stage.

Consequently, in most applications the optocoupler provides the best means to interface from industrial control systems to microprocessor systems. With this in mind, optocoupler applications will now be explored.

A basic optocoupler is of the configuration shown in Figure 1 (6N135). The application of this optocoupler provides the needed isolation between systems via the light path from LED emitter to photodiode. However, the level detection which is needed to distinguish noise from signal must be provided. Level detection can be performed at two possible locations. First, threshold detection can be performed at the output of the optocoupler as shown in Figure 2.

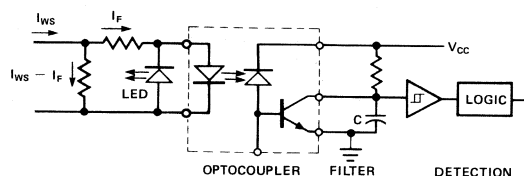


Figure 2. Threshold Detection After Optocoupler.

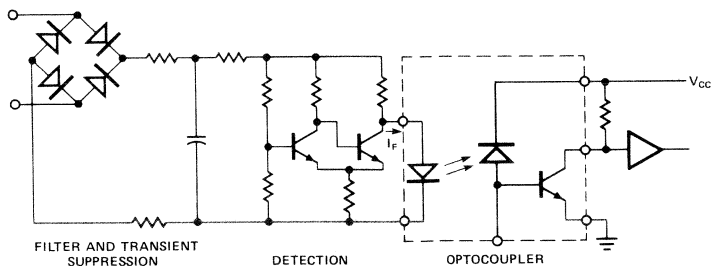


Figure 3. Threshold Detection Before Optocoupler.

This is a common method of detection. However, the detection level of the signal will change with time because of the change in CTR of the optocoupler over time or as a function of unit to unit. A better location for threshold detection would be prior to the optocoupler. Detection before the optocoupler eliminates the influence of CTR changes on the threshold levels as the circuit in Figure 3 illustrates.

The difficulty with simple level detection prior to the optocoupler is that of supplying power to the detection circuit from the signal while providing predictable threshold levels over temperature. Figure 4 shows a simple, discrete threshold detection circuit which is powered from the signal source. This circuit is used as an ac line monitor and complete analysis of this circuit is found in Hewlett-Packard's *Optoelectronics/Fiber-Optics Applications Manual*. This ac application requires an external rectification bridge and filter circuit.

An optimum optocoupler for providing isolation, insulation, and level detection is the HCPL-3700, a self-contained eight pin dual-in-line plastic package which houses an internal rectification bridge, temperature compensated threshold detection circuit, current source for LED, and photodiode detector circuit. Figure 5 is a schematic of the HCPL-3700. This device can be conveniently treated as a black box unit, i.e., specific voltage/current threshold levels can be easily obtained via simple Ohm's Law calculation. Application of a single resistor will program the device to operate at a desired threshold. Other simple resistive net-

works can be used at the input of the device to select any simultaneous combination of turn-on and turn-off thresholds.

With ac operation, filtering of the rectified ac can be performed at the input of the device which leaves the output a pure digital signal for TTL or CMOS logic. The internal bridge rectification circuit consists of Zener diodes which will clamp the input voltage level and shunt excess input current from stressing the LED. This is an advantage in high transient, industrial environments. Utilization of threshold detection prior to the optical isolation removes any CTR degradation influences upon the device thresholds. More detailed information about the interface applications of the HCPL-3700 optocoupler with microprocessors follows next.

Of the many interface applications possible with the HCPL-3700, both a dc and ac example will be shown. To illustrate the simplicity of setting a specific threshold, the following dc application is given.

Figure 6 illustrates a remote float switch which is monitored for reservoir tank level condition. This information needs to be communicated over a dedicated telephone line to the control processing unit. At the control unit, the HCPL-3700 optocoupler turn-on threshold is set for 75% ($V_+ = 36\text{ V}$) of the 48 V telephone line voltage to indicate a full reservoir tank. The threshold setting resistor is

$$R_X = \frac{V_+ - V_{TH+}}{I_{TH+}}$$

$$= \frac{36\text{ V} - 3.8\text{ V}}{2.5\text{ mA}} = 12.9\text{ K}\Omega$$

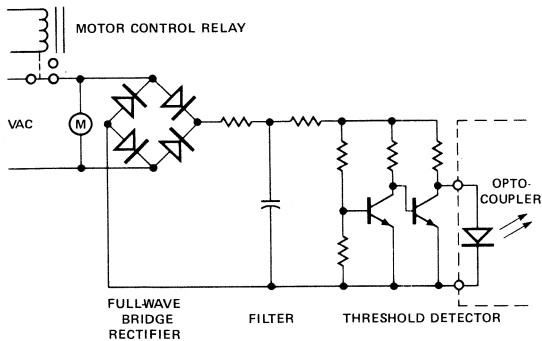


Figure 4. AC Motor Voltage Monitor with Threshold Detection Circuit Prior to Optocoupler.

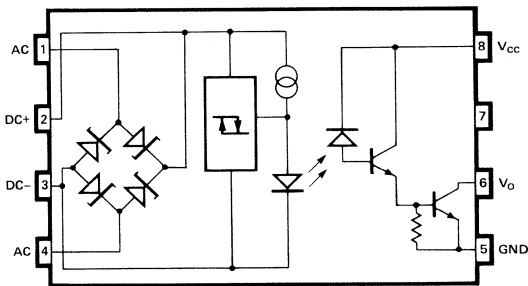


Figure 5. Schematic Diagram of HCPL-3700.

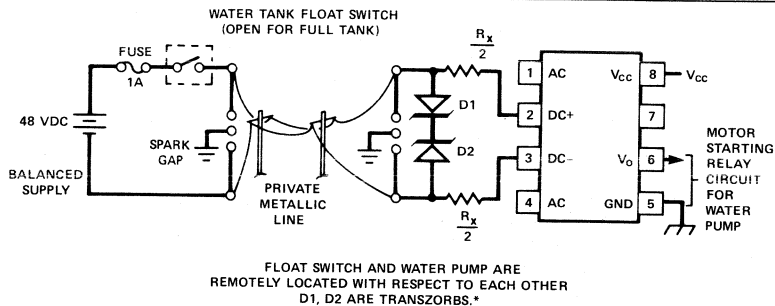


Figure 6. Application of the HCPL-3700 to Private Metallic Telephone Circuit for Remote Control of Equipment.

$$\begin{aligned} V_- &= R_X I_{TH-} + V_{TH-} \\ &= 13 \text{ K}\Omega (1.3 \text{ mA}) + 2.6 \text{ V} \\ V_- &= 19.5 \text{ V} \end{aligned}$$

This gives 16.5 V of noise immunity for this telephone line which could expect typically 10 V RMS or less of ac coupled voltage. The additional components prior to the optocoupler provide additional transient protection for telephone line equipment as well as for the optocoupler.

A commonly encountered ac application for interfacing from an industrial control environment to a microprocessor system is the need to monitor a limit switch located on a production line machine. This limit switch information must be interfaced to a process controller unit. This information is generally in the form of the presence or absence of available ac voltage from the production floor. Figure 7 displays the interface circuit. A peripheral interface adapter (P.I.A.) is used to interface to a microprocessor. As in the dc application, the single R_X resistor is determined by the desired external thresholds and device thresholds. Instantaneous ac voltage levels are used for calculation and maximum input current must be observed. Of course, this single resistor technique provides no filtering. The microprocessor must examine the periodic waveform from the optocoupler/P.I.A. to determine presence or absence of the ac input.

Another method by which to inform the microprocessor of ac presence is to filter the output of the optocoupler. This provides a constant low state for the P.I.A. Appropriate

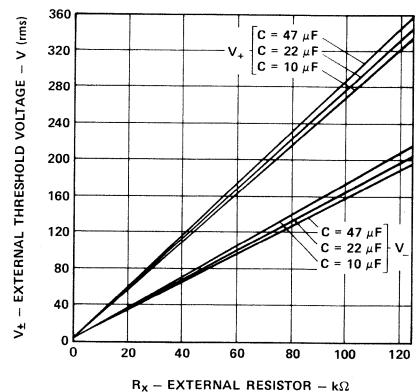


Figure 8.. External Threshold Voltage vs. R_X , C for AC Input Filter Applications.

R₁C_L combination will perform this task, but when ac is removed from the input, the optocoupler output will have a slow rise time. This can result in logic chatter problems, and delayed signal response.

A better method that can be used is to perform ac filtering at the input to the optocoupler. This is accomplished by placing a filter capacitor across the dc terminals while

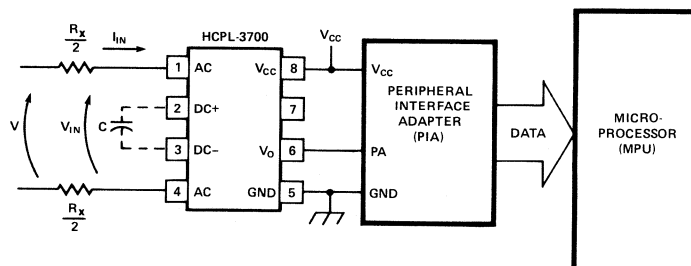


Figure 7. AC Application of HCPL-3700 Interface to Microprocessor Controller via a Peripheral Interface Adapter.

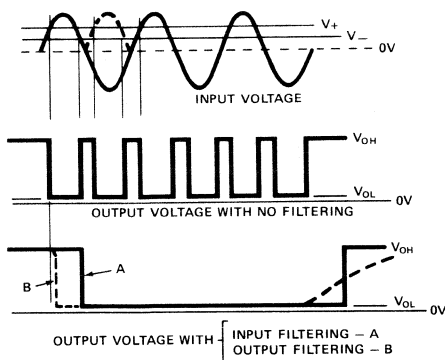


Figure 9. Comparison of Input-Output Waveforms of HCPL-3700 in AC Application.

supplying ac voltage to the series threshold setting resistor, R_X . The advantage of this technique is that the optocoupler output is purely digital, adaptable for TTL or CMOS logic levels. In addition, the voltage requirement for the filter capacitor would be that of the clamp level of the rectifier bridge. The value for R_X is obtained from Figure 8. The filter capacitor impedance complicates the simple R_X formula.

A comparison of timing of the ac input waveform with the three possible output waveforms of Figure 9 show the particular levels and time delays encountered with these filter techniques. The above examples are completely covered in Hewlett-Packard "Application Note 1004."

When specific turn-on and turn-off threshold levels are required, the single R_X resistor technique will not give this flexibility. This is not a limitation on the application of the HCPL-3700. Very simple networks can be used at the input to the optocoupler to obtain essentially any desired set of on and off thresholds. The principle of each network will be explained and specific applications of these networks will be shown next.

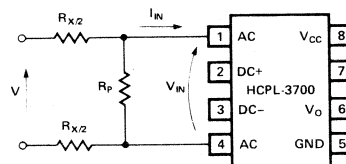


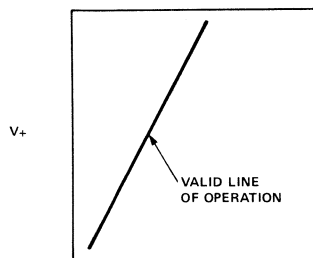
Figure 10. Two Resistor R_X , R_P Technique for Specific Turn-On and Turn-Off Threshold Levels.

The simplest network to use for simultaneous selection of turn-on and turn-off threshold levels is to use a series and parallel resistor combination, as shown in Figure 10.

This network provides a region for which a specified pair of thresholds can be obtained. Figure 11b displays a region of valid operation for the two resistor network, whereas Figure 11a shows a line of valid operation for the single resistor case. Outside the valid region of operation, the two resistor technique will not obtain a desired pair of V_{\pm} . For instance, gross detection of both a power line drop to 50% of nominal line level and presence of power line at 75% nominal level can be achieved, with R_X , R_P values shown in Figure 12.

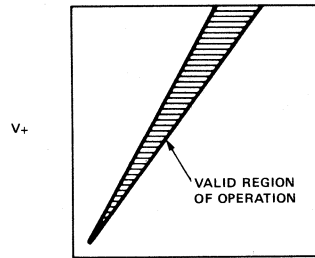
When the desired pair of turn-on and turn-off thresholds are not in the valid region of Figure 11b, but are widely separated, the addition of a correct offset voltage to the R_P resistor path will adjust the thresholds to the desired levels. Essentially, the boundaries of valid operation rotate to "capture" the desired pair of threshold points as shown in Figure 13.

An application of this R_X , R_P , V_{TO} technique is used in the petroleum products industry where a remote pump station interfaces to a microprocessor system. Figure 14 displays the dual use of 115 V ac line to sense the request switch as well as provide power to the amount reset motor. The sense thresholds level must be widely separated to allow for large noise levels, low ac line condition, while providing sufficient level detection for absence of line. Threshold levels of 80 V RMS for turn-on and 40 V RMS for turn-off are obtainable with the network shown in Figure 14.



V_-

(a)



V_-

(b)

Figure 11a,b. External Turn-On Threshold (V_+) vs. External Turn-Off Threshold (V_-) for Series Resistor R_X (a), for Series Resistor R_X and Parallel Resistor R_P (b).

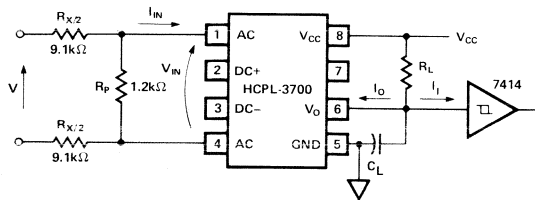


Figure 12. AC Power Line Monitor with Simultaneous Selection of Upper and Lower Threshold Levels and Output Filtering.

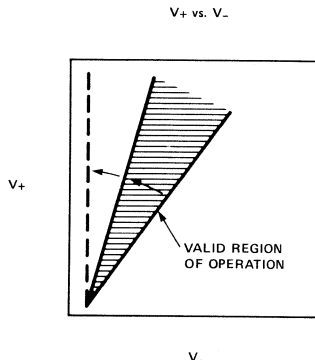


Figure 13. External Turn-On Threshold (V_+) vs. External Turn-Off Threshold (V_-) for Parallel Network Operation (R_X , R_P , V_{TO}).

There is the opposite situation where the desired threshold levels need to be close together, yielding small hysteresis. This can be obtained with the addition of an offset voltage (Zener diode) in series with the R_X resistor. Essentially, this

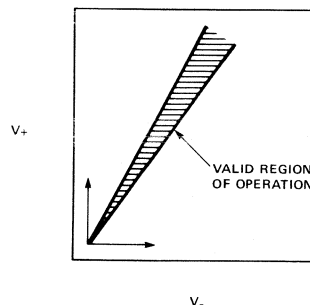


Figure 15. External Turn-On Threshold (V_+) vs. External Turn-Off Threshold (V_-) for Series Network Operation (R_X , R_P , V_Z).

effect translates the boundaries of Figure 15 to provide the small difference between turn-on and turn-off thresholds at the level desired.

An important application where small hysteresis at high voltage levels is needed is to monitor for failing power to a microprocessor system. Notification of failing power allows proper supply switch over to a backup battery unit. Figure 16 schematically shows the R_X , R_P , V_Z network for turn-on threshold of 260 V dc and turn-off of 228 V dc. Sensing at the filter capacitor of the switching power supply will give early indication of ac power loss and supply load demand. The carry over capability of the power supply will provide adequate time for an interrupt flag to warn the microprocessor to save special memory information through a proper power down sequence. The specific threshold levels are selected for turn-off at 70% of nominal filter capacitor voltage to provide adequate warning time, and turn-on at 80% level to indicate safe operating region for the switching supply. This allows for worst case low ac line condition as well (-15%).

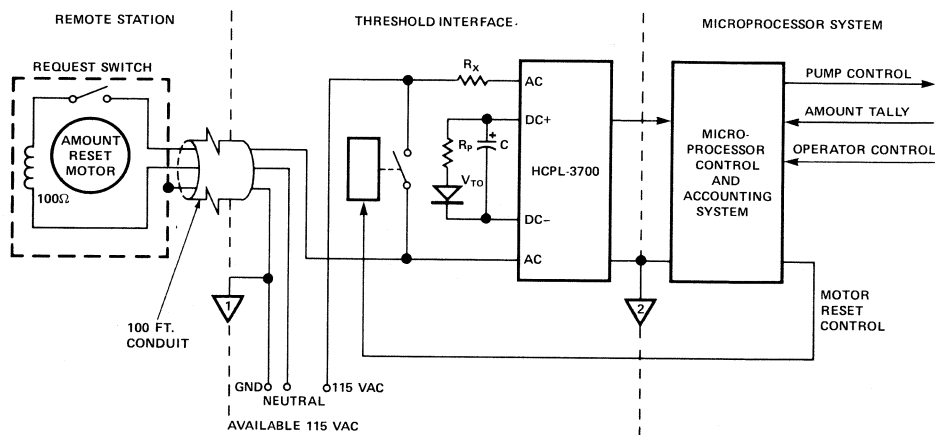


Figure 14. Threshold Interface Between Remote Amount Reset Motor and Microprocessor Control/Accounting System.

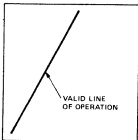
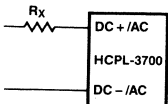
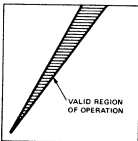
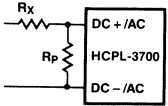
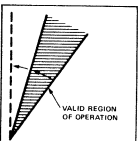
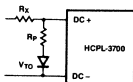
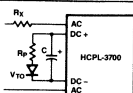
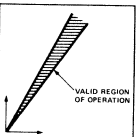
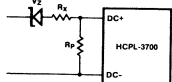
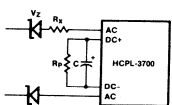
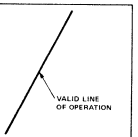
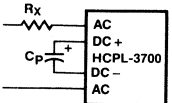
129

The need to provide isolation and level detection for interfacing from the industrial control environment to a microprocessor system is a must in order to ensure integrity of information and protection of equipment. The standard methods of isolation, such as relays and transformers, provide only a partial solution to the interface problems. As was discussed earlier, providing isolation and level detection is not an easy task to accomplish,

especially, if simplicity, versatility, and reliability are simultaneously required. The optocoupler isolation technique is the method which offers the best combinations. In particular, the advantages of the HCPL-3700 optocoupler provide an easy to design and nearly complete solution for interfacing to a microprocessor system from the industrial control world.

ADDENDUM TO INTERFACING FROM INDUSTRIAL CONTROL SYSTEMS TO MICROPROCESSORS

A SYNOPSIS OF TECHNIQUES FOR EXTERNAL THRESHOLD SELECTION

Network	$r = \frac{V_+ - V_{TH+}}{V_- - V_{TH-}}$		Mode	Theshold Selection	Region of Operation	Schematic
	Min.	Max.				
R_X	1.923		DC	Single		
	1.923		AC			
R_X, R_P	1.462	1.923	DC	Dual		 NO INPUT FILTERING
	1.342	1.923	AC			
Parallel Network R_X, R_P, V_{TO}	Overlap With Series Network	$r > 1.923$	DC	Dual		
		$r > 1.923$	AC			
Series Network R_X, R_P, V_Z	$r < 1.462$	Overlap With Parallel Network	DC	Dual		
	$r < 1.342$		AC			
R_X, C_P	1.56 ($C_P = 10 \mu F$) 1.71 ($C_P = 22 \mu F$) 1.81 ($C_P = 47 \mu F$)		AC	Single		

$V_+ > V_{TH+}$
 $V_- > V_{TH-}$ For DC mode: $V_{TH+} = 3.8 \text{ Vdc}$
 $V_{TH-} = 2.6 \text{ Vdc}$

For AC mode: $V_{TH+} = 5.1 \text{ V}$
 $V_{TH-} = 3.8 \text{ V}$ AC instantaneous voltage used with V_{\pm} instantaneous voltage

SERIES NETWORK CALCULATIONS

Step	Typical HCPL-3700 Thresholds*	$V_{TH+} = 3.8 \text{ V}, I_{TH+} = 2.5 \text{ mA}$ $V_{TH-} = 2.6 \text{ V}, I_{TH-} = 1.3 \text{ mA}$ $V_B = 1.33 \text{ V}$	Results
1	Desired External Thresholds	DC AC $V_+ = ? \text{ Vdc, or VRMS}_+$ $V_- = ? \text{ Vdc, or VRMS}_-$	260 Vdc 228 Vdc
2	AC (pins 1, 4)	$V_{P+} = \frac{2\sqrt{2}}{\pi} \text{VRMS}_+ - V_B$ $V_{P-} = \frac{2\sqrt{2}}{\pi} \text{VRMS}_- - V_B$	
	DC (pins 2, 3)	$V_{P+} = V_+$ $V_{P-} = V_-$	260 V 228 V
	DC (pins 1, 4)	$V_{P+} = V_+ - V_B$ $V_{P-} = V_- - V_B$	
3		$R_{TH} = \frac{V_{TH+} - V_{TH-}}{I_{TH-}}$	0.923 K Ω
4		$K_I = \frac{I_{TH+} - I_{TH-}}{I_{TH-}}$	0.923
5	AC (pins 1, 4)	$V_{Zmin} > \frac{\frac{V_{TH+}}{V_{TH-}} \left[\frac{2\sqrt{2}}{\pi} \text{VRMS}_- - (V_B + 0.7 \text{ V} + V_{TH-}) \right] - \left[\frac{2\sqrt{2}}{\pi} \text{VRMS}_+ - (V_B + 0.7 \text{ V} + V_{TH+}) \right]}{\frac{V_{TH+}}{V_{TH-}} - 1}$	
	DC (pins 2, 3)	$V_{Zmin} > \frac{\frac{V_{TH+}}{V_{TH-}} [V_- - V_{TH-}] - [V_+ - V_{TH+}]}{\frac{V_{TH+}}{V_{TH-}} - 1}$	158.7 V
	DC (pins 1, 4)	$V_{Zmin} > \frac{\frac{V_{TH+}}{V_{TH-}} [V_- - V_B - V_{TH-}] - [V_+ - V_B - V_{TH+}]}{\frac{V_{TH+}}{V_{TH-}} - 1}$	
6	AC (pins 1, 4)	$V_{Zmax} < \frac{\frac{I_{TH+}}{I_{TH-}} \left[\frac{2\sqrt{2}}{\pi} \text{VRMS}_- - (V_B + 0.7 \text{ V} + V_{TH-}) \right] - \left[\frac{2\sqrt{2}}{\pi} \text{VRMS}_+ - (V_B + 0.7 \text{ V} + V_{TH+}) \right]}{K_I}$	
	DC (pins 2, 3)	$V_{Zmax} < \frac{\frac{I_{TH+}}{I_{TH-}} [V_- - V_{TH-}] - [V_+ - V_{TH+}]}{K_I}$	192.0 V
	DC (pins 1, 4)	$V_{Zmax} < \frac{\frac{I_{TH+}}{I_{TH-}} [V_- - V_B - V_{TH-}] - [V_+ - V_B - V_{TH+}]}{K_I}$	
7	Choose V_Z	such that $V_{Zmin} < V_Z < V_{Zmax}$ Temperature Compensated Zener diode is best	175 V
8	AC (pins 1, 4)	Calculate new $V'_{P+} = \frac{2\sqrt{2}}{\pi} \text{VRMS}_+ - V_B - 0.7 \text{ V} - V_Z$ $V'_{P-} = \frac{2\sqrt{2}}{\pi} \text{VRMS}_- - V_B - 0.7 \text{ V} - V_Z$	
	DC (pins 2, 3)	Calculate new $V'_{P+} = V_+ - V_Z$ $V'_{P-} = V_- - V_Z$	85 V 53 V
	DC (pins 1, 4)	Calculate new $V'_{P+} = V_+ - V_B - V_Z$ $V'_{P-} = V_- - V_B - V_Z$	
9		$K'_V = \frac{V'_{P+} - V_{TH+}}{V'_{P-} - V_{TH-}} - 1$ ($K'_V < K_I$)	0.611
10		$R'_O = \frac{V'_{P-} - V_{TH-}}{I_{TH-}}$	38.8 K Ω
11		$v = \frac{V_{TH-}}{V_{TH+} - V_{TH-}}$ ($v > 0$)	2.167
12		$R_X = R'_O \left(\frac{1 - K'_V v}{1 - K_I v} \right)$	12.56 K Ω
13		$R_P = R_{TH} \left(\frac{1 - K'_V v}{K'_V - K_I} \right)$	0.959 K Ω
14	AC Operation (Filter Capacitor)	$C = 30.3 \left(1 + \frac{1.23}{R_P} \right) \mu\text{F}$ 60 Hz $C = 36.4 \left(1 + \frac{1.23}{R_P} \right) \mu\text{F}$ 50 Hz R_P in K Ω	

*Worst case values can be obtained from HCPL-3700 data sheet.

PARALLEL NETWORK CALCULATIONS

Step	Typical HCPL-3700 Thresholds*	$V_{TH+} = 3.8 \text{ V}, I_{TH+} = 2.5 \text{ mA}$ $V_{TH-} = 2.6 \text{ V}, I_{TH-} = 1.3 \text{ mA}$ $V_B = 1.33 \text{ V}$	Results
1	Desired External Thresholds	DC AC $V_+ = ? \text{ Vdc, or VRMS}_+$ $V_- = ? \text{ Vdc, or VRMS}_-$	80 VRMS 40 VRMS
2	AC (pins 1, 4)	$V_{P+} = \frac{2\sqrt{2}}{\pi} \text{ VRMS}_+ - V_B$ $V_{P-} = \frac{2\sqrt{2}}{\pi} \text{ VRMS}_- - V_B$	70.73 V 34.70 V
	DC (pins 2, 3)	$V_{P+} = V_+$ $V_{P-} = V_-$	
	DC (pins 1, 4)	$V_{P+} = V_+ - V_B$ $V_{P-} = V_- - V_B$	
3		$R_O = \frac{V_{P-} - V_{TH-}}{I_{TH-}}$	24.69 K Ω
4		$R_{TH} = \frac{V_{TH+} - V_{TH-}}{I_{TH-}}$	0.923 K Ω
5		$K_V = \frac{V_{P+} - V_{TH+}}{V_{P-} - V_{TH-}} - 1$	1.085
6		$K_I = \frac{I_{TH+} - I_{TH-}}{I_{TH-}}$	0.923
7		$V_K = V_{TH-} - \frac{V_{TH+} - V_{TH-}}{K_V}$	1.494 V
8		$V_K > 0$, Continue to Step 9 $V_K < 0$, Series Network must be employed	$V_K > 0$
9		$K_V < K_I$ go to Step 10 $K_V > K_I$ go to Step 11, or Step 16 if desire to move upper threshold only (see text) $K_V = K_I$ go to Step 15	$K_V > K_I$
10	Select V_{TO}	$0 < V_{TO} < V_K$ Skip Step 11	
11	Select V_{TO}	$V_K < V_{TO} < V_{TH-}$	1.65 V
12		$v = \frac{V_{TH-} - V_{TO}}{V_{TH+} - V_{TH-}}$ $(v > 0)$	0.792
13		$R_X = R_O \left(\frac{1 - K_V v}{1 - K_I v} \right)$	12.91 K Ω
14		$R_P = R_{TH} \left(\frac{1 - K_V v}{K_V - K_I} \right)$ Next Step 19, if AC operation is used (pins 1, 4)	0.802 K Ω
15		$R_X = R_O; R_P = \infty$ (For AC operation, pins 1, 4, $C_{min} = 10 \mu\text{F}$)	
16	Select V_{TO}	$V_{TH-} < V_{TO} < V_{TH+}$	
17		$v = \frac{V_{TH-} - V_{TO}}{V_{TH+} - V_{TH-}}$ $(-1 < v < 0)$	
18		$R_X = R_O; R_P = R_{TH} \left(\frac{1 + v}{K_V - K_I} \right)$	
19	AC OPERATION (pins 1, 4)	$C = 30.3 \left(1 + \frac{1.23 - 0.229 V_{TO}}{R_P} \right) \mu\text{F}$ 60 Hz $C = 36.4 \left(1 + \frac{1.23 - 0.229 V_{TO}}{R_P} \right) \mu\text{F}$ 50 Hz R_P in K Ω	62.5 μF 75.1 μF

*Worst case values can be obtained from HCPL-3700 data sheet.



Designing with the HCPL-4100 and HCPL-4200 Current Loop Optocouplers

PREFACE

Hewlett-Packard produces a comprehensive line of optocouplers which address different speed and current gain requirements for isolation interface circuits. New Hewlett-Packard optocoupler products build on the established base of optocoupler technology and expand with additional features that make optocouplers easier to use in special applications. The HCPL-4100 (transmitter) and the HCPL-4200 (receiver) optocouplers include specialized circuits for 20 mA digital current loop applications. These optocouplers are designed to easily interface TTL, LSTTL, and CMOS logic systems to current loop systems. An external current source is needed to complete the current loop system.

This application note will assist the circuit design engineer to achieve maximum performance from Hewlett-Packard HCPL-4100 and HCPL-4200 current loop optocouplers. Practical applications for interfacing to and from a current loop will be shown. In addition, overall current loop system aspects and current source designs will be discussed. Potential applications of current loops, configurations, types of current sources, and inherent tradeoffs between data rate and length of wire line are covered.

INTRODUCTION

Data transmission between electronic equipment, which are physically separated by distances of more than a few feet, can be accomplished in many ways. Wire links, microwave links, and fiber optic links are among the most common means. Each technology has inherent trade-offs in data rate, error rate, simplicity of use, reliability and cost. Of the wire techniques, a signal can be transmitted as a voltage signal or a current signal. Many popular industry standards exist for voltage signal transmission, such as RS-232-C, RS-422, RS-423 (serial data transmission), or IEEE-488 (parallel data transmission), etc. When compared to these voltage signal techniques, a current signal or current loop can provide an excellent alternative.

First, some basic definitions are in order. A current loop is a loop which carries a current, generally 20 mA or 60 mA, between electronic equipment via a twisted pair of wires. The loop can be opened and closed by a transmitter

within equipment connected to the loop. These interruptions of current are sensed by other equipment connected to the current loop (receiver). The convention used in this application note for a MARK, or logic 1, corresponds to a presence of loop current, e.g., 20 mA. A SPACE, or logic 0, corresponds to an absence of loop current, e.g., 0 mA. A current loop transmitter or receiver can be either of two types: active (source) or passive (sink). An active transmitter supplies current to the loop. Any receivers or other transmitters within that loop must then be passive units which accept the supplied loop current. Alternatively, an active receiver supplies current to passive transmitters or other passive receivers in the current loop.

Current sources used within a current loop vary in complexity. The simplest current source is a resistor and voltage source. More complex current sources will contain active elements or special integrated circuits to provide constant current under various power supply and load conditions. The compliance voltage of a current source is a term which is used to indicate at what level the current decreases to zero.

There are no widely accepted industry standards for current loops, only accepted conventions. Common digital current loops are 0-20 mA and 0-60 mA, while the analog current loop is 4-20 mA. These levels were originally associated with digital teleprinter equipment and analog industrial sensors such as thermocouples, strain gauges, etc. The HCPL-4100 and HCPL-4200 optocouplers address only the 20 mA digital current loop applications.

Basic Advantages of Current Loops

In voltage based transmission lines, a voltage signal attenuates over distance. A current loop design ensures constant current through the loop resulting in no signal attenuation. Noise immunity is higher with current loop systems. A constant current maintains a high signal-to-coupled noise ratio. The voltage signal attenuation reduces this ratio.

Even with expensive, low capacitance cable, RS-232-C wire communication over distances greater than 60 m (200 ft.) at 20 kBd is impractical. RS-232-C wire distances are severely limited when compared to current loop distances

at the same operating data rate. Current loop systems employ inexpensive twisted pair wire cable. Serial data transmission is accomplished by a simple two-wire arrangement. Multiple stations can be connected in series provided sufficient compliance voltage is available. Unlike voltage techniques, if a fault should open the loop, permanent loop current disruption could be sensed.

Optocouplers can be used in current loops to provide optical isolation of the logic circuits from the current loop circuit. This optical isolation prevents ground potential differences or common mode influences from affecting the current loop performance. Optocoupler construction and sophisticated integrated circuit processing achieve excellent common mode rejection ($10 \text{ kV}/\mu\text{s}$). Electrical independence between input and output circuits of an optocoupler permit different reference grounds on either side of the interface.

The maximum data rate of a 20 mA current loop system is determined by the characteristics of the transmitter and receiver and the length and characteristics of the transmission line. For short transmission lines, less than 40 m (131 ft.), the maximum data rate is approximately 120 kBd for the HCPL-4100 and approximately 4.5 MBd for the HCPL-4200.

The small eight pin dual-in-line plastic package results in a savings of printed circuit board space. Standard automatic insertion equipment can be used.

The easy design and implementation of a 20 mA current loop using the HCPL-4100 and HCPL-4200 permits rapid design, fabrication, and testing.

CURRENT LOOP APPLICATIONS

Current loops are used because they offer communications link lengths up to 10 km, have high immunity to errors caused by noise, and are low cost. Previous 20 mA current loop designs were often limited to 5 or 10 kBd speeds even for short line lengths. Hewlett-Packard 20 mA current loop transmitters and receivers are capable of 20 kBd at 400 metres.

In the industrial control industry, current loops are used when there is a need to communicate digital information. Because of the proliferation of the microprocessor and advances in digital circuitry and software, digital control of industrial processes is becoming widely accepted. Micro, mini, and mainframe computers are distributed throughout the factory and need to exchange information. The same considerations apply where distributed data processing equipment is used in a factory environment for inventory control or workflow monitoring. Hewlett-Packard 20 mA current loops are a natural choice for noisy environments.

For these applications, 20 mA current loops are desirable because they are resistant to errors caused by noise, they eliminate ground loops, can be used in communications links up to 10 km long, are low cost, and can be easily installed. No other common communications system can equal these features.

HEWLETT-PACKARD CURRENT LOOP OPTOCOUPLEDERS

General Design Considerations with Optocouplers

When ordinary optocouplers are used as the interface between logic systems and a current loop, and vice versa, careful design must be followed. The light emitting diode (LED) in a current loop receiver must be protected from

current overstress. A threshold needs to be established with hysteresis in order to define the MARK and SPACE conditions and to avoid possible noise effects. The threshold circuit should be located prior to the optical isolation to prevent the current transfer ratio (CTR) changes within an optocoupler over time from influencing established threshold levels. This input protection/threshold circuit should be powered solely by the current loop to maintain isolation and reduce power supply requirements. The receiver output circuit should be simple to interface to TTL or CMOS systems. The total current loop receiver circuit needs to occupy minimal board space within loop station equipment. Of course, the design must have good speed performance in order to meet ever increasing speed requirements.

Similar considerations exist for current loop transmitter design. The transmitter will operate from either a TTL or CMOS input data signal. The output of the transmitter should be protected and buffered to handle the loop current and compliance voltage level of the current source. Output protection needs to be provided to ensure against miswired connection of the current loop to the transmitter terminals. The output circuit must be powered by the current loop source. If power failure occurs to the transmitter, the transmitter must remain ON in order to prevent obstruction of data on the current loop. Other subtle effects such as the type of current source and termination used will also influence speed performance of the loop.

These design considerations have been incorporated into the HCPL-4100 and HCPL-4200 to simplify the circuit designer's task.

Features Common to the HCPL-4100 (Transmitter) and the HCPL-4200 (Receiver)

The Hewlett-Packard current loop optocoupler product family consists of two devices: a current loop transmitter (HCPL-4100) and a current loop receiver (HCPL-4200). Their unique characteristics will be explained by first discussing the features which are common to both devices; then particular characteristics of each device will be addressed.

Optical isolation is provided within each device to permit electrical independence of the logic systems from the current loop system. Electrical independence specifically means two concepts: 1. signal isolation capability between the two systems, 2. insulation capability between the two systems. Signal isolation is the ability of the device to reject common mode signal interference. The common mode rejection capability of both the HCPL-4100 and the HCPL-4200 is typically $10 \text{ kV}/\mu\text{s}$ with a specified minimum of $1000 \text{ V}/\mu\text{s}$. The device insulation capability is the ability to withstand a transient potential difference stress between the two systems. The Withstand Test Voltage is 3 kV DC for five seconds.

Speed performance of each device has a typical propagation delay of $0.2 \mu\text{s} - 0.3 \mu\text{s}$ with a specified maximum of $1.6 \mu\text{s}$ over 0°C to 70°C , excluding transmission line delay. Depending upon the location of the current source within a loop, data rates of 1.5 MBd for 250 metres loop length is achieved with the HCPL-4200 receiver. Up to 75 kBd for 100 metres of loop length with the HCPL-4100 transmitter is also achieved.

The transmitter input and receiver output are compatible with TTL, LSTTL and CMOS logic levels. Passive current

loop switching or monitoring is performed by integrated circuits (ICs) within each device which are powered from an external 20 mA current source. No additional design for power supplies or buffer circuitry is needed for either unit. Current protection of up to ± 30 mA is provided in each optocoupler. Specific, simple current sources which can be used are explained in a subsequent section.

The HCPL-4100 20 mA current loop transmitter and HCPL-4200 20 mA current loop receiver incorporate these features in eight pin dual-in-line plastic packages. The eight pin dual-in-line package allows for automatic insertion capability and conserves printed circuit board space.

Features of the HCPL-4100 Transmitter

The output integrated circuit of the HCPL-4100 transmitter directly controls a recommended 20 mA loop current. The minimum breakdown voltage of this IC, which determines the upper compliance voltage limit of the current source, is 27 V DC. At a recommended loop current of 20 mA, the MARK state voltage drop across the output terminals is typically 2.35 V DC. The SPACE state current level is typically 1.1 mA (maximum 2 mA) which powers the output integrated circuit. Should power fail to the input IC of the HCPL-4100 transmitter, the output IC will remain in the MARK state. This important feature is needed in multidrop current loop applications. A minimum capacitive loading of 1000 pF is required for the output IC (loop side) of the transmitter. This guarantees stability of the IC under all possible load conditions. In general, an external 1000 pF capacitor can be omitted for twisted wire cable lengths greater than 30 metres (100 ft.). If there is any possibility of using a wire loop length less than 30 metres (100 ft.), the 1000 pF capacitor must be connected. Good engineering practice is to use a bypassing capacitor (0.1 μ F) from V_{CC} to ground for the input IC of the transmitter. Data from directly connected TTL, LSTTL or CMOS units to the input of the HCPL-4100 transmitter will properly operate this device. A block diagram of the HCPL-4100 is given in Figure 1 and transfer characteristic is illustrated in Figure 2.

Features of the HCPL-4200 Receiver

The HCPL-4200 receiver input IC directly monitors the 20 mA loop current. Power for this IC is supplied by the current loop from the external current source. Loop current level detection is performed prior to the optical isolation.

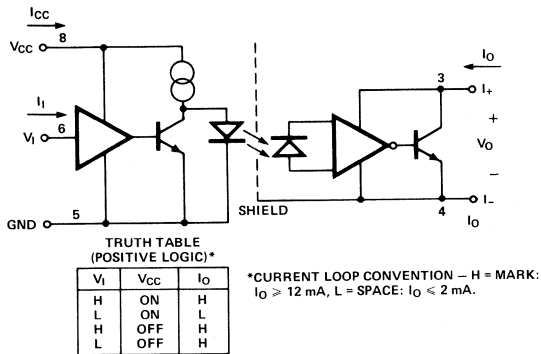


Figure 1. Block Diagram and Truth Table for HCPL-4100 Optocoupler

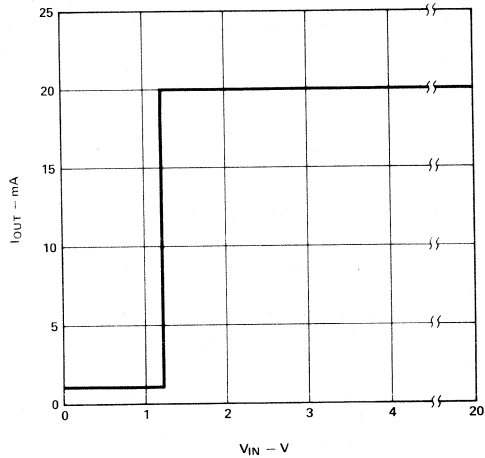


Figure 2. HCPL-4100 Typical Transfer Characteristic. Output Loop Current vs. Input Voltage. MARK State Loop Current is Provided by External Current Source.

Specified current thresholds are a minimum of 12 mA for MARK state and a maximum of 3 mA for SPACE state. The typical threshold for MARK state is 6.8 mA with 0.8 mA hysteresis. A guaranteed switching threshold level for loop current provides additional common mode and differential mode noise immunity, and prevents possible current transfer ratio (CTR) changes from affecting loop current threshold levels. At the recommended loop current of 20 mA, the MARK state voltage drop across the input terminals is typically 2.52 V DC.

The output integrated circuit of the HCPL-4200 receiver can have a voltage output (V_O) greater than the power supply voltage (V_{CC}). The absolute maximum voltage level for V_O and V_{CC} is 20 V DC. A third state (high impedance) output enable feature is available for use with buss interface applications or special inhibit functions. The output will remain at a high impedance level (third state) if V_{CC} is zero volts. A block diagram of the HCPL-4200 is given in Figure 3 and the transfer characteristic is illustrated in Figure 4. Conventional TTL and LSTTL logic devices can be directly connected to the output of the HCPL-4200 unit. A standard CMOS interface for the HCPL-4200 receiver is given in Figure 5.

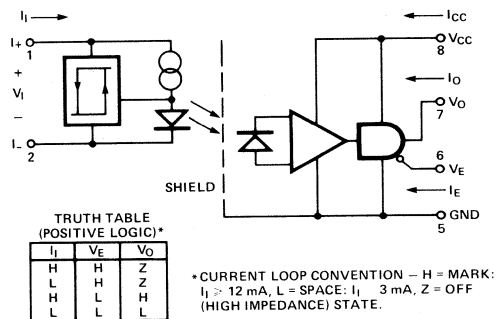


Figure 3. Block Diagram and Truth Table for HCPL-4200 Optocoupler

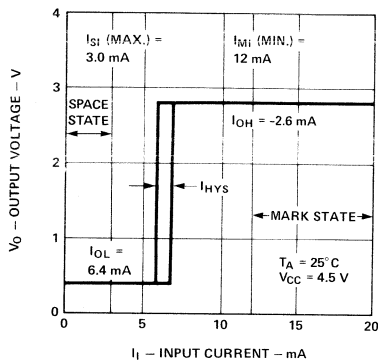


Figure 4. HCPL-4200 Typical Transfer Characteristic. Output Voltage vs. Input Loop Current

CURRENT LOOP CONFIGURATIONS

Current loop configurations can be arranged in three basic ways: simplex, half duplex and full duplex. Two variations within each configuration can exist, i.e., point-to-point or multidrop connections. Definitions for these terms, recommended interface circuits, performance trade-offs and measured performance data will be discussed and illustrated within this section.

Simplex

The most fundamental loop configuration is simplex point-to-point. The data flows in only one direction from the transmitter over the current loop to the remote receiver. This configuration is shown in Figures 6a and 6b. Figure 6a illustrates a non-isolated, active current loop transmitter used with an isolated HCPL-4200 receiver. Figure 6b shows an isolated HCPL-4100 current loop transmitter used with a non-isolated, active receiver. A possible point-to-point application is to use a 20 mA current loop for communication between a computer and remote printer. The simplex topology can be expanded from point-to-

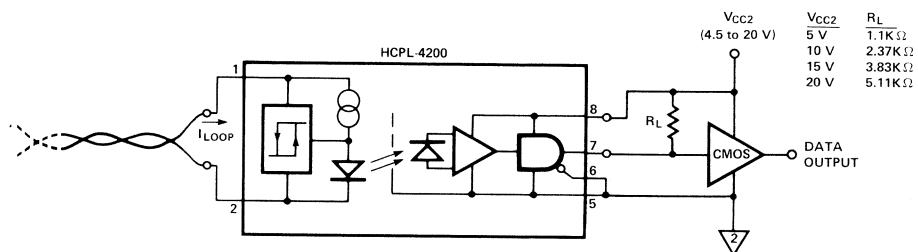
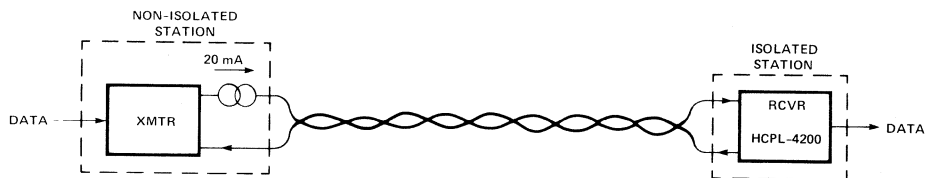
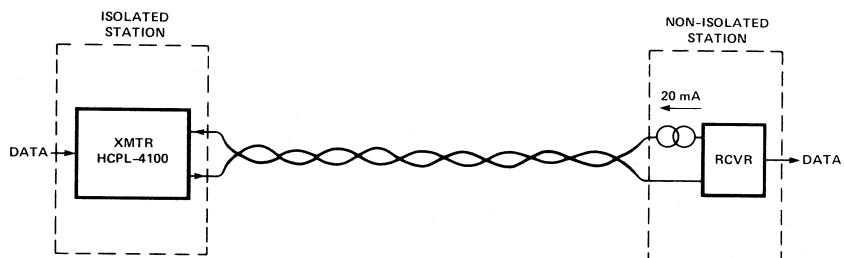


Figure 5. Recommended Interface from HCPL-4200 Receiver to CMOS Circuit

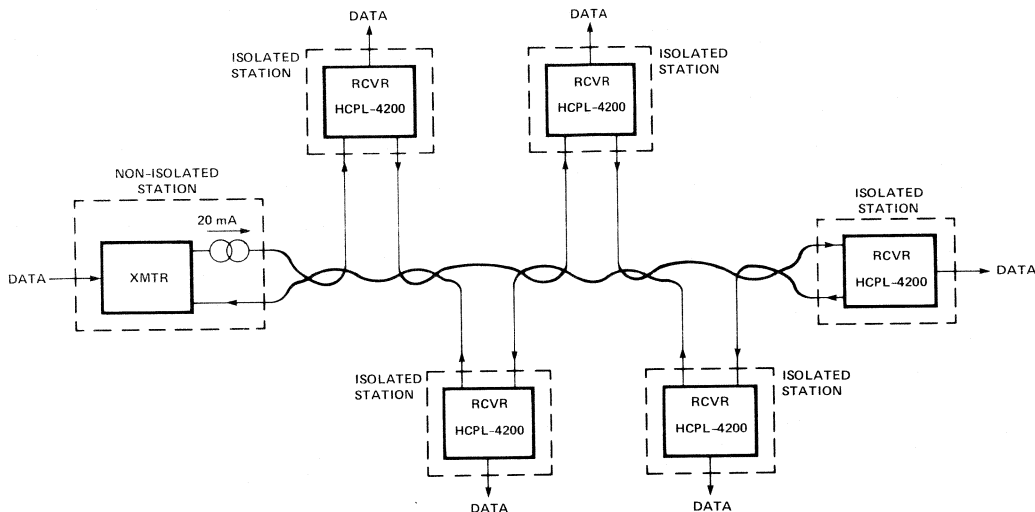


a. Simplex, Point-to-Point with Isolated Receiver



b. Simplex, Point-to-Point with Isolated Transmitter

Figure 6. Simplex Current Loop Configurations: Point-to-Point with Current Source Located at: a. Transmitter, b. Receiver; c. Multidrop



c. Simplex, Multidrop with Isolated Receivers

Figure 6. Simplex Current Loop Configurations: Point-to-Point with Current Source Located at: a. Transmitter, b. Receiver; c. Multidrop

point to multidrop. In a multidrop system, a number of receivers are in series on the loop which contains only one transmitter as illustrated in Figure 6c. A configuration with multiple transmitters and one receiver is possible as well. However, the priority of the operating transmitter must be established in that case.

Undesired ground loops are eliminated and common mode rejection is increased by providing electrical isolation of the current loop. This isolation can be provided at either the receiver or transmitter end of the loop as illustrated in Figures 6a and 6b respectively. The opposite end need not be isolated. The non-isolated unit will supply the current (active) for this simplex configuration. A circuit

diagram of a non-isolated, active transmitter connected to the HCPL-4200 receiver (Figure 6a) is given in Figure 7. The data rate performance versus the length of the current loop for this circuit is given in Figure 8.

The circuit for the alternate simplex arrangement of a non-isolated, active receiver connected to the HCPL-4100 transmitter is given in Figure 9. The trade-off of data rate versus loop length and compliance voltage is illustrated in Figure 10.

Comparing the data rate performance for each circuit shows that the active, non-isolated transmitter configuration is faster by a factor of 11 at 1000 metres (3281 ft.) of loop distance.

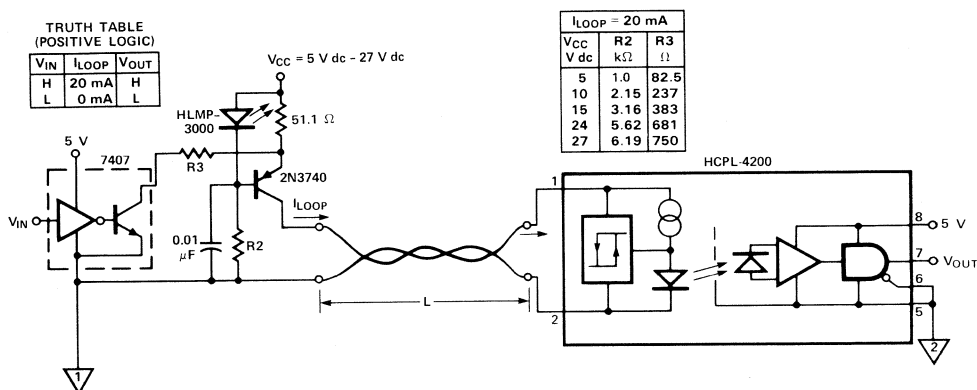


Figure 7. Recommended Non-Isolated Active Transmitter with HCPL-4200 Isolated Receiver for Simplex Point-to-Point 20 mA Current Loop

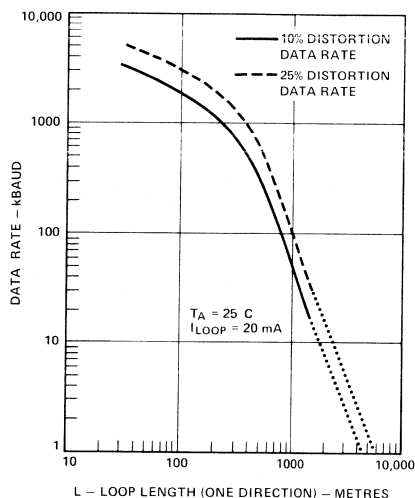


Figure 8. Typical Data Rate vs. Distance for Circuit of Figure 7

The design and location of the current source determine loop length and data rate performance. In both simplex configurations, the current source compliance voltage can be much lower than the HCPL-4100 device maximum of 27 V. However, limitation on the length of the loop (DC resistance) and data rate capability would dictate a minimum V_{CC} which can be used for the current source. With a $24\text{ V} \pm 10\%$ power supply, multidrop applications for very long loop lengths ($>3\text{ km}$) can be done. Device performance as a function of current source design is covered in a later section.

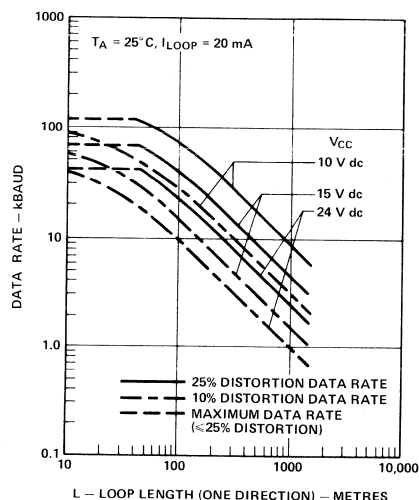


Figure 10. Typical Data Rate vs. Distance and Supply Voltage for Circuit of Figure 9

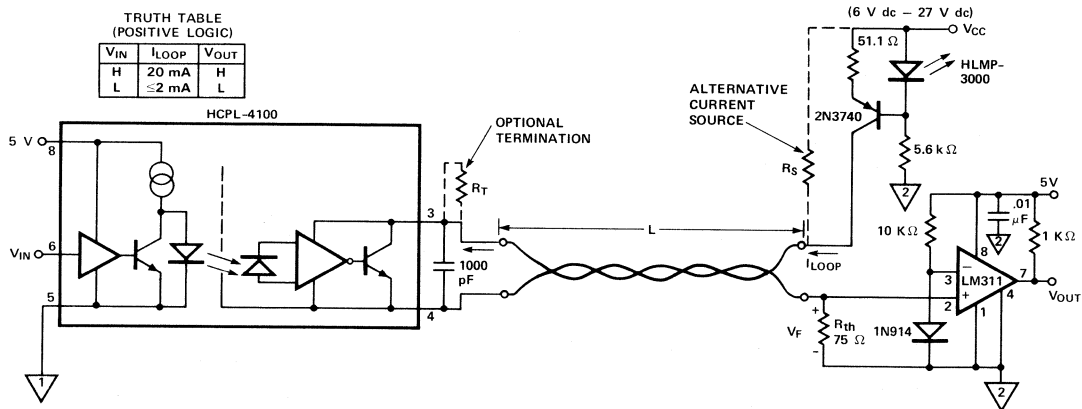


Figure 9. Recommended Non-Isolated Active Receiver with HCPL-4100 Isolated Transmitter for Simplex Point-to-Point 20 mA Current Loop

DC Performance

By summing the MARK state voltage drops around the current loop, a basic equation is derived for DC performance for the loop. This is expressed as the maximum distance over which a current loop can be operated.

$$L = \frac{V_{COMP} - \Sigma V_{RCVR} - \Sigma V_{XMTR}}{2 I_{LOOP} R_{LINE}} \quad (1)$$

- Where
- L = Length of wire in one direction
 - V_{COMP} = Compliance voltage of current source = (V_{CC} – V_{SAT})^[1]
 - V_{CC} = Supply voltage for current source;
 - V_{SAT} = Saturation voltage of current source
 - I_{LOOP} = Operating loop current
 - R_{LINE} = DC resistance of wire per length
 - ΣV_{XMTR}_{MARK} = Summation of voltage drops across each non-isolated and isolated transmitter current loop terminals when MARK state current flows.^[2]
 - ΣV_{RCVR}_{MARK} = Summation of voltage drops across each non-isolated and isolated receiver current loop terminals when MARK state current flows.^[2]

- Notes:
1. V_{COMP} must be less than the breakdown voltage rating of the transmitter unit in SPACE state.
 2. The non-isolated unit will supply loop current. If two or more non-isolated units are used, then only one of these units needs to supply loop current.

This equation can be solved for any particular parameter of interest if the other remaining parameters are known. For example, Equations (1) and (2) can be solved for minimum power supply voltage, V_{CC}, which can be used for current source of Figure 7 for the following conditions.

$$V_{COMP} = \Sigma V_{RCVR} + \Sigma V_{XMTR} + 2 L I_{LOOP} R_{LINE} \quad (3)$$

- Where,
- ΣV_{RCVR}_{MARK} = 2.76 V (One isolated receiver)
 - ΣV_{XMTR}_{MARK} = 0 V (Non-isolated transmitter voltage drop is incorporated in V_{COMP})
 - I_{LOOP} = 22 mA (20 mA + 10%),
 - R_{LINE} = 0.053 Ω/m (AWG No. 22),
 - L = 305 m
 - V_{COMP} = 2.76 V + 0 V + 2(305 m) (0.022 A) (0.053 Ω/m) = 3.47 V

- and using equation (2)
- V_{CC} = V_{COMP} + V_{SAT}; where V_{SAT} = 1.5 V = 3.47 V + 1.5 V
 - V_{CC} = 4.97 V

For the listed conditions, these calculations are for the worst case temperature and unit to unit variations.

To address device voltage breakdown concerns, the current source compliance level for the current loop and the SPACE state current need to be known. The SPACE state current is determined by the transmitter when it is in the OFF state. SPACE state current will not be necessarily equal to zero. Hence, when a current loop receiver is designed, the threshold must be set at a proper level to avoid detecting the SPACE state current as well as to provide a noise margin. With the HCPL-4200 receiver, SPACE state current of 3.0 mA or less is allowed. Should a larger noise current margin be desired for SPACE state, the maximum SPACE state current of the HCPL-4200 can be raised effectively by shunting the input with a resistor. Actual device current threshold does not change; only the loop current level required to reach SPACE state threshold increases. Use of a shunting resistor will reduce the noise current margin in the MARK state for the HCPL-4200.

Should the HCPL-4100 transmitter be used, the maximum SPACE state current is 2.0 mA. For half duplex applications, a noise margin of 1.0 mA is specified for SPACE state with the combination of the HCPL-4100/-4200 units.

AC Performance

AC performance of a current loop is influenced by many factors. Typical data rate capability for the simplex configurations shown in Figures 7 and 9 are shown in Figures 8 and 10 respectively. The 10% (25%) distortion data rate is defined as the rate at which 10% (25%) distortion occurs to the output bit interval with respect to the reference input bit interval. This is expressed by equation (4).

Distortion Data Rate

$$f_D = \frac{1}{t_{BIT}} \quad (4)$$

Where D = % distortion and t_{BIT} is bit time of the input signal when D distortion is present in the output bit interval.

A square wave as well as a 16 bit data stream was used to “exercise” the current loop system. In both simplex point-to-point configurations, the input data rate was adjusted to result in a 10% (25%) distortion to the output signal for either an input square wave or a 16 bit pattern.

The 16 bit pattern was used to provide two propagation delay test conditions for the current loop. One part of the 16 bit waveform tests for data rate distortion affected by a long duration in either a MARK or SPACE state prior to state change. The other part of the 16 bit waveform tests for effects on data rate distortion via short durations in either a MARK or SPACE state prior to a state change. In both simplex configurations, Figures 7 or 9, the transition from either a short or a long duration MARK state to a SPACE state affects the data rate distortion the most. The 16 bit exerciser circuit diagram and bit stream waveform are shown in Appendix A.

In the description of the AC performance that follows, an approximation has been made to simplify the analysis. The transmission line is treated as a lumped capacitance. A more complete analysis of AC performance would require rigorous treatment via transmission line theory.

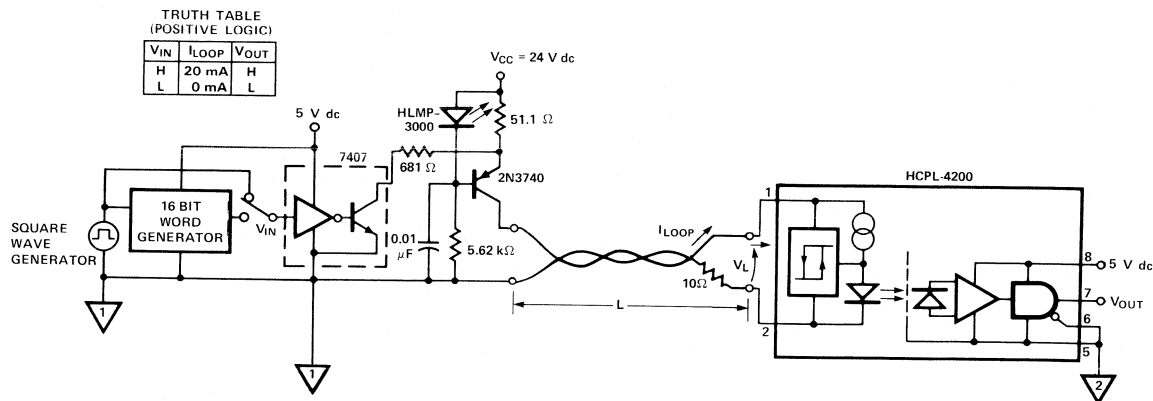


Figure 11. Data Rate Test Circuit for Non-Isolated Active Transmitter to Isolated HCPL-4200 Receiver

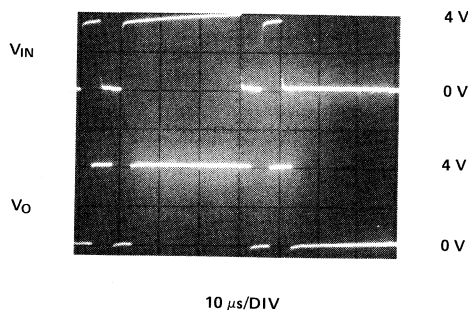


Figure 12. Timing Comparison of Output Signal (V_O) to Input Signal (V_{IN}) using 16-Bit Word at 10% Distortion with 305 m (1000 ft.) Loop Distance. Reference Figure 11.

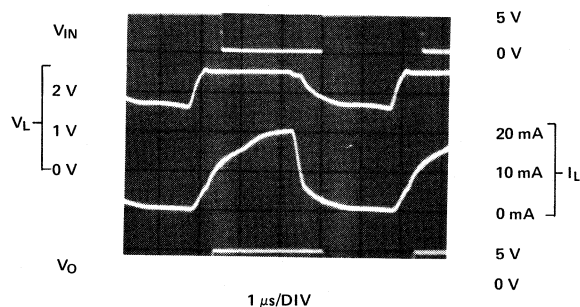


Figure 13. Characteristic Waveform Performance of Circuit in Figure 11 with 305 m (1000 ft.) Loop Distance, Square Wave Input and Output Distortion of 10%. a. Input Voltage (V_{IN}), b. Receiver Load Voltage (V_L), c. Loop Current (I_{LOOP}), d. Output Voltage (V_O)

Non-Isolated Active Transmitter with the HCPL-4200 Receiver

The typical waveforms for the non-isolated active transmitter used with the HCPL-4200 (Figure 11) are shown in Figures 12 and 13. The loop length is 305 metres (1000 ft.). Figure 12 shows 10% distortion when the input signal is a 16 bit pattern. The total propagation delay shown in Figure 12 for a SPACE to MARK transition is $2.4 \mu\text{s}$. The propagation delay of the transmitter and receiver is $0.3 \mu\text{s}$. Hence, the propagation delay for the transmission line is $2.1 \mu\text{s}$. Current and voltage waveforms for the current loop at the receiver end are shown in Figure 13 for a 10% distortion of data to an input square wave. Notice the loop current waveform delay of $2.4 \mu\text{s}$ before V_O follows V_{IN} . The important parameter to observe is loop current. When the loop current level exceeds the HCPL-4200 current threshold, V_O changes state. Loop voltage at the receiver only follows the current level and changes by approximately one volt. This simplex configuration provides the best speed performance.

Non-Isolated Active Receiver with the HCPL-4100 Transmitter

The typical waveforms for the non-isolated active receiver used with the HCPL-4100 (Figure 14) are shown in Figures 15 and 16. The loop length is 305 metres (1000 ft.). Figure 15 shows 10% distortion when the input signal is a 16 bit pattern. Figure 16 illustrates a 10% distortion for an input square wave. Recall that current level determines the switching point, not the voltage level.

At the input low to high state change, the loop current changes momentarily to the MARK state short circuit output current level, I_{sc} (typically 85 mA). A current spike appears at the receiver end after the inherent transmission line propagation delay of approximately $2 \mu\text{s}$, as expanded in Figure 17. The spike is caused by sudden discharge of cable capacitance. However, the loop current rapidly decreases from the I_{sc} level to a 20 mA level when line discharge is complete. Time duration of I_{sc} can be calculated by referring to the output power dissipation calculations for the HCPL-4100 in Appendix B.

TRUTH TABLE
(POSITIVE LOGIC)

V_{IN}	I_{LOOP}	V_{OUT}
H	20 mA	H
L	≤ 2 mA	L

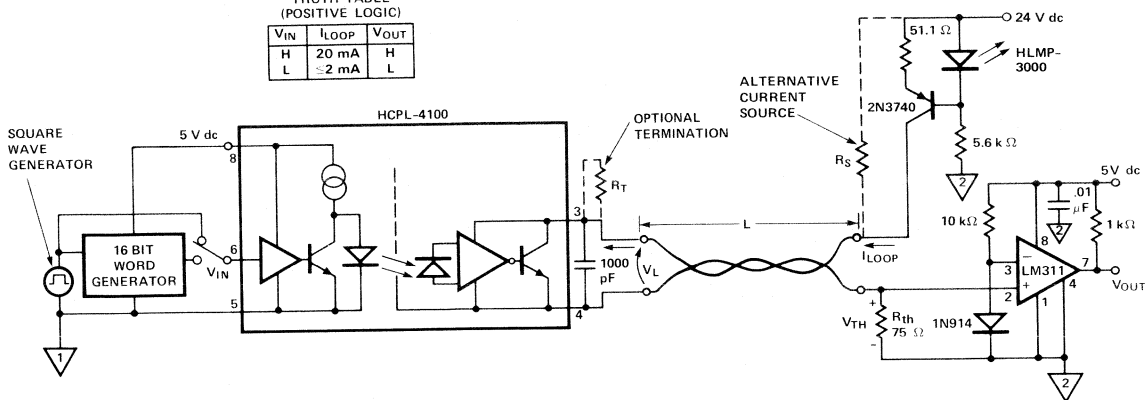


Figure 14. Data Rate Test Circuit for Isolated HCPL-4100 Transmitter to Non-Isolated Active Receiver

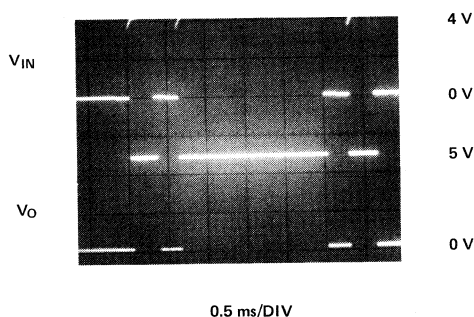


Figure 15. Timing Comparison of Output Signal (V_O) to Input Signal (V_{IN}) Using 16-Bit Word at 10% Distortion with 305 m (1000 ft.) Loop Distance. Reference Figure 14.

The non-isolated receiver switched states when loop current crossed approximately 10 mA level. Yet, the loop voltage took approximately 10 μ s to change from a current source voltage compliance level of 22.5 V to a MARK state voltage of 2.4 V at 20 mA. This loop voltage characteristic does not limit the turn on speed performance.

At the input signal high to low transition, the HCPL-4100 transmitter turns off after the device propagation delay. However, the loop current at the receiver does not change from 20 mA until approximately 30 μ s later. This is due to the current source charging the line capacitance at a fixed rate of 20 mA from essentially a MARK state voltage level (2.4 V) to the compliance level of the current source. Only after the compliance voltage is reached does the loop current fall below the 10 mA threshold of the receiver. As before, the current level at the receiver determines the switching time. In this example, the compliance voltage of the current source influences the turn off delay of the loop. This dependence is graphically illustrated in Figure 10.

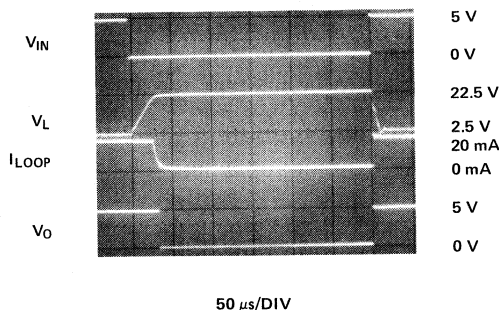


Figure 16. Characteristic Waveform Performance of Circuit in Figure 14 with 305 m (1000 ft.) Loop Distance, Square Wave Input and Output Distortion of 10%. a. Input Voltage (V_{IN}), b. Transmitter Load Voltage (V_L), c. Loop Current (I_{LOOP}), d. Output Voltage (V_O)

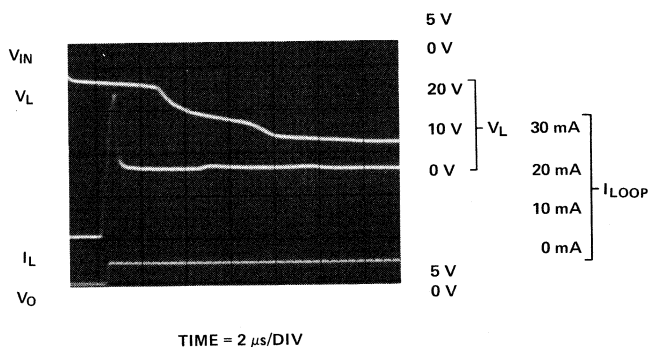


Figure 17. Expanded Waveform Response of Figure 16. Displayed are Details of I_{SC} Magnitude and Duration at Receiver as well as Transmitter Output Voltage (V_L)

General Factors Affecting Data Rate

Three factors which limit data rate and their corresponding trade-offs are:

1. **Loop length:** The length of the line will limit the speed performance of a current loop. This results mainly from the total capacitive loading effect of the cable upon the transmitter and receiver. The data rate versus length of line for the two simplex point-to-point configurations is illustrated in Figures 8 and 10. Shielded cable provides more noise immunity but, in general, the capacitance per unit length will be larger than unshielded cable. The characteristics of the cable used, such as wire size, twist, insulation material, etc. all influence the maximum data rate. (The characteristics of the cable used in the text applications are listed in Appendix C.)
2. **Current Source:** The location, type and compliance voltage of the current source used within a current loop can affect the system data rate. The primary limitation on data rate is the location of the current source within the loop. When the current source is located at the transmitter end of the loop rather than at the receiver end, the maximum data rate is much higher for a given loop length. This effect can be seen when comparing data in Figure 8 to Figure 10. The main reason for the lower data rate capability shown in Figure 10 is that the current source must charge the cable capacitance to the compliance voltage of the current source. The speed achieved in Figure 8 results because cable voltage changes by a small amount between the MARK and SPACE states. Practical applications of the HCPL-4100 and HCPL-4200 optocouplers generally will require the current source to be located at the non-isolated end of the loop. For best speed performance, an active non-isolated transmitter would be used with the HCPL-4200 receiver. However, in full duplex applications (two simplex loops), the non-isolated ends should be at a common location. Hence, overall bidirectional system data rates would be limited by the slowest loop, i.e., the one which contained a non-isolated, active receiver. More discussion of full and half duplex applications is found in subsequent sections.

The type of current source can affect speed performance. A simple resistor, when used with a voltage source at the non-isolated loop end, can set the loop current level. Improper source impedance or termination of the loop causes reflections which distort data resulting in a lower data rate capability. Termination of a current loop with an impedance equivalent to the characteristic impedance of the line can improve the data rate capability by approximately 20%. Termination resistance does reduce part of the voltage available for operating station(s) on the loop.

An active element current source can be controlled by current steering which allows for a higher speed of operation while providing consistently high on and off output impedance. Less variation in current source output impedance can help to reduce multiple signal reflections from occurring. Active element current sources are described in the Current Sources section of this application note.

The compliance voltage can influence the speed performance of the non-isolated, active receiver circuit shown in Figure 9. Data rate dependency upon the

compliance voltage is shown in Figure 10. Reducing the current source supply voltage from 24 V DC to 10 V DC for a simplex point-to-point current loop configuration increases the data rate by a factor of 3.5 in a 1000 metre (3281 ft.) loop. The reason for the improvement is that less time is required to charge the transmission line to the lower compliance voltage level at a constant charge rate. However, the opposite simplex arrangement of a non-isolated, active transmitter, Figure 7, has no data rate dependency on compliance voltage as illustrated in Figure 8. This is the result of the HCPL-4200 performing current threshold detection, not voltage level detection.

The maximum usable data rate for a given loop length and configuration is usually determined by the propagation delay differences of the current loop and the amount of skew that is allowed in the user's application. Propagation delay skew is $|t_{PLH} - t_{PHL}|$. Factors which contribute to the system propagation delay skew are the current source compliance voltage level, the current source location, the inherent propagation delay skew of the current source, as well as the optocoupler propagation delay skew. Detailed information on factors which affect distortion of data are discussed in the subsequent Half Duplex section.

3. **Device Performance:** The propagation delay of the transmitter and the receiver can influence data rates for short loop lengths (<100 metres) in high speed applications (>1 MBd). Generally, current loops are designed to operate over much greater distances than 100 metres. Consequently, the cable capacitance dominates the data rate limitations.

Another device performance consideration is the power dissipated in the HCPL-4100 transmitter. An example of power dissipation calculation for the HCPL-4100 is given in Appendix B. Derating may be required when operating the unit at large V_{CC} voltage.

Optional Device Protection Considerations

Specific end product applications may require additional device protection. A bridge rectifier can be included in order to remove loop polarity connection concerns. Current buffering can be designed for loop currents greater than 30 mA. Possibility of damage due to electrostatic discharge to the cable or interconnection points can be significantly reduced by the use of energy absorbing devices, such as TransZorbs® or metal oxide varistors (MOV).

Full Duplex

A common and useful extension of the simplex configuration is the full duplex configuration. Full duplex communication is defined as the simultaneous, bidirectional transmission of information between local and remote units. The block diagram in Figure 18 shows this point-to-point configuration.

Essentially, a full duplex arrangement is two point-to-point simplex loops (a four wire system) used simultaneously for back and forth data flow. A common current loop application for full duplex configuration is connecting remote terminals to an I/O interface section of a central computer system.

Implementation of optical isolation within a full duplex current loop system should be done at one common end

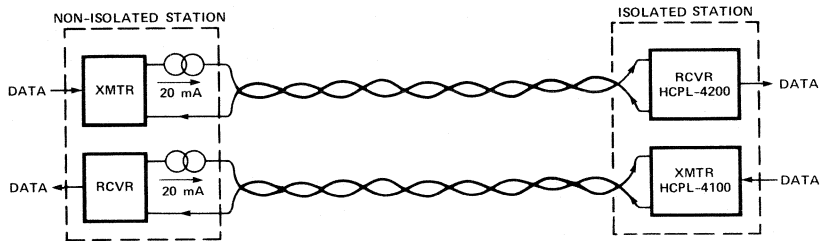


Figure 18. Full Duplex Point-to-Point Current Loop System Configuration

of the loops. Two separate, active, non-isolated units are located at the other end of the loops. Figure 18 illustrates these comments. Providing isolation at one common end will significantly reduce common mode coupling between the two loops. In most cases, the full duplex data rate is limited by the loop containing the HCPL-4100 and the non-isolated active receiver. This limitation can be circumvented by using an isolated current source at the HCPL-4100 end of the loop and a non-isolated passive receiver. The isolated current source increases the cost of the data link, but this increased cost may be justified by the speed improvement obtained. All information which is described in the Simplex section for the performance of a simplex point-to-point current loop configuration will apply to the full duplex applications as well.

Half Duplex

A half duplex current loop provides non-simultaneous, bidirectional data flow between remote and local equipment. This configuration utilizes a simpler two wire interconnection, compared to the four wire arrangement of the full duplex case. The half duplex system can easily be expanded from a point-to-point application to a multidrop application with multiple transmit and receive stations along the loop. The block diagrams of Figure 19 demonstrate the two cases of point-to-point and multidrop for half duplex.

A characteristic of the half duplex configuration is the need to establish priority of transmitters in the current loop whether the loop is point-to-point or multidrop. Protocol in the information being transferred will ensure that

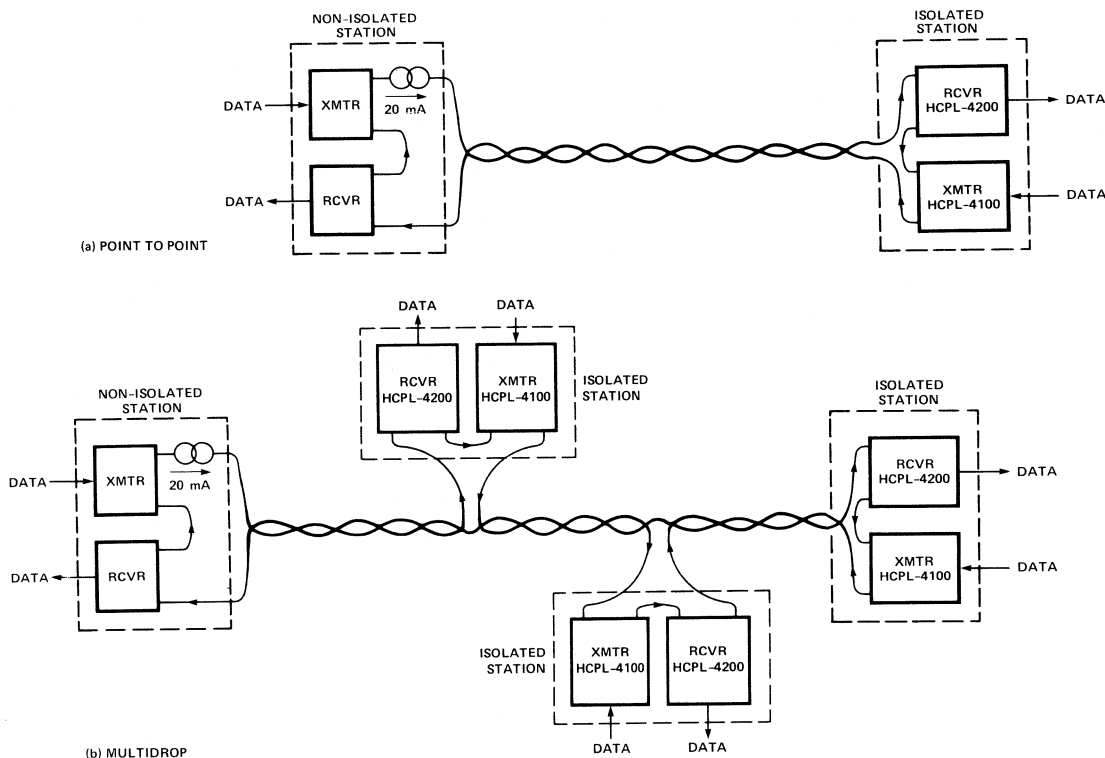


Figure 19. Half Duplex Current Loop System Configurations for: a. Point-to-Point, b. Multidrop

only one transmitter is sending data at any given time. Typical usage of a half duplex current loop parallels similar applications for the full duplex case.

DC Performance

As Figure 19 illustrates, isolation of the current loop from logic systems is easily implemented at one end of the loop by the use of the combination of the HCPL-4100 transmitter and the HCPL-4200 receiver. Significant reduction of common mode influences on the current loop, elimination of ground potential differences and specified loop current noise immunity are achieved by the use of these complementary optocouplers. For this combination of optocouplers, the loop current noise immunity is a minimum of 1 mA in the SPACE state and 8 mA in the MARK state. A non-isolated active transceiver (transmitter and receiver) with one current source operates at the opposite end of the current loop.

The maximum compliance voltage of the current source is limited by the breakdown voltage capability of any transmitter in the half duplex loop. The isolated HCPL-4100 transmitter has a maximum operating voltage of 27 V DC. However, in multidrop applications, each isolated HCPL-4200 receiver will share a portion of the compliance voltage during the SPACE state, worst case 0.9 V DC at a minimum SPACE state current of 0.5 mA. Also, each isolated conducting HCPL-4100 transmitter will share a

portion of the compliance voltage during SPACE state as well. Worst case, this is 0.95 V DC at 0.5 mA. For example, with four pairs of HCPL-4100 and HCPL-4200 units being used, an additional worst case 6.5 V DC can be added to increase the maximum compliance voltage value from 27 V DC to 33.5 V DC for the current source. The additional 6.5 V DC is calculated on the basis of one of the HCPL-4100 transmitters interrupting 22 mA loop current at 200 metre station intervals. This increase in the compliance voltage level can allow another isolated station to be used. Minimum V_{CC} required for the current source of Figure 20(b) with five isolated stations in the MARK condition with worst case parameters previously used yields 33.2 V DC. A higher compliance voltage can allow longer loop lengths but data rate will be slower. Precautions must be taken to prevent the removal of any stations from the loop in order to avoid an excessive compliance voltage from overstressing any transmitter remaining in the loop. A design compromise has to be determined for the benefits achieved at different compliance voltages. Equation (1) from the Simplex section can be used to determine any DC parameter in a half duplex application.

A specific active, non-isolated transceiver which can be used in point-to-point and multidrop applications with the HCPL-4100 and HCPL-4200 current loop optocouplers is shown in Figure 20.

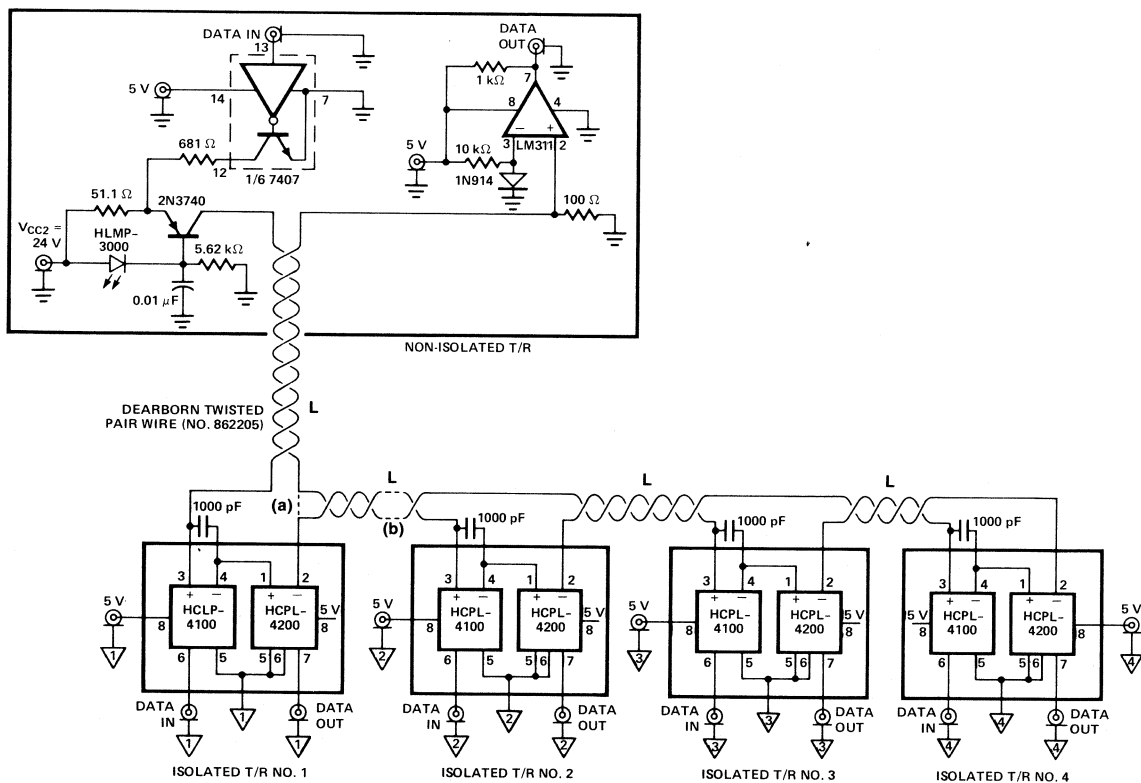


Figure 20. Circuit Schematic of Half Duplex Configurations: a. Point-to-Point, b. Multidrop

AC PERFORMANCE

Point-to-Point

The corresponding data rate performance versus loop distance and direction of data is given in Figure 21 for the half duplex point-to-point application. Definitions for 10% and 25% distortion data rate are given under the Simplex Configuration section.

Transmission of data from an isolated T/R (transmitter and receiver pair) to an active non-isolated T/R limits the half duplex data rate performance. This limitation is due to slower speed of a current loop when using an isolated transmitter. A lower current source compliance voltage will improve the data rate of an isolated T/R to a non-isolated T/R as discussed in the Simplex section.

Multidrop

The data rate performance for half duplex multidrop applications, as illustrated in Figure 20(b), is summarized in Tables 1 and 2. These tables compare data rate versus the loop distance between stations, total length of loop, direction of data, distortion data rate and data format. Table 1 illustrates at fixed distortion (10% or 25%) how data rate can be different at different stations along the loop. Table 2 shows the pulse width distortion that results when the multidrop loop is operated at several fixed data rates.

Comparison of data rates for point-to-point (half duplex) and multidrop configurations can appear contradictory. Data presented in Figure 21 and Table 1 illustrate this at a 25% distortion on a 915 m (3000 ft.) loop. A comparison shows the influence of multiple stations upon the data rate for a fixed loop length. In the point-to-point case, the data rate is 62.5 kBd from an active, non-isolated T/R to the isolated T/R No. 1. In the multidrop case, non-isolated T/R to the isolated T/R No. 3, data rate in the same direction is 25 kBd. As expected, the data rate in point-to-point is faster because the current source only needs to charge the line to a lower sum ($\approx 1/2$) of MARK state voltages than in the multiple station case. However, in the opposite direction of isolated T/R No. 1 to active, non-isolated T/R, the point-to-point data rate is 3.33 kBd while the multidrop data rate is 6.25 kBd. In this instance, multidrop is 2X faster than the point-to-point case over the same distance, contrary to "expected" results. The reason for this speed improvement results from the fact that when T/R No. 3 interrupts the loop current, the current source will continue to charge the loop until the compliance voltage is reached causing the current source to shut down. Fortunately, the voltage difference between the sum of all MARK state voltage drops and compliance voltage is small due to the total of four stations in the loop. Hence, a small voltage excursion requires considerably less charging time than if this charging occurred over a larger voltage excursion.

In addition, with the usage of multiple stations at a constant data rate, the data distortion can vary from station to station. This distortion varies with respect to the transmitting station. As an illustration from Table 2, the 915 m (3000 ft.) example with three remote stations [i.e., the isolated T/R No. 3 transmitting at 6.25 kBd to successive 305 m (1000 ft.) stations of T/R No. 2, T/R No. 1 and an active non-isolated transceiver] yields distortion levels of 19%, 31%, 25% respectively. Larger distortion at an interim station than at a station located at an end of a loop is due to different thresholds for each station. Identical current threshold levels at each station will provide progressively increasing distortion levels at each station along the loop. Also, reflection of signals between stations can account for inconsistent distortion levels at various stations on a loop system. The designer will be limited to a data rate that results in acceptable distortion for each station.

In general, data rate limitations in multidrop applications for data which flows from active non-isolated station to isolated stations will be caused by propagation delay time of the line and the charging or discharging time for the total line capacitance. Charging and discharging the line occurs over a voltage level which is equal to the difference between the sum of all MARK state voltages and the sum of all SPACE state voltages which are presented at the active non-isolated loop connection points. Data rate limitations in the opposite direction (isolated units to an active, non-isolated unit) are limited by propagation delay time of the line and by the time to charge total line capacitance over a voltage equal to the difference between the sum of MARK state voltages and compliance voltage of the current source.

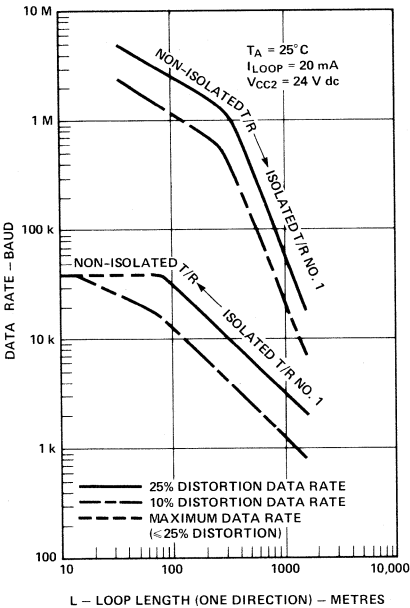


Figure 21. Half Duplex Point-to-Point (Figure 20a) Data Rate vs. Loop Length and Data Direction

Table 1. Constant % Distortion, Variable Data Rate for Half Duplex Multidrop Configuration.

Data In	Data Out	L Length between Data Input and Data Output points		L _T Total Loop Length	Data Rate kBd	% Distortion	Comments
Active Non-Isolated Transceiver	T/R #4	m	ft.	m (ft.)			Input Signal: Square Wave Current Source: 20 mA/24 V DC Half Duplex Current Loop Circuit Schematic: Figure 20b.
	T/R #3	122	400	122 (400)	250	25%	
	T/R #2	92	300		370		
	T/R #1	61	200		370		
		31	100		250		
	T/R #4	122	400		125	10%	
	T/R #3	92	300		167		
	T/R #2	61	200		167		
T/R #1	31	100	125				
Isolated T/R #4	Non-Iso. T/R	122	400	915 (3000)	62.5	25%	
	T/R #1	92	300		62.5		
	T/R #2	61	200		82.5		
	T/R #3	31	100		100		
	Non-Iso. T/R	122	400		25	10%	
	T/R #1	92	300		25		
	T/R #2	61	200		33.3		
	T/R #3	31	100		40		
Active Non-Isolated Transceiver	T/R #3	915	3000	915 (3000)	25	25%	
	T/R #2	610	2000		33.3		
	T/R #1	305	1000		25		
	T/R #3	915	3000		12.5	10%	
	T/R #2	610	2000		16.7		
	T/R #1	305	1000		12.5		
Isolated T/R #3	Non-Iso. T/R	915	3000	915 (3000)	6.25	25%	
	T/R #1	610	2000		5.0		
	T/R #2	305	1000		8.25		
	Non-Iso. T/R	915	3000		2.0	10%	
	T/R #1	610	2000		2.0		
	T/R #2	305	1000		3.33		

Table 2. Constant Data Rate, Variable % Distortion for Half Duplex Multidrop Configuration.

Data In	Data Out	L Length between Data Input and Data Output points		L _T Total Loop Length	Data Rate kBd	% Distortion	Comments
		m	ft.	m (ft.)			
Active Non-Isolated Transceiver	T/R #4	122	400	122 (400)	250	25%	Input Signal: Square Wave Current Source: 20 mA/24 V DC Half Duplex Current Loop Circuit Schematic: Figure 20b.
	T/R #3	92	300		250	30%	
	T/R #2	61	200		250	15%	
	T/R #1	31	100		250	25%	
	T/R #4	122	400		125	10%	
	T/R #3	92	300		125	6%	
	T/R #2	61	200		125	7.5%	
	T/R #1	31	100		125	12%	
Isolated T/R #4	Non-Iso. T/R	122	400	122 (400)	62.5	25%	
	T/R #1	92	300		62.5	25%	
	T/R #2	61	200		62.5	19%	
	T/R #3	31	100		62.5	6%	
	Non-Iso. T/R	122	400		25	10%	
	T/R #1	92	300		25	10%	
	T/R #2	61	200		25	7.5%	
	T/R #3	31	100		25	7.5%	
Active Non-Isolated Transceiver	T/R #3	915	3000	915 (3000)	25	25%	
	T/R #2	610	2000		25	17.5%	
	T/R #1	305	1000		25	25%	
	T/R #3	915	3000		12.5	10%	
	T/R #2	610	2000		12.5	7.5%	
	T/R #1	305	1000		12.5	12%	
Isolated T/R #3	Non-Iso. T/R	915	3000	915 (3000)	6.25	25%	
	T/R #1	610	2000		6.25	31%	
	T/R #2	305	1000		6.25	19%	
	Non-Iso. T/R	915	3000		2.0	10%	
	T/R #1	610	2000		2.0	8%	
	T/R #2	305	1000		2.0	12%	

APPLICATION
SPECIFIC
OPTOCOUPERS

CURRENT SOURCES

Resistor

Current sources used for current loop systems can vary in performance, complexity and cost. The most elementary and inexpensive technique for supplying loop current is to use a series resistor between the non-isolated station power supply and the loop. The resistance value (R_S) to use is a function of the desired loop current (I_{LOOP}), of the type of cable (resistance per length, R_{LINE}), the loop length (L), the number of stations on the loop with their respective MARK state terminal voltages (ΣV_{MARK}) and the power supply voltage (V_{CC}) for the non-isolated station. Equation (5) determines the resistor value. The simplicity of a single resistor yielding a 20 mA loop current is achieved at the expense of requiring that the loop configuration cannot be changed without changing the resistor value.

$$R_S = \frac{V_{CC} - (I_{LOOP})(R_{LINE})2L - \Sigma V_{MARK}}{I_{LOOP}} \quad (5)$$

Speed performance of a loop system using a current setting resistor is slower than with an active current source. This difference arises from an exponential current response versus a linear current response associated with an active current source. For a given current threshold level, the linear response will charge a capacitive line quicker than an exponential response. When a current setting resistor is used, termination resistance can be employed at the isolated stations in order to reduce somewhat the signal reflections along a loop. Up to a 20% speed improvement can be obtained with termination resistance equal to characteristic line impedance. However, with the use of termination resistance, allowance must be made for the additional MARK state voltage drop of the terminating resistor with respect to the available compliance range of the current loop.

LED/Transistor

The recommended current source to use is a simple, relatively inexpensive, active constant current source shown in Figure 22. The LED provides a stable voltage reference (V_F) for the transistor base and also helps to compensate the base-emitter junction voltage (V_{BE}) changes with temperature. This current source is fairly independent of the V_{CC} level if the LED bias current (I_F) is set so that the V_F only changes slightly with large variations in I_F (≈ 60 mV/decade of I_F). Regulation of 10% in output current can easily be achieved over a V_{CC} range of 5 V DC - 27 V DC.

When large V_{CC} is used with low MARK state voltage conditions, the use of a transistor with good thermal conduction to the ambient environment will minimize the variation in the source current because of the variation of V_{BE} with temperature. This state is the large power dissipation condition.

This current source can be easily current steered for fast switching. Current steering is illustrated in Figure 7. For applications of this current source at high data rates over short loop distances it is important that the difference in propagation delays from on-to-off and off-to-on be made as small as possible. Status indication is conveniently given by the LED.

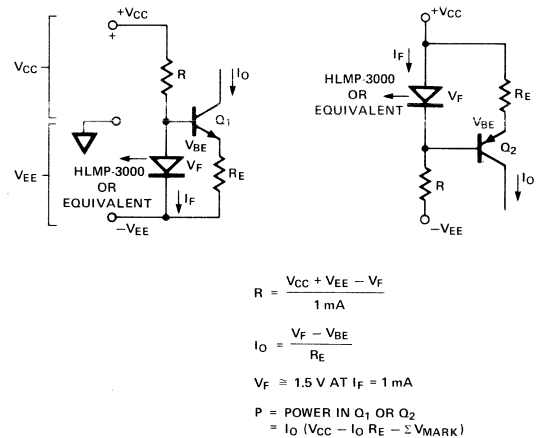


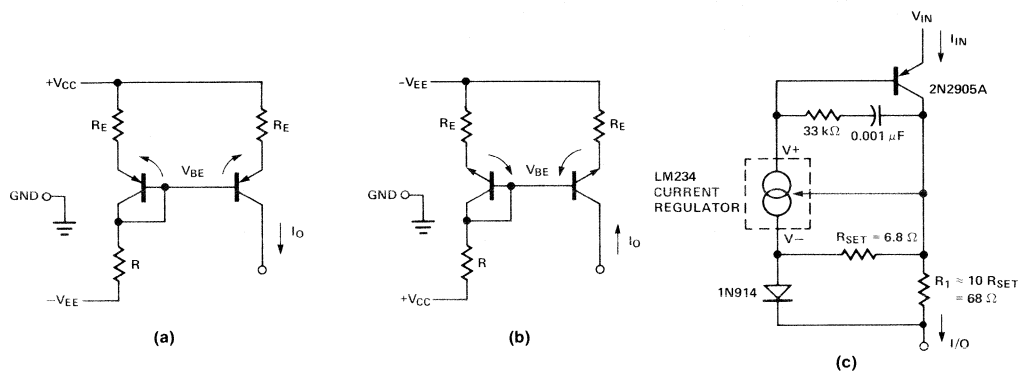
Figure 22. Recommended Constant Current Source

Specialized Integrated Circuits

More complicated current sources which are usable in current loops can be current mirrors or specialized integrated circuits. A current mirror displayed in Figure 23 requires the use of a matched pair of transistors in order to perform well.

In general, commercially available matched pairs are not designed for output collector currents greater than 10 mA. Additional components which are needed to obtain 20 mA results in greater complexity and higher cost with less reliability. In order to reduce power supply noise influences and improve thermal stability, significant transistor emitter degeneration resistance must be used. This degeneration sacrifices the available voltage range between the total MARK state voltage and the compliance voltage of the current mirror.

In Figure 23(c), the LM234 integrated circuit current source can be used. More components are required for temperature compensation to provide a proper current level and regulation over a wide temperature range as well as to prevent possible oscillations of this active device. In addition, switching characteristics of the LM234 must be considered with regard to the desired loop speed performance. Over all, the current source provides good regulation ($\pm 3\%$) for current loop usage, but the cost of additional components and space in an input-output module may detract from the design convenience of this device.



$$R_E = \frac{\Delta T (\Delta V_{BE} / \Delta T)}{\Delta I} \quad \left\{ \begin{array}{l} \Delta T = \text{TEMPERATURE CHANGE FROM ROOM TEMPERATURE IN } ^\circ\text{C} \\ \Delta I = \text{ACCEPTABLE DEVIATION FROM } I_O \text{ IN mA} \end{array} \right.$$

$$\Delta V_{BE} = \Delta V_{BE2} - \Delta V_{BE1}$$

$$I_O \approx \frac{V_{CC} + V_{EE} - V_{BE}}{R + R_E}$$

Figure 23. Specialized Integrated Circuit Current Sources. Current Mirrors: a. PNP, b. NPN. Current Regulator: c. LM234 plus Components

APPENDIX A.

16-Bit TTL Data Exerciser Circuit

The purpose of this circuit is to provide long (6 bits) and short (1 bit) durations of the logic one and logic zero states in different time sequences. Figure 24 illustrates the 16-bit TTL output waveform (Q_A).

APPENDIX B.

HCPL-4100 Power Dissipation Calculations

The power dissipation calculation for the HCPL-4100 transmitter is made using the standard method for determining the input power dissipation. Calculation of the output power dissipation must take into account power consumed in three different operating conditions. These conditions are: 1. power dissipated during transition from SPACE to MARK state, 2. power dissipated in MARK state, and 3. power dissipated in SPACE state. The worst case average power dissipated over two bit intervals should be calculated. The average output power dissipation is calculated from the following formula:

$$P_O = \frac{P_{SM} + P_{TM} + P_{STs}}{2 t_{BIT}} \quad (6)$$

where

P_O = Average output power dissipated during a worst case time interval.

P_{SM} = Power dissipated during SPACE to MARK transition

$$= \frac{I_{SC} (V_{COMP} + V_{MO})}{2} \quad (7)$$

I_{SC} = MARK state short circuit output current

V_{COMP} = Compliance voltage of current source

V_{MO} = MARK state output voltage

P_M = Power dissipated during MARK state
 $= V_{MO} I_{LOOP}$ (8)
 $I_{LOOP} = \text{Loop Current}$

P_S = Power dissipated during SPACE state
 $= V_{COMP} I_{SO}$ (9)

I_{SO} = SPACE state output current

t_{SM} = Duration time of power dissipated during SPACE to MARK transition

$$= \frac{C_L (V_{COMP} - V_{MO})}{I_{SC}} \quad (10)$$

C_L = Total load capacitance

t_M = Duration time of MARK state

t_S = Duration time of SPACE state

t_{BIT} = Time of bit interval

These formulas are based upon an assumption of a linear discharge of a capacitive load.

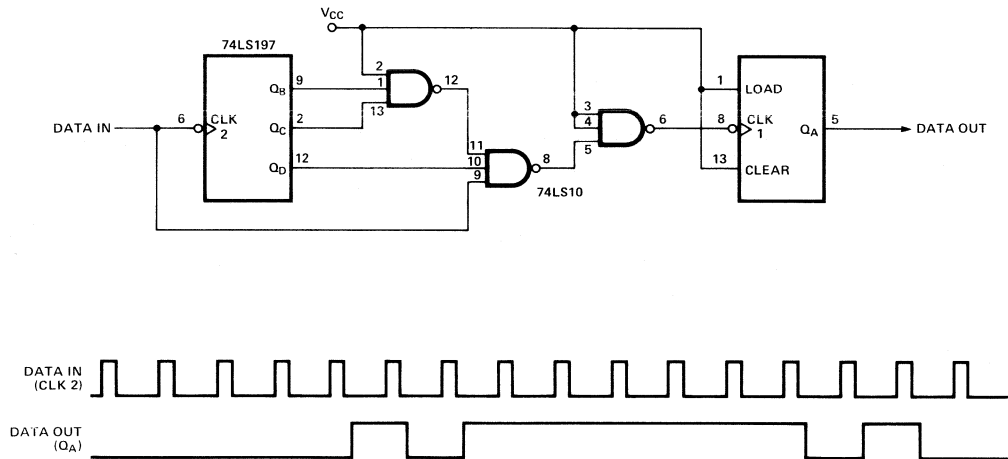


Figure 24. 16-Bit TTL Data Exerciser Circuit and Corresponding Waveforms

Using equations (6) through (10), the worst case output power dissipated in the HCPL-4100 transmitter can be calculated for the following operating conditions.

L = 200 metres (656 ft.)
 $C_L = 36,000 \text{ pF}$ (180 pF/m)
 $V_{COMP} = 23.5 \text{ V DC}$ ($V_{CC} = 24 \text{ V DC}$)
 $I_{LOOP} = 22 \text{ mA}$ (20 mA + 10%)
 $I_{SC} = 85 \text{ mA}$
 $T_A = 70^\circ \text{C}$

CMOS LOGIC (15 V \pm 5%)

HCPL-4100 Power Dissipation Limits at 70°C

$P_{IN} = 208 \text{ mW}$, $P_{TOTAL} = 283.5 \text{ mW}$

$V_{MO} = 2.75 \text{ V}$ at 22 mA

$I_{SO} = 2 \text{ mA}$

$t_{BIT} = 104.1 \mu\text{s}$

(9600 Baud, NRZ* alternating MARK and SPACE states.
 Reference Figure 25.)

*Non Return to Zero data format.

D = 25% Distortion

Calculation of maximum input power to the HCPL-4100 is based upon linear interpolation of maximum I_{CC} and I_{IH} .

$$\begin{aligned} P_{IN} &= V_{CC}I_{CC} + V_{IH}I_{IH} \\ &= (15.8 \text{ V}) (12.6 \text{ mA}) + (15.8 \text{ V}) (0.206 \text{ mA}) \\ &= 202.3 \text{ mW}. < 208 \text{ mW max} \end{aligned} \quad (11)$$

Consequently, maximum derated output power is

$$\begin{aligned} P_O &= P_{TOTAL} - P_{IN} \\ &= 81.2 \text{ mW} \end{aligned} \quad (12)$$

Applying given values to equations (7), (8), (9), and (10) results in

$$P_{SM} = 1115.6 \text{ mW}$$

$$P_M = 60.5 \text{ mW}$$

$$P_S = 47 \text{ mW}$$

$$t_{SM} = 8.8 \mu\text{s}$$

Equation (6) yields average output power per bit interval of

$$P_O = 98.4 \text{ mW} > 81.2 \text{ mW max}$$

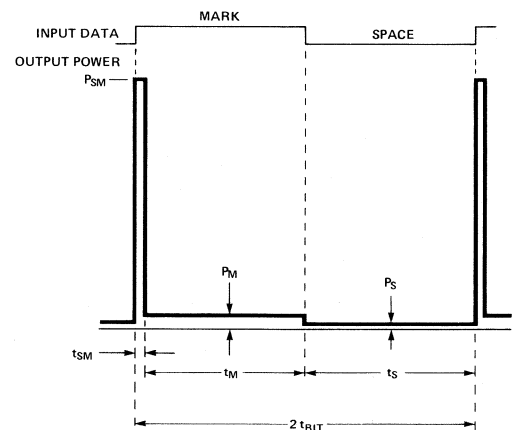


Figure 25. Output Power Dissipation over Two Bit Intervals in HCPL-4100 Transmitter

To circumvent this excess output power dissipation condition, V_{CC} of current source can be reduced from 24 V DC to 15 V DC. Recalculation with $V_{CC} = 15$ V DC yields

- $P_{SM} = 733.1$ mW
- $P_M = 60.5$ mW
- $P_S = 29$ mW
- $t_{SM} = 5.0$ μ s
- $P_O = 60.9$ mW < 81.2 mW max

The major compromises which would be given up are:
a. maximum loop length is reduced by one half, and
b. less capability for multidrop applications. However, data rate can be doubled to 20 kBd at $V_{CC} = 15$ V DC over 200 metres.

APPENDIX C.

Cable Data

The cable which was used throughout this application note contained five pairs of unshielded, twisted, 22 AWG wire (Dearborn No. 862205). Typical measured properties of this cable are listed below. Other manufacturers provide cable with similar characteristics (Belden No. 9745). Consult cable manufacturer catalogs for detailed information.

- $Z_O = 75$ Ω , Characteristic Impedance – line to line
- $R_{LINE} = 52.91$ Ω /1000 m, DC Resistance – single conductor
- $C = 174$ pF/m, Capacitance – line to line
- $t_{DELAY} = 5.9$ nsec/m

APPENDIX D.

List of Parameters

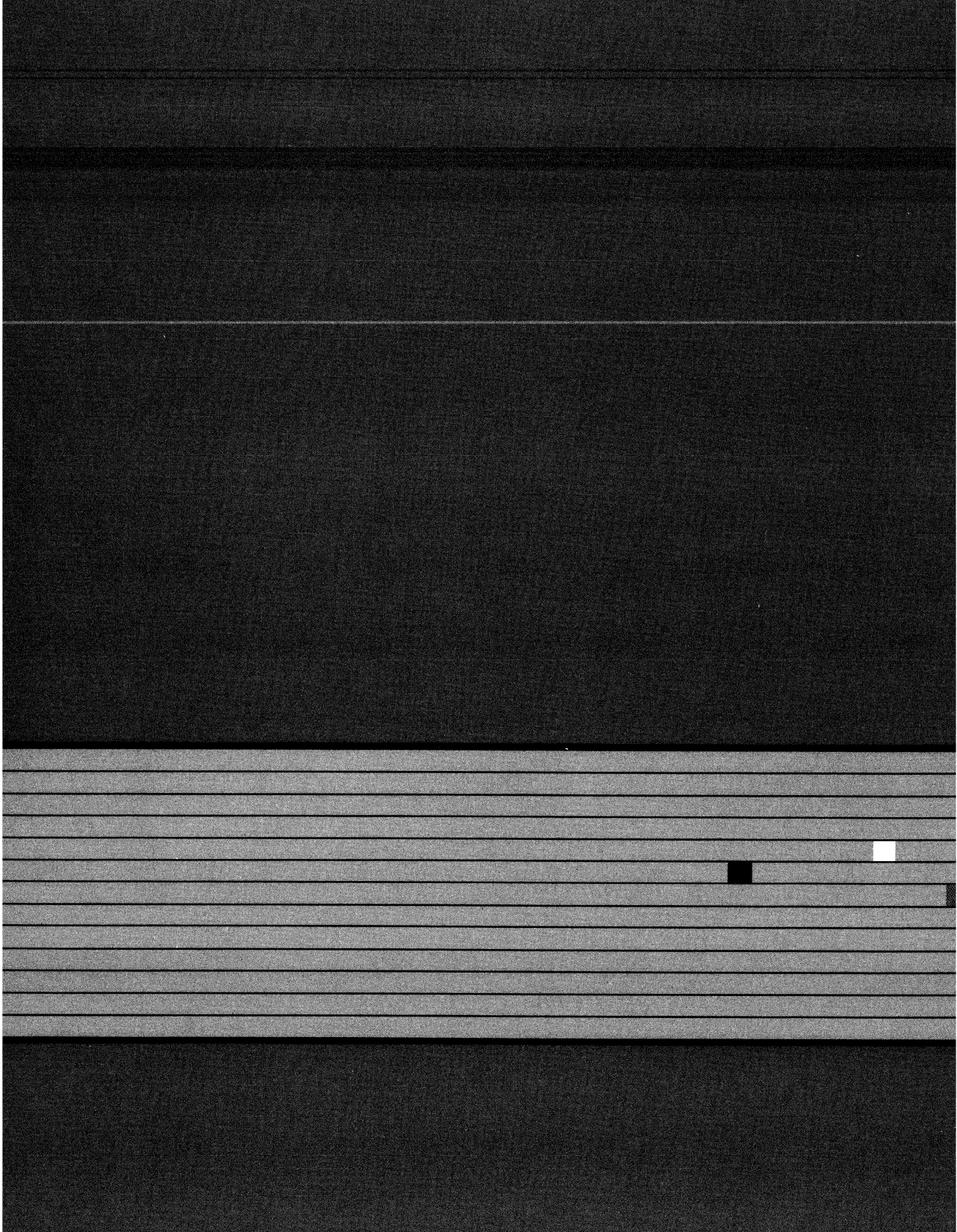
- $C_L =$ Total load capacitance
- $f_D =$ Data rate at which D% output pulse distortion occurs
- $I_{LOOP} =$ Operating loop current
- $I_{SC} =$ MARK state short circuit output current
- $I_{SO} =$ SPACE state output current
- $L =$ Length of wire in one direction
- $P_S =$ Power dissipated during SPACE state

- $P_O =$ Average output power dissipated over a time interval
- $P_{SM} =$ Power dissipated during SPACE to MARK transition
- $P_M =$ Power dissipated during MARK state
- $R_{LINE} =$ DC resistance of wire per length
- $R_S =$ Current setting resistor from non-isolated power supply
- $t_{BIT} =$ Time of bit interval
- $t_S =$ Duration time of SPACE state
- $t_M =$ Duration time of MARK state
- $t_{SM} =$ Duration time of SPACE to MARK transition
- $V_{CC} =$ Power supply voltage
- $V_{COMP} =$ Compliance voltage of current source
- $V_{MO} =$ MARK state output voltage
- $V_{RCVR} =$ Voltage across current loop receiver terminals when MARK state current flows
- $V_{SAT} =$ Saturation voltage of current source
- $V_{XMTR} =$ Voltage across current loop transmitter terminals when MARK state current flows

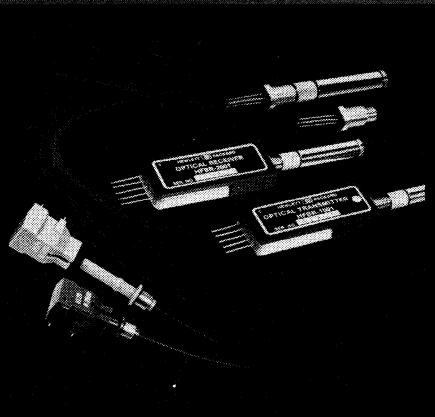
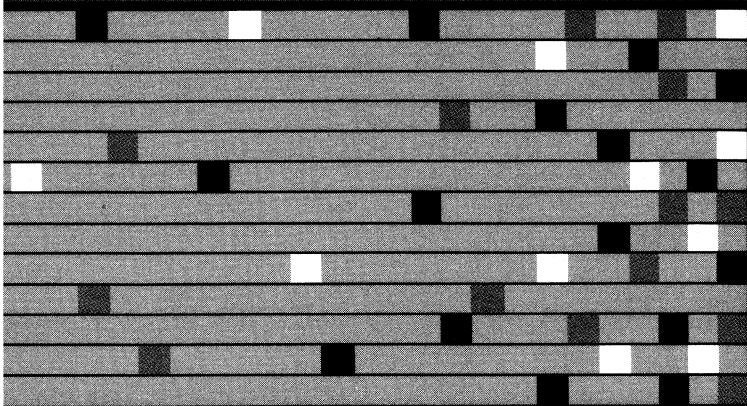
APPENDIX E.

References

1. *Optoelectronics/Fiber Optics Application Manual*, Hewlett-Packard Company, Second Edition, McGraw-Hill, New York, 1981, pp. 3.1–3.77, 10.1–10.8.
2. True, Kenneth M., *The Interface Handbook – Line Drivers and Receivers*, Fairchild Semiconductor Components Group, Mountain View, CA., 1975, pp. 1-1 – 5-12.
3. McNamara, John E., *Technical Aspects of Data Communications*, Second Edition, Digital Equipment Corporation, Bedford, MA., 1982, pp. 13–21, 233–242.
4. Larsen, David G., Ronz, Peter R., Titus, Jonathan A., “INWAS: Interfacing with Asynchronous Serial Mode,” *IEEE Transactions on Industrial Electronics and Control Instrumentation*, Vol. IECI-24, No. 1, February 1977, pp. 2–10.
5. *HP 13266A Current Loop Converter User's Manual*, Hewlett-Packard Company, Palo Alto, CA 1979



Fiber Optic Technology



HP Fiber Optic Families: A Description

Three major families of fiber optic components offer a wide range of application solutions. The design and specification of each of these three families allow easy design-in and provide guaranteed end-to-end performance.

Hewlett-Packard's method of specification assures guaranteed link performance and easy design-in. The transmitter optical output power and receiver sensitivity are specified at the end of a length of test cable. These specifications take into account variations over temperature and connector tolerances. The guaranteed distance and data rates for various transmitter/receiver pairs are shown in Figure 2.

Hewlett-Packard offers a choice of fiber optic cable, either glass fiber or plastic, simplex or duplex, factory-connected or bulk. Connector attachment in each case has been designed for your production-line economy.

The performance of the three fiber optic families can be evaluated easily. Kits are

available for the first-time user along with reliability data and detailed product specification literature.

HP Fiber Optic Performance

Characteristics — The charts on this page and the facing page illustrate the performance ranges of Hewlett-Packard's fiber optic components. Both charts are color-coded by family. To determine which family is appropriate for your design, use the distance/data rate chart (Figure 1). The performance of each family incorporates the entire area below each boundary. Specific component choices and their associated optical-power budget are indicated in Figure 2.

The optical-power budget is determined by subtracting the receiver sensitivity (dBm) from the transmitter optical output power (dBm). The distance specification can be calculated simply by dividing the optical-power budget (dBm) by the cable attenuation (dB/km).

Figure 1.

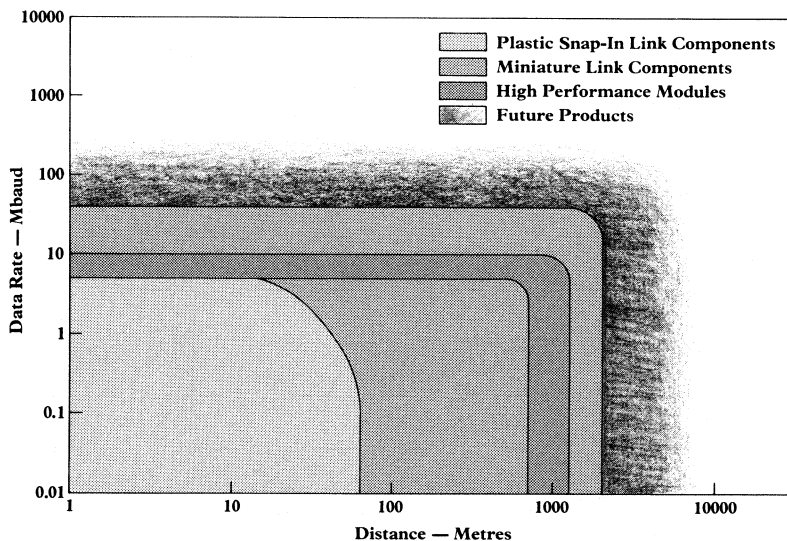


Figure 2.

1. Optical power budget calculations are at 25°C.
2. For link performance with other fiber sizes contact your local HP Sales Office.

Sensitivity (dBm)

**FIBER OPTIC
TECHNOLOGY**



HEWLETT
PACKARD

*Copyright Wire Journal International;
reprinted with permission.*

Optical Fiber or Wire: The Designer's Dilemma or a Clear Choice

The attractions of optical fibers — no electromagnetic interference or short circuits, long-distance transmission without relays — are numerous. But don't forget the problems — hidden costs and a lack of standardization.

Until now electronic system designers had little choice when connecting systems together. Wire cables had been the standard or the only choice until the advent of fiber optic cable and modules for transmitting and receiving optical flux.

The designer is now faced with a choice of using wire or fiber optic cable. What follows is a description of the shortcomings of wire communication, typical solutions already tried, and the advantages and limitations of fiber optics. A summary includes some cost considerations for the designer before he makes a final decision.

WIRE COMMUNICATIONS

Wire communications have handled the bulk of data interchange ever since the earliest telegraphs of the 1840s. Craftsmen are familiar with wire, standards have evolved and there are many choices of wire cable for almost any use, from aerial-strung cable to submarine applications. Standard wire connectors vary from precision exotic microwave interconnects to simple single or multipin plug-in devices.

With all of the wire cable and connectors available, why is there so much interest in fiber optics?

WIRE LIMITATIONS

Wire communications inherently have problems due to the conductive metallic path of the interconnecting wires.

Radio Frequency Interference (RFI) from radio, TV stations, diathermy machines and RF heaters can cause errors in data communications where the wire cable is acting as an antenna picking up the RF signals. Stories were circulated a number of years ago of early automobiles using electronic controls and either the engine

going dead or the brakes inadvertently being applied when driving near a radio transmitter.

Electromagnetic Interference (EMI) in wire systems could be caused by inductive pick up of power line current or interference from industrial machinery. In the case of a numerical controlled (NC) lathe or mill, corrupted data from its computer could be received due to the EMI generated from its own motors. Traditional methods of solving these problems have been to use heavy twisted shielded cable or balanced lines with differential driver and receivers.

So far external sources are shown to affect wire communications. But, conversely, the high-speed data driving the wire cable can also be radiated with the interconnecting wire cable acting as a transmitting antenna, possibly causing interference to neighboring circuits.

When data is transmitted over any distance, ground loops can be a problem. A ground loop is caused by using "ground" as a reference on both the transmit side and the receive side of the wire cable when the two "grounds" are not at the same potential. The ground loop is manifested as current flowing through the shield or ground wire of the interconnecting cable. Tying the "ground" of each unit to a common point or using very heavy grounding wires as is done in computer installations can sometimes solve this problem. However, it may be impractical when cable lengths approach tens of meters. Balanced lines, differential circuits and optocouplers have long been used to solve ground loop and other common mode voltage problems. But the transmission medium is still wire and the optocoupler limitation is the common mode capacitance (C_{CU}) of the device, which results in a frequency dependent interference path.

In cases where an intended voltage offset is required, as in the feedback of isolated power supplies, or data transmission between two points differing in potential as in ion or plasma physics experiments, electrically conductive paths cannot be used at all. The solution up to this time has been expensive isolation transformer coupling. A differential line receiver's common mode rejection voltage is typically 15 V and optocouplers used in these circuits would be limited to 3,000 V. In some instances microwave radios have been used to transmit data from power grid monitors to collection stations several meters away due to the high voltage potential differences.

The use in data communication of many integrated circuits (ICs), which have a low breakdown voltage rating, has led many designers to study way of minimizing electrostatic discharge (ESD). Common forms of ESD are, of course, lightning, discharge of a spark by a person due to static voltage accumulation in the body capacitance and deliberate high voltage discharge as in a Xenon lamp firing in a paper copier. Again, the interconnecting wires act as antennas, funneling the destructive voltage to the sensitive circuits. Careful attention to layout and good grounding techniques are required to minimize a circuit's sensitivity to static discharge.

Capacitance between wire cables can cause coupling between data lines and if the interference is great enough, the data will be corrupted. Also, because of the inductive wire and distributed capacitance of the cable, the wire transmission medium is a distributed low pass filter with a particular three dB frequency.

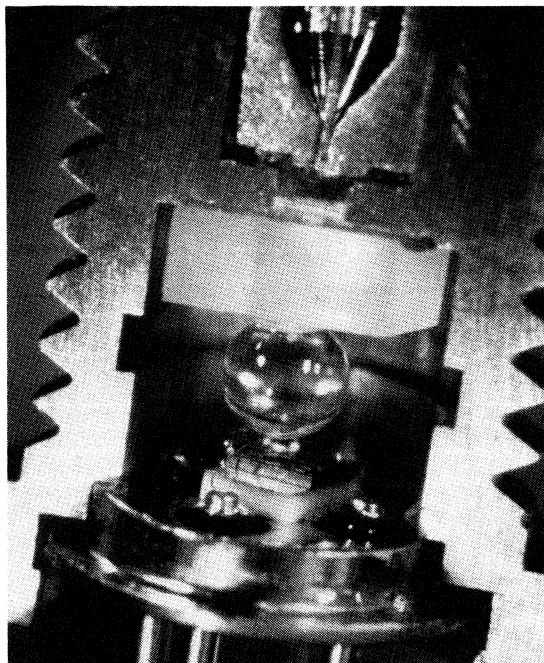
The wire's skin effect, though, has a pronounced effect on the bandwidth of the cable. The three dB wire cable bandwidth varies inversely as the square of the length. Systems requiring long distance transmission are then required to use either a low bit rate or, for high bit rate systems, have repeaters regenerate the signals at intermediate points along the transmission path.

For many systems to operate at their intended speed, the low bandwidth of the wire cable has forced designers to send data in parallel bits so that each wire cable need only carry $1/n$ of the bit rate of the total system. This wire limitation has caused many computer installations to have long runs of expensive, heavy multiconductor wire cable as their data transmission facility.

The above examples have shown many instances where extra precaution was required for systems to operate in difficult environments. Many times the designer had no choice. Wire was the only method and the extra circuitry was mandatory.

FIBER OPTIC CABLE

Fiber optic electro/optical components and fiber cables are readily available now and fiber optic systems interfaces are as easy to use as interfacing to TTL gates. The difficult part of fiber optic design (the electro/optical-opto/electrical interface) has been done by the various module manufacturers. The advantages of using fiber optics over wire lies in the nonmetallic, totally dielectric fiber optical cable. Information is transmitted in the optical waveguide by packets of photons, which have no charge and are not affected by radio frequencies or other electromagnetic interference.



A miniature fiber optic logic link.

The totally dielectric fiber cable medium allows the designer to transmit data with complete isolation from end to end. Data can be transmitted between points of vastly different potential, eliminating any ground loop or common mode voltage problems. Applications in programming floating power supplies, Supervisory Control and Data Acquisition (SCADA) systems, or control of high voltage lab experiments is now feasible, inexpensive and usually faster due to elimination of the limited bandwidth isolation transformers.

A non-dielectric medium with no current flowing also has beneficial safety considerations. If the fiber cable is cut, there is no possibility of sparks and no short circuits. Hazardous areas with volatile chemicals can use fiber optics for control and for gathering data. The chemical plant and petroleum industries are specifically intrigued by the safety aspects of fiber optics. Also, many Computer Automated Measurement and Control (CAMAC) systems are being implemented with fiber optics as the transmission link in the serial data highway. Several computer installations in areas with high thunderstorm activity and long runs to terminals can now be operated during lightning storms without worrying about having to disconnect the cables to prevent the computer from crashing.

Contrasting metallic wire cable and fiber cable made of non-dielectric materials, a significant factor is the reduction of weight. Non-metallic materials give typical fiber optic cable a 1/6 weight advantage over typical coaxial cable, which results in significantly less pulling force when installing the fiber cable in conduit, not to mention the ease of use by the craftsmen working with lighter materials. Since 1,000 meters of fiber weighs about six kg, the military is very interested in optical fiber for fast and easy deployment in tactical applications.

Fiber optic transmission lends itself quite naturally to applications where wire communication systems have shortcomings.

The inherent immunity to RFI and EMI have spawned fiber optic applications for data transmission through areas of high RFI. Industrial control motors in rolling steel mills, milling machines and robotics controlled with fiber optics would be immune to the electromagnetic interference radiated by the machines themselves.

Optical communications in fibers are essentially waveguide communications with the optical flux contained totally within the waveguide; therefore, no RF radiation is possible from the cable. Hence, fiber optics are used where there are restrictions on radiated electromagnetic interference. Increased governmental restrictions on emitted EMI radiation have forced several manufacturers to stop shipment of products until corrective measures were taken. VDE or FCC restrictions on radiated interference from cables can easily be met with fiber optics. Applications for transmission between a data terminal and its keyboard, calculators to peripherals, CPUs and peripherals, and digital microwave radios to multiplexers are easily handled with fiber optics and there are no emissions from the interconnecting fiber optic cable. Other applications where no radiation is permissible would be in military applications for secure data or voice transmission.

Fiber optic cables have the advantage of a very large length bandwidth product. One factor is that the three dB bandwidth is inversely proportional to the length, whereas for wire the bandwidth is inversely proportional to the length squared. This is best illustrated by comparing a typical fiber optic cable with RG-58 coax. At 1,000 meters the coaxial cable has a three dB bandwidth of 300 KHz. For the optical fiber, the bandwidth is typically greater than 20 MHz.

Long distance, high-speed transmission without repeaters is then possible with fiber optics. This is very beneficial in the telephone industry where typical distances between central offices can be four to 10 km. Trends in computers are faster memories and CPUs communicating over distributed networks, which will require higher data rates and longer distances than are available now with wire.

Computer applications, now restricted to parallel data interchange due to limited cable bandwidth, can now be serialized and transmitted over a single optical fiber, eliminating a heavy, expensive multi-conductor cable.

FIBER OPTIC LIMITATIONS

Fiber optic data communications appear to have many of the problems of wire communication solved. Obviously, as in all technologies, there is some apprehension to switch unless all factors are known. There are limitations in fiber optics, and system designers should be aware of these limitations and make thoughtful and careful design trade-offs.

Most fiber used for data communication is about the size of a human hair. Any dirt obscuring the optical port would

be detrimental to the transmission path. Therefore, the optics of a system must be kept clean.

At this time there is little standardization; each manufacturer offers its own modules, cable or connectors. Few manufacturers offer a complete system. Most specialize in connectors or cables or modules and leave the fiber optic system design to the buyer. Depending on the manufacturers, fiber optic components may be specified with min/max values 0 to 70°C, or just typical specifications at room temperature. The system designers should be aware of all parameters and their effect on system performance.

Some fiber optic component designs may require special coding of the data signal due to the use of AC coupled receiver circuits, whereas some manufacturers offer DC coupled receivers or incorporate internal coding schemes to pass data with no restrictions in format.

Data networks such as loops or stars or multidrop implementations that are easy with wire are limited in fiber optics due to the losses of the network elements.

Mechanically, the fiber optic cables are strong for their weight. The area of concern, though, is the bend radius of the cable, the radius beyond which the glass fiber may break.

Safety considerations are another factor. The optical flux from most emitters is not harmful to the eyes of a person looking directly into it. However, this practice should not become a habit due to newer and more powerful emitters — such as lasers and high power operation in the infrared with no visible wavelengths present to warn the person.

Connecting fiber optic cables can be a tedious task. Manufacturers are now introducing kits for fiber optic connectors on cables in the field. Only with these kits will fiber optics be field-supportable and viable for production use.

THE DESIGNER'S CHOICE

The bottom line for fiber optics versus wire is usually cost, and high performance fiber optic systems have a high selling price. However, there are medium performance systems on the market and even all-plastic, low cost systems available for system designs which compete very favorably with wire technology. The future looks bright, too, for fiber costs are decreasing due to increased competition, quantity manufacturing and research into cost-effective production methods.

The hidden costs that often are incalculable in system design should be "factored in" also. These are the costs involved in making a system "work" if there are ground loop problems — if there is interference from a nearby transmitter, electrical machinery or even the soft drink dispensing machine in the next room. Fiber optics can solve systems problems right at the beginning or open up new capabilities. Fibers and wire both have a place in system designs and they will complement each other. The choice will depend on the systems designers and the particular application.



HP's Connector Assembly Tooling Kit Simplifies Connector Attachment to Fiber Optic Cables

Fiber optic systems have been used in the laboratory for many years as specialized communication systems in high voltage and electromagnetic studies. The inherent properties of a non-dielectric communications medium were quickly realized by the scientific community. Fiber optics in the lab had highly skilled personnel to prototype, calibrate, and maintain systems. Only with the advent of production fiber optic components that are easily incorporated in systems, low in cost, and maintainable, will fiber optics be in widespread use.

Many manufacturers are offering fiber optic modules, several cable vendors offer a wide variety of fiber cable designs, and connector manufacturers are attempting to standardize their products to the popular fiber sizes on the market.

Few manufacturers have addressed the installation and maintainability of fiber optic systems.

Hewlett-Packard has seen the need to provide their customers with the support required for field installation and maintenance of the Hewlett-Packard fiber optic systems. An HFBR-0100 Connector Assembly Tooling (CAT) kit is available now which provides all of the necessary tools, components, and detailed instructions for installing the precision Hewlett-Packard fiber optic connector on their optical glass cable. Connectors can now be field installed and have the same low loss as compared to production assembled connectors.

The CAT kit is offered as a convenience to customers, for most tools are available commercially and any specialty machined components are fully described with machine drawings in the User's Manual. The kit is contained in a molded case designed to survive even the roughest airline baggage handler. Hewlett-Packard has made the HFBR-0100 CAT kit available through distributors but has elected to drop ship all kits to minimize the problems with the limited shelf-life components of the kit.

The goals of the connector assembly project from the beginning were to support the line of fiber optic modules and connected cable.

The recent availability of 1000 metre transmitters necessitated the requirement for field repairable cable. Until this time any broken cable was returned to the factory and repaired. Now the case of a 1000 metre fiber optic cable installed in conduit and the cable breaks at the connector *must be considered*.

For customers installing their own cabling from bulk spools, connector kits are an essential part of the installation for most cables installed in conduit are "pulled in" unconnected.

The HFBR-0100 CAT kit project also spawned several other products, namely Hewlett-Packard is now selling its HFBR-4000 connectors as a separately available part and also HP is making its unconnected simplex and duplex cable available to the public.

The significant contribution to the market though is the User's Manual — a detailed picture guide giving step-by-step instructions for the first time user.

As written in the beginning general instructions, the first time user can expect to spend several hours assembling a fiber optic connector. While the manual was written to guide the user around the pitfalls, it seems inevitable that a few connectors will be ruined by mistakes or a misunderstanding. Therefore several extra connector parts have been included to account for the mistakes. An experienced user can expect to assemble a connector in twenty minutes which includes ten minutes of epoxy cure time.

The objective of the HFBR-0100 Connector Assembly Tooling kit was to provide a safe, easy to use kit for fiber optic connector assembly. Since the kit would be used anywhere in the world, all material for the assembly process would have to be provided and the kit had to be easily transportable and rugged for field service use.

Early investigations and field trials with numerous people of various backgrounds from secretaries to engineers brought out the fact that although the directions were clear, a person needed the manual dexterity and familiarity with common tools in order to assemble a connector with ease.

When the glass cable is assembled in the connectors, the glass fiber is staked in the metal ferrule with epoxy. Because only the tip of the ferrule need be filled with epoxy, a syringe and flat-tipped needle is used to inject the epoxy into the connector ferrule. Several complaints regarding the amount of preparation required to move the syringe plunger when filled with the highly viscous epoxy led to the design of a syringe vise for dispensing epoxy from the syringe. Since no manual syringe vises were found commercially, a machinist's vise was modified to provide a mechanical advantage when dispensing the epoxy.

During the early development steps of the CAT kit, fiber cleaving and fiber polishing, the two main types of fiber-end preparation, were tried. While the production fiber-end preparation is the polishing method, several factors such as no polishing and possibly no epoxy adhesive made the cleaving technique very attractive. Several Hewlett-Packard fiber optic connectors were modified so that a cleaved fiber could be aligned flush with the end of the ferrule tip, depending on how far the cable was screwed into the body. A portable fiber cleaving mechanism was also built for the field trials. The end results were disappointing, for while the connector assembly was relatively easy, the fiber alignment and cleave repeatability was poor with respect to the polishing technique. The insertion loss of connected fiber cables from the cleave trials varied with a σ of 2.0 dB whereas cables from the polishing technique had a σ of 0.5 dB.

Clearly, to obtain performance equal to production cables the polishing technique was preferred even though the assembly was slightly more involved.

The original plans called for a one hour cure from the epoxy staking the glass fiber. Although the time seemed slightly on the long side, it was generally thought that an hour was tolerable and even quite acceptable considering no heater for curing the epoxy would be required. The CAT kit, meant to be used anywhere in the world, would then require no outside sources of power. Once again the field trials made an abrupt change in plans.

Upon inspecting the finished fiber ends, many of the glass fibers had epoxy smears obstructing the optical path. This was caused by the polishing step being performed before the epoxy had cured. At first it was thought the assemblers were impatient and were polishing before the cure time was over. Questioning the assemblers though led to other areas of investigation. Several of the conference rooms which were used for the field trials tend to be cooler than the main building due to the small enclosed environment. After experimenting with the epoxy alone, a knee was found in the temperature versus time cure curve. The temperature of the conference rooms was just below the knee and a time of two to three hours would have been required to cure the epoxy.

A simple heater was then enlisted to insure a cure no matter what the condition of the environment. The side benefit of the heater is that now the cure time is only ten minutes due to the elevated temperatures involved.

It turns out that any source of low grade heat is quite acceptable for curing the epoxy, even that provided by a baby bottle warmer. The only requirement is that any moisture be kept away from the epoxy and that the cure not be in direct sunlight.

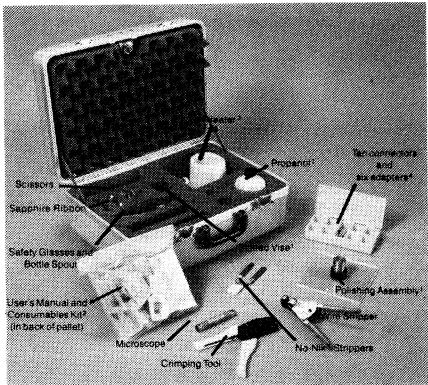
The Users Manual guides the assembler through three main areas; 1) cable preparation; 2) connector assembly and, 3) fiber polishing.

International symbols are used to guide or caution the assembler when working on various sections and photomicrographs in the fiber polishing section give the assembler a reference when inspecting the cables.

A sample page from each major section gives an indication of the detailed step-by-step procedure of the User's Manual. Note the full size metric gauge lengths supplied and the boxes for checking off each step.

The User's Manual is meant for the novice assembler of Hewlett-Packard fiber optic connectors. After several connectors are assembled one quickly becomes an expert at the assembly of fiber optic connectors.

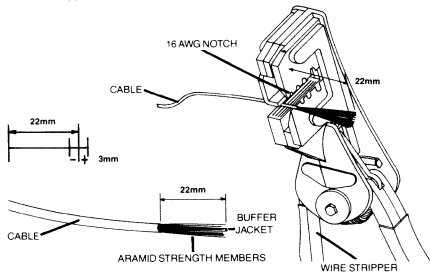
HEWLETT-PACKARD
HFBR-0100 Fiber Optic Connector Assembly Tooling Kit



1. Custom tools, available as HFBR-0102 (drawings for these parts appear in Appendix II).
2. Consumables Kit, containing sufficient materials for assembling 10 connectors, available as HFBR-0101.
3. Available in 110VAC (option 001) or 220VAC (option 2XX).
4. Individual, unassembled connectors, available as HFBR-4000 and adapter, HFBR-3099.
5. For a detailed description of the contents of this kit, refer to Appendix I.

PAGE 5

STEP 8 ☐ Remove 22mm of the outer jacket with the 16 AWG notch of the wire stripper. The cable end should now appear as shown below.

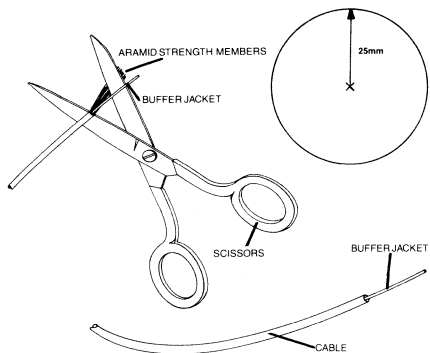


STEP 9 ☐ Carefully cut off all of the exposed aramid strength members with the scissors. The cable end should now appear as shown below.

CAUTION

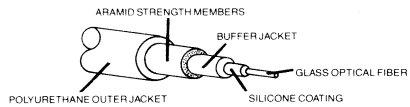


Do not cut or excessively bend the buffer jacket. (The minimum bend radius is 25mm.)

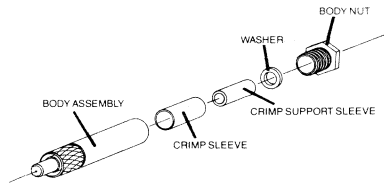


PAGE 10

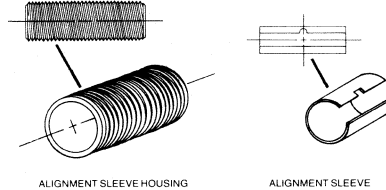
HEWLETT-PACKARD
HFBR-3000 THRU 3400 SERIES CABLE*



HEWLETT-PACKARD
HFBR-4000 CONNECTOR*



HEWLETT-PACKARD
HFBR-3099 ADAPTER*



*SEE DATA SHEETS FOR DETAILED SPECIFICATIONS.

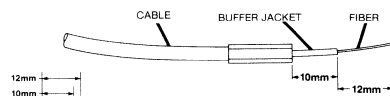
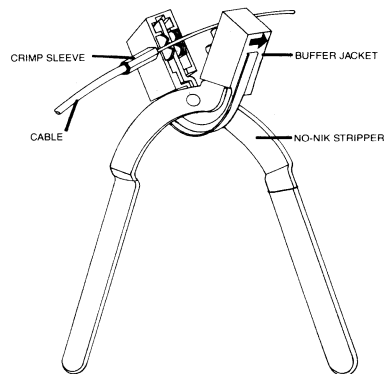
PAGE 4

STEP 18 ☐ Remove all but 10mm of the buffer jacket from the glass fiber with the No-Nik® strippers. To avoid breaking the fiber, point the arrow on the No-Nik® strippers toward the cable end and remove the buffer jacket in short sections, approximately 6mm long. Clear the No-Nik® stripper jaws of debris after each strip. The cable should appear as shown below.

CAUTION



THE FIBER CAN BREAK IF IT IS STRIPPED AGAINST THE DIRECTION OF THE ARROW ON THE NO-NIK STRIPPERS OR IF THE JAWS ARE NOT CLEANED OUT AFTER EACH STRIP TAKE CARE NOT TO VIOLATE THE MINIMUM BEND RADIUS OF 25mm.



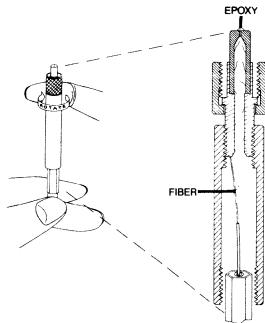
PAGE 16

CAUTION



Step 28 is critical. If not done properly, the glass fiber may break, making it necessary to start the procedure over again at step 1.

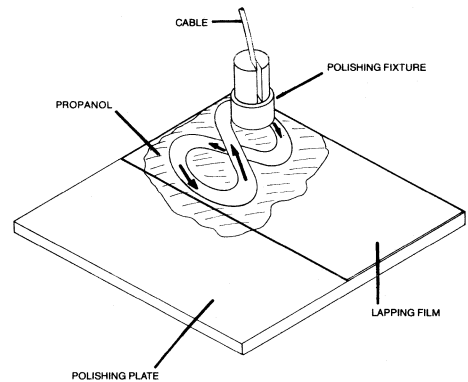
- STEP 28** □ While holding the cable vertically, carefully lower the epoxy-filled connector body onto the glass fiber. Ease the connector onto the fiber while slowly rotating the body with the index finger. This will allow the fiber to work its way into the ferrule through the epoxy. Allow only the connector's weight to apply pressure on the glass fiber. Avoid side or downward pressure when sliding the fiber through the epoxy. Continue until the glass fiber protrudes through the hole in the connector body ferrule tip. Some epoxy on the ferrule tip is allowable, but avoid getting the epoxy on the sides of the ferrule. Approximately 7 mm of glass fiber should protrude from the ferrule tip. If the connector feels springy before the glass fiber exits through the ferrule tip, the fiber may be blocked. If this occurs, remove the fiber and repeat this insertion procedure. If the fiber breaks during this procedure, prepare the cable end again starting at step 1, using a new connector body, as the semi-cured epoxy remaining in the used connector body will block the ferrule.



Fiber blocked by Ferrule — remove fiber and repeat insertion procedure

PAGE 22

- STEP 36** □ Hold only the polishing assembly and move the fixture in a figure-eight pattern on the lubricated lapping film for approximately 30 strokes. Try to use only half of the lapping film area for the initial polish in case a second polish is required. Add more propanol if the polishing fixture begins to stick to the lapping film. The propanol will aid in preventing metal particles from becoming imbedded in the fiber end.



PAGE 28

- STEP 42** □ Point the exposed fiber end opposite the connector being inspected at a bright light source. Inspect the back lit fiber end in the center of the ferrule tip.

If it is uniformly illuminated with a flat matte finish as in figure A, proceed to step 43. If any defects such as the following are observed, repeat steps 35 through 38 until they are polished away.

1. Chip-outs as in figure B
2. Scratches as in figure C
3. Imbedded metal particles as in figure D

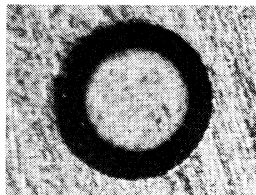


FIGURE A
ACCEPTABLE FLAT
MATTE FINISH
50X

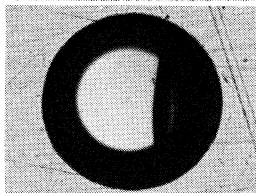


FIGURE B
CHIP OUT
50X

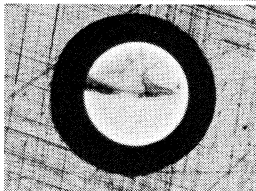


FIGURE C
CRACK
50X

PAGE 30



Design Considerations for Fiber Optic Data Communications Systems

INTRODUCTION

Fiber optics is an attractive choice for the transmission medium in local data communications (LDC) systems because of the benefits it offers:

1. Satisfies FCC/VDE requirements
2. High bandwidth — distance product
3. EMI/RFI immunity
4. No sparks
5. Satisfies Tempest and secure data requirements
6. Light weight and small size

In particular, the recently introduced FCC (Part 15) and VDE radiation requirements are often quite difficult to meet even with short wire cables, and the development and test effort required to meet the radiation requirements for all possible system configurations is normally substantial. Fiber optics not only eliminates radiation due to interconnects but also virtually eliminates the need for EMI testing beyond what is necessary for the individual pieces of computer and peripheral equipment.

Local data communications refer to communications within a building or between buildings on a common site. Data rates range from very low to up to hundreds of mega-Baud. The area covered is typically less than 2 km in diameter. Local Area Networks (LANs) are a subset of LDCs and are designed to interconnect a broad spectrum of data nodes, e.g. computers, terminals, mass storage devices, plotters, printers, and gateways to other networks within a restricted area.

TECHNOLOGY CHOICES

Figure 1 summarizes the attenuation versus bandwidth-distance parameters of available fibers and Figure 2 summarizes the fiber parameter options in the numerical aperture versus core diameter plane^[1]. The pros and cons of selecting fibers in the four corners of this plane are listed. Figure 3 shows the attenuation versus wavelength for glass fiber and which source and detector materials are used for different wavelengths^[2].

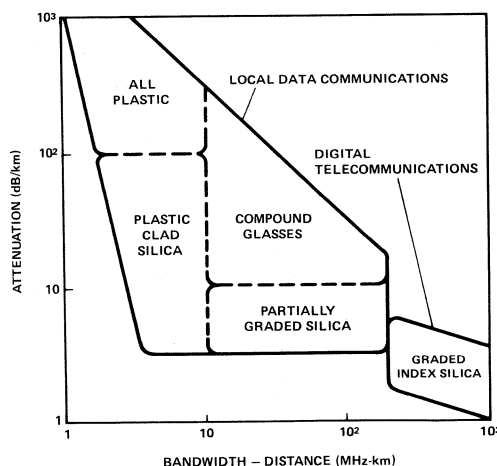


Figure 1. Fiber Transmission Parameters (at $\lambda_0 = 825$ nm)
vs. Technology Choices

SYSTEM REQUIREMENTS

The fiber technology choices have to be carefully considered in light of the systems requirements. To assure successful system performance, the designer must address the key issues of standardization, ease of implementation, reliability, servability, and cost.

Standardization is crucial in data communications because many types of equipment from different vendors are connected together. Certain fiber standards have been proposed or are in the process of being proposed. In the case of telecommunications, the standard fiber is 50/125 with numerical aperture of 0.22. Higher cost, greater precision

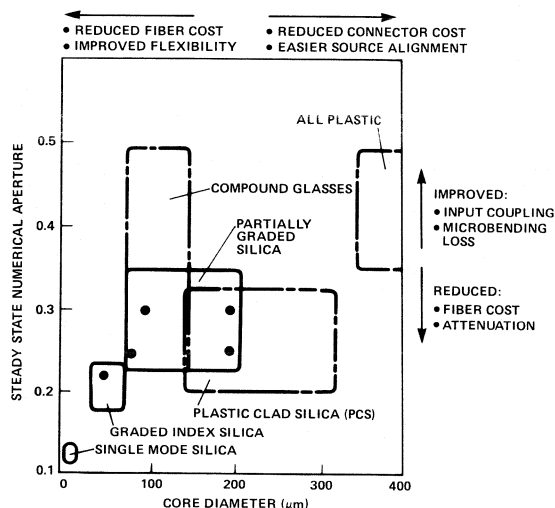


Figure 2

connectors are acceptable with this relatively small core fiber since fiber cost for long cable lengths between repeaters is reduced.

Because of the shorter link lengths involved in LDC, there is a desire to utilize lower cost, less precision connectors and larger area sources. As a result, the evolving standards have core area stepping by factors of four, i.e. core diameters increment from 50 to 100 to 200 μm . There is also interest in a 60 to 85 core/125 cladding fiber in order to use the same connector hardware as in telecommunications. For applications requiring less than 200 MHz-km, 100/140 is usually chosen because its large diameter results in improved coupling and its high N.A., 0.28, results both in improved coupling and reduced bending loss. However, there is a slight penalty of increased fiber cost and attenuation with increased N.A.

The significant attenuation windows for glass fiber are 820 nm, 1300 nm, and 1500 nm. Today, low cost 820 nm LEDs are available and are widely used in LDC. There is a trend to use 1300 nm LEDs for applications requiring data rates in the hundreds of megaBaud range and distances of a kilometer. LEDs are preferred over lasers because they have at least an order of magnitude higher lifetime and lower cost.

A tight tube cable structure is the best choice for office environments because it is crush, impact, and kink resistant. This construction consists of an optical fiber surrounded by a soft buffer coating (typically silicone) and an inner buffer jacket. Aramid strength members, typically Kevlar, surround the inner cable jacket and provide load bearing and impact protection. The outer jacket, typically made of polyurethane or PVC, provides abrasion resistance and structural rigidity.

All-plastic fiber with a 1 mm core is advantageous in applications requiring distances less than 50 m and rela-

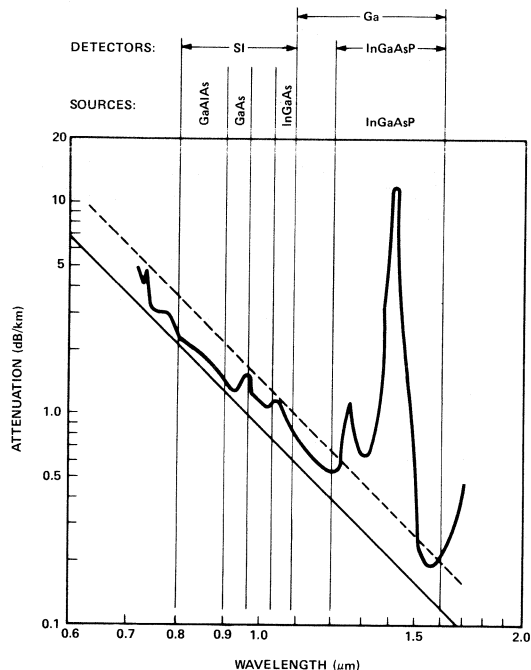


Figure 3

tively low data rates because it is less expensive, easier to connector, and more rugged than glass cable³.

The large core diameter and high N.A. of plastic fiber reduces the source coupling loss compared to other fiber types. However, this advantage is rapidly lost with increasing distance because of the much higher attenuation of the plastic fiber. See Figure 4⁴. The plastic fiber exhibits lowest attenuation in the visible wavelength region with significant windows around 650 nm and 570 nm.

Low cost sources emitting in the 650 nm wavelength region are available today. These sources are based on

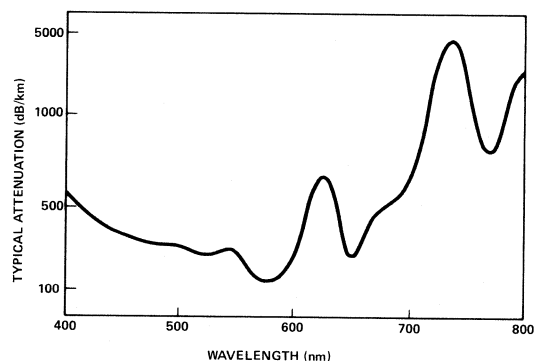


Figure 4. Plastic Fiber Attenuation

GaAsP technology. Monolithically integrated photodetectors in silicon are available which provide direct TTL interfacing with terminal equipment. The large core size allows moderate tolerance requirements on packaging and connectorization so low cost molded plastic parts can be used.

The emerging connector standards are not yet as clear as the fiber standards. Because of recent advances, the SMA connector (1/4-36 threads) has become cost efficient and is now widely used with glass cables. It appears it will become a standard.

An important unresolved standardization issue that affects ease of implementation is how the performance of the transmitters and receivers is specified. If only the transmitter output and the receiver input are specified, the designer must calculate the area, numerical aperture, and index grading mismatch losses plus alignment losses to determine the flux budget for the specific fiber used. On the other hand, when the transmitter output power is measured at the end of a meter of connected cladding-mode-stripped cable and the required receiver input is measured emerging from a connected cable, the flux budget is simply the difference in dB between the required receiver power and the transmitter power.

Component reliability is a key concern of a designer because down time, repair costs, and redundancy can significantly add to the total system cost. It is usually unacceptable for one or two component failures to bring the system down. Service cycles and replacement schedules can be determined from experimentally measured MTBF (Mean Time Between Failures). The failure rate of the system is:

$$\text{Failure Rate} = \sum \frac{1}{\text{MTBF}}$$

Figure 5 is a cross section of a package for LED based components that was designed to maximize active device reliability⁵. The package maximizes the electro-optical conversion efficiency (optical power launched into the fiber per milliamp of drive current). In the case of the transmitter, this efficiency allows the emitters to be driven at lower

current levels, which can be related directly to longer device life. In the receiver, this efficiency results in consistently higher sensitivity.

The key element of the package architecture is the precisely machined metal housing. It maintains the axial optical alignment of the emitter or detector and lens with the mating fiber and connector assembly. This architecture minimizes the accumulated assembly tolerances normally associated with the discretely packaged emitter and detector chips requiring intermediate hardware to ensure mechanical alignment with the terminated fiber. The resulting accurate and repeatable connecting results in a smaller portion of the receiver dynamic range required to be budgeted for coupling tolerances. This is especially important for high speed receivers which have a limited dynamic range. The initial design for the lensing geometry was optimized for maximum optical power coupling into a 100µm core fiber with an approximate numerical aperture of 0.28. The exact geometry was determined through the use of a computer ray tracing model.

The sapphire lens is suspended above the die surface by a stainless steel lens clip. This placement eliminates scratching and mechanical stress on die surface associated with designs that mount the lens directly on the emitter or detector. The lens clip also maintains accurate centering of the lens. The LED chip is then actively aligned. The header is positioned while the LED is turned on and the light out of a fiber stub is monitored. When the output is maximized, the header is epoxied to the housing. The epoxy contains an alumina compound which provides additional thermal mass behind the header. This lowers the overall thermal resistance of the package for increased heat dissipation.

The coupling efficiency was also enhanced by applying a conformal coating to the surfaces of the emitters and detectors which provides an intermediate refractive index that increases coupling between the die surfaces and the surrounding air.

Fiber optics is increasingly becoming cost competitive with wire. Figure 6 summarizes the results of comparing coax and fiber costs for different link lengths. As indicated

FIBER OPTIC
TECHNOLOGY

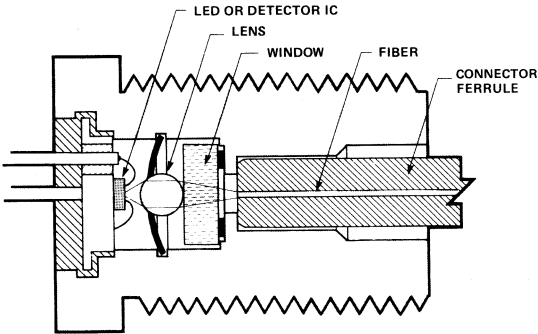


Figure 5. Miniature Fiber Optic Transmitter

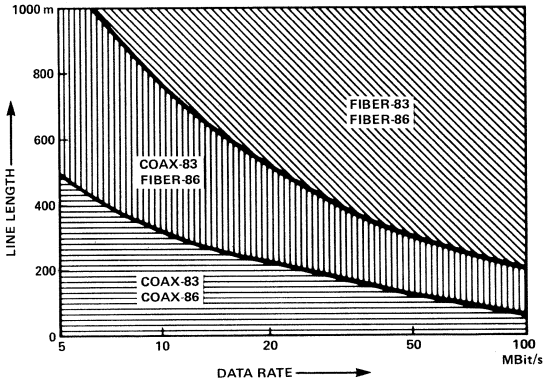


Figure 6. Application Areas for Fiber Optic and Coax Links

by this drawing, fiber optics is cost competitive with coax today in many local data communications applications³. Furthermore, this application area is rapidly expanding with the decreasing costs of fiber optic technology.

SUMMARY

This paper discussed the different design parameters, i.e. fiber material, size, and numerical aperture; cable configuration; source and detector type; and connector style, in terms of the requirements of system performance, i.e. standardization ease of implementation, reliability, serviceability, and cost.

REFERENCES

1. Hanson, Delon: *Fiber Optics in Local Area Network Applications*, Advances in Electronics and Electron Physics, Vol. 57, Academic Press, 1981.
2. Kao, Charles: *Optical Fiber Systems, Technology, Design and Applications*, pg. 12, McGraw-Hill, 1982.
3. Fredricsson, Staffan: *Fiber Optic Single Channel and Multichannel Communication Links*, IEEE Recent Developments in Fiber Optic Communication Systems, N.Y., May 12, 1983.
4. Mitsubishi Rayon Co., Ltd. Eska Extra, High Performance Plastic Optical Fiber. Technical Data 1983.
5. Bloom, Cynthia and Krusi-Thom, Douglas: *Package Design for Miniature Link Components*, Laser Focus, Dec. 1982.
6. Hewlett-Packard: Reliability Data HFBR-1201, HFBR-1202, September 1982.

General Concerns for LAN Fiber Optic Cable Installation

ABSTRACT

Within all local area networks (LAN) there is the requirement to install an interconnecting medium. Often overlooked, or given low emphasis, in network systems is what type of fiber optic cable to use, where to locate that cable, and how to install such a fiber optic cable. Brief discussion of different cable constructions is given with regard to the application requirement along with common connector styles which may be used. Most importantly, the main topic of concentration for this article is how to properly install a fiber optic cable for optimum results. Installation topics which are covered range from the stress limitations of a fiber optic cable, installing a cable with or without connectors, techniques to facilitate pulling a cable, support mechanisms for cable, configuration and redundancy concerns, confirming performance of cable and estimating the reliability of a cable after installation.

INTRODUCTION

An important component of a local area network (LAN) is the medium by which signals are conveyed. A critical, but often overlooked, phase of a successful LAN operation occurs during installation of the signalling medium. Whether this medium is twisted pair or coaxial wire or a fiber optic cable, important guidance and techniques should be followed in order to have a "first time" operation occur after installation. The subsequent topic areas will address the concerns of basic fiber optic cable characteristics, connector aspects, actual installation issues and techniques as well as the reliability of a fiber optic cable/cable installation. This discussion about proper fiber optic cable installation is mainly for data communication (<5 km) applications, rather than for telecommunication applications.

FIBER OPTIC CABLES

Of the glass fiber types of cables, there are basically two types of construction: tight tube construction, and loose tube construction. A third category which is actually a subset of the above is the multiple optical fiber cable.

As for tight tube construction, an optical fiber within a cable structure is tightly bounded by a buffer jacket,

typically Hytrel® (Dupont Chemical Corp.), which acts as a mechanical shock absorber for the fiber. Beyond this tight tube jacket are the strength members, typically Kelvar® material (Dupont Chemical Corp.), and outer environmental jacket which can vary in material from polyurethane to various PVC varieties. Figure 1A illustrates these generic styles of construction. Hewlett-Packard supplies tight tube style of cable. Common glass fiber

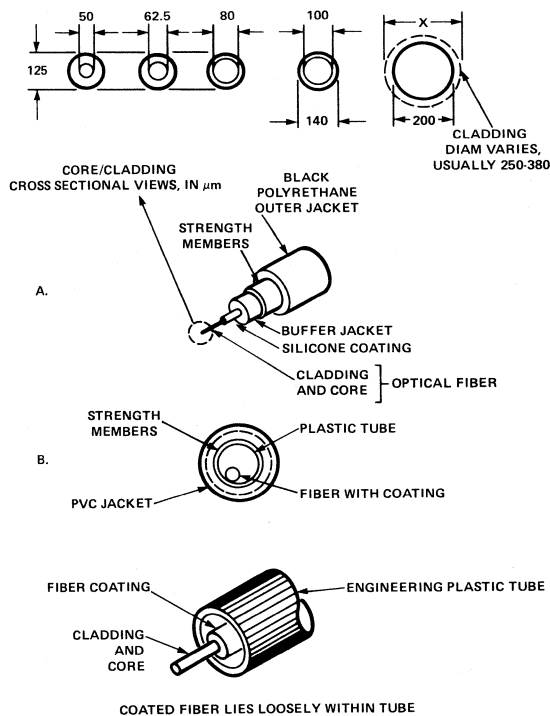


Figure 1. A. Tight tube fiber optic cable construction with corresponding core/cladding fiber sizes. B. Loose tube fiber optic cable construction.

sizes are found in this construction style, i.e., 50/125 μm , 100/140 μm , even 200 μm plastic clad silica (PCS) fiber. The basic advantage of tight tube construction is that the fiber is tightly supported by the buffer jacket to prevent microbending. Microbending promotes growth of microcracks on the fiber when significant temperature excursions occur. This support prevents more attenuation from occurring within the fiber as well as protects the fiber from long term catastrophic breakage, especially while under simultaneous mechanical stress (more about stress later). The only major disadvantage of tight tube construction is that the cable is not as capable of tolerating abuse during installation in comparison to loose tube construction. However, as will be seen later, proper care during installation of a fiber optic cable, whether it be tight or loose tube construction, should avoid any excessive abuse to the cable.

Loose tube construction has a large, hollow tube which allows the fiber to rest freely within that tube. Corresponding strength members and outer jacket are similar to the tight tube construction, see Figure 1B. More installation abuse can be permitted (≈ 500 lbs.) without passing the stress onto the internal fiber. However, the thermal coefficient of expansion difference between loose tube and fiber material promote microbending to occur over temperature extremes which jeopardies the reliability of the optical fiber.

Multiple optical fiber cable can incorporate both styles of construction. Basic advantage is that one cable supports all individual fibers. Disadvantage is that this style of assembly is not as mechanically flexible for convenient installation needs and that special multiple fiber optic connector must be used (expensive) or special arrangements need to be done for distribution of individual fiber connections.

Applications where fiber optic cables are used can vary widely from short to long distance needs. There are tradeoffs with regard to fiber size and their associated characteristics (numerical aperture, multimode graded fiber, attenuation/length, etc.) which influence the available choice and cost for fiber optic connectors (amount of precision needed). In selecting a fiber optic cable, many aspects need to be considered beside optical performance, because configuration and environmental factors must be considered too. Is the configuration going to be a point to point link, a multidrop link, a loop, will redundant cabling be needed, will the network be used for upgrade capability with better transmitters and receivers, all these factors need to be determined wisely beforehand. Whether the environment is going to be of a commercial application requiring less expensive cable, or an industrial environment where better cable performance is needed or a military environment where hermetic and radiation hardened fiber is needed with a tough protective jacket are all factors which influence cable selection and installation.

FIBER OPTIC CONNECTORS

Brief comments will be made at this point about fiber optic connectors because their selection may influence the ease by which a fiber optic cable is installed. There are different styles of detachable connectors. The common type of alignment is by use of a ferrule to hold and align the optical fiber which couples to another fiber (butt couple) or to an optical lense system (lense couple). This ferrule

style of connector provides reasonable loss ≈ 1 -1.5 dB, via a semi-precision connector, has moderately low cost, can be epoxy or epoxyless connector, and may be re-useable.

A common data comm fiber optic connector is the subminiature style A (SMA) version which uses a ferrule. This connector was modeled after the wire equivalent connector. Hewlett-Packard makes a ferrule style connector as well. Figure 2 shows a chart of part numbers for some of the possible vendors. These ferrule type of connectors require a mechanism by which the ferrule to ferrule aligns properly. Hence, only one hermaphroditic connector is used. There are other ferrule sizes for different fiber sizes and these connectors are constructed in plastic material as well.

Many various techniques of alignment are used in non-ferrule connectors ranging from multiple pin or rod alignment to V groove techniques. Tradeoffs with these styles range with regard to their precision for low loss to ease of manufacture and cost.

The basic concern with connectors during installation of a fiber optic cable is that a tension, or stress, not be transmitted from the cable to the fiber at or near the connector. If the connector is an epoxy style of connector, then it is possible to misapply a tension from the cable to the fiber and cause the fiber to kink or snap in the neighborhood of the connector. If the connector is epoxyless, it is possible for the same phenomenon to happen, or the fiber may experience some movement or pistoning of the fiber in the ferrule. A situation similar to pistoning which occurs due to temperature excursions placed upon the connector. If no breakage occurs, but pistoning does, optical loss in the connector can be increased with potential degradation of optical link performance.

A secondary aspect with respect to installation of cable with connectors already installed is that the outside diameter of the connector will dictate how many connectors may be pulled together through a conduct or duct at one time.

RELIABILITY OF FIBER AND CABLE INSTALLATION

Prior discussion about cable construction and of connectors leads one to wonder how can a fiber optic cable fail. What are the mechanisms which promote failure and how best to reduce or eliminate them, especially during the installation of a cable.

The major factor which causes a fiber within a cable to fail is the STATIC stress that is applied to it. Flexing, or dynamic stress, is not a problem to a fiber because, essentially, glass is a very viscous liquid, not a solid. Again, excessive, long term static stress is the killer of glass fiber.

FIBER SIZE	XX/125		100/140		200PCS	
	HP	SMA	HP	SMA	HP	SMA
VENDOR						
HP	—	—	HFBR-4000	HFBR-4001	—	—
PALO ALTO, CA						
AMPHENOL	906-120-5001	906-110-5017	906-120-5000	906-110-5018	906-120-5002	906-113-5003
OAK BROOK, ILL.					250 μm O.D.	250 μm O.D.
OFTI	—	252-S-RB-1	—	255-S-RB-1	—	2010-S-RB-1
BILLERICA, MASS.						250 μm O.D.

OFTI - OPTICAL FIBERS TECHNOLOGY INC.
CONNECTORS LISTED ARE FOR TIGHT TUBE CABLE CONSTRUCTION AS ILLUSTRATED IN EARLIER FIGURE.

Figure 2. Commercially available connectors for XX/125 μm , 100/140 μm glass and 200 μm plastic clad silica fibers.

The form in which the static stress can exist is either through a tension force in the glass fiber causing a distortion to the length of the fiber, or via a bending of the fiber which produces a radial distortion to the fiber. Where and how long the stress is applied will definitely influence the longevity of the fiber. The effect of static stress is to promote microcracks to propagate which result in more attenuation or eventual outright failure of the fiber. Hence, during installation as well as afterwards, locations which will produce the most tension or bending will affect stress levels and stress time must be controlled. As a result, the overall fiber optic cable will have a specification for maximum applied tension (pull force) allowed as well as the minimum bending radius permitted. As a numerical example, pure glass has a maximum stress level of approximately 800 kpsi, for Hewlett-Packard 100/140 μm glass cable at 1% distortion would correspond to 100 kpsi proof test, which would require that the pull force be limited to 135 lbs. (dual fiber cable), or if no tension exists, the minimum bend radius be 20 mm.

When both stresses are present, tension and bending, the total stress is the sum of the two stresses as illustrated in Figure 3.

Proof testing must be done over the full length of the fiber in order to ensure that the fiber is of sufficient quality that it can withstand the applied tension and bending expressed upon that cable. Since the microcracks are located randomly along the fiber, the worse case testing must allow for these microcracks to be located everywhere and that the probability of the stress being applied at exactly a microcrack is equal to one. A proof test applies a static proof stress, S_O , (tension and bending) for a specific test time t_O .

For Hewlett-Packard fiber (100/140 μm), as an example, an empirical relationship exists between absolute minimum operating lifetime (t_{\min}) and applied stress (S) to proof test stress (S_O) and test time (t_O) i.e.,

$$t_{\min} \geq t_O \left(\frac{S}{S_O} \right)^{-18} \tag{1}$$

This equation can be re-expressed in terms of parameters which are more conveniently measurable, i.e.,

$$t_{\min} \geq t_{DS} \left(\frac{F}{F_{DS}} + \frac{r_{DS}}{r} \right)^{-18} \tag{2}$$

Where t_{DS} , F_{DS} , r_{DS} are the allowable application time (t_{DS}) for the maximum pull force (F_{DS}) and minimum bend

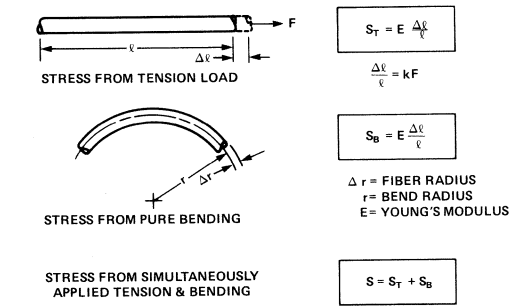


Figure 3. Tension and bending stress applied to an optical fiber.

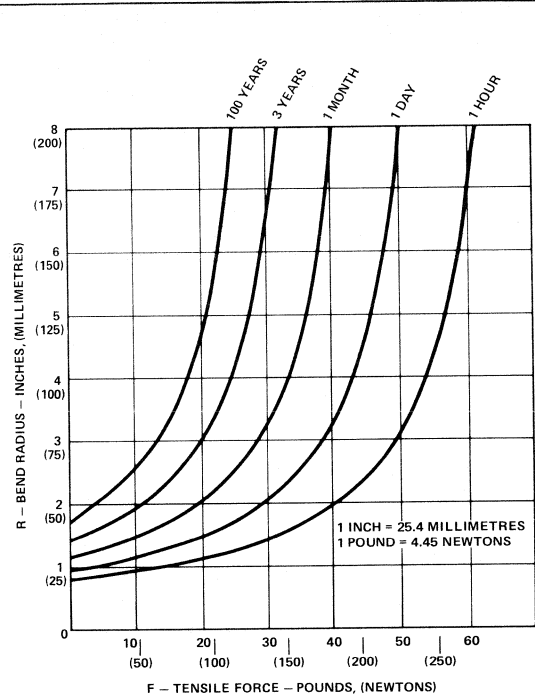


Figure 4. Minimum operating life versus cable bend radius and tensile force for HFBR-3000 series fiber optic cable.

radius (r_{DS}) from the cable data sheet. F and r are actual applied tension and bend radius experienced. Figure 4 graphically illustrates the combination of tension plus bending stress versus minimum operating lifetime for HP fiber. If a fiber is needed which must tolerate more stress at a given tension and bending, then a purer glass fiber should be found which has a more negative exponent than that given in equations (1) and (2). When comparing fiber of different manufacturers the test stress level and duration must be compared simultaneously to ensure a correct comparison.

CABLE INSTALLATION

Properly installed fiber optic cable will serve well the system equipment requirement. The key word is "properly" installed cable for optimum results. The details of how to properly install a fiber optic cable will now be examined.

The first place to begin is to select the "best" layout which can be used for the cable network being installed. Scale a layout drawing in order to plan the efficient use of the available conduits or ducts that will be used or needed. If a choice of configuration arrangement is possible, the scaled drawing will help optimize the interconnection of the network.

Secondly, the actual installation of the cable can be done with or without connectors. If the choice is possible and experimentation with attaching connectors is not preferred, then order fiber optic cable with connectors factory assembled on the cable. Guaranteed performance is then assured initially.

To install cable with connectors attached, a commercial pulling grip (such as a Kellems grip) can be obtained which will house the connectors. The pulling grip has a wire mesh after the pulling head which frictionally grips the fiber optic cable beyond the connectors in order to transfer the pulling force to the cable strength members. The nose of the grip (a hollow tube) has a ball bearing swivel to prevent the cable(s) from becoming twisted helically as it is pulled. Depending upon the size of the cable and connector an appropriate pulling grip can be obtained. A five inch long, 7/8 inch diameter pull head can house four HP connectors and be pulled through standard 20" radius conduits.

If a cable is to be installed without attached connectors, the cable can be stripped back to expose the strength members. These members can be directly attached to a swivel which, in turn, ties to the pull rope. If multiple cables are being pulled at once, all strength members can be attached to that swivel. Use a braided pull rope to avoid any helical action. An 1/8 inch diameter pull rope should be pulled by installers with no gloves for installation of HP fiber optic cable.

If the threshold of pain is quite high with a particular installer, provide a short "fishing line" leader in series with the pull rope which has a known and proper "pound" test limit.

Before pulling a cable through a conduit, an estimate of the total pulling force needed can be done with respect to either pull end of the conduit. This allows a simple initial choice on which end to begin pulling in order to help keep the stress lower.

A brief discussion is needed about frictional pull effects before performing an actual calculation of the total pull force. For straight pull through ducts the pull force (F_P) is given by equation (3).

$$F_P = F_D + \mu WL \quad (3)$$

Where F_D = drag force (retarding force prior to entering conduit)

W = weight/unit length of cable

L = length of straight duct

μ = coefficient of friction cable/duct boundary

Notice that this pull force is purely additive. To measure coefficient of friction, μ , place a sample of cable in a conduit, the bends multiply the incoming drag force to that can be tilted. Tilt the conduit with respect to the horizontal until the sample cable begins to slide. Record the tilt angle between the horizontal and tilted conduit. Take the tangent of that angle and it will be a very close approximation for μ value.

As for bends which are incurred by the cable in the conduit, the bends multiply the incoming drag force to that bend by the factor given in equation (4).

$$F_P = F_D e^{\mu \theta} \quad (4)$$

Where θ equals angle of the bend. If $\mu = 0.58$, then a 45° bend is 1.6 times the incoming drag force and if the bend is 90° then the factor is 2.5.

Now, to estimate a pull force, an example with a set of given conditions is shown in detail in Figure 5. If the additive and multiplicative factors are applied as the cable is pulled from left to right through the conduit, example shown in the upper left corner of Figure 5, the pull force is

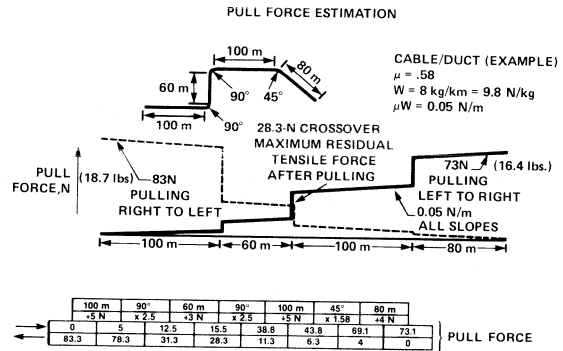


Figure 5. Graphical estimation of pull force for a given conduit layout.

73.1 N. If cable was pulled right to left, the pull force is 83 N. Just by starting on the right side and pulling to the right, a savings in stress to the cable can be achieved. However, if the cable had to be removed at a later time, the removing pull force would be larger. It would be nice to have nearly equal forces in both directions. The point to learn from this is that the bends, which will be incurred during pulling the cable, should occur early, then mostly straight pulling afterwards will allow a net lower pull force on the cable.

As a last calculation, the residual tension in the cable residing inside the conduit can be determined by finding the cross over point for the graphically plotted pull forces as shown in Figure 5 (when calculating for both directions). In this example, the cross over point was 28.3 N. This amount is the tension remaining within the cable after all pulling has ceased. This comes about because the conduit bends and friction of cable/conduit surface do not allow cable to fully relax to zero tension. Hence, this residual tension value at the corresponding bend location (or applied bend radius) will allow a calculation of minimum operating lifetime of the fiber optic cable by using this data and the data of Figure 4. Equation (2) can be used instead of Figure 4 if desired. All of these estimates allow one to wisely pull cable and predict cable operating life.

For installation of cable over spans with supports which are of a radius below the recommended minimum bend radius for the fiber optic cable, the following can be done. Two conditions can occur with a span installation as illustrated in Figure 6. One condition is that a certain span (D) with small sag (C) are required. This condition places the cable under a tension-limited condition. If the opposite case were to apply, the same span (D) can be done with a large sag (C), the cable would be under a bend-radius-limited condition. Data taken for both conditions for the Hewlett-Packard HFBR-3000 fiber optic cable is graphed in Figure 6. The optimum condition for span and sag is shown as a negative sloping straight line through the peaks of each curve. The weight and rigidity of the cable shape this family of curves which are shown. A good rule of thumb for HP cable is that a span of ≤ 24 m is wise for 100 year operating life and that a sag of approximately 100 mm (4 inches) should be used regardless of the span length.

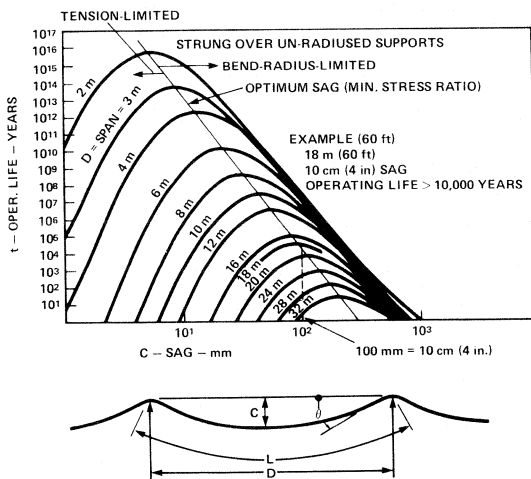


Figure 6. Minimum operating lifetime versus span and sag of HFBR-3000 series fiber optic cable.

AIDS TO CABLE INSTALLATION

A number of suggestions will follow which assist in promoting proper installation techniques.

One of the simplest ways to facilitate an installation of fiber optic cable is to place junction boxes at strategic intervals along the route the cable will follow. These junction boxes provide advantages by allowing the cable to be pulled through short segments of conduit, to allow reduced residual tension within the cable after installation, and to allow easy access to slack cable for equipment movement or repair of cable in the future. When using junction boxes, cable should be pulled without sharp edges of the box damaging the cable. One technique is to install a simple, single pulley in the junction box which forces a proper and constant bend radius on the cable as the cable is pulled out of or into the box. The common electrical junction boxes (5" x 5") allow storage of HP cable in a 100 mm (4 in.) diameter coil for >100 year life. Storage of cable at as large a diameter as possible will reduce significantly the bending stress and add dramatically to the operating life of the cable as Figure 4 indicates. A radius of 76 mm (3 in.) with 90 N (20 lbs.) yields 3 years operating cable life. Change the radius to 194 mm (4.5 in.) with same tension and minimum operating life of cable becomes 100 years, a factor x 33.3 time improvement!

If installation of cable needs to be underground, a conduit should be used. For example, direct burial of Hewlett-Packard fiber optic cable is not recommended. A conduit provides moisture protection, rodent protection as well as some margin of preventing physical damage that could occur when repairs are excavating in the area.

Installing multiple cables at once is wise to do whether there is a need for all cables or just that an extra cable be installed for redundancy or future expansion of a system. Installation cost of installing one cable or many cables at once is nearly equal. A good rule of thumb for estimating the amount of unconnected fiber optic cables (N) which can be pulled into a conduit is given by equation (5).

$$N \approx 0.5 \left(\frac{\text{inside duct diameter}}{\text{outside F.O. cable diameter}} \right)^2 \quad (5)$$

Additional help in installing cables in difficult conduits may be accomplished by use of lubricants. Generally, lubricants can be of help in long distance, linear pulls of cable, but if many bends are experienced during the pulling of cable, lubricants usually provide little, if no, help. A lubricant is of no assistance if it does not reach the area of constriction or bind. A number of ways are available for putting lubricants on a cable: "paint" onto cable, blow into a conduit, attach a lubricant bag to a pull rope for expected breakage of the bag at the point of constriction, etc. Suggested lubricants used in the cabling industry are "Polywater"® (American Polywater Co.) and "Moon grease" (Ideal 77®, Ideal Co.). The basic point about lubricants is that one should not expect miracles from their use.

When installing cable into conduits, excess cable which is not on a take-up reel may need to be stored on a floor or ground as this cable is passed through a conduit system. In order to prevent the cable from twisting, or curling, as it is temporary laid aside, the cable should be laid in a figure eight pattern. This greatly eliminates curling-twisting action from occurring to the fiber optic cable. This technique is sometimes referred to as "faking" the cable.

Always insure that installers observe the maximum pull force and minimum bend radius of the cable during installation. If pulling is done by hand, don't use gloves, monitor actual pull force by a gauge device.

TROUBLESHOOTING A CABLE INSTALLATION

Sometimes it is necessary to troubleshoot a cable installation after the work was "completed". Unfortunately, not all precautions may have been followed and a search must ensue as to where the trouble spot lies. One way to assist in determining if a fiber optic cable is good is to perform a simple initial optical measurement on the cable prior to actual installation. If connectors are already installed, connect the transmitter and measure the optical power at the opposite end of the cable. This calibrates the cable for a remeasurement after cable installation to provide a confirmation that cable performance is what it should be. Simple portable power meters are available from Photodyne (XE-11 model) for example. If no connectors are available, a simple gross optical check can be done prior and after installation by shining light from a light bulb or flashlight into the fiber and observing light existing from the fiber at the other end of the cable.

If a cable was broken during installation the following things should be looked for to identify the fault.

Under certain circumstances when fiber optic cable is installed with connectors attached and proper pulling of cable was not done, the break generally occurs near the connector end which experienced the pulling action. Fortunately, this location is usually accessible and a section of cable can be cut back a few metres to remove the broken cable and associated connector. This happens because the rigidly held fiber in an epoxy connector is kinked by a pull force. The pull force was not frictionally coupled well enough to the cable and allowed motion of the fiber to occur.

Also, examine any areas of stress to the cable in the form of sharp corners exceeding minimum bend radius, or chafed jacket of cable, kinked cable, etc.

Look for structure damage or change to conduit or duct locations where cable is housed.

If accessibility to the installed cable is difficult and the cable is long, an optical time domain reflectometer (OTDR) can be used to locate a fault within 2 metres out of 2 km. OTDR performance is conceptually similar to wire TDRs. Tektronix, Photodyne, Orionics, etc. all make these devices which are generally quite expensive.

When no convenient technique can be used to find the problem, sometimes an educated guess has to be made and a portion of the cable must be cut (half way point?) with removal of the damaged portion. Last resort is to replace the whole fiber optic cable.

RELIABILITY ENHANCEMENTS FOR CABLE INSTALLATION

Some basic comments on reducing the possibility of failure can be mentioned. Most obvious is to reduce the residual static stress within the cable, i.e., reduce tension force to as low a level as possible and to store fiber optic cable in as large a radius as physically possible (> 100 mm, 4 in. diameter). Avoid constant moisture or soak conditions occurring to the cable, unless such cable is designed for those conditions.

Select a fiber optic cable which is best designed for a specific application. Which conditions are important can vary, but some examples are listed for interest. Within an office environment, a flame retardant cable or plenum acceptable cable, may be needed. For outdoor applications where interconnection of a network between buildings requires a cable which can tolerate weathering abuse from sun radiation, temperature extremes, ice loading, moisture etc. should be sought. For military applications, radiation hardened fiber may be needed as well as tolerance to harsh physical conditions. Within the oil exploration industry, high temperature, pressure, moisture fiber optic cable is needed in that application.

Best protection during and after cable installation is to provide additional cable for relocation of equipment or repair. Provide a redundant cable that will allow quick service for cable substitution in order to prevent system "down-time" problems.

SUMMARY AND CONCLUSIONS

Fiber optic communication links fulfill well local area network needs. Initial success of operation of a network relies not only upon the electrical/optical performance, but also upon the care which was taken during cable installation. Proper choice of a fiber optic cable for the specific application must be selected. Types of common connectors were reviewed for data communication applications, but no standardized connector has been accepted to date.

Understanding of the stress mechanisms (tension and bending) that a fiber can undergo and how to reduce or eliminate those influences to extend the operating lifetime of a fiber were reviewed. Supportive characteristic data on Hewlett-Packard cable was given. Some often overlooked but common concerns of cable installation were highlighted to help promote easier and more reliable installation. Troubleshooting suggestions were made with regard to potential problems that may occur. The fiber optic cable industry is really no different that the wire cable industry with respect to installation concerns. In fact, quality fiber optic cables provide easier installation than wire cable because of smaller weight per unit length and smaller bend radius permitted. As the natural resources for metals become scarce, glass fiber optic cable will become more plentiful and less expensive which will result in overall lower cable and installation cost.

ACKNOWLEDGEMENTS

For assistance with respects to research, testing and reviewing of this paper, my appreciation is given to Hans Sørensen of Hewlett-Packard Optical Communication Division.

REFERENCE

1. Application Staff, Optical Communication Application Seminar Follow Along Booklet, Hewlett-Packard Company, Palo Alto, CA April 1984, section 2E.



Use of Standard Modulation Codes for Fiber Optic Link Optimization

SUMMARY

A modulation code is the rule by which serial binary data (ones and zeroes) are converted to a signal suitable for transmission. There is a variety of codes in current usage and for some of these there is a sufficiently broad understanding of their rules that they have a status as de-facto standards. For others there remains a good deal of variability in nomenclature and definition. One purpose of this paper is to describe what, in the author's opinion, represents a consensus on nomenclature and definition. Because of their special properties relative to fiber optic link application, emphasis is given to MILLER and MFM codes. The main purpose of the paper is to describe how code selection can optimize data rate (bits per second) while not necessarily optimizing symbol rate (symbols per second, or baud). In conclusion a description is made of specific results obtained using the MFM code.

CODE DESCRIPTIONS

In the usual sense of the term "standard" there exists a document describing certain broadly supported definitions. For modulation codes there is no single document collecting and describing all the codes in current usage. Individual code descriptions appear in some of the literature^[1, 2, 3] but there is sometimes disagreement in terminology, nomenclature, and definition.

Figure 1 summarizes a few of the more popular codes and their properties, relative to a stream of serial data shown in the top row. In binary signaling, a "symbol" is a signal level (low or high) that is held for a length of time (symbol width or symbol time). The capacity of a channel for signaling is its symbol rate (inverse of symbol time) in symbols per second or baud. Note that the often-heard expression "baud rate" is no more correct when describing binary channel capacity than would be the never-heard "hertz rate" when describing bandwidth. Binary channel capacity or symbol rate has the units symbols per second or baud; analog bandwidth has the units cycles per second or hertz. There are some modulation codes requiring several "symbols" to define a "bit"; these are used in error-detection or error-correction applications and are not con-

sidered in this paper. Some of the codes in Figure 1 have two symbols per bit, for purposes of self-clocking, power conservation, or, in the case of MFM, reducing the effects of distortion in transmission. The descriptions given in order of their appearance in Figure 1, represent what seems to be most widely accepted. The first three are not self-clocking because there may be indefinite periods without timing edges.

NRZ is a level-type code, and is perhaps the one most widely known and used for serialized data. A "zero" is a low level and a "one" is a high level that does not return to zero between successive "ones", hence the name non-return to zero (NRZ). Note that inversion of the signal changes all "one" to "zeroes" and vice versa, so it is not invertible.

RZ is an impulse-type code in which "ones" are represented by a high level that returns to zero between successive "ones". Consequently, it requires a channel capable of signaling two symbols (high and low) per bit. Its main advantage is in power conservation, since energy is required only for transmitting "ones". Invertibility is not an issue.

NRZI is an edge-type code in which a "zero" is represented by an edge while "one" is represented by no-edge. Since the edges may be either rising or falling, inversion of the signal does not change the sense of the code and it is therefore invertible.

BIPHASE-MARK is an edge-type code requiring a channel capability of two symbols per bit. Each bit cell begins with an edge; then, for a "one", an additional edge occurs during the bit cell while for a "zero" there is no edge during the bit cell. Because there is always an edge at the beginning of the bit cell, clock recovery from this code is possible by either phase-lock or one-shot techniques. There is no rule for polarities of the edges, so the signal may be inverted without changing the sense of what is encoded.

BIPHASE-SPACE is also an edge-type, invertible, self-clocking code, differing from BIPHASE-MARK only in that

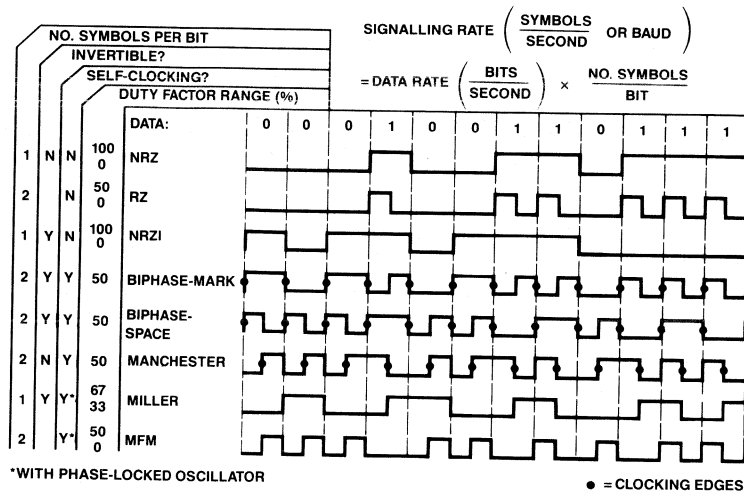


Figure 1. Modulation Code Descriptions

"zeroes" (rather than "ones") have the additional edge during the bit cell. Both BIPHASE codes are sometimes called "f/2f" because the additional mid-cell edge may be regarded as a cycle of a frequency which is twice that for the absence of the mid-cell edge.

MANCHESTER is a level-type code in which a "one" has a high level at the beginning of the bit cell with high-to-low transition at mid-cell, while a "zero" starts at a low level with low-to-high transition at mid-cell. This code also requires a channel capability of two symbols per bit. Because there is a mid-cell transition in each bit, clock recovery is possible by either phase-lock or one-shot techniques. Although the coded signal resembles BIPHASE, the MANCHESTER code is not invertible because of the polarity rules on levels and transitions. A variety of nomenclature (e.g. "Bi-Phase-Level"[1]) and rules exists for this type of code, some of which have opposite polarity.

MILLER is an edge-type code often called "delay modulation"[1]. Each "one" in the serial data is encoded as a mid-cell edge. The "zeroes" either have no edge (following a "one") or are encoded as edges at the beginning of the bit cell. In this manner the encoded data have edges occurring at intervals of 1.0, 1.5, or 2.0 bit times. Because there are no edges occurring at intervals less than one bit time the channel capability required is only one symbol per bit. With edges occurring regularly at integral multiples of half a bit time, clock recovery is possible with a phase-locked oscillator running at a frequency which is twice the data rate. There can be no more than four cycles of this oscillator without a phase-locking edge because edges occur at no more than two bit times. With a data sequence 110110 repeated, the duty factor is either 33% or 67% but with pseudo-random data and in most actual situations the duty factor is very close to 50%.

MFM is an impulse-type code similar to MILLER in that impulses occur at intervals of 1.0, 1.5, or 2.0 bit times. For this reason, clock recovery is possible. Because of the impulse nature, the channel capability required is two symbols per bit. With impulse duration much less than a bit time, duty factor approaches zero, but cannot exceed 50%. These properties provide some distinct advantages in the design of some types of fiber optic links. The name MFM (Modified Frequency Modulation) comes from its similarity to MILLER, which is also sometimes called MFM[2, 3].

FIBER OPTIC LINK OPTIMIZATION

Fiber optic link optimization deals with maximizing the data rate and the dynamic range. In most low cost links the data rates are limited by the transmitter and receiver circuits. Their limitations are in the form of either bandwidth or distortion or both. Distortion is here defined as the difference between propagation delays for rising and falling edges.

Situations in which the limitation is mainly bandwidth (i.e. very little distortion) are found in links having ac coupled amplification in the receiver so the threshold (slicing level) is close to halfway between positive and negative excursions. These situations would benefit mainly from use of the MILLER code because it employs the channel capability most efficiently. As seen in the lower portion of Figure 2, a MILLER-coded signal is easily generated from a MANCHESTER signal by having each falling edge of the MANCHESTER toggle a divide-by-two flip-flop. Decoding is a little trickier, but is similar to that employed for MFM, and is described later.

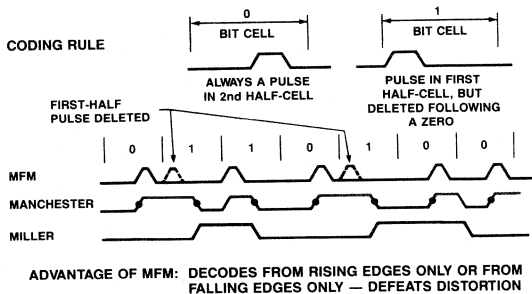


Figure 2. MILLER and MFM Codes Related to MANCHESTER

Distortion has adverse effects on both data rate and dynamic range. Dynamic range is the ratio (usually in dB) of the maximum to the minimum power to the receiver within which range satisfactory performance is obtained. At any given power level the signaling rate is limited by distortion to the minimum symbol time that allows adequate margin for decoding. The usual rule is that minimum symbol time must be four times the distortion. In many types of fiber optic links distortion varies as the receiver input signal power varies — usually increasing with increase in power. In this way distortion limits the dynamic range at a particular data rate.

With MFM coding, distortion problems are greatly reduced because the decoder operates from only rising edges or only falling edges. The only limit is that the distorted (widened) impulse must not be so large as to encroach on a following pulse. In the MFM waveform of Figure 2 it is clear that the minimum pulse interval is a full bit time. This waveform, when compared with the MANCHESTER waveform shows how MFM is easily generated by producing an impulse at each rise of the MANCHESTER coded data.

Decoding of either MFM or MILLER can be done as shown in Figure 3. Only the MFM receiver output is shown; if MILLER code is employed it must be in a link having sufficiently small distortion that the pulses from the "either-edge" sensor (waveform S) are close enough to the desired interval spacing (1.0, 1.5, 2.0 bit times) that decoding is possible. As an absolute limit the timing spread must be less than a half bit time, but as a practical matter it should be less than a quarter bit time. The phase-locked oscillator is synchronized with the "S" pulses and its output is applied to a divide-by-two counter which is the decoding clock. The clock will have proper frequency but might start up in the wrong phase. Clock phase correction is done by a 2-bit counter that is reset each time an "S" pulse occurs. If the time between pulses extends beyond 1.5 bit times the counter sets the clock phase, based on the fact that occurrence of an "S" pulse after an interval of 2.0 bit times is associated with a particular edge of the transmitter clock. Only those "S" pulses that occur when the decode clock is high can toggle the decoder flip-flop (No. 2). At the next fall of the clock, the state of the decoder flip-flop is transferred to the output flip-flop (No. 3) to yield clock-synchronized NRZ serial data.

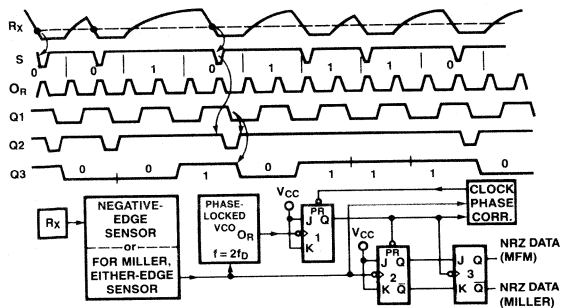


Figure 3. MILLER or MFM Demodulation

ANALYSIS OF BENEFIT FROM MFM

To show the potential improvement in data rate that can be obtained from use of MFM code, a timing analysis is made. For the comparative analysis, BIPHASE (or MANCHESTER) code is used because, like MFM, it requires a channel capability of two symbols per bit. For decoding BIPHASE, the decoding clock edge must occur at a time when the distorted received signal is at proper level, as seen in Figure 4. Applying the rule that minimum symbol time must be four times the distortion leads to the result that if the distortion is 50 ns then the margin for clocking is 75 ns and maximum data rate is 2.5 Mb/s.

With MFM, the margin requirement is not two-sided as it is for BIPHASE; as mentioned earlier it is only necessary that any given pulse not encroach on the next pulse, which may follow in as little as 1.0 bit times. For the analysis in Figure 5 there is application of the same values of distortion (50 ns) and margin (75 ns) as were applied in the BIPHASE analysis of Figure 4. Then applying the limit that pulse width is a half bit time leads to the result that the minimum bit time is twice the sum of distortion plus margin, or 250 ns for a data rate 4.0 Mb/s, which is clearly better than the 2.5 Mb/s obtained using BIPHASE. The pulse width may be much shorter than a half bit time, however, and in Figure 5 a pulse width of 50 ns was applied, leading to the 5.7 Mb/s shown.

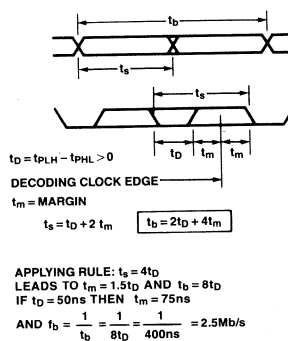


Figure 4. Timing Analysis of Distortion in BIPHASE

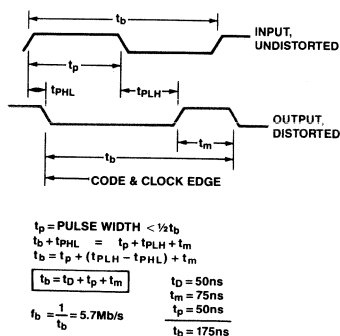


Figure 5. Timing Analysis of Distortion in MFM

ACTUAL RESULTS

To establish validity of the advantages of MFM coding, a system was constructed for serial transmission of multiplexed 16-bit words. A block diagram of the system is shown in Figure 6. Synchronizing pulses for the demultiplexer were obtained by generating a code violation in the MFM modulator. This violation consisted of an interval of 3.0 bit times between pulses, formed by deleting the two middle pulses from a four-zero sequence. Thus a multiplexing "overhead" of four bits was added; i.e., to send 16 bits required 20 bit times.

Pulse widths of 10 ns were used, and, applying the formula from Figure 5, an estimate was made that the system could be operated at 7.4 Mb/s. Actual waveform observation showed that the margin could be much less than 75 ns and consequently the system was operated at 10 Mb/s. As indicated in Figure 6, a number of different types of transmitters and receivers were used, having different distortion properties. Dynamic range was checked using cable lengths ranging from 0.2 to 20 metres of plastic cable. Although this produced a large variation in the amount of distortion, it had no effect on the data rate capability.

CONCLUSION

For enhancement of understanding in verbal communication it would be helpful to have documented standards of nomenclature, and description of modulation codes.

Regardless of what they are called in other literature the modulation codes called MILLER and MFM in this paper

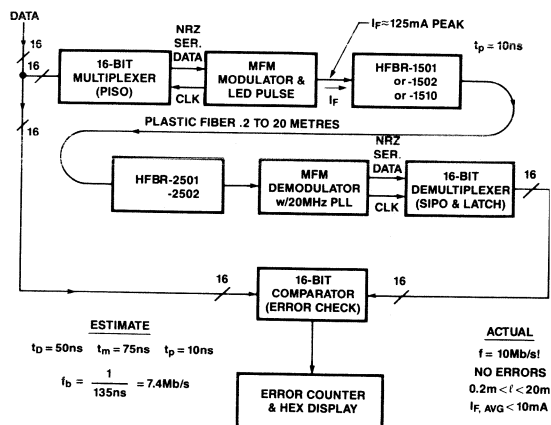


Figure 6. Diagram of System for Optimization Check

have much to offer in the design of fiber optic systems requiring clock recovery from the received signal. In links having little distortion, MILLER coding can double the data rate over what is possible with BIPHASE or MANCHESTER. Where distortion and dynamic range present limitations, MFM coding is superior.

ACKNOWLEDGEMENTS

Special credit goes to Robert P. Warnock III who shared his considerable knowledge of the MFM, especially as applied to fiber optics; formerly with Fortune System, Inc., Mr. Warnock is presently a computer architecture consultant in Redwood City, California. Also deserving mention is Gary Mayes, the technician at Hewlett-Packard, Optical Communication Division, who not only made the MFM circuits work, but devised a simple error-checking circuit to prove it.

REFERENCES

1. Lindsey, William C., and Simon, Marvin K., Telecommunication System Engineering, Prentice-Hall, 1973, page 11
2. Mallinson, J.C., and Miller, J.W., "Optimal codes for digital magnetic recording", Radio and Electronics Engineer, Vol. 47, No. 4, April 1977, pp. 172-176.
3. Batey, Robert M., and Becker, James D., "Second-Generation Disc Read/Write Electronics", Hewlett-Packard Journal, January 1984, pp. 7-12.



Reliability Considerations in Designing Fiber Optic Transmitters

SUMMARY

In LED-driven fiber optic transmitters the reliability is usually limited by the operating life of the LED, and can be enhanced by proper considerations for mechanical stress, temperature, and current density. LED degradation history suggests operation at low current density but this has unacceptable performance limitation in driving optical fibers. Changes in device design and manufacture allow higher current density while maintaining high reliability, and virtually eliminating gradual degradation. Package improvement further increases the MTBF. The validity of the reliability enhancements is shown in a comparison with fiber optic receivers in identical packaging.

HISTORY OF LED DEGRADATION

A great deal of information has been gathered on the performance of LEDs in lamps and optocouplers.^[1] The phenomenon of LED degradation results from defects in crystal structure. Such defects within the junction area of

an LED allow current to pass through the junction without producing photons (non-radiative current). This alone would not be a problem, but there is a tendency for such defects to grow during operation of the LED. The rate of growth increases with current density and temperature. Consequently, of total LED current, the fraction which is non-radiative increases as a function of time, current density, and temperature. Under high magnification, these growing defects can be seen on visible LEDs as dark lines, hence the term Dark Line Defect (DLD) is often used to describe them.

With the LED operated at a fixed current, the rising fraction of the current that is non-radiative results in decreasing optical output as a function of time. This characteristic is shown in Figure 1 for operation at a current density of approximately 25 A/cm² at 25°C (Curve A) and 85°C (Curve B), and at 75 A/cm², 25°C (Curve C).

LIMITATIONS OF OPERATING AT LOW CURRENT DENSITY

Performance of an LED as a fiber optic driver when operated at a current density, $J = 25 \text{ A/cm}^2$ can be computed. The optical power density, $M \text{ (W/cm}^2\text{)}$ at the outside surface of an LED is the product of current density, photon energy, and external quantum efficiency. At 700 nm, photon energy is 1.77 electronvolts per photon (1240 divided by wavelength in nanometres). External quantum efficiency^[2] is the ratio of the number of photons radiated to the total number of electrons passed through the device; a typical value is 0.005 photons per electron. Multiplying these:

$$M \left(\frac{\text{W}}{\text{cm}^2} \right) = J \left(\frac{\text{A}}{\text{cm}^2} \right) \times 1.77 \left(\frac{\text{eV}}{\text{photon}} \right) \times .005 \left(\frac{\text{photon}}{\text{electron}} \right)$$

$$= .221 \text{ W/cm}^2 \text{ for } J = 25 \text{ A/cm}^2$$

Butt-coupled to a fiber with core diameter smaller than the LED radiating area requires multiplying the optical power density by the core area, and since the NA of an LED is unity, the square of the fiber NA is another factor. Fresnel loss at the fiber is small, and therefore ignored.

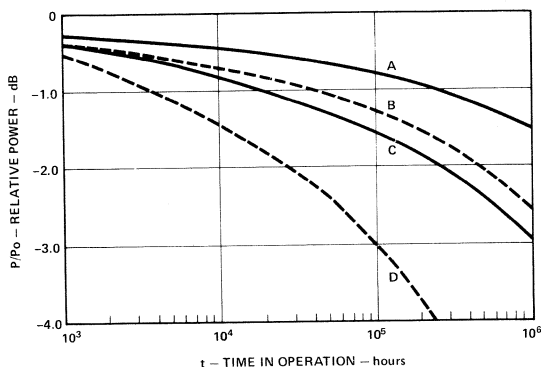


Figure 1. Optical Power Degradation (average). Predicted from optocoupler history.^[1]

A — at 25 A/cm², 25°C C — at 75 A/cm², 25°C
B — at 25 A/cm², 85°C D — at 75 A/cm², 85°C

For a fiber having NA = .5 and core diameter = 200 μm (.02 cm)

221	mW/cm ² power density
x.25	square of NA
55.2	
x314	E-6 area of core (cm ²)
17.4	μW coupled into the fiber

Seventeen microwatts is large enough to be useful, but if the same LED were used with a fiber having a smaller NA ($\approx .3$) and smaller core diameter such as 100 μm (.01 cm), the results are:

221	mW/cm ²
x.09	square of NA
19.9	
x78.5	E-6 area of core (cm ²)
1.56	μW

This amount of power is so small as to be useless, except for very low data rates and/or very short fiber length.

FACTORS PERMITTING HIGHER CURRENT DENSITY

Clearly, a higher current density is necessary, but unless something else is done, the rate of degradation would be unacceptable (Curve C in Figure 1). The "something else" consists of three important factors in the design and manufacture of LEDs for use as fiber optic drivers.

First, there is control of the crystal defect density permitted in the materials on which the LEDs are fabricated. This is helpful, but not sufficient for some applications in which current density over 1000 A/cm² is required. The second factor is reduction of the size of the junction area, which has two effects: (1) it reduces the absolute current needed to achieve high current density and (2) it lowers the probability of including a crystal defect within the junction area. The third factor is the use of a burn-in period on LEDs before they are accepted for assembly into fiber optic transmitters.

During pre-assembly burn-in the LEDs are operated at a current density high enough to cause measurable degradation if there is a significant defect in the junction area. It is characteristic of the LEDs accepted for assembly that they exhibit little or no degradation after many thousands of hours of operation.

DEVICE RELIABILITY AT HIGHER CURRENT DENSITY

The absence of slow degradation does not imply everlasting life, but requires a different approach to defining reliability. After many thousands of hours there is a sharp, though not catastrophic, decrease in optical output. The only way to deal with this situation in describing their reliability is to define the MTBF (Mean Time Before Failure) in terms of operating current and operating temperature, with failure noted as the time at which the sharp change in light output reduces it by 50%.

A study was performed^[3] on devices made as described above, operating them at current densities ranging from 300 A/cm² to more than 8000 A/cm², and at 85°C, 125°C,

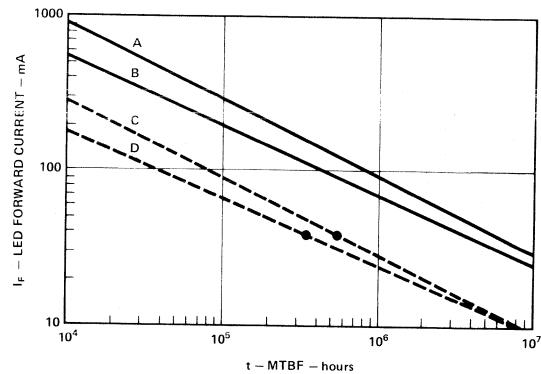


Figure 2. MTBF vs. Current at Temperature. Predicted from device study^[3] with equation (1). At 40 mA, $J = 1200 \text{ A/cm}^2$, both devices.

A — Burros 25°C C — Burros 70°C
B — Planar 25°C D — Planar 70°C

150°C temperatures. The conclusion drawn is that the MTBF can be described as:

$$\text{MTBF} = k_1 I^n \exp(E_a/kT)$$

k_1 = rationalizing constant, depending on choice of units for time and current

I = operating current (or current density, J)

E_a = activation energy = .458 eV

K = Boltzmann's constant = $8.614 \times 10^{-5} \text{ eV/}^\circ\text{K}$

T = absolute temperature (Kelvin) = $273^\circ + T_A (^\circ\text{C})$

$n = -2$ for Burros type

$n = -2.3$ for planar type

From this expression a family of MTBF characteristics can be plotted, as in Figure 2. The only other information needed is MTBF for a particular set of conditions, so the rationalizing factors can be evaluated. At 40 mA and 70°C the MTBF was found in the study to be 350,000 hours for the planar device and 530,000 hours for the Burros type. For MTBF in hours, and current in milliamperes, the values are:

$K_1 = 314$, planar device

$K_1 = 157$, Burros device

EFFECTS OF PACKAGING

In the study mentioned above, the devices were not actually assembled into fiber optic transmitters, but were mounted on TO-46 headers. This was necessary to allow observation of the effect of aging on surface emission characteristics and far-field emission patterns. The effects of packaging could improve or degrade the MTBF, depending on how well the factors of mechanical stress and thermal stress (heat sinking) are controlled.

The Burros devices have been designed into a transmitter in which the optical output is obtained through butt-coupling a fiber stub to the optical port of the LED, which is mounted on a ceramic standoff. Mechanical stress is minimized by having the fiber stub spaced away from the LED surface, with no epoxy or other optical coupling

material which might transmit mechanical stress from the stub to the LED surface.^[4] Direct comparison of the transmitter's MTBF with the result of applying equation (1) derived from the study is clouded by two issues: First, the operating current is not fixed; however, the average value is very close to the 40 mA for which the rationalizing constant applies. Second (and more important), is the inclusion in the transmitter package of an integrated circuit driver and other components which not only contribute to reduction of the overall MTBF, but also affect the thermal environment of the LED.

The planar devices were designed into the package shown in Figure 3, which provides several important features that enhance reliability with little sacrifice of performance. The TO-46 header on which the LED is mounted has tight thermal coupling to the massive heat sink surrounding it. Mechanical stress is relieved by having the coupling lens spaced away from the surface of the LED. This spacing also permits formation of a real image of the LED to be focused on the face of the optical fiber in the ferrule of a connector seated in the package. Except for approximately 1 dB of fresnel loss, this is the optical equivalent of pressing the fiber face against the surface of the LED, so there is little sacrifice of performance. Furthermore, the package contains only the LED, so the reliability of the transmitter is more directly comparable with the results of the study mentioned earlier.

RELIABILITY COMPARISON

Reliability figures for the devices above, as obtained in the study, are not necessarily accurate in describing the reliability of the transmitters in which they are packaged. Nevertheless, the figures obtained from packaged devices exhibit expected directions when their MTBFs are compared with MTBFs of receivers in the same style of package.

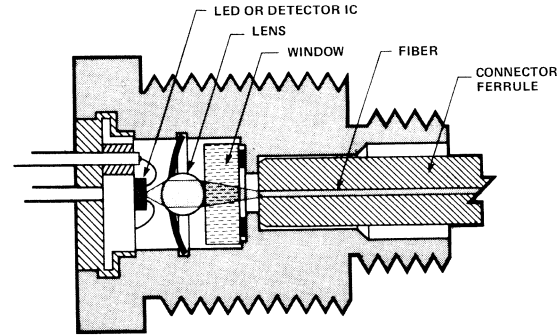


Figure 3. Cross Sectional View of Fiber Optic Transmitter (not to scale). This package preserves optical efficiency while minimizing mechanical and thermal stress. Using planar devices, MTBF = 585,000 hours at 70° C and 40 mA (1200 A/cm²).

In particular, for the Burrus device, the transmitter in which it is used has factors other than current density that impact the MTBF. This would include the integrated circuit driver, and other components, whose power dissipation

affects the thermal environment. In the comparison table, the 459,000 hours is what would be predicted, based on the average operating current in the LED. Relative to this, the 60,000 hours obtained in operation of the transmitter seems dismal, but when it is compared with the 94,000 hours for a receiver in the same style of package, it seems reasonable. The conclusion drawn is that the transmitter reliability is not limited severely by the MTBF of the LED.

RELIABILITY COMPARISON TABLE

	MTBF (k hours)	
	Burrus	Planar
Result of device study at 40 mA, 70° C	530	350
Predicted from Eq. (1) for device in transmitter package	459	350
Actual transmitter reliability at 70° C	60	585
RECEIVER in same package at 70° C	94	373

In the case of the planar device, the transmitter package appears to enhance the MTBF — most likely from improved heat sinking. A more direct comparison is possible here because the package contains no other electronic components or devices. The predicted MTBF is the same as that obtained in the study because identical drive condition and ambient temperature was applied. The somewhat lower MTBF for the receiver in the same package is probably due to its greater complexity.

CONCLUSION

With proper consideration for effects of current density, temperature, and mechanical stress, LED-driven fiber optic transmitters are capable of adequate reliability along with satisfactory performance. With LEDs of small junction area, current density greater than 1000 A/cm² (at 40 mA) make the power density adequate for driving small size fibers with enough power to operate over long distances at high data rates. Package improvement has raised the MTBF above 500,000 hours.

REFERENCES

1. Hewlett-Packard Application Note, AN-1002 "Considerations of CTR Variations in Optocoupler Circuit Designs", page 8.
2. "Optoelectronics/Fiber Optics Applications Manual", 2nd Edition, McGraw-Hill, 1981, Page 2.3.
3. B. Twu and H. Kung, "Reliability of Fiber Optic Emitters", Proceedings of S.P.I.E., Vol. 321, Integrated Optics II, 1982)
4. Hewlett-Packard, Application Note AN-1000, "Digital Data Transmission With the HP Fiber Optic System", Figure 16.
5. Hewlett-Packard Reliability Data Sheets for:
HFBR-1002
HFBR-2001
HFBR-1201/02
HFBR-2201/02

FIBER OPTIC TECHNOLOGY



HEWLETT
PACKARD

Reprinted from *Electronics*, March 24,
1982. Copyright © 1982, McGraw-Hill, Inc.
All rights reserved.

Fiber-Optic Multiplexer Clusters Signals from 16 RS-232-C Channels

**Operating at rates up to 19.2 kb/s, link transmits
data between a computer and terminals over 1 km apart**

A multiplexed fiber-optic link can provide fast relief for a big headache in data processing. It can link clusters of terminals and other peripherals to a central processing unit in a high-speed, wideband channel having the advantages of an all-dielectric transmission medium.

Such point-to-point communication is possible with the 39301A time-division data multiplexer. This full-duplex part operates independently of the asynchronous protocols of any CPU or peripheral because its time-division multiplexing allows each of its 16 input channels to operate by protocol-independent signal sampling.

Operating at speeds up to 19.2 kilobits per second with an error rate of less than 1 bit in 10^9 , the 39301A is more than

adequate for most office applications (Fig. 1). Its electrical interface adheres to the widely used RS-232-C standard, which is limited by its governing specifications to a 15-meter cable length at 20 kb/s. That limit does apply to the distance between the peripheral devices and the multiplexer, but the fiber-optic transmission channel to the CPU can be up to 1 kilometer long with no decrease in data rate for any of the multiplexed lines.

The cost of the multiplexer and fiber-optic link is amortized over the number of data lines. Thus this approach combines the benefits of fiber optics with a per-channel cost that is less than that of a multiple-wire approach (see "In praise of fiber-optic multiplexers," p. 126).

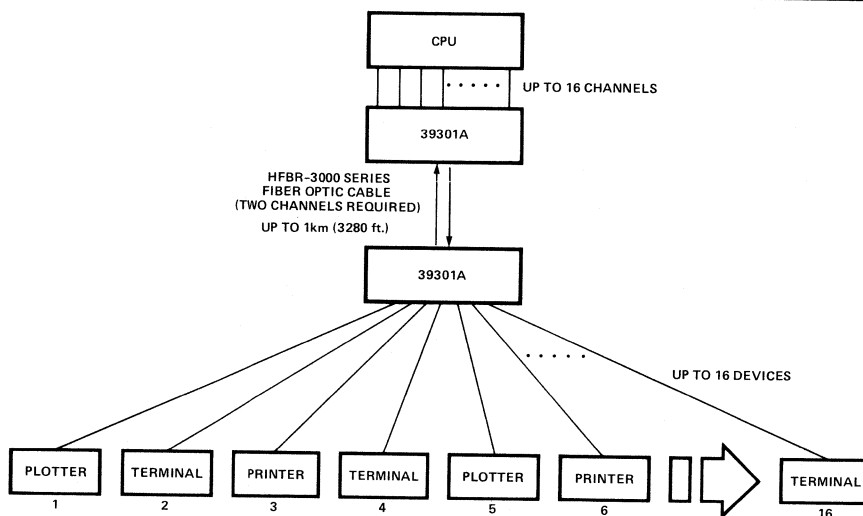


Figure 1. Combinations. The HP 39301A fiber-optic multiplexer can link 16 peripheral devices to a central processing unit independently of the data-communication protocols used by either the CPU or its terminals. Transmission distances of up to 1 km are possible.

The 39301A (Fig. 2) has eight input connectors, each of which can handle two data channels. It samples these channels at a 200-kilohertz rate, loading their contents into a 16-bit parallel-to-serial shift register. These 16 bits are shifted into the biphase encoder, which creates a serial stream of pulses containing both timing information and data.

AT THE OTHER END

After transmission, a second 39301A decodes the optical bit stream into separate clock and data signals and feeds them to a serial-to-parallel shift register. When the synchronization signal is detected, the demultiplexer loads the data from the shift register into an output latch. The outputs are then converted to RS-232-C electrical levels with standard integrated circuits.

The multiplexer's output data rate is 3.5 megabit/s, and since it is encoded in a biphase format, it requires a 7-Mb/s channel. The fiber-optic link, rated at 10 Mb/s, provides enough margin for transmitting this signal. The link is based on the standard Hewlett-Packard fiber-optic data-channel components [Electronics, Dec. 18, 1980, p. 83].

One consideration in setting the transmission channel's data rate is the biphase (Manchester) encoding that provides an easily recoverable clock signal for the demultiplexer. Such encoding requires twice as wide a bandwidth as does the same data with nonreturn-to-zero encoding. Therefore, the data transmission rate with this fiber link must be less than 5 Mb/s.

This data rate plays a part in determining the number of input data channels, as do the 19.2-kb/s maximum input rate and the 200-kHz sampling rate. (Although theory states that a rate twice the input signal's highest frequency is sufficient for sampling, digital signal sampling at least 10 times the highest frequency is appropriate in order to avoid distortion.)

To determine the number of input data channels that can be served, the 39301A's designers relied on an analysis showing that the product of the number of channels (n), the maximum per-channel data rate, and the number of samples taken per data bit must be no more than the fiber-optic transmission channel's data rate. In this case, $n(20 \times 10^3) 10 \leq 5 \times 10^6$, or $n = 25$. However, for a multiplexed system with low pulse distortion, the designers settled on a conservative 16 channels plus a synchronizing channel. This distortion is well within the specifications of the data link, and the 16 channels are compatible with the standard ICs needed to convert to the electrical signal in the demultiplexer.

CODE PATTERNS

The serial bit stream that is the multiplexer's output consists of pulses that are either 143 or 286 nanoseconds in length, as determined by the biphase modulator. Two short pulses represent a high level on the corresponding input line, and a single long pulse represents a low level. A short pulse followed by a long pulse is used as a synchronization signal to guarantee that the data corresponding to

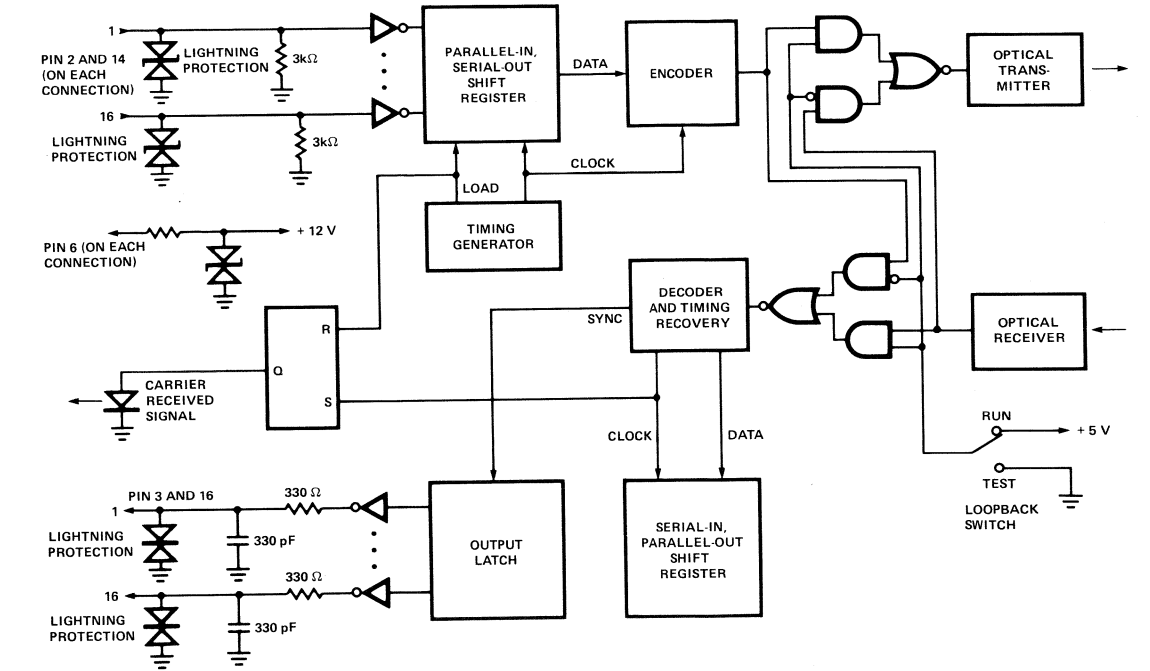


Figure 2. Inside story. The 39301A multiplexer has two separate cables to provide full-duplex transmission. The heart of its simple electronics are 16-channel parallel-in-serial-out and serial-in-parallel-out shift registers and a biphase encoder in the transmit section.

FIBER OPTIC TECHNOLOGY

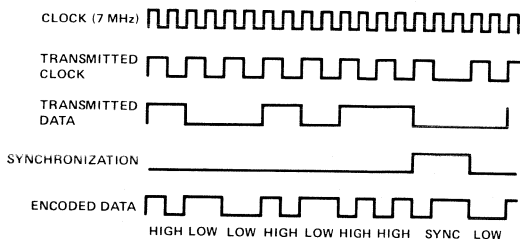


Figure 3. Timing. The multiplexer's data-coding pattern requires that two short pulses represent a high level on the corresponding input line. A single long pulse represents a low level and a short pulse followed by a long one is a synchronization signal.

each input is demultiplexed to the proper output. Figure 3 shows these data-coding patterns.

Since all 16 outputs are sampled simultaneously and the outputs are latched simultaneously, the data skew between any two channels is at most one sample period (5 microseconds) plus the time for any mismatches in the delays of the output drivers. This specification makes the part suitable for transmission systems in which control over data skew is important, such as an application with parallel bit streams and synchronous data transmission where both clock signal and data are provided.

VERSATILE UNIT

Channel usage in the 39301A may be split in several ways. Perhaps the most common split will be eight channels for data from eight peripheral devices and eight secondary channels for accompanying housekeeping signals like handshaking. In other installations, where synchronous data transmission is required and where the peripherals can provide the clock signal, the secondary channels can transmit this signal.

Still other configurations can be accommodated. For example, in applications where only a three-wire interface is required, the multiplexer can link up to 16 independent peripheral devices to a computer.

The multiplexer was designed from the start for ease of troubleshooting in systems applications. Thus loopback testing at the optical level enables an entire multiplexer's operation to be verified. At the same time, bidirectional loopback testing at the electro-optical interface facilitates a remote loopback for another 39301A, as well as serving

to locate boards in the host multiplexer that may require service. Light-emitting diodes both monitor the +5-volt power supply and indicate the presence of received data.

A short fiber-optic cable provided with the unit facilitates the loopback test at the optical level. This test uses data from an RS-232-C source, such as a cathode-ray-tube terminal. An electrical switch under the instrument's top panel loops back the electrical signal before the fiber-optic board and returns the electrical outputs of this board, thereby retransmitting the received optical signal. This feature, used primarily to isolate a failure in a unit to the optical or electrical level, verifies the optical path once each 39301A in the data-communications link is deemed to be operating satisfactorily.

Several 39301A systems in use at HP provide intra- and inter-building communications. In one case, several terminals in the manufacturing area of a building are connected to the main computers in the administrative building. They provide remote word-processing and production-scheduling capabilities. Research and development areas connected to their own computer are able to gain access to files and data bases of the manufacturing and accounting areas through system links.

In another application, a company occupying three floors of a high-rise office building uses a 39301A system to connect three clusters of terminals to a computer. Order processing, accounts receivable, and shipping coordination are now all tied directly to the main computers with no sacrifice in terminal or computer speed over the 300-m distances.

OTHER USES

A large complex of manufacturing buildings could use these systems to send signals from bar-code readers to the main computer system. Still another application might have remote terminals in a typesetting area connected to a CPU and a second cluster at editors' and reporters' desks on another floor of a newspaper office.

There are still other possibilities. Clusters of numerically controlled machines on a large factory floor can be downloaded from the main computer where program development is done. The long-distance data communications and noise immunity of fiber optics keep data error-free in the factory environment and from the programmer stations to the CPU. Finally, a large manufacturing building may have remote printers, plotters, and terminals connected to the CPU, providing graphics capability in the drafting areas and plotter printouts of the designs directly on the manufacturing floor.

IN PRAISE OF FIBER-OPTIC MULTIPLEXERS

More and more, the users of computer systems want to extend standard data-communications lines beyond their typical specified length and still operate at a high bit rate. That is, they want to push the bandwidth-length products of their systems to new levels. The inherently large bandwidth-length product of fiber-optic systems makes them the preferred candidate over telecommunication-based methods and wireless approaches.

In a typical RS-232-C installation, extending the terminal-to-computer distance beyond the specification of 15 meters can cause problems if error-free operation is called for: the data rate must be reduced, not increased. What's more, the system's manufacturer will not support this out-of-spec application.

For communication over a 50- to 1,000-m distances, systems installers may go to the newer RS-449 standard and its subsets. In a balanced configuration with special cables, data transmission can extend to 1,200 m. However, for the highest bit rate of 10 megabits a second, the transmission distance is still limited to 12 m or so, and the common-mode noise immunity is a mere ± 7 volts.

A short-haul modem can operate at speeds up to 19.2 kilobit/s, but it generally requires dedicated low-noise telephone lines for high-performance applications and may be susceptible to lightning damage.

These three transmission schemes either employ low-speed individual data channels for each peripheral, or they depend upon a statistical multiplexer to transmit active signals alternately over the low-speed data channel. Simultaneous operation of all peripherals is not possible with such a multiplexing scheme, and per-channel cost ranges from \$300 to \$1,000.

Wireless transmission schemes using infrared and microwave technology can transmit data at high rates over long distances. However, they may be too costly, and they are limited to line-of-sight transmission.

Thus, fiber-optic systems, with their typical bandwidth-length products of 20 megahertz-kilometer look promising, particularly since their all-dielectric nature puts an end to interference problems from lightning. On the other hand, dedicating that wide bandwidth to a single computer peripheral would be expensive, rather like chartering a wide-body jet plane for one person.

Therefore, a multiplexer that allows full-duplex transmission can be a cost-effective solution. In applications with a cluster or clusters of peripherals, fiber-optic multiplexers situated with each cluster can gang the data signals for transmission over a single wide-bandwidth channel to the central processing unit. Per-channel costs might be in the \$200 range.

*After publication of this article, HP improved cable bandwidth-length specifications to 40 megahertz-kilometer.



Threshold Detection of Visible and Infrared Radiation with PIN Photodiodes

Traditionally, the detection and demodulation of extremely low level optical signals has been performed with multiplier phototubes. Because of this tradition, solid-state photodetectors are often overlooked even though they have a number of clear functional advantages and in some applications provide superior performance as well. Some of these advantages are summarized below and become even more apparent in the following discussion.

ADVANTAGES OF PIN PHOTODIODES VERSUS MULTIPLIER PHOTOTUBES

1. **Size and weight:**
PIN photodiodes are approximately three orders of magnitude smaller and lighter. This greatly simplifies and reduces the cost of mounting.
2. **Power Supply:**
Multiplier phototubes require more than 1000 volts, which must be precisely regulated and divided among the dynodes. By comparison, PIN photodiodes and associated amplifiers operate stably on less than 20 volts, which does not require precise regulation.
3. **Cost:**
The cost, including that of the necessary amplifier, is lower for the PIN photodiode because of lower power supply requirements.
4. **Spectral Response:**
Broad skirts of the PIN photodiode make it useful from the ultra-violet, through the visible, and well into the infrared region. This exceeds the range of any other device of comparable sensitivity.
5. **Sensitivity:**
Noise equivalent power of the PIN photodiode is lower than that of any other type of photodetector. The signal levels are extremely low, however, and to achieve low level performance they require a high gain, high input resistance amplifier. Multiplier phototubes have built-in gain and do not require additional low-noise amplification. Moreover, the high input resistance needed for sensitive performance precludes fast response, whereas the response time of multiplier phototubes may be in the nanosecond region even in the sensitive mode.

6. **Stability:**

The characteristics of noise, responsivity, and spectral response of the PIN photodiode are not dependent on time, temperature, or other environmental considerations. The same conditions may be hazardous to multiplier phototubes.

7. **Overloading:**

In the presence of excessive signal, multiplier phototubes of comparable sensitivity are capable of destroying themselves as a result of excessive output current. The PIN photodiode is unaffected by exposure to room light or even direct sunlight.

8. **Ruggedness:**

PIN photodiodes can tolerate exposure to extreme levels of shock and vibration. Typical shock capability is 1500 G's for 0.5 millisecond.

9. **Magnetic Fields:**

Multiplier phototube gain is affected by fields as small as one gauss. If the interfering field is fluctuating, the output will be modulated by it. The PIN photodiode is insensitive to magnetic fields.

10. **Precision:**

The responsivity of the PIN photodiode is inherently precise and repeatable. Within a given type, the characteristics agree (from unit to unit) within plus or minus 0.1 decade. Responsivity of multiplier phototubes may vary over more than a decade from one unit to another.

11. **Sensitive Area:**

The small sensitive area of the PIN photodiode makes it unnecessary to establish an aperture which may be required for some applications. However, in some applications good optical alignment is imposed by the small area.

PIN PHOTODIODE DETECTORS

At the present time a variety of different types of solid-state photodetectors are available. Of these, the Silicon PIN Photodiode has the broadest applicability and is the subject of this note. The PIN photodiode's main advantages are: broad spectral response, a wide dynamic range, high speed, and extremely low noise. With appropriate terminal circuits it is well suited for many applications that require converting an optical signal to an electrical signal. The

present discussion, however, will be limited to the description of the PIN photodiode's threshold detection sensitivity and the design of suitable terminal circuits that will realize this capability.

PHOTODIODE DESCRIPTION
Construction

A brief description of the PIN photodiode will be helpful in understanding its performance and the principles for designing appropriate circuits to be used with it. Figure 1 shows a typical construction of the PIN photodiode. This figure is for the purpose of explanation only and is not to scale. The relative proportions have been deliberately distorted for the sake of clarity.

The PIN structure is produced by diffusion through an oxide (SiO_2) mask which also serves to protect the surface. Since most metals are very opaque to optical radiation, especially at infrared wavelengths, the gold contact is deposited only around the perimeter of the P-layer, and the gold contact pattern provides for lead attachment a short distance away from the junction region, so the lead is not in the light path.

Mode of Operation

When a photon is absorbed by the silicon it produces a hole and an electron. If the absorption of the photon occurs in the I-layer, as shown in Figure 1, the hole and the electron are separated by the electric field in the I-layer. For the highest quantum conversion efficiency (electrons per photon) it is desirable to have the P-layer as thin as possible and the I-layer as thick as possible. The thickness of the P-layer also determines the value of the parasitic series resistance (R_s in Figure 2). The thinner the P-layer the higher the R_s . Since R_s affects high frequency performance there is therefore a design trade-off between quantum efficiency and bandwidth. Once the trade-off is settled, the desired thickness is then controlled during the diffusion process. The effective thickness of the I-layer is controlled partly by the manufacturing diffusion process and partly by the magnitude of the electric field applied to the diode—the higher the field, the thicker will be the effective I-layer. It is therefore desirable to operate the diode with an external reverse bias, as shown in Figure 2. As the reverse bias voltage is increased from zero, there are three beneficial effects: hole and electron transit time decreases; conversion efficiency increases slightly; and most importantly, the capacitance decreases sharply with bias up to about ten volts and continues to decrease slightly up to about twenty volts reverse bias.

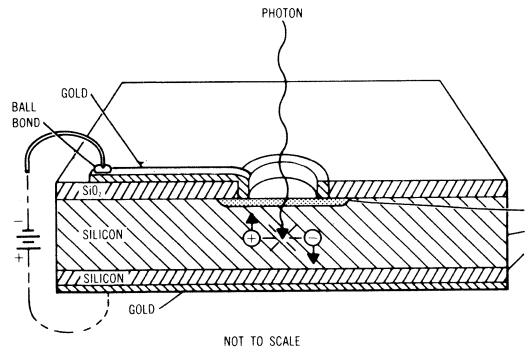


Figure 1. PIN Photodiode Cutaway View

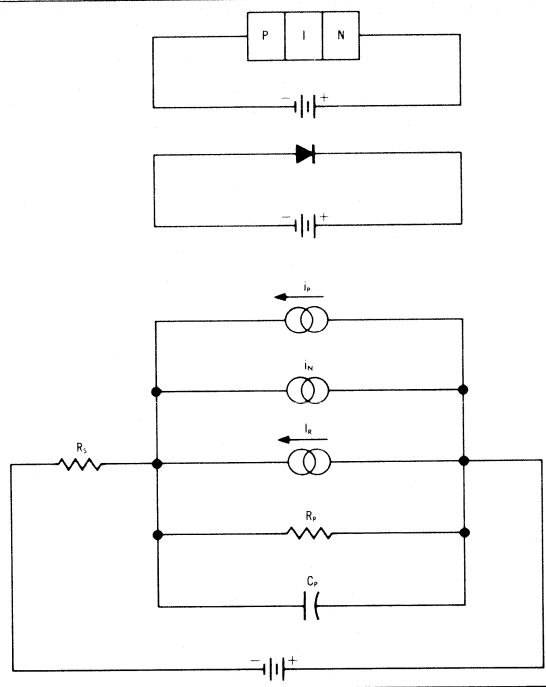


Figure 2. PIN Photodiode Schematic Symbol, and Equivalent Circuit

In the presence of optical signals there is a slight modulation of the shunt conductance as the presence of photon-produced holes and electrons in the I-layer modulate its conductivity. This effect can be quite significant at very high levels of illumination since the I-layer may become saturated, resulting in a decrease in quantum efficiency and an increase in rise time. Saturation can be prevented by applying a very high reverse bias voltage (up to 200 volts). However, such a high voltage, applied over a long period of time, may cause a degradation of the diode's leakage properties. Since our present concern is with threshold performance, reverse bias voltages greater than twenty volts need not be considered.

Equivalent Circuit

When properly biased, the PIN photodiode can be accurately represented by the equivalent circuit shown in Figure 2. Here i_p is the external current resulting when the diode is illuminated. It has a time constant of 10 picoseconds and a value of approximately 0.5 amp per watt of input at a wavelength of 8000 angstroms (800 nanometers). This corresponds to a quantum efficiency of 75%, that is, 0.75 electrons per photon. The quantum efficiency is constant from 500 nanometers to 800 nanometers (5,000 Å to 8,000 Å).

i_n is the noise current of the PIN photodiode. Since the diode is reverse biased, the shot noise formula is applicable, so that the noise current can be computed from:

$$\frac{i_n^2}{B} = 2qI_{dc} \tag{1}$$

where B = system output bandwidth, Hz
 q = electron charge, 1.6×10^{-19} coulombs
 I_{dc} = dc current, Amp.

In the case of the photodiode, I_{dc} is simply the dark current, I_R , which has a value determined by the construction and dimensions of the particular diode type. Maximum values are: 100 picoamps for 5082-4204, 150 picoamps for 5082-4205 and 2 nanoamps for 5082-4203.

Shunt resistance, R_p , is very large, being usually greater than 10 gigaohms (10,000 megohms), and its noise current may therefore be neglected. Shunt capacitance, C_p , has a value from two to five picofarads, depending upon the diode type and reverse bias. For high frequency operation it is important to minimize C_p because the cutoff frequency is determined by:

$$f_c = \frac{1}{2\pi R_p C_p} \quad (2)$$

Although our present concern is with low frequency threshold operation, there is another reason for minimizing C_p . This will be discussed later, when circuit design principles are presented.

Performance

Threshold performance can and has been specified in a number of different ways. The most commonly understood and usable expression takes the form of a noise equivalent input signal. This is the input signal which produces an output signal level that is equal in value to the noise level that is present when no input signal is applied. The noise equivalent input in watts is called Noise Equivalent Power (NEP) and is defined by:

$$NEP = \frac{\text{NOISE CURRENT (amps per root hertz)}}{\text{CURRENT RESPONSIVITY (amps per watt)}} \quad (3)$$

which has the units of watts per root hertz. Devices for photo-detection could then be compared on the basis of NEP. The lower the NEP the more sensitive is the device.

Another method of defining threshold sensitivity is on the basis of signal-to-noise ratio for given input signal power levels. Taking a power level of one picowatt, for example, the signal-to-noise ratio at the output can be obtained from:

$$SNR = \frac{\text{RESPONSIVITY} \left(\frac{\text{amps}}{\text{watts}} \right) \times \text{INPUT (watts)}}{\text{NOISE CURRENT (amps)}} \quad (4)$$

This is a ratio of currents. To express it in dB we would take twenty times its log to base ten, even though the expression converts linearly to a power ratio. This is because the devices respond *linearly* to input *power*.

Figure 3 shows spectral sensitivity characteristics of several PIN photodiodes and multiplier phototubes. Sensitivity is given in terms of SNR and NEP. The latter is in terms of dBm. Several interesting features are evident in Figure 3. Although the quantum efficiency for PIN photodiodes is constant from 500 to 800 nanometers, the sensitivity curve is not. This is due to the fact that the energy per quantum (photon) of radiant energy varies with wavelength.

The curves for the three different PIN photodiodes also show the dependence of sensitivity on leakage current. Here the highest sensitivity is obtained with the 5082-4204 which has a maximum leakage current of 100 picoamps. Next is the 5082-4205 with 150 picoamps and finally the 5082-4203 with maximum leakage of 2 nanoamps. The three curves are in effect displaced by the magnitude of the noise current difference because quantum efficiency is equal for all. These curves also show the inherent broad response of PIN photodiodes with respect to multiplier phototubes. Therefore, the power responsivity of the PIN photodiode

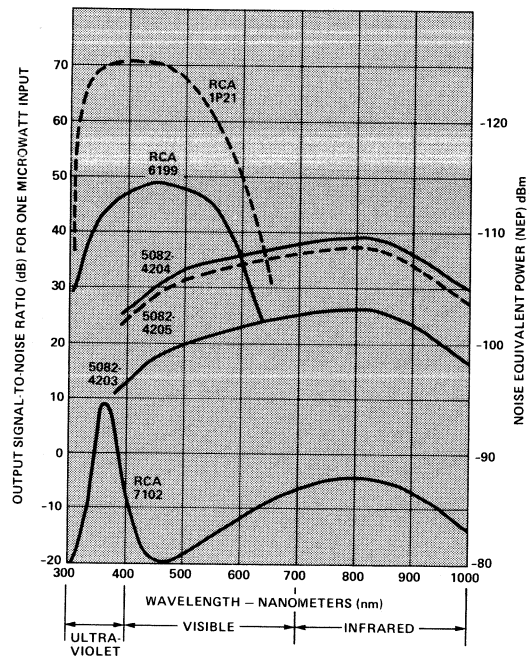


Figure 3. Spectral Sensitivity Comparisons of Photodetectors

has a corresponding slope. Notice how the inherently broad response of silicon, enhanced by the thick I-layer construction, extends the range of useful performance over the response ranges of two types of photocathodes.

Although the threshold sensitivity of multiplier phototubes is superior in the visible region, nevertheless for many applications the advantage is not significant enough to outweigh the disadvantages of generally unstable and temperature-sensitive gain, large size and weight, and the need of very high and stable power supply voltages. On the other hand, the superior red and infrared threshold performance of the PIN photodiode does not necessarily mean it is better in any application, because one must take into account its small sensitive area and low signal levels. Realization of the performance capability described in Figure 3 also requires fairly careful attention to the design of the terminal circuits into which the PIN photodiode operates.

TERMINAL CIRCUIT DESIGN PRINCIPLES

The design of the terminal amplifier must consider the usual design objectives of low noise, broad band, wide dynamic range, etc. In addition, there are two fundamental considerations which are dictated by the PIN photodiode:

1. High Reverse Voltage:

The diode must be operated at ten to twenty volts of reverse bias to reduce shunt capacitance.

2. High Input Resistance:

This is a fundamental consideration in the sensitivity/rise time trade-off.

The effects of reverse voltage on capacitance have been discussed earlier. However, the effect is sufficiently important to deserve a re-emphasis here.

A high input resistance is necessary in order to maintain a high signal-to-noise ratio. Since the output signal from the photodiode is a current, and its own internal noise is repre-

sented by a current, it is appropriate to represent the noise of the terminal amplifier as an equivalent noise current at the input. The smallest value of resistor which may be connected to the input is then limited by its noise current according to the formula for thermal noise:

$$\frac{i_N^2 \text{ (thermal)}}{B} = \frac{4kT}{R} \tag{5}$$

By comparing eq(1), relating diode noise current to leakage current, with eq(5), relating resistor noise current to its resistance value, it is clear that there is some value of resistance below which the NEP of the system, i.e., threshold sensitivity, would be degraded at the rate of 5 dB per decade of decreasing resistance. For example, in the case of the 5082-4203, assuming a maximum leakage current of 2 nanoamps, the value of resistance should be greater than 25 megohms, to avoid degrading the threshold sensitivity.

TRANSISTOR AMPLIFIER

In addition to keeping the input noise current low by using large values of input resistance, it is also important to keep other sources of noise in the amplifier at a minimum. Using ordinary transistors (PNP or NPN) it is not possible to approach the ultimate sensitivity of which the PIN photodiode alone is capable, even when low-noise transistors, such as the 2N2484, are used. However, in those applications where it is possible to sacrifice sensitivity for simplicity, transistors may be used. A typical transistor circuit is shown in Figure 4. With this circuit, a sensitivity corresponding to an NEP of -95 dBm was obtained. In this case, Q1 was operated at the lowest possible collector current which would still give adequate gain. A high loop gain was desired in order to compensate, with negative feedback, for the long open-loop rise time produced by the high input resistance. A resistance higher than 10 megohms was not necessary here, since the transistor itself sets the fundamental noise limitation. A PNP transistor was selected for Q2 in order to balance out most of the base-to-emitter voltage of Q1, so that the output would tend to be near zero without any zero adjustment. A slight zero adjustment, provided by R2 and R3,

gives the necessary range without appreciably attenuating the feedback current. As the photocurrent, I_2 , increases, the amplifier causes the voltage at the emitter of Q3 to decrease, which causes a current in R1 to flow out of the node (base of Q1) into which I_2 flows.

Basic Amplifier Arrangements

For linear operation, the photodiode should be operated with as small a load resistance as possible. Figure 5 shows the recommended amplifier arrangement. The negative-going input is at virtual ground; the dynamic resistance seen there by the photodiode is R_1 divided by loop gain. If the op-amp has extremely high input resistance, loop gain is very nearly the forward gain of the op-amp. R_2 can be omitted if the photocurrent is reasonably high — its purpose is only to balance off the effect of offset current. As shown, the output voltage will rise in response to the optical signal. If it is preferable to have the output drop in response to optical input, then both the photodiode and E_C should be reversed. E_C may, of course, be zero. Speed of response is usually limited by the time constant of R_1 with its own capacitance, so it is improved by using a string of two or more resistors in place of a single R_1 .

Logarithmic operation requires the highest possible load resistance — at least 10GΩ. With an FET-input op-amp, this is

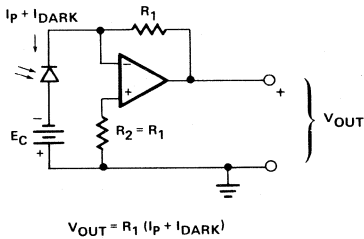


Figure 5. Linear Response; Photodiode and Amplifier Circuit Arrangement

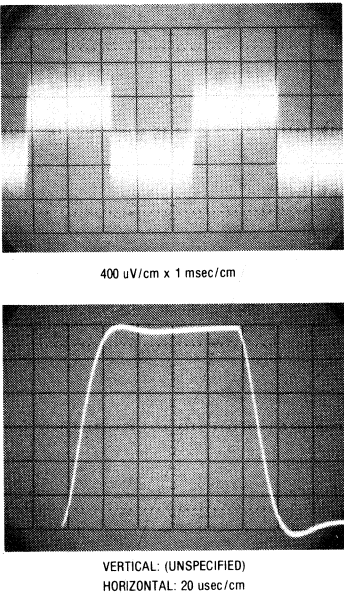
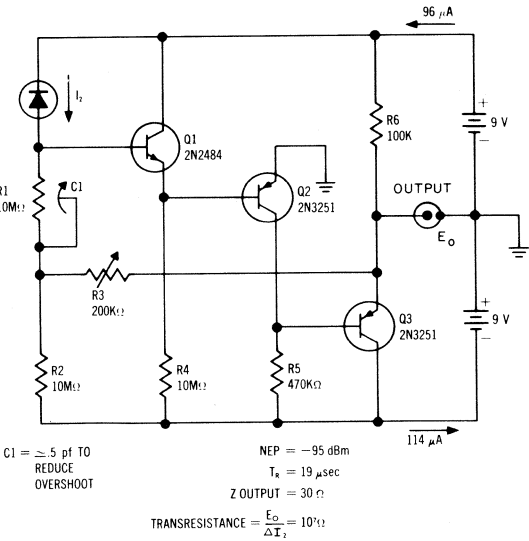


Figure 4. Transistor Photodiode Amplifier Schematic



easily achieved as in Figure 6. If the offset current of the amplifier poses a problem, a resistor can be added between the positive- and negative-going inputs. Its value should not be less than $10G\Omega$ divided by loop gain. If the amplifier has a very high input resistance, loop gain is equal to the forward gain of the amplifier divided by $(1 + R/R_1)$ so making $R_2 = 0$ allows the smallest possible resistance between the inputs. The speed of response of this amplifier will be very low, with a time constant

$\tau \approx 0.1s$. If high speed logarithmic operation is required, it is best to use the linear amplifier of Figure 5 followed by a logarithmic converter.

High Speed Photodiode Amplifier

Applications that call for high speed data signaling, such as CRT light pens, require amplifiers that have a wider bandwidth than the circuit shown in Figure 5.

Using a five transistor array (RCA CA3127E) it is possible to construct a high speed, high gain photodiode amplifier. This circuit is shown in Figure 8. It is configured as a two stage amplifier. The first stage is composed of transistors Q1-Q3, where Q1 is an input emitter follower with feedback obtained from the emitter of Q3. Q2 functions as an inverting amplifier interconnecting Q1 to Q3. The second stage consists of Q4 and Q5 which provide additional gain and output buffering, of the first stage. These two stages provide an equivalent transresistance of 420K ohms. This means that the output voltage V_o is equal to the photocurrent, I_p , times 420K ohms.

When high speed circuit layout techniques are used it is possible to obtain the rise and fall time performance shown in Figure 7. This speed is equivalent to a bandwidth of 9.5MHz with an input flux of $1.9\mu W$. This flux level can be obtained from a HEMT-6000 700nm High Intensity Subminiature Emitter when it is operated at 10mA, at a distance of 1cm from the 5082-4207 PIN photodiode.

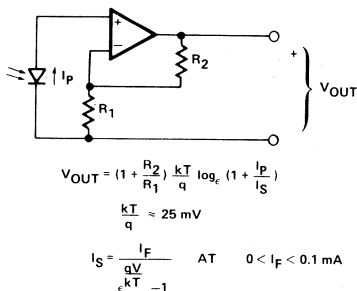


Figure 6. Logarithmic Response; Photodiode and Amplifier Circuit Arrangement

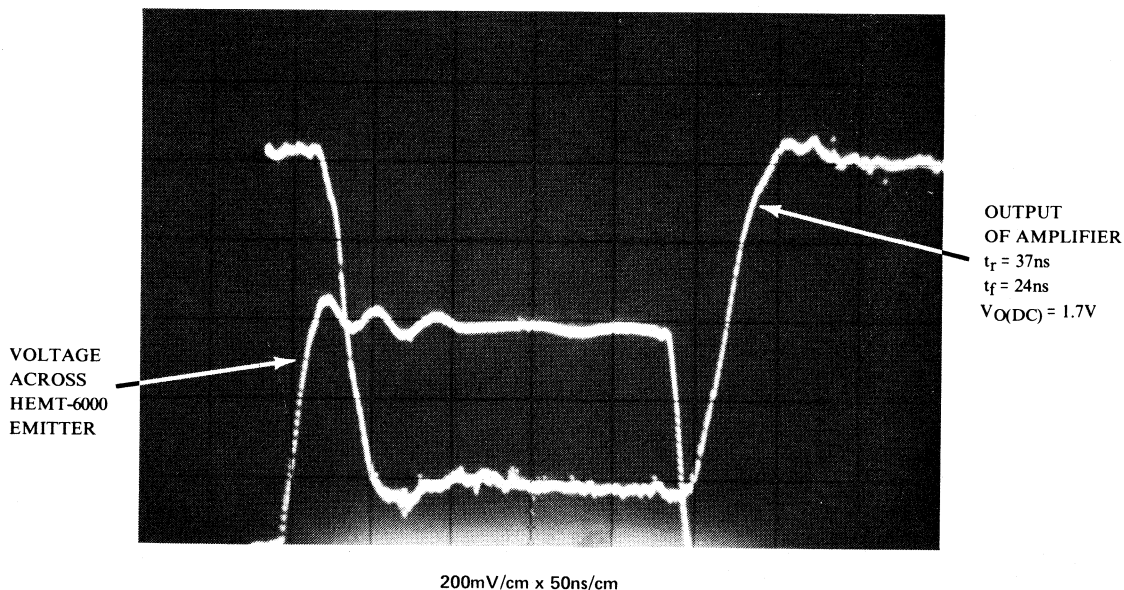
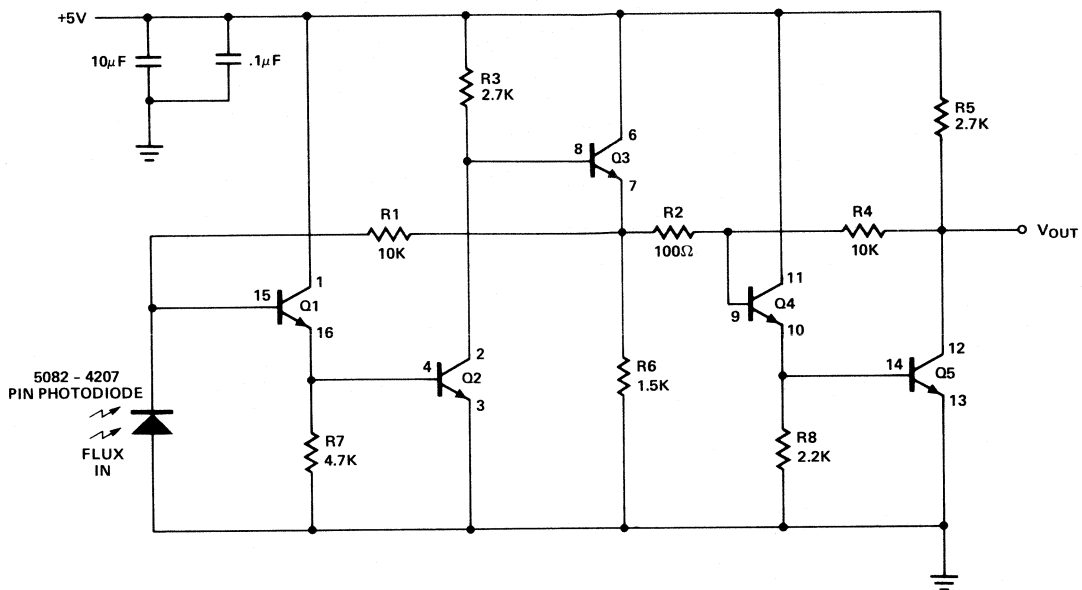
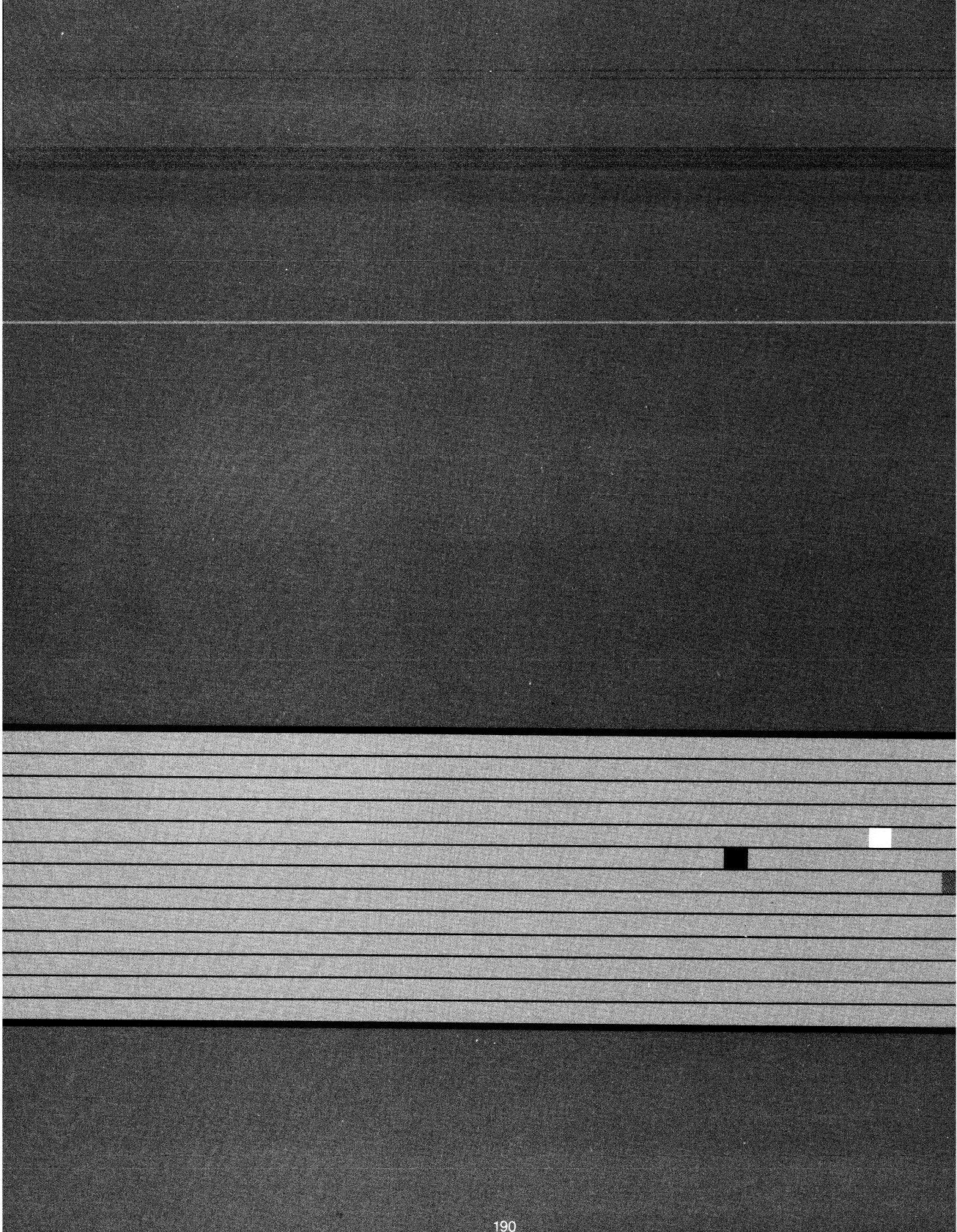


Figure 7. Pulse Response of Photodiode Amplifier

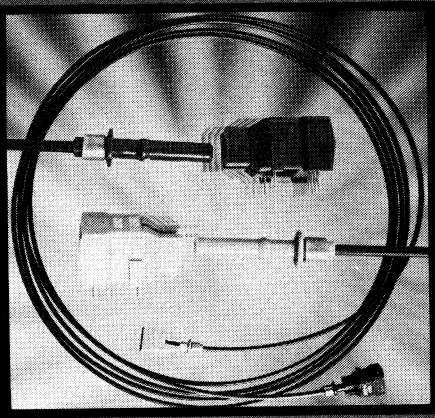
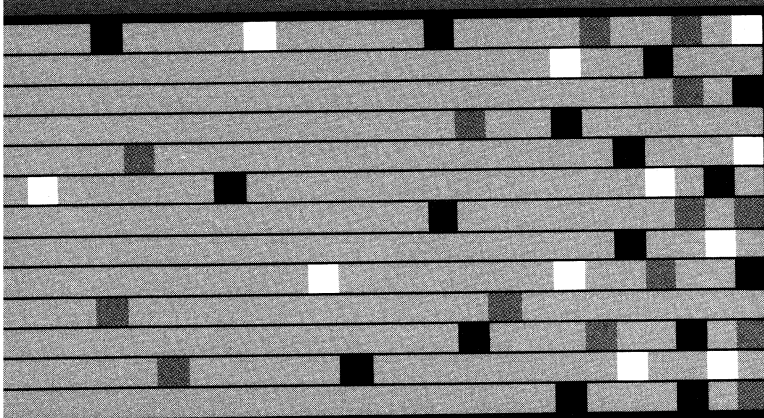


NOTES: TRANSISTORS ARE SINGLE PACKAGE, CA3127E. PINS LABELED FOR EACH. PIN 5 IS SUBSTRATE.

Figure 8. High Speed, High Gain Photodiode Amplifier



*Plastic Snap-in
Fiber Optic Components*



Plastic Snap-in Fiber Optic Components

Low cost and ease of use make this family of link components well-suited for applications connecting computers to terminals, printers, plotters and industrial-control equipment. These links use rugged, 1 millimetre diameter plastic fiber cable. Assembling the plastic

snap-in connectors onto the cable is extremely easy. The HFBR-0500 evaluation kit contains a complete working link including transmitter, receiver, 5 metres of connected cable, extra connectors, polishing kit and technical literature.

Snap-In Link Family: Features — Plastic fiber (1 mm dia.), Plastic Snap-in connectors, TTL compatible output.

Products/Part Nos.	Description
Evaluation Kit HFBR-0500	HFBR-1510 Transmitter, HFBR-2501 Receiver, 5 metre connected cable, connectors, bulkhead feedthrough polishing kit, literature.

Transmitter/Receiver Pairs	Data Rate	Guaranteed Distance, -20°C to 70°C	
		HFBR-3530 Cable	HFBR-351X Cable
HFBR-1510/-2501	5 MBd	17 m	12 m
HFBR-1502/-2502	1 MBd	34 m	24 m
HFBR-1512/-2503 (extended distance link)	40 KBd	82 m	60 m
HFBR-1512/-2503 (low current link)	40 KBd	11 m	8 m
HFBR-1512/-2503 (photo interrupter link)	20 KHz	NA	NA
HFBR-1502/-2502 (photo interrupter link)	500 KHz	NA	NA

Products/Part Nos	Description
Low Loss Cable	<div> <div>Cable Length</div> <div> 0.1 metre 0.5 metre 1.0 metre 5.0 metre 10.0 metre 20.0 metre 30.0 metre 45.0 metre 60.0 metre </div> <div>connected</div> </div>
Simplex	
HFBR-3511	
HFBR-3512	
HFBR-3513	
HFBR-3514	
HFBR-3515	
HFBR-3516	
HFBR-3517	
HFBR-3518	
HFBR-3519	
HFBR-3579	
HFBR-3580	
HFBR-3581	
Super Low Loss Cable	
HFBR-3530	
HFBR-3582	
Connectors	
HFBR-4501	
HFBR-4511	
Polishing Kit	<div> <div>Plastic polishing fixture, abrasive paper</div> <div>Metal polishing fixture</div> </div>
HFBR-4595	
HFBR-4596	
Bulkhead Feedthrough/in-line Splice	<div> <div>Gray Bulkhead Feedthrough</div> <div>Blue Bulkhead Feedthrough</div> </div>
HFBR-4505	
HFBR-4515	

*Link performance at 25°C.

An Introduction to Plastic Fiber Optic Technology

Plastic optical fiber provides an excellent transmission medium for short distance communication. Several industrial, computer, medical and automotive applications utilize low cost plastic fiber optic components. The purpose of this discussion is to present a detailed description of plastic fiber optic components. Differences between plastic and glass fiber optic systems, as well as information concerning factory applications of plastic fiber optic components are discussed.

PLASTIC FIBER OPTIC COMPONENTS

CABLES

Plastic fiber optic cable consists of a plastic fiber surrounded by a polyurethane outer jacket. The fiber contains both core and cladding material; core sizes range from 250 to 2000 micrometres in diameter. The outer jacket can be made flame retardant by selecting an appropriate jacket material. Typical cable construction is shown in Figure 1.

The large fiber diameter allows for easy launching of light into the fiber, and typical numerical aperture specifications are on the order of 0.5. Attenuation of several hundred dB/Km limits the cable length of plastic cable to under 70 metres. Note in Figure 2 that there have been improvements made in this area to accommodate longer distance cable especially in the transmission of visible light, green in particular (570 nm). Plastic Fiber Optic cable provides high voltage insulation between transmitter and receiver due to its low electrical conductivity.

CONNECTORS

The cable must be interfaced to a transmitter, receiver or another cable by means of a connector. There are several varieties in existence today, and are usually quite simple. In Figure 3, exemplary snap-in and locking connector styles are shown. The snap-in connector grants quick attachment and detachment, while the locking connector provides a more permanent interface. Bulkhead feedthrough connectors furnish the addition of an in-line splice to a plastic cable. Typically, it is very straightforward to install a

connector on to a plastic fiber. The cable can be cut with a knife or wire cutters, the jacket stripped with wire strippers, and the connector can usually be crimped directly on the cable with a crimping tool, if necessary. Some connectors require the end be polished lightly, but even so, the total process usually requires less than 30 seconds to complete.

PACKAGE CONSIDERATIONS

The transmitter and receiver circuits are inserted into plastic packages of various styles. The packages are molded to be compatible with the connectors on the cable. Mechanical considerations play an important role in the design process. Does the package require additional screws to attach to a printed circuit board, and is drilling of screw holes required? Will the package be compatible with the footprint of a conventional dual-in-line package socket? Will the package fit into a sufficiently small space? Does the package have a locking connector? Figure 4 illustrates a few examples of package styles. Depending upon the application, a designer can choose the package style which best addresses his concerns.

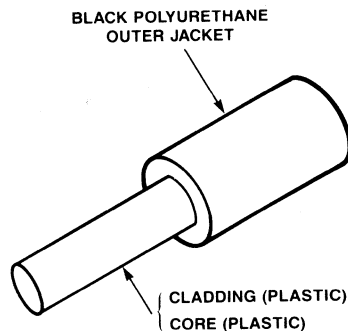
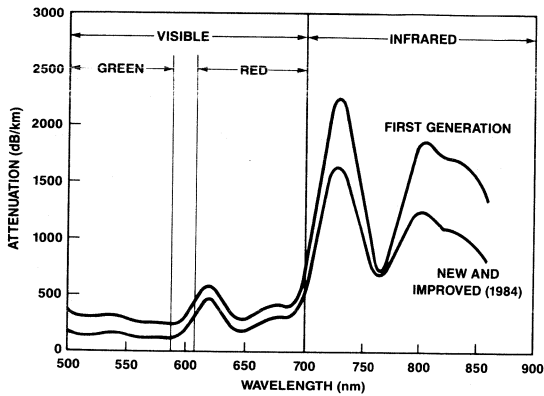


Figure 1. Typical Plastic Fiber Optic Cable Construction

PLASTIC FIBER CABLE ATTENUATION VS WAVELENGTH



GLASS FIBER CABLE ATTENUATION VS WAVELENGTH

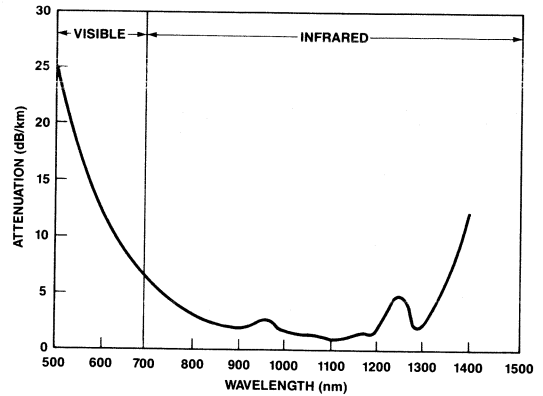
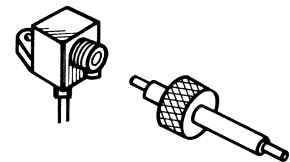
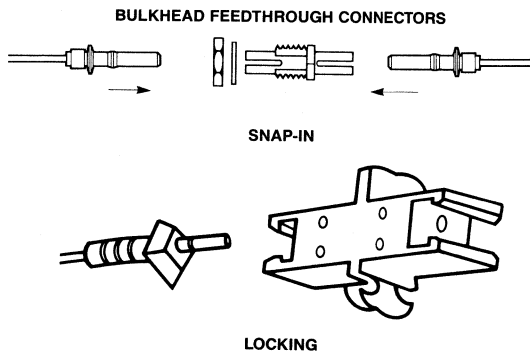
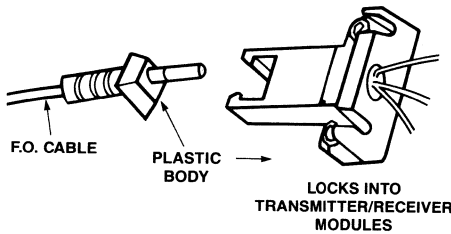
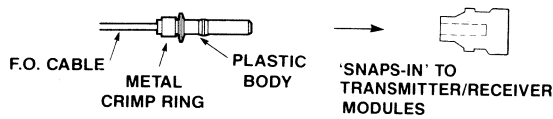
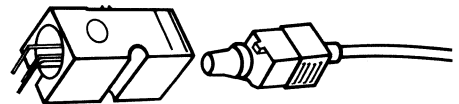


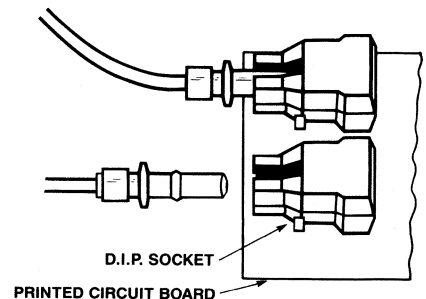
Figure 2. Attenuation Characteristics of 1000 Micrometre Plastic Fiber Optic Cable and 100/140 μm Glass Fiber Optic Cable vs. Wavelength



SCREW-IN STYLE PACKAGE



SNAP-IN STYLE PACKAGE



SNAP-IN STYLE PACKAGE INSERTED INTO CONVENTIONAL D.I.P. SOCKET

Figure 3. Various Plastic Fiber Optic Connectors

Figure 4. Various Plastic Fiber Optic Package Styles

TRANSMITTERS

An LED transmits optical energy in most plastic fiber optic systems. Light Emitting Diodes are simple, low cost, rugged, and proven reliable, as compared to most lasers. An LED which emits light in the visible range of 550 nm to 700 nm (green-red) will encounter the least cable attenuation, and drive up to 70 metres of plastic cable. These LED crystals are grown from GaP or GaAsP for green and red, respectively. GaAIAs technology has been recently developed, and has been found to exhibit higher electrical bandwidth and switching capabilities than GaP or GaAsP. Diffused PUP junction GaAIAs emitters can exhibit 3dB bandwidth capabilities of up to 40 MHz. However, the GaAIAs LED emits from 820-850 nm (infrared), and will support cable lengths under 10 metres due to the great increase of attenuation at that wavelength. Figure 2 will illustrate that longest distances (70 m) are possible with a 570 nm (green) LED, followed by the 665 nm (red) LED (30 m). Higher data rates (40 MBd) are achieved using a GaAIAs 820 nm (infrared) LED, provided the receiver has adequate electrical bandwidth, but only very short cable lengths are possible due to high cable attenuation at that wavelength.

RECEIVERS

All plastic fiber optic receivers provide a photon to electron interface, but range in complexity from discrete PIN photodiodes, phototransistors and photodarlington receivers to those which contain detector, amplifier, logic, and buffer circuitry all on one integrated circuit. There are tradeoffs encountered in receiver design. Discrete PIN detectors offer the fastest speed of response, with 3 dB bandwidth capabilities exceeding 50 MHz, but require external support circuitry to translate the low levels of photocurrent to useable TTL or CMOS logic standards. The response speed of a PIN photodiode is directly proportional to the reverse bias voltage, and must be considered, especially in five volt TTL designs. Photodarlington feature high sensitivity levels because of the two transistor configuration, but do so at the expense of response speed. Photodarlington are not directly compatible to TTL logic, because logic low output voltage exceeds the TTL defined threshold levels. If the fiber optic link is to be interfaced to TTL logic, direct compatibility with high fanout and response speed usually offers the designer the least overall cost and greatest ease of implementation.

COMPARISON BETWEEN PLASTIC AND GLASS FIBER OPTIC COMPONENTS

Now that a detailed description of plastic fiber optics is understood, a comparison to glass fiber optic components will be made. Plastic fiber optic components cost less than glass fiber optic components because of simpler cable construction, packages are molded plastic rather than precisely machined metal, and optical alignment between cable and optoelectronic interface is less crucial because of the larger diameter fiber core. Also, receiver design is simple because of lower (5 MBd) data rate expectations. Plastic cable lends itself well to installation because of its ruggedness and ease of connector attachment. Cable lengths are much shorter in plastic systems because of cable attenuation, and data rates are lower because of low cost fiber optic receiver design. Table 1 provides the reader with a summary of the differences between plastic and glass fiber optic systems.

FACTORY APPLICATIONS OF PLASTIC FIBER OPTIC COMPONENTS

Today, factories are becoming highly dependent on the use of electronic systems to perform several key operations. Fiber Optics has been proven effective in the factory environment, where its immunity to EMI has solved the problem of erroneous data transmission in the proximity of noisy electric motors and heavy equipment. Plastic fiber optics lends itself well to other "factory" applications as well — those regarding high voltage insulation.

Consider the AC motor. It's inexpensive, rugged design has made it the workhorse of American industry. The motor's speed, however, depends on the input electrical frequency. As a result, gear reduction systems have been used to create a "variable speed" motor, at considerable cost and inefficiency. In the area of AC motor control, CMOS logic circuitry can manipulate electrical power and vary its frequency, all with the turn of a dial^[1]. In Figure 5, the block diagram of a popular AC motor control system is shown. Note that the plastic fiber optic link protects the +12 volt CMOS logic from the +650 volt AC motor potential. The immunity of plastic fiber to electrical noise eliminates the concern of erroneous switching of the unit's power section. The short distance plastic fiber optic link permits the high voltage section of the controller to be physically separated from the logic section. In this particular application, plastic fiber optics offers improved performance, greater personal safety, and easier serviceability than previous solutions.

Slot interruptors are used in factory applications as card readers, position sensors, and explosion proof switches. For example, a fuel level monitor can be located inside a tank, where a spark would be hazardous. The electronic components can be located outside of the volatile environment, offering greater personal safety.

In automated machining operations, such as die press, drill press, lathe operations, and automatic welding, etc., a computer controls a piece of heavy equipment operating at high voltage potentials. A plastic fiber optic link that sends information from the control unit to the heavy equipment provides insulation and protection of the computer circuits from the high voltages present in the heavy equipment. Certain applications require two printed circuit boards to be referenced to different grounds, where differences in potential could be on the order of several thousand volts. A typical plastic fiber optic cable has an electrical conductivity of only 2 μ A/m at 50 kV, and therefore can provide a communications link between two systems operating at tremendous potential differences and prohibit the flow of electric current between the two.

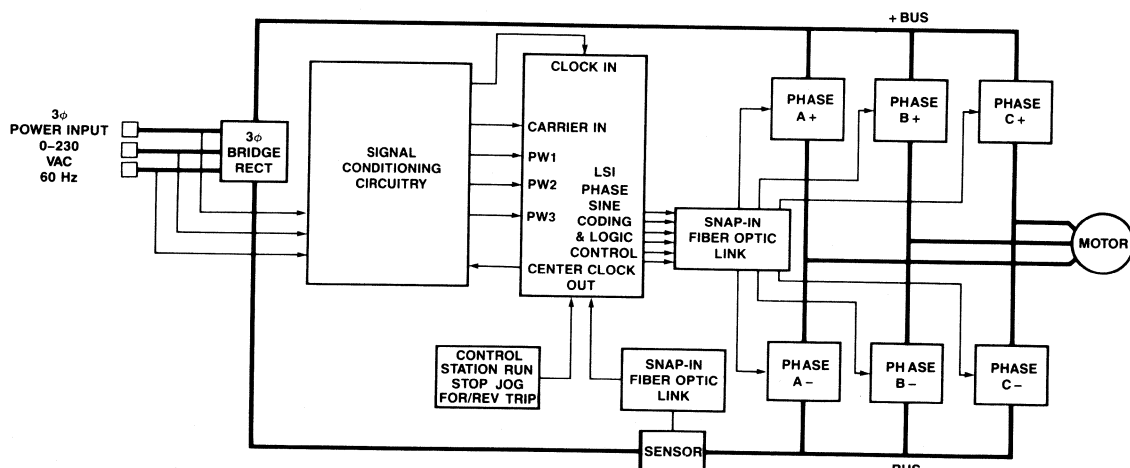
CONCLUSION

This discussion has presented a detailed description of plastic fiber optic components. A comparison between systems utilizing glass fiber optic products and plastic fiber optic products will allow the reader to effectively choose the appropriate technology to satisfy his needs. In particular, the discussion pertaining to factory applications of plastic fiber optic components illustrates the versatility of this rapidly growing technology.

PLASTIC
SNAP-IN
FIBER OPTICS

Table 1: Comparison between Plastic and Glass Fiber Optic Components

	PLASTIC	GLASS
COST	Low	Moderate to High
DISTANCE	Short (< 70 m)	Long (500 m to Several km)
DATA RATE	Low (D.C. to 15 MBaud)	High (D.C. to > 200 MBaud)
CONNECTOR COMPLEXITY	Low	Moderate to High
CABLE CONSTRUCTION	Plastic Clad Plastic Large Fiber Diameter Simple fiber, outer jacket	Glass Clad Glass or Plastic Clad Glass Small Fiber Diameter Complex fiber, buffer jacket, tensile strength members, outer jacket
TRANSMITTER	Visible LED (GaP, GaAsP) (570 nm — 700 nm) Near Infrared (GaAlAs) (820 nm — 850 nm)	Infrared LED (GaAlAs, In GaAlAs) (750 nm — 1550 nm)
RECEIVER	Simple TTL Interface	Simple to Complex TTL, ECL Interface



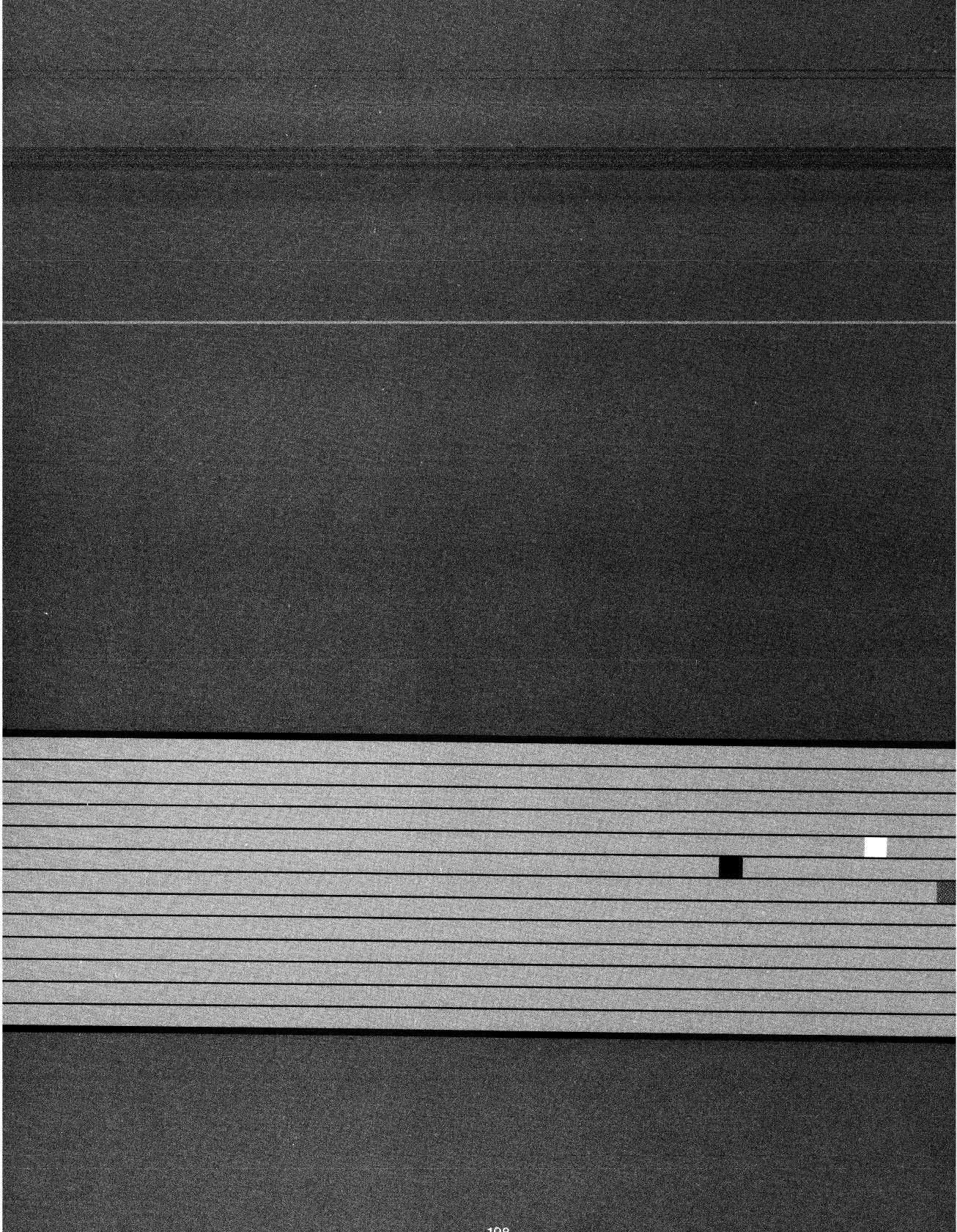
- PLASTIC FIBER OPTICS ISOLATES CMOS CONTROL LOGIC FROM HIGH VOLTAGE AC MOTOR
- PROVIDES GREATER LINE NOISE IMMUNITY, HIGHER DEGREE OF PERSONAL SAFETY, AND EASIER FIELD SERVICEABILITY

Figure 5. Block Diagram of AC Motor Control System Utilizing Plastic Fiber Optics

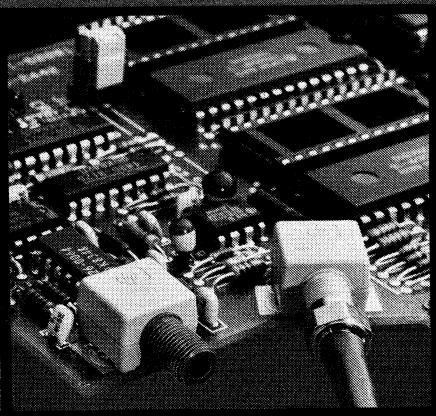
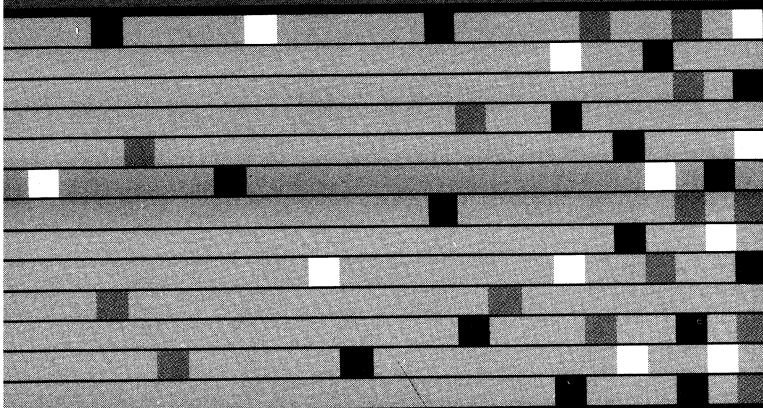
REFERENCES

1. Andreiev, Nikita, "Software Driven LSI Chips are Key to Future AC Drives", *Control Engineering*, November, 1981.
2. AMP Incorporated, *Designer's Guide to Fiber Optics*, AMP Incorporated, Harrisburg, PA, 1982.
3. Lombaerde, Robert, "Fiber Optic Data Link Snaps In Place", *Electronics*, McGraw Hill, November, 1982.
4. SAE Technical Paper Series, "Optical Link for Automotive Multiplex Wiring", February, 1984.
5. *Optoelectronics Designer's Catalog*, Hewlett-Packard Company, January, 1984.

Notes



*Low Cost, Miniature
Fiber Optic Components*



Low Cost, Miniature Fiber Optic Components

This family offers a wide range of price/performance choices for computer, industrial-control and military applications. The unique design of the lensed optical coupling system makes this family of components very reliable. The low cost, miniature line (HFBR-0400 series) features a

dual-in-line package which requires no mounting hardware or receptacle for use with SMA-style connectors. It is also specified for use with five fiber sizes: 100/140 μm , 85/125 μm , 62.5/125 μm , 50/125 μm , and 200 μm Plastic Coated Silica (PCS) cable.

Low Cost Miniature Link Family: Features — Dual-in-line package interfaces directly with SMA-style connectors specified for use with 50/125 μm , 62.5/125 μm , 85/125 μm , 100/140 μm , and 200 μm Plastic Coated Silica (PCS) cable. No mounting hardware required.

Products/Part Nos.	Description
Transmitter/Receiver Pairs	Guaranteed Optical Power Budget* Guaranteed Data-Rate*
HFBR-1402/2402	14 dB (200 μm PCS) 5 MBd
	9 dB (HFBR-3000 100/140 μm cable) 5 MBd
	6 dB (85/125 μm cable) 5 MBd
HFBR-1404/2402	9 dB (62.5/125 μm cable) 5 MBd
	4 dB (50/125 μm cable) 5 MBd
HFBR-1402/2404 (HFBR-0422 Transceiver Board)	12 dB (HFBR-3000 100/140 μm cable) 50 MBd
HFBR-1402 Standard Transmitter	Optimized for large size fiber such as 85/125 μm , 100/140 μm , or 200 μm PCS cable
HFBR-1404 High-Performance Transmitter	Optimized for small size fiber such as 50/125 μm or 62.5/125 μm cable
HFBR-2402 5 MB Receiver	TTL/CMOS Compatible receiver with -25.4 dBm sensitivity
HFBR-2404 25 MHz Receiver	PIN-preamp receiver for data rates up to 50 MBd

*Link performance at 25°C.



Using 200/PCS Optical Fiber with Hewlett-Packard Components

INTRODUCTION

In some applications, use of 200/PCS optical fiber has advantages over the standard HP 100/140- μm fiber ("200/PCS" stands for 200- μm core diameter Plastic Clad Silica.) Both fibers are used in local data communications with typical link lengths ranging from 100 to 2000 metres. By virtue of its larger core, it is easier to couple light into the 200/PCS fiber than the 100/140- μm fiber. On the other hand, the 200/PCS fiber has a higher attenuation (8.2 dB/km) and lower bandwidth (15-20 MHz-km) with an LED source.

The purpose of this Application Bulletin is to illustrate typical transmission distance using 200/PCS fiber and Hewlett-Packard fiber optic components. The HP Optoelectronics Designer's Catalog and Application Note 1000 ("Digital Data Transmission with the HP Fiber Optic System") provide further description and design aid.

DESIGN CONSIDERATIONS

A fiber optic system consists of a transmitter, receiver, cable, and connectors, as shown in Figure 1.

In this system, connector losses occur at each end of the link, as well as attenuation loss along the fiber itself. However, since Hewlett-Packard specifies transmitter power in the form of coupled power, i.e. useful optical power measured at the end of a 1 metre cable, loss at the transmitter end is already accounted for in the data sheet. Similarly the loss at the receiver end is included in the receiver sensitivity specification. If dispersion loss is small, the cable attenuation becomes the only system loss that a designer will have to deal with in

determining maximum transmission distance. In designing the actual system, care must be taken to ensure that enough optical power reaches the receiver, i.e. that it is not "under-driven." The following equation, which applies to any fiber optic system design, can be used to calculate a maximum link length.

$$P_T - \alpha_O l \geq P_R + \alpha_M \quad (\text{Eq. 1})$$

P_T = Transmitter Power (dBm) measured at the end of 1m cable

α_O = Fiber cable attenuation per length. (dB/km)

l = Cable length. (km)

$P_R(\text{min})$ = Minimum optical power required by receiver. (dBm)

α_M = Optical power margin set by user, should be > 1 dB.

TEST CONDITIONS

Empirical tests were performed using the 200/PCS fiber specified in Table 1. The cable was cut into two 1 metre lengths and connected on both ends with identical connectors.

Table 1. Test Cable Specifications

Core Diameter	200- μm
Outside Cladding Diameter	330- μm
Numerical Aperture, NA	0.4
Attenuation at 820 nm	8.2 dB/km
Bandwidth	20 MHz-km

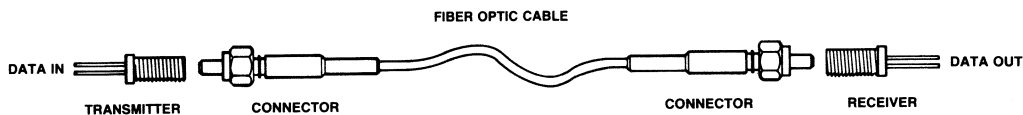


Figure 1. A Fiber Optic System.

These connectors are commonly used with 200/PCS fiber. The cable was connected according to manufacturer's specification.

Upon connecting, the fiber protective jacket was removed and an epoxy having a greater index of refraction than the cladding was used ($n = 1.394$). With the cladding modes thus stripped, the measured light was from the core only.

The test set up is shown in Figure 2. The links were connected to random samples of HP transmitters. Optical power was measured at the end of the 1 m links while operating the transmitters at various drive currents.

RESULTS

For each transmitter, measured and typical data sheet values of coupled power at 1 m are listed in Table 2.

Typical link lengths using each T/R pair can be obtained from Figures 3-9. These graphs are constructed with no optical power margin (α_M in Eq. 1 = 0).

Included in the test results is information on the performance of each T/R pair using HP 100/140- μm size fiber.

A review of the data will confirm the following points when comparing the performance of HP T/R pairs with 100/140- μm fiber and 200/PCS fiber:

- Hewlett-Packard transmitter and receiver specifications greatly simplify link design calculations.
- Transmitter coupled power is roughly 3 dB higher when using 200/PCS fiber, reflecting its advantage in coupling power due to larger core diameter and NA. In short distance applications this allows for more in-line connectors (splices) or lower LED drive current.
- Link distance is roughly 700 metres longer with 100/140- μm fiber, reflecting its lower attenuation.

The graphs (Figures 3-9) allow the designer to predict the typical value of optical power available from a given fiber at a specific length for a certain transmitter. All graphs are constructed from measured values.

Typical link lengths can be obtained by noting the intersection of the fiber attenuation line and the receiver sensitivity threshold. The x-coordinate of this point is the link length obtainable under typical conditions.

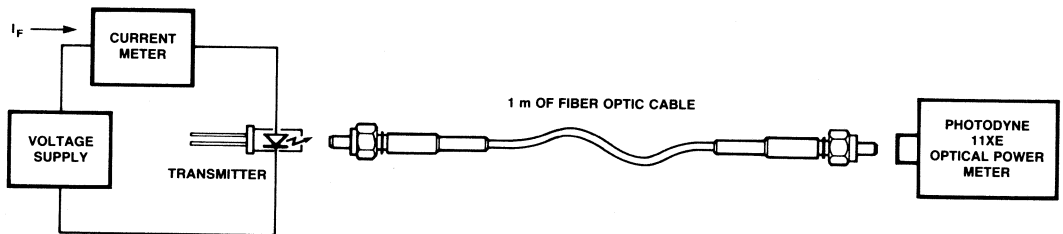


Figure 2. Test Set Up.

Table 2. Test Results

Transmitter	Cable/Connector [Note 1]	P_T (Measured)	P_T (Data Sheet Typical)	Link Length, Km [Notes 3, 6]	Conditions [Note 2]
HFBR-1002	100/140- μ m/ HFBR-4000	-13.3 dBm 47 μ W	-12.5 dBm 56 μ W	2.7	HFBR-2001 Receiver Used @ 10 MBaud $P_R = -31$ dBm
	200- μ m PCS/ Amphenol 906-120-5002	-13.1 dBm 49 μ W	-12.5 dBm 56 μ W	1.8	
HFBR-1201	100/140- μ m/ HFBR-4000	-14.6 dBm 3.5 μ W	-46.0 dBm 25 μ W	2.8	(Note 4) HFBR-2203/4 Receiver Used
	200- μ m PCS/ Amphenol 906-120-5002	-11.9 dBm .65 μ W	-15.5 dBm 28 μ W	2.2	
HFBR-1202	100/140- μ m/ OFTI 455B (SMA Style)	-16.4 dBm 23 μ W	-16.0 dBm 25 μ W	2.4	
	200- μ m PCS Amphenol 905-222-5000	-12.0 dBm 63 μ W	-15.5 dBm 28 μ W	2.2	
HFBR-1203	100/140- μ m/ HFBR-4000	-6.4 dBm 229 μ W	-7.4 dBm 182 μ W	4.3	I _F = 100 mA @ 10 MBaud $P_{R(min)} = -32.8$ dBm (Note 4) HFBR-2203/4 Receiver Used
	200- μ m PCS Amphenol 906-120-5002	-3.9 dBm 407 μ W	-5.9 dBm 257 μ W	3.2	
HFBR-1204	100/140- μ m/ OFTI 455B (SMA Style)	-7.6 dBm 174 μ W	-7.4 dBm 182 μ W	4.0	
	200- μ m PCS Amphenol 905-222-5000	-3.2 dBm 479 μ W	-5.9 dBm 257 μ W	3.2	
HFBR-1402	100/140- μ m/ OFTI 455B (SMA Style)	-11.5 dBm 71 μ W	-11.5 dBm 71 μ W	2.0	I _F = 60 mA $P_{R(min)} = -25.4$ dBm (Note 5)
	200- μ m PCS/ Amphenol 905-222-5000	-6.5 dBm 224 μ W	-6.5 dBm 224 μ W	1.9	
HFBR-1404	100/140- μ m/ OFTI 455B (SMA Style)	-7.1 dBm 195 μ W	-7.1 dBm 195 μ W	2.8	
	200- μ m PCS/ Amphenol 905-222-5000	-3.1 dBm 490 μ W	-3.1 dBm 490 μ W	2.4	
HFBR-1402	100/140- μ m/ OFTI 455B (SMA Style)	-11.5 dBm 71 μ W	-11.5 dBm 71 μ W	3.3	I _F = 60mA @ 10 MBaud HFBR-2404 Receiver Used $P_{R(min)} = -32.8$ dBm (Note 4)
	200- μ m PCS/ Amphenol 905-222-5000	-6.5 dBm 224 μ W	-6.5 dBm 224 μ W	2.8	
HFBR-1404	100/140- μ m/ OFTI 455B (SMA Style)	-7.1 dBm 195 μ W	-7.1 dBm 195 μ W	4.1	
	200- μ m PCS/ Amphenol 905-222-5000	-3.1 dBm 490 μ W	-3.1 dBm 490 μ W	3.2	

Notes:

1. The attenuation of the 100/140- μ m fiber used = 5.5 dB/km. The attenuation of the 200- μ m PCS fiber used = 8.2 dB/km @ λ 820 nm.
2. Tests were made at ambient temperature of 25° C and BER 10⁻⁹. For guaranteed operation at -40° C \leq T \leq 85° C. See HP Optoelectronics Designers Catalog for transmitter and receiver data sheets.
3. Link lengths are predicted using eq. 1, the measured value of P_T and the appropriate HP receiver and cable.
4. Reference Optoelectronics Designer's Catalog, 1985, Pg. 6-38 to 6-39.
5. HFBR-2402 receiver used.
6. A 3 dB optical power margin (α_m) is already included.

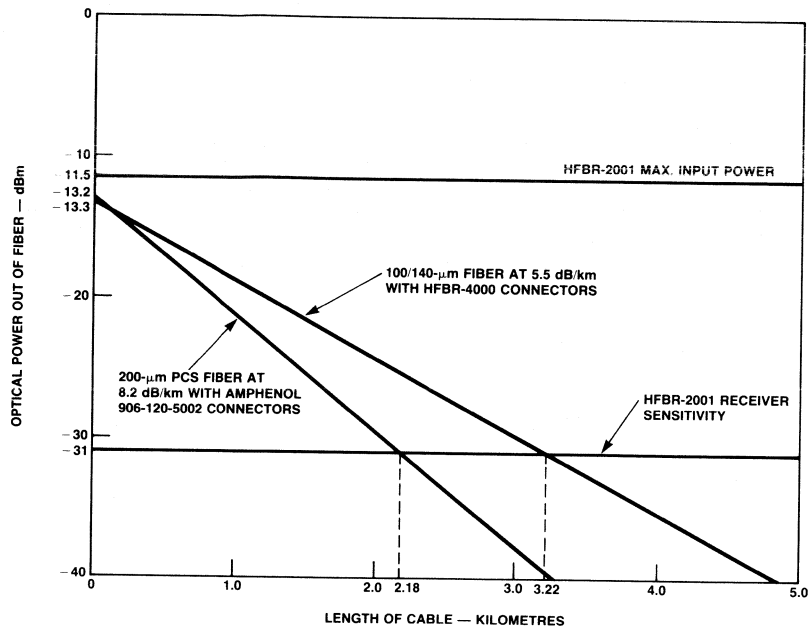


Figure 3. Expected Optical Power out of a Given Length of Cable using the HFBR-1002 Transmitter.

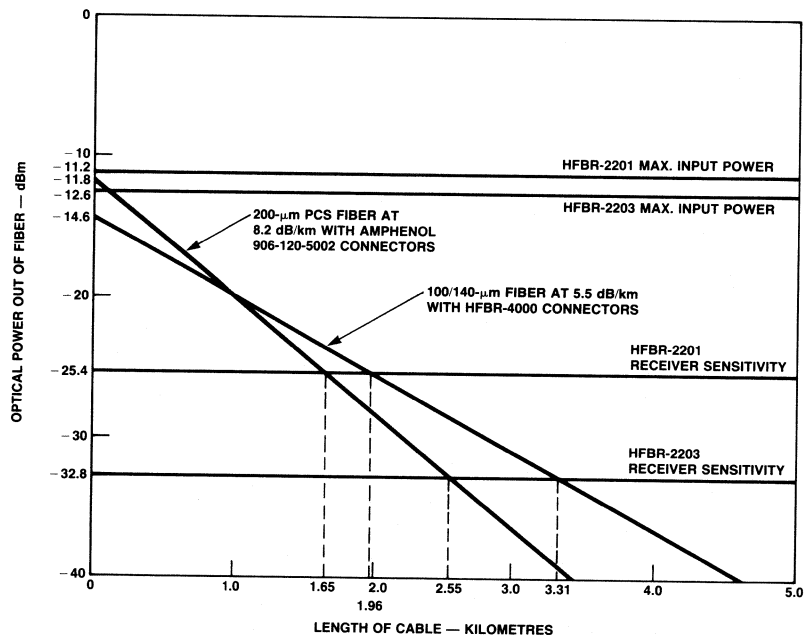


Figure 4. Expected Optical Power out of a Given Length of Cable using the HFBR-1201 Transmitter.

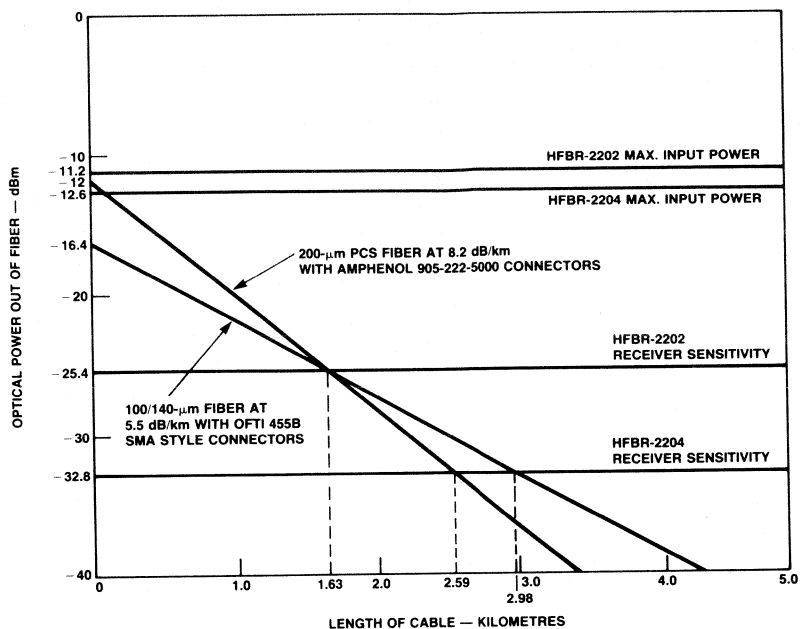


Figure 5. Expected Optical Power out of a Given Length of Cable using the HFBR-1202 Transmitter.

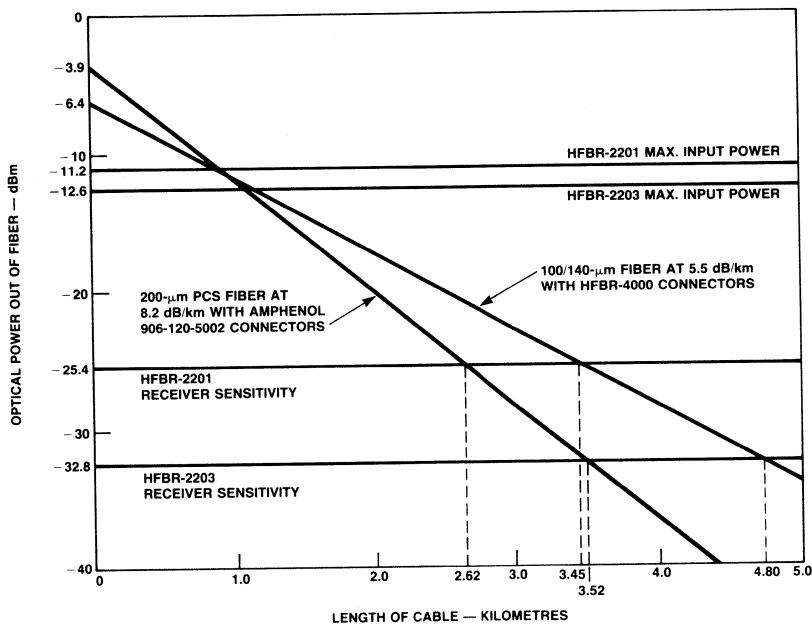


Figure 6. Expected Optical Power out of a Given Length of Cable using the HFBR-1203 Transmitter.

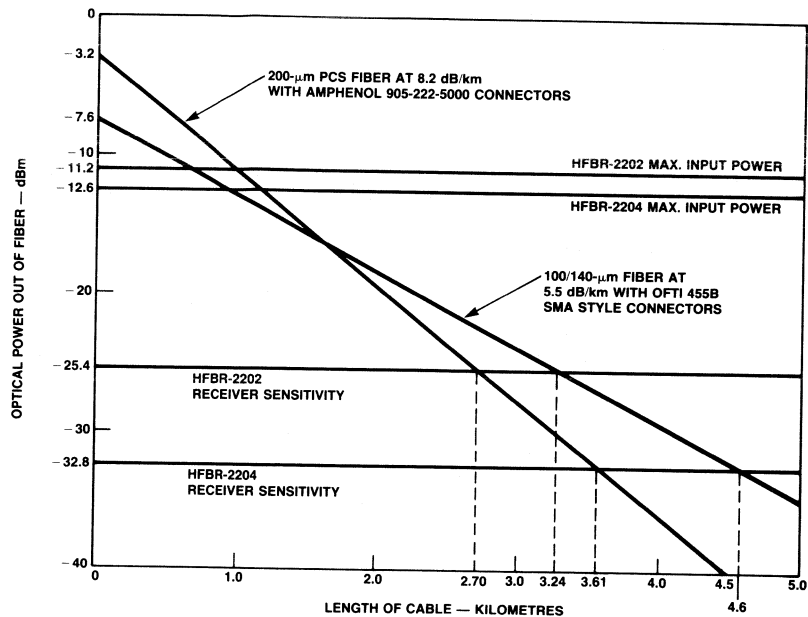


Figure 7. Expected Optical Power out of a Given Length of Cable using the HFBR-1204 Transmitter.

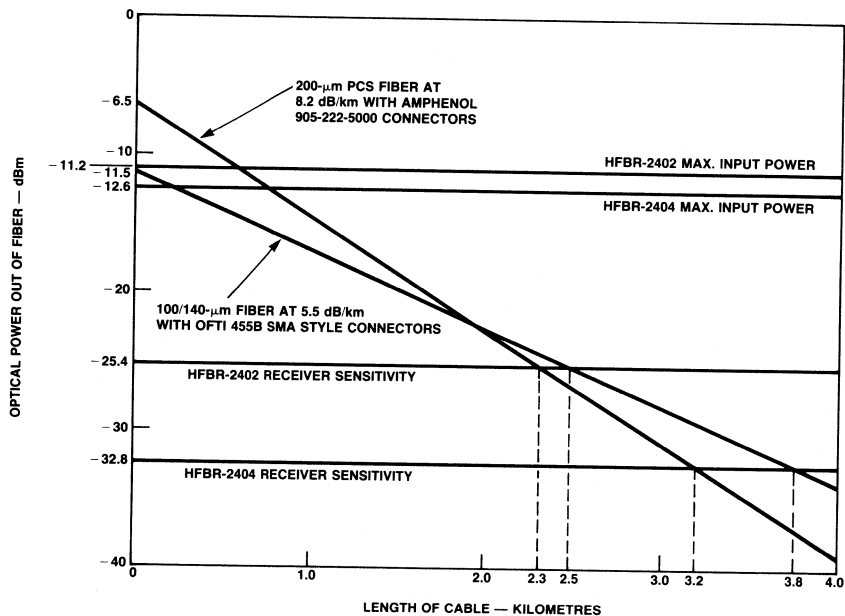


Figure 8. Expected Optical Power out of a Given Length of Fiber Using the HFBR-1402 Transmitter.

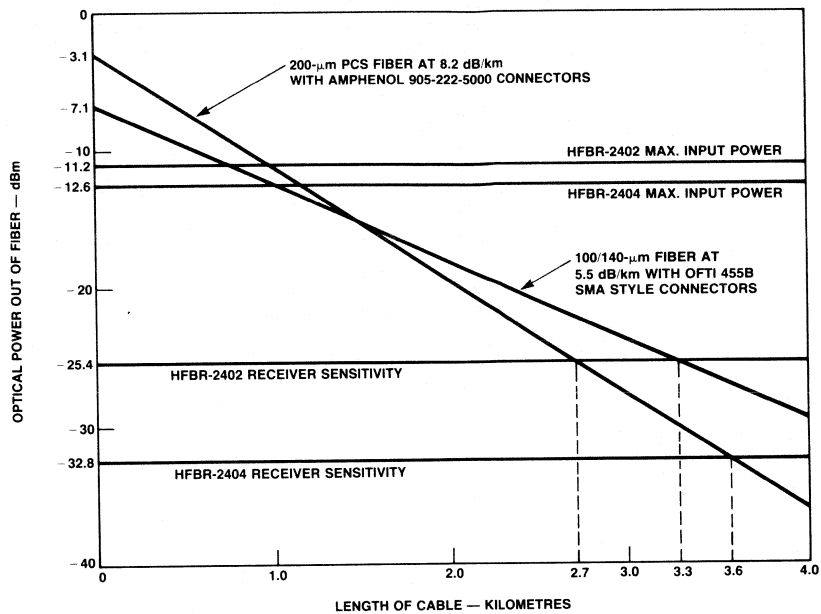


Figure 9. Expected Optical Power Out of a Given Length of Fiber Using the HFBR-1404 Transmitter.



Fiber Optic SMA Connector Technology

INTRODUCTION

The availability of low cost miniature fiber optic components such as HP's new HFBR-1402/1404 transmitter and HFBR-2402/2404 receivers increases the need for inexpensive, easily installed SMA connectors. This Tech Brief addresses the performance tradeoffs of different connecting techniques offered by the major SMA connector suppliers. The data for different connectors was gathered from published literature as of the date of this publication. For more comprehensive data regarding a specific connector, please contact the connector manufacturer directly.

CONNECTORING TECHNIQUES

There are a variety of connecting techniques but they all have the following basic steps in common:

1. Strip cable/clean the exposed fiber.
2. Fix the fiber in the connector ferrule (epoxy or crimp).
3. Anchor the cable strength members to the connector body to prevent direct stress on the fiber.
4. Prepare the fiber face to achieve a good optical finish (polish or cleave).

TRADEOFFS

The main tradeoffs are in steps 2 and 4. The fiber can be fixed in the ferrule using epoxy or mechanical crimping techniques, and the fiber face can be finished using polishing techniques or by simply cleaving the end of the fiber. Secondly, there are differences in materials and fabrication techniques among the various connectors. Die cast connectors offer the lowest cost, while machined or ceramic ferrule connectors offer the lowest coupling loss. Prices range from \$4 to \$5 for low cost connectors that have losses of 2 dB per splice, precision connectors that have losses on the order of 0.6 dB per splice can cost as much as \$25.

The use of epoxyless connectors or connectors utilizing cleave preparation of the optical interface results in reduced assembly time at the expense of larger performance variations over time relative to terminations that require polishing and epoxy. For a low cost, low loss rugged termination, it is still hard to beat the conventional SMA connector where the fiber is staked using epoxy. However, no polish and no epoxy connectors do provide an alternative that could be useful for rapid field repairs where the use of adhesives or polishing are impractical or impossible.

For further assistance in the selection of fiber optic SMA connectors, consult the handy table found on the reverse side of this page.

Table 1. Effects of Various Techniques on End User

	Epoxy	No Epoxy	Polish	Cleave
Installation Time	curing time required	reduction in assembly time	time required for polishing	reduction in assembly time
Tooling Required	heat gun	crimp tool	polishing fixture	cleaving tool
Electrical Power Required	yes	no	no	no
Optical Loss	lowest	higher loss	lowest	technique and tool dependent
Optical Loss Repeatability	high	lower	high	technique and tool dependent
Temperature Range	-20 to +70	restricted*	no effect	no effect
Mechanical Properties	most rugged SMA style	fiber pistons when temp. cycled*	no effect	no effect

Note: * Pistoning is affected by the connector design and the fiber type. For detailed temperature performance of a specific connector and fiber, please consult the connector manufacturer.

Table 2. Popular Connector Types

Manufacturer	Epoxy	No Epoxy	Polish	Cleave	Die Cast	Ceramic	Precision SMA	Fiber Type
AMP P.O. Box 3608 Harrisburg, PA 17105 Tel: (717) 564-0100	X		X					A, B, C
Amphenol/Bendix 2122 York Road Oak Brook, IL 60521 Tel: (321) 986-2300		#	X					A, B, C
Ensign-Bickford 16-18 Ensign Dr. Avon, CT 06001 Tel: (203) 678-0371		X		X				D
Interoptics 770 Airport Blvd. Burlingame, CA 94010 Tel: (415) 347-7727		X		X			X	A, B, C
Optelecom Inc. 15940 Luanne Dr. Gaithersburg, MD 20877 Tel: (301) 840-2121		X		X				A, B, C
Optical Fiber Technologies Inc. P.O. Box 148 Nutting Lake, MA 01865 Tel: (617) 663-6629	X	X	X		X	X	X	A, B, C
Radiall 101 Rue Philibert Hoffman Rosny Sous Bois 93116 France		X		X			X	C
Switchcraft Inc. 5555 N. Elston Ave. Chicago, IL 60630 Tel: (312) 792-2700		*		X				A, B, C

Notes:

- # denotes non epoxy adhesive required.
* denotes U.V. cured adhesive required.
- A denotes 50, 62.5, 85/125 μm GCS
B denotes 100/140 μm GCS
C denotes 200 PCS
D denotes Ensign-Bickford Hard Clad Silica



Fiber/Cable Selection for LED Based Local Communications Systems

INTRODUCTION

The purpose of this tech brief is to assist the first time fiber optic link designer with the selection of a fiber and cable for specific local communications applications. The data included here reflects fiber/cable performance at the time of publication and it is strongly recommended that the potential link designer contact the fiber/cable manufacturers directly to ensure that they obtain current product data.

COMMON FIBER TYPES

1. Glass clad silica (GCS)
 - Graded index
50/125, 62.5/125, 85/125, 100/140
(core cladding dia. in μm)
 - Single mode
2. Plastic clad silica (PCS)
 - 200 μm core dia.

FIBER TRADEOFFS

1. PCS has a larger core diameter and is capable of coupling a greater amount of power from the emitter into the fiber core, for a given numerical aperture, at the expense of higher attenuation and a lower modal bandwidth than GCS fibers. PCS is step index fiber since the index of refraction changes in a step function manner at the interface between the silica core and the plastic cladding.
2. Graded index GCS exhibits a higher modal bandwidth due to the gradually decreasing index of refraction from the center of the core to the cladding. This gradual reduction in the refractive index reduces the propagation time of high angle or skew rays since they propagate at higher velocities in the lower index material. This tends to equalize the time of arrival of all the rays at the end of the lightguide. As a result of the nearly equal propagation times for all modes, the pulses coupled into the fiber are not dispersed with respect to time when they reach the end of the fiber, provided a narrow spectral line width source, such as a laser, was used to produce the pulses. This reduction in modal dispersion of the optical pulses allows the use of graded index GCS fibers at higher data rates than step index PCS types.

3. Single mode GCS fiber minimizes dispersion caused by different propagation times for various modes, since the core diameter is so small that it will support only one mode of propagation. Single mode fiber is widely accepted in the long haul telecommunications field where the use of laser diodes and precision optical coupling combine to produce high performance systems. Reliable, lower cost LED emitters may be suitable for future use with single mode fiber as improved emitters and sensitive receivers are developed.

EFFECTS OF LED EMITTERS ON FIBER PERFORMANCE

Chromatic dispersion, caused by different propagation velocities for light of different wavelengths, is the dominant bandwidth limiting factor for LED driven fiber optic links since light emitting diodes have a broad emission spectrum, on the order of 40 to 60 nm full width at half maximum amplitude centered at 820 nm. When selecting a fiber the buyer should be aware of how the bandwidth, expressed in MHz-km, was determined. The bandwidth of a fiber measured using a narrow spectrum emitter, such as a laser diode, is the modal bandwidth. This will be higher than the chromatic bandwidth obtained using an LED. Both the wavelength and spectral width of the emitter used to drive a fiber will impact the final system bandwidth. A chromatic dispersion null which occurs in silica fiber at about 1300 nm, implies that pulse propagation near this wavelength will experience the minimum possible dispersion. Specifications for HP HFBR-3000 fiber reflect system performance that will be obtained using 820 nm LED sources. The effective bandwidth of fiber is a factor of both chromatic and modal bandwidth and can be calculated by using the following equation:

$$\text{B.W. FIBER} = \left[\frac{1}{\left(\frac{1}{\text{B.W. MODAL}} \right)^2 + \left(\frac{1}{\text{B.W. CHROMATIC}} \right)^2} \right]^{1/2}$$

COUPLED POWER VERSUS NUMERICAL APERTURE AND CORE DIAMETER

Numerical aperture (N.A.) is the sine of the cone half angle through which the fiber will accept light. Light incident on the fiber core at angles greater than this acceptance angle will not propagate through the fiber. Thus, fibers with a larger N.A. will have a higher coupled power since they will accept more of the high angle modes radiated from an emitter. Unfortunately the method used to measure the acceptance cone angle varies throughout the industry. The most common method of determining N.A. involves measuring the exit cone of light coupled out of a 1 to 2 metre section of fiber over the angle through which the intensity is $\geq 5\%$ of the peak intensity. However, some manufacturers specify N.A. as the sine of the half angle to zero intensity through a process of extrapolation. Hewlett-Packard specifies the N.A. of HFBR-3000 fiber in terms of links >500 metres in length, where the intensity in the exit cone must be $\geq 10\%$ of the peak intensity. This measurement is a better representation of long link fiber performance since the effective N.A. of long fibers is reduced to approximately 85% of the short length N.A. due to high order mode losses that approach a steady state value for fibers >500 metres in length. The power coupled into a specific fiber is related to the core diameter and numerical aperture of the particular fiber used. If the fiber is uniformly overfilled so that the N.A. and spot diameter of the emitter exceeds the N.A. and core diameter of the fiber, as is the case for the HP HFBR-1402/4 fiber optic transmitter, then the approximate change in the coupled power into a specific fiber relative to HFBR-3000 100/140 μm fiber can be determined as follows:

$$\Delta P_T = 20 \log \left(\frac{D_{\text{FIBER}}}{100 \mu\text{m}} \right) + 20 \log \left(\frac{\text{N.A.}_{\text{FIBER}}}{0.3} \right)$$

If the core diameter of the selected fiber is greater than the LED spot size, as is the case when 200 PCS is used with the HFBR-1402/4 transmitter, the increase in relative coupled power will be less than calculated by the above equation.

SELECTING A CABLE

The selection of the cable type is dependent on the configuration of the local communications system and the intended environment into which the cable will be installed.

- 1. Simplex duplex and multichannel fiber optic cables are available to meet the various local communications system requirements.
- 2. Plenum cables with Teflon® outer jacketing are available for industrial applications where cables are installed in open cable trays.
- 3. Armored cable is available for systems that require direct burial.
- 4. Flame retardant cables are available whose characteristics meet the UL VW-1 specifications.
- 5. Cables are available with loose and tight tube construction. Tight tube construction, where the fiber is in intimate contact with a plastic jacket, is better suited to installations where small bend radii are required and is slightly easier to connector than its loose tube counterpart. Loose tube fiber has better performance over temperature than tight tube cable. The intimate contact between the lightguide and the buffer materials in tight tube cable induces strain in the lightguide due to the dissimilar temperature coefficients of the plastic buffer and silica fiber that result in increased optical attenuation at low ambient temperatures.
- 6. Connector selection will be influenced by the type of cable chosen. The best resources to determine what connectors will fit a given cable are the cable and connector manufacturers listed in this publication and Tech Brief 101 which addresses SMA connector technology.

®Teflon is a registered trademark of the E.I. duPont Company.

Table 1. Typical Fiber Characteristics

	100/140 μm	85/125 μm	62.5/125 μm	50/125 μm	200 μm Core PCS
Attenuation (dB/Km) @ $\lambda_0 = 820 \text{ nm}$	3-10	3-6	3-6	2-10	5-50
Coupled PWR into 1 metre relative to 100/140 fiber using HP HFBR-1402/4 (dB)	0	-3.5	-5.0	-10.4	+5.0
Modal BW (MHz-km) @ $\lambda_0 = 820 \text{ nm}$	5-200	200	200	100-500	5-30
820 nm LED Chromatic BW (MHz-km)	50	50	50	50	50
Numerical Aperture	0.30	0.29	0.28	0.20	0.40

LOW COST
MINIATURE
FIBER OPTICS

Table 2. Suppliers Versus Cable Type

	GCS	PCS	Simplex	Duplex	Multi-Fiber	Flame Retardant	Plenum	Dir. Burial
Belden Wire & Cable 2000 S. Batavia Ave. Geneva, IL 60134 Tel: (312) 232-8900	X	X	X	X	X	X		X
Ensign-Bickford Industries Inc. 16 Ensign Dr. Avon, CT 06001 Tel: (203) 678-0371		X	X	X	X			
EOTec Corp. 420 Frontage Rd. West Haven, CT 06516 Tel: (203) 934-7961	X	X	X	X		X		X
FORT Fiber Optics Research & Technology 3767 Birch St. Newport Beach, CA 92660 Tel: (714) 852-9110	X	X	X	X	X			
General Cable Co. Fiber Optics Div. 160 Field Crest Ave. P.O. Box 7810 Edison, NJ 08818 Tel: (201) 225-4780	X		X	X	X	X	X	X
Hewlett-Packard Optical Communications 640 Page Mill Rd. Palo Alto, CA 94304 Tel: (415) 857-6560	X		X	X		X		
ITT Electro Optics Products Division 7635 Plantation Rd. Roanoke, VA 24019 Tel: (703) 563-0371	X		X	X	X	X	X	X
Pilkington Fiber Optic Technologies Ltd. Kimnel Park, Bodgwyddan, Rhyl Choyd LL 18 Sty. UK Telex: 61148	X	X	X	X				
Quartz Products Corp. P.O. Box 1347 Plainfield, NJ 07061 Tel: (201) 757-4545	X	X	X					
Siecor Corp. 489 Siecor Pk. Hickory, NC 28603 Tel: (704) 327-5000	X		X	X	X	X	X	X
Sumitomo Electric USA Inc. 551 Madison Ave. New York, NY 10022 Tel: (212) 308-6444	X		X	X	X	X		X

Baseband Video Transmission with Low Cost Fiber Optic Components

INTRODUCTION

The transmission of video signals over fiber optic links offers several advantages relative to comparable wire distribution systems. The immunity of fiber to external noise sources allows video to be transmitted over links that are located in electrically noisy environments such as factories. Some additional advantages that fiber has relative to wire are: no undesired phase shift that can distort chroma information in long transmission lines and no possibility of ground loops and reflections that can result from the improper termination of coax distribution systems. Fiber will inherently provide better picture quality in electrically noisy applications and is insensitive to termination changes made by system end users which can upset the performance of wire cable video distribution systems.

BASEBAND VIDEO TRANSMISSION

A simple baseband transmitter is shown in Figure 1. This circuit allows the transmission of high resolution baseband video since it has a 3dB bandwidth of 34 Hz to 20 MHz. An interesting advantage of this transmitter circuit is that modulation depth, which is the change in the LED current above and below its quiescent value, is unaffected by variations in LED forward voltage. The independence of LED forward voltage and modulation depth assures that the peak to peak amplitude of the optical signal produced by the transmitter will not be a function of the LED selected. The depth of modulation is an important parameter to control since this change in the peak to peak optical flux determines the amplitude of the analog output voltage at the receiver.

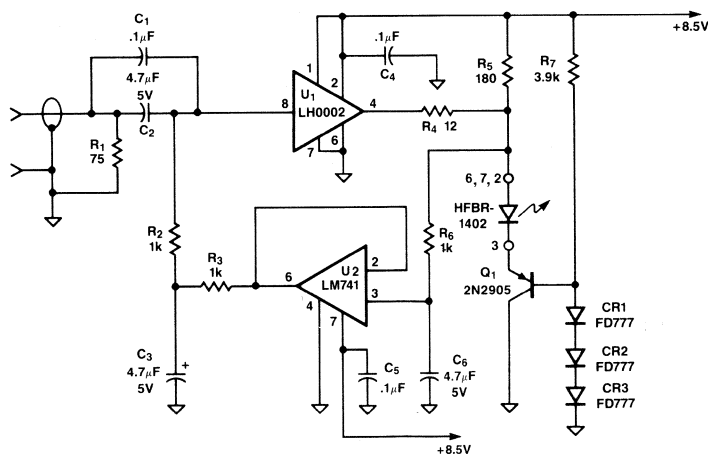


Figure 1. Analog Video Transmitter

LOW COST
MINIATURE
FIBER OPTICS

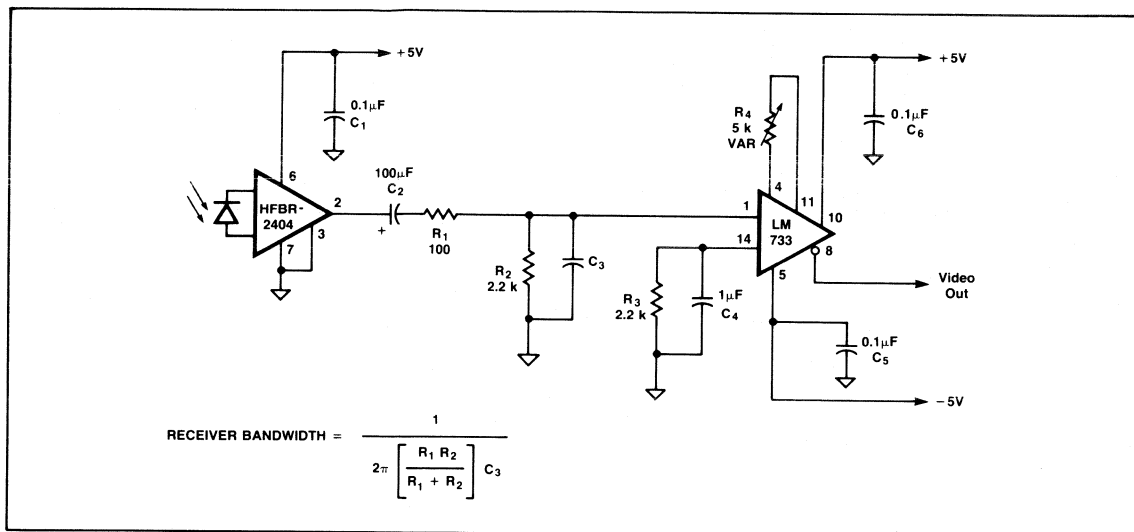


Figure 2. Video Receiver

The fiber optic receiver for the 20 MHz baseband video is shown in Figure 2. The gain of this receiver can be adjusted using potentiometer R4 for a standard 1 Vpp composite video output for distribution systems that vary from 1 metre to greater than 1k metres in length. Various alternatives to the LM-733 amplifier could be combined with a peak detector, a loop amplifier and a low pass filter to build a simple video receiver with AGC.

CONCLUSION

The prototype baseband fiber optic link shown in this Tech Brief was tested in a 25°C environment using H-P HFBR-3000 100/140 µm fiber cable and was capable of sending high quality color video signals over distances that varied from 1 metre to 2,300 metres.

High Performance Low Cost 3rd Generation Fiber Optic Components

INTRODUCTION

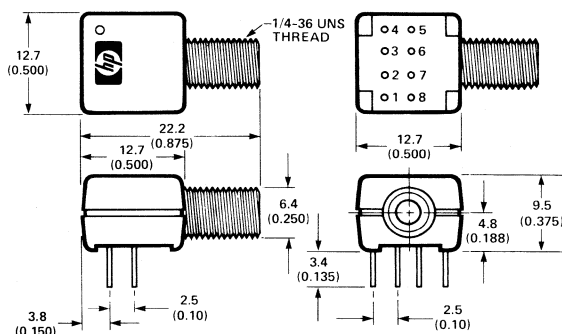
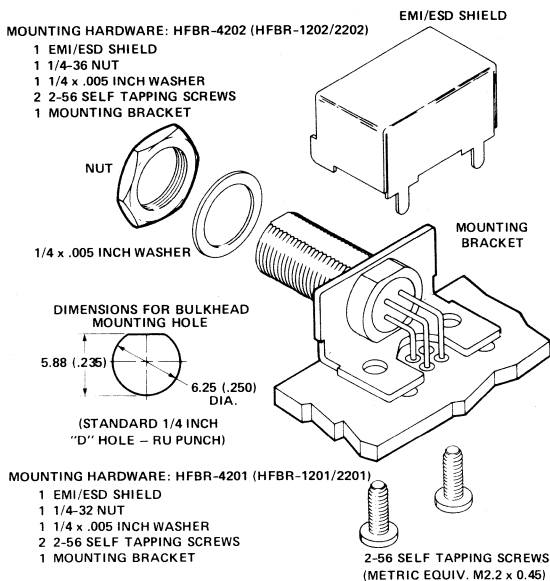
Hewlett-Packard first introduced fiber optic products in 1975 in the form of a line of hybrid modules which incorporated an internal encoding option. These modules required no external components and were designed for applications requiring maximum data rates of 10 MBd at distances up to 1.25 k metres.

The second generation of fiber optic components was the 0200 family of LED transmitters and receivers. The transmitters used in this family consisted of LED emitters that

were actively aligned in the metal housing of the optical port which allowed use of either the HP or SMA style fiber optic connectors. Receivers utilized the same metal housing as the transmitters and were available with a fully integrated TTL compatible output, or as a 25 MHz bandwidth PIN transimpedance preamplifier. In 1984 a new 0200 component was added to this line in the form of a PIN diode which can be combined with the appropriate supporting circuitry to enable designers to construct fiber optic receivers that have bandwidths in the hundreds of MHz region. The 0200 product line offers improved applications flexibility relative to the older hybrid modules, but an improved package was deemed necessary since the 0200 components required the assembly of the optical port, a supporting bracket, and a cover with associated mounting hardware thus requiring assembly techniques that are not compatible with automated manufacturing processes.

Enter the new 0400 low cost miniature fiber optic components from HP. The 0400 component family features a new high efficiency emitter that utilizes a sophisticated optical system and a high tech plastic package that significantly reduces the cost of high performance LED based fiber

LOW COST
MINIATURE
FIBER OPTICS



NOTE: ALL DIMENSIONS IN MILLIMETRES AND (INCHES).

Figure 1. Assembly of 0200 Components

Figure 2. One Piece 0400 Component Package

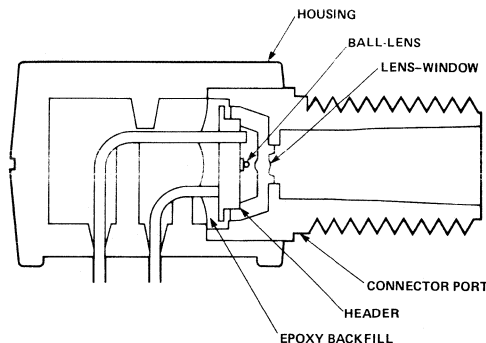


Figure 3. Improved SMA Optical Port

optic systems. These components require no assembly and feature a dual inline footprint that allows them to be installed in printed circuits using automated loading techniques.

This paper discusses the technical features of this exciting new line of fiber optic components and briefly reviews some possible applications circuits.

ADVANTAGES OF THE NEW 0400 COMPONENTS

One of the improved features of the 0400 product family is the high efficiency LED emitter which utilizes a sophisticated optical system to provide high coupling efficiency into fibers whose core diameters can vary from 50 to 200 μm . The optical system consists of a spherical lens that is attached to the cathode contact ring on the LED die and a lens window that is welded to the optical port by an ultrasonic process. The use of this multi element optical port allows the LED to be operated at lower forward current while maintaining high coupled power into the fiber. Operation of the LED at lower currents is allowed by the high coupling efficiency of the improved optical port which results in a significant improvement in the emitter reliability, since the MTBF of an LED is related to the forward current as shown in the following proportionality:

$$\text{MTBF} \propto (I_F)^N \exp(E_A/kT)$$

Improved reliability due to the lower drive currents allowed by the use of high efficiency optics is evident in initial tests which indicate that the HFBR-1402/4 transmitter will have an MTBF in excess of 2 million hours.

Materials used in the new 0400 package were chosen to produce a component that is both mechanically and environmentally rugged. This ruggedness is demonstrated by the fact that this new component family is specified to operate over a temperature range of -40 to $+85^\circ\text{C}$. In addition to a wide operating temperature range these new low priced plastic transmitters and receivers are mechanically quite rugged as exemplified by their ability to survive a mechanical shock of 1500G, vibrations of 50G peak from 20Hz to 2kHz, 500 reconnects, a side load of 1kg applied to the optical port and a connector securing torque of 6 kg-cm (5.25 in-lb) with no thread damage. Resistance of the low cost miniature package to solvents exceeds requirements set by MIL-STD-883C, however, HP recom-

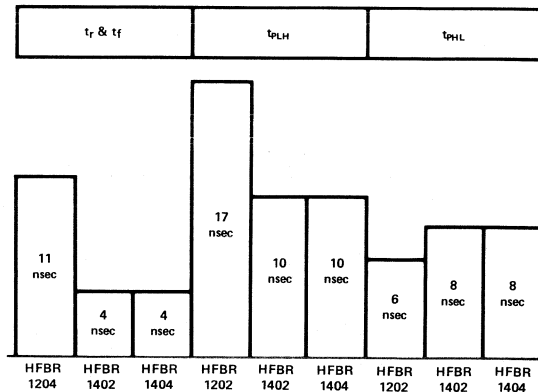


Figure 4. Relative Speed of LED Emitters

mends that the user avoid prolonged contact with solvents that fall into the category of partially halogenated hydrocarbons. Freon TF is considered to be a suitable solvent but it is recommended that specific solvents such as trichloroethene, methelene-chloride, chloroform, freon TMC, acetone and butyl cellusolve should be avoided since it is known that prolonged exposure to these substances will cause damage to the plastics used in the new 0400 package. To ensure the ruggedness of the bond that secures the spherical lens to the LED cathode metalization ring TO-46 headers to which the LED die and the lens had been bonded were subjected to a constant acceleration of up to 30kG with no failures. Additional reliability tests conducted on this new package include a penetrant dye gross leak test (Zygly test), a solderability test per MIL-STD-883C that subjects the part to lead temperatures of 260°C for 10 sec, accelerated life tests where the components are operated at maximum electrical stress at temperatures of 85°C , high temperature storage tests, thermal shock tests and an ESD (electrostatic discharge) test that subjects the part to static voltage stresses up to 10,000 volts. In addition to these tests HP will perform additional tests or select components to meet a specific customers need when this is possible and the dollar volume warrants such special testing.

The new HFBR-1402/1404 LED transmitter has excellent performance relative to previous HP miniature fiber optic components in terms of speed, coupled power and cost.

The rise fall times for the new HFBR-1402/1404 transmitter is typically 4.0 n seconds and has a worst case maximum value of 5.5 n seconds. This compares to typical rise fall times of 11 n seconds for the older HFBR-1204 Burrus transmitter. Another important parameter to consider when specifying a high speed emitter is propagation delay. The delay time between a positive current step applied to the LED and a corresponding step increase in the optical output is referred to as t_{PLH} and the delay between a negative current step into the LED and the resulting step decrease in the optical output is defined as t_{PHL} . An earlier HP LED transmitter, the HFBR-1202, had a specified t_{PLH} of 17 n seconds and a t_{PHL} of 6 n seconds. By comparison the new HFBR-1402/1404 transmitters have a t_{PLH} of 10 n

seconds and a t_{PHL} of 8 n seconds. The propagation delay and rise fall parameters are sensitive to the forward current through the LED. The data published in the HFBR-1402/4 data sheet was obtained at a forward current of 60 mA. Some reduction in the high speed performance of the emitter occurs as the forward current is reduced, however these effects can be minimized by using drive circuits that employ some form of current peaking or prebias. Suitable drive circuits, that optimize the high speed performance of the new HP fiber optic transmitters, will be discussed in detail in the applications portion of this presentation. The nearly equal propagation times from low to high and high to low coupled with the short rise fall times make these new fiber optic transmitters significantly faster than previous offerings, thus allowing designers to develop a new generation of high speed LED based local communications systems.

The new HFBR-1402/1404 transmitter has been designed for use with various fiber sizes that range from 50/125 up through 200PCS. Prior to development of the new 0400 transmitters, only the HFBR-1204 LED emitter had been specified into any fiber diameter other than 100/140. After the power coupled into a specific fiber of known core diameter and N.A. has been determined, the change in the coupled power into other fiber sizes can be calculated using the following equation:

$$\Delta P_t = 20 \log (D_2/D_1) + 20 \log (N.A.2/N.A.1) + \text{Fresnel loss}$$

The preceding expression assumes that the fiber is uniformly overfilled so that the N.A. and spot diameter of the emitter exceeds the N.A. and core diameter of the fiber, but since the optical flux is highly unlikely to remain at a constant intensity throughout the acceptance cone of the fiber, this equation will only provide the approximate change in the coupled power. The HFBR-1402/1404 transmitter allows the system designer to select any of the commonly available fiber types since the datasheet shows typical power coupled into 50/125, 62.5/125, 85/125, 100/140 and 200PCS fibers. By specifying the power coupled into various fiber sizes the difficulty associated with determin-

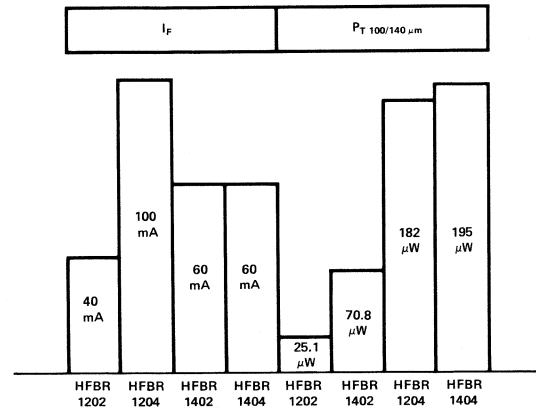


Figure 5. Relative Efficiency of LED Emitters

ing the coupled power when different fiber sizes are used is avoided, this allows potential link designers to choose the fiber type that best fits their particular application without the need to expend considerable effort to determine what coupled power will result. In addition to the ease of design these new emitters outperform older HP LED's by coupling a greater amount of optical power into the fiber than previously possible while using less current. The most dramatic increase is evident when the power coupled into 50 μm fiber is examined. The HFBR-1204 typically coupled -19.1 dBm into 50 μm core fiber at an I_F of 100 mA while the new HFBR-1404 couples -17.5 dBm in for a 1.7 dB increase at a lower I_F of 60 mA.

Another critical area where these new plastic components have an advantage over the older metal case miniature components is in the area of pricing. The HFBR-1402 couples 6.5 dB more power into a fiber than the HFBR-1202 at a cost reduction of 77% of the price of the older part. The higher powered HFBR-1404 has an advantage over the older Burrus LED emitter in both coupled power and speed at a cost that is less than 43% of the HFBR-1204 pricing. The receivers used in the new 0400 series components are the same I.C.s that were used in the older 0200 component family. Due to the lower cost to manufacture these components in the plastic package the HFBR-2402, which is the equivalent of the HFBR-2202, costs only 57% as much while the HFBR-2404 equivalent of the older HFBR-2204 is available for 59% of the price of its metal case predecessor.

APPLICATIONS FOR LOW COST F.O. COMPONENTS

Applications engineering at HP Optical Communications Division has expended considerable effort to support the new low cost high performance 0400 components. The introduction of this new product line has resulted in increased efforts to develop better digital drive circuitry that will take advantage of the improved high speed characteristics of the HFBR-1402/1404 emitter. In addition to new digital drivers, an improved method of analog current modulating LED transmitters for baseband analog transmission was developed. For the receiving end of the video link Applications has developed a preliminary analog receiver that uses the HFBR-2404 and has additional support circuitry that produces an AGC function. In addition to these circuits work is ongoing to develop support circuitry

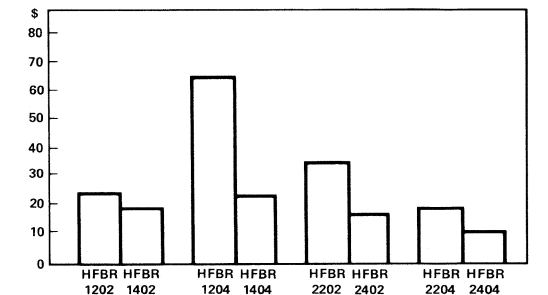
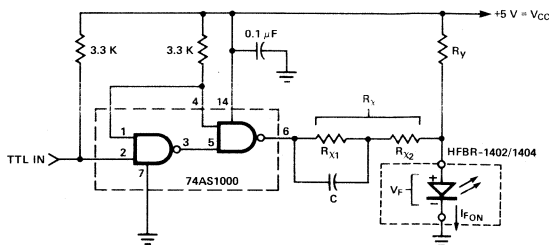


Figure 6. Relative Cost of Fiber Optic Components

LOW COST
MINIATURE
FIBER OPTICS



$$R_Y = \frac{(V_{CC} - V_F) + 6.6 (V_{CC} - V_F - 1.4 V)}{I_{FON}}$$

$$R_X = \left(\frac{R_Y}{6.6} - 10 \Omega \right)$$

$$R_{X1} = \frac{R_X + 10 \Omega}{2}$$

$$R_{X2} = R_{X1} - 10 \Omega$$

$$C = \frac{2.0 \text{ nsec}}{R_{X1}}$$

Figure 7. 74AS1000 LED Drive Circuit

that will linearly modulate LED transmitters for multi-channel video applications, and continuing effort is also being spent to make digital receivers using the HFBR-2404 that will work at data rates up to 50 MBd. For digital links faster than 50 MBd OCD Applications can provide supporting literature that explains how to use the HFBR-2208 PIN detector to construct optical receivers with bandwidths in the hundreds of MHz.

Some specific examples of the circuits developed to support the new line of plastic components are as follows. The circuit shown in Figure 7 is a high speed digital driver implemented using an I.C. that costs approximately 50 cents that has a pulse width distortion of less than 15% at a data rate of 120 MBd. Figure 8 shows the steady state response of the driver implemented using the 74AS1000 quad two input nand line driver.

The excellent performance of this drive circuit is substantiated when the impulse response as shown in Figure 9 is examined revealing that there is no readily observable change between the impulse and steady state response of the optical output. Careful scrutiny of the waveforms reveals that some subtle changes do however occur during the impulse test. The observed t_{PLH} of the combined driver and LED remain constant between the steady state and the two impulse conditions, but a slight reduction in t_{PHL} from 12.5 n seconds to 11.5 n seconds occurs when the output is held low for a long period of time and then briefly pulsed high.

Another change in response that at first might not be apparent is a .5 n second increase in the rise fall times that occurs when the output is held high for a long period of time then briefly pulsed low.

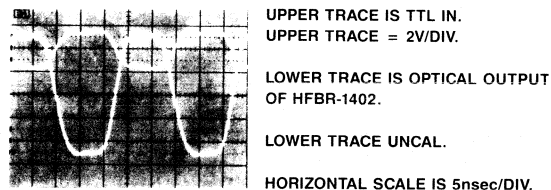


Figure 8. Steady State Response of 74AS1000 Drive Circuit

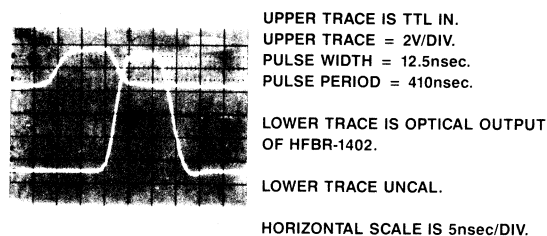


Figure 9a. Positive Impulse Response of 74AS1000 Drive Circuit

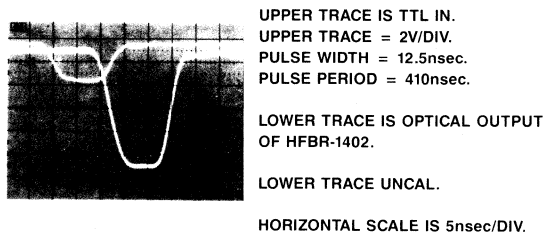
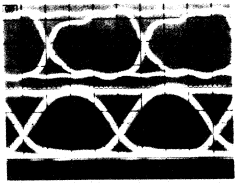


Figure 9b. Negative Impulse Response of 74AS1000 Drive Circuit

Observations of the total eye closure that results due to changes in propagation distortion and rise fall times for the 74AS1000 LED driver indicate that pulse width distortion will typically be 15% at 120 MBd as shown in Figure 10.

A drive circuit similar to the one just discussed can be constructed using the 74F3037 quad two input nand line driver as shown in Figure 11. Small changes in the network connecting the line driver totem pole output to the LED will be required to compensate for the higher pull up output impedance and slower edge speeds of the 74F output stages. Driving the HFBR-1402/1404 LED transmitter with the 74F3037 also allows operation at 120 MBd with

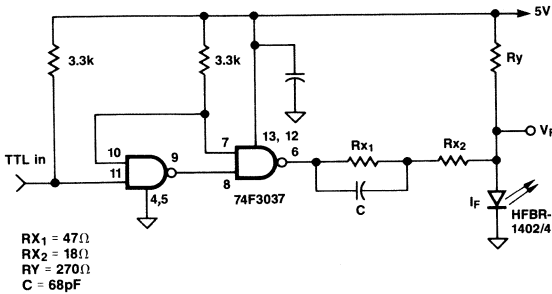


TTL INPUT TO
74AS1000 TRANSMITTER
UPPER TRACE 1V/DIV
LOWER TRACE UNCL
HORIZONTAL 2nsec/DIV

OPTICAL OUTPUT OF
HFBR-1402/4 AT
120MBd MEASURED
USING AN HP 81519A
OPTICAL RECEIVER

$R_{X1} = 47\Omega$; $R_{X2} = 33\Omega$; $R_Y = 287\Omega$; $C = 43\text{pF}$

Figure 10. 120 MBd Eye Pattern for the 74AS1000 Drive Circuit



$R_{X1} = 47\Omega$
 $R_{X2} = 18\Omega$
 $R_Y = 270\Omega$
 $C = 68\text{pF}$

Figure 11. 74F3037 LED Drive Circuit

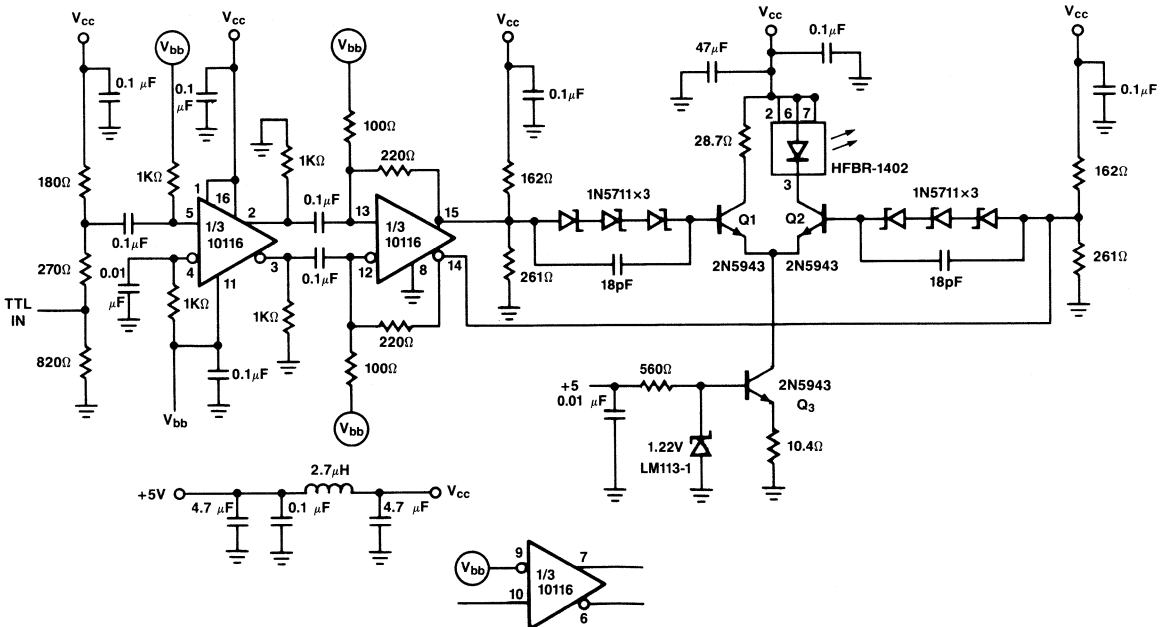


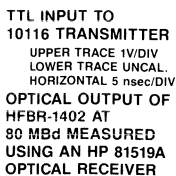
Figure 12. Constant Supply Current LED Driver

typical pulse distortion of 5% and total propagation delay from digital input to optical output is on the order of 1 n second less than possible with the 74AS1000 due to the shorter internal delay of the 74F gates.

An alternative drive circuit that uses the 10116 ECL line receiver can be implemented as shown in Figure 12. This circuit is complex when compared to the TTL line drivers discussed in the previous sections but has the advantage of drawing a constant current from its power supply regardless of whether the LED is on or off. This constant power requirement substantially reduces the chances of undesired crosstalk from the transmitter to the receiver when these components are mounted close to one another as required by many system configurations such as full duplex or LAN applications. The performance of this circuit is shown in Figure 13 which shows the eye pattern for this transmitter as measured at 80 MBd.

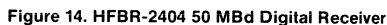
Digital receivers using the HFBR-2402 will work for both level and edge coded data at speeds up to 5 Mb/s. The HFBR-2402 is a complete DC coupled receiver that requires one external pull up resistor to interface to TTL logic. If the output of the HFBR-2402 is to be interfaced to a higher voltage logic such as CMOS, the open collector output of this receiver can be pulled up to the desired logic families positive supply using an external resistor, provided that the 25 mA maximum collector current rating is not exceeded.

LOW COST
MINIATURE
FIBER OPTICS



For data speeds up to 50 MBd the HFBR-2404 analog receiver combined with a simple external quantizing circuit will produce a low cost simple digital receiver. The circuit shown in Figure 14 produces an inexpensive TTL compatible receiver that will yield a BER $< 10^{-9}$ for an average optical flux input of ~ 30.8 dBm.

emitter configured as a linear analog transmitter suited for use in a local area communications of baseband video or other small signal linear information. The 3 dB bandwidth of



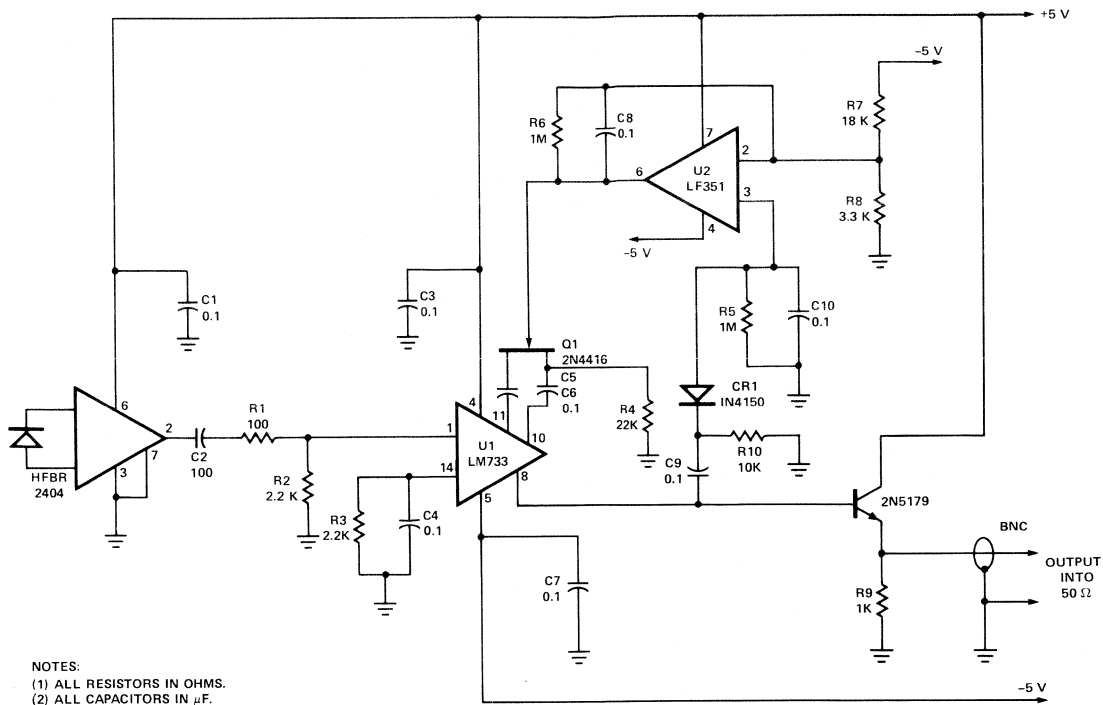


Figure 16. Prototype Analog Receiver with AGC

this particular transmitter is 27 Mhz as limited by the LH-0002 analog driver. Total harmonic distortion measured for a 1 Vpp sine wave input was 2.2% at a frequency of 5 MHz.

This transmitter can be combined with the circuit shown in Figure 16, which uses the HFBR-2404 PIN preamplifier, to make an analog receiver which allows construction of systems capable of transmitting baseband analog signals. Variations in the link length are accommodated by varying the gain of the LM-733 video amplifier with an AGC loop comprised of a peak detector, loop error amplifier and an N channel junction type FET operated below pinchoff to form a voltage controlled resistance. The performance of this receiver is sufficient to allow link length variations, from 1 metre to 2.33 k metres, when used with the transmitter circuit described earlier. This receiver is not an optimal design and is only intended to demonstrate the feasibility of constructing an analog receiver using the HFBR-2404. Improved performance relative to what has been discussed here should be possible with a carefully designed receiver that has a post amplifier with a higher gain than the LM-733. This is so since the receiver discussed here is not noise limited, but has insufficient gain to produce the 1 Vpp required for NTSC composite video output when used with fiber links in excess of the 2.33 k metres.

A transmitter that utilizes current feedback can be implemented, as shown in Figure 17, for systems that require improved linearity by using discrete transistors. This ver-

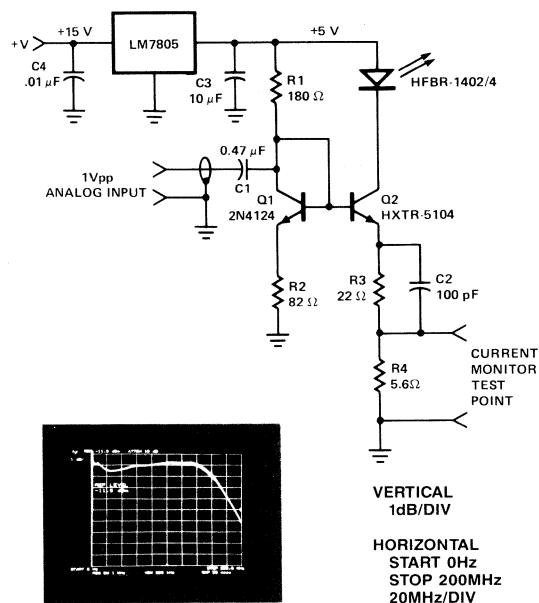


Figure 17. Wideband Linear LED Transmitter

sion of the analog transmitter has a 3 dB bandwidth of 180 MHz and a low distortion factor due to the large amount of current feedback inherent in this type of scaled current mirror LED driver. The clean linear response of this prototype LED driver combines with the wide bandwidth of the circuit shown in Figure 17 to make this transmitter a suitable candidate for use with frequency division multiplexed analog signals without introducing excessive intermodulation distortion thus allowing the transmission of 36 simultaneous television channels over one LED driven fiber optic link.

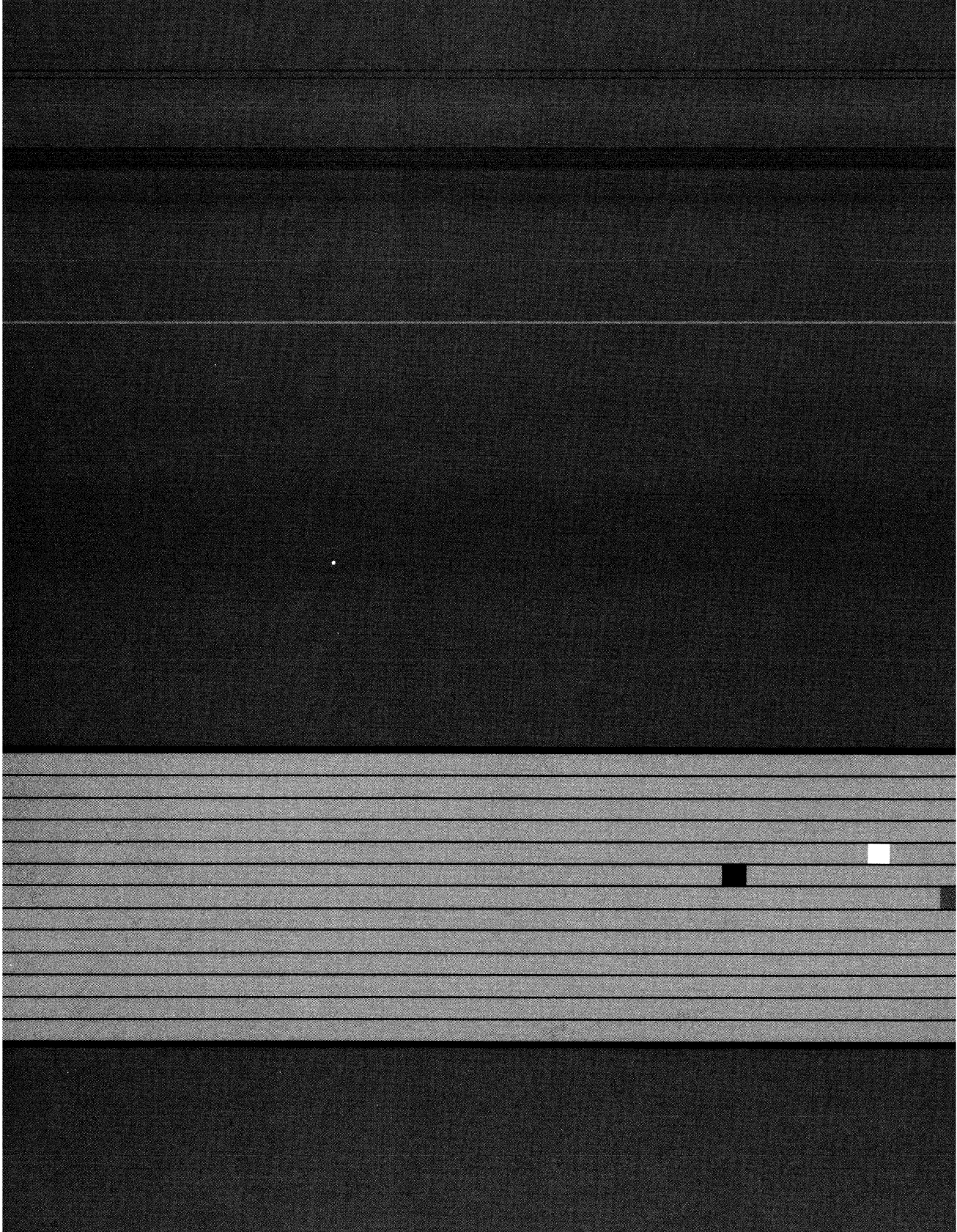
PUBLICATIONS AND TECHNICAL TRAINING

In addition to all the support circuitry that was developed for the new 0400 family of transmitters and receivers, the OCD applications department has written two new short form publications that address cable and connector selection to assist the first time user of fiber optic components. Tech Brief 101 discusses the latest in SMA connector technology and Tech Brief 102 addresses issues related to selection of fiber and cable for use in local communications systems. To further reduce the time required to select

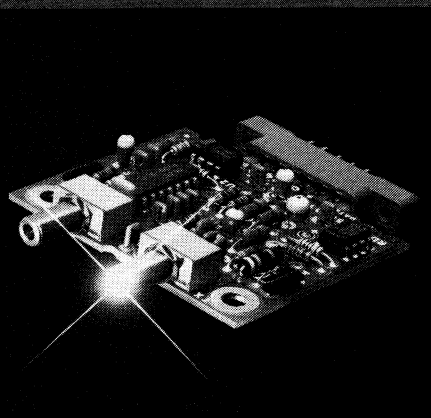
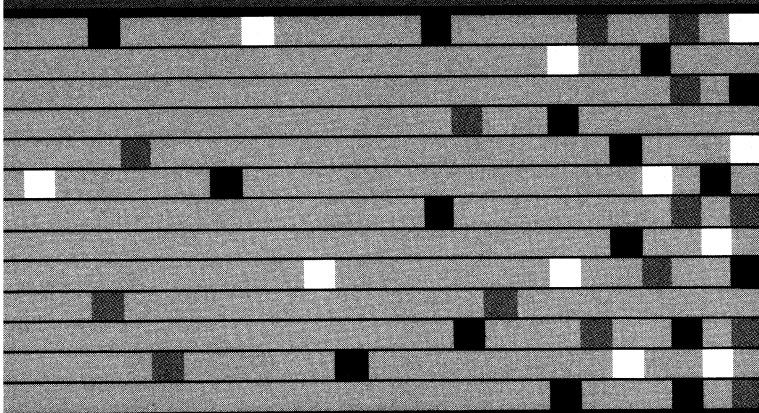
a cable or connector, these two tech briefs contain a contact matrix showing the addresses and phone numbers of the various manufacturers versus the types of products offered. Tech Brief 101 and 102 are just the beginning; users of the 0400 family of fiber optic components can look forward to continued support for these new components in the form of future application notes and tech briefs.

The Applications Engineering Department at HP Optical Communications Division is interested in assisting potential users of the new low cost 0400 family of products with their specific system design problems. Hewlett-Packard's determination to improve local communication products is demonstrated by the seven years of commitment required to get from the first generation hybrid modules to the new low cost high performance components. For the latest information regarding HP fiber optic components contact your local HP sales representative who will be able to provide the latest product or applications information. Hewlett-Packard's experience with fiber optics is also available through an ongoing seminar program conducted by the OCD Applications department that is accessible by contacting your local HP Components Field Service Engineer for the time and place of future seminars.

This image shows a full page of blank, lined paper. It features approximately 28 horizontal black lines spaced evenly across the page, typical of standard notebook paper. The lines are thin and extend from the left edge to the right edge. There is no handwriting or other markings on the page.



*Miniature
Fiber Optic
Components*



Miniature Fiber Optic Components

The standard miniature line (HFBR-0200 series) features a precision metal package for rugged applications. Both HP-style and SMA-style connectors are available for this line. An evaluation kit is available for sampling purposes. The HFBR-0200 kit contains transmitter, receiver, 10 metres of cable and technical literature.

Miniature Link Family: Features — Glass fiber (100/140 μm). Precision metal connectors.

Products/Part Nns.	Description
Evaluation Kit HFBR-0200	HFBR-1201 Transmitter, HFBR-2201 Receiver, 10 metre connected cable Mounting Hardware
Transmitter/Receiver Pairs HP Style Connectors SMA Style Connectors HFBR-1201/-2201 HFBR-1202/-2202 HFBR-1201/-2203 HFBR-1202/-2204 HFBR-1203/-2201 HFBR-1204/-2202 HFBR-1203/-2203 HFBR-1204/-2204 HFBR-1203/-2207 HFBR-1204/-2208	Guaranteed Distance* Guaranteed Data Rate* 800 metre 5 MBd 1200 metre 40 MBd 1800 metre 5 MBd 2100 metre 40 MBd 500 metre (typical) 125 MBd (typical)
Transceivers, 20 MBd (to 40 MBd) HP Style Connectors SMA Style Connectors HFBR-0221 HFBR-0222 HFBR-0223 HFBR-0224	Guaranteed Distance Data Format 1100 metre 33 to 67% duty factor (for use with code schemes such as Manchester) 625 metre STD 95% duty factor (for use with code schemes such as NRZ)
Cables Simplex Duplex HFBR-3000 HFBR-3100 (OPT001) (OPT001) HFBR-3000 HFBR-3100 (OPT002) (OPT002) HFBR-3200 HFBR-3300 HFBR-3001 HFBR-3021	Customer specified length, connected (HFBR-4000 connector) Customer specified length, connected (SMA style connector) Customer specified length, unconnected 10 metres connected (HFBR-4000 connector) 10 metres connected (SMA style connector)
Connectors HFBR-4000 HFBR-3099	Metal body, metal ferrule Connector-connector junction, bulkhead feedthrough for HFBR-4000 connector
Connector Assembly Tools HFBR-0100 HFBR-0101 HFBR-0102	Field installation kit for HFBR-4000 connectors (includes case, tools, consumables) Replacement consumables for HFBR-0100 Kit Custom tool set only
Mounting Hardware HFBR-4201 HFBR-4202	PCB mounting bracket, EMI shield, misc. hardware for HFBR-1201/-1203/-2201/-2203 PCB mounting bracket, EMI shield, misc. hardware for HFBR-1202/-1204/-2202/-2204

*Link performance at 25°C.



Using 50/125 μm Optical Fiber with Hewlett-Packard Components

INTRODUCTION

In some applications, 50/125 μm size optical fiber may be more advantageous to use than 100/140 μm size optical fiber. 100/140 μm fiber is used primarily in the local data communications area where link lengths typically run anywhere from 500 metres to 2000 metres. 100/140 μm fiber, having a larger core diameter, is easier to launch light into but the attenuation per unit length is higher than the 50/125 μm . The 50/125 μm fiber, having a lower attenuation per unit length, is used more in the telecommunications area where links typically run several kilometres.

Tests were made with three HP metal packaged fiber optic transmitters using 50/125 μm fiber, and this application bulletin documents those test results to aid in designing a fiber optic system using 50/125 μm fiber. Use of this bulletin in conjunction with the HP Optoelectronics Designers Catalog and Application Note 1000, "Digital Data Transmission with the HP Fiber Optic System", is suggested to help in understanding, in more detail, the design parameters required to determine typical transmission distance.

A fiber optic system is defined as a transmitter, receiver, cable and connectors as shown in Figure 1.

In constructing a system, there are optical and mechanical losses incurred at the transmitter to connector interface, the connector to receiver interface, and there is also the steady state cable attenuation which contributes to losses. In using 50/125 μm size fiber with HP components, as will be shown, most of the coupling losses occur at the trans-

mitter to connector interface. This is where tests were made, to determine what the typical losses are. Using the data from these tests, a full system performance can be predicted.

In designing a fiber optic system, concern must be taken to ensure enough optical power will reach the receiver for it to operate correctly. The following equation is used to predict losses and an expected link length. The equation applies to any fiber optic system design.

THE OPTICAL POWER BUDGET

$$10 \log \frac{\Phi_T}{\Phi_R} \geq \alpha_o \ell + \alpha_{TC} + \alpha_{CR} + \alpha_M \quad (1)$$

The optical power ratio should be greater than or equal to the system losses.

Φ_T = Optical power available from the transmitter (μW)

Φ_R = Minimum optical power required by the receiver (μW)

$$10 \log \frac{\Phi_T}{\Phi_R} = \text{Optical power ratio} \quad (\text{dB})$$

System Losses	{	$\alpha_o \ell$ = Steady state fiber loss	(dB/km · length)
		α_{TC} = Transmitter to connector coupling loss	(dB)
		α_{CR} = Connector to receiver coupling loss	(dB)
		α_M = Optical power margin (set by user, should be > 1 dB)	

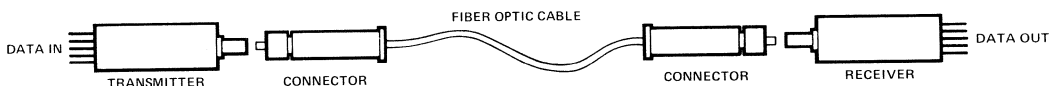
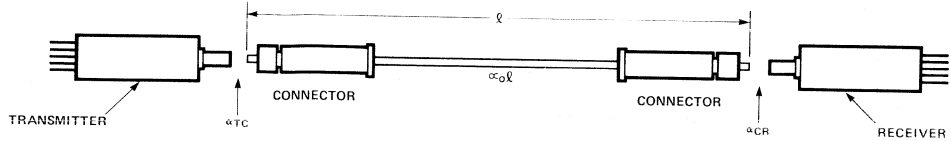


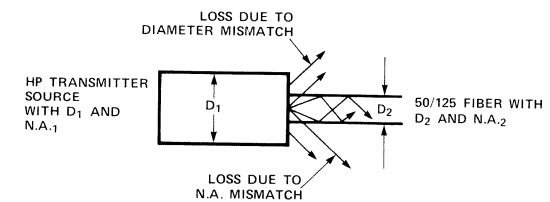
Figure 1. A Fiber Optic System

WHERE THE LOSSES OCCUR



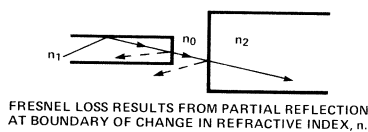
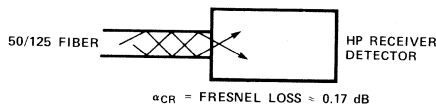
In a fiber optic link using HP transmitters/receivers and 50/125 μm fiber, all HP transmitters have a larger source area and larger N.A. than the 50/125 μm fiber. Therefore a large optical loss is obtained at the transmitter/connector interface.

HP receivers have a larger detecting area and larger N.A. than the 50/125 μm fiber, therefore all light is accepted into the receiver and the only optical loss is due to Fresnel loss which is about 0.17 dB. The diagrams below illustrate the calculations required to predict the optical losses across each interface.



$$\alpha_{TC} = 20 \log \frac{D_1}{D_2} + 20 \log \frac{N.A.1}{N.A.2} + \text{Fresnel loss} \quad (2)$$

Loss due to diameter mismatch (See Note 1). Loss due to effective N.A. mismatch



Note:

1. D_1 , D_2 , $N.A.1$, $N.A.2$ can be obtained from their respective data sheets.

Empirical tests were performed with the 50/125 μm fiber optic cable specified in Table 3. The cable was cut into

two 1 metre lengths and connected on both ends with identical connectors listed in Table 1.

Table 1. Connectors Used in Test

Amphenol 906-120-5001	HP style thread
Amphenol 906-110-5017	SMA style thread

These connectors are commonly used for 50/125 μm optical fiber. The cable was connected according to the procedures documented with each connector when purchased.

Upon connecting, an epoxy having a greater index of refraction than the fiber cladding was used. This removed light from the cladding and allowed light to be measured within the core only (i.e. the fiber was mode stripped).

The links were connected to random samples of HP transmitters and optical power was measured at the end of the 1 m links while driving the transmitters at various currents. Figure 2 shows the test set up.

Before empirical tests were performed, theoretical data was calculated to determine losses, using data from the HP transmitter data sheets and data from the specific cable used.

Table 2 lists the HP transmitters used in the tests.

Table 2. HP Transmitters Tested

Transmitter
HFBR-1002
HFBR-1203
HFBR-1204

Table 3 lists the specifications of the 50/125 μm fiber used in the tests.

Table 3. Test Cable Specifications

Core Diameter	50 μm
Outside Cladding Diameter	125 μm
Numerical Aperture, N.A.,	0.21
Attenuation at $\lambda = 820 \text{ nm}$, α_o ,	4.09 dB/km
Index Grading Coefficient, g,	2

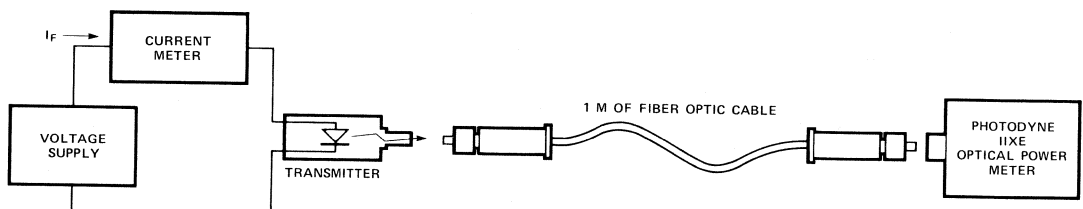


Figure 2. Test Set Up

An example theoretical calculation to determine optical power out of a 1 metre of cable is shown below using the HFBR-1002 transmitter and the 50/125 μm fiber. Optical power out of the transmitter (ΦT) minus the transmitter to connector coupling loss (αTC) minus the attenuation of $\ell = 1\text{ m}$ of cable ($\alpha\text{o}\ell$) equals the optical power out of 1 metre of cable (Φ1m).

$\Phi\text{1m} = \Phi\text{T} - \alpha\text{TC} - \alpha\text{o}\ell$ (3)

$\Phi\text{T} = -12.5\text{ dB}$

Typical, from HFBR-1002 data sheet (including 1.5 dB fixed coupling loss)

$\alpha\text{TC} = 9\text{ dB}$

$= 20\text{ Log } \frac{100}{50} + 20\text{ Log } \frac{0.3}{0.21}$

$D_1 = 100\text{ }\mu\text{m}$, $\text{N.A.}_1 = 0.3$ for HFBR-1002

$D_2 = 50\text{ }\mu\text{m}$, $\text{N.A.}_2 = 0.21$ for the 50/125 μm fiber

Fresnel loss is included in the 1.5 dB fixed coupling loss.

$\Phi\text{1m} = -12.5\text{ dB} - 9\text{ dB} - [4.09\text{ dB/km} (0.001\text{ km})] = -21.5\text{ dB}$

Knowing ΦR (from HFBR-2001 receiver data sheet) and using the equation below, a link length can be predicted.

$\Phi\text{1m} - \alpha\text{CR} - \alpha\text{o}\ell \geq \Phi\text{R}$

$\ell = (-\Phi\text{R} + \Phi\text{1m} - \alpha\text{CR})/\alpha\text{o}$ (4)

$\Phi\text{R} = -30.9\text{ dB}$ minimum from HFBR-2001 data sheet

$\alpha\text{CR} = 0.17\text{ dB}$

$\ell = (30.9\text{ dB} - 21.5\text{ dB} - 0.17\text{ dB})/4.09\text{ dB/km}$

$\ell = 2.25\text{ km}$

Typical link lengths using each T/R pair can be obtained from Figures 4, 5, and 6.

For each transmitter, measured and typical data sheet values of Φ1m are listed in Table 4.

Included in the test results is information on the expected performance of each T/R pair using HP 100/140 μm size fiber.

A review of the data will confirm the following points when comparing the performance of HP T/R pairs with 100/140 μm and 50/125 μm size fibers:

- Φ1m is reduced by approximately 10 dB when using 50/125 μm fiber
- Link distance will be longer with 100/140 μm fiber

The graphs (Figures 4, 5, and 6) allow the designer to predict the optical power available from a given fiber at a specific length, for typical transmitters.

Typical links lengths can be obtained by noting where the slope of the fiber attenuation line crosses the receiver sensitivity and extrapolating down.

Table 4. Test Results

Transmitter	Cable/Connector [Note 2]	Φ1m (Measured)	Φ1m (Data Sheet Typical)	Link Length, m [Note 4]	Conditions [Note 3]
HFBR-1002	100/140 μm / HFBR-4000	-10.5 dBm 89 μW	-12.5 dBm 56 μW	3.6 k	T = 25°C V _{CC} = 5 V I _F = 83.6 mA
	50/125 μm / Amphenol 906-120-5001	-20.3 dBm 9.3 μW	-21.5 dBm 7.1 μW	2.5 k	
HFBR-1203	100/140 μm / HFBR-4000	-8.6 dBm 138 μW	-7.4 dBm 182 μW	3.1 k	T = 25°C I _F = 100 mA
	50/125 μm / Amphenol 906-120-5001	-19.0 dBm 12.6 μW	-19.3 dBm 11.7 μW	1.7 k	
HFBR-1204	100/140 μm / OFT1 455B (SMA Style)	-8.5 dBm 141 μW	-7.4 dBm 182 μW	3.1 k	T = 25°C I _F = 100 mA
	50/125 μm / Amphenol 906-110-5017	-17.2 dBm 19.3 μW	-19.3 dBm 11.7 μW	2.1 k	

Notes:

2. The attenuation of the 100/140 μm fiber used = 5.5 dB/km. The attenuation of the 50/125 μm fiber used = 4.09 dB/km.
3. Tests were made at ambient temperature of 25°C. For guaranteed operation at -40°C ≤ T ≤ 85°C, see HP Optoelectronics Designers Catalog for transmitter and receiver data sheets.
4. Link lengths are predicted using eq. 4, the measured value of Φ1m , and the appropriate HP receiver and cable. See Figures 4, 5, and 6 for graphical representation.

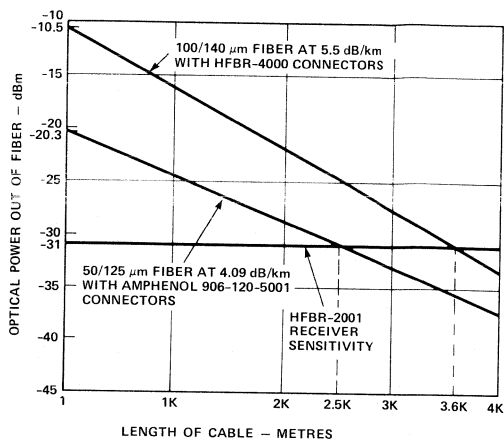


Figure 4. Expected Optical Power out of a Given Length of Cable Using the HFBR-1002 Transmitter

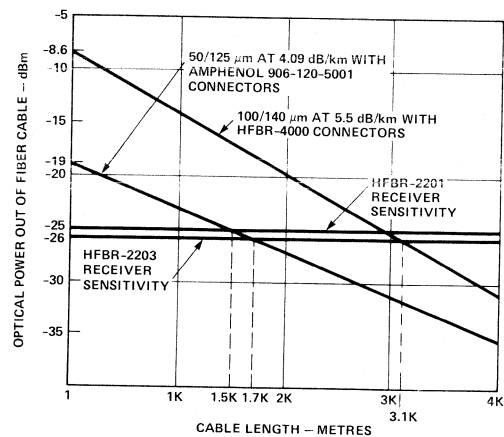


Figure 5. Expected Optical Power out of a Given Length of Cable Using the HFBR-1203 Transmitter

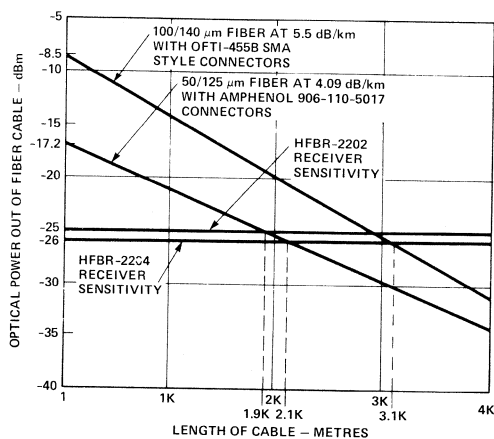


Figure 6. Expected Optical Power out of a Given Length of Cable Using the HFBR-1204 Transmitter

Note: All graphs are constructed from measured values.

High Speed Fiber Optic Link Design with Discrete Components

INTRODUCTION

Fiber optic components can be divided into three categories based upon the level of functional integration of the optical source, the photodetector and the associated circuitry.

Category I is a complete functional module supplying an output electrical or optical signal given a specified input optical or electrical signal. Power and data are generally the only concerns left to the designer. Functional modules in this category are typically TTL or ECL logic compatible. Category II is a group of components which are incorporated into a single package to provide a particular function that is generally difficult to achieve by the system designer. A PIN photodiode with an integrated transimpedance amplifier is an example of this type of component. Category III is a set of discrete components such as an LED or a photodetector. Components in the latter categories perform generally only a portion of the system function. Circuit design must be provided to complete the fiber optic link. Table 1 collates the relative costs of the categories. The lowest cost discrete components require correspondingly more support circuitry.

Table 1. Categories of Fiber Optic Components

Category	Example	Relative Cost
I Modules	Transmitter Module Receiver Module	Highest
II Hybrid/ Integrated	PIN with pre-amp LED with driver	Medium
III Discrete Components	PIN, LED	Lowest

The purpose of this application note is to demonstrate a 100 MBd, 100 metre fiber optic communication link using low cost, reliable discrete components of category III.

No attempt is made to recommend a best design but rather typical performance data of the link is shown. Variations in component parameters and printed circuit layout will affect the actual results in your implementation. System design

and testing at these high data rates can be complex and Hewlett-Packard Optical Communication Division (HP OCD) would like to encourage you to discuss these issues with our Application Engineering staff. HP OCD has a large development effort ongoing in high speed fiber optics. Future products will include fully logic compatible transmitter and receiver modules for cost effective high volume usage.

A high efficiency LED was used as the transmitter and a PIN photodiode was used as a detector. A driver circuit was designed for the LED, and a low-noise pre-amp coupled to a post-amp and comparator was designed for the receiver. These circuits were constructed on printed circuit boards using discrete and commercially available ICs. Careful consideration was given to the layout and assembly of these circuits because of the problems with parasitic interactions which are inherent at these frequencies.

The design was intended to satisfy these requirements:

Data Rate: 100 MBd NRZ 2⁷-1 PRBS⁽¹⁾
 Distance: 100 Metres
 Bit-Error Ratio (BER): 10⁻⁹
 I/O: ECL
 Operating Temp: 0-70 °C
 Cable: Hewlett-Packard HFBR-3000
 100/140 µm, g = 2
 Bandwidth @ 1 km = 40 MHz

This design was also used to evaluate link parameters such as dynamic range, sensitivity and pulse width distortion.

Applications for such a link range from computer/mass storage communications and time domain multi-channel data multiplexing to LAN and high resolution digitized video.

The remainder of this note is organized as four sections. The Transmitter and the Receiver sections discuss their respective designs and trade offs. The Test section documents the test methods and summarizes results. Finally the Conclusion and Recommendation section describes the system limitations and offers some suggestions for possible performance improvements and related issues.

TRANSMITTER

An LED presents many advantages as a fiber optic transmitter. It is physically small and rugged. It only needs a low voltage to operate. Most of all, LEDs are easy to make, reliable and inexpensive.

The material composition and device structure of an LED will affect its emitting wavelength, speed and cost. Table 2 compares some of the common fiber optic LEDs.

Table 2. LED as a Fiber Optic Source

Material	GaAsP	GaAlAs		InGaAsP
Device	Surface LED	Surface LED	Etched-Well LED	Transparent Substrate LED
1. Wavelength (nm)	665	820	820	1300
2. Spectral Linewidth (nm)	30	40	40	120
3. Ext. Quantum Efficiency $\eta(\%)$	0.1-0.2	1.5-2.0	4	4
4. Response Time (nsec)	<40	5-15	<15	<10
5. Relative Cost	Low	Medium	Higher	Highest

For the Transmitter, switching the LED with a large amount of forward current with good rise/fall time is an important consideration. A Hewlett-Packard etched well type LED, the HFBR-1204, was selected for its high optical power output and low forward-biased junction capacitance. It is fabricated by mounting the chip upside down and etching a well in the substrate. Mounting the chip upside down puts the active region closer to the mounting frame, which acts as a heat sink. This allows higher current density and therefore more optical power output. The etched well in the substrate (now on top) enables the light to travel through the thinner layer with less absorption and scattering. Figure 1 illustrates the etched well structure.

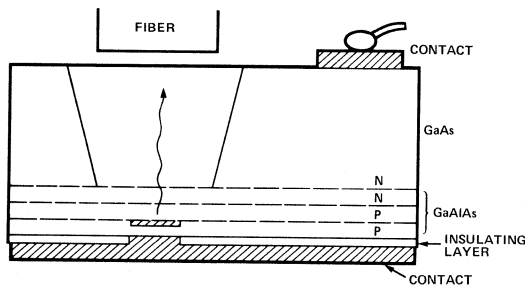


Figure 1. Etched-Well Emitter

In order to achieve the desired 100 metre distance the link must have adequate optical power. With the HFBR-3000 cable, the maximum cable loss is 8 dB/km or 0.8 dB for the 100 metres. Assuming two in-line connector-to-connector junctions each with 2 dB insertion loss and allowing a 3 dB margin, the total system optical power loss is (average optical power is used throughout this note):

$$0.8 \text{ dB} + 2(2 \text{ dB}) + 3 \text{ dB} = 7.8 \text{ dB.}$$

Suppose the receiver sensitivity is -24 dBm , the minimum optical power required from the LED is:

$$X \text{ dBm} - 7.8 \text{ dB} = -24 \text{ dBm}$$

$$X = -24 \text{ dBm} + 7.8 \text{ dB} = -16.2 \text{ dBm or } 24 \mu\text{W}$$

Table 3 lists the key typical characteristics of the HFBR-1204 fiber optic transmitter.

Table 3. Typical Key HFBR-1204 Fiber Optic Transmitter Characteristics

Parameter	Symbol	Typ.	Units	Conditions
Peak Emission Wavelength	λ_P	820	nm	
Output Optical Power Coupled into 100/140 μm Fiber	P_T	-7.4	dBm	$I_F = 100 \text{ mA}$
		182	μW	$T_A = 25^\circ \text{C}$
Rise Time, Fall Time (10 to 90%)	t_r, t_f	11	nsec	
Junction Capacitance	C_j	100	pF	$V_F = 1.25 \text{ V}$

At the 100 MBd data rate the LED will have to respond to a pulse width of 10 ns. The specified 11 ns rise/fall time is obviously inadequate to handle the 10 ns pulse width required by the 100 MBd data rate. Some form of frequency response compensation is necessary to extend the natural LED corner frequency. Figure 2 illustrates the idea.

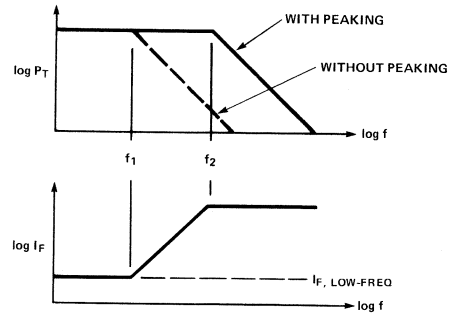


Figure 2. LED Frequency Response and Equalization

The uncompensated LED output power P_T decreases as the modulation frequency is increased. However, if LED forward current I_F is also increased as a function of modulation frequency then P_T is extended from f_1 to some f_2 determined by the compensation network.

To realize such a circuit, the important criteria are:

1. Good gain and phase stability at the operating frequency. This leads to the selection of transistors with high f_T .
2. Minimum gain variation over the intended operating temperature range.

- Must not drive the LED beyond its maximum allowable forward current.
- Must be small in size and simple to implement.

The circuit chosen consists of a current mirror with the LED as the collector load as shown in Figure 3. The input signal developed at the emitter of Q_1 is "mirrored" at the emitter of Q_2 . The Q_2 V_{BE} variation due to temperature is compensated by Q_1 connected as a diode.

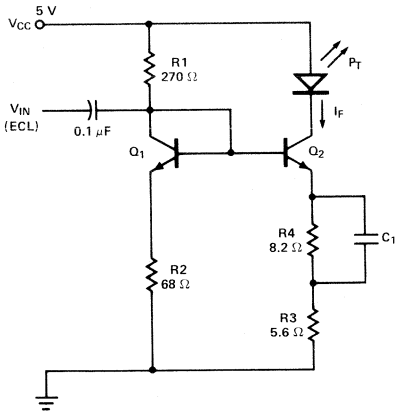


Figure 3. Analog Compensation of LED

At frequencies below f_1 the LED forward current I_F is controlled by R_3 and R_4 . R_4C_1 combination is chosen to provide the 20 dB/decade roll off beyond about 100 MHz. R_1 and R_2 determine the dc operating point. The compensation circuit shown here is analog, in other words, Q_2 is never in saturation or cut off. The LED current I_F follows the input voltage causing the optical output to be modulated accordingly. Consequently this same circuit can be used to transmit analog signals such as video or multiplexed audio.

In addition to the frequency domain it is possible to compensate the LED in the time domain. Figure 4 demonstrates such a scheme. The open-collector transistor is turned on to shunt current away from the LED to turn it off. When the transistor is off, initial I_F is controlled by R_1 while the steady state current is determined by R_1 and R_2 . R_2C_p provides the time constant for the peaking. The peaking current overcomes the junction capacitance to force the LED on. The speed of this type of digital peaking circuit is limited by the driver device used. A Schottky TTL type gate with open collector output can act as a driver for the HFBR-1204 up to about 25 MHz. The FAST series or the AS1000 series logic families can improve the performance of such a circuit. The common problem with this digital approach is the removal of current from both the LED junction and the saturated output stage of the driver causing optical fall time of the transmitter to suffer.

RECEIVER

The receiver section is comprised of a PIN photodiode detector, a transimpedance pre-amp, a post amplifier, and a high speed differential comparator.

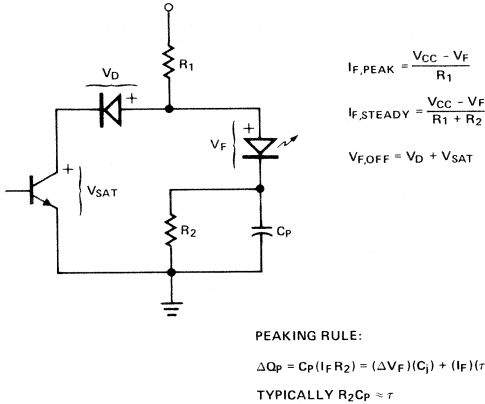


Figure 4. LED Peaking

The advantages of the PIN photodiode over an avalanche photodiode are low cost, circuit simplicity, wide bandwidth, and low variation of sensitivity with temperature and bias. Figure 5 shows a PIN structure. An additional intrinsic region is used to separate the heavily doped p and n layers of a diode structure. The wide intrinsic layer increases the photodiode sensitivity by increasing the probability that incident photons will create electron-hole pairs within the depletion region. The PIN photodiode is the most practical for moderate distance and data rate (e.g. up to about 200 MBd and 2 km).^[2]

The HFBR-2208 is a silicon PIN photodetector, factory mounted and dynamically aligned in a rugged, low capacitance, metal SMA port. The low noise, low capacitance and efficient coupling make the HFBR-2208 well suited for high speed fiber optic applications. The responsivity specification includes the coupling losses from the fiber onto the PIN photodiode, as well as the responsivity of the PIN photodiode itself.

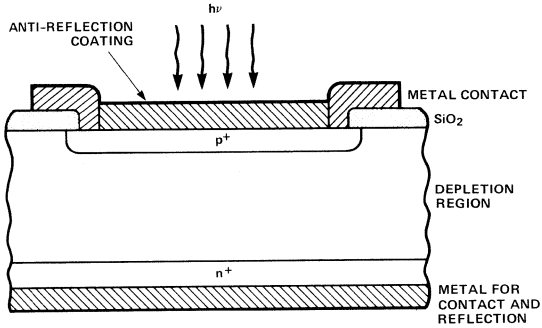


Figure 5. Structure of a Typical Si PIN Photodiode

Table 4. Typical Characteristics of HFBR-2208 PIN Photodetector

Parameter	Symbol	Typ.	Units	Conditions
Responsivity	R _p	0.38	A/W	
3dB Bandwidth	BW	100	MHz	V _{BIAS} = 5 V
Peak Spectral Response		820	nm	
Dark Current	I _D	50	pA	V _{BIAS} = 20 V P _R = 0
Total Capacitance	C _T	1.3	pF	

Table 4 shows the typical characteristics of the HFBR-2208 PIN photodetector and Figure 6 illustrates its packaged cross sectional view.

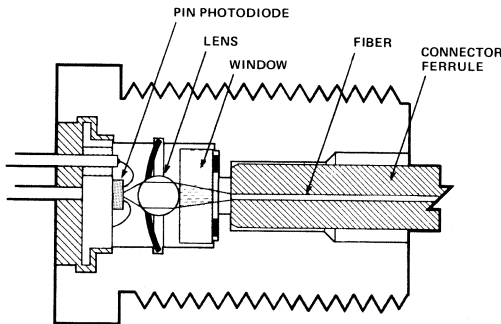


Figure 6. HFBR-2208 Cross Sectional View

The popular bipolar transistor feedback transimpedance amplifier approach was chosen in order to achieve wide bandwidth and dynamic range, with acceptable sensitivity and gain. This approach is also more amenable to later design specialization, such as bandwidth or gain adjustments, since complex equalization circuits are not required. The major disadvantage of such a feedback amplifier is that thermal noise generated in the feedback resistor adds directly to the amplifier input, thereby degrading the sensitivity. Larger values of feedback resistor contribute less input noise, although the bandwidth is correspondingly decreased.

In a realistic digital fiber optic link, the receiver sensitivity is a measure of the minimum optical power level required at the receiver to achieve a desired bit-error ratio. A bit-error ratio of 10^{-9} is often specified for data communication systems. Since the receiver consists of the PIN photodetector, the pre-amp, the post-amp and the comparator, this definition is a measure of their combined performance, and therefore, is practical and useful.

The sensitivity of the receiver can be calculated based on the amplifier (mainly the pre-amp) noise level. For BER = 10^{-9} and unipolar signalling, the signal to noise ratio must

be a minimum of 12. In other words, better noise performance at the front end of the receiver leads to better sensitivity. However, it must be recognized that hysteresis and threshold setting in the comparator is reflected as input optical power consumed. This sensitivity definition is, therefore, not an absolute measure of the PIN photodiode and its amplifier. It has been documented that a sensitivity of -40 dBm (NRZ, BER = 10^{-9}) is achievable with a short wavelength PIN photodetector diode and a bipolar transistor transimpedance amplifier at 100 Mb/s data rate^[3].

While the minimum optical power at the receiver input is determined by the receiver sensitivity, in a practical system, the receiver has to operate not only at the minimum detectable power level but also at optical power levels which can be significantly larger. This wide range of received power levels is caused by variations in link lengths, fiber losses, connector and splice losses, transmitter output changes with temperature and aging, etc.

The receiver dynamic range is the difference (in decibels) between the minimum power level determined by the receiver sensitivity and the maximum allowable input power level without amplifier saturation. As the received optical power increases to the minimum required, the receiver bit-error ratio decreases to the desired level because adequate signal-to-noise ratio is obtained. This improved performance continues until saturation or overloading occurs at the receiver. At this point, the received signal waveform becomes distorted and the error ratio starts to increase once again due to intersymbol interference^[3].

The maximum allowable optical power at the receiver input is then defined to be the level where the measured error ratio starts to be worse than the desired value; normally 10^{-9} . However, as defined, the dynamic range includes some nonlinear operation of the amplifier at the high power level end. This nonlinear operation is difficult to predict and may not be repeatable between different amplifiers (of the same design)^[3]. Thus a conservative margin must be used in determining the maximum allowable receiver input power level. The advantage of this dynamic range definition is that bit-error ratio is easy to verify throughout the entire operational limit.

The dynamic range is a function of the feedback resistor of the front-end transimpedance amplifier. As the feedback resistor decreases, the maximum allowable received optical power increases to widen dynamic range. However, a reduction in the feedback resistance results in an increase in the amplifier noise level which affects sensitivity. Thus there is a tradeoff between high receiver sensitivity and wide dynamic range.

Circuit Description

The pre-amp circuit is shown in Figure 7. The circuit consists of a common-collector-common-emitter pair with shunt-shunt feedback, followed by a common-collector buffer stage. The advantages of this configuration are:

- High front-end gain to minimize noise contributed by succeeding stages
- Compact layout to control circuit board parasitics and spurious oscillation
- Elimination of input Miller effect capacitance
- Single source biasing

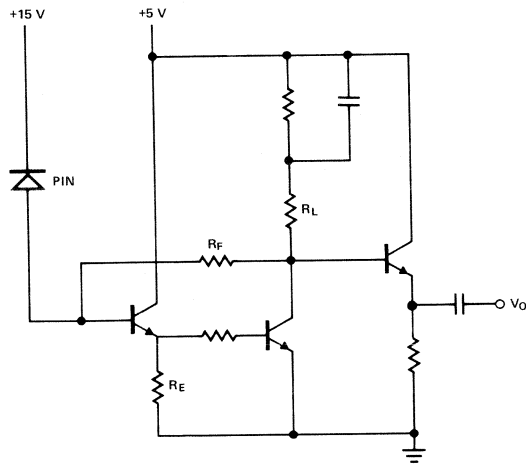


Figure 7. Impedance Pre-Amplifier Circuit Diagram

Sensitivity Calculations

If the signal gain of the first transistor stage is sufficiently high, the sensitivity of the pre-amp can be determined by summing the noise generated by the input circuit, the equivalent input noise generated by the first transistor stage and the noise generated by the feedback resistor.

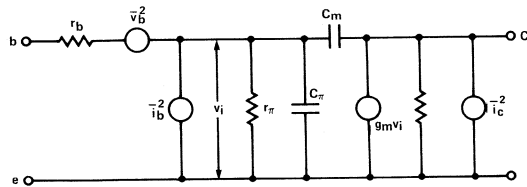


Figure 8. Noise Source Model of Bipolar Transistor

The circuit model shown in Figure 8 can be used to calculate the noise generated by the first transistor stage. The primary noise sources in bipolar transistors are shot noise due to the collector and base bias currents and thermal noise generated by the base resistance. Since the noise sources arise from separate physical mechanisms, they may be considered uncorrelated with mean square values given by:

$$\begin{aligned} \overline{V_b^2} &= 4kT r_b \Delta f && \text{Thermal noise due to base resistance} \\ \overline{i_b^2} &= 2qI_B \Delta f && \text{Shot noise due to base bias} \\ \overline{i_c^2} &= 2qI_C \Delta f && \text{Shot noise due to collector bias} \end{aligned}$$

To obtain a direct comparison of the internal noise generated by an amplifier with the input signal strength, the internal noise sources can be expressed in terms of external generators at the input of a noiseless amplifier.

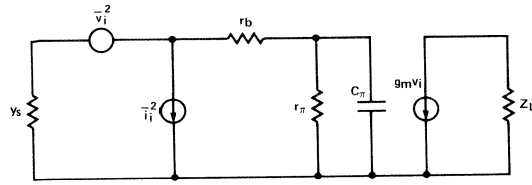


Figure 9. Bipolar Transistor Model with Noise Sources Referred to Input

Figure 9 shows an equivalent circuit where the internal noise generators have been referred to the input. The equivalent input voltage and current noise generators as shown are given by:

$$\overline{V_i^2} = \overline{i_b^2} r_b^2 + \overline{V_b^2} + \left| \frac{\overline{i_c^2}}{g_m^2} \right| \left| \frac{Z_\pi + r_b}{Z_\pi} \right|^2 \quad (2)$$

$$\overline{i_i^2} = \overline{i_b^2} + \overline{i_c^2} / |g_m Z_\pi|^2 \quad (3)$$

The circuit model of the HFBR-2208 PIN photodiode is shown in Figure 10.

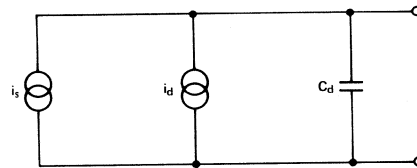


Figure 10. Simplified Circuit Model of a PIN Photodiode

Using this model with Equations 2 and 3 the internal noise can be represented by an equivalent input current generator with mean squared value:

$$\begin{aligned} \overline{i_n^2} &= 4kT(r_b + 1/2g_m)(B/R_L^2 + 4\pi^2 B^3 C_d^2/3) \\ &+ 2qB(I_d + I_B + I_C/\beta^2 + B^2 I_C/3\beta f_T^2) \end{aligned} \quad (4)$$

where

B is the analog bandwidth,
I_d is the photodiode leakage current, and
f_T is the transistor unity current gain frequency.

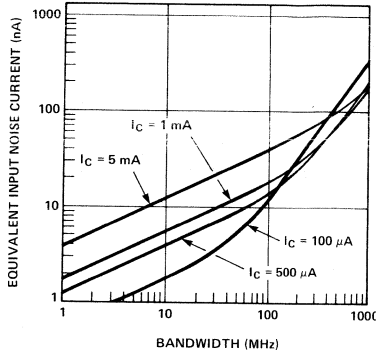


Figure 11. Equivalent Input Noise Current vs. Bandwidth

Equations 2 and 3 may also be used to solve for a bias current which minimizes the transistor generated noise. This is given by:

$$I_C = 2\pi C_T V_T B \sqrt{\beta_O} / (3 + \beta B^2 \tau_f^2)^{1/2} \quad (5)$$

where

- β_O is the dc current gain,
- B is the bandwidth
- V_T is the junction thermal voltage, kT/q
- τ_f is the forward base transit time, and
- C_T is the sum of the diode junction capacitance C_d , the emitter-base depletion region capacitance C_{je} , and collector-base capacitance C_{μ} .

For the HXTR-3615 transistor $\tau_f \approx 27 \times 10^{-12}$ sec, $C_{je} \approx 1.1$ pF, $C_{\mu} \approx 0.8$ pF, and $\beta_O \approx 50$ at low bias current. Using 2 pF for the diode capacitance and a bandwidth of 100 MHz, Equation 5 yields $I_C = 0.27$ mA for minimum transistor generated noise.

Solutions of Equation 4, for various bias values, using HXTR-3615 transistor parameters are shown in Figure 11. If feedback is used in the front-end circuit the feedback resistor will produce an additional noise term equal to:

$$\overline{i_{n^2 F.B.}} = 4 kT \Delta f / R_f \quad (6)$$

which adds to the input noise current of Equation 4.

By summing the separate noise currents at the input, the required signal power to achieve a desired bit-error ratio may be determined. The BER of a digital string corresponds to an analog signal-to-noise ratio (S/N). For example, for a NRZ binary waveform in the presence of Gaussian noise, a BER of 10^{-9} is equivalent to an S/N (power ratio) of 72, or an amplitude ratio of $12 (i_{in-PEAK} / \sqrt{i_n^2})^{1/4}$.

From Figure 11, it is seen that at 100 MHz, the equivalent input noise of the PIN/transistor front-end circuit, at 500 μ A bias, is about 15 nA. Assuming a 10 K ohm feedback resistor, which produces an additional noise current of 18 nA at 25°C, gives an equivalent input noise current of 23 nA in a 100 MHz bandwidth. The input signal must therefore be 12×23 nA = 276 nA or larger.

The photodiode responsivity is the signal current generated by incident light on the photodiode and is given by:

$$I = q \eta \Phi \lambda / hc \quad (7)$$

where

- Φ = INCIDENT OPTICAL POWER
- q is electron charge,
- η is the detector efficiency,
- λ is the wavelength of incident light,
- h is Planck's constant, and
- c is the velocity of light.

For the HFBR-2208 PIN photodiode the responsivity at $\lambda = 820$ nm is between 0.3 to 0.4 μ A/ μ W. The required optical input power is therefore 937 nW or -30.3 dBm.

Transfer Function

The transfer function of the pre-amp circuit of Figure 7, using hybrid-pi parameters is given by:

$$A_z = \frac{V_O}{i_{in}} \approx \frac{-R_f (1 + s r_{\pi 1} C_{\pi 1} / \beta_{O1})}{1 + R_f / A_O + s [(R_f / A_O) (C_{in} r_{\pi 2}' \beta_{O1} + r_{\pi 2}' C_{\pi 2}') + r_{\pi 1} C_{\pi 1} / \beta_{O2}] + s^2 (R_f / A_O) [r_{\pi 1} r_{\pi 2}' (C_{\pi 1} C_{\pi 2}' + C_{in} C_{\pi 1} + C_{in} C_{\pi 2}')]}$$

where r_b has been neglected, and

β_{O1} = D.C. beta of Q_1

β_{O2} = D.C. beta of Q_2

$r_{\pi 1}$ = r_{π} of Q_1

$r_{\pi 2}' = (r_{\pi} \text{ of } Q_2) || (R_E \text{ of } Q_1)$

$C_{in} = C_{\text{junction of pin}} + C_{\mu} \text{ of } Q_1$

$C_{\pi 1} = C_{\pi} \text{ of } Q_1$

$C_{\pi 2}' = C_{\pi 2} + (1 + g_{m2} R_L) C_{\mu 2}$

A_O = low frequency open loop gain

$$= \beta_{O1} \beta_{O2} R_L$$

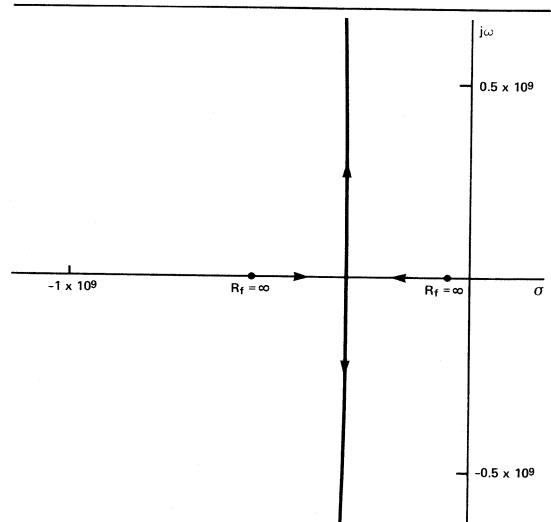


Figure 12a. Poles of Amplifier Transfer Function

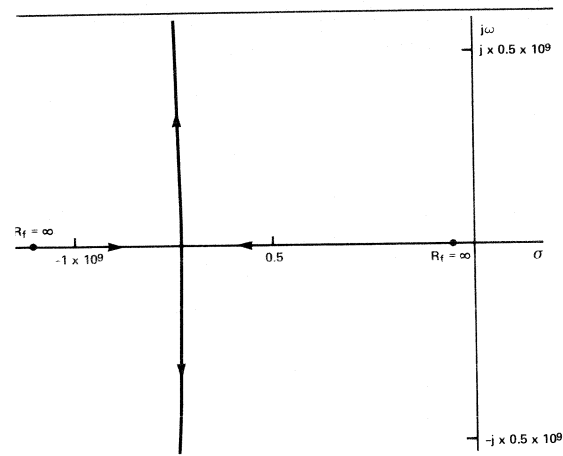


Figure 12b. Poles of Amplifier Transfer Function with Compensation Capacitance

From the form of the denominator it is seen that the amplifier has two poles, which can be complex. As R_f is decreased the feedback loop gain increases. Figure 12a shows how the poles of the transfer function move in the S-plane with feedback resistor R_f . When the imaginary part of the conjugate poles increases with respect to the real part, the amplitude response becomes peaked and the step response becomes damped-oscillatory. Although the amplifier is technically stable, large loop-gain can place the amplifier dangerously close to oscillation for practical implementation.

An effective means of controlling this peaking is to add a compensation capacitor in parallel with R_f . This increases the phase margin of the frequency response at the peaking frequencies, thereby decreasing the peaking and the possibility of oscillation.

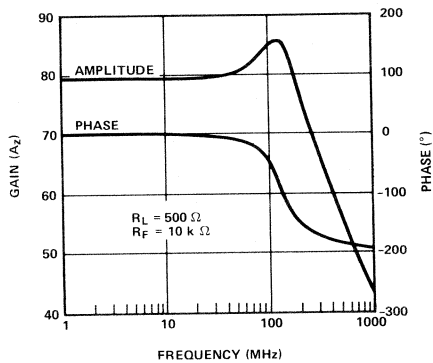
The transfer function now becomes:

$$A_z = \frac{V_O}{i_{in}} \approx \frac{-R_f (1 + s r_{\pi 1} C_{\pi 2} / \beta_{O1})}{1 + R_f / A_O + s \left[(R_f / A_O) (C_{in} r_{\pi 2}' \beta_{O1} + r_{\pi 2}' C_{\pi 2}' + (r_{\pi 1} C_{\pi 1} / \beta_{O2} + R_f C_f)) \right] + S^2 \left[(R_f / A_O) (r_{\pi 1} r_{\pi 2}' (C_{\pi 1} C_{\pi 2}' + C_{in} C_{\pi 1} + C_{in} C_{\pi 2}')) + R_f C_f r_{\pi 1} C_{\pi 1} / \beta_{O2} \right]} \quad (9)$$

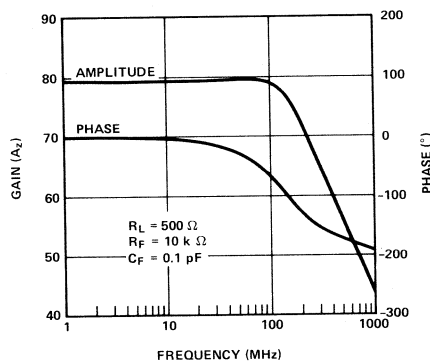
where C_f is the compensation capacitor.

Figure 12b shows how the poles of the transfer function are modified by C_f . It is seen that as C_f increases, the distance of the poles to the $j\omega$ axis increases for a given value of R_f , and that the locus of poles bends more strongly away from the $j\omega$ axis. Figure 13 shows the effect of C_f on the amplitude peaking and the phase margin of the amplifier. These plots were obtained from circuit simulations based on measured small signal two-port parameters of HXTR-3615 transistors.

The values of C_f which were found to be necessary to control potential oscillation of the pre-amp circuit were on the order of 0.02 to 0.05 pF. From bench tests it was found that capacitance values of this order occur as parasitic elements of some resistor types, and that 1/8 watt carbon film



(a)



(b)

Figure 13. Computer Simulated Amplifier Response

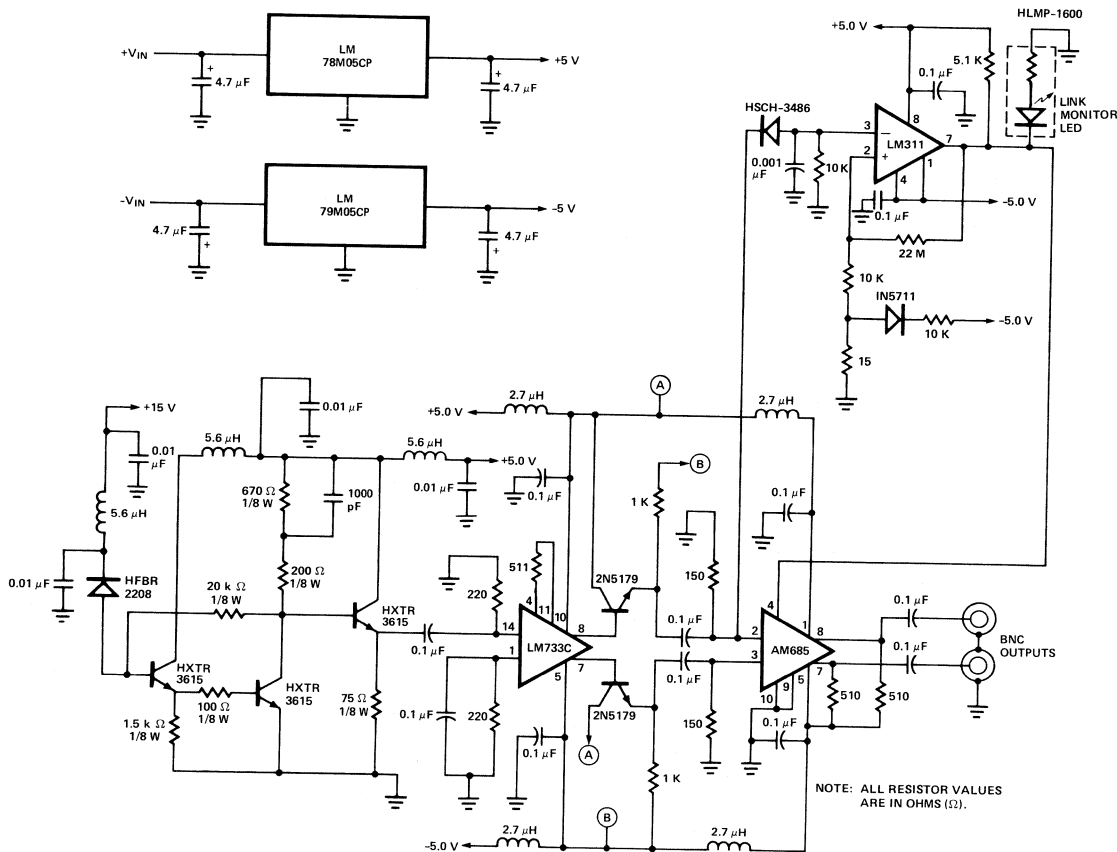
resistor worked better than metal film or carbon composition resistors.

It can be seen from Equation 5 that the PIN photodetector diode dark current I_D adds to the pre-amp input equivalent noise current. This contribution becomes significant if the bit rate is high (B is larger than 500 MHz in the equation). The HFBR-2208 is guaranteed with a maximum dark current of 300 pA which is low compared to the other terms in the equation so that it can be ignored for practical consideration in a PIN/bipolar transimpedance pre-amp combination at this bit rate as shown in Figure 11.

Furthermore, low detector capacitance C_D also will reduce bipolar transistor transimpedance amplifier input equivalent noise current. This is evident in Equation 4 since C_D is multiplied by the cube of the bit rate. This effect causes noise current to increase rapidly as a function of bit rate especially at low bias current as seen in Figure 11. The low capacitance of the HFBR-2208 at 1.5 pF helps to reduce overall receiver noise and improve sensitivity.

The gain of the amplifier is easily adjusted by just one external resistor, R8. Emitter follower stages are used to buffer its outputs to interface to the low impedance inputs of the AM685 differential comparator. The buffer stages help the post-amp maintain its frequency response. No hysteresis is used in the comparator so that sensitivity can be maximized. The outputs of the comparator are ECL compatible.

There are other wide bandwidth amplifiers suitable in this post-amp application but generally at higher cost. The microwave type gain blocks are usually single ended and also with fixed gain. On the other hand these gain blocks only require a single power supply. Equally true for the comparators, there are faster ECL comparators available at possibly higher cost.



238

The transmitter and the receiver circuits were laid out on separate printed circuit boards. Twenty (20) links were built and tested.

```

graph LR
    WG[WORD GEN HP 3760A] --> XDC[XMTR DRIVE CKT]
    XDC -- ECL --> UUT[UUT]
    ED[ERROR DET HP 3761A] --> PM[PHOTODYNE 11 XE POWER METER]
    UUT -- "HFBR-3000 1 METRE" --> PM
  
```

```

graph LR
    XMTR_UUT[XMTR UUT] --- PD[PHOTODYNE 1600 XP WAVEFORM ANALYZER]
    PD --- HP_Scope[HP SCOPE 1726A]
  
```

Figure 17. Transmitter Driver

Table 5. Summarized Transmitter/Receiver Performance Measured with PRBS 10⁷-1 BER = 10⁻⁹

Parameter	Temperature — °C								
	−5	5	15	25	35	45	55	65	75
Transmitter Output Optical Power (dBm)	−11.3	−11.3	−11.4	−11.5	−11.6	−11.7	−11.9	−12.1	−12.3
Transmitter PWD (ns) t _{PHL} − t _{PLH}				1.21					1.05
Link Sensitivity (dBm)	−24.0	−23.8	−24.2	−24.3	−23.9	−23.7	−23.5	−23.2	−23.0
Link PWD (ns) t _{PHL} − t _{PLH}	1.4	1.2	1.3	1.3	1.1	1.2	1.3	1.7	1.5

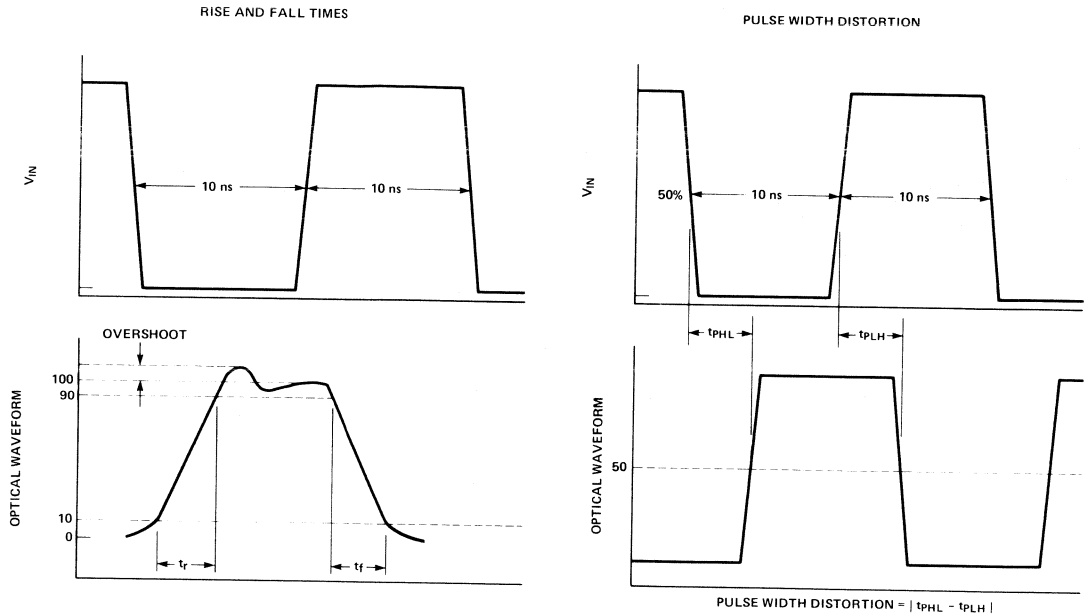


Figure 18. Pulse Width Distortion

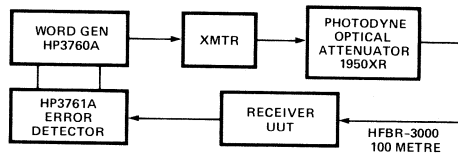


Figure 19. BER Measurement Set-up

CONCLUSIONS AND RECOMMENDATIONS

To summarize the concepts demonstrated:

- It is shown that the HFBR-1204 fiber optic transmitter can be compensated for higher speed data transmission than its natural cutoff frequency might have allowed.
- A properly compensated HFBR-1204 LED can provide close to constant optical power output through the 0 – 70°C temperature range.
- The HFBR-2208 PIN photodiode is proved to be a practical detector. It is reliable and easy to use. Furthermore it only requires a low bias voltage.
- The transimpedance amplifier required to convert the photo current is implemented discretely using microwave type bipolar transistors with low noise and high gain at low bias current.
- Commercially available integrated circuits can be used as post-amp and comparator.

The mean measured average optical output power from the transmitter is –11 dBm with 90 mA of peak LED drive current at 25°C. This corresponds to a –8 dBm of dc optical

output power which agrees with the data sheet typical of –7.4 dBm at 100 mA of drive current.

The measured receiver sensitivity is different than the theoretically calculated performance and the computer simulation. The pre-amp sensitivity was calculated to be –30.4 dBm but the measured receiver is –24 dBm at 25°C. The analog bandwidth of the transimpedance amplifier is measured to be approximately 60 MHz instead of 100 MHz in the computer simulation. This mainly is attributed to the printed circuit layout and the use of discrete components in the pre-amp section. Parasitic coupling and feedback are the limiting factors. Components placement, therefore, is found to be extremely critical. It is also important to use carbon film type low capacitance resistors. Ceramic capacitors are suitable for high frequency applications because of their low inductance.

There are several possible system improvements:

1. If the pre-amp is hybridized it can better realize the theoretical sensitivity and bandwidth limits.
2. An AGC circuit can be implemented to improve dynamic range.
3. A shield over the sensitive pre-amp circuit reduces coupled noise and improved sensitivity. The shield must be grounded to the electrical ground of the circuit close to the pre-amp.
4. An appropriate type of line code can improve the efficiency of the fiber optic link. The commonly used Manchester code requires two transitions per data bit therefore it is relatively inefficient. No one standard code will always provide an optimized link performance under different system environments. 4B/5B, MFM and Miller are some of the codes currently being examined.^[5]

The sensitivities of the fiber optic link were also measured at 50 MBd and 120 MBd over a 1 metre length of 100/140 μm fiber. They were found to be -25 dBm and -22 dBm at 25°C respectively. At data rates up to about 50 MBd, fiber optic transmission distance is primarily cable attenuation

limited. From 50 to about 500 MBd, transmission distance is primarily chromatic dispersion limited. Beyond 500 MBd modal dispersion also needs to be considered. Proper choices of fiber characteristics therefore influence data rate and distance severely.^[2]

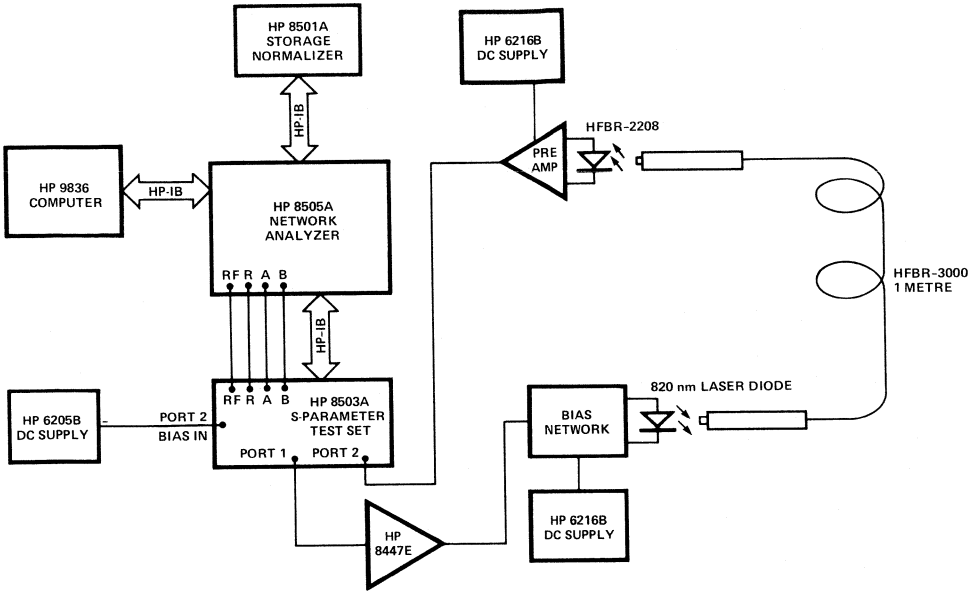


Figure 20. Bandwidth Measurement Set-up

APPENDIX

The pre-amp was constructed separately from the rest of the receiver circuit so that variability in the layout and the effect of using chip capacitors could be studied.

The result showed that the compact layout and the use of chip capacitors had indeed allowed the amplifier to better approach the computer simulated performance. The average measured frequency response was 90 MHz and the sensitivity derived from the noise measurement was -30 dBm . Figure 20 illustrates the bandwidth measurement equipment set up and Figure 21 shows the frequency response of one of the amplifiers.

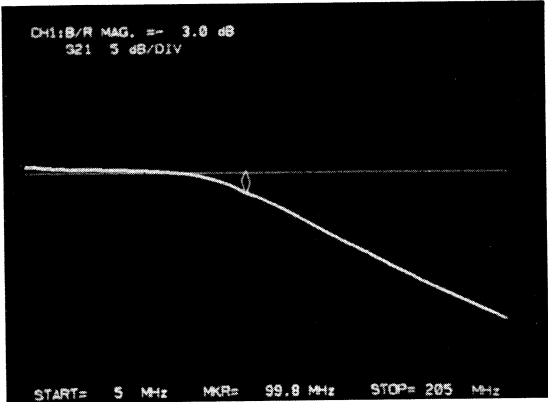


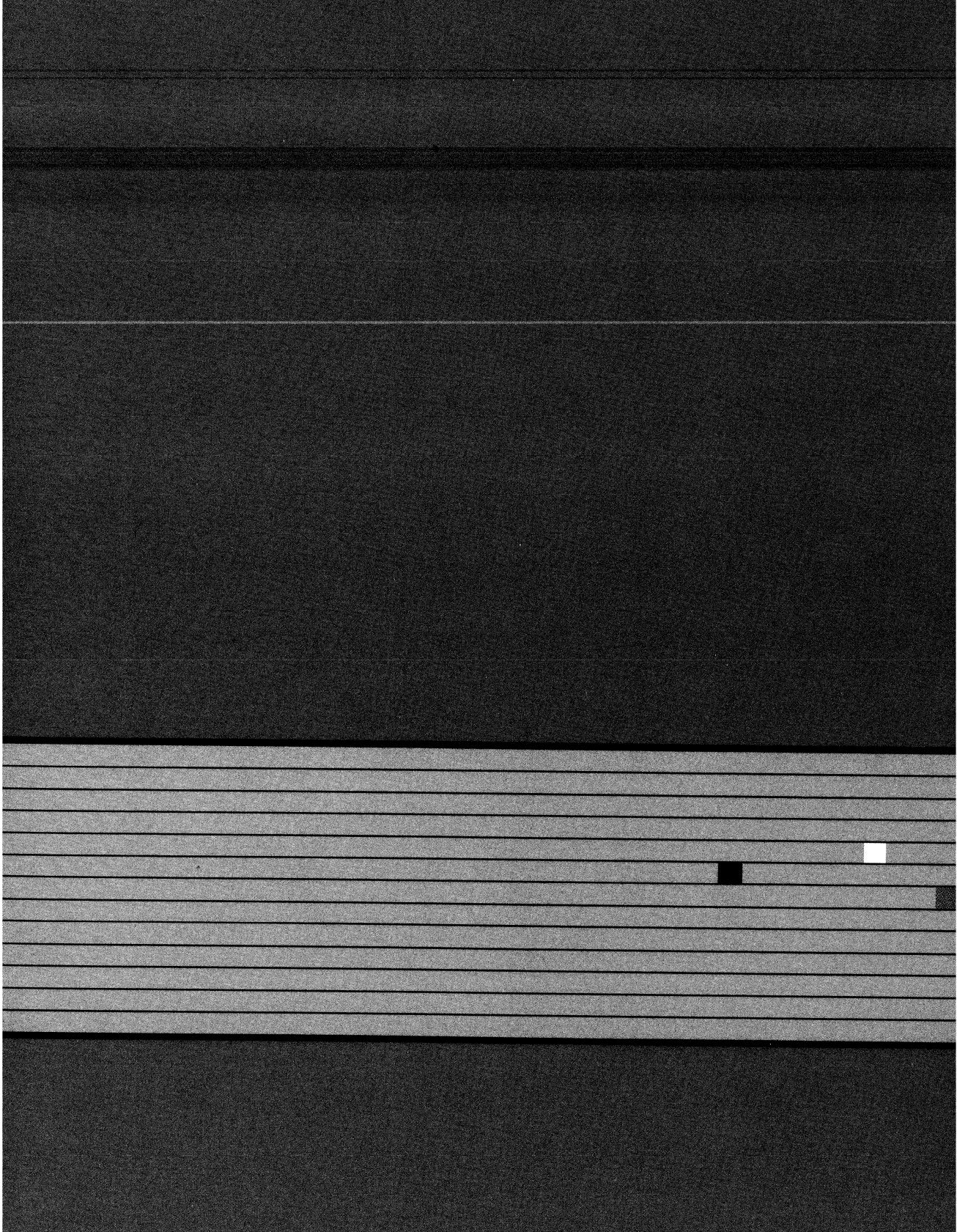
Figure 21. Pre-Amp Frequency Response

References

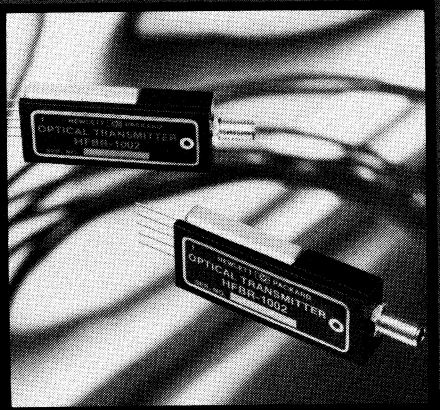
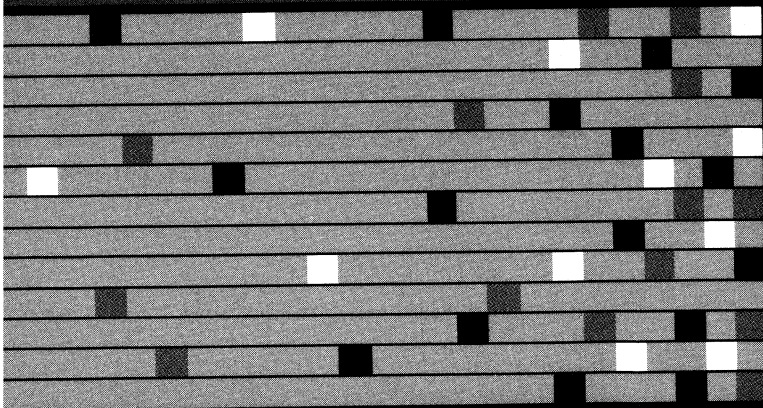
1. *Operating Manual, 150 Mb/s Error Rate Measuring System 3760/61A*, Hewlett-Packard Company, 1973.
2. Keiser, Gerd. *Optical Fiber Communications*. New York: McGraw-Hill, 1983.
3. Muoi, Tran Van. "Receiver Design for High-Speed Optical-Fiber Systems." *Journal of Lightwave Technology*, Vol. Lt-2, NO. 3, June 1984, P243-265.
4. Carlson, A.B. *Communication Systems*. New York: McGraw-Hill, 1968.
5. *Use of Standard Modulation Codes for Fiber Optic Link Optimization*. Proc of FOC/LAN, 17-21 Sept. 1984. Boston: Information Gatekeepers, Inc.

Notes

MINIATURE FIBER OPTICS



High Performance Fiber Optic Modules



High Performance Fiber Optic Modules

Transparent TTL — TTL link capability and independence from data format restrictions make this family of modules easy to use in a variety of applications. A link monitor on the receiver provides a digital indication of link continuity, independent of the presence of

data. The modules are compatible with HP-style connectors and small-diameter glass fiber cable. A transmitter, receiver, 10 metres of connected cable and technical literature are contained in the HFBR-0010 evaluation kit.

High Performance Module Family: Glass fiber (100/140 μm). Precision metal connectors, TTL compatible output, Link monitor. Transparent 3-level code.

Products/Part Nos.	Description		
Evaluation Kit HFBR-0010	HFBR-1001 Transmitter, HFBR-2001 Receiver, 10 metre connected cable, literature		
Transmitter/Receiver Pairs HFBR-1001/-2001 HFBR-1002/-2001	Guaranteed Distance* 180 metre 1500 metre	Guaranteed Data Rate* 10 MBd 10 MBd	Connector Style HFBR-4000 HFBR-4000
Cables Simplex HFBR-3000 (OPT001) HFBR-3200 HFBR-3001 HFBR-3021 Duplex HFBR-3100 (OPT001) HFBR-3300	Customer specified length, connected (HFBR-4000 connector) Customer specified length, unconnected 10 metres connected (HFBR-4000 connector) 10 metres connected (SMA style connector)		
Connectors HFBR-4000 HFBR-3099	Metal body, metal ferrule Connector-connector junction, bulkhead feedthrough for HFBR-4000 connector		
Connector Assembly Tools HFBR-0100 HFBR-0101 HFBR-0102	Field installation kit for HFBR-4000 connectors (includes case, tools, consumables) Replacement consumables for HFBR-0100 Kit Custom tool set only		

*Link performance at 25°C.



Digital Data Transmission With the HP Fiber Optic System

Fiber optics can provide solutions to many data transmission system design problems. The purpose of this application note is to aid designers in obtaining optimal benefits from this relatively new technology. Following a brief review of the merits, as well as the limitations, of fiber optics relative to other media, there is a description of the optical, mechanical, and electrical fundamentals of fiber optic data transmission system design. How these fundamentals apply is seen in the detailed description of the Hewlett-Packard system. The remainder of the note deals with techniques recommended for operation and maintenance of the Hewlett-Packard system, with particular attention given to deriving maximum benefit from the unique features it provides.

ELECTRICAL WIRE VS. FIBER OPTICS

In fiber optic cables, the signals are transmitted in the form of energy packets (photons) which have no electrical charge. Consequently, it is physically impossible for high electric fields (lightning, high-voltage, etc.) or large magnetic fields (heavy electrical machinery, transformers, cyclotrons, etc.) to affect the transmission. Although there can be a slight leakage of flux from an optical fiber, shielding is easily done with an opaque jacket, so signal-bearing fibers cannot interfere with each other or with the most sensitive electric circuits, and the optically-transmitted information is, therefore, secure from external detection. In some applications, optical fibers carry signals large enough to be energetically useful (e.g., for photocoagulation) and potentially harmful, but in most data communication applications, economy dictates the use of flux levels of $100\mu\text{W}$ or less. Such levels are radiologically safe and in the event of a broken or damaged cable, the escaping flux is harmless in explosive environments where a spark from a broken wire could be disastrous. Jacketed fiber optic cables can tolerate more mechanical abuse (crush, impact, flexure) than electrical cables of comparable size; moreover, fiber optic cables have an enormous weight and size advantage — for equivalent information capacity. Properly cabled optical fibers can tolerate any kind of weather and can, without ill-effect, be immersed in most fluids, including polluted air and water.

Bandwidth considerations clearly give the advantage to fiber optics. In either parallel- or coaxial-wire cable, the

bandwidth varies inversely as the square of the length, while in fiber optic cable it varies inversely as only the FIRST power of the length. Here are some typical values for length, ℓ , in metres:

$$(1) f_{3dB} = \frac{12,000}{\ell} \text{ MHz for HFBR-3000/-3100 cables}$$

$$(2) f_{3dB} = \frac{225,000}{\ell^2} \text{ MHz for typical } 50\Omega \text{ coax (RG-59)}$$

For example, if $\ell = 100\text{m}$, the 3dB frequency is only 22.5MHz for the coax cable, but for the fiber optic cable it is 120MHz.

The limitations of fiber optics arise mainly from the means for producing the optical flux and from flux losses. While the power into a wire cable can easily and inexpensively be made several watts, the flux into a fiber optic cable is typically much less than a milliwatt. Wire cable may have several signal "taps"; multiple taps on fiber optic cables are economically impractical at present.

The losses in a point-to-point fiber optic system are insertion loss at the input and output, connector loss, and transmission loss proportional to cable length. Variations in these losses require a receiver with a dynamic range capable of accommodating these variations and yet able to provide adequate BW (bandwidth) and SNR (signal-to noise) ratio at the lowest flux level. Fortunately, no noise is picked up by a fiber optic cable so the receiver SNR at any BW is limited only by the noise produced within the receiver.

Fiber optics is not the best solution to every data transmission problem; but where safety, security, durability, electrical isolation, noise immunity, size, weight, and bandwidth are paramount, it has a clear advantage over wire.

FIBER OPTIC FUNDAMENTALS

Flux coupled into an optical fiber is largely prevented from escaping through the wall by being re-directed toward the center of the fiber. The basis for such re-direction is the index of refraction, n_1 , of the core relative to the index of refraction, n_2 , of the cladding.

Index of refraction is defined as the ratio of the velocity of light in a given medium to the velocity of light in a vacuum.

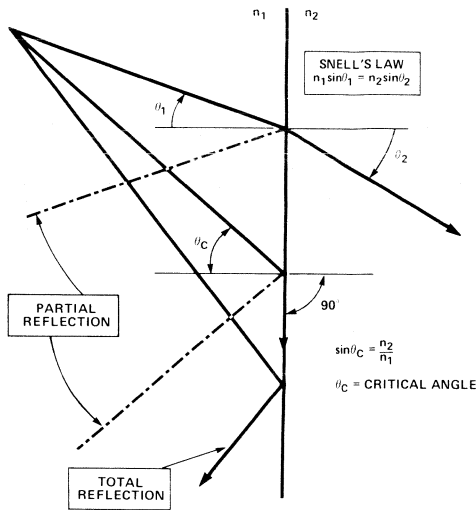


Figure 1. Snell's Law.

As a ray of light passes from one medium into another of a different index of refraction, the direction changes according to Snell's Law:

$$(3) \quad n_1 \sin \theta_1 = n_2 \sin \theta_2 \quad \boxed{\text{SNELL'S LAW}}$$

This is illustrated in Figure 1. Notice that the relationship between the angles is the same, whether the ray is incident from the high-index side (n_1) or low-index side (n_2). For rays incident from the high-index side, there is a particular incidence angle for which the exit angle is ninety degrees. This is called the critical angle. At incidence angles less than the critical angle, there is only a partial reflection, but for angles greater than the critical angle, the ray is totally reflected. This phenomenon is called TOTAL INTERNAL REFLECTION (TIR).

Numerical Aperture.

Rays within the core of an optical fiber may be incident at various angles, but TIR applies only to those rays which are incident at angles greater than the critical angle. TIR prevents these rays from leaving the core until they reach the far end of the fiber. Figure 2 shows how the reflection angle at the core/cladding interface is related to the angle at which a ray enters the face of the fiber. The acceptance angle, θ_A , is the maximum angle, with respect to the fiber axis, at which an entering ray will experience TIR. With respect to the index of refraction, n_0 , of the external medium, the acceptance angle is related to the indices of refraction of the core and cladding. When the external medium is air ($n_0 \approx 1$), the sine of the acceptance angle is called the NUMERICAL APERTURE (N.A.) of the fiber:

$$(4) \quad \text{NUMERICAL APERTURE, N.A.} = \sin \theta_A$$

The derivation in Figure 2 applies only to meridional rays, i.e., rays passing through the axis of the fiber; skew rays (non-meridional) can also be transmitted, and these account for the observation that the reception and

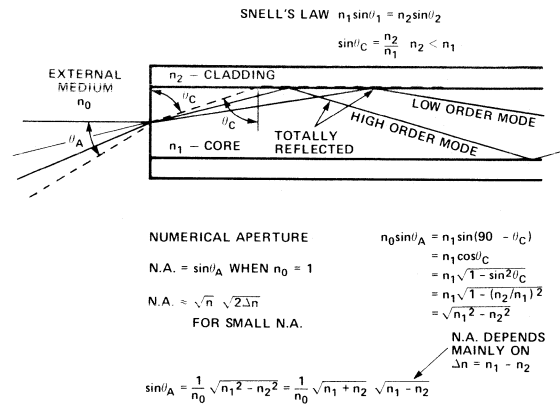


Figure 2. Total Internal Reflection.

radiation patterns of optical fibers are not perfect step functions at the acceptance angle. For this reason, the practical definition of N.A. is somewhat arbitrary.

Modes of Propagation

Within the limits imposed by the N.A., rays may propagate at various angles. Those propagating at small angles with respect to the fiber axis are called LOW-ORDER MODES, and those propagating at larger angles are called HIGH-ORDER MODES. These modes do not exist as a continuum. At any given wavelength, there are a number of discrete angles where propagation occurs. SINGLE-MODE fibers result when the core area and the N.A. are so small that only one mode can propagate.

In addition to high- and low-order modes, there are others, called LEAKY MODES, which are trapped as skew rays — partly in the core, but mostly in the cladding where they are called CLADDING MODES. As implied by the term, leaky modes do not propagate as well as the more nearly meridional modes; their persistence, depending mainly on the structure of the optical fiber, ranges from less than a metre to more than fifty metres. The presence of leaky modes will, of course, affect the results obtained in measurement of N.A. and transmission loss, making them both artificially high. For this reason, N.A. is usually specified in terms of the EXIT N.A. for a fiber of length adequate to assure that leaky modes have effectively disappeared. Since most leaky mode propagation is in the cladding, it can be "stripped." Such cladding mode stripping is done by surrounding the unjacketed fiber with a material having a refractive index higher than that of the cladding.

EXIT N.A. is defined as the sine of the angle at which the radiation pattern (relative intensity vs. off-axis angle) has a particular value. This value is usually taken at 10% of the axial (maximum) value.

ransmission Loss

egular core (non-leaky) modes also exhibit transmission losses. These are due to (1) scattering by foreign matter, (2) molecular (material) absorption, (3) irregularities at the core/cladding interface, and (4) microbending of the optical fiber by the cable structure. The first two loss mechanisms depend on the length of path taken by a ray; the third depends on the number of reflections of the ray before it emerges. It is clear from Figure 2 that the higher order modes have longer paths and more reflections with consequently higher loss. Larger N.A. fibers permit higher-order-mode propagation and, therefore, exhibit generally a higher transmission loss. Transmission loss is exponential and is, therefore, usually expressed in "dB per m." Coupling loss consideration usually favors larger N.A.

The four main loss mechanisms for coupling between fibers or between fibers and the optical ports of other devices are: (1) relative N.A.'s, (2) relative areas, (3) relative index gradings of the optical ports, and (4) Fresnel (reflection) loss. In addition to these, there may be coupling loss due to misalignment and/or separation of optical ports.

Relative N.A. loss can be ignored (\approx zero dB) whenever the N.A. of the receiving port (fiber or detector) is larger than the N.A. of the source port (flux generator or fiber), otherwise:

5) N.A. LOSS (dB) = $20 \log \frac{\text{N.A. of Source Port}}{\text{N.A. of Receiver Port}} = \alpha_{NA}$

Relative area loss can be ignored whenever the area of the receiver port is larger than the area of the source port, otherwise:

6) AREA LOSS (dB) = $20 \log \frac{\text{Diam. of Source}}{\text{Diam. of Receiver}} = \alpha_A$

In applying equation (6) to coupling between single fibers, the diameter to be used is the CORE DIAMETER.

Relative index grading loss can be ignored whenever the index grading coefficient for the receiving port is larger than the index grading coefficient of the source port, otherwise:

7) INDEX GRADING LOSS (dB) = $10 \log \frac{1 + \frac{2}{\alpha_R}}{1 + \frac{2}{\alpha_S}} = \alpha_I$

where

α_R = index grading coefficient of the receiving port

and

α_S = index grading coefficient of the source port

The index grading coefficient is described later under Construction of Fiber Optics.

Fresnel loss occurs when a ray passes from one medium to another having a different index of refraction. Part of the flux is reflected; the fraction transmitted is described by the transmittance, τ , so the loss is:

8) FRESNEL LOSS (dB) = $10 \log \frac{1}{\tau} = 10 \log \frac{2 + \frac{n_x}{n_y} + \frac{n_y}{n_x}}{4}$

n_x = index of refraction of medium x

n_y = index of refraction of medium y

It is clear from equation (8) that the loss is the same in either direction. If two fibers are joined with an air gap between their faces, taking $n_x = 1$ for air and $n_y = 1.49$ for

the cores of the fibers, the fiber-to-air Fresnel loss is 0.17dB. The air-to-fiber loss is the same, so the total airgap loss is 0.34dB. If several such connections are made, the loss could be high enough to make it worthwhile to use a coupling medium, such as silicone, to remove the air gap.

The use of a coupling medium is more significant when a fiber is coupled to an LED or IRED source. These sources are usually of gallium arsenide, or related substances, with a refractive index of 3.6. With such a high index of refraction, the use of an epoxy cement can reduce coupling loss by approximately 1dB. Figure 3 shows how the flux coupling is derived.

At the receiving end, where the silicon of the detector has an index of refraction of nearly 3.6, the Fresnel loss is also very high.

Fresnel losses at the emitter and detector surfaces can generally be ignored in designing systems with components having either connectors or pigtail fiber optic ports. This is possible because performance of such components is usually specified with reference to the external optical port so the internal Fresnel losses have already been taken into account.

Rise Time Dispersion

Bandwidth limitation in fiber optics is the result of a phenomenon called DISPERSION, which is a composite of MATERIAL dispersion and MODAL dispersion. Both of these relate to the velocity of flux transmission in the core. Velocity varies inversely as the index of refraction, and if the index of refraction varies over the wavelength spectrum of the source, the flux having a wavelength at which the refractive index is lower will travel faster than the flux having a wavelength at which the index is higher. Thus, all portions of the spectrum of flux launched simultaneously will not arrive simultaneously, but will suffer time dispersion due to differences in travel time. This is MATERIAL DISPERSION. It is reduced by using sources of narrow spectrum (e.g., lasers) or fibers with a core index of refraction which is constant over the source spectrum.

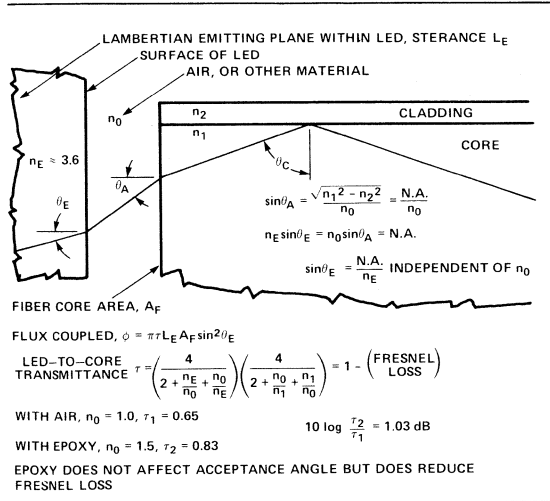


Figure 3. Acceptance Angle and Fresnel Loss Effects.

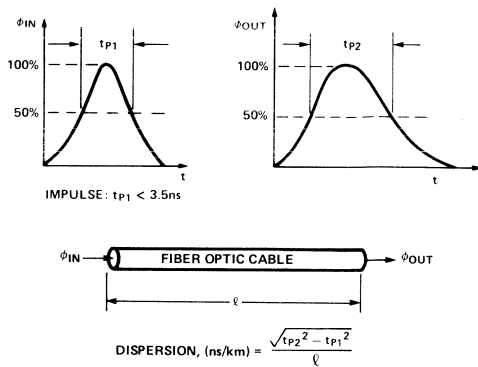


Figure 4. Rise Time Dispersion.

In Figure 2, notice that rays moving parallel to the axis travel a path length which is shorter than that of rays which are not paraxial. Those rays propagating in the higher-order modes will, therefore, have a longer travel time than those in lower-order modes, and simultaneously launched rays will suffer dispersion of their arrival times. This is MODAL DISPERSION. It can be reduced by reducing the N.A. (smaller acceptance angle) to allow only lower-order modes to propagate, or by using graded-index fiber.

Whether the dispersion is material or modal (or both), it is measured, as shown in Figure 4, by applying an impulse of flux and measuring the 3dB pulse widths at the input and output of a fiber long enough to exhibit significant dispersion. Time dispersion is then defined as

(9) RISE TIME DISPERSION

$$\frac{\Delta t}{\ell} \text{ (ns/km)} = \frac{1}{\ell} [tp_2^2 - tp_1^2]^{0.5}$$

where ℓ is the length (in kilometers) of the fiber and tp_1 and tp_2 are the 3dB widths in nanoseconds (or FWHM) of the pulses into and out of the fiber.

Modulation frequency response of a fiber has a 6dB per octave roll-off, so the effect of rise time dispersion can also be described in terms of a length-bandwidth product:

$$\text{(10) 3dB BANDWIDTH} \cdot \text{LENGTH (MHz} \cdot \text{km)} = \frac{350}{\text{DISPERSION (ns/km)}}$$

Construction of Fiber Optics

Fibers having a sharp boundary between core and cladding, as in Figure 2, are called STEP INDEX fibers. The reflection at the boundary is not a "zero-distance" phenomenon — the ray, in being reflected, is actually entering a minute distance into the cladding and there is some loss. This loss can be seen as a faint glow along the length of unjacketed lossy fibers carrying visible flux. To reduce such reflection loss, it is possible to make the rays turn less sharply by reducing the index of refraction gradually, rather than sharply, from core to cladding. A fiber of such a form is called a GRADED INDEX fiber and the rays propagate as shown in Figure 5. Graded index fiber has not only a very low transmission loss, but modal dispersion is also very low. Higher-order modes do travel longer paths, but in the off-axis, lower-index regions they travel faster so the travel time differential between high-order and low-order modes is not as large as it is in step index fibers.

From the center of the core to the outer limit of the core (inner wall of the cladding) the grading of the index of refraction is described by the index grading coefficient, α , with this approximate relationship:

$$\left(\frac{n_1^2 - n_2^2}{n_1^2 - n_2^2} \right) = \left(\frac{r}{a} \right)^\alpha \quad \text{at radius, } r \\ 0 < r < a$$

where

$$\begin{aligned} a &= \text{radius of the core} \\ n &= \text{index of refraction at } r \\ n_2 &= \text{index of refraction at } r = a \\ n_1 &= \text{index of refraction at } r = 0 \end{aligned}$$

With $\alpha = 2$, the index of refraction profile is approximately parabolic, and modal dispersion is minimized. This is called fully graded index. However, as seen in Equation (7), there is additional coupling loss when flux is sent from a high-index fiber into a low-index fiber. For moderate distances and data rates there is some value of the index grading coefficient ($\alpha \approx 8$) that optimizes performance, resulting in what is called partially graded index. In step index fiber the grading coefficient is so high ($\alpha \approx 100$) that the index grading loss can be ignored.

Graded index fiber has higher coupling loss and may be more costly than step index fiber. It is, therefore, used mainly in applications requiring transmission over many kilometres at modulation bandwidths over 50MHz. For shorter distances and/or lower bandwidths, a variety of step index fibers are available at a variety of costs.

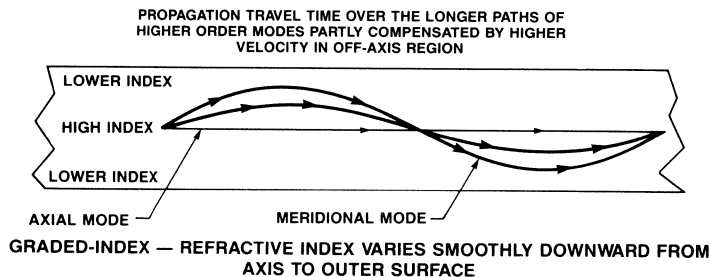


Figure 5. Graded Index Fiber Modes.

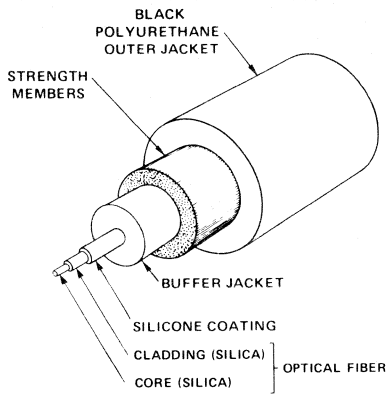


Figure 6. Step Index Fiber Optic Cable Construction.

Figure 6 shows the construction of a Hewlett-Packard fiber optic cable. Over the fused-silica, step-index, glass-clad fiber there is a silicone coating to protect the thin (20 μ m) cladding from scuffing. Over the buffer jacket are the tensile strength members, which allow the cable to be pulled through long conduits, and an outer jacket to protect the cable against crush and impact damage. This cable tolerates far more abuse than most wire cable. A sample was laid across the main entrance to the Hewlett-Packard headquarters and factory at 1501 Page Mill Road, Palo Alto. After several weeks of being driven over, night and day, there was no impairment of performance.

Other materials used in step index fibers are glass-clad glass, plastic-clad glass or fused silica, and plastic-clad plastic. These have N.A.'s ranging from less than 0.2 to more than 0.5, and transmission losses from less than 10dB/km to more than 1000dB/km. Some manufacturers offer bundled fibers in which the individual glass fibers are small enough to allow the cable to be very flexible. In earlier days of fiber optic development, bundled fibers were considered necessary for reliability because breakage of one or more fibers could be tolerated without total loss of signal transmission. Also, the large diameter of the fiber bundle allowed more tolerance in connector alignment. The popularity of fiber bundles has dwindled because the single-fiber cable durability is better than had been anticipated, and connectors are now available which are capable of providing the precise alignment required for low coupling loss with small-diameter single fibers.

Flux Budgeting

Flux requirements for fiber optic systems are established by the characteristics of the receiver noise and bandwidth, coupling losses at connectors, and transmission loss in the cable.

The flux level at the receiver must be high enough that the signal-to-noise ratio (SNR) allows an adequately low probability of error, P_e . In the Hewlett-Packard fiber optic system, the receiver bandwidth and noise properties allow a $P_e < 10^{-9}$ with a receiver input flux of 0.8 μ W under worst-case conditions. At higher flux levels, the P_e is reduced.

From the receiver flux requirement (for given P_e), the flux which the transmitter must produce is determined from the expression for a point-to-point system:

$$(11) \quad 10 \log \left(\frac{\phi_T}{\phi_R} \right) = \alpha_0 \ell + \alpha_{TC} + \alpha_{CR} + n \alpha_{CC} + \alpha_M$$

where ϕ_T is the flux (in μ W) available from the transmitter
 ϕ_R is the flux (in μ W) required by the Receiver at P_e
 α_0 is the fiber attenuation constant (dB/km)
 ℓ is the fiber length (km)
 α_{TC} is the Transmitter-to-Fiber coupling loss (dB)
 α_{CC} is the Fiber-to-Fiber loss (dB) for in-line connectors
 n is the number of in-line connectors; n does not include connectors at the transmitter and receiver optical ports
 α_{CR} is the Fiber-to-Receiver coupling loss (dB)
 α_M is the Margin (dB), chosen by the designer, by which the Transmitter flux exceeds the system requirement

Equation (11) is called the FLUX BUDGET and it is represented graphically in Figure 7. The same basic units (watts) are used for flux and for power, so it is correct and convenient to express flux in "dBm".

$$(12) \quad \phi(\text{dBm}) = 10 \log \left(\frac{\phi(\text{mW})}{1 \text{ mW}} \right) = 10 \log \left(\frac{\phi(\mu\text{W})}{1000 \mu\text{W}} \right)$$

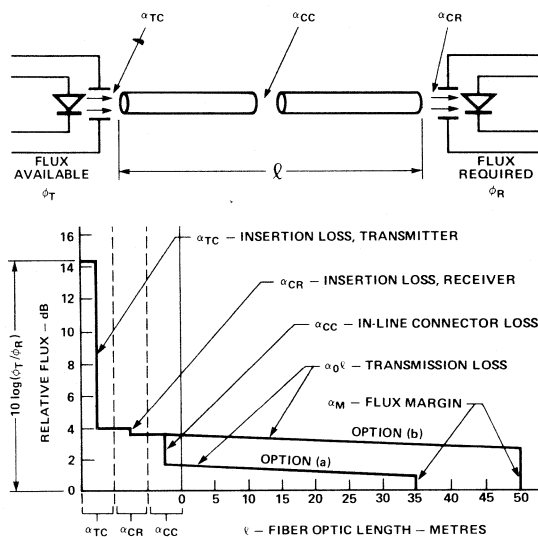


Figure 7. Flux Budget — Graphical Representation.

Here is an example of how the flux budget works:

1. Transmitter $\phi_T = 44 \mu\text{W}^*$
 2. Receiver $\phi_R = 1.6 \mu\text{W}^*$
- *peak-to-peak

Transmitter optical port: N.A. = 0.5, diam. = 200 μ m, $\alpha = 100$

Optical fiber (cable): N.A. = 0.3, core diam. = 100 μ m, $\alpha = 10$

3. From Equations (5), (6), (7):

$$\begin{aligned} \alpha_{TC} &= \alpha_{NA} + \alpha_A + \alpha_I \\ &= 20 \log \left(\frac{0.5}{0.3} \right) + 20 \log \left(\frac{200}{100} \right) + 10 \log \left(\frac{1 + \frac{2}{10}}{1 + \frac{2}{100}} \right) \\ &= 4.44\text{dB} + 6.02\text{dB} + 0.71\text{dB} = 11.17 \text{ dB} \end{aligned}$$

Receiver optical port: N.A. = 0.5, diam. = 200 μ m, $\alpha = 100$

4. Because the N.A., diameter, and α of the receiver are all larger than those of the fiber, there remains only a small amount of Fresnel loss, making $\alpha_{CR} \approx 0.17 \text{ dB}$.

5. Apply equation (11) to see what the flux budget allows:

$$14.39\text{dB} = \alpha_0 \ell + 11.17\text{dB} + \alpha_{\text{CC}} + 0.17\text{dB} + \alpha_{\text{M}}$$

$$\alpha_0 \ell + \alpha_{\text{CC}} + \alpha_{\text{M}} = (14.39 - 11.17 - 0.17)\text{dB} = 3.05\text{dB}$$

6. In accounting for cabling losses, two options are considered:

- (a) with one in-line connector, possibly to allow for later insertion of a repeater. Taking 2.0dB for the connector leaves:

$$\alpha_0 \ell + \alpha_{\text{M}} = 3.05 - 2.0 = 1.05\text{dB}$$

With cable having attenuation of 20dB/km a length of 35 metres leaves:

$$\alpha_{\text{M}} = 1.05 - (0.02\text{dB/m}) (35\text{m}) = 0.35\text{dB}$$

- (b) Without in-line connector, there is only attenuation to consider. A length of 50 metres leaves:

$$\alpha_{\text{M}} = 3.05 - (0.02\text{dB/m}) (50\text{m}) = 2.05\text{dB}$$

In flux budgeting, α_{M} should always be large enough to allow for degradation of the efficiency of the flux generator in the transmitter (LED, IRED, laser, etc.). On the other hand, in dealing with more powerful transmitters, α_{M} must not be so large that it exceeds the dynamic range of the receiver.

Dynamic Range

The dynamic range of the receiver must be large enough to accommodate all the variables a system may present. For example, if the system flexibility requirement is for transmission distances ranging from 10 metres to 1000 metres with 12.5dB/km cable, and up to two in-line connectors, the dynamic range requirement is:

$$\begin{aligned} \alpha_0 \ell &= 1\text{km} \times 12.5\text{dB/km} = 12.5\text{dB} \\ \alpha_{\text{CC}} &= 2 \times 2\text{dB} = 4.0\text{dB} \\ \alpha_{\text{M}} &= 3.0\text{dB} \\ \text{thermal variations} &= \frac{1.0\text{dB}}{20.5\text{dB}} \text{ (estimated)} \end{aligned}$$

Accommodating a 20dB dynamic range plus providing high sensitivity requires the receiver to have two important features: automatic level control, and a-c coupling or its equivalent. The a-c coupling keeps the output of the amplifier at a fixed quiescent level, relative to the logic thresholds, so that signal excursions as small as the specified minimum can cause the amplifier output to exceed the logic threshold. This function can also be called d-c restoration.

ALC (automatic level control) adjusts the gain of the amplifier. Low-amplitude excursions are amplified at full gain; high-amplitude excursions are amplified at a gain which is automatically reduced enough to prevent saturation of the output amplifier. Saturation affects propagation delay adversely so ALC is needed to allow high speed performance at high, as well as low, signal levels.

HEWLETT-PACKARD'S FIBER OPTIC SYSTEM

A number of objectives were established as targets for this development. Convenience and simplicity of installation and operation were the primary objectives, along with a probability of error $P_e < 10^{-9}$ at 10Mb/s NRZ, over moderate distances. In addition, there were the traditional

Hewlett-Packard objectives of rugged construction and reliable performance. Manufacturing costs had to be low enough to make the system attractively priced relative to its performance.

Electrical convenience is provided by several system features. The Receiver and the Transmitter require only a single +5-volt supply. All inputs and outputs function at TTL logic levels. No receiver adjustments are ever necessary because the dynamic range of the Receiver is 21dB or more, accommodating fiber length variations as well as age and thermal affects. When the system is operated in its internally coded mode, it has NRZ (arbitrarily timed data) capability and is no more complicated to operate than a non-inverting logic element. Built-in performance indicators are available in the Receiver; the Link Monitor indicates satisfactory signal conditions and the Test Point allows simple periodic maintenance checks on the system's flux margin.

There are also several optical and mechanical convenience features. The optical ports of the Transmitter and Receiver are well defined by optical fiber stubs built into receptacles that mate with self-aligning connectors. Low-profile packaging and low power dissipation permit the modules to be mounted without heat-sink provision on P.C. boards spaced as close as 12.5mm (0.5 in.).

The internally-coded mode of operation is the simplest way to use the Hewlett-Packard system. This mode places no restriction on the data format as long as either positive or negative pulse duration is not less than the minimum specified. The simplicity is achieved by use of a 3-level coding scheme called a PULSE BI-POLAR (PBP) code. This mode is selected simply by applying a logic low (or grounding) to the Mode Select terminal on the Transmitter — no conditioning signal or adjustment is necessary in the Hewlett-Packard Receiver because it automatically responds to the PBP code.

The externally coded mode makes the waveform of the output flux a digital replica of the Data Input signal. This 2-level mode is called the FULL ON-OFF (FOO) mode; it is selected by applying a logic high (or V_{CC}) to the Mode Select terminal. When used with the Hewlett-Packard Receiver, the FOO mode must have a Data Input signal with a 50% duty factor, as seen later.

Transmitter Description

Figure 8 shows symbolically the logical arrangement of the Transmitter, and waveforms for the output flux. The arrangement shown is logically correct but circuit details are not actually realized as shown. For example, the current sources actually have partial compensation for the negative temperature coefficient of the LED (or IRED). In Figure 8, there are five important things to notice.

First, notice that the bias current, I_{C} , is never turned off — not even when the Transmitter is operated in the externally coded mode (Mode Select "high"). This is done to enhance the switching speed of the LED (or IRED) in either internally- or externally-coded mode. The bias current also stabilizes the flux excursion ratio (k in Equation 14) symmetry in the internally-coded mode.

Second, notice that

- ϕ_{L} , the low-level flux, is produced by I_{C}
- ϕ_{M} , the mid-level flux, requires $I_{\text{B}} + I_{\text{C}}$
- ϕ_{H} , the high-level flux, requires $I_{\text{A}} + I_{\text{B}} + I_{\text{C}}$

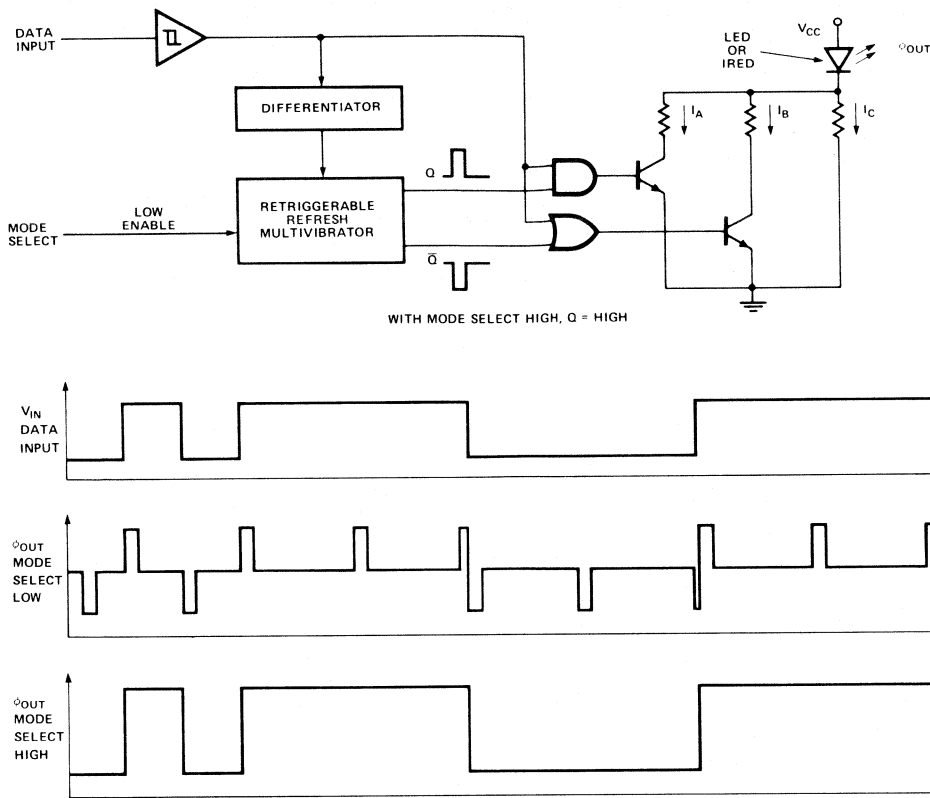


Figure 8. Transmitter Block Diagram and Waveforms.

As far as the Receiver is concerned, the excursion flux, $\Delta\phi$, produced by switching I_A and I_B , is the important parameter of the Transmitter. Average flux is, of course, related to excursion flux but is not as important in establishing the SNR of the system.

Third, notice that with Mode Select "low" and a 500kHz signal at Data Input, there will be only one refresh pulse generated in each logic state. The excursions ($\phi_H - \phi_M$) and ($\phi_M - \phi_L$) are nearly balanced so an average-reading flux meter will indicate the mid-level flux, ϕ_M , within $\pm 0.6\%$ or -0.6% depending on whether the flux excursion ratio, k , is at its maximum or at its minimum limit.

Fourth, notice that, with Mode Select "low", any Data Input transition (either H-L or L-H) retriggers the Refresh Multivibrator to start a new train of pulses. All refresh pulses for either logic state have the same duration. This keeps the average flux very near the mid-level even when the duration in either logic state of arbitrarily timed input data is very short. Notice also that any refresh pulse is overridden (abbreviated) by the occurrence of a Data Input transition so there is additional jitter ($\approx 15\text{ns}$) when the duration of the Data Input in either state is the same length of time as the refresh interval. The refresh interval is very long, relative to the refresh pulse duration, making a duty factor of approximately 2%, this also is done to keep the average flux near mid-level regardless of how long

Data Input remains in either logic state. The only condition under which the average flux can deviate significantly from the mid-level occurs when Data Input remains in one state for a period of time LESS than the duration of the refresh pulse. If this is likely to occur, the format should be configured so the numbers of 1's and 0's are balanced as they would be in Manchester code. Observing this data format allows the use of the internally-coded mode of the Hewlett-Packard system at data rates ranging from arbitrarily low to higher than 10M baud, with the absolute limit being that at which the signal intervals become as short as t_{PHL} and/or t_{PLH} .

Fifth, notice that with Mode Select "high," the Q output of the Refresh Multivibrator is "high" (and \bar{Q} is "low"). Under this condition, I_A and I_B are both ON when Data Input is "high" and both OFF when it is "low". This makes the output flux excursion a logical replica of the Data Input.

Flux Measurement

The Transmitter has two important flux parameters, flux excursion and flux excursion ratio. The flux excursion is defined as half of the peak-to-peak value:

$$(13) \text{ FLUX EXCURSION, } \Delta\phi = \frac{\phi_H - \phi_L}{2}$$

necessary to avoid "pulling" the receiver dc restorer voltage too far away from the value corresponding to the average flux, and possibly losing occasional bits.

Receiver Description

The Hewlett-Packard Receiver block diagram is shown in Figure 9. There are four functional blocks:

- 1. The amplifier, including a gain-control stage and split-phase outputs with a voltage divider for each.
- 2. The dc-restorer with a long time constant.
- 3. Logic comparators with an R-S latch.
- 4. Positive and negative peak comparator with single-ended output for the ALC and link monitor circuits.

Optical flux at the input is converted by the PIN photodiode to a photocurrent, I_P , which is converted to a voltage by the PREAMPLIFIER. This voltage is amplified to a positive-going output, V_{P1} , and a negative-going output, V_{N1} . A rising input flux will cause V_{P1} to rise and V_{N1} to fall. These voltages are applied to the differential inputs of the DC RESTORER AMPLIFIER whose output, V_T , falls until it is low enough to draw the average photocurrent away from the preamplifier via the 25k resistor. This makes $V_{P1} \approx V_{N1}$ when the input flux is at the average level. The output impedance of the dc restorer amplifier is very high, making a long time constant with the filter capacitor, C_T . The long time constant is required for loop stability when input flux levels are so low that there is little or no ALC gain reduction, with consequently high loop gain. With no input flux, $V_T = V_{TMAX}$; as input flux rises, V_T falls proportionately, so the voltage at the TEST POINT can be used as an indicator of the average input flux. With respect to the Receiver optical port, the responsivity of the PIN photodiode is approximately 0.4A/W, leading to the expression:

(17) AVERAGE INPUT FLUX, $\phi_{AV}(\mu W) \approx \frac{[V_{TMAX} - V_T] (mV)}{10}$

where V_{TMAX} = Test Point Voltage with no optical input signal.

The instrument for observing V_T must not load the Test Point significantly, so an input resistance of 10MΩ is recommended.

As described above, when the input flux is at the average level, the positive-going and negative-going output voltages V_{P1} and V_{N1} are approximately equal. Notice that this makes the outputs of both logic comparators low. A positive flux excursion, rising faster than the dc restorer (with its long time constant) can follow, will cause V_{P1} to rise and V_{N1} to fall. If the positive flux excursion is high enough, the LOGIC HIGH COMPARATOR input voltage ($V_{P2} - V_{N1}$) becomes positive, and a SET pulse is produced for the R-S flip-flop. [Similarly, a negative flux excursion of such amplitude would make ($V_{N2} - V_{P1}$) become positive and a RESET pulse would be produced.] A larger amplitude of positive flux excursion would make the POSITIVE PEAK DETECTOR input voltage ($V_{P3} - V_{N1}$) change from negative to positive and cause current to flow into the ALC FILTER capacitor. When the voltage V_A starts to rise above V_{REF} , the ALC AMPLIFIER output will operate on the GAIN CONTROL AMPLIFIER to limit the Receiver's forward gain. Notice that the ALC action is the same for a negative flux excursion, so that the Receiver's gain limitation is determined EITHER by positive flux

excursion OR by negative flux excursion — whichever is the larger. For this reason, the positive and negative excursions must be nearly balanced with respect to the average flux. The allowable imbalance is determined by the values of the resistors in the negative and positive voltage dividers. The ALC action limits the maximum excursion to a voltage $I_0 (R_1 + R_2)$, whereas the logic threshold is only $I_0 R_1$. Actual limits are established by the tolerances on the resistors and current sources. Notice that the ALC voltage, V_A , activates both the ALC COMPARATOR and the LINK MONITOR COMPARTOR. Therefore, a "high" LINK MONITOR signifies two conditions:

- 1. The input flux excursions are high enough to cause ALC action (gain limitation).
- 2. The excursions are more than adequate for operation of the logic comparator.

Notice that the LINK MONITOR could be "high," but k could be outside the specified limits such that P_e exceeds 10^{-9} . Conversely, because of safety margin in the Receiver design, it is also possible to have $P_e < 10^{-9}$ when the flux excursions are too small to make the LINK MONITOR "high".

OPERATION OF THE HEWLETT-PACKARD SYSTEM

With Hewlett-Packard Components Exclusively

The main concern in a fiber optic link is the flux budget. Other areas of concern are: data rate, data format, and the interface with other elements of a data transmission system.

Flux budgeting, using the Hewlett-Packard Transmitter, Receiver, Connector, and Cable components is very straight forward for most applications. It is necessary only to use the data sheet information correctly in making the coupling loss and transmission loss allowances.

When used with other Hewlett-Packard components, the optical characteristics of the Receivers are not critical. Their optical ports have a diameter and N.A. which are both greater than the size and N.A. of the Hewlett-Packard Cable. The Receivers also have a high responsivity and the spectral response is nearly constant over the spectrums radiated by Hewlett-Packard Transmitters.

With Components From Other Manufacturers

When using the Hewlett-Packard Receivers with other cables, it may be necessary to account for N.A. loss and/or area mismatch loss. When other sources are used, it may be necessary to compute an effective flux ratio:

(18) EFFECTIVE FLUX RATIO, $EFR_s = \frac{\int \phi_\lambda R_{r\lambda} d\lambda}{\int \phi_\lambda d\lambda}$
(Source Spectrum)

where $R_{r\lambda}$ is the relative response of the Receiver (from data sheet)

ϕ_λ is the spectral flux function of the source

If the transmission loss of the cable varies sharply over the wavelength range of the source spectrum, then the spectral transmittance of the cable should be included in the computation of EFR. The spectral transmittance varies

with cable length, so the integration must be performed using the cable length required in a particular installation:

$$(19) \text{ EFFECTIVE FLUX RATIO, } EFR_{CS} = \frac{\int \tau_{\lambda} \phi_{\lambda} R_{r\lambda} d\lambda}{\int \tau_{\lambda} \phi_{\lambda} d\lambda}$$

(Cable and Source)

where τ_{λ} is the spectral transmittance of the installed length of fiber optic cable, computed as:

$$(20) \tau_{\lambda} = 10^{-\left(\frac{\ell}{10}\right) \alpha_{0\lambda}}$$

where $\alpha_{0\lambda}$ is the spectral function in (dB/km) of the fiber optic cable and ℓ is the installed cable length (km)

Notice that as the length is reduced, τ_{λ} becomes more nearly a constant and may be factored out of both numerator and denominator of Equation (19). When EFR is significantly less than unity, it enters the flux budget expression, Equation (11).

$$(21) 10 \log \left(\frac{\phi_T}{\phi_R} \right) = \alpha_{TC} + \alpha_{CR} + n \alpha_{CC} + \alpha_0 \ell + \alpha_M$$

-10 log (EFR)

See Equations 11, 18, and 19 for definition of terms.

The optical ports of Hewlett-Packard Transmitters are designed for mating with Hewlett-Packard Cable/Connector assemblies, but their characteristics require a little more attention than do the Receiver optical ports. The Transmitter and Cable/Connector data sheets should be consulted for the correct values of size and N.A., or for the directly-given value of transmitter-to-fiber coupling loss, α_{TC} , to use in flux budgeting. In applications having very short transmission distances, but requiring a number of in-line (cable-to-cable) connections, it is likely to be advantageous to use fiber optics of larger core diameter and N.A., such as some of the plastic types. The larger core diameter reduces the likelihood of losses in connectors due to misalignment. Depending on the size and N.A. of the Transmitter optical port, a larger core diameter and N.A. in the fiber optic cable may also reduce α_{TC} , but if the cable core diameter is too large, the cable-to-receiver loss, α_{CR} , may be excessive.

Data Rate and Format

The other areas of concern (data rate, data format, and interface) are interactive, depending on system requirements. In any single transmitter-to-receiver link, the flux budget along with probability of error P_e , establish the signaling rate, in baud units (symbols per second), while the data rate, in bits per second, depends also on the data format, or transmission code. NRZ (Non-Return-to-Zero) is the term for a transmission code in which the signal does not periodically return to zero. If a stream of NRZ data contains a series of consecutive "1s", the signal remains at the "1" level; similarly, the signal remains at the "0" level for consecutive "0s". RZ (Return-to-Zero) code signals a "1" by changing from low level to high level and back, never remaining at high level for a period of time longer than half a bit interval. Some examples of codes are given in Figure 10. Notice that NRZ code uses the channel capacity most efficiently since it requires only one code symbol per bit. The RZ code illustrated uses two code symbols per bit while other codes may require an even higher channel capacity for a given data rate. NRZ code requires a clock signal at the receiving end to define, for each interval, the point in time at which the

data is valid. The time at which the data is clocked must be sufficiently clear of the interval edges to avoid phase-shift errors due to jitter, rise time, or propagation delay. Since the clock signal is separately transmitted, phase shift in the clock channel can contribute to the phase-shift error unless it is equal, in direction and magnitude, to the phase shift in the data channel. For this reason, fiber optic channels carrying clock signals should use the same type of cable and the same length, unless the transmission distance is very short. Note that the transmission time delay in an optical fiber depends on the core index of refraction:

$$(22) \text{ TRANSMISSION DELAY, } t_{\ell} = \left(\frac{1}{c} \right) \ell n$$

where c is the velocity of light in a vacuum, $c = 3 \times 10^8 \text{ m/s}$
 ℓ is the fiber optic cable length (m)
 n is the core index of refraction

and differential delay between a data channel and a clock channel is:

$$(23) \text{ DIFFERENTIAL DELAY, } t = \left(\frac{1}{c} \right) [\ell_2 n_2 - \ell_1 n_1]$$

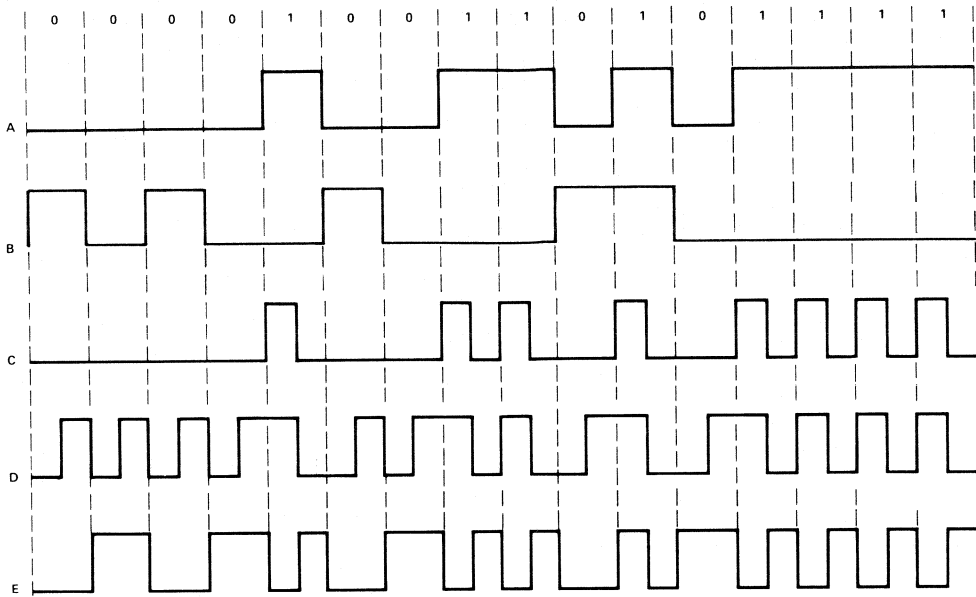
Some codes are self-clocking — i.e., a separate channel to transmit the clock signal is not required, so there is no problem with differential delay. For this reason, self clocking codes may be preferred even though the data rate is less than that of NRZ. Note that in its internally coded mode, the Hewlett-Packard fiber optic system transmits either NRZ or codes of arbitrary format and duty factor. In the externally coded mode, the system requires the duty factor of the code to be 50% and the signal must remain LESS than $5 \mu\text{s}$ in either high state or low state.

The Hewlett-Packard system is capable of a 10 Mbaud signaling rate. If a higher data rate is required, the data stream can be divided among additional channels. If each channel is coded, such as with Manchester code, the capacity of each channel is 5Mb/s and if the total data rate requirement is 20Mb/s, four channels are required. Using NRZ, the 20Mb/s data can be transmitted on two channels, with a third channel for the clock signal. Thus, if the data rate requirement exceeds 15Mb/s, the NRZ format requires fewer fiber optic channels.

System Configuration

The simplex arrangement in Figure 11 allows data in one direction only, and the format should, therefore, include error checks, such as parity bits. The full duplex arrangement requires two Transmitter/Receiver (T/R) pairs and two cables but allows data to go in both directions simultaneously. If, at a given time, Station 1 is transmitting, the return transmission from Station 2 can be unrelated to the information from Station 1, but could also be a relay or re-transmission of the data received by Station 2, so a logic delay and comparator circuit in Station 1 can check for errors and allow corrections. The same is true for the full triplex arrangement. Extension to larger numbers of stations is possible and the benefits are the same, but the number of T/R pairs increase rapidly, as shown by the series in Figure 11, requiring $n(n-1)$ T/R pairs for n stations.

Half-duplex (not illustrated) is a means for allowing two stations to alternately use the same transmission medium. With a wire cable, half-duplex operation is commonly and easily done; it can also be done with fiber optic cable but



CODE		DESCRIPTION	CHANNEL REQUIRED	REQUIRES DC?	REQUIRES CLOCK?
A	NRZ (NON-RETURN TO ZERO)	High during entire "mark", low during entire "space" interval	1 Mbaud per Mb/s	YES	YES
B	NRZ I (NRZ INVERTABLE) (SELF-CLOCKING)	Transition for "space" No transition for "mark"	1 Mbaud per Mb/s	YES	NO*
C	RZ (RETURN TO ZERO)	Low during entire "space", momentarily high during "mark" interval	2 Mbaud per Mb/s	NO	YES
D	MANCHESTER (SELF-CLOCKING)	Positive transition for "space", negative transition for "mark"	2 Mbaud per Mb/s	NO	NO
E	BIPHASE MARK (MANCHESTER II) (SELF-CLOCKING)	Each bit period begins with a transition. "Space" has NO transition during bit period – "mark" has one transition during bit period	2 Mbaud per Mb/s	NO	NO

NOTE THAT C, D, E HAVE 50% DUTY FACTOR ($k = 1.00$)
 *WITH PHASE-LOCK LOOP AND BIT STUFFING

Figure 10. Examples of NRZ and RZ Code Patterns.

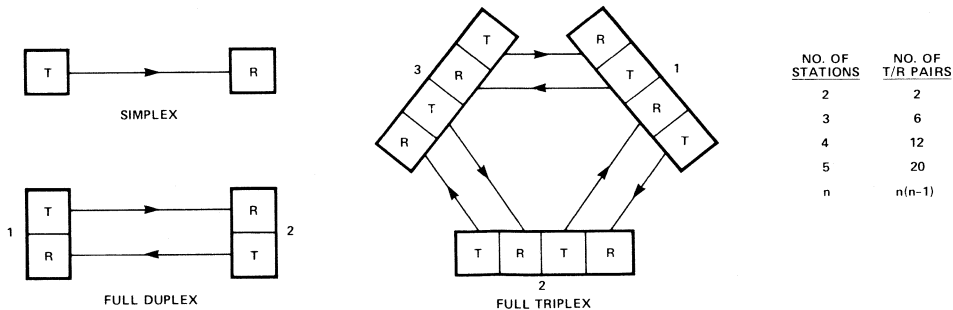


Figure 11. Simplex, Full-Duplex, Full Triplex, Full-n-plex Fiber Optic Links.

the fiber-furcating couplers for accomplishing it are very lossy, are not commonly available, and will not be discussed.

Data interchange among a large number of stations can be accomplished with fewer T/R pairs by using the Master Station Multiplex (MSM) arrangement in Figure 12. The MSM arrangement requires only $2(n-1)$ T/R pairs for n stations (master + $(n-1)$ slaves). Its operation differs from the full n -plex arrangement of Figure 11 in that only the master station transmits directly to all other stations. Data from any slave station is transmitted to master and re-transmitted to all slave stations according to the "re-transmit enable" ($E_1 \dots E_x$) selection made in the master station. Thus, a complete error check is possible. Regardless of how many slave stations are added, the transmission delay from any slave to any other slave is just the delay of two fiber optic links plus the propagation delay in the master station's relay circuit. The time delay between re-transmission from the master and the error-check return transmissions from the slaves is the same if each link length is the same, i.e., two links plus relay time. Notice that a complete error check requires an error check in the master, plus an error check in the station where the data originated. Another feature of the MSM system is that any slave station can be disconnected or turned off without affecting the other stations. With slightly more complicated relay control logic in the master stations, the MSM system can provide even more flexibility in the control of data movement — the schematic in Figure 12 is intended only to illustrate the potential flexibility of MSM.

At the expense of less flexibility and longer transmission delay, multiplex operation can be done with an even smaller number of T/R pairs by means of Looped-Station Multiplexing (LSM) as in Figure 13. In addition to requiring only n T/R pairs for n stations, LSM offers the advantage that an error check is required only at the station from which the data originates. There are some disadvantages. A relatively minor disadvantage is the data delay around the loop to where the data originated. A less minor disadvantage is the fact that, even if one of the stations in the loop is designated for loop control, it does not have

control as absolute as that of the master station in MSM. A major disadvantage is that removal of one or more stations from the loop may require a re-run of the fiber optic cable unless the flux budget allows insertion of a connector to replace the station(s) removed. There is some error accumulation around the loop, but this is not a disadvantage if error correction is applied.

Error Accumulation

Where error correction is inconvenient or impossible, the accumulation of error through data relay units may be significant. With Hewlett-Packard components operated within the limits prescribed by the data sheet parameters and the flux budget, any point-to-point link has a probability of error $P_e < 10^{-9}$. This means that $P_e < 10^{-9}$ as long as the loss margin, $\alpha_M(\text{dB})$ is above zero. With a number, n , of repeater links, the worst case estimate of cumulative probability of error is the RMS value:

(24) CUMULATIVE PROBABILITY OF ERROR,

$$P_{e,n} = 1 - \prod_{i=1}^n (1 - P_{e,i}) \approx \sum_{i=1}^n P_{e,i}$$

where $P_{e,i}$ is the probability of error in link "i"

If each link has the same probability of error, P_e , then the cumulative value of P_e is estimated at:

(25) CUMULATIVE PROBABILITY OF ERROR FOR EQUAL P_e 's

$$P_{e,n} \approx nP_e$$

However, as in any chain, the probability of error is usually just that of the "weakest link," that is, the link having the highest probability of error.

Measuring the probability of error can be very time-consuming if P_e has a very low value. For instance, if $P_e = 10^{-9}$ at 10 Mbaud ($\text{BER} = 10^{-9}$), this suggests that if the system is operated for 100 seconds at 10 Mbaud (accumulate 10^9 bits) with one error, the $P_e = 10^{-9}$ is verified. This is not necessarily true. The significance of $P_e = 10^{-9}$ is that over several such periods the average error is one per 100 seconds. A less time-consuming procedure is to lower the signal (flux) level until the error rate, $P_e N$ is measurably high in a comfortable period of time, and note

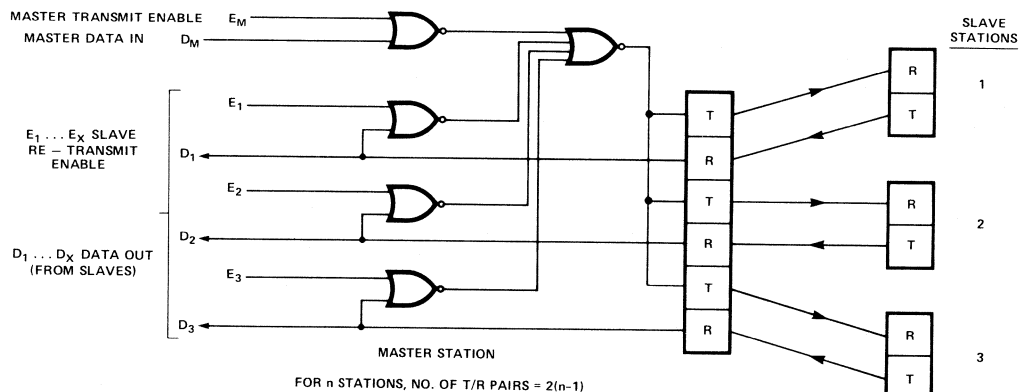


Figure 12. Master Station Multiplex Arrangement for Fiber Optic Links.

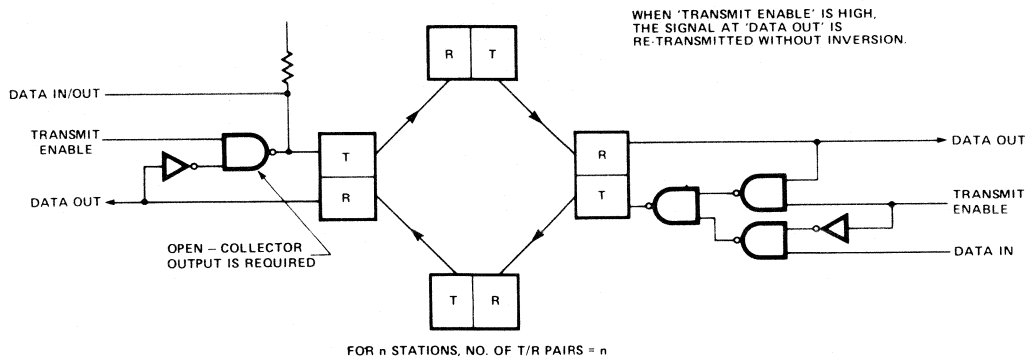


Figure 13. Looped-Stations Multiplex Arrangement for Fiber Optic Links.

the Bit Error Rate (BER) as a function of flux level into the Receiver. At these lower levels of flux, the Probability of Error (P_e) is:

$$P_e = \text{BER} = \frac{\text{NO. OF ERRORS IN A PERIOD}}{\text{NO. OF BITS IN SAME PERIOD}}$$

Since the occurrence of error is random, the probability of error can be described by the Complementary Error Function, erfc :

$$(26) P_e = 0.5 \text{erfc} \left[(\phi - C) / \sigma \sqrt{2} \right]$$

where

σ = standard deviation (W) referred to Receiver input.
 c = logic comparator level as referred to Receiver input (W)
 ϕ = input flux (W)

With the BER observations made at two or more flux levels, the arguments of the Complementary Error Function values corresponding to these data points can be used to form a set of simultaneous equations to be solved for " c " and " σ ". Due to the randomness of the data, a curve-fitting approach is recommended, using:

$$\text{erfc}^{-1}(2 P_e) = y_i = [(x_i - b) / \sigma \sqrt{2}]$$

where x_i = flux level

Values of the inverse of the Complementary Error Function can be obtained from a table, but when $P_e < 10^{-4}$ adequate precision is obtained from the approximation:

$$\text{erfc} X \approx 0.54 / (X e^{X^2}) = 0.54 e^{-(X^2 + \ln X)}$$

(see Appendix)

INSTALLATION, MEASUREMENT, AND MAINTENANCE

The shielded metal packages of Hewlett-Packard Fiber Optic Modules are very sturdy and can be mounted in any position. Both Transmitter and Receiver dissipate very low power, so heat sinking is not required. A cool location is preferred, especially for the Transmitter. The main concern in selecting the locations of both modules is accessibility of the optical ports.

Mounting

The preferred mounting is with two #2-56 screws on a printed circuit board. Clearance must be provided for the Lock Nut, which protrudes 0.5mm to 1.0mm (depending on angular position) beyond the plane of the module's bottom surface. The usual way to deal with this is to allow the Lock Nut to overhang the edge of the P.C. board as in Figure 14. Lock Nut clearance could also be provided by

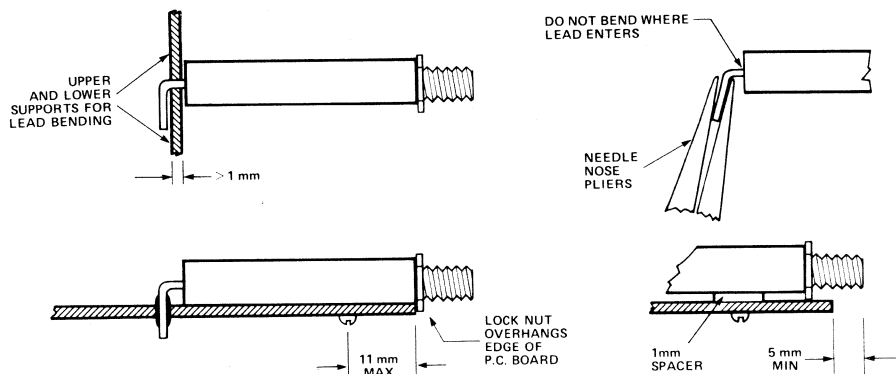


Figure 14. Lead Bending and P.C. Board Mounting.

an opening in the board, or by using washers of 1mm thickness on the #2-56 mounting screws to space the Module bottom 1mm from the board. Screws entering the #2-56 tapped holes **MUST NOT TOUCH BOTTOM AS THIS MAY DAMAGE THE MODULE.** The #2-56 tapped hole is 5.6mm (0.22 in.) deep, which provides an ample purchase on the thread.

P.C. Board Thickness		Recommended Screw Length — mm (in.)	
mm	in.	W/O Spacer	W/1-mm Spacer
0.79	1/32	4.78 (.188)	6.35 (.250)
1.59	1/16	6.35 (.250)	6.35 (.250)
2.38	3/32	6.35 (.250)	6.35 (.250)

The #2-56 holes near the front of the package are the only screw holes that may be used for mounting the module. **UNDER NO CIRCUMSTANCES MAY THE SCREWS ALREADY INSTALLED OR THE SET SCREW BE DISTURBED.** Disturbing these may cause interior damage.

For additional support, the electrical leads may be bent down and soldered into the P.C. board. In bending the leads, care must be taken to avoid strain at the point where the leads enter the glass seal. This can be done by applying mechanical support between the module and the bending point which should be at least 1.0mm (0.04 in.) from the end of the module. A needle-nose pliers can also be used to bend the leads individually, providing no bending moment is transferred to the seal. See Figure 14 for details for these techniques.

Panel mounting can also be used. This is an especially attractive mounting when R.F. shield integrity must be maintained. As seen in Figure 15, the panel thickness must be less than 4mm (5/32 in.) and have a counter-bore to receive the Lock Nut. This will make the mounting secure and leave enough of the Barrel outside the panel to permit installation of an external mounting nut as well as the Cable Connector.

Fiber Optic Cable Connections

The data sheet cautions against disturbing the Lock Nut and Barrel. This is to prevent damage by someone who has not read the following material:

As seen in Figure 16, there is a clearance between the interior end of the Barrel and a shoulder on the Fiber

Alignment Sleeve. If this clearance is not maintained, there is a risk that a force applied to the Barrel may be transmitted by the Fiber Alignment Sleeve to the optical fiber stub, forcing the stub against the face of the source or detector. The source (or detector) is an extremely fragile semiconductor device and even a very small force can cause severe damage. Should it be necessary to remove the Lock Nut and Barrel, they should be reinstalled with this procedure:

- 1. Lightly and carefully thread the Barrel into the Module body until it comes against the shoulder of the Fiber Alignment Sleeve.
- 2. Back the Barrel **OUT ONE FULL TURN**, then **HOLD THE BARREL FROM TURNING** while seating the Lock Nut securely against the body. During final tightening of the Lock Nut, the Barrel may be allowed to enter no more than **HALF A TURN**. Final barrel position must be between a **HALF-TURN** and a **FULL TURN** from the alignment sleeve shoulder.

When Hewlett-Packard Cable Connectors are joined, either to each other or to the optical port of a Transmitter or Receiver, there is a cylindrical spring Sleeve that aligns the Ferrules. This is shown in Figures 16 and 17. It may be difficult to see, but the Sleeve does have a slightly flattened "leaf" on either side of a notch. The notch makes the leaves spring separately, allowing the Ferrules at

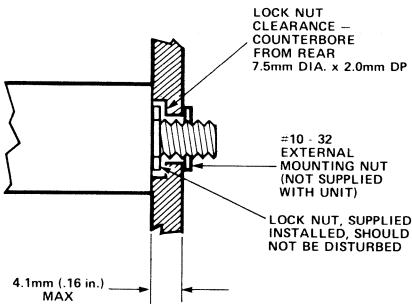


Figure 15. Panel Mounting.

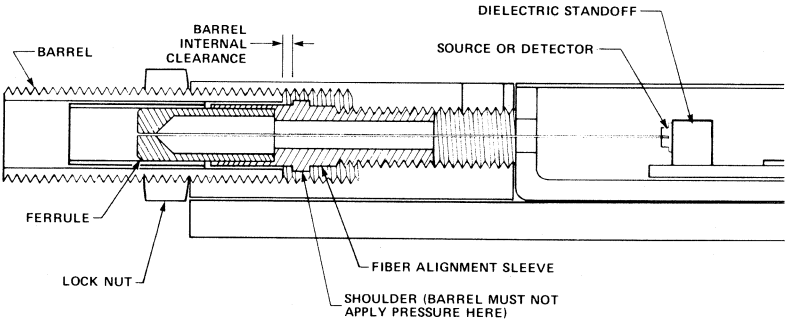


Figure 16. Opto-Mechanical Structure of T/R Modules.

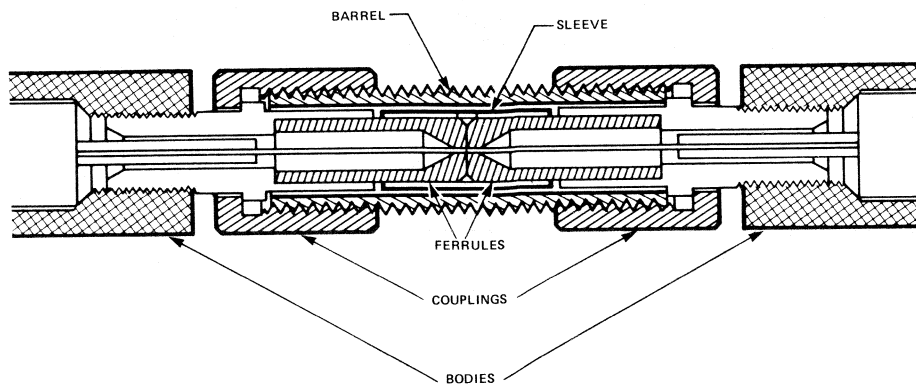


Figure 17. In-Line Connector Arrangement.

opposite ends of the sleeve to have slightly different diameters and yet be firmly aligned by the curved interior wall. A chamfer on the edge of the Ferrule aids insertion. In making temporary Cable-to-Cable connection, it is permissible, and often convenient, to omit the Barrel, since it does not perform an alignment function. When the Barrel is used for a more sturdy joint, the connection procedure is:

1. Install the Sleeve and Barrel on one Connector, using only FINGER TIGHTNESS of the Coupling on the Barrel.
2. Start the Ferrule of the second Connector into the Sleeve.
3. Engage the Coupling on the Barrel threads and tighten FINGER TIGHT.

Alignment of the Ferrules (and hence the fiber optics) is performed by the Sleeve; the Barrel and Couplings are intended only for tensile support, but if they are OVER tightened, they may cause misalignment. Loss of coupling due to misalignment can be observed at the V_T (Test Point) on the Receiver when the System is active:

$$\Delta V_T / \Delta \phi \approx 10 \text{ mV} / \mu \text{W}.$$

The procedure above applies also to making Cable connection at the Receiver and Transmitter, except that the Sleeve and Barrel are already installed. In manufacture, the Sleeve in the Module is pre-stressed for a tighter fit on the Ferrule in the Module than on the Ferrule in the Connector. The Sleeve is not likely to be pulled out when the Module is disconnected, but if that does happen, it can be reinstalled without removing the Barrel by using the Connector Ferrule to guide and support it.

In connecting fiber optics other than those from Hewlett-Packard to a Hewlett-Packard module, it is necessary to center the fiber in a cylinder with the same outside diameter as the Hewlett-Packard Ferrule over a length (to first shoulder) equal to half the length of the Sleeve, i.e., 3.5mm. This is adequate for a temporary connection. For a more permanent connection, add a coupling to fit the #10-32 thread on the Barrel.

Power Supply Requirements

Power supply lines for the Transmitter and the Receiver should each have a pi filter of two $60\mu\text{F}$ shunt capacitors and a $2.2\mu\text{H}$ ($<1\Omega$) inductor. The Transmitter needs this filter to prevent transients from reaching other equipment when the LED (or IRED) currents are switched. The Receiver needs the filter to keep line transients from interfering with its extremely sensitive amplifier. In addition, the Receiver may need its own regulator, as shown in the data sheet, to prevent low-frequency transients or ripple from interfering with the data stream. If a regulator is used, the pi filter should be between the regulator output and the Receiver supply terminal. The Transmitter needs no regulator if the supply voltage is in the specified range.

System Performance Evaluation

System performance checks may be done by using error-detection equipment, such as the Hewlett-Packard Mod. 3760A Word Generator and 3761 Error Detector as indicated in Figure 18. The Mod. 3780A Pattern Generator/Error Detector which contains both word generator and error detector is also usable, although it has less flexibility in word generation and a lower data rate capability. These instruments have low-impedance (50Ω and 75Ω) inputs and outputs. The outputs have adequate voltage swing to drive the Fiber Optic Transmitter Data Input, but ringing may occur unless the signal line is properly terminated. The low-impedance inputs require a buffer amplifier between the Receiver output and the Error Detector input. Here also the voltage swing is ample, so a simple emitter follower will do as a buffer.

With Mode Select "low" (on the Fiber Optic Transmitter), the Word Generator may be set for either NRZ or RZ code, and there is no restriction of any kind on word length or composition (pseudo random or selected). With Mode Select "high", the code selection must be such that:

1. No interval $> 5\mu\text{s}$ of consecutive marks or consecutive spaces
2. Duty factor: $.44 < DF < .57$ or $.75 < k < 1.25$

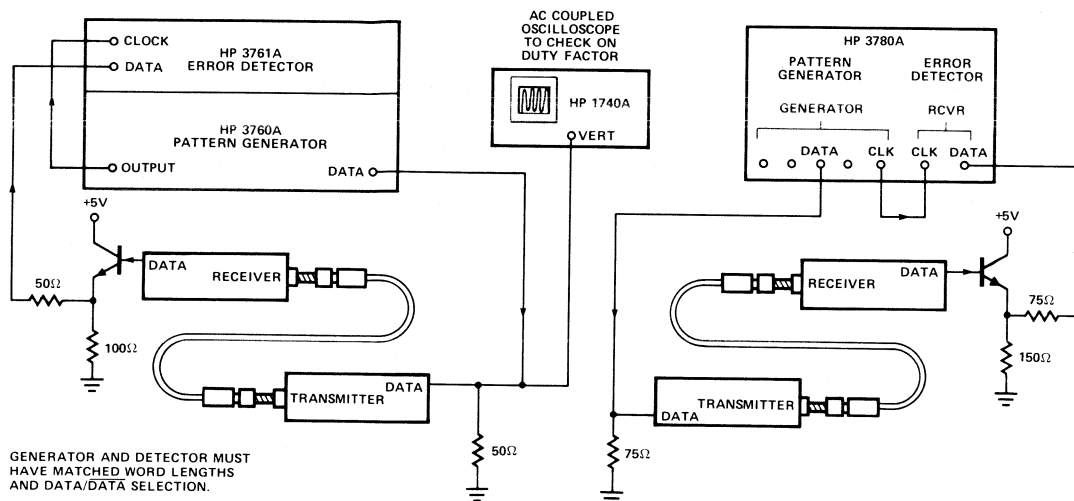


Figure 18. Bit Error Rate Measurement Arrangement.

The first condition can be examined with an oscilloscope, but if word length is such that:

$$\frac{\text{word length (bits)}}{\text{data rate (bits/second)}} < 5 \text{ microseconds}$$

then there is no way that any consecutive marks or spaces can extend over 5μs.

The easiest way to check duty factor is by observing k directly on an ac coupled oscilloscope: first establish the baseline position (e.g., center of scope face) with zero signal input, then with the data signal applied:

$$k = \frac{\text{excursion above baseline position}}{\text{excursion below baseline position}}$$

where the oscilloscope deflects upward for positive input. For this observation, the oscilloscope need not be synchronized — it could be free-running. The word composition should be adjusted to bring k within the specified limits. The word composition can be adjusted by adding zeroes, changing word length, or by handselecting the bit sequence.

Either error detector has two modes of operation: BER (Bit Error Rate) mode and "count" mode. The count mode is simplest to use and gives an earlier indication of the result of any system adjustment.

With the System at normal operating flux level, the error rate is so low that it would take several hours or even days to make an accurate BER measurement. If the flux level is reduced, SNR falls and BER rises until it becomes measurable. Then the error function [see Equation (26)] can be applied to determine the BER at the normal flux level in terms of the constants "a" and "b". The problem now is that the flux may be too low to measure with equip-

ment at hand. The solution is in the Receiver Test Point voltage, V_T , which varies linearly as Receiver input flux — see Equation (17). But even this method has limits: when the flux becomes a small fraction of a microwatt, the voltage difference ($V_{TMAX} - V_T$) cannot be accurately observed. The solution to this problem is in the Transmitter-to-Cable connection. Just back off the Coupling, noting the number of turns while observing V_T , then plot a curve like that of Figure 19. The curve is quite repeatable if care is taken to avoid backlash and rotation of the Connector Body (rotate Coupling only) but the curve is not the same for each System.

Operating Margin Measurement

The approximate flux margin, α_M , for a system can be found using the Connector on the Transmitter as an adjustable attenuator as described above, proceeding as follows:

1. Prepare a curve similar to Figure 19.
2. Count the turns, N , needed to get measurable error, $P_e, N \approx 10^{-6}$
3. Find $\alpha_N(\text{dB})$ from N and the curve from Step 1.

$$(27) \alpha_M(\text{dB}) = \alpha_N(\text{dB}) - 0.5\text{dB}$$

The 0.5 dB in Equation (27) is to allow for the fact that the operating BER should be 10^{-9} , but the BER at which error is easily observed is near 10^{-5} . At $\text{BER} = 10^{-5}$ the flux level is 0.5 dB below the flux level needed for $\text{BER} = 10^{-9}$.

If any kind of relative flux indicator is available (e.g., a photodiode or radiometer) the flux margin can be observed in a similar manner, but the counting of turns, N ,

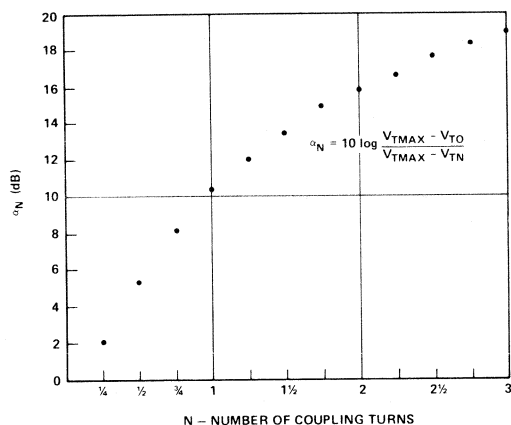


Figure 19. Flux Decoupling by Rotation of Connector Coupling.

and use of Figure 19 become unnecessary. The procedure is:

1. Unscrew the Transmitter connector until error is observed at the Receiver.
2. Transfer the Receiver connector to the flux indicator and note indication I_1 then, without changing the coupling to the flux indicator, reseal the Transmitter connector and note indication I_2 .
3. α_M (dB) = $10 \log (I_2/I_1) - 0.5$ dB

Absolute flux levels at "N" turns can be found by measuring the flux level when $N=0$ and applying a ratio. A rough measurement can be made using the Test Point voltage, V_T , and Equation (15). A more precise measurement requires a calibrated radiometer, such as the EG&G Mod. 550, used as shown in Figure 20a. With its "flat" filter installed, the EG&G Mod. 550 reads the radiant incidence, E , in W/cm^2 on an aperture area, $A_D = 1$ cm^2 and N.A. = 1. With the filter removed, a fiber optic cable can be placed so close to the aperture that there is no flux loss, and since the radiometer N.A. exceeds the fiber N.A., the radiometer will have a reading in W/cm^2 which is numerically equal to the flux in watts. However, a correction must be made for the removal of the filter.

The insertion loss of the filter must be evaluated at the measurement wavelength because it varies with wavelength to compensate for spectral variation in the response of the silicon detector. The arrangement shown in Figure 20 for measurement of radiant intensity is a good one for measuring insertion loss of the filter. Two observations are made — one with and one without the filter. Error due to ambient radiation is avoided by working in subdued ambient and for each observation taking two radiometer readings (source off and source on); the difference in readings is the observation of the radiant incidence, E_e , produced by the radiant intensity, I_e , of the source. The ratio of the two observations gives:

$$(28) \text{ FILTER INSERTION LOSS, } \alpha_F = 10 \log \frac{E_e(\text{filter out})}{E_e(\text{filter in})}$$

This same arrangement can be used to measure the average flux of the Transmitter as shown in Figure 20b. From the observation of E_e with the filter IN:

$$(29) \text{ AVERAGE INTENSITY, } I_e \left(\frac{\mu W}{sr} \right) = E_e \left(\frac{\mu W}{cm^2} \right) \times d^2 \text{ (cm}^2\text{)}$$

$$(30) \text{ AVERAGE FLUX, } \phi_e(\mu W) = I_e \left(\frac{\mu W}{sr} \right) \left[\frac{\phi(\theta)}{I(0)} \right] (\text{MAX})$$

from Equation (29)
value from radiation pattern integral in Transmitter Data Sheet

SYSTEM MAINTENANCE

Preventive Maintenance

Good system performance requires clean surfaces at the faces of the optical fibers to avoid obstruction of the optical path. This is true for the fiber faces in the Transmitter/Receiver modules, as well as in the Cable Connectors. Compressed air is often sufficient to remove particles of foreign matter; methanol or Freon™ on a cotton swab also works well. If it is necessary to remove the threaded barrel and lock nut to clean the Transmitter (or Receiver) optical port, refer to the earlier section "Fiber Optic Cable Connections" for re-assembly instructions. Severely ground-in or adhering foreign material may require repeated cleaning efforts to restore original optical performance.

Long-term degradation occurs in any LED and LED degradation affects the Hewlett-Packard Fiber Optic System in two ways: reduced average flux, affecting either externally- or internally-coded mode, and altered flux excursion ratio, affecting only the internally-coded mode. Significant degradation of either the flux or the flux excursion ratio can be detected by regular observation of the flux margin, α_M , and of k .

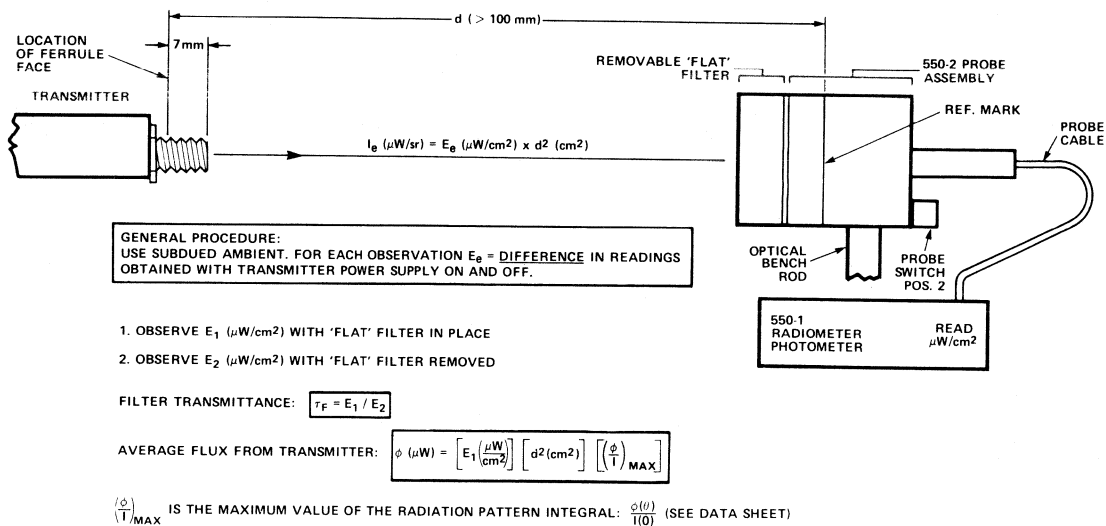
α_M is evaluated as explained under Operating Margin Measurement from Equation (27). A plot of α_M against the logarithm of the cumulative hours of operation will allow an estimate to be made of the operating time remaining until $\alpha_M = 0$ FOR THE P_e DESIRED.

k must be evaluated by measuring ϕ_H , ϕ_M , and ϕ_L as explained in the Transmitter description. The Test Point voltage can be used in making this measurement — see Equation (15). The upper and lower margins on k for a particular Receiver can be found by operating the Transmitter with Mode Select "high" and a rectangular signal ($f \approx 500$ kHz) at Data Input. As the duty factor of the signal is varied, the limits on k are found as those at which the Receiver fails to follow the Data Input signal.

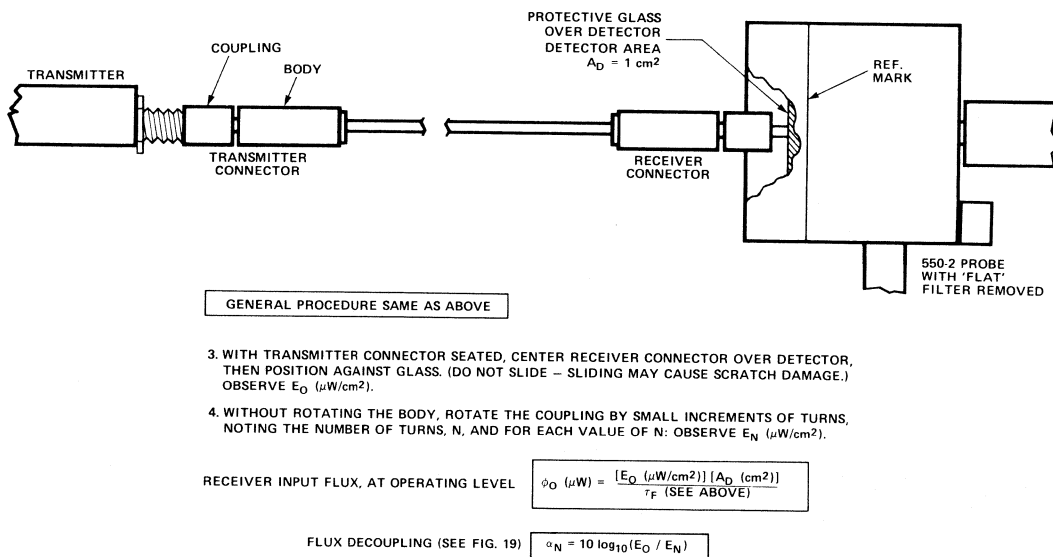
$$(31) k = \left(\frac{1}{ft_p} \right) - 1 = \frac{1}{ft_n - 1}$$

where ft_p is the positive-pulse duty factor
 ft_n is the negative-pulse duty factor

Changes in k of the Transmitter do not affect the Receiver performance in externally-coded (FOO) mode, and if this mode is used, then flux margin, α_M , is the only concern.



(a) MEASUREMENT OF TRANSMITTER AVERAGE FLUX



(b) MEASUREMENT OF AVERAGE RECEIVER INPUT FLUX AND FLUX DECOUPLING AT TRANSMITTER CONNECTOR.

Figure 20. Flux Measurement with EG&G Mod 550 Radiometer.

Corrective Maintenance

Trouble in the System may range from complete breakdown to excessive BER. The flux used in the Hewlett-Packard System is visible so the cause of complete breakdown can sometimes be localized by simply looking at the output of the Cable and the Transmitter. If there is visible output from the cable, then, when the Cable is connected to the Receiver, there should be an 8mV change in Test Point voltage, V_T , as the Transmitter (Mode Select "low") is turned on and off by switching V_{CC} . If ΔV_T is more than 8mV but the system is not working, then either the Receiver logic is not functioning properly or the flux excursion ratio, k , is either too high or too low. Excursion ratio can be checked as described above, using V_T . If k is satisfactory, the logic malfunction could be due to incorrect supply voltage or output loading.

If the System is functioning but has excessive BER, either the flux and flux excursion ratio are marginal (can be checked as described above) or there is too much interference from noise or other effects. If the Data Input voltage levels are correct, either random noise is high or errors are occurring due to incorrect supply voltage or output loading, or due to noise on the supply line. Random noise effects can be checked by lowering the flux level to a point where P_e is measurably high. If P_e varies with flux level according to $P_e = \text{erfc}(X)$, as in Equation (26), then the problem is excessive random noise. Random noise can also be checked by changing the data rate while the flux level is low enough to make P_e measurable. If P_e is the same at any data rate, the problem is excessive random noise. Excessive random noise is more likely to occur in the Receiver than in the Transmitter; the best way to check is by replacement of the Receiver. Noise on the supply line is difficult to trace. If there is any doubt, the Receiver should be operated from its own supply (e.g., a 5V regulator). Receiver noise should be low enough to make $P_e < 10^{-9}$ at 10 Mbaud with normal flux level ($\Delta V_T > 8$ mV by the method described above indicates normal flux level).

APPENDIX

Find the values of the constants, c and σ for Equation (26) by least-squares curve fitting to data of errors vs. input flux level, using the approximation:

$$(A1) Y = \text{erfc } X \approx 0.54 e^{-X^2 + \ln X} = 0.54 / (X e^{X^2})$$

which has adequate precision for $10^{-3} < Y < 10^{-12}$

The value of X corresponding to a given Y is easily obtained by repetitively computing:

$$(A2) X_{m+1} = \sqrt{\ln \frac{0.54}{Y} + \ln \frac{1}{X_m}}$$

until $X_{m+1} = X_m$ (4 to 10 loops for 9-place accuracy)

then, $X \approx \text{erfc}^{-1} Y$

$$\begin{matrix} n \\ \text{DATA} \end{matrix} \left\{ \begin{matrix} X_i = \text{flux level } (\mu W) \\ P_{ei} = \text{bit error rate at } X_i \end{matrix} \right\} 1 \leq i \leq n$$

PAIRS

Using Equation (A2) with $Y = 2 P_{ei}$, compute:

$$(A3) Y_i \approx \text{erfc}^{-1} (2 P_{ei})$$

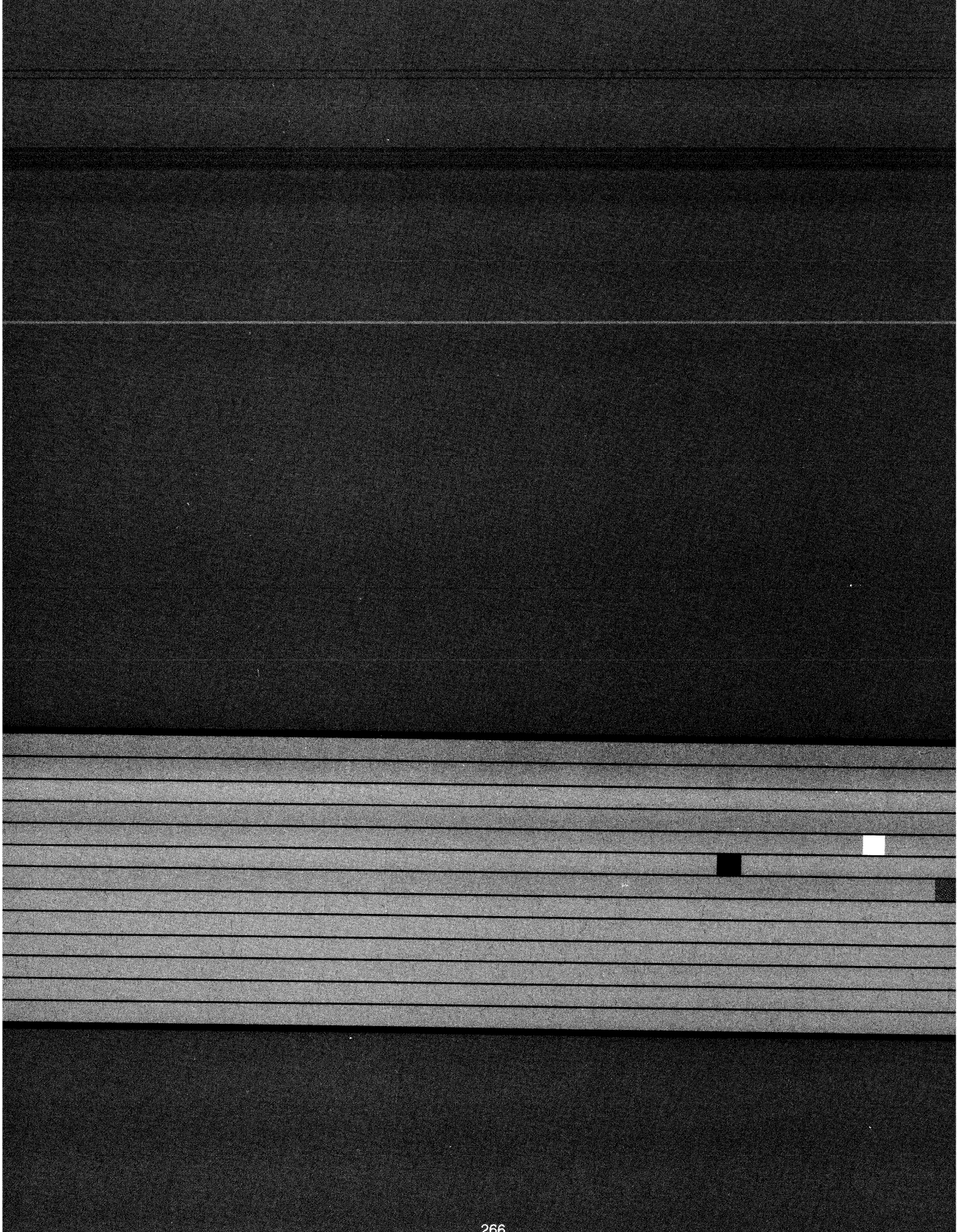
Then, for the n data pairs, prepare the summations:

$$\sum_{i=1}^n X_i, \sum_{i=1}^n X_i^2, \sum_{i=1}^n Y_i, \sum_{i=1}^n X_i Y_i, n = \sum_{i=1}^n 1$$

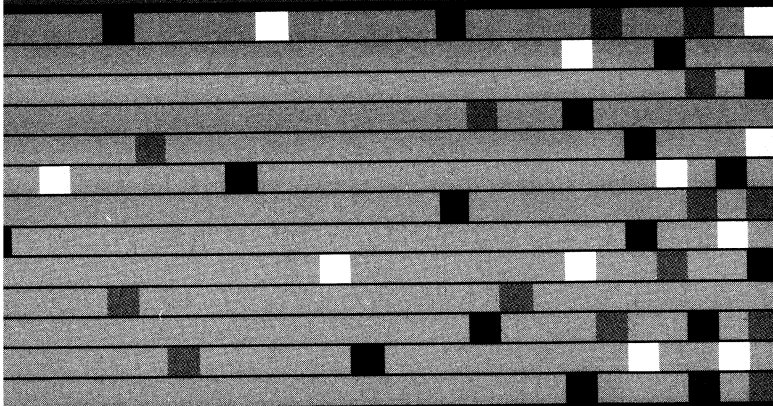
The constant for a least-squares fit to Equation (26) are:

$$(A4) \sigma = \frac{1}{\sqrt{2}} \left[\frac{n (\sum X_i^2) - (\sum X_i)^2}{n (\sum X_i Y_i) - (\sum X_i) (\sum Y_i)} \right]$$

$$(A5) c = \frac{(\sum X_i) (\sum X_i Y_i) - (\sum Y_i) (\sum X_i^2)}{n (\sum X_i Y_i) - (\sum X_i) (\sum Y_i)}$$



Appendix



HP Components Sales and Service

Alabama

P.O. Box 7700
420 Wynn Dr., N.W.
Huntsville 35805
Tel: (205) 830-2000

Arizona

8080 Pointe Parkway West
Phoenix 85044
Tel: (602) 273-8000

California

1421 So. Manhattan Ave.
Fullerton 92631
Tel: (714) 999-6700

9606 Aero Dr.
P.O. Box 23333
San Diego 92123
Tel: (714) 279-3200

3003 Scott Blvd.
Santa Clara 95050
Tel: (408) 988-7000

2150 West Hillcrest Dr.
Thousand Oaks 91320
Tel: (805) 373-7000

Colorado

24 Inverness Place East
Englewood 80110
Tel: (303) 649-5000

Connecticut

47 Barnes Industrial Rd. So.
P.O. Box 5007
Wallingford 06492
Tel: (203) 265-7801

Florida

P.O. Box 13910
6177 Lake Ellenor Dr.
Orlando 32809
Tel: (305) 859-2900

Georgia

P.O. Box 105005
2000 South Park Place
Atlanta 30348
Tel: (404) 955-1500

Illinois

5201 Tollview Dr.
Rolling Meadows 60008
Tel: (312) 255-9800

Indiana

11911 No. Meridian Street
Carmel 46032
Tel: (317) 844-4100

Maryland

3701 Koppers St.
Baltimore 21227
Tel: (301) 644-5800

P.O. Box 1648
4 Choke Cherry Rd.
Rockville 20850
Tel: (301) 948-6370

Massachusetts

1775 Minuteman Rd.
Andover 01810
Tel: (617) 682-1500

Michigan

39550 Orchard Hill Place Dr.
Novi 48050
Tel: (313) 349-9200

Minnesota

2025 W. Larpenteur Ave.
St. Paul 55113
Tel: (612) 644-1100

Missouri

1001 East 101 Terr.
Suite 120
P.O. Box 24796
Kansas City 64131
Tel: (816) 941-0411

New Jersey

20 New England Ave. West
Piscataway 08854
Tel: (201) 981-1199

W. 120 Century Rd.
Paramus 07652
Tel: (201) 265-5000

New Mexico

7801 Jefferson St., NE
Albuquerque 87109
Tel: (505) 823-6100

New York

7641 Henry Clay Blvd.
Liverpool 13088
Tel: (315) 451-1820

200 Cross Keys Office
Fairport 14450
Tel: (716) 223-9950

2975 Westchester Ave.
Purchase 10577
(914) 935-6300

3 Crossways Park West
Woodbury 11797
Tel: (516) 921-0300

North Carolina

305 Gregson Dr.
Cary 27511
Tel: (919) 467-6600

Ohio

15885 Sprague Rd.
Cleveland 44136
Tel: (216) 243-7300
675 Brooksedge Blvd.
Westerville 43081
Tel: (614) 891-3344
9080 Springboro Pike
Miamisburg 45342
(513) 433-2223

Oregon

9255 S.W. Pioneer Ct.
P.O. Box 328
Wilsonville 97070
Tel: (503) 682-8000

Pennsylvania

2750 Monroe Blvd.
P.O. Box 713
Valley Forge 19482
Tel: (215) 666-9000

Texas

1826-P Kramer Lane
Austin 78758
Tel: (512) 835-6771

10535 Harwin
Houston 77036
Tel: (713) 776-6400

930 E. Campbell Rd.
P.O. Box 831270
Richardson 75083-1270
Tel: (214) 231-6101

Washington

Bellefield Office Pk.
15815 S.E. 37th St.
Bellevue 98006
Tel: (206) 643-4000

International Sales Offices and Representatives

Product Line Sales/Support Key

Key Product Line
A Analytical
CM Components
C Computer Systems Sales Only
CH Computer Systems Hardware Sales and Services
CS Computer Systems Software Sales and Services
E Electronic Instruments & Measurement Systems
M Medical Products
P Personal Computation Products

IMPORTANT: These symbols designate general product line capability. They do not insure sales or support availability for all products within a line, at all locations. Contact your local sales office for information regarding locations where HP support is available for specific products.

+ Indicates main office

HP distributors are printed in italics.

Arranged Alphabetically by country

ANGOLA

Telectra
Empresa Tecnica de Equipamentos
R. Barbosa Rodrigues, 41-1 DT.
Caixa Postal 6487
LUANDA
Telex: 35515,35516
E.P.

ARGENTINA

Hewlett-Packard Argentina S.A.
 Montaneses 2140150
 1428 **BUENOS AIRES**
 Tel: 783-4886/4836/4730
 4705/4729
 Cable: HEWPAKARG
 A,E,CH,CS,P

Biotron

S.A.C.I.M. e.l.
Av Paso Colon 221, Piso 9
*1399 **BUENOS AIRES***
Tel: 541-333-490
541-322-587
Telex: 17595 BIONAR

ESANCO S.R.L.

A/ASCO 2328
 1416 **BUENOS AIRES**
 Tel: 581981, 592767
 Telex: c/o 9400 HPARGENTINA
 A

AUSTRALIA

Adelaide, South Australia Office

Hewlett-Packard Australia Ltd.
 153 Greenhill Road
PARKSIDE, S.A. 5063
 Tel: 272-5911
 Telex: 82536
 Cable: HEWPAKD Adelaide
 A,CH,CS,CM,E,M,P

Brisbane, Queensland Office

Hewlett-Packard Australia Ltd.
 10 Payne Road
THE GAP, Queensland 4061
 Tel: 30-4133
 Telex: 42133
 Cable: HEWPAKD Brisbane
 A,CH,CS,CM,E,M,P

Canberra, Australia Capital Territory Office

Hewlett-Packard Australia Ltd.
 121 Wollongong Street
FYSHWICK, A.C.T. 2609
 Tel: 80 4244
 Telex: 62650
 Cable: HEWPARD Canberra
 C,CH,CM,CS,E,P

Melbourne, Victoria Office

Hewlett-Packard Australia Ltd.
 31-41 Joseph Street
BLACKBURN, Victoria 3130
 Tel: 895-2895
 Telex: 31-024
 Cable: HEWPAKD Melbourne
 A,CH,CM,CS,E,M,P

Perth, Western Australia Office

Hewlett-Packard Australia Ltd.
 261 Stirling Highway
CLAREMONT, W.A. 6010
 Tel: 383-2188
 Telex: 93859
 Cable: HEWPAKD Perth
 A,CH,CM,CS,E,M,P

Sydney, New South Wales Office

Hewlett-Packard Australia Ltd.
 17-23 Talavera Road
 P.O. Box 308
NORTH RYDE, N.S.W. 2113
 Tel: 888-4444
 Telex: 21561
 Cable: HEWPAKD Sydney
 A,CH,CM,CS,E,M,P

AUSTRIA

Hewlett-Packard Ges.m.b.H.
 Grottenhofstrasse 94
 A-8052 **GRAZ**
 Tel: (0316) 291 5 66
 Telex: 32375
 CH,E

+ Hewlett-Packard Ges.m.b.H.
 Liebigasse 1
 P.O. Box 72
 A-1222 **VIENNA**
 Tel: (0222) 23 65 11-0
 Telex: 134425 HEPA A
 A,CH,CM,CS,E,M,P

BAHRAIN

Green Salon
P.O. Box 557
Manama
BAHRAIN
Tel: 255503-255950
Telex: 84419
 P

Wael Pharmacy
P.O. Box 648

BAHRAIN
Tel: 256123
Telex: 8550 WAEI BN
 E,M

BELGIUM

Hewlett-Packard Belgium S.A./N.V.
 Blvd de la Woluwe, 100
 Woluwedal
B-1200 BRUSSELS
 Tel: (02) 762-32-00
 Telex: 23-494 paloben bru
 A,CH,CM,CS,E,M,P

BERMUDA

Applied Computer Technologies
Atlantic House Building
Par-La-Ville Road
HAMILTON 5
 Tel: 295-1816
 Telex: 380 3589/ACT BA
 P

BOLIVIA

Arrellano Ltda
Av. 20 de Octubre #2125
Casilla 1383
LA PAZ
 Tel: 368541
 A

BRAZIL

+ Hewlett-Packard do Brasil I.e.C.
 Ltda.
 Alameda Rio Negro, 750
ALPHAVILLE
 06400 Barueri SP
 Tel.: (011) 421.1311
 Telex: (011) 33872 HPBR-BR
 Cable: HEWPAKD Sao Paulo
 A,CH,CM,CS,E,M,P

Hewlett Packard do Brasil I.e.C.Ltda.
 Praia de Botafogo 228-
 6° andar-conj 614
 Edificio Argentina - Ala A
 22250 - **RIO DE JANEIRO**
 RJ
 Tel: (021) 552.6422
 Telex: (021) 21905 HPBR-BR
 Cable: HEWPAKD Rio de Janeiro
 A,CH,CM,E,M,P

Convex/Van Den
Rua Jose Bonifacio
458 Todos Os Santos
CEP 20771

RIO DE JANEIRO, RJ
Tel: (021) 5910197
Telex: 33487 E6LB BR
 A

ANAMED I.C.E.I. Ltda.
Rua Bago, 103
*04012 **SAO PAULO, SP***
Tel: (011) 572.6537
Telex: 24740
 M

CANADA

Alberta
 Hewlett-Packard (Canada) Ltd.
 3030 3rd Avenue N.E.
CALGARY, Alberta
 T2A 6T7
 Tel: (403) 235-3100
 A,CH,CM,E,M,P

Hewlett-Packard (Canada) Ltd.
 11120-178th Street
EDMONTON, Alberta
 T5S 1P2
 Tel: (403) 486-6666
 A,CH,CM,CS,E,M,P

British Columbia

Hewlett-Packard (Canada) Ltd.
 10691 Shellbridge Way
RICHMOND,
 British Columbia
 V6X 2W7
 Tel: (604) 270-2277
 A,CH,CM,CS,E,M,P

Hewlett-Packard (Canada) Ltd.
 121 - 3350 Douglas Street
VICTORIA, British Columbia
 V8Z-3L1
 Tel: (604) 381-6616
 CH,CS

Manitoba

Hewlett-Packard (Canada) Ltd.
 1825 Inkster Blvd.
WINNIPEG, Manitoba
 R2X 1R3
 Tel: (204) 694-2777
 A,CH,CM,E,M,P

New Brunswick

Hewlett-Packard (Canada) Ltd.
 37 Shediac Road
MONCTON, New Brunswick
 E1A 2R6
 Tel: (506) 855-2841
 CH,CS

Nova Scotia

Hewlett-Packard (Canada) Ltd.
 900 Windmill Road
DARTMOUTH, Nova Scotia
 B3B 1L2
 Tel: (902) 469-7820
 CH,CM,CS,E,M,P

Ontario

Hewlett-Packard (Canada) Ltd.
 3325 N. Service Rd., Unit #3
BURLINGTON, Ontario
 L7N 3G2
 Tel: (416) 335-8644
 CH,M

Hewlett-Packard (Canada) Ltd.
 496 Days Road
KINGSTON, Ontario
 K7M 5R4
 Tel: (613) 384-2088
 CH,CS

Hewlett-Packard (Canada) Ltd.
 552 Newbold Street
LONDON, Ontario
 N6E 2S5
 Tel: (519) 686-9181
 A,CH,CM,E,M,P

+ Hewlett-Packard (Canada) Ltd.
 6877 Goreway Drive
MISSISSAUGA, Ontario
 L4V 1M8
 Tel: (416) 678-9430
 Telex: 069-8644
 A,CH,CM,CS,E,M,P

CANADA (Cont'd)

Hewlett-Packard (Canada) Ltd.
2670 Queensview Dr.
OTTAWA, Ontario
K2B 8K1
Tel: (613) 820-6483
A,CH,CM,CS,E,M,P

Hewlett-Packard (Canada) Ltd.
The Oaks Place, Unit 9
2140 Regent Street
SUDBURY, Ontario
P3E 5S8
Tel: (705) 522-0202
CH

Hewlett-Packard (Canada) Ltd.
3790 Victoria Park Avenue
WILLOWDALE, Ontario
M2H 3H7
Tel: (416) 499-2550
CH,E

Quebec
Hewlett-Packard (Canada) Ltd.
17500 Trans-Canada Highway
South Service Road
KIRKLAND, Quebec
H9J 2X8
Tel: (514) 697-4232
Telex: 058-21521
A,CH,CM,CS,E,M,P

Hewlett-Packard (Canada) Ltd.
1150, rue Claire Fontaine
QUEBEC CITY, Quebec
G1R 5G4
Tel: (418) 648-0726
CH, CS

Hewlett-Packard (Canada) Ltd.
#7-130 Robin Crescent
SASKATOON, Saskatchewan
S7L 6M7
Tel: (306) 242-3702
CH,CS

CHILE

ASC Ltda.
Austria 2041
SANTIAGO
Tel: 223-5946, 223-6148
Telex: 340192 ASC CK
P,C

Isical Ltda.
Av. Italia 634 Santiago
Casilla 16475
SANTIAGO 9
Tel: 222-0222
Telex: 440283 JCYCL CZ
CM,E,M

Metrolab S.A.
Monjitas 454 of. 206
SANTIAGO
Tel: 395752, 398296
Telex: 340866 METLAB CK
A

Olympia (Chile) Ltda.
Av. Rodrigo de Araya
Casilla 256-V
SANTIAGO
Tel: 225-5044
Telex: 340892 OLYMP
Cable: Olympachile Santiagochile

CHINA, People's Republic of

China Hewlett-Packard Ltd.
P.O. Box 9610, Beijing
4th Floor, 2nd Watch Factory Main Bldg.
Shuang Yu Shu, Bei San Huan Road
Hai Dian District
BEIJING
Tel: 28-0567
Telex: 22601 CTSHP CN
Cable: 1920 Beijing
A,CH,CM,CS,E,M,P

China-Hewlett-Packard Co. Ltd.
China Resources Building, 47/F
26 Harbour Road, Wanchai
HONG KONG
Tel: 5-8330833
Telex: 76793 HEWPA HX
A,C,CH,CS,E,M,P

CHINA (Cont'd)

China Hewlett-Packard Rep. Office
P.O. Box 418
1A Lane 2, Luchang St.
Beiwei Rd., Xuanwu District
BEIJING
Tel: 33-5950
Telex: 22601 CTSHP CN
Cable: 1920
A,CH,CM,CS,E,M,P

COLOMBIA

Instrumentacion
H.A. Langebaek & Kier S.A.
Carrera 4a, A No. 52 A 26
Apartado Aereo 6287
BOGOTA 1, D.E.
Tel: 212-1466
Telex: 44400INST CO

Nefromedicas Ltda.
Cable 123 No. 98-31
Apartado Aereo 100-958
BOGOTA D.E., 10
Tel: 213-5267, 213-1615
Telex: 43415 HEGAS CO
A

Compumundo
Avenida 15 # 107-80
BOGOTA D.E.
Tel: 214-4458
Telex: 45466 MARCO
P

Carvajal S.A.
Calle 29 Norte No. 6A-40
Apartado Aereo 46 CALI
Tel: 3681111
Telex: 55650

COSTA RICA

Cientifica Costarricense S.A.
Avenida 2, Calle 5
San Pedro de Montes de Oca
Apartado 10159
SAN JOSE
Tel: 24-38-20, 24-08-19
Telex: 2367 GALGUR CR
CM,E,M

CYPRUS

Telexra Ltd.
P.O. Box 4809
14C Stassinos Avenue
NICOSIA
Tel: 62698
Telex: 2894 LEVIDO CY
E,M,P

DENMARK

Hewlett-Packard A/S
Datavej 52
DK-3460 **BIRKEROD**
Tel: (02) 81-66-40
Telex: 37409 hpas dk
A,CH,CM,CS,E,M,P

Hewlett-Packard Iceland
Hoefdabakka 9
110 Reykjavik
Tel: (1) 67 1000
A,CH,CM,CS,E,M,P

Hewlett-Packard A/S
Rølgshedsvej 32
DK-8240 **RISSKOV**, Aarhus
Tel: (06) 17-60-00
Telex: 37409 hpas dk
CH,E

DOMINICAN REPUBLIC

Microprog S.A.
Juan Tomas Mejia y Cotes No. 60
Arroyo Hondo
SANTO DOMINGO
Tel: 565-6268
Telex: 4510 ARENTA DR (RCA) P

ECUADOR

CYEDE Cia. Ltda.
Avenida Eloy Alfaro 1749
y Belgica
Casilla 6423 CCI
QUITO
Tel: 450-975, 243-052
Telex: 22548 CYEDE ED
P,E

Ecuador Overseas Agencies C.A.
Calle 9 de Octubre #818
P.O. Box 1296
GUAYAQUIL
Tel: 306022
Telex: 3361 PBCGYE ED
M

Hospitalar S.A.
Robles 625
Casilla 3590
QUITO
Tel: 545-250, 545-122
Telex: 2485 HOSPTL ED
Cable: HOSPITALAR-Quito
M

Meditronics
Valladolid 524 Madrid
P.O. box 9171
QUITO
Tel: 2-238-951
Telex: 2298 ECUAME ED
A

EGYPT

Sakrcro Enterprises
P.O. Box 259
ALEXANDRIA
Tel: 802908,808020, 805302
Telex: 54333

Egyptian International
Office for Foreign Trade
P.O. Box 2558
42 El-Zahraa Street
Dokki, **CAIRO**,
Tel: 712230
Telex: 93337 EGFOR UN
Cable: EGYPOR
P,A

International Engineering Associates
24 Hussein Hegazi Street
Kasr-el-Aini
CAIRO
Tel: 23829, 21641
Telex: 93830 IEA UN
Cable: INTEGASSO
E

Sakrcro Enterprises
P.O. Box 1133
7, El Boustani El Saidy Str.
Talaat Harb Square
CAIRO
Tel: 762162,765189, 756071
Telex: 93156

S.S.C. Medical
40 Gezerat El Arab Street
Mohandessin
CAIRO,
Tel: 803844, 805998, 810263
Telex: 20503 SSC UN
M

EL SALVADOR

IPESA de El Salvador S.A.
29 Avenida Norte 1223
SAN SALVADOR
Tel: 26-6858, 26-6868
Telex: 20539 IPESA SAL
A,CH,CM,CS,E,P

FINLAND

Hewlett-Packard Oy
Piispankalliontie 17
02200 **ESPOO**
Tel: 00358-0-88721
Telex: 121563 HEWPA SF
CH,CM,CS,P

FRANCE

Hewlett-Packard France
Z.I. Mercure B
Rue Berthelot
F-13763 Les Milles Cedex
AIX-EN-PROVENCE
Tel: (42) 59-41-02
Telex: 410770F
A,CH,E,M,P

Hewlett-Packard France
64, rue Marchand Saillant
F-61000 **ALENCON**
Tel: (33) 29 04 42

Hewlett-Packard France
Boite Postale 503
F-25026 **BESANCON**
28 rue de la Republique
F-25000 **BESANCON**
Tel: (81) 83-16-22
Telex: 361157
CH,M

Hewlett-Packard France
13, Place Napoleon III
F-29000 **BREST**
Tel: (98) 03-38-35

Hewlett-Packard France
Chemin des Mouilles
Boite Postale 162
F-69130 **ECULLY** Cedex (Lyon)
Tel: (78) 833-81-25
Telex: 310617F
A,CH,CS,E,M,

+ Hewlett-Packard France
Parc d'Activite du Bois Briard
Ave. du Lac
F-91040 **EVRY** Cedex
Tel: 6 077-8383
Telex: 692315F
E

Hewlett-Packard France
5, avenue Raymond Chanas
F-38320 **EYBENS** (Grenoble)
Tel: 76 62-67-98
Telex: 980124 HP GREN0B EYBE
CH

Hewlett-Packard France
Centre d'Affaire Paris-Nord
Batiment Ampere 5 etage
Rue de la Commune de Paris
Boite Postale 300
F-93153 **LE BLANC MESNIL**
Tel: (1) 865-44-52
Telex: 211032F
CH,CS,E,M

Hewlett-Packard France
Parc d'Activites Cadera
Quartier Jean Mermoz
Avenue du President JF Kennedy
F-33700 **MERIGNAC** (Bordeaux)
Tel: (56) 34-00-84
Telex: 550105F
CH,E,M

Hewlett-Packard France
Immeuble "Les 3 B"
Nouveau Chemin de la Garde
ZAC de Bois Briard
F-44085 **NANTES** Cedex
Tel: (40) 50-32-22
Telex: 711085F

Hewlett-Packard France
125, rue du Faubourg Bannier
F-45000 **ORLEANS**
Tel: (38) 68 01 63

Hewlett-Packard France
Zone Industrielle de Courtabœuf
Avenue des Tropiques
F-91947 Les Ulis Cedex **ORSAY**
Tel: (6) 907-78-25
Telex: 600048F
A,CH,CM,CS,E,M,P

Hewlett-Packard France
Paris Porte-Maillot
15, Avenue de L'Amiral Bruix
F-75782 **PARIS CEDEX 16**
Tel: (1) 502-12-20
Telex: 613663F
CH,M,P

Hewlett-Packard France
124, Boulevard Tournasse
F-64000 **PAU**
Tel: (59) 80 38 02

Hewlett-Packard France
2 Allée de la Bourgonnette
F-35100 **RENNES**
Tel: (99) 51-42-44
Telex: 740912F
CH,CM,E,M,P

FRANCE (Cont'd)

Hewlett-Packard France
98 Avenue de Bretagne
F-76100 **ROUEN**
Tel: (35) 63-57-66
Telex: 770035F
CS

Hewlett-Packard France
4 Rue Thomas Mann
Boite Postale 56
F-67033 **STRASBOURG** Cedex
Tel: (88) 26-36-46
Telex: 890141F
CH,E,M,P

Hewlett-Packard France
Le Peripole
20 Chemin du Pigeonnier de la C
epiere
F-31083 **TOULOUSE** Cedex
Tel: (61) 40-11-12
Telex: 531639F
A,CH,CS,E,P

Hewlett-Packard France
9, rue Baudin
F-26000 **VALENCE**
Tel: (75) 42 76 16

Hewlett-Packard France
Carolor
ZAC de Bois Briand
F-57640 **VIGY** (Metz)
Tel: (8) 771 20 22
CH

Hewlett-Packard France
Immeuble Pericentre
F-59658 **VILLENEUVE D'ASCO**
Cedex
Tel: (20) 91-41-25
Telex: 160124F
CH,E,M,P

GERMAN FEDERAL REPUBLIC

Hewlett-Packard GmbH
Geschäftsstelle Berlin
Keithstrasse 2-4
1000 **BERLIN** 30
Tel: (030) 219904-0
Telex: 183405 hpbm
A,CH,E,M,P

Hewlett-Packard GmbH
Zentralbereich Marketing
Herrenberger Strasse 130
7030 **BOBLINGEN**
Tel: (7031) 14-0
Telex: 7265739 hep
A,CH,CM,CS,E,M,P

Hewlett-Packard GmbH
Vertriebszentrum Boblingen
Schickardstrasse 2
7030 **BOBLINGEN**
Postfach 1427
Tel: (7031) 645-0
Telex: 7265743 hep

Hewlett-Packard GmbH
Geschäftsstelle Dortmund
Schloßstr. 28
4600 **DORTMUND** 41
Tel: (0231) 45001-0
Telex: 822858 hepdod

Hewlett-Packard GmbH
Reparaturzentrum Frankfurt
Berner Strasse 117
6000 **FRANKFURT** am Main 60
Tel: (069) 5004-1
Telex: 413249 hpfm
A,CH,CM,CS,E,M,P

Hewlett-Packard GmbH
Vertriebszentrale Deutschland
Hewlett-Packard Strasse
Postfach 1641
6380 **BAD HOMBURG** v.d.H.
Tel: (06172) 400-0
Telex: 410844 hpbhg

Hewlett-Packard GmbH
Vertriebszentrum Nord
Kapstadtring 5
2000 **HAMBURG** 60
Tel: (040) 63804-0
Telex: 2163032 hphh
A,CH,CS,E,M,P

Hewlett-Packard GmbH
Geschäftsstelle Hannover
Heidering 37-39
3000 **HANNOVER** 61
Tel: (0511) 5706-0
Telex: 823259 hphn
A,CH,CM,E,M,P

Hewlett-Packard GmbH
Geschäftsstelle Mannheim
Rosslauer Weg 2-4
6800 **MANNHEIM** 31
Tel: (0621) 7005-0
Telex: 462105 hpmhm
A,C,E

Hewlett-Packard GmbH
Geschäftsstelle Neu Ulm
Messerschmittstrasse 7
7910 **NEU ULM**
Tel: (0731) 7073-0
Telex: 712816 hpulm
A,C,E

Hewlett-Packard GmbH
Geschäftsstelle Nürnberg
Emmericher Strasse 13
9500 **NÜRNBERG** 10
Tel: (0911) 5205-0
Telex: 623860 hpnbg
CH,CM,E,M,P

Hewlett-Packard GmbH
Vertriebszentrum Ratingen
Berliner Strasse 111
4030 **RATINGEN** 4
Postfach 31 12
Tel: (02102) 494-0
Telex: 589070 hprad

Hewlett-Packard GmbH
Vertriebszentrum München
Eschenstrasse 5
8028 **TAUFKIRCHEN**
Tel: (089) 61207-0
Telex: 524985 hpmch
A,CH,CM,E,M,P

Hewlett-Packard GmbH
Geschäftsstelle Karlsruhe
Ermisallee
7517 **WALDBRONN** 2
Postfach 1251
Tel: (07243) 602-0
Telex: 782838 hepk

GREAT BRITAIN (See United Kingdom)

GREECE

Hewlett-Packard Hellas
178, Kifissias Avenue
6th Floor
Halandri: **ATHENS**
Greece
Tel: 6471673, 6471543, 6472971
A,CM,E,M,P

Kostas Karayannis S.A.
8 Omirou Street
ATHENS 133
Tel: 32 30 303, 32 37 371
Telex: 215962 RKAR GR
A,CH,CM,CS,E,M,P

PLAISIO S.A.
Ellipoulas Brothers Ltd.
11854 **ATHENS**
Tel: 34-51-911
Telex: 216286
P

GUATEMALA

IPESA
Avenida Reforma 3-48, Zona 9
GUATEMALA CITY
Tel: 316827, 314786
Telex: 4192 TELTRO GU
A,CH,CM,CS,E,M,P

HONG KONG

Hewlett-Packard Hong Kong, Ltd.
G.P.O. Box 795
5th Floor, Sun Hung Kai Centre
30 Harbour Road, **HONG KONG**
Tel: 316827, 314786
Telex: 5-8323211
Cable: HEWPAC HX
Cable: HEWPAC HONG KONG
E,CH,CS,P

CET Ltd.
10th Floor, Hua Hsia, Bldg.
64-66 Gloucester Road
HONG KONG
Tel: (5) 200922
Telex: 85148 CET HX
CM

Schmidt & Co. (Hong Kong) Ltd.
18th Floor, Great Eagle Centre
23 Harbour Road, Wanchai
HONG KONG
Tel: 5-6330222
Telex: 74766 SCHMC HX
A,M

ICELAND

Eliding Trading Company Inc.
Hafnarvöll Tryggvagotu
P.O. Box 885
IS **REYKJAVIK**
Tel: 1-58-20, 1-63-03
M

INDIA

Blue Star Ltd.
Sabri Complex 2nd Floor, 24 Residency
Rd.
BANGALORE 660 025
Tel: 55660, 578881
Telex: 0845-430
Cable: BLUESTAR
A,CM,E

Blue Star Ltd.
Band Box House, Prabhadevi
BOMBAY 400 025
Tel: 4933101 4933222
Telex: 011-71051
Cable: BLUESTAR
A,M

Blue Star Ltd.
Sahas, 41/42 Vir Savarkar Marg
Prabhadevi
BOMBAY 400 025
Tel: 422-6155, 422-6556
Telex: 011-71193 BSSS IN
Cable: FROSTBLUE
A,CM,E,M

Blue Star Ltd.
Kalyan, 19 Vishwas Colony
Alkapuri, **BARODA**, 390 005
Tel: 65235
Cable: BLUE STAR
A

Blue Star Ltd.
7 Hare Street
CALCUTTA 700 001
Tel: 230131, 230132
Telex: 021-7655
Cable: BLUESTAR
A,M

Blue Star Ltd.
133 Kodambakkam High Road
MADRAS 600 034
Tel: 472056, 470238
Telex: 041-379
Cable: BLUESTAR
A,M

Blue Star Ltd.
13, Community Center
New Friends Colony
NEW DELHI 110 065
Tel: 633773
Telex: 031-61120
Cable: BLUEFROST
A,CM,E,M

Blue Star Ltd.
15/16 C Wellesley Rd.
PUNE 411 011
Tel: 22775
Cable: BLUE STAR
A

Blue Star Ltd.
2-247/1108 Bolarum Rd.
SECUNDERABAD 500 003
Tel: 72057
Telex: 0155-645
Cable: BLUESTAR
A,E

Blue Star Ltd.
T.C. 7/603 Poornima, Maruthankuzhi
TRIVANDRUM 695 013
Tel: 65799
Telex: 0884-259
Cable: BLUESTAR
E

INDONESIA

BERCA Indonesia P.T.
P.O. Box 496/Jkt.
Jl. Abdul Muis 62, **JAKARTA**
Tel: 21-373009
Telex: 46748 BERSAL IA
Cable: BERSAL JAKARTA
P

BERCA Indonesia P.T.
P.O. Box 2497/Jkt.
Antara Bldg., 12th Floor
Jl. Medan Merdeka Selatan 17
JAKARTA-PUSAT
Tel: 340417, 341445
Telex: 46748 BERSAL IA
A,CS,E,M

BERCA Indonesia P.T.
Jl. Kutai no. 24, **SURABAYA**
Tel: (031) 67118
Telex: 31146 BERSAL SB
Cable: BERSAL-SURABAYA
A,E,M,P

IRAQ

Hewlett-Packard Trading S.A.
Service Operation
Al Mansoor City 9B/37
BAGHDAD
Tel: 551-49-73
Telex: 212-455 HEPAIRAQ IK
CH,CS

IRELAND

Hewlett-Packard Ireland Ltd.
82/83 Lower Leeson Street
DUBLIN 2
Tel: 0001 608800
Telex: 30439
CH,CS,E,P

Cardiac Services Ltd.
Kilmore Road
Artane
DUBLIN 5
Tel: (01) 351820
Telex: 30439
M

ISRAEL

Eldan Electronic Instrument Ltd.
P.O. Box 1270
JERUSALEM 91000
16, Ohaliav St.
JERUSALEM 94467
Tel: 533 221, 553 242
Telex: 25231 AB/PAKRO IL
A,M

Computation and Measurement
Systems (CMS) Ltd.
11 Masad Street
TEL-AVIV
Tel: 388 388
Telex: 33569 Motil IL
CM,CH,CS,E,P

ITALY

Hewlett-Packard Italiana S.p.A.
Traversa 99C
Via Giulio Petroni, 19
I-70124 **BARI**
Tel: (080) 41-07-44
CH,M

Hewlett-Packard Italiana S.p.A.
Via Martin Luther King, 38/III
I-40132 **BOLOGNA**
Tel: (051) 402394
Telex: 511630
CH,CS,E,M

Hewlett-Packard Italiana S.p.A.
Via Principe Nicola 436/C
I-95126 **CATANIA**
Tel: (095) 37-10-87
Telex: 970291
CH

Hewlett-Packard Italiana S.p.A.
Via G. Di Vittorio 9
I-20063 **CERNUSCO SUL NAVIGLIO**
(Milano)
Tel: (02) 923691
Telex: 334632
A,CH,CM,CS,E,M,P

ITALY (Cont'd)

Hewlett-Packard Italiana S.p.A.
Via C. Colombo 49
I-20090 TREZZANO SUL
NAVIGLIO
(Milano)
Tel: (02) 4459041
Telex: 322116
CH,CS

Hewlett-Packard Italiana S.p.A.
Via Nuova San Rocco a
Capodimonte, 62/A
I-80131 NAPOLI
Tel: (081) 7413544
Telex: 710698
CH,CS,E,M

Hewlett-Packard Italiana S.p.A.
Viale G. Modugno 33
I-16156 GENOVA PEGLI
Tel: (010) 68-37-07
Telex: 215238
E,C

Hewlett-Packard Italiana S.p.A.
Via Pelizzo 15
I-35128 PADOVA
Tel: (049) 664888
Telex: 430315
A,CH,CS,E,M

Hewlett-Packard Italiana S.p.A.
Viale C. Pavese 340
I-00144 ROMA EUR
Tel: (06) 54831
Telex: 610514
A,CH,CS,E,M,P

Hewlett-Packard Italiana S.p.A.
Via di Casellina 57/C
I-50018 SCANDICCI-FIRENZE
Tel: (055) 753863
CH,E,M

Hewlett-Packard Italiana S.p.A.
Corso Svizzera, 185
I-10144 TORINO
Tel: (011) 74 4044
Telex: 221079
A,CS,CH,E

JAPAN

Hewlett-Packard Ltd.
152-1, Onna
ATSUGI, Kanagawa, 243
Tel: (0462) 25-0031
CM,C,E

Hewlett-Packard Ltd.
Meiji-Seimei Bldg. 6F
3-1 Hon Chiba-Cho
CHIBA, 280
Tel: (0472) 25 7701
E,CH,CS

Hewlett-Packard Ltd.
Yasuda-Seimei Hiroshima Bldg.
6-11, Hon-dori, Naka-ku
HIROSHIMA, 730
Tel: (082) 241-0611

Hewlett-Packard Ltd.
Towa Building
2-3, Kaigan-dori, 2 Chome Chuo-ku
KOBE, 650
Tel: (078) 392-4791
C,E

Hewlett-Packard Ltd.
Kumagaya Asahi 82 Bldg.
3-4 Tsukuba
KUMAGAYA, Saitama 360
Tel: (0485) 24-6563
CH,CM,E

Hewlett-Packard Ltd.
Asahi Shinbun Daichi Seimei Bldg.
4-7, Hanabata-cho
KUMAMOTO, 860
Tel: (0963) 54-7311
CH,E

Hewlett-Packard Ltd.
Shin-Kyoto Center Bldg.
614, Higashi-Shiokoji-cho
Karasuma-Nishiru
Shiokoji-dori, Shimogyo-ku
KYOTO, 600
Tel: 075-343-0921
CH,E

Hewlett-Packard Ltd.
Mito Mitsui Bldg.
4-73, Sanno-maru, 1 Chome
MITO, Ibaraki 310
Tel: (0292) 25-7470
CH,CM,E

Yokogawa-Hewlett-Packard Ltd.
Meiji-Seimei Kokubun Bldg. 7-8
Kokubun, 1 Chome, Sendai
MIYAGI, 960
Tel: (0222) 25-1011
C,E

Yokogawa-Hewlett-Packard Ltd.
Nagoya Kokusai Center Bldg.
47-1 Nagano 1 Chome
Nakamura-ku
NAGOYA, 460
Tel: (052) 571-5171
CH,CM,CS,E,M

Yokogawa-Hewlett-Packard Ltd.
Chuo Bldg.
4-20 Nishinakajima, 5 Chome
Yodogawa-ku
OSAKA, 532
Tel: (06) 304-6021
Telex: YHPOSA 523-3624
A,CH,CM,CS,E,M,P

Yokogawa-Hewlett-Packard Ltd.
27-15, Yabe, 1 Chome
SAGAMIHARA Kanagawa, 229
Tel: 0427 59-1311

Yokogawa-Hewlett-Packard Ltd.
Daichi Seimei Bldg.
7-1, Nishi Shinjuku, 2 Chome
Shinjuku-ku, TOKYO 160
Tel: 03-348-4611
CH,E,M

Yokogawa Hewlett-Packard Ltd.
9-1, Takakura-cho
Hachioji-shi, TOKYO, 192
Tel: 0426-42-1261
CH,E

Yokogawa-Hewlett-Packard Ltd.
29-21 Takaido-Higashi, 3 Chome
Suginami-ku TOKYO 168
Tel: (03) 331-6111
Telex: 232-2024 YHPTOK
A,CH,CM,CS,E,P

Yokogawa-Hewlett-Packard Ltd.
Meiji-Seimei Utsunomiya Odori Bldg.
1-5 Odori, 2 Chome
UTSUNOMIYA, Tochigi 320
Tel: (0286) 34-1175
CH,CS,E

Yokogawa-Hewlett-Packard Ltd.
Yasuda Seimei Nishiguchi Bldg.
30-4 Tsuruya-cho, 3 Chome
YOKOHAMA 221
Tel: (045) 312-1252
CH,CM,E

JORDAN

Scientific and Medical Supplies Co.
P.O. Box 1387
AMMAN
Tel: 24907, 39907
Telex: 21456 SABCO JO
CH,E,M,P

KENYA

ADCOM Ltd., Inc., Kenya
P.O. Box 30070
NAIROBI
Tel: 331955
Telex: 22639
E,M

KOREA

Samsung Hewlett-Packard Co. Ltd.
Dongbang Yeouido Bldg.
12-16th Floors
36-1 Yeouido-Dong
Youngdeungpo-ku
SEOUL
Tel: 784-4666, 784-2666
Telex: 25166 SAMSAN K
A,CH,CM,CS,E,M,P

Dongbang Healthcare Products Co. Ltd.
Suite 301 Medical Supply Center
Bldg. 1-31 Dongsungdong
Jong Ro-gu, SEOUL
Tel: 764-1171
Telex: K25706 TKBKO
Cable: TKBEEKPO
M

Young-in Scientific Co. Ltd.
Younguha Bldg.
547 Shinsa-Dong
Kangnam-Ku, SEOUL
Tel: 546-7771
Telex: K23457 GINSCO
A

KUWAIT

Al Khaldiya Trading
& Contracting
P.O. Box 830
SAFAT
Tel: 424910, 411726
Telex: 22481 AREEG KT
Cable: VISCOUNT
E,M,A

Photo & Cine Equipment
P.O. Box 270
SAFAT
Tel: 2445111
Telex: 22247 MATIN KT
Cable: MATIN KUWAIT
P

W.J. Towell Computer Services
P.O. Box 5897
SAFAT
Tel: 2462640/1
Telex: 30336 TOWELL KT
C

LEBANON

Computer Information Systems
P.O. Box 11-6274
BEIRUT
Tel: 89 40 73
Telex: 42309
C,E,M,P

LUXEMBOURG

Hewlett-Packard Belgium S.A./N.V.
Blvd. de la Woluwe, 100
Woluwedall
B-1200 BRUSSELS
Tel: (02) 762-32-00
Telex: 23-494 paloben bru
A,CH,CM,CS,E,M,P

MALAYSIA

Hewlett-Packard Sales (Malaysia) Sdn.Bhd.
9th Floor, Chung Khaw Bank Building
46 Jln Raja Laut
KUALA LUMPUR
Tel: 986555
Telex: HPSM MA 31011
A,CH,E,M,P

Protel Engineering
P.O. Box 1917
Lot 6624, Section 64
23/4 Pending Road
Kuching, SARAWAK
Tel: 36299
Telex: MA 70904 PROMAL
Cable: PROTELENG
A,E,M

MALTA

Philip Toledo Ltd.
P.O. Box LL
Notabile Rd.
MRIEHEL
Tel: 447 47, 455 66, 4915 25
Telex: Media MW 649
E,P,M

MEXICO

Hewlett-Packard de Mexico, S.A.
de C.V.
Av. Periferico Sur No. 6501
Tepepan, Xochimilco
16020 MEXICO D.F.
Tel: 6-76-46-00
Telex: 17-74-507 HEWPAK MEX
A,CH,CS,E,M,P

Hewlett-Packard de Mexico, S.A.
de C.V.
Czda del Valle
409 Ote. - 4th Piso
Colonia del Valle
Municipio de Garza Garcia Nuevo Leon
66220 MONTERREY
Tel: 78 42 41
Telex: 038 410
CH

Hewlett-Packard de Mexico, S.A.
Francisco J. Allen #30
Colonia Nueva
Los Angeles 27140
COAHUILA, Torreon
Tel: 37220
Microcomputadoras Hewlett-Packard S.A.
Monte 115 Pelvoux de C.V.
Mexico, D.F. LOS LOMAS
Tel: 520-9127

Equipos Cientificos de Occidente,
S.A.
Av. Lazaro Cardenas 3540
GUADALAJARA
Tel: 21-66-91
Telex: 0684 186 ECOME
A
Infograficas y Sistemas del
Noreste, S.A.
Rio Orinoco #171 Oriente
Despacho 2001
Colonia Del Valle
MONTERREY
Tel: 782499, 781259
A,E

Hewlett-Packard de Mexico (Polanco)
Avenida Ejercito Nacional #579
2do y 3er Piso
COLONIA GRANADA 11520
Mexico, D.F.
Tel: 211-3683

MOROCCO

Dolbeau
81 rue Karatchi
CASABLANCA
Tel: 3041-82, 3068-38
Telex: 23051, 22822
E

Gerep
2 rue d'Agadir
Boite Postale 156
CASABLANCA
Tel: 272093, 272095
Telex: 23 739
P

Sema-Maroc
Rue Lapebie
CASABLANCA
Tel: 26.09.80
CH,CS,P

NETHERLANDS

Hewlett-Packard Nederland B.V.
Startbaan 16
1187 XR Amstelveen
P.O. Box 667
NL-1180 AR AMSTELVEEN
Tel: (20) 547 6911
Telex: 13216 hepa nl
A,CH,CM,CS,E,P

Hewlett-Packard Nederland B.V.
Bongard 2
NL-2906VK CAPELLE A/D IJSSEL
P.O. Box 41
NL-2900AA CAPELLE A/D IJSSEL
Tel: (10) 51-64-44
Telex: 21261 HEPAC NL
A,CH,CS,E

Hewlett-Packard Nederland B.V.
Pastoor Petersstraat 134-136
NL-5612 LV EINDHOVEN
P.O. Box 2342
NL-5600 CH EINDHOVEN
Tel: (040) 326911
Telex: 51484 hepae nl
A,E,M

NEW ZEALAND

Hewlett-Packard (N.Z.) Ltd.
5 Owens Road
P.O. Box 26-189
Epsom, AUCKLAND
Tel: 687-159
Cable: HEWPAK Auckland
CH,CS,CM,E,P
Hewlett-Packard (N.Z.) Ltd.
4-12 Cruickshank Street
Kilbirnie, WELLINGTON 3
P.O. Box 9443
Courtenay Place, WELLINGTON 3
Tel: 877-139
Cable: HEWPAK Wellington
CH,CS,CM,E,P

Northrop Instruments & Systems
Ltd.
369 Khyber Pass Road
P.O. Box 8602
AUCKLAND
Tel: 794-091
Telex: 80605
A,M

NEW ZEALAND (Cont'd)

Northrop Instruments & Systems Ltd.

110 Mandeville St.

P.O. Box 8388

CHRISTCHURCH

Tel: 488-873

Telex: 4203

A,M

Northrop Instruments & Systems Ltd.

Sturdee House

85-87 Ghuznee Street

P.O. Box 2406

WELLINGTON

Tel: 850-091

Telex: NZ 3380

A,M

NORWAY

Hewlett-Packard Norge A/S

Folke Bernadottes vei 50

P.O. Box 3558

N-5033 FYLLINGSDALEN (Bergen)

Tel: 0047/516 55 40

Telex: 76621 hpnas n

CH,CS,E,M

+ Hewlett-Packard Norge A/S

Osterndalen 16-18

P.O. Box 34

N-1345 OSTERAS

Tel: 0047/217 11 80

Telex: 76621 hpnas n

A,CH,CM,CS,E,M,P

OMAN

Khunji Ramdas

P.O. Box 19

MUSCAT

Tel: 722225, 745601

Telex: 5289 BROKER MB MUSCAT

P

Suhail & Saud Bahwan

P.O. Box 169

MUSCAT

Tel: 734 201-3

Telex: 5274 BAHWAN MB

E

Imtat LLC

P.O. Box 8676

MUTRAH

Tel: 601695

Telex: 5741 Tawoos On

A,C,M

PAKISTAN

Mushko & Company Ltd.

House No. 16, Street No. 16

Sector F-6/3

ISLAMABAD

Tel: 824545

Telex: 54001 MUSKI PK

Cable: FEMUS Islamabad

A,E,P

Mushko & Company Ltd.

Osman Chambers

Abdullah Haroon Road

KARACHI 0302

Tel: 524131, 524132

Telex: 2894 MUSKO PK

Cable: COOPERATOR Karachi

A,E,P

PANAMA

Electronico Balboa, S.A.

Calle Samuel Lewis, Ed. Alfa

Apartado 4929

PANAMA 5

Tel: 642700

Telex: 3483 ELECTRON PG

A,C,M,E,M,P

PERU

Cia Electro Medica S.A.

Los Flamencos 145, San Isidro

Casilla 1030

LIMA 1

Tel: 41 4325, 41-37015

Telex: Pub. Booth 25306 PEC PISIDR

CME,M,P

SAMS S.A.

Avenida Republica de Panama 3534

SAN ISIDRO, Lima

Tel: 419928/417108

Telex: 20450 PE LIBERTAD

PHILIPPINES

The Onine Advanced Systems

Corporation

2/F Electra House

Esteban Street

Legaspi Village

Makati

Metro MANILA

Tel: 815-38-11 (up to 16)

Telex: 63274 Online PN

A,CH,CS,E,M,P

PORTUGAL

Mundinter

Intercambio Mundial de Comercio

S.A.R.L.

P.O. Box 2761

Av. Antonio Augusto de Aguiar 138

PLISBON

Tel: (19) 53-21-31, 53-21-37

Telex: 16691 munter p

M

Soquimica

Av. da Liberdade, 220-2

1298 LISBON Codex

Tel: 56 21 81/2/3

Telex: 13316 SABASA

P

Telectra-Empresa Tecnica de

Equipamentos Electronicos S.A.R.L.

Rua Rodrigo da Fonseca 103

P.O. Box 2531

P.LISBON 1

Tel: (19) 68-60-72

Telex: 12598

CME

Rarcentro Ltda

R. Costa Cabral 575

4200 PORTO

Tel: 499174/495173

Telex: 26054

CH,CS

QATAR

Computer Arabia

P.O. Box 2750

DOHA

Tel: 428555

Telex: 4806 CHPARB

P

Nasser Trading & Contracting

P.O. Box 1563

DOHA

Tel: 422170

Telex: 4439 NASSER DH

M

SAUDI ARABIA

Modern Electronic Establishment

Hewlett-Packard Division

P.O. Box 281

Thuobah

AL-KHOBAR

Tel: 895-1760, 895-1764

Telex: 671 106 HPMEEK SJ

Cable: ELECTA AL-KHOBAR

CH,CS,E,M

Modern Electronic Establishment

Hewlett-Packard Division

P.O. Box 1228

Redec Plaza, 6th Floor

JEDDAH

Tel: 644 9628

Telex: 4027 12 FARNAS SJ

Cable: ELECTA JEDDAH

A,CH,CS,CM,E,M,P

+ Modern Electronic Establishment

Hewlett-Packard Division

P.O. Box 22015

RIYADH

Tel: 491-97 15, 491-63 87

Telex: 202049 MEERYD SJ

CH,CS,E,M

Abdul Ghani El Ajou

P.O. Box 78

RIYADH

Tel: 40 41 717

Telex: 200 932 EL AJOU

P

SCOTLAND

See United Kingdom

SINGAPORE

Hewlett-Packard Singapore (Sales)

Pte. Ltd.

#08-00 Inchcape House

450-2 Alexandra Road

P.O. Box 58 Alexandra Rd. Post

Office

SINGAPORE, 9115

Tel: 4731788

Telex: HPSGSO RS 34209

Cable: HEWPACK, Singapore

A,CH,CS,E,M,P

Dynamar International Ltd.

Unit 05-11 Block 6

Kalam Ayer Industrial Estate

SINGAPORE 1334

Tel: 747-6188

Telex: RS 26283

CM

SOUTH AFRICA

Hewlett-Packard So Africa (Pty.)

Ltd.

P.O. Box 120

Howard Place CAPE PROVINCE

7430

Pine Park Center, Forest Drive,

Pinelands

CAPE PROVINCE 7405

Tel: 53-7954

Telex: 57-20006

A,CH,CM,E,M,P

Hewlett-Packard So Africa (Pty.)

Ltd.

P.O. Box 37099

Overport Drive 92

DURBAN 4067

Tel: 28-4178

Telex: 6-22954

CH,CM

Hewlett-Packard So Africa (Pty.)

Ltd.

6 Linton Arcade

511 Cape Road

Linton Grange

PORT ELIZABETH 6001

Tel: 041-301201

CH

Hewlett-Packard So Africa (Pty.)

Ltd.

Fountain Center

Kalkden Str.

Monument Park

Ext 2

PRETORIA 0105

Tel: 45-5723

Telex: 32163

CH,E

+ Hewlett-Packard So Africa (Pty.)

Ltd.

Private Bag Wendywood

SANDTON 2144

Tel: 802-5111, 802-5125

Telex: 4-20877

Cable: HEWPACK Johannesburg

A,CH,CM,CS,E,M,P

SPAIN

Hewlett-Packard Espanola S.A.

Calle Entenza, 321

E-BARCELONA 29

Tel: 322.24.51, 321.73.54

Telex: 52603 hpbce

A,CH,CS,E,M,P

Hewlett-Packard Espanola S.A.

Calle San Vicente S/No

Edificio Albia II - 7B

E-BILBAO 1

Tel: 423.83.06

A,CH,E,M

+ Hewlett-Packard Espanola S.A.

Crta. de la Corona, Km. 16, 400

Las Rozas

E-MADRID

Tel: (1) 637.00.11

Telex: 23515 HPE

CH,CS,M

Hewlett-Packard Espanola S.A.

Avda. S. Francisco Javier, S/No

Planta 10. Edificio Sevilla 2,

E-SEVILLA 5

Tel: 66.44.54

Telex: 72933

A,CS,M,P

Hewlett-Packard Espanola S.A.

C/Isabel La Catolica, 8

E-46004 VALENCIA

Tel: 0034/6/351 59 44

CH,P

SWEDEN

Hewlett-Packard Sverige AB

Ostra Tullgatan 3

S-21128 MALMO

Tel: (040) 70270

Telex: (854) 17886 (via Spanga office)

Hewlett-Packard Sverige AB

Vastra Vintergatan 9

S-70344 OREBRO

Tel: (19) 10-48-80

Telex: (854) 17886 (via Spanga office)

CH

+ Hewlett-Packard Sverige AB

Skallholtsgratan 9, Kista

Box 19

S-16393 SPANGA

Tel: (08) 750-2000

Telex: (854) 17886

Telefax: (08) 7527781

A,CH,CM,CS,E,M,P

Hewlett-Packard Sverige AB

Frotallsgatan 30

S-42132 VASTRA FROLUNDA

(near Gothenburg)

Tel: (31) 49 09 50

Telex: (854) 17886 (via Spanga office)

A,CH,CM,CS,E,M,P

SWEDEN (Cont'd)

Hewlett-Packard Sverige AB
Frottallsgatan 30
S-42132 **VASTRA-FROLUNDA**
Tel: (031) 49-09-50
Telex: (854) 17886 (via Spanga office)
CH,CS,P,E

SWITZERLAND

Hewlett-Packard (Schweiz) AG
Clarastrasse 12
CH-4057 **BASEL**
Tel: (61) 33-59-20
A

Hewlett-Packard (Suisse) SA
7, rue du Bois-du-Lan
Case Postale 365
CH-1217 **MEYRIN 2**
Tel: (0041) 22-83-11-11
Telex: 23984 HPAG CH
CH,CM,CS

+ Hewlett-Packard (Schweiz) AG
Allmend 2
CH-8967 **WIDEN**
Tel: (0041) 57 31 21 11
Telex: 53933 hpag ch
Cable: HPAG CH
A,CH,CM,CS,E,M,P

SYRIA

General Electronic Inc.
Nuri Basha Ahnaf Ebn Kays Street
P.O. Box 5781
DAMASCUS
Tel: 33-24-87
Telex: 411 215
Cable: ELECTROBOR DAMASCUS
E

Middle East Electronics
P.O. Box 2308
Abu Rumanneh
DAMASCUS
Tel: 33-45-92
Telex: 411 304
M

TAIWAN

Hewlett-Packard Taiwan
Kaohsiung Office
11/F 456, Chung Hsiao 1st Road
KAOSHIUNG
Tel: (07) 2412318
CH,CS,E

+ Hewlett-Packard Taiwan
8th Floor Hewlett-Packard Building
337 Fu Hsing North Road
TAIPEI
Tel: (02) 712-0404
Telex: 24439 HEWPACK
Cable: HEWPACK Taipei
A,CH,CM,CS,E,M,P

Ing Lih Trading Co.
3rd Floor, 7 Jen-Ai Road, Sec. 2
TAIPEI 100
Tel: (02) 3948191
Cable: INGLIH TAIPEI
A

THAILAND

Unimesa Co. Ltd.
30 Patpong Ave., Suriwong
BANGKOK 5
Tel: 235-5727
Telex: 84439 Simonco TH
Cable: UNIMESA Bangkok
A,CH,CS,E,M

TOGO

Societe Africaine De
Promotion
B.P. 12271
LOME
Tel: 21-62-88
Telex: 5304
P

TRINIDAD & TOBAGO

Caribbean Telecoms Ltd.
Corner McAlister Street &
Eastern Main Road, Laventille
P.O. Box 732
PORT-OF-SPAIN
Tel: 624-4213
Telex: 22561 Cartel WG
Cable: CARTEL, PORT OF SPAIN
C,M,E,M,P,A

Computer and Controls Ltd.
P.O. Box 51
66 Independence Square
PORT-OF-SPAIN
Tel: 623-4472
Telex: 3000 POSTLX WG, ACCT LOOGO
AGENCY 1264
P,A

TUNISIA

Tunisie Electronique
31 Avenue de la Liberté
TUNIS
Tel: 280-144
CH,CS,E,P

Corema
1 ter. Av. de Carthage
TUNIS
Tel: 253-821
Telex: 12319 CABAM TN
M

TURKEY

E.M.A.
Mediha Eldem Sokak No. 41/6
Yenisehir
ANKARA
Tel: 319175
Telex: 42321 KTX TR
Cable: EMATRADE ANKARA
M
Kurt & Kurt A.S.
Mithatpasa Caddesi No. 75
Kat 4 Kizilay
ANKARA
Tel: 318875/6/7/8
Telex: 42490 MESR TR
A

Saniva Bilgisayar Sistemleri A.S.
Buyukdere Caddesi 103/6
Gayrettepe
ISTANBUL
Tel: 1673180
Telex: 26345 SANI TR
C,P

Teknim Company Ltd.
Iran Caddesi No. 7
Kavaklidere
ANKARA
Tel: 275800
Telex: 42155 TKNM TR
E,CM

UNITED ARAB EMIRATES

+ Emitac Ltd.
P.O. Box 1641
SHARJAH
Tel: 591181
Telex: 68136 EMITAC EM
Cable: EMITAC SHARJAH
E,C,M,P,A

Emitac Ltd.
P.O. Box 2711
ABU DHABI
Tel: 820419-20
Cable: EMITACH ABUDHABI

Emitac Ltd.
P.O. Box 8391
DUBAI
Tel: 377591

Emitac Ltd.
P.O. Box 473
RAS AL KHAIMAH
Tel: 28133, 21270

UNITED KINGDOM

GREAT BRITAIN

Hewlett-Packard Ltd.
Trafalgar House
Navigation Road
ALTRINCHAM
Cheshire WA14 1NU
Tel: 061 928 6422
Telex: 668066
A,CH,CS,E,M,P

+ Hewlett-Packard Ltd.
Miller House
The Ring, **BRACKNELL**
Berkshire RG12 1XN
Tel: (0344) 424898
Telex: 848733
C,M,P

Hewlett-Packard Ltd.
Elstree House, Elstree Way
BOREHAMWOOD, Herts WD6 1SG
Tel: 01 207 5000
Telex: 8952716
E,CH,CS

Hewlett-Packard Ltd.
Oakfield House, Oakfield Grove
Clifton **BRISTOL**, Avon BS8 2BN
Tel: 0272 736806
Telex: 444302
CH,CS,E

Hewlett-Packard Ltd.
Bridewell House
Bridewell Place
LONDON EC4V 6BS
Tel: 01 583 6565
Telex: 298163
CH,CS,P

Hewlett-Packard Ltd.
Harman House
1 George Street
Uxbridge,
MIDDLESEX, UB8 1YH
Tel: 0895 72020
Telex: 893134/5
E,CH,CM,M

Hewlett-Packard Ltd.
Pontefract Road
NORMANTON, West Yorkshire
WF6 1RN
Tel: 0924 895566
Telex: 557355
CH,CS

Hewlett-Packard Ltd.
The Quadrangle
106-118 Station Road
REDHILL, Surrey RH1 1PS
Tel: 0737 68855
Telex: 947234
CH,CS,E

Hewlett-Packard Ltd.
Avon House
435 Stratford Road
Shirley, **SOLIHULL**, West Midlands
B90 4BL
Tel: 021 745 8800
Telex: 339105
CH,CS

Hewlett-Packard Ltd.
West End House
41 High Street, West End
SOUTHAMPTON
Hampshire SO3 3DQ
Tel: (0703) 476767
Telex: 477138
CH,CS

Hewlett-Packard Ltd.
King Street Lane
Winnersh, **WOKINGHAM**
Berkshire RG11 5AR
Tel: 0734 784774
Telex: 847178
CH,CS,E

Hewlett-Packard Ltd.,
Customer Support Centre
Eskdale Road,
Winnersh, **WOKINGHAM**
Berkshire, RG11 5D2
Tel: (0734) 696622
Telex: 848884
A

SCOTLAND

Hewlett-Packard Ltd.,
15 Carden Place,
ABERDEEN
AB1 1UR
Tel: 0224 638042
E,CH

Hewlett-Packard Ltd.
SOUTH QUEENSFERRY
West Lothian, EH30 9TG
Tel: 031 331 1188
Telex: 72682/3
A,CH,CM,CS,E,M,P

URUGUAY

Pablo Ferrando S.A.C. e I.
Avenida Italia 2877
Casilla de Correo 370
MONTEVIDEO
Tel: 80-2586
Telex: Public Booth 901
A,CM,E,M

Olympia de Uruguay S.A.
Maquinas de Oficina
Avda. del Libertador 1997
Casilla de Correos 6644
MONTEVIDEO
Tel: 91-1809, 98-3807
Telex: 6342 OROU UY
P

VENEZUELA

+ Hewlett-Packard de Venezuela C.A.
3A Transversal Los Ruices Norte
Edificio Segre 2 & 3
CARACAS 1071
Tel: 239-4133
Telex: 251046 HEWPACK
A,CH,CS,E,M,P

Hewlett-Packard de Venezuela C.A.
Centro Ciudad Comercial Tamanaco
Nivel C-2 (Nueva Etapa)
Local 53H05
CHUAO, Caracas
Tel: 928291
P

Hewlett-Packard de Venezuela C.A.
Residencias Tia Betty Local 1
Avenida 3 y con Calle 75
MARACAIBO, Estado Zulia
Apartado 2646
Tel: (061) 75801-75805-75806-
80304
Telex: 62464 HPMAR
C,E

Hewlett-Packard de Venezuela C.A.
Urb. Lomas del Este
Torre Trebol — Piso 11
VALENCIA, Estado Carabobo
Apartado 3347
Tel: (041) 222992/223024
CH,CS,P

Albis Venezolana S.R.L.
Av. Las Marias, Qta. Alix,
El Pedregal
Apartado 81025
CARACAS 10804
Tel: 747984, 742146
Telex: 24009 ALBIS VC
A

Tecnologica Medica del Caribe,
C.A.
Multicentro Empresarial del Este
Ave. Libertador
Edif. Libertador
Nucleo "C" — Oficina 51-52
CARACAS
Tel: 339867/333780
M

YUGOSLAVIA

Hermes
General Zdanova 4
Telex: YU-11000 BEOGRAD
A,C,H,E,P

Hermes
Titova 50
Telex: YU-31583 LJUBLJANA
CH,CS,E,M,P

Elektrotehna
TITOVA 50
Telex: YU-61000 LJUBLJANA
CM

ZAMBIA

R.J. Tilbury (Zambia) Ltd.
P.O. Box 32792
LUSAKA
Tel: 215590
Telex: 40128
E

ZIMBABWE

Field Technical Sales
45 Kelvin Road, North
P.O. 3458
SALISBURY
Tel: 705 231
Telex: 4-122 RH
E,P

REGIONAL HEADQUARTERS OFFICES

If there is no sales office listed for your area, contact one of these headquarters offices.

AFRICA AND

MIDDLE EAST

Hewlett-Packard S.A.
Mediterranean and Middle East
Operations
Atrina Centre
32 Kifissias Ave.
Paradissos-Amarousion, ATHENS
Greece
Tel: 682 88 11
Telex: 21-6588 HPAT GR
Cable: HEWPACKSA Athens

NORTH CENTRAL

AFRICA

Hewlett-Packard S.A.
7, Rue du Bois-du-Lan
CH-1217 MEYRIN 2, Switzerland
Tel: (022) 83 12 12
Telex: 27835 hpse
Cable: HEWPACKSA Geneva

ASIA

Hewlett-Packard Asia Ltd.
47/F, China Resources Bldg.
26 Harbour Rd., HONG KONG
G.P.O. Box 863,
Tel: 5-8330833
Telex: 76793 HPA HX
Cable: HPASIALTD TO

EASTERN EUROPE

Hewlett-Packard Ges.m.b.h.
Liebigasse 1
P.O. Box 72
A-1222 VIENNA, Austria
Tel: (222) 2365110
Telex: 1 3 4425 HEPA A

NORTHERN EUROPE

Hewlett-Packard S.A.
Uilenstede 475
P.O. Box 999
NL-1180 AZ AMSTELVEEN
The Netherlands
Tel: 20 437771

SOUTH EAST EUROPE

World Trade Center
110 Avenue Louis Casal
1215 Cointrin, GENEVA
Switzerland
Tel: (022) 98 96 51
Telex: 27225 hpser

OTHER INTERNATIONAL

AREAS

Hewlett-Packard Co.
Intercontinental Headquarters
3495 Deer Creek Road
PALO ALTO, CA 94304
Tel: (415) 857-1501
Telex: 034-8300
Cable: HEWPACK

ABOUT HEWLETT-PACKARD

David Packard and William Hewlett founded the company as a partnership in Palo Alto, California in 1939. Worldwide sales in fiscal year 1984 totalled U.S. \$6.04 billion. International sales accounted for almost 43% of this figure.

PEOPLE

Worldwide employment is over 83,000 with 26,000 employees outside the United States.

PRODUCTS

The company designs, manufactures, and markets measurement and computation products and systems used in business, industry, science, engineering, education, and medicine.

FACILITIES

Hewlett-Packard has manufacturing facilities the United States, Canada, Latin America, Europe, and Asia. The company has established joint ventures in Japan, the People's Republic of China, Mexico, and South Korea. Hewlett-Packard has 330 sales and support activities in 76 countries. Intercontinental Operations headquarters and HP's corporate offices are located in Palo Alto, California. European Operations are headquartered in Geneva, Switzerland.

HP Components

Authorized Distributor and Representative Directory

United States

Alabama

Hall-Mark Electronics
4900 Bradford Drive
Huntsville 35807
(205) 837-8700

Hamilton/Avnet
4940 Research Drive N.W.
Huntsville 35805
(205) 837-7210

Schweber Electronics
4930A Corporate Drive
Huntsville 35805
(205) 895-0480

Arizona

Hamilton/Avnet
505 South Madison
Tempe 85281
(602) 231-5100

Schweber Electronics
11049 N. 23rd. Drive
Suite 100
Phoenix 85029
(602) 997-4874

California

Hall-Mark Electronics
8130 Remmet Avenue
Canoga Park 91304
(818) 716-7300

Hall-Mark Electronics
1110 Ringwood Court
San Jose 95131
(408) 946-0900

Hall-Mark Electronics
19220 S. Normandie
Torrance 90502
(213) 217-8400

Hall-Mark Electronics
14831 Franklin Avenue
Tustin 92680
(714) 669-4700

Hamilton/Avnet
9650 De Soto Avenue
Chatsworth 91311
(818) 700-6500

Hamilton/Avnet (Corp)
10950 W. Washington Blvd.
Culver City 90230
(213) 558-2020

Hamilton/Avnet
3002 East G Street
Ontario 91764
(714) 989-4602

California (cont.)

Hamilton/Avnet
4103 Northgate Blvd.
Sacramento 95834
(916) 925-2216

Hamilton/Avnet
4545 Viewridge Avenue
San Diego 92123
(619) 571-7510

Hamilton/Avnet
1175 Bordeaux Drive
Sunnyvale 94086
(408) 743-3355

Hamilton Electro Sales
3170 Pullman Street
Costa Mesa 92626
(714) 641-4100

Hamilton Electro Sales
1361 "B" West 190th Street
Gardena 90248
(213) 217-6700

Schweber Electronics
21139 Victory Blvd.
Canoga Park 91303
(818) 999-4702

Schweber Electronics
1225 W. 190th Street
Suite 360
Gardena 90248
(213) 327-8409

Schweber Electronics
17822 Gillette Avenue
Irvine 92714
(714) 863-0200

Schweber Electronics
1771 Tribute Road
Suite B
Sacramento 95815
(916) 929-9732

Schweber Electronics
6750 Nancy Ridge Drive
Bldg. 7, Suites D & E
San Diego 92121
(619) 450-0454

Schweber Electronics
90 East Tasman Drive
San Jose 95134
(408) 946-7171

Colorado

Hamilton/Avnet
8765 East Orchard
Suite 708
Englewood 80111
(303) 779-9998

Colorado (cont.)

Schweber Electronics
8955 E. Nichols Avenue
Highland Tech Business Plaza
Englewood 80112
(303) 799-0258

Connecticut

Hall-Mark Electronics
Barnes Industrial Park
33 Village Lane
P.O. Box 5024
Wallingford 06492
(203) 269-0100

Hamilton/Avnet
Commerce Drive
Commerce Industrial Park
Danbury 06810
(203) 797-2800

Schweber Electronics
Finance Drive
Commerce Industrial Park
Danbury 06810
(203) 748-7080

Florida

Hall-Mark Electronics
15301 Roosevelt Blvd.
Suite 303
Clearwater 33520
(813) 530-4543

Hall-Mark Electronics
7648 Southland Blvd.
Suite 100
Orlando 32809
(305) 855-4020

Hall-Mark Electronics
3161 S.W. 15th Street
Pompano Beach 33069-4800
(305) 971-9280

Hamilton/Avnet
6801 N.W. 15th Way
Ft. Lauderdale 33309
(305) 971-2900

Hamilton/Avnet
3197 Tech Drive North
St. Petersburg 33702
(813) 576-3930

Hamilton/Avnet
6947 University Blvd.
Winter Park 32792
(305) 628-3888

Florida (cont.)

Schweber Electronics
317 S. North Lake Blvd.
Suite 1024
Altamonte Springs 31701
(305) 331-7555

Schweber Electronics
2830 N. 28th Terrace
Hollywood 33020
(305) 927-0511

Georgia

Hall-Mark Electronics
6410 Atlantic Boulevard
Suite 115
Norcross 30071
(404) 447-8000

Hamilton/Avnet
5825 D. Peachtree Corners East
Norcross 30092
(404) 447-7507

Schweber Electronics
303 Research Drive
Suite 210
Norcross 30092
(404) 449-9170

Illinois

Hall-Mark Electronics
1177 Industrial Drive
Bensenville 60106
(312) 860-3800

Hamilton/Avnet
1130 Thorndale Avenue
Bensenville 60106
(312) 860-7700

Schweber Electronics
904 Cambridge Drive
Elk Grove Village 60007
(312) 364-3750

Indiana

Hall-Mark Electronics
4275 W. 96th Street
Indianapolis 46268
(317) 872-8875

Hamilton/Avnet
485 Gradle Drive
Carmel 46032
(317) 844-9333

Iowa

Hamilton/Avnet
915 33rd Avenue S.W.
Cedar Rapids 52404
(319) 362-4757

Schweber Electronics
5270 North Park Place N.E.
Cedar Rapids 52402
(319) 373-1417

Kansas

Hall-Mark Electronics
10815 Lakeview Drive
Lenexa 66215
(913) 888-4747

Hamilton/Avnet
9219 Quivira Road
Overland Park 66215
(913) 888-8900

Schweber Electronics
10300 W. 103rd. Street
Suite 200
Overland Park 66214
(913) 492-2922

Maryland

Hall-Mark Electronics
10240 Old Columbia Road
Columbia 21046
(301) 988-9800

Hamilton/Avnet
6822 Oak Hall Lane
Columbia 21045
(301) 995-3500

Schweber Electronics
9330 Gaither Road
Gaithersburg 20877
(301) 840-5900

Massachusetts

Hall-Mark Electronics
6 Cook Street
Pinehurst Park
Billerica 01521
(617) 935-9777

Hamilton/Avnet
100 Centennial Drive
Peabody 01960
(617) 532-3701

Schweber Electronics
25 Wiggins Avenue
Bedford 01730
(617) 275-5100

Michigan

Hamilton/Avnet
2215 29th Street S.E.
Grand Rapids 49508
(616) 243-8805

Hamilton/Avnet
32487 Schoolcraft Road
Livonia 48150
(313) 522-4700

Michigan (cont.)

Schweber Electronics
12060 Hubbard Drive
Livonia 48150
(313) 525-8100

Minnesota

Hall-Mark Electronics
10300 Valley View Road
Suite 100
Eden Prairie 55344
(612) 941-2600

Hamilton/Avnet
10300 Bren Road E.
Minneapolis 55343
(612) 932-0600

Schweber Electronics
7424 W. 78th Street
Edina 55435
(612) 941-5280

Missouri

Hall-Mark Electronics
13750 Shoreline Drive
Earth City 63045
(314) 291-5350

Hamilton/Avnet
13743 Shoreline Court
Earth City 63045
(314) 344-1200

Schweber Electronics
502 Earth City Expwy.
Suite 203
St. Louis 63045
(314) 739-0526

New Hampshire

Hamilton/Avnet
444 East Industrial Park Dr.
Manchester 03103
(603) 624-9400

Schweber Electronics
Bedford Farms, Bldg. 2
Kilton & South River Road
Manchester 03102
(603) 625-2250

New Jersey

Hall-Mark Electronics
107 Fairfield Road
Suite 1B
Fairfield 07006
(201) 575-4415

Hall-Mark Electronics
1000 Midlantic Drive
Mt. Laurel 08054
(609) 235-1900

Hamilton/Avnet
1 Keystone Avenue
Cherry Hill 08003
(609) 424-0100

Hamilton/Avnet
10 Industrial Road
Fairfield 07006
(201) 575-3390

New Jersey (cont.)

Schweber Electronics
18 Madison Road
Fairfield 07006
(201) 227-7880

New Mexico

Hamilton/Avnet
2524 Baylor S.E.
Albuquerque 87106
(505) 765-1500

New York

Hall-Mark Electronics
1 Comac Loop
Ronkonkoma 11779
(516) 737-0600

Hamilton/Avnet
933 Motor Park Way
Hauppauge 11788
(516) 231-9800

Hamilton/Avnet
333 Metro Park Drive
Rochester 14623
(716) 475-9130

Hamilton/Avnet
103 Twin Oaks Drive
Syracuse 13206
(315) 437-2641

Schweber Electronics
3 Town Line Circle
Rochester 14623
(716) 424-2222

Schweber Electronics
Jericho Turnpike
Westbury 11590
(516) 334-7474

North Carolina

Hall-Mark Electronics
5237 North Boulevard
Raleigh 27604
(919) 872-0712

Hamilton/Avnet
3510 Spring Forest Road
Raleigh 27604
(919) 878-0810

Schweber Electronics
1 North Commerce Center
5285 North Boulevard
Raleigh 27604
(919) 876-0000

Ohio

Hall-Mark Electronics
5821 Harper Road
Solon 44139
(216) 349-4632

Hall-Mark Electronics
400 E. Wilson Bridge Rd.
Suite S
Worthington 43085
(614) 888-3313

Ohio (cont.)

Hamilton/Avnet
4588 Emery Industrial Parkway
Cleveland 44128
(216) 831-3500

Hamilton/Avnet
954 Senate Drive
Dayton 45459
(513) 439-6700

Hamilton/Avnet
777 Brooksedge Blvd.
Westerville 43081
(614) 882-7004

Schweber Electronics
23880 Commerce Park Road
Beachwood 44122
(216) 464-2970

Schweber Electronics
7865 Paragon Road
Suite 210
Dayton 45459
(513) 439-1800

Oklahoma

Schweber Electronics
4815 S. Sheridan
Suite 109
Tulsa 74145
(918) 622-8000

Oregon

Hamilton/Avnet
6024 S.W. Jean Road
Bldg. C, Suite 10
Lake Oswego 97034
(503) 635-8831

Pennsylvania

Hamilton/Avnet
2800 Liberty Avenue
Pittsburgh 15222
(412) 281-4150

Schweber Electronics
231 Gibraltar Road
Horsham 19044
(215) 441-0600

Schweber Electronics
1000 R.I.D.C. Plaza
Suite 203
Pittsburgh 15238
(412) 782-1600

Texas

Hall-Mark Electronics (Corp.)
11333 Pagemill Drive
Dallas 75234
(214) 343-5000

Hall-Mark Electronics
12211 Technology Blvd.
Austin 78727
(512) 258-8848

Hall-Mark Electronics
10375 Brookwood Road
Dallas 75238
(214) 553-4300

Hall-Mark Electronics
8000 Westglen
Houston 77063
(713) 781-6100

Texas (cont.)

Hamilton/Avnet
2401 Rutland
Austin 78758
(512) 837-8911

Hamilton/Avnet
8750 West Park
Houston 77063
(713) 780-1771

Hamilton/Avnet
2111 W. Walnut Hill Lane
Irving 75062
(214) 659-4111

Schweber Electronics
6300 La Calma Drive
Suite 240
Austin 78752
(512) 458-8253

Texas (cont.)

Schweber Electronics
4202 Beltway Drive
Dallas 75234
(214) 661-5010

Schweber Electronics
10625 Richmond Avenue
Suite 100
Houston 77042
(713) 784-3600

Utah

Hamilton/Avnet
1585 West 21st S.
Salt Lake City 84119
(801) 972-2800

Washington

Hamilton/Avnet
14212 N.E. 21st Street
Bellevue 98006
(206) 453-5844

Wisconsin

Hall-Mark Electronics
16255 West Lincoln Ave.
New Berlin 53151
(414) 797-7844

Hamilton/Avnet
2975 Moorland Road
New Berlin 53151
(414) 784-4510

Schweber Electronics
150 S. Sunnyslope Road
Brookfield 53005
(414) 784-9020

International

Australia

VSI Electronics Pty. Ltd.
Office 4
116 Melbourne Street
North Adelaide
South Australia 5006
(61) 8 267 4848

VSI Electronics Pty. Ltd.
Suite 3, Bell Court
Cnr. Water & Brunswick Streets
Fortitude Valley
Brisbane, Queensland 4006
(61) 7 52 5022

VSI Electronics Pty. Ltd.
Unit 1
25 Brisbane Street
East Perth, W.A. 6000
(61) 9 328 8499

VSI Electronics Pty. Ltd.
16 Dickson Avenue
Artarmon, N.S.W. 2064
(61) 2 439 8622

VSI Electronics Pty. Ltd.
6/417 Ferntree Gully Road
Mt. Waverley
Melbourne, Victoria 3149
(61) 3 543 6445

Austria

Transistor V.m.b.H
Auhofstr. 41a
A-1130 Wien
(43) 222 829451

Belgium

Diode Belgium
Luchtschipstraat 2
Rue De L'Aeronef 2
B-1140 Brussels
(32) 2 216 2100

Brazil

Datatronix Electronica LTDA
c/o MC-Microcircuits Ctd.
Rua Madeira, 42
03033 - Sao Paulo
(55) 11 543766
(55) 11 229845

Canada

Hamilton/Avnet
Electronics Ltd.
6845 Rexwood Drive
Units 3, 4 & 5
Mississauga, Ontario L4V 1R2
(416) 677-7432

Hamilton/Avnet
Electronics Ltd.
2795 Halpern Street
St. Laurent
Montreal, Quebec H4S 1P8
(514) 335-1000

Hamilton/Avnet
Electronics Ltd.
190 Colonnade Road
Nepean, Ontario K7E 7J5
(613) 226-1700

Hi-Tech Sales Limited (REP)
Box 115
339 10th Avenue S.E.
Calgary, Alberta T2G 0W2
(403) 239-3773

Hi-Tech Sales Limited (REP)
7510B Kingsway
Burnaby, B.C. V3N 3C2
(604) 524-2131

Hi-Tech Sales Limited (REP)
102-902 St. James Street
Winnipeg, Manitoba R3G 3J7
(204) 786-3343

Zentronics, Ltd.
8 Tilbury Court
Brampton, Ontario L6T 3T4
(416) 451-9600

Canada (cont.)

Zentronics, Ltd.
Bay #1
3300 14th Avenue, N.E.
Calgary, Alberta T2A 6J4
(403) 272-1021

Zentronics, Ltd.
155 Colonnade Road
Units 17 & 18
Nepean, Ontario K2E 7K1
(613) 226-8840

Zentronics, Ltd.
817 McCaffrey Street
Ville St. Laurent
Montreal, Quebec H4T 1N3
(514) 737-9700

Zentronics, Ltd.
Unit 108
11400 Bridgeport Road
Richmond, B.C. V6X 1T2
(604) 273-5575

Zentronics, Ltd.
546 Weber St. N.
Unit 10
Waterloo, Ontario N2L 5C6
(519) 884-5700

Zentronics, Ltd.
590 Berry Street
Winnipeg, Manitoba R3H 0S1
(204) 775-8661

China

(Peoples Republic of China)

China HP Rep Office
4th Floor, 2nd Watch Factory
Shuang Yu Shu
Bei San Huan Lu
Hai-Dian District, Beijing
(560) 280-567

Denmark

Interelko APA
Silovej 18
DK-2690 Karlslunde
(45) 3 140700

Finland

Field-OY
Veneentekijantie 18
SF-00210 Helsinki 21
(358) 0 6922577

France

Almex
Zone Industrielle d'Antony
48, rue de l'Aubepine
92160 Antony
(33) 1 6662112

F. Feutrier
8, Benoit Malon
F-92150 Suresnes
(33) 1 7724646

F. Feutrier
Rue des Trois Glorieuses
42271 St. Priest En Jarez
(33) 7 7746733

S.C.A.I.B.
80 rue d'Arceuil
Zone Silic 137
94523 Rungis Cedex
(33) 1 6872313

Germany

Distron GmbH
Behaimstrasse 3
D-1000 Berlin 10
(49) 30 3421041

EBV-Elektronik
Oberweg 6
D-8025 Unterhaching
Munich
(49) 89 611051

Germany (cont.)

Ingenieurbuero Dreyer
Flensburger Strasse 3
D-2380 Schleswig
(49) 4621 23121

Jermyn GmbH
Postfach 1180
D-6277 Bad Camberg
(49) 6434 230

SASCO GmbH
Hermann-Oberth Strasse 16
D-8011 Dutzbrunn
Munich
(49) 89 461 1211

Hong Kong

CET Ltd. (REP)
10/F Hua Hsia Bldg.
64-66 Gloucester Road
(852) 5 200922

India

Blue Star Ltd. (REP)
Sabri Complex II Floor
24 Residency Road
Bangalore 560 025
(91) 812-55660

Blue Star Ltd. (REP)
Sahas
414/2 Vir Savarkar Marg
Prabhadevi
Bombay 400 025
(91) 22-430-6155

Blue Star Ltd. (REP)
Bhandari House,
7th/8th Floors
91 Nehru Place
New Delhi 110 024
(91) 11-633-773

Blue Star Ltd. (REP)
2-2-47/1108 Bolarum Road
Secunderabad 500-003
(91) 842-72057

Israel

Computation & Measurement
Systems. Ltd. (REP)
11 Masad Street
P.O. Box 25089
Tel Aviv
(972) 3 388456

Italy

Celdis Italiana S.p.A.
Via Fratelli Gracchi, 36
I-20092 Cinisello Balsamo
Milano
(39) 2 6120041

Eledra 3S S.p.A.
Viale Elvezia, 18
I-20154 Milano
(39) 2 349751

Japan

Ryoyo Electric Corporation
Meishin Building
1-20-19 Nishiki
Naka-Ku, Nagoya, 460
(81) 52 2030277

Ryoyo Electric Corporation
Taiyo Shoji Building
4-6 Nakanoshima
Kita-Ku, Osaka, 530
(81) 6 4481631

Ryoyo Electric Corporation
Konwa Building
12-22 Tsukiji, 1-Chome
Chuo-Ku, Tokyo
(81) 3 543771

Tokyo Electron Company, Ltd.
Sinjuku-Nomura Building
Tokyo 160
(81) 3 3434411

Korea

Supertek Korea Inc. (REP)
Han Hyo Building
34-2 Yoido-Dong
Youngdungpo-Ku, Seoul
(82) 2 782-9076/8

Netherlands

Koning en Hartman
Elektrotechniek BV
Koperwerf 30
2504 AE Den Haag
(31) 70 210101

New Zealand

VSI Electronics Pty. Ltd.
#7 Beasley Ave., Penrose
Auckland
(64) 9593603

VSI Electronics Pty. Ltd.
Box 21-239
Christchurch
(64) 60928

VSI Electronics Pty. Ltd.
P.O. Box 11145
Wellington
(64) 4848922

Norway

HEFRO Teknisk A/S
P.O. Box 6596, Rodeløkk
N-0501 Oslo 5
(47) 2 380286

Singapore

Dynamar International Ltd. (REP)
12, Lorong Bakar Batu, #05-11
Kolam Ayer Industrial Park
Singapore 1334
(65) 747-6188

So. Africa

Advanced Semiconductor Devices
(Pty) Ltd.
P.O. Box 2944
Johannesburg 2000, S.A.
(27) 11 802-5820

Spain

Diode Espana
Avda. Brasil 5, 1st Planta
Madrid 20
(34) 14553686

Sweden

TRACO AB
Box 103
123 22 Farsta
(46) 8930000

Switzerland

Baerlocher AG
Foerlibuckstrasse 110
CH-8037 Zurich
(41) 1 429900

Fabrimex Ag
Kirchenweg 5
CH-8032 Zurich
(41) 1 251 2929

Taiwan (Republic of China)

Morrihan International Inc.
9F, No. 176
Fu, Hsing N. Road
Taipei
(886) 2 7151083

United Kingdom

Celdis Ltd.
37-39 Loverock Road
Reading, Berkshire
RG3 1ED
(44) 734 585171

Farnell Electronic
Components Ltd.
Canal Road
Leeds LS12 2TU
(44) 532-636311

Jermyn Distribution
Vestry Estate
Otford Road
Sevenoaks, Kent
TN14 5EU
(44) 732 450144

Macro Marketing Ltd.
Burnham Lane
Slough, Berkshire
SL1 6LN
(44) 628 64422

Yugoslavia

Elektrotehna
Do Junel O.Sol.O.
Tozd Elzas O.Sol.O.
Titova 81
61001 Ljubljana
(38) 61 347749
(38) 61 347841

Application Note Number/Title

Cross Reference

	Page
Application Bulletin 60: Applications Circuits for HCPL-3700 and HCPL-2601	105
Application Bulletin 65: Using 50/125 μ m Optical Fiber with Hewlett-Packard Components	227
Application Bulletin 69: CMOS Circuit Design Using Hewlett-Packard Optocouplers	76
Application Bulletin 71: Using 20 μ m PCS Optical Fiber with HP Components	201
Application Note 915: Threshold Detection of Visible and Infrared Radiation with PIN Photodiodes	184
Application Note 947: Digital Data Transmission Using Optically Coupled Isolators	19
Application Note 948: Performance of the 6N135, 6N136 and 6N137 Optocouplers in Short to Moderate Length Digital Data Transmission Systems	79
Application Note 951-1: Applications for Low Input Current, High Gain Optocouplers	98
Application Note 951-2: Linear Considerations of Optocouplers	88
Application Note 1000: Digital Data Transmission with the HP Fiber Optic System	247
Application Note 1002: Consideration of CTR Variations in Optically Coupled Isolator Circuit Designs	3
Application Note 1004: Threshold Sensing for Industrial Control Systems with the HCPL-3700 Interface Optocoupler	107
Application Note 1018: Designing with HCPL-4100 and HCPL-4200 20 mA Optocouplers	133
Application Note 1022: High Speed Fiber Optic Link Design with Discrete Components	231
Application Note 1023: Radiation Immunity of HP Optocouplers	69
Application Note 1024: Ring Detection with the HCPL-3700 Optocoupler	120
Technical Brief 101: Fiber Optic SMA Connector Technology	208
Technical Brief 102: Fiber/Cable Selection for LED Based Local Communications Systems	210
Technical Brief 103: High Speed Optocouplers vs. Pulse Transformer	92
Technical Brief 104: Baseband Video Transmission with Low Cost Fiber Optic Components	213

Solder Flux Considerations

In order to avoid Chloride corrosion of optocoupler leadframes, a halide-free flux is recommended for use in soldering operations. Recommended fluxes are shown below.

Summary of Recommended Halide-Free Fluxes

<u>Manufacturer</u>	<u>Flux</u>	<u>Description</u>
Kenco Alloy & Chemical Co., Inc. 418 W. Belden Addison, Ill. 60101 (312) 543-2510	Kenco 183	Citric acid based halide free flux, used by OCD
Alpha Metals, Inc. 600 Rte 440 Jersey City, NJ 07304 (201) 434-6778	250-MP TL 33M 433 Thinner 244A Saponifer	Organic acid flux system
London Chemical Co., Inc. P.O. Box 806 Beneville, Ill. 60196 (312) 766-5902	CF 350 CF 340 RF 9000D 1 PA Longoterge 520 Longoterge 530	Organic acid flux system Activated rosin flux system

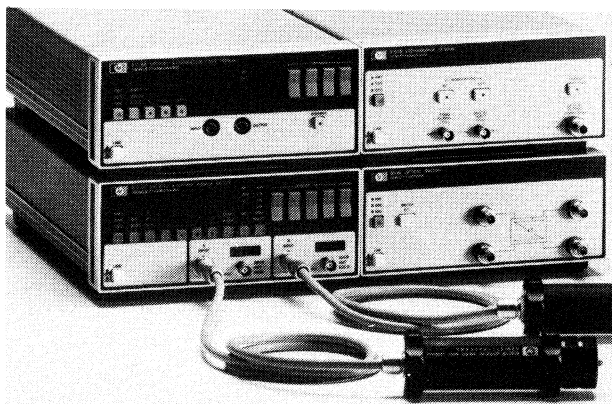
HP Offers the Fiber Optic Test Instruments You've Been Looking for . . .

. . . . when you need

high accuracy. to measure other than the standard wavelength. ratio measurements. full specifications.	The HP 8152A Optical Average Power Meter provides an accuracy of 0.15dB between 0dB and -50dBm full scale. and individual wavelength calibration for every Optical Head. two optical inputs for direct insertion loss and ratio measurement. full specifications over wavelength and all measurement ranges between 0 and 55°C.
high stability of output power.	The HP 8154B LED Source provides a stability of 0.02dB over 1 hour and 0.3dB over 1 year.
to adapt to different fiber types. to measure at different wavelengths. high resolution. high repeatability.	The HP 8158B Optical Attenuator provides measurements with single- and multimode fibers from 9 μ m to 85 μ m diameter. calibration at 1300nm and at 1550nm, and a typical curve between 1200 and 1650nm. a resolution of 0.01dBm. measurement repeatability of 0.04dB.
control measurements.	The HP 8159A Optical Switch provides an elegant way to avoid manual reconections.
automation of your tests.	The whole family provides Fuyll HP-IB control.

. . . and the literature.

Recently Christian Hentschel of the Boeblingen Instruments Division of HP wrote the paper "How to Make Accurate Fiber Optic Power Measurements." This paper is available to order in the U.S. from Hewlett-Packard, 1820 Embarcadero Road, Palo Alto, CA 94303, or in Europe from Hewlett-Packard, Nederland BV, Central Mailing Dept., P.O. Box 529, 1180 AM Amstelveen, The Netherlands. Use the publication number shown below when ordering.



Clockwise from top left are: The HP 8158B, the HP 8154B, the HP 8152A, the HP 8159A and the HP 81521B optical heads (foreground)

How to Make Accurate Fiber Optic Power Measurements.

(Publication Number 5952-9594)

At a first glance, optical power measurement appears simple. Most optical engineers learn about the limitations and inaccuracies of this measurement after discovering inconsistencies. These problems may be caused by the meter. But there is an equally high probability of problems outside of the meter, such as reflections, interferences and laser sensitivity to back-reflections.

The purpose of this paper is to give information about the effects involved when measuring optical power, and to show practical improvements both inside and outside the power meter.



**HEWLETT
PACKARD**

5954-8417

For more information call your local HP sales office listed in the telephone directory white pages. Ask for the Components Department. Or write to Hewlett-Packard: **U.S.A.** — P.O. Box 10301, Palo Alto, CA 94303-0890. **Europe** — P.O. Box 999, 1180 AZ Amstelveen, The Netherlands. **Canada** — 6877 Goreway Drive, Mississauga, L4V 1M8, Ontario. **Japan** — Yokogawa-Hewlett-Packard Ltd., 3-29-21, Takaide Higashi, Suginami-ku, Tokyo 168. **Elsewhere** in the world, write to Hewlett-Packard Intercontinental, 3495 Deer Creek Road, Palo Alto, CA 94304.

Printed in U.S.A.

Data Subject to Change

HPBK-5000 (7/86)